Mitochondrial Metabolism Elucidated by Rapid Fractionation from Tissue

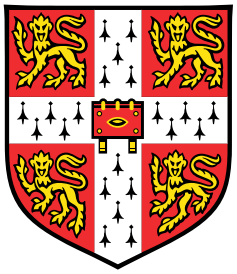

Fay Marie Allen

Department of Clinical Medicine
MRC Mitochondrial Biology Unit
University of Cambridge

This dissertation is submitted for the degree of
Doctor of Philosophy

Darwin College September 2019

Declaration

I hereby declare that except where specific reference is made to the work of others, the contents of this dissertation are original and have not been submitted in whole or in part for consideration for any other degree or qualification in this, or any other university. This dissertation is my own work and contains nothing which is the outcome of work done in collaboration with others, except as specified in the text and Acknowledgements. This dissertation contains fewer than 65,000 words including appendices, bibliography, footnotes, tables and equations and has fewer than 150 figures.

Fay Marie Allen
September 2019

Acknowledgements

Firstly, I would like to thank my supervisor, Prof. Mike Murphy, for the opportunity of completing my PhD in his lab. Thank you for your support and guidance, I have learnt so much and have relished the challenges the PhD has offered me.

I would also like to extend my thanks to AJ for his patient advice on many topics (in science and life in general!).

The MitoDys lab has taught me a lot and I am thankful for the technical support I have received from them and others at the MBU, including Carlo Viscomi for providing the animals. I am grateful to Tracy and Georgina for their support and running of the lab. Thank you to Tom and Georgina for assisting with the rapid isolations. Thank you to Liz, Hiran and Nils for reading parts of this thesis and for their insightful comments.

I am grateful to Christian Frezza and all in his lab who ran my MS samples: Sofia, Effie and Laura, thank you for your time and efforts with my samples, and for all of your advice.

I'm so grateful to everyone in SynBio at GSK for my introduction to science, I would not be where I am today without you all. A very special thanks to Andy Fos for his continued support and friendship (and for toning down the embarrassment - a bit).

To my Cambridge pals Cloudy, Cyan and Victoria – thanks for all your support, laughter and baking over the years. To darling Noor, thank you for fuelling my PhD with coffee! To Liz, thanks for your wise advice and always finding an excuse to celebrate/commiserate together over too much pasta. Anja, thank you for brightening up the lab and my entire PhD!

Mum, Dad and Nathan have been a constant source of support throughout my PhD. Mum, thank you for always, always being there. Nathan, you really are the best big brother, thanks for inspiring me and for your unfaltering belief in me, it means a lot. Dad, thanks for celebrating my every achievement and always being up for chatting science!

And lastly, to Phil. I am so happy we could experience Cambridge together. Thank you for being my rock and making me smile even in the harder times and for being by my side through everything.

Abstract

Mitochondria are metabolic hubs, with many diseases found to have altered metabolism and mitochondrial dysfunction, such as ischaemia-reperfusion injury. A detailed understanding of the metabolic changes in different cellular pools would aid diagnosis and treatment. However, the current methods of mitochondrial isolation are too slow to provide a snapshot of purely mitochondrial metabolism, meaning that current metabolic data is only from whole cell. This project has developed and used a novel technique to rapidly isolate mitochondria from tissue by density centrifugation through silicone oil, with a view to assess the mitochondrial metabolic changes during ischaemia-reperfusion injury. This method has minimal cytosolic contamination and is completed in under 5 minutes, and mass spectroscopy analysis has shown enrichment of mitochondrial metabolites. Seahorse and Oroboros analysis have shown that the mitochondria are functional and capable of coupled respiration. Data is presented on how the method optimisation was analysed and developed. This largely reduced time frame gives the advantage over other methods to enable the study of metabolism in mitochondria.

All abbreviations, unless listed, are as described in the "Instructions to Authors" of the Biochemical Journal (http://www.biochemj.org).

Δp: Proton motive force
ΔpH: pH gradient
$\Delta\psi$: Membrane potential
AAC: ATP/ADP carrier
AB: Ammonium bicarbonate
ABC: ATP-binding cassette
AcCoA: Acetyl CoA
ACL: ATP citrate lyase
AGC: Aspartate-glutamate carrier
AlaM: Alamethicin
APC: ATP-Mg/P_i carrier
BCA: Bicinchoninic acid
BME: β-Mercaptoethanol
BSA: Bovine serum albumin
BTM: Butylmalonate
CAC: Carnitine/acylcarnitine carrier
CATR: Carboxyatractyloside
cGPDH: Cytosolic glycerol-3-phosphate dehydrogenase
CI: Cold ischaemia
CIC: Citrate carrier
CPT1: Carnitine acyltransferase I
CPTII: Carnitine acyltransferase II
CS: Citrate synthase
Cyt *c*: Cytochrome *c*
DHAP: Dihydroxyacetone phosphate
DIC: Dicarboxylate carrier
DOP: Dioctyl phthalate
DSMPS: Poly(dimethylsiloxane-co-methyl-phenyl siloxane) oil
DTNB: 5,5'-dithio-bis-[2-nitrobenzoic acid]
DTT: Dithiothreitol
e^-: Electron
E_h: Reduction potential
ER: Endoplasmic reticulum

ESI: Electrospray ionisation
ETC: Electron transport chain
ETF: Electron-transferring flavoprotein
FA: Formic acid
FCCP: Carbonyl cyanide-p-trifluoromethoxyphenylhydrazone
FMN: Flavin mononucleotide
G3P: Glycerol-3-phosphate
G6P: Glucose-6-phosphate
Gpx: Glutathione peroxidase
GR: Glutathione reductase
Grx: Glutaredoxin
GSH: Glutathione
GSSG: Glutathione disulphide
GST: Glutathione-S-transferase
HIF: Hypoxia inducible factor
HILIC: Hydrophilic interaction liquid chromatography
HSAB: Heavy seahorse assay buffer
IDH: Isocitrate dehydrogenase
IMS: Intermembrane space
IRI: Ischaemia-reperfusion injury
IVC: Inferior vena cava
IP: Immunopurification
LAD: Left anterior descending artery
LC-MS: Liquid chromatography-mass spectrometry
LDH: Lactate dehydrogenase
MAS: Malate-aspartate shuttle
MACS: Magnetic cell sorting
mGPDH: Mitochondrial glycerol-3-phosphate dehydrogenase
MIM: Mitochondrial inner membrane
MLM: Mouse liver mitochondria
MOM: Mitochondrial outer membrane
MPC: Mitochondrial pyruvate carrier
MPS: Poly(methylphenylsiloxane) oil
MPTP: Mitochondrial permeability transition pore
mtDNA: Mitochondrial DNA
m/z: Mass:charge ratio

MVI: Missing value imputation
NBD: Nucleotide-binding domain
NEM: N-ethylmaleimide
NMR: Nuclear magnetic resonance
NO: Nitric oxide
NOS: Nitric oxide synthase
OAA: Oxaloacetate
OCR: Oxygen consumption rate
OGC: Oxoglutarate carrier
ORC: Ornithine carrier
OXPHOS: Oxidative phosphorylation
PBS: Phosphate-buffered saline
PC: Pyruvate carboxylase
PCA: Perchloric acid
PDH: Pyruvate dehydrogenase
PEP: Phosphoenolpyruvate
PEPCK: Phosphoenolpyruvate carboxykinase
PHD: Prolyl hydroxylase
P_iC: Phosphate carrier
PK: Pyruvate kinase
PNC: Purine nucleotide cycle
PM: Plasma membrane
PRP: Pyridoxal phosphate
Prx: Peroxiredoxin
PPP: Pentose phosphate pathway
PVDF: Polyvinylidene difluoride
Q: Ubiquinone
QH_2: Ubiquinol
RET: Reverse electron transfer
RLM: Rat liver mitochondria
ROS: Reactive oxygen species
SAB: Seahorse Assay Buffer
SDH: Succinate dehydrogenase
SDS: Sodium dodecyl sulphate
SOD: Superoxide dismutase
SSA: 5-Sulfosalicyclic acid

TA: Tris-acetate buffer
TAG: Triacylglycerol
TCA: Tricarboxylic acid cycle
TClA: Trichloroacetic acid
TIM: Translocase of the inner membrane
TOM: Translocase of the outer membrane
TM: Transmembrane
TMRM: Tetramethylrhodamine, methyl ester
TR: Thioredoxin reductase
Trx: Thioredoxin
UCP: Uncoupling protein
VDAC: Voltage-dependent anion channel
WI: Warm ischaemia XO: Xanthine oxidase

Table of contents

Chapter 1

Introduction

1.1 General Introduction

Mitochondria are endosymbiotic organelles present inside most eukaryotic cells which perform the vital role of ATP production by oxidative phosphorylation (OXPHOS), as well as many other important functions. Mitochondria are thought to have evolved over 2 billion years ago when oxygen-utilising α-proteobacteria were engulfed by early eukaryotic cells, forming a symbiotic relationship (Gray, 2012; Lane, Martin, 2010; Margulis, 1981). Gradually, many of the genes from this engulfed cell were transferred to the host genome, forming a relationship in which the oxygen-metabolising cell became a sub-cellular organelle that provided an energy source to the host cell. The organelle maintained some of its own genes and therefore the ability to use gene expression to modify certain factors independently, such as the proton motive force (Δp). The basis of the endosymbiotic theory is that this relationship enabled the host cell to increase in complexity and size, allowing the evolution of modern eukaryotic cells (Lane, Martin, 2010). Mitochondria have become so embedded in the function of eukaryotic cells that survival is dependent on fully functioning mitochondria that are able to respond and adapt quickly to changes in the external environment so that a steady energy supply can be maintained.

The division of labour in animals is achieved by specialised organs which perform specific functions. Organs are composed of multiple cell types, which contain multiple organelles,

which can be further compartmentalised by their spatial location within the cell. Organelles perform different metabolic functions, and this generates discrete metabolite pools across the cell, which are regulated by numerous, highly conserved metabolite transporters. This compartmentation has allowed the development of complexity in animals, with many metabolic reactions able to occur simultaneously across different locations (Zecchin et al., 2015). Some pathways require both intra- and extra-mitochondrial enzymes, such as the urea cycle. Mitochondrial subcellular localisation has been found to be important for cancer metastasis, with mitochondria at the leading front of migrating epithelial cancer cells (Desai 2013), suggesting the ATP required for actin remodelling during migration is supplied by mitochondria. Metabolism can also be compartmentalised temporally, for example glycolysis activity peaks during the S phase of the cell cycle (Zecchin et al., 2015).

The study of the compartmentalisation of metabolism is still an emerging field, partly due to a lack of techniques to study metabolic pathways in real time and also due to caveats to methods of visualising metabolic compartments. One such method is Förster resonance energy transfer (FRET) (Hou et al., 2011). Limitations to the use of this method are that the cells must be genetically modified and there are currently only a few reporter molecules. At present, the most comprehensive method for studying cellular metabolism is metabolic profiling by LC-MS or GC-MS methods.

Subcellular compartmentalisation delivers many advantages for metabolism. The unique subcellular microenvironments allow specific enzymes to function at their optimal capacity. For example, the enzymes of the lysosome, such as cathepsins, function optimally at an acidic pH (Voet, Voet, 2011). Furthermore, substrates and cofactors required for the activity of certain enzymes can be accumulated to the required concentrations in these smaller subcompartments, compared to the larger space of the cytosol. These reactions would otherwise be diffusion-limited due to substrate availability. Conversely, compartmentalisation also generates compartments that are distinct from the cytosol. For example, the high NADPH/$NADP^+$ ratio in the cytosol allows fatty acid synthesis to take place. Similarly, a membrane-bound compartment prevents the diffusion of metabolic intermediates, maximising efficiency. Some metabolic reactions produce toxic by-products, which can be sequestered away from the rest of the cell and disposed of. For example, hydrogen peroxide is contained and disposed of inside peroxisomes. Compartmentalisation also prevents futile cycling of metabolites by physically separating opposite reactions.

Mitochondria are able to respond to short-term energy demands of the cell by increasing or decreasing ATP production by OXPHOS, regulated by the magnitude of the Δp (Brown, 1992; Chance, Williams, 1956; Mitchell, 1961; Murphy, Brand, 1987). Mitochondrial ATP production is also regulated by the supply of electrons to the mitochondrial respiratory complexes, which themselves generate the Δp, as well as by the quantity of mitochondria in the cell. Responding to cellular energy demands requires effective communication between the mitochondria and other sub-cellular organelles. For example, an important signal that the cell must respond to is oxygen. Cells have evolved multiple mechanisms to cope with decreased oxygen levels, which include physiological responses such as vasodilation, angiogenesis and erythropoiesis, as well as metabolic responses, such as the activation of hypoxia-inducible transcription factors (HIFs) which promote glycolysis and allow the continued production of ATP in the absence of oxygen. This is an important example of communication between the mitochondria and the rest of the cell, as the HIF pathway can be activated by mitochondrial succinate exported to the cytosol (Tannahill et al., 2013). The release of succinate from mitochondria is also involved in downstream activation of the immune response (Mills et al., 2017).

The release of two other important nutrients, glucose and fatty acids, from their respective storage tissues liver and adipose tissue, is controlled by hormones. Once these are taken up by the cell there are many processes in the cytosol that facilitate the uptake of these nutrients or their downstream metabolites to the mitochondria, where they are substrates for the tricarboxylic acid (TCA) cycle and fatty acid oxidation, which both occur in the mitochondria and provide electrons to the respiratory complexes. A further example is the export of mitochondrial citrate to the cytosol to engage in lipid synthesis. Also, mitochondrial biogenesis (the growth and division of mitochondria) requires the synchronised transcription of mitochondrial genes encoded by both the mitochondrial and nuclear genomes (Lane, Martin, 2010).

A recently emerging form of communication between mitochondria and the cell is redox signalling, in the form of reactive oxygen species (ROS). Mitochondria are major producers of ROS, which in excess can overwhelm antioxidant responses, leading to oxidative damage and cell death (Smith et al., 2012). However, there is growing consensus that the release of ROS from mitochondria in controlled amounts can act as an important signal, informing the rest of the cell of mitochondrial redox status. In particular, ROS generated by reverse electron transport (RET) is potentially a signal involved in metabolic adaptation, and is

tightly regulated and responsive to mitochondrial redox status (Chouchani et al., 2014, 2016; Mills et al., 2016).

A key attribute of communication between mitochondria and the rest of the cell is energy sensing. AMP-activated protein kinase (AMPK) is an energy-sensing enzyme and a master regulator of energy metabolism (Jornayvaz, Shulman, 2010). It senses energy demand through an increase in AMP and ADP relative to ATP, triggering activation of ATP-producing mechanisms and inhibition of ATP-requiring mechanisms to limit energy demand (Carling et al., 2011; Garcia, Shaw, 2017; Hardie et al., 2012).

Despite numerous adaptive mechanisms, mitochondrial dysfunction occurs in certain conditions and plays a key role in many pathologies. Ischaemia-reperfusion injury (IRI) is caused by the blockage and subsequent return of blood flow to an organ. It is a disease whose pathology is dictated, in part, by mitochondrial dysfunction. There have been many studies looking at how cell and mitochondrial metabolism is altered in IRI (Chouchani et al., 2014; Ferrari, 1995; Heather et al., 2013; Martin et al., 2019) but these have all looked at metabolism at the whole cell level. This could mask any changes at the mitochondrial level. This project aimed to identify the metabolic changes in mitochondria during IRI and identify the key differences to the response of the rest of the cell.

In order to study the mitochondrial metabolic response, in either normal conditions or during IRI, the mitochondria must be isolated from the rest of the cell. The challenge here is that metabolites are interchanged and distributed throughout the cell by the action of enzymes and transporters. Therefore, to look at the level of a metabolite at any one time the isolation method must be performed quickly and coolly enough to limit the action of these enzymes and transporters. Unfortunately, no method met these fundamental criteria sufficiently at the start of this project.

The first aim of this project was to develop a method of isolating mitochondria from tissue that would enable me to obtain a true reading of the status of mitochondrial and cytosolic metabolites during normoxia, IRI and other conditions. The second aim was to implement the method in control tissue samples and analyse the metabolite levels by LC-MS. The third aim was to measure the metabolic response of mitochondria and the whole cell in ischaemic tissue. In the next sections, I give an overview of mitochondrial energy metabolism and transport before focusing on existing methods of mitochondrial isolation.

1.2 Structure and functions of mitochondria

1.2.1 Mitochondrial architecture, biogenesis and dynamics

According to the widely accepted endosymbiont theory, mitochondria originated from α-proteobacteria which were enveloped by a primordial eukaryotic cell, leading to an endosymbiotic relationship (Gray, 2012; Lane, Martin, 2010; Margulis, 1981). Mitochondria have retained some of the original structure and functions that they performed early on in the endosymbiosis, namely central metabolism and ATP generation for the rest of the cell, but they have also acquired new functions such as apoptotic signalling (Rasola, Bernardi, 2011) and innate immune responses (Mills et al., 2017). In this way they have become fully integrated into the metabolic and signalling pathways of the cell.

A few decades ago mitochondria were generally depicted as static rods, based on transmission electron microscopy (TEM) studies (see **Figure 1.1A and B**), but due to work with electron tomography and confocal microscopy they are now known to be far more dynamic, and that it is more accurate to consider mitochondria as part of a fused, elongated and dynamic network (Lee, Yoon, 2016) (**Figure 1.1C and D**). These networks can undergo fission and fusion, depending on their function and the metabolic demands of the cell (Civitarese et al., 2007).

Mitochondria consist of two membranes and two aqueous spaces. The mitochondrial outer membrane (MOM) is the outer barrier and separates the intermembrane space (IMS) from the cytosol. The mitochondrial inner membrane (MIM) separates the IMS from the matrix. The MOM is the primary barrier between the cytosol and the mitochondrion. It contains thousands of copies of the pore-forming protein porin or voltage-dependent anion channel (VDAC). This is a 31-kDa protein which forms a β-barrel structure with a central pore of $\sim$3.5 nm (Mannella, 1992). The pore allows the passage of metabolites across the MOM. Besides acting as a permeability barrier to proteins, the MOM has functions in cell death, mitochondrial fission and fusion, mitophagy and inflammation (Arnoult et al., 2011; Friedman, Nunnari, 2014). The IMS contains cytochrome *c* (Cyt *c*), a protein which is involved in electron transfer on the MIM and is released into the cytoplasm during apoptosis (**Section 1.3.7**). The IMS also contains other proteins such as Cu/Zn superoxide dismutase (SOD), which detoxifies superoxide ($O_2^{\cdot -}$), a potentially harmful by-product of oxygen metabolism, discussed in more detail later. The MIM is a protein-rich membrane which is highly folded into cristae. These sub-structures provide a large surface area to house the

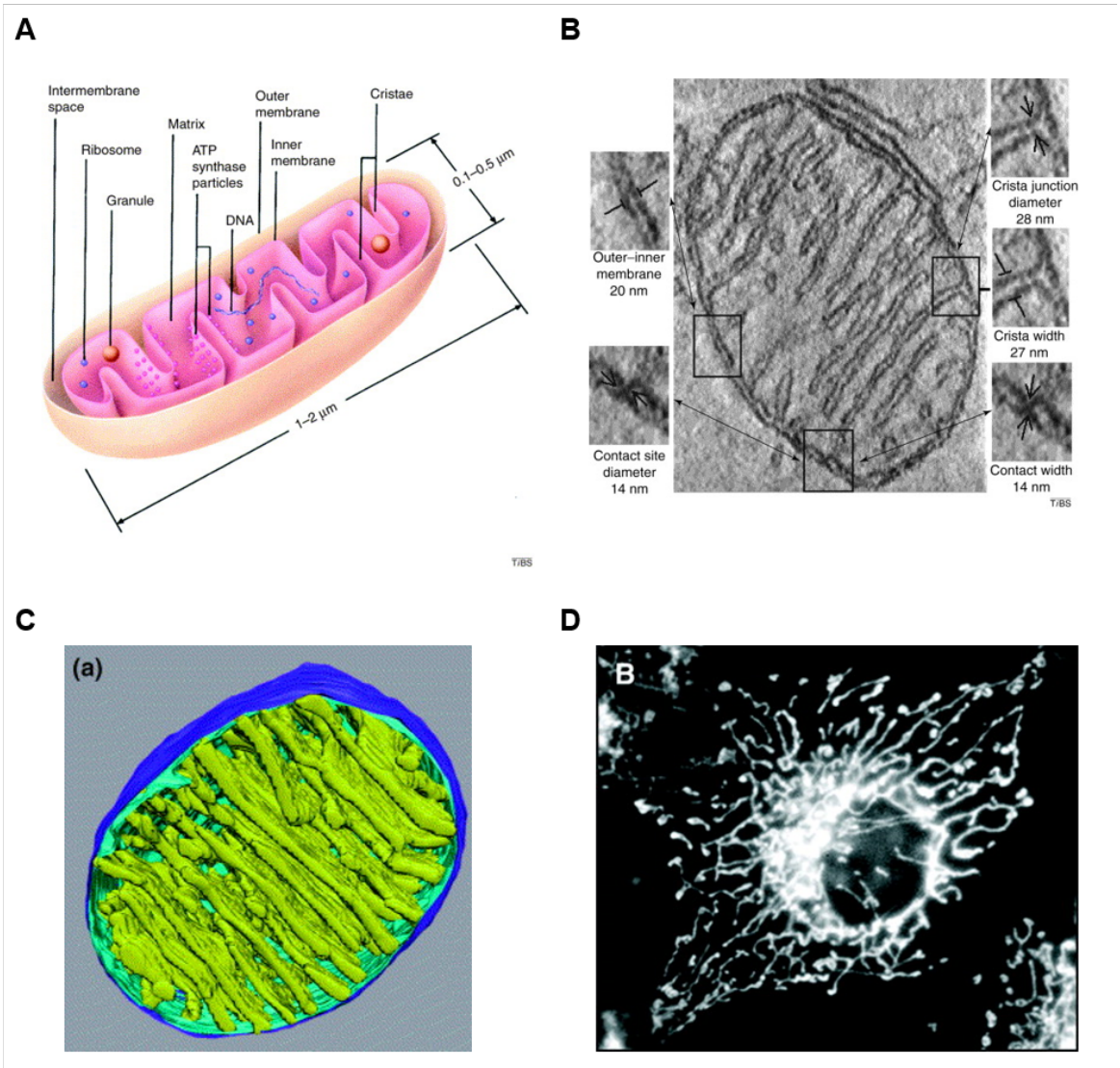

Fig. 1.1 Mitochondrial morphology. ***A)*** Cartoon model of mitochondrion (from Lodish et al. (2007)). ***B)*** Electron micrograph of a mitochondrion. ***C)*** Computer model generated from segmented 3D tomograms of a mitochondrion showing their 3D structure. ***D)*** Extended and interconnected mitochondrial network in an african green monkey fibroblast (COS-7 cell). Pictures A-C taken from Frey, Mannella (2000); D from Westermann (2002).

electron transfer chain (ETC) and ATP synthase, maximising the area available for oxidative phosphorylation and generating a high local concentration of H^+, which is discussed later.

The matrix is a viscous, protein-rich compartment containing membrane-bound projections of some respiratory complexes and the F_oF_1-ATP synthase as well as soluble enzymes (e.g. those involved in the TCA cycle, amino acid, fatty acid and ROS metabolism), nucleotide cofactors and many copies of the mitochondrial DNA (mtDNA) genome. The matrix also contains replication, transcription and translation machinery for expression and maintenance of mtDNA.

The human mitochondrial genome is a circular, double-stranded 16,569 bp molecule (Gustafsson et al., 2016). In mammals it encodes 37 genes: 22 transfer RNAs, 2 ribosomal RNAs and 13 polypeptides. All 13 polypeptides are components of respiratory chain complexes (I, III and IV) or the F_oF_1-ATP synthase, with their remaining subunits encoded by nuclear DNA. Complex II is entirely encoded by nuclear DNA. Despite having their own genome, 99 % of the ∼1,000 mitochondrial proteins are encoded by nuclear genes (Schmidt et al., 2010). This necessitates protein import systems (**Figure 1.2**). Many, but not all, nucleus-encoded mitochondrial proteins have an N-terminal targeting signal to direct them to the correct destination. The majority of mitochondrial proteins cross the MOM through the translocase of the outer membrane (TOM) complex. Once in the IMS, proteins destined for the matrix are imported by the presequence translocase of the inner membrane (TIM23) complex and the presequence translocase-associated motor (PAM). This presequence import is driven by the Δp. Mitochondrial processing peptidase (MPP) removes the presequence. IMS proteins are imported and folded by the mitochondrial intermembrane space assembly (MIA) machinery. Inner membrane proteins, such as metabolite carriers like the ADP/ATP carrier (AAC), contain transmembrane segments that are hydrophobic. They are imported through the TOM complex but then require the action of the chaperones in the IMS and the carrier translocase, the TIM22 complex (Schmidt et al., 2010; Wiedemann, Pfanner, 2017).

The current structure of mitochondria contains vestiges of their past as α-proteobacteria. The MOM and MIM have different lipid compositions. The MOM is more similar to the endoplasmic reticulum (ER) membranes of the host eukaryotes and the MIM is more similar to bacterial cell membranes, as it contains cardiolipin but no cholesterol (Cavalier-Smith, 2006). Much of the mitochondrial DNA replication machinery and ribosomes are similar to bacteria (Gustafsson et al., 2016).

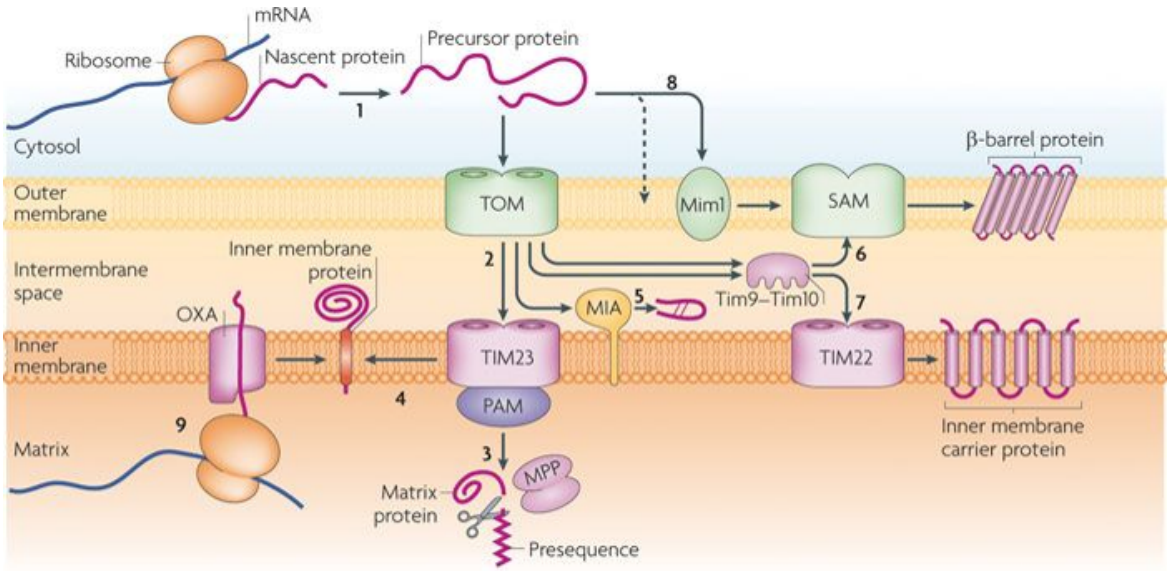

Fig. 1.2 Mitochondrial protein import systems. The majority of mitochondrial proteins are imported through the translocase of the outer membrane (TOM) complex. Once inside the IMS, targeting signals direct the precursor proteins to different sorting machineries. Matrix proteins are imported from the IMS to the matrix by the presequence translocase of the inner membrane (TIM23 complex) and the presequence translocase-associated motor (PAM). Once in the matrix the presequences are removed by mitochondrial processing peptidase (MPP). IMS proteins are imported and folded by the mitochondrial intermembrane space assembly (MIA) machinery. Inner membrane proteins such as carrier proteins are inserted into the inner membrane by the carrier pathway, with the action of chaperones and the carrier translocase TIM22. From (Schmidt et al., 2010).

As mitochondria are essential to the cell, there are many mitochondrial quality control mechanisms that help prevent mitochondrial dysfunction. One such mechanism is fission and fusion of the mitochondrial network (Lee, Yoon, 2016). Fusion of mitochondria generates continuous reticulated networks, which are hypothesised to maximise OXPHOS efficiency, but the details of this remain obscure. Fusion and fission are both driven by membrane-remodelling enzymes which are part of the dynamin family of large GTPases, including: Dynamin-related/-like protein 1 (Drp1); mitofusin (Mfn) and optic atrophy 1 (OPA1) (Lee, Yoon, 2016). Fusion is Δp-dependent and so only polarised mitochondria can fuse together, meaning that dysfunctional mitochondria with low Δp are excluded and prevented from damaging healthy networks of mitochondria (Twig et al., 2008). Whilst fusion is inhibited in these depolarised mitochondria, increased fission occurs, resulting in a mixture of damaged and healthy daughter organelles. This quality control mechanism means that damaged mitochondria are physically sequestered away from healthy mitochondria, before the damaged daughter organelles are targeted for removal by mitophagy (Gottlieb, Gustafsson, 2011). The healthy, polarised mitochondria are then able to recommence fusion and fission cycling.

Mitochondrial biogenesis is a complex process that involves the coordination of many pathways, such as nuclear-mitochondrial communication, mitochondrial protein expression and import, mtDNA gene expression, assembly of multi-subunit enzyme complexes, mitochondrial turnover, and regulation of mitochondrial fission and fusion (Diaz, Moraes, 2008). The expression of nuclear-encoded mitochondrial proteins is regulated by transcription factors and transcriptional coactivators. For example, peroxisome proliferator-activated receptor γ-coactivator-1α (PGC-1α) is an important transcriptional coactivator that coordinates mitochondrial biogenesis through the activation of different transcription factors (Scarpulla, 2002). Two important transcription factors are the nuclear respiratory factors 1 and 2 (NRF-1 and NRF-2) (Virbasius et al., 1993a,b) which activate the nuclear transcription of mitochondrial genes (Diaz, Moraes, 2008). NRF-1 and -2 also activate mitochondrial transcription factor A (Tfam), which further drives transcription and replication of mitochondrial DNA. The PGC-1 family regulates a number of metabolic pathways involved in mitochondrial biogenesis, including cellular respiration, thermogenesis and hepatic glucose metabolism. Mitochondrial biogenesis is often upregulated in mitochondrial disorders, which are the result of either nuclear or mtDNA mutations (Diaz, Moraes, 2008). These disorders often exhibit abnormal mitochondrial proliferation in an attempt to compensate for deficiencies, such as dysfunctional OXPHOS. As a result, these disorders often affect tissues with high energy demands, such as brain, heart and skeletal muscle (Diaz, Moraes, 2008).

Mitochondrial turnover must be carefully balanced with mitochondrial biogenesis to maintain cellular homeostasis. In older literature, figures for mitochondrial turnover of 9.3, 17.5 and 24.4 days for mitochondria in liver, heart and brain respectively can be found (Menzies, Gold, 1971). However, these data are hard to interpret as mitochondrial turnover includes turnover of whole mitochondria and individual proteins. The main way defective mitochondria are removed is by a specialised form of autophagy termed mitophagy, whereby mitochondria are selectively targeted for lysosomal degradation (Kim et al., 2007; Lee et al., 2012).

1.2.2 Oxidative phosphorylation

A major function of mitochondria is oxidative phosphorylation (OXPHOS), which is the energy transducing process by which F_oF_1-ATP synthase phosphorylates ADP to generate ATP (Chance, Williams, 1956). The energy used to drive this process comes from an electrochemical proton potential gradient across the MIM called the proton motive force (Δp). The Δp comprises two components: a pH gradient (ΔpH) (more basic in the matrix) and the membrane potential ($\Delta\Psi$) (more negative in the matrix) and was first described by Peter Mitchell in his chemiosmotic hypothesis (Mitchell, 1961). Metabolic substrates such as glucose, fatty acids or amino acids are oxidised by passing their electrons to the electron carriers NADH or $FADH_2$ (Wilson, 2017). These factors then pass their electrons to a series of respiratory complexes in the electron transport chain (ETC), which are arranged in order of increasing reduction potential (E_h) (Nicholls, Ferguson, 2013; Sazanov, 2015). The electron carriers ubiquinone (Q) in the MIM and Cyt *c* in the IMS are also involved in transferring electrons down the ETC. At the end of the ETC, complex IV reacts with the terminal electron acceptor O_2, which is reduced to H_2O. Electron transport is exergonic, and the energy released enables complexes I, III and IV to pump protons across the MIM from the matrix to the IMS against the growing proton electrochemical gradient, thereby generating the Δp. The Δp drives the flow of protons back through F_oF_1-ATP synthase, down the proton electrochemical gradient, and the energy of this is used to phosphorylate ADP to ATP (Watt et al., 2010). Thus, substrate oxidation is coupled to ATP synthesis, via the Δp and electron transfer to O_2. This process is depicted in **Figure 1.3** and outlined in more detail below.

Electrons from NADH enter the ETC via complex I (NADH:Q oxidoreductase) (Brandt, 2006). NADH binds to complex I on the matrix side of the MIM at a flavin mononucleotide (FMN), which accepts 2 electrons (e^-) from NADH to generate $FMNH_2$. The e^- are then

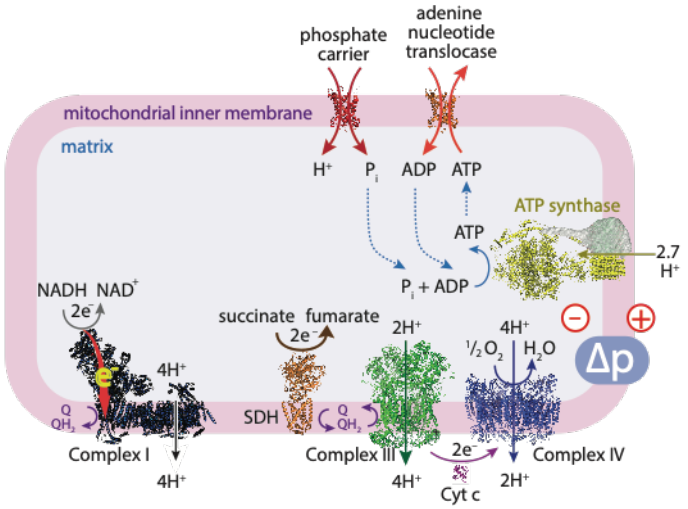

Fig. 1.3 The electron transport chain and oxidative phosphorylation. Electrons are donated to Complex I or Complex II by the electron carriers NADH and $FADH_2$ respectively. Electrons are passed along the respiratory chain, which is composed of complexes arranged in order of increasing reduction potential (E_h) (i.e more oxidising). The electron carriers ubiquinone (Q) and cytochrome *c* (Cyt *c*) move the electrons down the chain. Finally, electrons reach Complex IV and are passed onto the terminal electron acceptor O_2, which is reduced to H_2O. Electron transport is exergonic, providing energy to complexes I, III and IV to pump protons across the MIM from the matrix to the IMS, generating the Δp. The Δp drives H^+ back down its gradient through the F_oF_1-ATP synthase, which harnesses the energy of this movement to phosphorylate ADP to ATP. Adapted from Chouchani et al. (2016).

passed along a chain of 7 Fe-S clusters with increasing E_h within the hydrophilic arm of complex I to Q forming ubiquinol (QH_2). During this electron transfer process, complex I pumps $4H^+$ from the matrix to the IMS.

Complex II (succinate:Q oxidoreductase) also donates electrons to Q. Complex II oxidises succinate to fumarate and the e^- are passed on to the cofactor FAD, generating $FADH_2$. This is re-oxidised by passing its electrons along a series of Fe-S clusters within the complex to Q (Iverson, 2013). Unlike the other respiratory chain complexes, complex II does not pump protons across the MIM.

Besides the NADH/complex I- and succinate/complex II-mediated pathways, there are at least 3 other enzymes in mammalian mitochondria that donate electrons to the Q pool: electron-transferring flavoprotein (ETF)-ubiquinone oxidoreductase; *s,n*-glycerophosphate dehydrogenase (discussed further in **Section 1.5.4.6**) and dihydroorotate dehydrogenase. Although they do not have the "complex" nomenclature of the other respiratory chain enzymes, both ETF-ubiquinone oxidoreductase and *s,n*-glycerophosphate dehydrogenase are connected to the respiratory chain. Electron-transferring flavoprotein (ETF) is located in the mitochondrial matrix. It has 1 FAD cofactor and can accept electrons from a range of flavin-containing dehydrogenases, such as enzymes involved in fatty acid oxidation. The resulting $FADH_2$ on ETF is oxidised by ETF-ubiquinone oxidoreductase, which houses an FAD, an Fe-S and a Q binding site. ETF-ubiquinone oxidoreductase then passes its electrons directly to Q (Watmough, Frerman, 2010). $FADH_2$ is also produced during fatty acid oxidation and is an intermediate of the TCA cycle from oxidation of acetyl CoA, and can therefore transfer electrons directly to Q. The enzymes dihydroorotate dehydrogenase (involved in pyrimidine biosynthesis) and *s,n*-glycerophosphate dehydrogenase are thought to contain an FAD and donate electrons from $FADH_2$ to Q (Nicholls, Ferguson, 2013).

QH_2, from complex I, complex II, or the other enzymes mentioned above, binds to complex III (cytochrome *bc1* complex) at its Q_o site near the cytosolic side of the MIM (Crofts, 2004). One e^- from the bound QH_2 is passed to the 1 e^- carrier protein Cyt *c* via an Fe-S cluster and a cytochrome c_1 centre, with $1H^+$ released into the IMS. The other e^- is passed through 2 *b*-type cytochromes. The oxidised Q then binds to the Q_i site (near the matrix) and the electron on the *b*-type cytochrome is returned, generating the radical $QH^{\cdot}$. Another QH_2 molecule binds to the Q_o site and passes one electron to another Cyt *c*, and the second to the radical, fully reducing it to QH_2. This is known as the Q cycle and its net result is 1 reduced QH_2 and 1 oxidised Q which can return to complex I to pick up more electrons (Nicholls,

Ferguson, 2013). $4H^+$ are pumped from the matrix to the IMS per QH_2 oxidised. Cyt *c* then transfers electrons to complex IV (cytochrome *c* oxidase).

The final step in the electron transfer chain of mitochondria is the passage of 4 electrons from Cyt *c* and 4 protons from the matrix to molecular oxygen (O_2) in complex IV to generate 2 H_2O (Hosler et al., 2006). As the protons required for this are in the mitochondrial matrix (the N-side of the membrane) and the electrons come from the IMS (the P-side), this results in the transfer of 4 positive charges from the N-side to the P-side per O_2 reduced. In addition, complex IV is a proton pump and translocates 2 additional protons per 2 electrons from the N- to the P-phase (Kaila et al., 2010; Nicholls, Ferguson, 2013).

Complex V (F_oF_1-ATP synthase) then harnesses this proton electrochemical potential gradient to generate ATP. F_oF_1-ATP synthase is a proton translocating complex made from 2 substructures: F_o and F_1 (Walker, 2013). F_o is an insoluble transmembrane (TM) protein with a proton-translocation channel and F_1 is a soluble peripheral membrane protein that protrudes into the matrix. F_o and F_1 are joined by a 50 Å central stalk and a smaller peripheral stalk. ADP and P_i bind to the β-subunit on one of three $\alpha\beta$-protomers in the F_1 component. These protomers can exist in one of 3 conformational states that favour: binding of ADP and P_i, phosphorylation of ADP or release of ATP (Watt et al., 2010). In a process called the binding change mechanism, the protomers cycle through each of these conformational states. This is driven by the rotation of the c-ring (which has 8 subunits in mammals) in the F_o component relative to the central stalk. This rotation is itself driven by the return of H^+ from the IMS into the matrix through F_oF_1-ATP synthase. 2.7 protons are required to make 1 ATP molecule in the matrix (Watt et al., 2010).

The ATP is transported to the cytosol for use in energy requiring processes via the AAC, in a 1:1 exchange for ADP. This is an electrogenic process because ATP is exported as ATP^{4-} and ADP is imported as ADP^{3-}. The $\Delta\psi$ drives this electrogenic exchange. The AAC only translocates ADP for ATP and is not able to change the total adenine pool size. Therefore, the action of the ATP-Mg/P_i carrier (APC) is also required to change total pool sizes, by catalysing the electroneutral exchange of $ATP.Mg^{2-}$ for $HPO_4{}^{2-}$ (Klingenberg, 2008). P_i for phosphorylation of ADP is imported into the matrix via the phosphate carrier (P_iC). This transport is electroneutral, with most evidence favouring an $H_2PO_4{}^-$:H^+ symport mechanism driven by the ΔpH (Nicholls, Ferguson, 2013). The relationship of these carriers is depicted in **Figure 1.4**. Continuous ATP synthesis requires the coordinated activity of the ATP synthase, the AAC, and the PiC. The PiC and the AAC result in the import of one

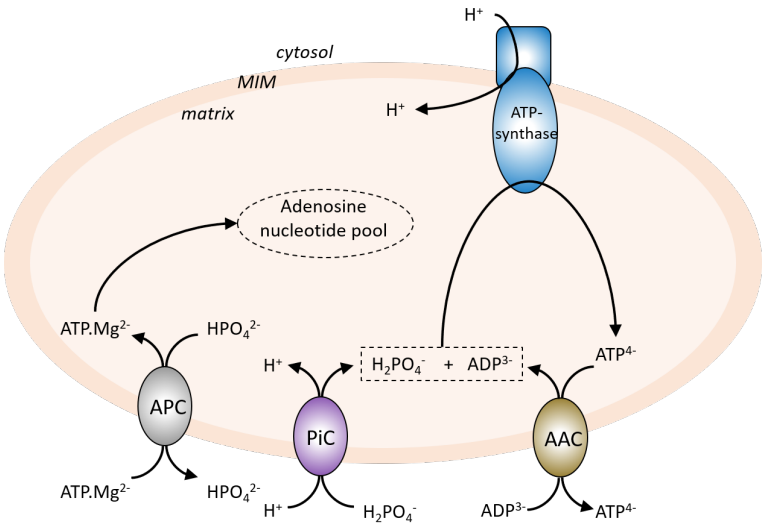

Fig. 1.4 Adenine nucleotide and phosphate transport in mitochondria. Phosphate ($H_2PO_4^-$) required for phosphorylation of ADP is imported into the mitochondria by the phosphate carrier (PiC) in an electroneutral symport mechanism with H^+. The ADP is imported into the mitochondria in an electrogenic exchange with ATP catalysed by the ADP/ATP carrier (AAC). ATP synthase phosphorylates ADP to ATP, concomitantly importing a proton into the matrix. As the AAC is a strict 1:1 exchanger it does not provide a mechanism for changing the total adenine nucleotide pool size. This is fulfilled by the ATP-Mg/Pi carrier (APC), which catalyses the import of $ATP.Mg^{2+}$ via an electroneutral exchange with HPO_4^{2-}.

additional proton to compensate for the charge imbalance of the AAC, so the H^+/ATP is 3.7. The P/O ratio is the ratio of the number of moles of ADP phosphorylated to ATP per 2 electrons in a defined segment of the electron transfer chain.

1.3 The role of mitochondria in cellular metabolism

Aerobic respiration in mitochondria requires several interconnecting pathways that converge to donate electrons to the ETC. Below, I outline the major metabolic pathways of cellular metabolism, with a particular emphasis on those that are either partly, or completely, housed within mitochondria and which feed products to mitochondria.

1.3.1 Glycolysis

Glycolysis is a cytosolic pathway but its intermediates, such as pyruvate and (indirectly) NADH, can be shuttled into mitochondria for use in energy transduction and biosynthesis (Bar-Even et al., 2012). The pathway generates ATP without using oxygen and is used in both aerobic and anaerobic conditions (Chandel, 2015). It is comprised of 10 enzymatic reactions that can be broadly split into ATP-requiring and ATP-generating reactions (**Figure 1.5**). Glycolysis begins with the phosphorylation of glucose and its end product is pyruvate, with many of its intermediates able to enter other biosynthetic pathways. Each molecule of glucose generates 2 molecules of pyruvate, with a net generation of 2 x ATP (4 generated and 2 invested) and 2 x NADH (Rich, Maréchal, 2010). In the presence of oxygen, both pyruvate and NADH are shuttled into the mitochondria. As NADH cannot cross the MIM and does not have a transporter, it enters the mitochondria indirectly through various mechanisms, such as the malate-aspartate shuttle (MAS). Once inside the mitochondria, NADH is oxidised by complex I of the ETC and pyruvate is decarboxylated by pyruvate dehydrogenase (PDH). This generates 1 x acetyl CoA (AcCoA) and 1 x NADH per pyruvate molecule. In the absence of oxygen, pyruvate cannot enter the ETC as the terminal electron acceptor, O_2, is not present. Instead, pyruvate is reduced to lactate by lactate dehydrogenase (LDH), coupled to NADH oxidation. Anaerobic glycolysis to lactate regenerates NAD^+ pools so that glycolysis, and thus ATP synthesis, can occur in the absence of O_2. In aerobic conditions, pyruvate is converted to malate before entry into the mitochondria via the MAS, which consists of several steps.

1.3.2 Gluconeogenesis

Glucose is stored in the body as glycogen in the liver, but the storage capacity of the liver is not sufficient to meet the glucose demands of the body, particularly under fasting conditions. Therefore, a further source of glucose is required: gluconeogenesis, which synthesises glucose from non-carbohydrate metabolites (Chandel, 2015). These include glycolytic lactate and pyruvate, TCA cycle intermediates and many amino acid carbon skeletons. The entry point for these precursors is oxaloacetate (OAA) (**Figure 1.5**). Fatty acids are not able to enter gluconeogenesis because their complete breakdown yields AcCoA, and there is no pathway for AcCoA conversion to oxaloacetate in mammals. Gluconeogenesis is also a way of regenerating glycolytic intermediates for the synthesis of other molecules,

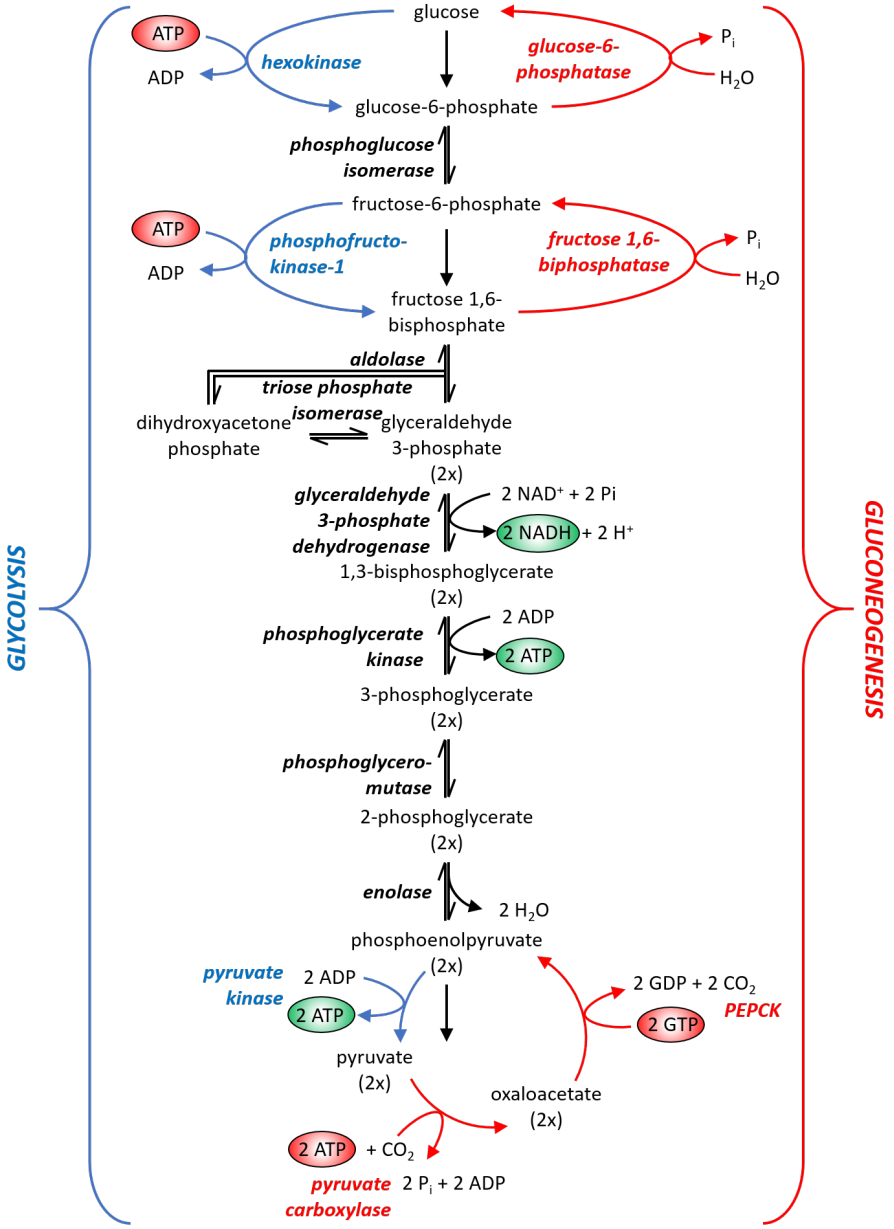

Fig. 1.5 Glycolysis and gluconeogenesis. The 10 steps of glycolysis are shown are shown alongside the steps of gluconeogenesis. Enzymes exclusive to glycolysis are shown in blue, with blue arrows depicting their reactions, and enzymes exclusive to gluconeogenesis are shown in red, with red arrows depicting their reactions. Enzymes and the reactions which are common to both glycolysis and gluconeogenesis are depicted in black. ATP and GTP molecules invested are shown in red circles and ATP and NADH molecules generated are shown in green circles. PEPCK: phosphoenolpyruvate carboxykinase.

such as lipids. The primary site of gluconeogenesis is the liver, and its reactions occur in both the mitochondrial matrix and the cytosol (Zhang et al., 2019). The majority of gluconeogenesis uses glycolytic enzymes, but three of the steps are catalysed by different enzymes (depicted in red in **Figure 1.5**) as these must overcome large negative free energy changes in the direction of glycolysis. The first reaction catalysed by a separate enzyme is catalysed by pyruvate carboxylase and phosphoenolpyruvate carboxykinase (PEPCK), which generates PEP from pyruvate. The second is catalysed by fructose 1,6-bisphosphatase, which converts fructose 1,6-bisphosphate to fructose-6-phosphate. The final reaction is catalysed by glucose-6-phosphatase, and generates glucose from glucose-6-phosphate. The biosynthetic gluconeogenesis and degradative pathway glycolysis differ in 3 reactions, which allows both directions to be simultaneously thermodynamically favourable under the same conditions (Chandel, 2015).

1.3.3 The tricarboxylic acid cycle

Pyruvate from glycolysis can enter the mitochondria and there be converted to AcCoA by PDH, which joins a larger pool of AcCoA from the oxidation of amino acids and fatty acids, and enters the TCA cycle. This is a central metabolic pathway of 8 enzymatic reactions that occurs in the mitochondrial matrix (**Figure 1.6**). The cycle generates the energy equivalents ATP or GTP and the reducing equivalents NADH and $FADH_2$, which ultimately generate ATP via OXPHOS (Akram, 2014). The cycle begins with AcCoA which is oxidised in a stepwise manner during the 8 reactions to yield 3 x NADH, 1 x $FADH_2$, 1 x GTP and 2 x CO_2. Glycolysis generates 2 x ATP (net) from 1 molecule of glucose, whereas aerobic respiration can theoretically generate an additional $\sim$36 x ATP from 1 molecule of glucose: 2 x ATP from TCA cycle and $\sim$34 x ATP from OXPHOS (10 x NADH and 4 x $FADH_2$). Thus it can be seen that aerobic respiration of glucose is more energy efficient in terms of ATP production than glycolysis alone (Rich, Maréchal, 2010).

The TCA cycle is positioned at the core of cellular metabolism and acts as a biosynthetic hub. It forms a bridge between metabolism and oxidative phosphorylation because one of its enzymes, SDH, is an enzyme of the TCA cycle and also a respiratory complex of the ETC. Furthermore, TCA cycle intermediates can feed into other metabolic pathways, acting as precursors for many other biomolecules such as haem, from succinyl-CoA, and lipids, from AcCoA (Akram, 2014; Chandel, 2015). The intermediates that are removed must be replenished, so that the cycle can continue. This is referred to as anaplerosis and

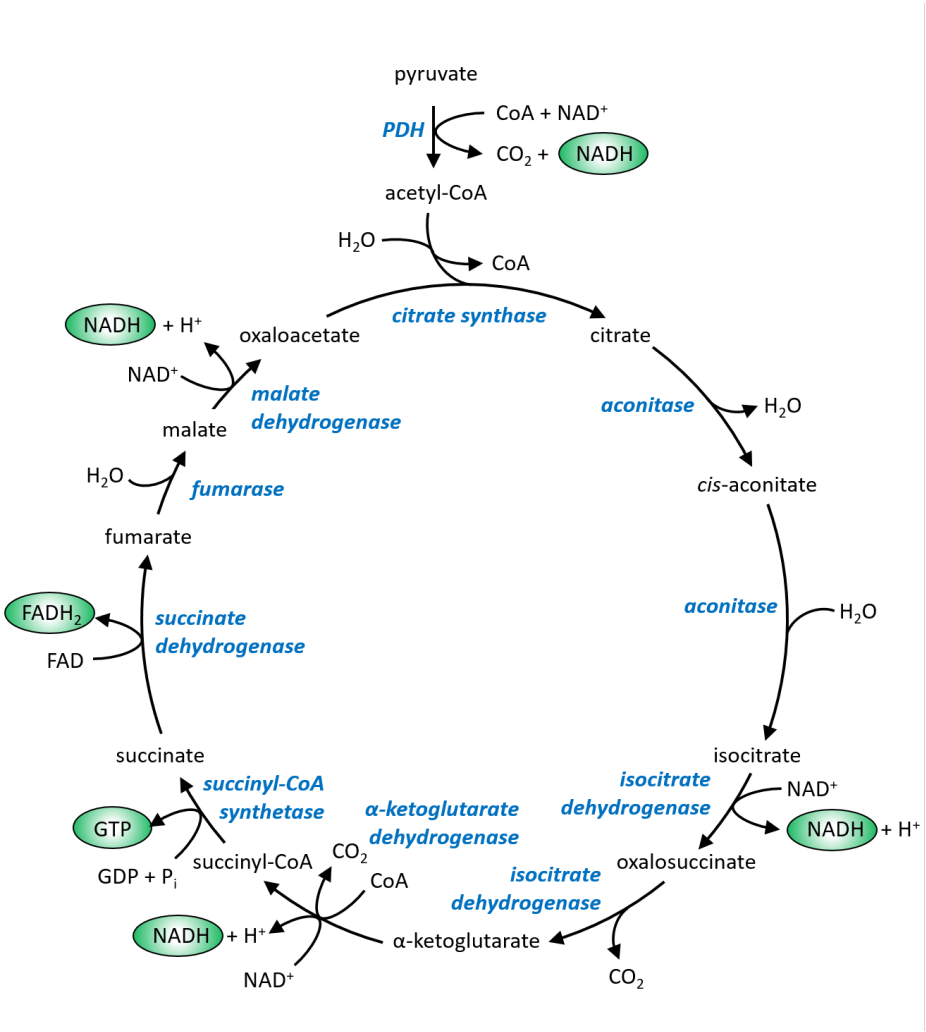

Fig. 1.6 The citric acid cycle. The cycle begins when acetyl CoA (AcCoA) is reduced to citrate. The cycle generates 3 x NADH, 1 x $FADH_2$, 1 x GTP and 2 x CO_2. Reducing equivalents (NADH and $FADH_2$) and energy equivalents (GTP) generated during the cycle are shown in green circles. Enzymes are written in blue. PDH: pyruvate dehydrogenase; CoA: Coenzyme A.

can occur because many different substrates can be broken down to enter the TCA cycle at various points, including fatty acids, amino acids and pyruvate. One important anaplerotic process is the conversion of pyruvate to OAA by pyruvate carboxylase. Another major input is glutaminolysis. This is the conversion of glutamine to glutamate and finally to α-ketoglutarate, which can enter the TCA cycle. Glutaminolysis is an important mechanism during lipid synthesis, as citrate is exported from the mitochondria to participate in the lipid synthesis. The removal of citrate limits the formation of downstream α-ketoglutarate (Chandel, 2015). The TCA cycle allows mitochondria to monitor and respond to the needs of cellular metabolism, and synthesise the biomolecules they need to carry out their own functions and for export for cellular functions.

1.3.4 Amino acid metabolism

There are 20 amino acids, nine of which are "essential" in humans and must be obtained from the diet, whilst the rest can be synthesised from glycolytic and TCA cycle intermediates. Amino acids are important for protein synthesis but also have roles in the generation of glucose, ATP and fatty acids and are precursors for haem groups and signalling molecules such as neurotransmitters (Chandel, 2015). Amino acid metabolism occurs in both the cytosol and the mitochondrial matrix.

In the heart, amino acids are metabolised under normal and pathological conditions. They have an anaplerotic role and can be metabolised to TCA cycle intermediates to generate energy (Drake et al., 2012). For example, glutamate can be transaminated to α-ketoglutarate, which can either enter the TCA cycle to generate NADH and GTP or be further metabolised to alanine, aspartate and arginine. Asparagine can be used as a mechanism to remove excess nitrogen from the cell, or be converted to aspartate. Aspartate can then be transaminated to oxaloacetate and enter the TCA cycle. This transamination reaction is reversible, allowing aspartate and asparagine to act as sinks for excess oxaloacetate. Alanine can be transaminated to pyruvate, whose oxidation yields NADH and GTP. The branched-chain amino acids (BCAAs) can be metabolised to AcCoA, pyruvate and succinyl-CoA, which has been suggested to be cardioprotective during ischaemia. Other amino acids can also be catabolised by the heart, with varying energy recovery yields. It should be noted that under normal conditions amino acid metabolism contributes only a small amount to cardiac ATP production. However, in certain conditions, such as when oxygen levels fall during

ischaemia, the heart relies on a broader range of fuel sources, including amino acids (Drake et al., 2012).

Besides energy generation, amino acid metabolism has important biosynthetic roles in the cell. For example, the mitochondrial enzyme aminolevulinate synthase (ALAS) is the rate-limiting enzyme in haem synthesis (Dwyer et al., 2009). Furthermore, mitochondrial glycine is a precursor in haem synthesis. Glycine and glutamate serve as neurotransmitters, with glutamate also generating the neurotransmitter γ-aminobutyric acid (GABA). Glutamate, glycine and cysteine generate the antioxidant glutathione. The metabolism of arginine by nitric oxide synthase (NOS) generates nitric oxide (NO), an important signaling molecule in the heart. Methionine provides the methyl group necessary for DNA and histone methyltransferases which regulate epigenetics. Glutamate is important for the interconversion of many different amino acids because it can act as both a nitrogen donor and acceptor (Chandel, 2015).

1.3.5 The urea cycle

Free amino acids cannot be stored and are deaminated, generating a carbon skeleton and ammonium (NH_4^+). Ammonium at high levels is toxic and must be removed. It is converted to urea by the urea cycle and excreted via the kidneys in mammals. The urea cycle consists of 5 enzymatic reactions and is mostly found in the liver, in both the mitochondria and the cytosol (**Figure 1.16**). The first two steps occur in the mitochondrial matrix: carbamoyl phosphate synthetase I generates carbamoyl phosphate from NH_4^+ and HCO_3^-, using 2 ATP molecules and sequestering the first nitrogen atom. Ornithine transcarbamoylase combines ornithine and carbamoyl phosphate to form citrulline. Citrulline is exported from the mitochondrial matrix to the cytosol in exchange for ornithine by the ornithine carrier (ORC). Citrulline and aspartate are converted to argininosuccinate in the cytosol by argininosuccinate synthetase, using another ATP molecule and incorporating the second nitrogen atom. Argininosuccinase metabolises argininosuccinate to arginine and fumarate. Finally, arginine is converted to ornithine by arginase, generating urea (Chandel, 2015; Morris, 2002). The fumarate produced in the cytosol is converted to malate by cytosolic fumarase. Malate can then enter the mitochondria and its conversion to oxaloacetate generates NADH, which is able to generate ATP through OXPHOS.

1.3.6 Fatty acid oxidation

Fatty acids are important structural and metabolic components of the cell. They are incorporated into many different types of lipids, such as the energy storing triacylglycerols (TAGs) (glycerol attached to saturated and unsaturated fatty acids) and the membrane components phospholipids (a glycerol molecule with two fatty acid tails attached to a polar molecule, such as choline, via a phosphate bond) (Chandel, 2015). Lipids also have metabolic roles in the cell. For example, the fatty acid arachidonic acid is a precursor of prostaglandins, These are a subclass of eicosanoids with hormone-like effects in mammals, and can be inflammatory and act as vasodilators (Kuehl, Egan, 1980).

Mitochondria have a role in both fatty acid synthesis and breakdown (termed β-oxidation). Although fatty acid synthesis occurs in the cytosol, where the high NADPH/$NADP^+$ ratio drives the reactions, mitochondrial citrate is required to provide the building blocks. Citrate is exported from the mitochondria to the cytosol, where it is metabolised to AcCoA by ATP citrate lyase (ACL)(Kastaniotis et al., 2017). AcCoA is then carboxylated to malonyl-CoA by AcCoA carboxylase (ACC), which is an irreversible reaction. The synthesis pathway then enters the elongation phase, whereby malonyl-acyl carrier protein (ACP) is formed from malonyl-CoA and acetyl-ACP is formed from AcCoA, catalysed by malonyl transacylase and acetyl transacylase respectively. Malonyl-ACP and acetyl-ACP then react in a series of 7 enzymatic reactions to form palmitate, catalysed by fatty acid synthase. In mammals these enzymes are collectively termed type II fatty acid synthase (FAS-II). Palmitate can then be further modified to other fatty acids.

A key difference between fatty acid synthesis and β-oxidation is the electron donor. β-oxidation uses FAD, whereas synthesis utilises NADPH. The metabolism of citrate by ACL yields oxaloacetate and AcCoA, which is directly involved in fatty acid synthesis. Malate dehydrogenase reduces this oxaloacetate to malate, which can be oxidised to pyruvate in the cytosol. This generates cytosolic NADPH which drives many of the reactions of fatty acid synthesis. The pentose phosphate pathway (PPP), 1-carbon metabolism and isocitrate dehydrogenase 1 (IDH1) also generate NADPH needed for fatty acid synthesis. Besides citrate, AcCoA can also be generated in the mitochondria from pyruvate (either from glycolysis or amino acid metabolism).

Stored TAGs can be broken down to generate fatty acids and glycerol. The glycerol backbone enters glycolysis through dihydroxyacetone phosphate. The fatty acids enter the mitochondria

which house the enzymes required for β-oxidation, which is an ATP-generating process. For β-oxidation to occur, the fatty acids must be transported into the mitochondrial matrix from the cytosol, via the carnitine transport cycle (**Figure 1.7**)(Kerner, Hoppel, 2000). This requires the fatty acid to first be converted to a fatty acyl-CoA by the action of fatty acyl-CoA synthetase in the cytosol. Carnitine acyl transferase (CPT1) can then replace CoA with a carnitine molecule, forming a fatty acyl carnitine molecule. This is translocated into the mitochondrial matrix by carnitine-acylcarnitine translocase in the MIM via an exchange mechanism with carnitine. Once in the matrix carnitine acyltransferase II removes the carnitine from the fatty acylcarnitine, generating fatty acyl-CoA. The carnitine is shuttled back across the membrane to act as a tag for another fatty acyl-CoA (Kerner, Hoppel, 2000).

The fatty acyl-CoA in the matrix can then enter the β-oxidation pathway. The long chains of fatty acyl-CoAs are degraded by the sequential removal of 2-carbon acetyl-CoA, concomitantly generating NADH and $FADH_2$ (Adeva-Andany et al., 2019; Houten et al., 2016). After each removal, the subsequent 2-carbon shorter acyl-CoA becomes the substrate for another round of β-oxidation. As each acetyl-CoA generates 3 NADH, 1 $FADH_2$ and 1 GTP, for the 16-carbon fatty acid palmitate, its complete β-oxidation generates 31 NADH (24 from acetyl-CoA + 7 from 7 x rounds of β-oxidation), 15 $FADH_2$ (8 from acetyl-CoA + 7 from 7 x rounds of β-oxidation) and 8 GTP. NADH and $FADH_2$ can enter OXPHOS to generate ATP, and GTP can be converted to ATP by nucleoside diphosphate (NDP) kinase. As each NADH generates 2.5 ATP, $FADH_2$ generates 1.5 ATP, and 1 GTP can be converted to 1 ATP, 108 molecules of ATP are generated from palmitate oxidation. Subtracting the 2 ATP used for the activation step gives a net ATP yield of 106 ATP molecules from palmitate oxidation.

Some tissues, such as the heart, rely on β-oxidation all the time, whereas other tissues switch to β-oxidation when cellular glucose levels are low, and glycolysis cannot generate acetyl-CoA (Houten et al., 2016). Fatty acid oxidation then steps in to generate the acetyl-CoA needed to maintain the TCA cycle. The heart is described as a "metabolic omnivore" and switches rapidly between fuel sources according to supply (Grynberg, Demaison, 1996). The heart uses fatty acid as its main fuel source because storage of fatty acids as TAGs in the body as an energy store is more efficient than glucose storage. This is because the energy density of fatty acids is much higher compared to glucose, stored as glycogen. The oxidation of these energy-rich molecules yields around twice as much energy as glucose (39 kJ/g for palmitate compared to 15 kJ/g for glucose). This is because fatty acid oxidation (or β-oxidation) occurs by the stepwise release of AcCoA from the acyl-CoA, generating 1 x NADH and 1 x $FADH_2$. Each AcCoA then yields 3 x NADH, 1 x $FADH_2$ and 1 x GTP in the TCA cycle. This means

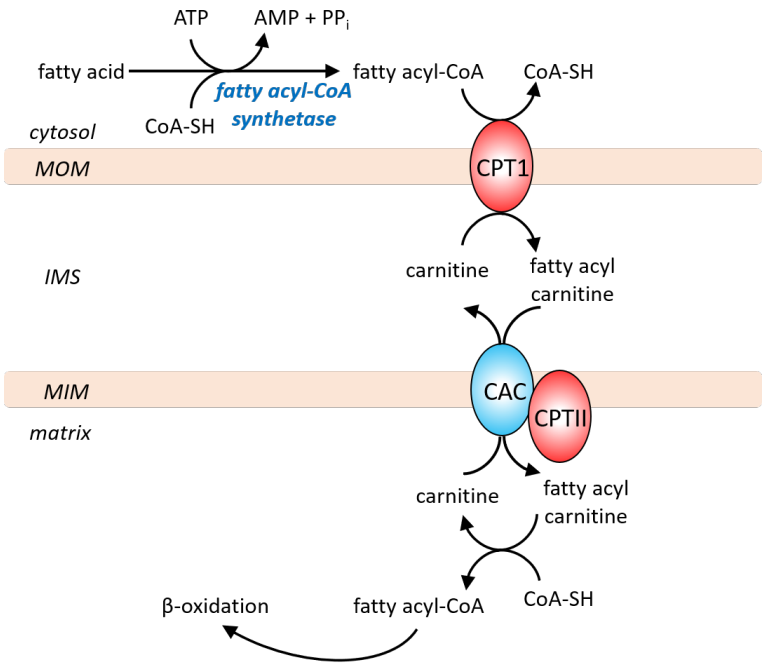

Fig. 1.7 The carnitine shuttle imports fatty acids into the mitochondria. Fatty acids in the cytosol are converted to a fatty acyl-CoA by fatty acyl-CoA synthetase. The fatty acyl-CoA can then be tagged with a carnitine by carnitine acyltransferase I (CPT1) in the MOM, generating a fatty acyl carnitine. The carnitine/acylcarnitine carrier (CAC) in the MIM catalyses the exchange of the fatty acyl carnitine for matrix carnitine. Once in the matrix, the fatty acyl carnitine is converted to to fatty acyl-CoA by carnitine acyltransferase II (CPTII). This releases carnitine, which is shuttled back to the cytosol to tag another fatty acyl-CoA for transport.

the oxidation of the 16-carbon fatty acid palmitate yields ∼106 x ATP (Röhrig, Schulze, 2016).

1.3.7 Other functions of mitochondria

Mitochondria are involved in a plethora of cellular processes besides the above mentioned roles in carbohydrate, fatty acid and amino acid metabolism. Below I describe other mitochondrial processes that are crucial for cellular function.

Mitochondria are essential for the assembly of iron-sulphur (Fe-S) clusters and for haem biosynthesis (Paul, Lill, 2015; Ye, Rouault, 2010). Fe-S clusters are small, highly conserved inorganic protein cofactors, which act as electron carriers in a range of redox reactions (e.g. in respiratory complexes) and have catalytic activity in some chemical reactions (e.g. aconitase). They are found in the mitochondria, the cytosol and the nucleus, but they are all synthesised in the mitochondria using the conserved iron-sulphur cluster (ISC) assembly machinery. Cytosolic and nuclear Fe-S proteins also require the action of the cytosolic iron-sulphur protein assembly (CIA) machinery (Paul, Lill, 2015). Iron-containing haem groups are synthesised solely in the mitochondria, where they are used in cytochromes or are exported from the mitochondria for use in haemoglobin and myoglobin (Ye, Rouault, 2010).

Mitochondria have a role in calcium storage and signalling. Mitochondria form intimate connections with the ER (Lebiedzinska et al., 2009; Murley, Nunnari, 2016), which rapidly takes up calcium to maintain calcium homeostasis. Mitochondria are also able to take up calcium into the matrix through the mitochondrial calcium uniporter (MCU) on the MIM, thereby acting as a calcium buffer. Movement of calcium into the mitochondria modulates mitochondrial ATP production (Brand, Murphy, 1987; Mammucari et al., 2011; McCormack et al., 1990).

Mitochondrial calcium is a major factor in a further role of mitochondria: the regulation of cell survival. Mitochondria are key players in both programmed cell death by apoptosis and necrotic cell death. In the mitochondrial pathway of apoptosis the release of mitochondrial factors, such as Cyt *c* from the IMS, is a critical step in committing the cell to activating apoptosis (Tait, Green, 2010). Necrosis often involves the opening of the mitochondrial permeability transition pore (MPTP) and is triggered by the accumulation of calcium inside mitochondria as well as ROS (Halestrap, 2005; Rasola, Bernardi, 2011). The opening of

the MPTP causes the loss of ATP and the collapse of ion gradients, as the dysfunctional mitochondria are unable to use ATP to maintain these gradients.

Mitochondria also play a range of roles in the immune response. Mitochondria release various signals that act as damage-associated molecular patterns (DAMPs). For example, mtDNA is released by damaged or necrotic cells and binds to the TLR9 receptor, leading to activation of the NF-κB signalling pathway and proinflammatory gene transcription (Mills et al., 2017). In this way the mitochondria signal to the nucleus that there is damage, enabling the cell to adapt and kickstart repair mechanisms. Furthermore, the MOM acts as a platform for signaling molecules such as mitochondria-associated viral sensor (MAVS), triggering immune responses (Arnoult et al., 2011). Mitochondrial succinate can be released from the cell, where it can act as an extracellular signal by binding to its receptor SUCNR1 (Rubic et al., 2008), triggering an immune response. Once in the cytosol succinate can also stabilise HIF1α (Murphy, O'Neill, 2018), discussed in more detail later.

1.4 Mitochondrial ROS production

Mitochondria are major sources of reactive oxygen species (ROS) within the cell, such as H_2O_2 and $O_2^{\cdot-}$ (Arnoult et al., 2011; Murphy, 2009; Tormos et al., 2011). Uncontrolled, aberrant ROS production can overwhelm antioxidant defences and lead to oxidative damage, both within the mitochondria and the rest of the cell, because ROS are damaging to lipids, proteins and DNA (**Figure 1.8**). This oxidative damage contributes to a range of pathologies (Smith et al., 2012). Lipid peroxidation can increase the permeability of the MIM to protons, uncoupling OXPHOS and inhibiting ATP production (Murphy, 2012). Damage to mtDNA can lead to mutations and deletions, contributing to the transformation and development of cancer. ROS also have a beneficial redox signalling role within the cell, enabling communication between the mitochondria and the cytosol and nucleus. For example, the cytosolic transcription factor HIF is stabilised by mitochondrial ROS and leads to transcriptional adaptation (Mills et al., 2016; Murphy, O'Neill, 2018).

The primary ROS produced by mitochondria is the superoxide anion $O_2^{\cdot-}$ (Murphy, 2009), which is formed by the one-electron reduction of O_2. Despite there being many electron donors within mitochondria they generally only donate or 'leak' an electron to O_2 under certain conditions, termed mode 1 and mode 2. Mode 1 occurs when there is a high

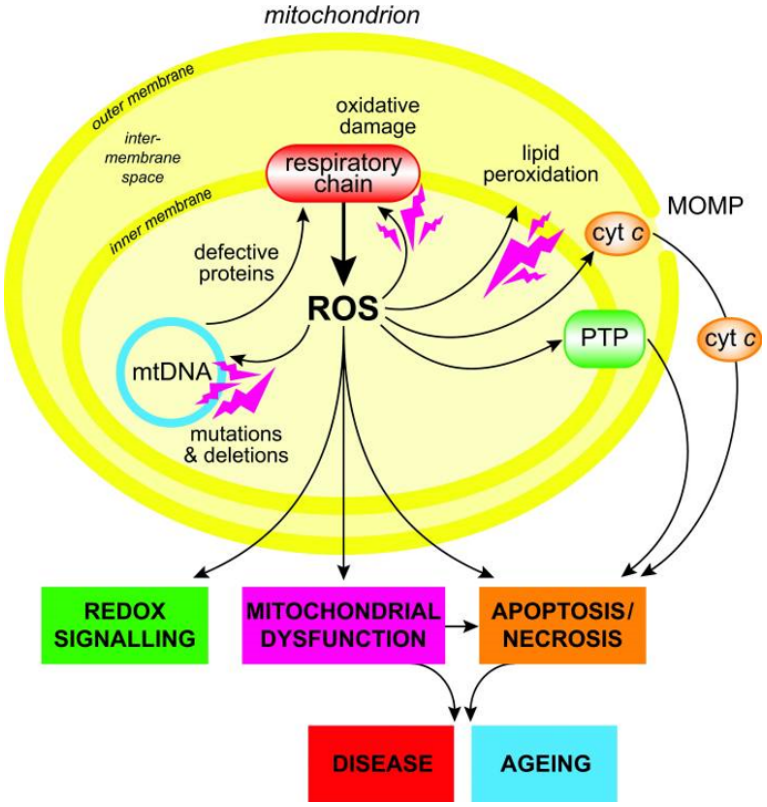

Fig. 1.8 Overview of ROS production and its downstream effects in the cell. Mitochondrial ROS production can cause oxidative damage to mitochondrial proteins, such as the respiratory chain complexes, membranes and DNA. This damage can prevent the mitochondria from performing their essential metabolic functions and ATP synthesis. Mitochondrial ROS can also lead to the release of cytochrome *c* (Cyt *c*) via the mitochondrial outer membrane permeabilisation (MOMP), as well as opening of the permeability transition pore (PTP), leading to apoptotic and necrotic cell death. ROS can also act as a redox signal. From Murphy (2009).

$NADH/NAD^+$ ratio in the matrix and mode 2 occurs when ATP synthase cannot operate, resulting in a high Δp and reduced CoQ pool. Some ROS synthesis occurs when mitochondria are making ATP (mode 3), but this rate is much lower. In the following sections, I outline the sources of mitochondrial ROS, their metabolism and their role in redox signalling.

1.4.1 Sources of mitochondrial ROS

Complex I is one of the main sources of mitochondrial $O_2^{\cdot-}$. It is capable of producing $O_2^{\cdot-}$ during both forward and reverse electron transfer (RET) (Chouchani et al., 2014, 2016; Murphy, 2009; Pryde, Hirst, 2011). $O_2^{\cdot-}$ is produced during forward electron transfer when O_2 reacts with fully reduced FMN on Complex I. The proportion of FMN that is fully reduced is set by the $NADH/NAD^+$ ratio (as NADH is the electron donor to Complex I). A high $NADH/NAD^+$ ratio occurs when the respiratory chain is blocked by damage, mutation, ischaemia, loss of cytochrome c or low ATP demand. $O_2^{\cdot-}$ production by RET occurs when mitochondria are operating in mode 2: a highly reduced CoQ pool combined with a high Δp forces electrons back into Complex I, reducing NAD^+ to NADH at the FMN site. This can lead to the transfer of e^- to O_2, forming $O_2^{\cdot-}$. $O_2^{\cdot-}$ production by RET at Complex I has been shown to occur during IRI (Chouchani et al., 2014) (**Section 1.9**).

Complex III is also capable of producing ROS under certain conditions (Murphy, 2009; Quinlan et al., 2011). The $UQ^{\cdot-}$/UQ couple formed during the Q cycle is highly reducing, making it thermodynamically capable of donating an electron to O_2, forming $O_2^{\cdot-}$. Under normal physiological conditions, complex III produces only a small amount of ROS. However, in the presence of its inhibitor antimycin, complex III can produce ROS by stabilisation of a semiquinone radical at the Q_o site (Nicholls, Ferguson, 2013; Quinlan et al., 2011).

1.4.2 Mitochondrial superoxide and hydrogen peroxide metabolism

Superoxide produced in the mitochondrial matrix cannot diffuse through membranes and is thus contained in the matrix. However, superoxide can be metabolised to generate other, more damaging ROS (**Figure 1.9**). Superoxide dismutases (SODs) catalyse the dismutation of $O_2^{\cdot-}$ to oxygen and hydrogen peroxide (H_2O_2) (Murphy, 2009). $O_2^{\cdot-}$ can also form peroxynitrite by spontaneous reaction with nitric oxide ($^{\cdot}NO$) produced by nitric oxide synthases (NOSs).

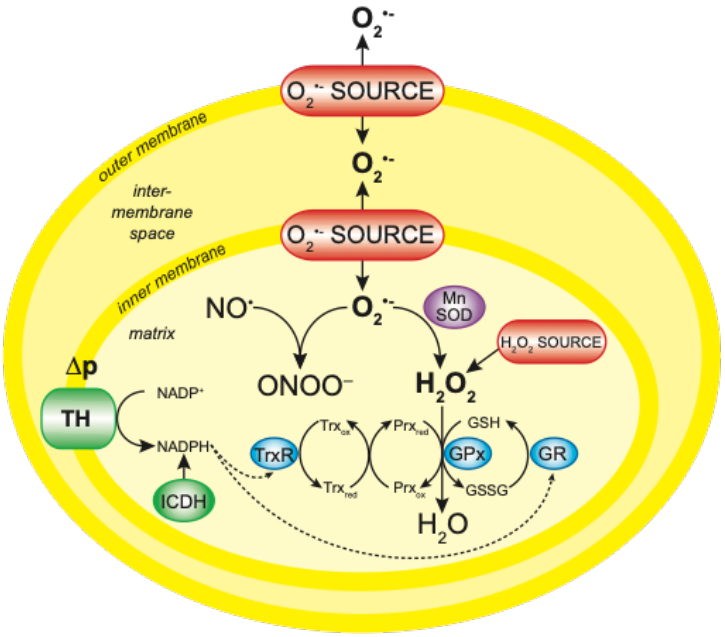

Fig. 1.9 Overview of mitochondrial superoxide and hydrogen peroxide metabolism. Superoxide ($O_2^{\cdot-}$) is produced in the matrix and metabolised to hydrogen peroxide (H_2O_2) by manganese superoxide dismutase (MnSOD). H_2O_2 is metabolised to H_2O by the peroxidases peroxiredoxin (Prx) and glutathione peroxidase (Gpx). Oxidised Prx can be regenerated by thioredoxin (Trx). Reduced Trx levels are controlled by thioredoxin reductase (TrxR), which in turn is regulated by the NADPH/NADP$^+$ pool. Gpx uses GSH to reduce oxidised peroxidases, such as Prx. The oxidised Gpx is recycled by glutathione reductase (GR). Furthermore, H_2O_2 can leave the mitochondria as it is membrane permeable. TH: transhydrogenase. Figure adapted from Murphy (2009).

In the presence of Fe^{2+}, H_2O_2 can form the hydroxyl radical ($^{\cdot}OH$) by the Fenton reaction (Murphy, 2012).

$O_2^{\cdot-}$, whether produced during pathological processes or for signalling purposes, must be removed by conversion to H_2O_2 to stop it causing uncontrolled damage. As well as being responsible for a large amount of ROS production, mitochondria also house a number of pathways for ROS metabolism. In addition, many mechanisms to remove ROS also exist in the cytosol. $O_2^{\cdot-}$ is converted to H_2O_2 and O_2 by SODs. Mammals possess 3 SODs: SOD1 (CuZn-SOD) is mostly cytoplasmic; SOD2 (Mn-SOD) is found in the matrix; SOD3 is extracellular. Loss-of-function (LOF) SOD2 mutations in mice cause early mortality, highlighting the importance of this mitochondrial defence mechanism (Nicholls, Ferguson, 2013). H_2O_2 can oxidise thiols on proteins, which is the basis of thiol-dependent redox signalling. For redox signalling to occur there must also be mechanisms to re-reduce thiols.

A group of mitochondrial thiol systems in the mitochondrial matrix are responsible for transmitting, modulating and sensing redox signals, as well as preventing oxidative damage by removing ROS. This "firewall" is dependent on a continued NADPH supply, which is maintained by the transhydrogenase, malic enzyme and NADP-dependent IDH enzymes (Murphy, 2009). As the electrons of NADPH are also used in the biosynthesis of fatty acids, cholesterol, amino acids and nucleotides (Chandel, 2015), NADPH may serve as a link between cellular metabolism and redox signalling, relevant in both the mitochondrial matrix (from IDH2 and malic enzyme 3) and the cytosol (from IDH1, malic enzyme 1 and the PPP).

1.4.2.1 The peroxiredoxin/thioredoxin system

Peroxiredoxins (Prx) are thiol peroxidases that act to maintain the redox balance of the cell by scavenging H_2O_2 (Murphy, 2012). Mammals possess 6 Prx isoforms with different subcellular locations. Prx1, 2 and 6 are cytoplasmic, Prx3 is mitochondrial, Prx4 is found in the ER and Prx5 is found in multiple locations, including the mitochondria and peroxisomes, although Prx3 is the highest capacity mitochondrial Prx. A redox-sensitive cysteine in the Prx active site is oxidised by H_2O_2, generating H_2O. When oxidised, the Prx forms homodimers through reversible inter-protein disulphide bridges and a sulfenic acid (-SOH) on the Prx. These oxidised Prxs are temporarily inactivated. This can be readily reversed by thioredoxin (Trx), which reduces the disulphide bond to a dithiol (-SH) (Chae et al., 1994; Cox et al., 2010; Murphy, 2012). Persistent oxidation can lead to other thiol modifications, such as sulfinic acid ($-SO_2H$), reversible by sulfiredoxin, and sulfonic acid ($-SO_3H$), which is an irreversible modification.

Trxs reduces disulphide bonds on proteins, including Prxs. Trx2 is found in the mitochondrial matrix and Trx1 is cytosolic. An active thiol within Trx acts as a nucleophile to attack the disulphide bond, forming a transient disulphide bridge with the protein. A second Trx2 is required to reduce this intermediate, reducing the target protein's disulphide bond. The resulting disulphide bond on Trx2 is reduced by the enzyme thioredoxin reductase (TR2), which requires NADPH as a reducing modality (Murphy, 2012) (**Figure 1.10**).

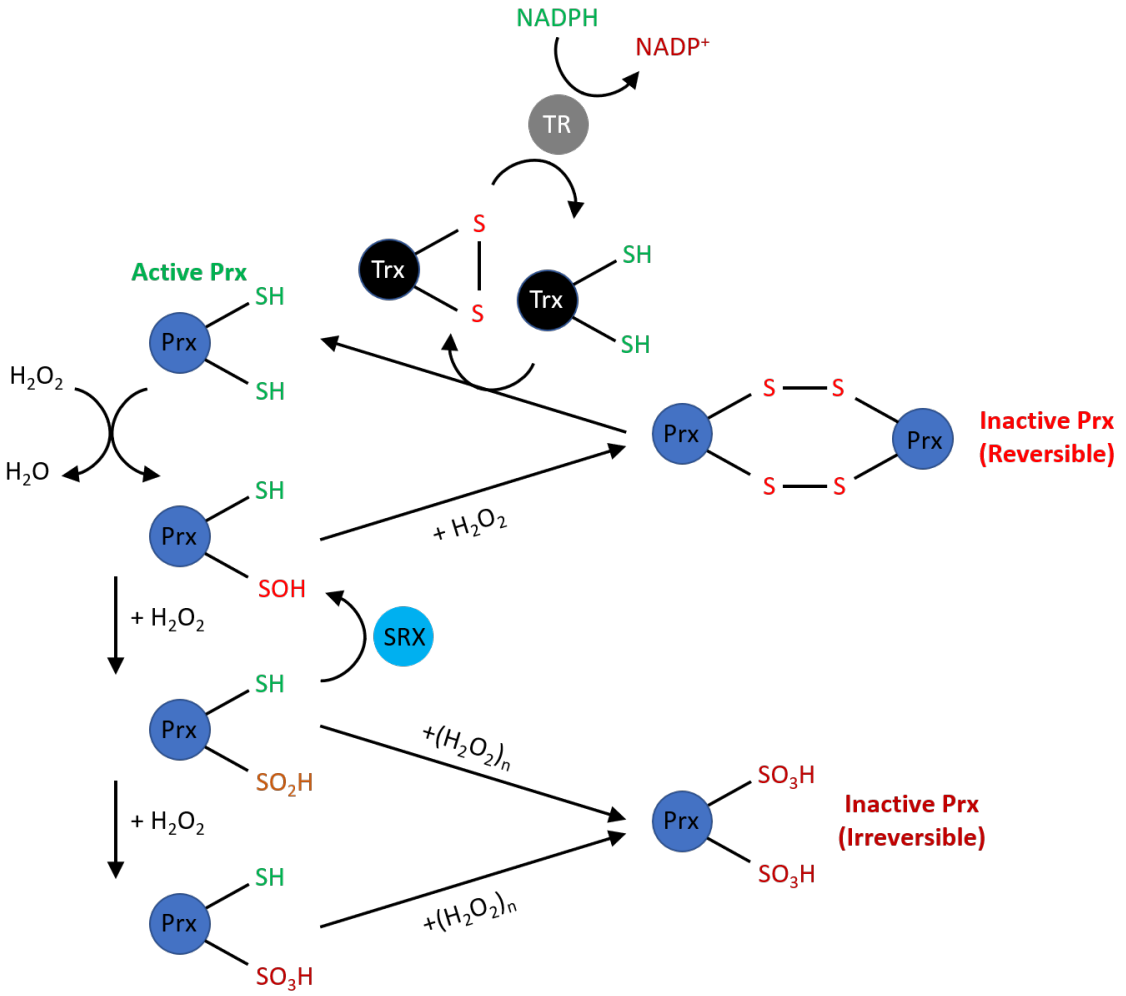

Fig. 1.10 The peroxiredoxin/thioredoxin system. Peroxiredoxins (Prxs) reduce H_2O_2 to H_2O, generating a sulfenic acid (-SOH) on the Prx. This can lead to inter-molecular homodimers of Prx, linked by disulphide bridges. Hyperoxidation can generate sulfinic acid ($-SO_2H$) and sulfonic acid ($-SO_3H$) modifications. Sulfinic acid modifications are reversible by sulfiredoxin (SRX) whereas sulfonic acid modifications are irreversible. Hyperoxidised Prxs are inactive (irreversibly or reversibly) and are a marker of oxidative damage. Prx dimers are reduced by thioredoxins (Trx), which are in turn regenerated by thioredoxin reductase (TR) and NADPH.

1.4.2.2 The mitochondrial glutathione system

Glutathione (GSH) is a small peptide that has protective roles in antioxidant defence, maintenance of thiol status and detoxification (Mari et al., 2009; Murphy, 2012). It is synthesised in the cytoplasm by γ-glutamylcysteine synthetase and glutathione synthetase and imported into the mitochondria. The matrix pool of GSH is thought to be 1-5 mM (Booty et al., 2015) and the cytosolic pool 5-15 mM (Mari et al., 2009; Smith et al., 1996). It was previously thought that GSH was transported into mitochondria by the dicarboxylate carrier (DIC) and the oxoglutarate carrier (OGC), but Booty et al. (2015) suggests this is not the case. Once in the matrix, GSH is oxidised to glutathione disulphide (GSSG) through the action of glutathione peroxidase (Gpx1) which reduces H_2O_2 to H_2O. GSSG is reduced back to GSH by glutathione reductase (GR), using NADPH as an electron donor. GR maintains the mitochondrial matrix GSH pool highly reduced (95-99 %) with some oxidised GSSG. The $NADP^+$ pool is in turn reduced by transhydrogenase and IDH (Murphy, 2012; Nicholls, Ferguson, 2013).

Glutathione peroxidase (Gpx1) uses GSH to detoxify peroxides (**Figure 1.11**). There are 2 Gpx isoforms in the matrix: soluble Gpx1 degrades H_2O_2, whilst Gpx4 is adsorbed to the MIM (on the matrix side) and degrades phospholipid hydroperoxides, preventing lipid peroxidation (Murphy, 2012; Nicholls, Ferguson, 2013).

Glutaredoxins (Grx) catalyse protein deglutathionylation, which occurs when oxidised protein thiols react with GSH. Grx2 is mitochondrial and Grx1 is located in the cytosol. Glutathione-S-transferases (GSTs) use GSH to detoxify electrophiles such as xenobiotics and products of oxidative damage (Murphy, 2012).

1.4.3 Mitochondrial redox signalling

Mitochondria are now understood to be signalling hubs which are essential to the health and fate of the cell. A key way they interact with the rest of the cell and modulate cellular function is through redox signalling.

H_2O_2 is a ROS signal. It can diffuse through membranes, unlike superoxide. In order to be an effective signal, it must be rapidly responsive to changes in mitochondrial status so that a meaningful and accurate message is relayed to the rest of the cell (Finkel, 2012; Holmström,

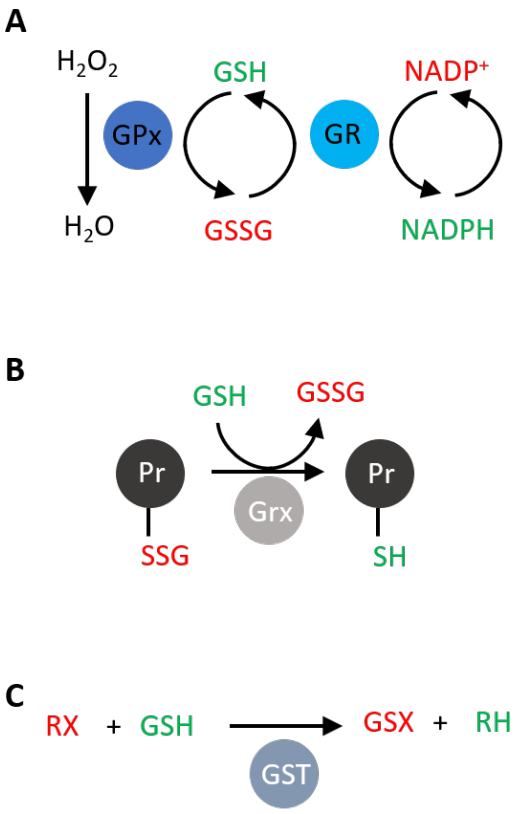

Fig. 1.11 The mitochondrial glutathione system. ***A)*** Glutathione peroxidase (Gpx) uses reduced glutathione (GSH) to reduce H_2O_2 to H_2O. The oxidised glutathione (GSSG) is reduced to GSH by glutathione reductase (GR). ***B)*** Glutaredoxin (Grx) catalyses the exchange of GSH with protein (Pr) thiols. ***C)*** Glutathione-S-transferase (GST) detoxifies electrophiles (RX) using GSH.

Finkel, 2014; Janssen-Heininger et al., 2008). This is achieved because the generation of superoxide by RET at complex I (one process by which H_2O_2 can be made) is extremely sensitive to the Δp and the redox state of the Q pool, as discussed above (Chouchani et al., 2016; Murphy, 2009). Both of these vary in direct response to mitochondrial activity: when mitochondria are inactive and become overloaded with electrons ROS production is increased, and is decreased when mitochondria are active (Chouchani et al., 2016; Murphy, 2009).

The level of ROS produced by RET can also be modulated by other, more physical, changes to complex I. One of these is post translational modifications (PTMs) to complex I such as phosphorylation (Covian, Balaban, 2012). Furthermore, RET is affected by the proportion of complex I in the active state. Complex I is known to adopt the deactive state during ischaemia (Gorenkova et al., 2013) but it is not known whether this is a mechanism to regulate RET and ROS signalling. Complex I can function as an isolated complex or as part of a supercomplex with other respiratory chain complexes (Moreno-Loshuertos, Enríquez, 2016). The physiological role of supercomplexes is not known (Blaza et al., 2014) but it is postulated that they increase efficiency of OXPHOS and reduce aberrant ROS production (Moreno-Loshuertos, Enríquez, 2016). Complex I incorporation into supercomplexes is proposed to be related to changes in mitochondrial ROS formation (Lopez-Fabuel et al., 2016). There are thought to be different supercomplex assemblies, each with different specificities for receiving electrons from NADH or $FADH_2$, meaning that they can respond to the NADH/$FADH_2$ ratio derived from available fuel sources. The adaptation of the superassemblies is postulated to be mediated by redox signalling. For example, the incorporation of complex II into the supercomplexes was increased by phosphorylation of its subunit FpSDH by the tyrosine-kinase enzyme Fgr, which is activated by H_2O_2 (Acín-Pérez et al., 2014).

RET is biologically relevant, both positively and negatively, in a range of physiological conditions. It is involved in the metabolic adaptation of macrophages during inflammation (Mills et al., 2016), triggering the immune response during viral infection (Buskiewicz et al., 2016) and in extending lifespan in fruit flies (Scialo et al., 2016). RET plays a major pathological role during reperfusion, the return of blood flow after a period of ischaemia, such as during a heart attack, stroke or surgery. The RET that occurs generates a burst of superoxide through complex I which leads to tissue damage, termed ischaemia-reperfusion injury (IRI). This is discussed in greater detail in **Section 1.9**.

H_2O_2 can diffuse out of the mitochondria into the cytosol, although at present it is unclear whether this is through a protein-mediated process (as for the transport of H_2O_2 across

the PM) or merely direct permeation through the MIM (Murphy, 2009). If the transport is protein-mediated this would confer an extra layer of control over H_2O_2 signalling. Once in the cytosol, it can alter enzyme activity by reversible oxidation of cysteine thiols or by acting on redox sensitive proteins such as Prxs and Trxs. H_2O_2 can also alter mitochondrial metabolism, such as acting on metal-centre proteins (Winterbourn, 2013) such that another signal is produced that can leave the mitochondria and signal to the rest of the cell.

H_2O_2 primarily acts as a signal by affecting the activity of proteins. The main way it achieves this is the redox modification of a cysteine residue on the target protein. Cysteine residues contain active thiol groups, which are maintained under a reduced state in normal physiological conditions (Menger et al., 2015). Changes in cellular redox state can lead to oxidative thiol modifications, such as disulphide bonds, *S*-sulfenylation, *S*-nitrosation, *S*-acetylation or *S*-glutathionylation (Paulsen, Carroll, 2013). These modifications affect the function of the protein by changing its activity, binding interactions, lifetime and subcellular localisation (Holmström, Finkel, 2014). Most of these redox modifications are reversible, meaning that the proteins can respond to the cellular redox state, such as the reversible inactivation of tyrosine phosphatases via cysteine thiol oxidation (Meng et al., 2002).

1.5 Mitochondrial metabolite transport

In order for mitochondria to perform these roles, metabolic substrates such as keto acids, amino acids, nucleotides, cofactors, vitamins and protons need to be imported into, and excreted from, the mitochondria. The MIM has to be impermeable to proteins, metabolites and protons to maintain its electrochemical potential gradients. Therefore, carriers are needed to move metabolites in and out of the mitochondria, across the MIM. The combined action of the impermeable MIM and the selective action of metabolite transporters on the MIM enable the coupling of metabolism between the mitochondria and the cytosol (**Figure 1.12**). Below, I outline mitochondrial transporters in general and describe some specific transporters and their role in metabolism and compartmentalisation.

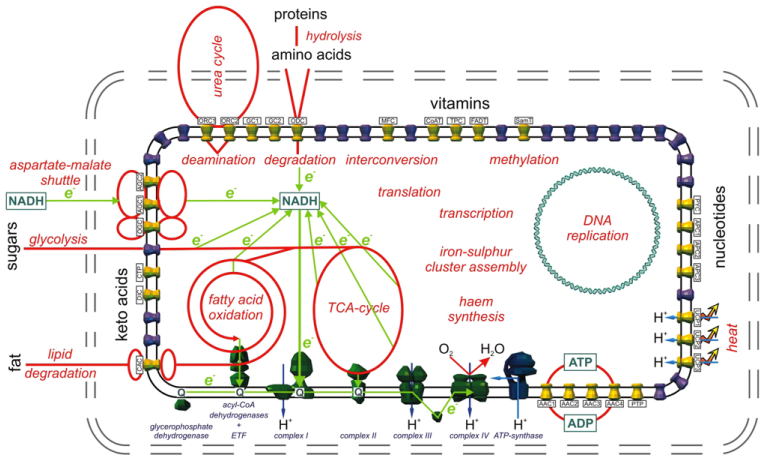

Fig. 1.12 Mitochondrial carriers. Schematic representation of a mitochondrion depicting the various carriers of the mitochondrial inner membrane (MIM) as well as the major metabolic pathways that they contribute to (shown in red). ATP synthase and respiratory chain complexes are blue and green respectively. Known mitochondrial carriers are depicted in yellow whilst unknown carriers are depicted in purple. Blue arrows show the direction of proton transport over the MIM. From Kunji, Robinson (2010).

1.5.1 Mitochondrial carriers

There are many different types of mitochondrial carriers in humans, and their mutation can lead to an array of diseases, exemplifying their importance for the maintenance of normal metabolism (Palmieri, 2008). For example, a deficiency in AAC caused by mutations in the SLC25A4 gene results in exercise intolerance, lactic acidosis and hypertrophic cardiomyopathy (Palmieri, 2008). As many metabolites are charged, their transport is affected by the $\Delta\psi$ and/or ΔpH across the MIM, and transporters often use these gradients to drive the accumulation of a metabolite on one side of the MIM. There are different strategies that can be used to harness or exploit the $\Delta\psi$ and/or ΔpH to influence transport. Proton symport with a neutral species is driven by the Δp. Proton symport with a negative species is an electroneutral mechanism, driven by ΔpH only. Uniport of either a positive or negative species, such as Ca^{2+}, is an electrogenic process driven by the $\Delta\psi$. The exchange of two metabolites can be electrogenic or electroneutral depending on their respective charges and is a useful mechanism of accumulating highly negatively charged species, such as ATP and ADP, that would otherwise be excluded due to the high inside negative membrane potential. The antiport of an anion or positively charged metabolite with protons is electroneutral.

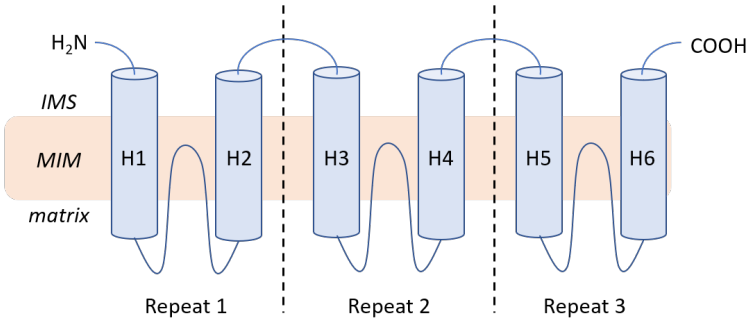

Fig. 1.13 SLC25A carrier monomer structure. A topological model of the structure of an SLC25A carrier monomer. SLC25A carriers have 6 transmembrane helices arranged in 3 repeats of 2 helices. Each repeat is connected to the next by a long hydrophilic matrix loop which protrudes into the membrane. Both the N- and C-termini face the cytosol.

Below, I outline the SLC25A mitochondrial carrier family, the largest mitochondrial carrier family in humans, and cover some of the main carriers of this family, before discussing other important carriers that are not part of this family.

1.5.2 The SLC25A carrier family

The SLC25A family is the largest family of mitochondrial carriers in humans, with 53 transporters (Palmieri, 2014). These are nuclear-encoded single polypeptide chain proteins with 6 TM α-helices and 3 matrix helices (**Figure 1.13**). It is thought that they generally function as monomers, with a single substrate binding site in a large central water-filled cavity formed by the TM helices. Access to the binding site is controlled by 2 gates made from 2-3 salt bridges. At any one time only one of these gates is open, avoiding an open channel which would dissipate ion gradients across the MIM (Kunji, Robinson, 2010; Palmieri, 2004).

Some carriers are expressed in all tissues (e.g. the ADP/ATP carrier and the phosphate carrier), whereas some are tissue specific or have isoforms with different tissue distributions, reflecting the different metabolic roles mitochondria play in different tissues (Palmieri, 2004).

Most transporters function as exchangers (substrate in/product out) but some are uniporters or exchange H^+ (driven by the Δp). Carriers that perform substrate-proton symport possess negatively charged residues (e.g. aspartate or glutamate) in the substrate binding site. Proton coupling allows the movement of the substrate against its concentration gradient by using the

Δp to power it (Kunji, Robinson, 2010). **Tables 1.1 and 1.2** outline the substrates, transport mechanism and tissue distribution of some of the major SLC25A family carriers.

Human gene name	Protein name	Predominant substrates	Transport type*/coupling ions	Tissue distribution
SLC25A1	CIC	Citrate, malate, PEP	E Citrate-H^+/malate	Liver, kidney, pancreas (also brain, lung, heart)
SLC25A2	ORC2	Ornithine, citrulline, lysine, arginine, histidine	E Ornithine/Citrulline + H^+ Ornithine/H^+	Liver, testis, spleen, lung, pancreas, small intestine, brain, kidney
SLC25A3	PiC	Phosphate	C Phosphate + H^+ E Phosphate/OH^-	Isoform A: heart, skeletal muscle, diaphragm Isoform B: liver, kidney, brain, thymus, lung, heart, skeletal muscle, diaphragm
SLC25A4	AAC1	ADP, ATP	E ADP/ATP	Heart, skeletal muscle, much less in brain, pancreas, prostate, kidney, lung, thymus
SLC25A5	AAC2	ADP, ATP	E ADP/ATP	Brain, lung, kidney, pancreas, heart, skeletal muscle, spleen
SLC25A6	AAC3	ADP, ATP	E ADP/ATP	Brain, lung, kidney, liver, pancreas, heart, skeletal muscle, spleen, thymus
SLC25A7	UCP1	H+	F	Brown adipose tissue
SLC25A8	UCP2	H^+	F	Brain, lung, kidney, spleen, heart
SLC25A9	UCP3	H^+	F	Skeletal muscle, lung

Table 1.1 The SLC25 mitochondrial carrier family. *Transport type - E: exchanger; C: cotransporter; F: facilitated transporter. CIC: Citrate carrier; ORC2: Ornithine carrier; PiC: Phosphate carrier; AAC1: ADP/ATP carrier 1; AAC2: ADP/ATP carrier 2; AAC3: ADP/ATP carrier 3; UCP1: Uncoupling protein 1; UCP2: Uncoupling protein 2; UCP3: Uncoupling protein 3. Adapted from Palmieri (2004).

Human gene name	Protein name	Predominant substrates	Transport type*/coupling ions	Tissue distribution
SLC25A10	DIC	Malate, phosphate, succinate, sulphate, thiosulphate	E Malate/phosphate	Liver, kidney, heart, brain, lung, pancreas
SLC25A11	OGC	Oxoglutarate, malate	E Oxoglutarate/malate	Heart, skeletal muscle, liver, kidney, brain, pancreas
SLC25A12	AGC1	Aspartate, glutamate	E Aspartate/glutamate + H^+	Brain, heart, skeletal muscle, lung, pancreas, kidney, but not in liver
SLC25A13	AGC2	Aspartate, glutamate	E Aspartate/glutamate + H^+	Liver, kidney, pancreas, heart, skeletal muscle, brain
SLC25A15	ORC1	Ornithine, citrulline, lysine, arginine	E Ornithine/ citrulline + H^+ Ornithine/H^+	Liver, pancreas, lung, testis, small intestine, spleen, kidney, brain, heart
SLC25A20	CAC	Carnitine, acylcarnitines	E Carnitine/acylcarnitines F (at slow rate)	Heart, skeletal muscle, liver (also in lung, kidney, brain, pancreas, placenta)
SLC25A22	GC1	Glutamate	C Glutamate + H^+ E Glutamate/OH^-	Pancreas, brain, liver, testis, spleen, kidney, heart, lung, small intestine

Table 1.2 The SLC25 mitochondrial carrier family (ctd.) *Transport type - E: exchanger; C: cotransporter; F: facilitated transporter. DIC: Dicarboxylate carrier; OGC: Oxoglutarate carrier; AGC1: Aspartate/glutamate carrier 1; AGC2: Aspartate/glutamate carrier 2; ORC1: Ornithine carrier 1; CAC: Carnitine/acylcarnitine carrier; GC1: Glutamate carrier. Adapted from Palmieri (2004).

1.5.2.1 The ADP/ATP carrier

The ADP/ATP carrier (AAC) exchanges cytosolic ADP^{3-} for mitochondrial ATP^{4-} (**Figure 1.4**) (Klingenberg, 2008) and serves to link energy metabolism between the mitochondria and the cytosol (where ATP is consumed). It is inhibited by carboxyatractyloside (CATR) which binds to the cytosolic-facing conformation, and by bongkrekic acid (BKA) which binds to the mitochondrial-facing conformation (Nicholls, Ferguson, 2013). There are 3 isoforms of the AAC in humans, with different tissue specificity: AAC1 (heart and skeletal muscle); AAC2 (ubiquitous); AAC3 (low in main tissues and abundant in highly proliferative cells). The expression levels of the carriers are regulated by the energy requirements of the cell, which maps onto the tissue specificity (Palmieri, 2004). Deficiency in AAC has been reported in some cases of myopathy or cardiomyopathy, as well as in autosomal dominant progressive external ophthalmoplegia (adPEO).

1.5.2.2 The phosphate carrier

The mitochondrial phosphate carrier (PiC) catalyses the electroneutral transport of $H_2PO_4^-$, with current evidence pointing towards it acting as a H^+ symporter (**Figure 1.4**). It has 2 isoforms (A and B). P_i transport, at the expense of the pH gradient across the MIM, is essential for OXPHOS (Klingenberg, 2008). P_i also has other roles in the mitochondria, such as its involvement in the conversion of succinyl CoA to succinate, catalysed by succinyl-CoA synthetase (Palmieri, 2004). P_i also facilitates the uptake of other metabolites into mitochondria by exchange. The tissue specificity of the carrier matches that of the AACs.

1.5.2.3 The citrate carrier

The citrate carrier (CIC) catalyses the electroneutral exchange of tricarboxylates (e.g. citrate, isocitrate, malate or phosphoenolpyruvate (PEP), **Figure 1.14**). It has high activity in liver and low activity in heart and brain. Its activity is affected by hormones and starvation status, with reduced activity during starvation and diabetes that can be corrected by exogenous insulin (Palmieri, 2004). The CIC is essential for fatty acid and sterol biosynthesis because it exports mitochondrial citrate to the cytosol, which is needed for fatty acid and sterol biosynthesis.

1.5.2.4 The dicarboxylate carrier

The dicarboxylate carrier (DIC) catalyses the electroneutral exchange of dicarboxylates (e.g. succinate and malate), P_i and inorganic sulphur compounds (e.g. sulphite, sulphate and thiosulphate) (**Figure 1.14**) (Dolce et al., 2014). One main function of the DIC is anaplerotic: it supplies substrates for the TCA cycle to the matrix. It can also play a role in gluconeogenesis by exporting TCA cycle intermediates to the cytosol, which are converted to PEP. Consistent with its role in gluconeogenesis the DIC is most abundant in liver and kidney (Nicholls, Ferguson, 2013; Palmieri, 2004). OAA in the matrix is converted to malate which is transported by the DIC to the cytosol, where it is converted back to OAA and then to PEP. In ischaemia, it is thought that succinate leaves the mitochondria via the DIC to act as a signal. The DIC is inhibited by substrate analogues such as butylmalonate.

1.5.2.5 The ornithine carrier

The ornithine carrier (ORC) transports ornithine, lysine, arginine and citrulline via an exchange mechanism. It has 2 isoforms in man: ORC1 and ORC2 (Nicholls, Ferguson, 2013; Palmieri, 2004). ORC1 has higher levels of expression in most tissue and ORC2 is basically absent in brain, heart and kidney. The import of lysine, arginine and histidine also allows for synthesis of mitochondrially translated proteins. Arginine hydrolysis (when there is excess arginine from diet) generates ornithine, which is then metabolised by ornithine aminotransferase in the matrix. Polyamine biosynthesis in the cytosol requires the export of ornithine. The ORC plays a role in the urea cycle, discussed in **Sections 1.3.5 and 1.5.4.4**.

1.5.2.6 The oxoglutarate carrier

The oxoglutarate carrier (OGC) catalyses the electroneutral exchange of mitochondrial oxoglutarate for cytosolic dicarboxylates (Palmieri, 2004). The OGC plays an important role in the MAS.

1.5.2.7 The glutamate carrier

The glutamate carrier catalyses the neutral symport of glutamate and a proton into the mitochondria (Palmieri, 2004). This carrier has a major role in metabolism because glutamate is an important metabolite, especially in cancer cell metabolism (Chandel, 2015).

1.5.2.8 Uncoupling proteins

Uncoupling proteins (UCPs) are a family of carriers with 5 different isoforms (UCP1-5). Despite their structure being known for some time, the function and physiological role of most of the isoforms is still under debate. The isoforms are known to have different tissue specificities: UCP1 (brown adipose tissue), UCP2 (ubiquitous); UCP3 (skeletal muscle); UCP4 and UCP5 (brain). UCP1 is known to transport H^+ across the MIM from the cytosol into the mitochondria, thus dissipating the electrochemical proton gradient and uncoupling the mitochondria (Busiello et al., 2015) and has a role in thermogenesis (Chouchani et al., 2019). The mild uncoupling mediated by UCP2 and UCP3 is thought to regulate mitochondrial ROS production (Brand, Esteves, 2005).

1.5.2.9 The aspartate-glutamate carrier

Humans have 2 aspartate/glutamate carriers (AGC): AGC1 is predominantly expressed in brain, skeletal muscle and heart, whereas AGC2 is primarily found in heart and liver (Nicholls, Ferguson, 2013). AGC1 is involved in the MAS (**Section 1.5.4.5**) whilst AGC2 exports aspartate from the mitochondria to participate in the urea cycle. Both isoforms catalyse the exchange of aspartate, glutamate and cysteinesulphinate, with aspartate and cysteinesulphinate transported as anions and glutamate cotransported with an H^+ (Palmieri, 2004). Therefore, aspartate export and glutamate import is stimulated when the membrane potential is positive inside.

1.5.2.10 The carnitine-acylcarnitine carrier

Acylcarnitines enter the mitochondria in exchange for matrix carnitine via the acylcarnitine-carnitine carrier (**Figure 1.7**). Acylcarnitines are cleaved by carnitine N-acyltransferase II in

the matrix, generating acyl-CoA for β-oxidation and carnitine, which is transported back across the membrane in exchange for more acylcarnitines (Nicholls, Ferguson, 2013).

1.5.3 Other transporters

Despite the SLC25A family being the largest, several other important mitochondrial metabolite carriers are not in this family. Some of these carriers are discussed below.

1.5.3.1 The pyruvate carrier

The mitochondrial pyruvate carrier (MPC) family imports pyruvate formed in glycolysis into the mitochondrial matrix across the MIM (Bricker et al., 2012; Herzig et al., 2012). Pyruvate is at a branch point of metabolism (Bender, Martinou, 2016), as it has roles in both the cytosol and the mitochondria. In the cytosol it can be converted to lactate by LDH, regenerating NAD^+ and allowing glycolysis to continue. When in the mitochondrial matrix, pyruvate can be carboxylated to oxaloacetate by pyruvate carboxylase (PC), which can enter gluconeogenesis or be shunted into anaplerosis, or metabolised to AcCoA by PDH, which can feed in to OXPHOS and ATP generation. Therefore, the decision to enter the mitochondria or not is a crucial determinant of metabolic homeostasis. The subunits MPC1 and MPC2 are inner mitochondrial membrane proteins and both are required for pyruvate transport (Bricker et al., 2012; Herzig et al., 2012). It is proposed that the functional carrier is a heterodimer. The MPC family is structurally distinct from the SLC25A carrier family, but shares some homology and three-dimensional structure with a bacterial family of transporters called SemiSWEET (Vanderperre et al., 2015; Xu et al., 2014). However, the exact three-dimensional structure of the MPC is yet to be solved. The MPC adopts a proton symport mechanism and is therefore driven by the Δp. It is involved in various shuttles, including the citrate-pyruvate shuttle (**Figure 1.14**) and the pyruvate-malate shuttle (**Figure 1.15**).

1.5.3.2 The ATP-binding cassette proteins

The ATP-binding cassette (ABC) transporters are a diverse family of membrane proteins, found in bacteria, archaea, fungi, plants and mammals. They are comprised of a pair

of conserved cytoplasmic ABC domains, or nucleotide-binding domains (NBDs) which hydrolyse ATP to power conformational changes in the transmembrane domains (Locher, 2016). This conformational change switches the NBD dimer between an open and closed state, allowing the movement of substrate across the membrane. Humans have 48 ABC transporters, present in the MIM and other cellular membranes. Unlike bacteria, mitochondria contain only a few ABC transporters, suggesting they were lost during their evolution from α-proteobacteria. 5 mammalian ABC transporters have been localised to the mitochondria (Lill, Kispal, 2001). ABC7 and MTABC3 are functionally homologous to the yeast Atm1p and are thought to have a role in the maturation of cytosolic Fe/S proteins (Lill, Kispal, 2001).

1.5.4 Transport shuttles

Often the SLC25A and other transporters are grouped into 'shuttles' and their combined action forms a cycle with the net transport of a specific metabolite from one side of the MIM to the other and the replenishment of substrates needed to keep the shuttle going. However, this is complicated *in vivo* and the actual contributions to metabolism of these shuttles are unknown.

1.5.4.1 The citrate-pyruvate shuttle

In the cytosol citrate is cleaved by ATP-citrate lyase (ACL) to oxaloacetate (OAA) and AcCoA. AcCoA is used for fatty acid and sterol syntheses. OAA produced in the cytosol is reduced to malate which is converted to pyruvate (via malic enzyme). This generates cytosolic NADPH and H^+ which are also required for fatty acid and sterol synthesis. Pyruvate re-enters the mitochondria via the citrate-pyruvate shuttle (Palmieri, 2004). Malate needs to be returned to the cytosol to enable citrate to leave the mitochondria, so it is exported via the DIC in exchange for P_i. P_i is returned to the cytosol via exchange with H^+, enabling the continued export of citrate to the cytosol for fatty acid synthesis (see **Figure 1.14**). NADPH production is important for fatty acid synthesis (Chandel, 2015; Kastaniotis et al., 2017). It is thought that NADPH is generated in the cytosol by malic enzyme, the isocitrate-αketoglutarate shuttle and the pyruvate-malate shuttle and pentose-phosphate pathway. The CIC is also involved in the isocitrate-oxoglutarate shuttle which results in the net import of

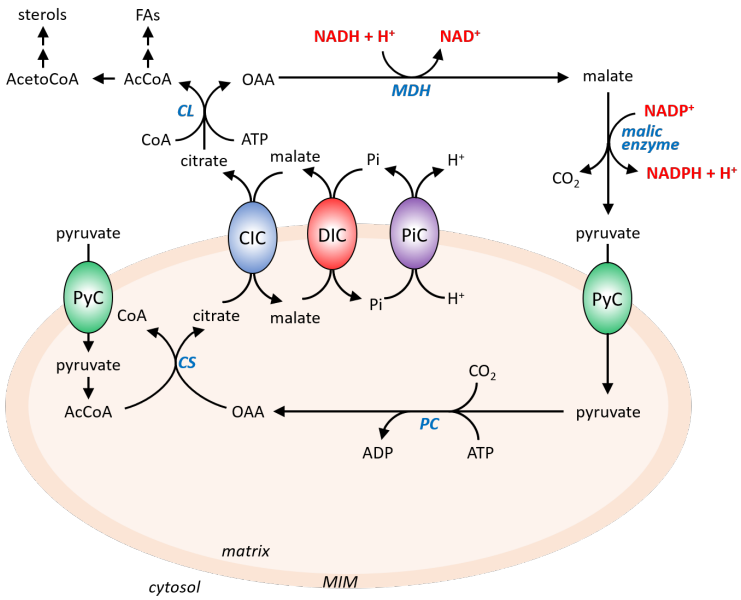

Fig. 1.14 The citrate-pyruvate shuttle. Pyruvate re-enters the mitochondria and malate is recycled across the MIM to drive citrate out of the matrix into the cytosol where it is required for fatty acid synthesis. The cycling of malate across the MIM requires the concerted action of the CIC, the DIC and the PiC. Enzymes are written in blue. PyC: pyruvate carrier; CIC: citrate carrier; DIC: dicarboxylate carrier; PiC: phosphate carrier; CL: ATP-citrate lyase; CS: citrate synthase; MDH: malate dehydrogenase; PC: pyruvate carboxylase.

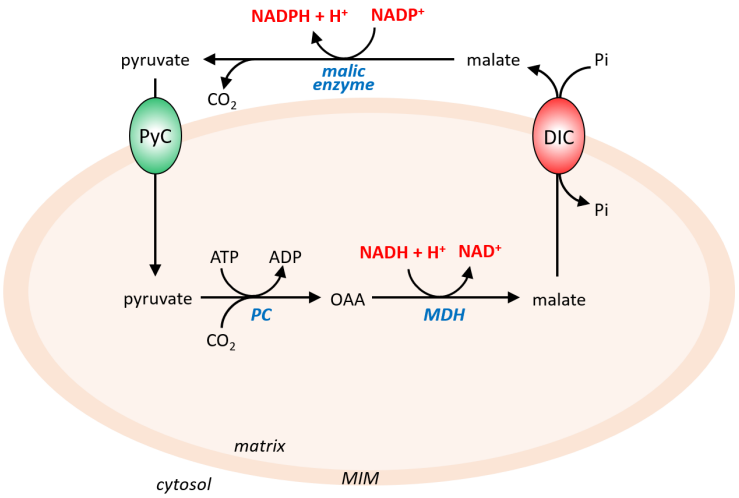

Fig. 1.15 The pyruvate-malate shuttle. The pyruvate-malate shuttle results in the generation of cytosolic NADPH. PyC: pyruvate carrier; DIC: dicarboxylate carrier; PC: pyruvate carboxylase; MDH: malate dehydrogenase. Enzymes are written in blue.

αKG into the mitochondria and export of isocitrate, and cytosolic NADPH generation by IDH.

1.5.4.2 The pyruvate-malate shuttle

The DIC is involved in the pyruvate-malate shuttle, whereby pyruvate is imported by the pyruvate carrier (MPC) and converted to malate inside the mitochondria (Palmieri, 2004). Malate is exported by the DIC in exchange for phosphate, and converted to pyruvate again by malic enzyme in the cytosol, generating cytosolic NADPH (**Figure 1.15**).

1.5.4.3 The citrate-malate shuttle

The citrate-malate shuttle is proposed to import cytosolic malate in exchange for citrate via the CIC and the reconversion of citrate to malate via OAA would generate the electron acceptor NAD^+ which can be used in glycolysis (Palmieri, 2004).

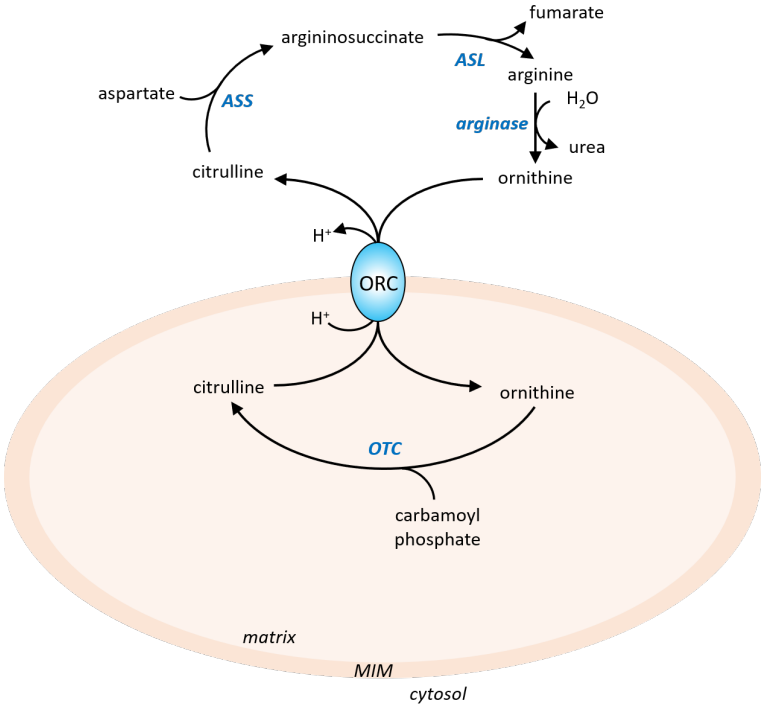

Fig. 1.16 The urea cycle. Urea is synthesised in the liver to remove excess nitrogen generated from amino acid breakdown. ORC: ornithine carrier; ASS: argininosuccinate synthase; ASL: argininosuccinate lyase; OTC: ornithine transcarbamoylase.

1.5.4.4 The urea cycle

The urea cycle synthesises urea in the liver in order to excrete nitrogen generated from amino acid breakdown, discussed in **Section 1.3.5** (Morris, 2002). The cycle occurs in both the cytosol and the mitochondrial matrix. ORC exchanges cytosolic ornithine for mitochondrial citrulline. Ornithine is combined with carbamoyl phosphate to make more citrulline **Figure 1.16**.

1.5.4.5 The malate-aspartate shuttle

The malate-aspartate shuttle (MAS) serves to transport cytosolic NADH electrons into the mitochondria and requires the combined action of the OGC and the AGC (Barron et al., 1998; Palmieri, 2004; Wiesner et al., 1988). The MAS can be split into 2 phases: the transport of electrons into the matrix and the regeneration of cytosolic OAA (**Figure 1.17**). NADH reduces cytosolic OAA to malate, which is transported into the mitochondria via

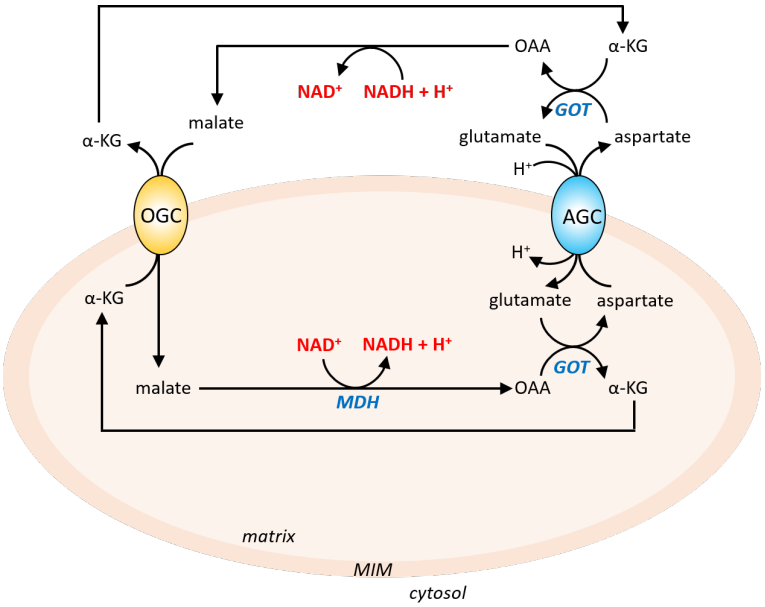

Fig. 1.17 The malate-aspartate shuttle. The malate-aspartate shuttle is a mechanism of importing NADH electrons into the mitochondria. It requires the concerted action of 2 carriers: the OGC and the AGC. AGC: aspartate-glutamate carrier; OGC: oxoglutarate carrier; GOT: glutamate oxaloacetate transaminase; MDH: malate dehydrogenase.

the OGC, in exchange for αKG (also known as oxoglutarate). Once in the matrix, malate is reoxidised by NAD^+, regenerating NADH and OAA. OAA is converted to aspartate, concomitantly converting glutamate to αKG. The aspartate is exported to the cytosol by the AGC in exchange for glutamate and a proton. Cytosolic aspartate is converted to OAA and αKG is converted to glutamate.

1.5.4.6 The glycerophosphate shuttle

The glycerophosphate shuttle is a mechanism that links glycolysis, oxidative phosphorylation and fatty acid metabolism (**Figure 1.18**) and as such is important in cell bioenergetics. It is comprised of two glycerol-3-phosphate dehydrogenases: the soluble cytosolic form (cGPDH) which is NADH-dependent, and the membrane-bound mitochondrial form (mGPDH), which is FAD-dependent. They catalyse oxidation of glycerol-3-phosphate (G3P) to dihydroxyacetone phosphate (DHAP), regenerating cytosolic NAD^+ from glycolytic NADH so that ATP production may continue. Concomitantly, electrons are transferred to CoQ and $FADH_2$ is generated inside the mitochondria (Mráček et al., 2013).

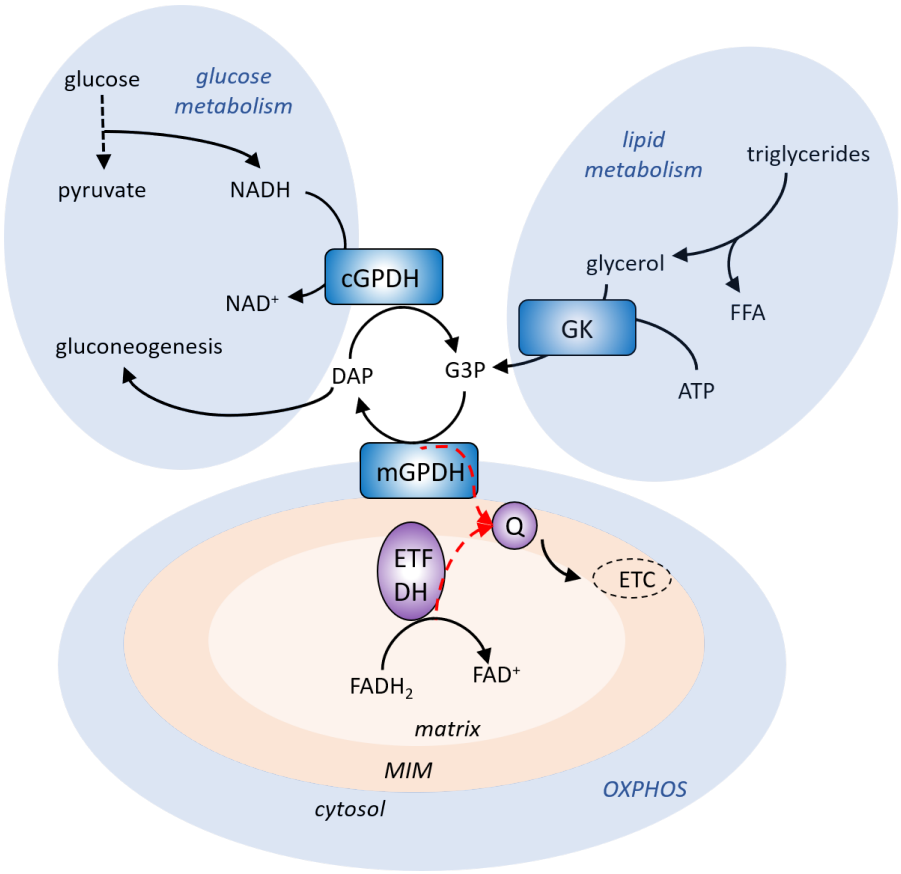

Fig. 1.18 The glycerophosphate shuttle. The enzymes of the glycerophosphate shuttle (cytosolic glycerol-3-phosphate dehydrogenase (cGPDH) and mitochondrial GPDH (mGPDH)) and glycerol kinase (GK) are shown in blue. Direction of electron transfer is depicted by red dotted lines. DAP: dihydroxyacetone phosphate; ETC: electron transfer chain; ETF DH: ETF:Q dehydrogenase; FFA: free fatty acids; G3P: glycerol-3-phosphate; Q: Coenzyme Q. Figure adapted from Mráček et al. (2013).

1.6 Compartmentalisation of metabolism

Metabolism is compartmentalised by physical containment within membrane-bound organelles, or within the cytosol (i.e. separated from organelles). Furthermore, metabolic enzymes can be organised into large quaternary structures, such as the fatty acid synthase homodimer or the glutamine synthetase polymer. This spatial organisation facilitates the movement of the product of one enzyme to the next enzyme, creating an "assembly line" and maximising metabolic output and efficiency (Zecchin et al., 2015).

Metabolic compartmentalisation is an important area to study because an understanding of the compartments, and how they are altered in diseases, could lead to the development of therapies. Drugs could be targeted to, and specifically activated in, particular subcellular compartments by their specific conditions. For example, hereditary leiomyomatosis and renal cell cancer (HLRCC) is caused by a heterozygous loss-of-function mutation in fumarate hydratase (FH) (Czibik et al., 2014). FH catalyses the conversion of fumarate to malate, thus its mutation leads to the accumulation of fumarate. Currently it is not known where this fumarate accumulates and what its downstream implications are, although it has been suggested to stabilise HIF-1α (Czibik et al., 2014). There is further evidence that fumarate hydratase and succinate dehydrogenase can act as tumour suppressors and that their mutation can activate tumour maintenance pathways (King et al., 2006). A deeper understanding of the compartmentalisation of these two metabolites and others would thus help in the development of cancer therapies.

The above points highlight the need for isolating mitochondria in some way from the rest of the cell in order to study their metabolism. Below, I outline historic and current methods of mitochondrial isolation from tissue and cultured cells before discussing work that attempted to measure mitochondrial metabolism from isolated mitochondria.

1.7 Mitochondrial Isolation Methods

1.7.1 Isolation of mitochondria from mammalian tissues

The majority of mitochondrial isolation methods from tissue used today stem from the work of Pallade and Hogeboom (Hogeboom et al., 1948), whose method was developed from Bensley, Hoerr (1934). A key component of Bensley's method was the use of differential centrifugation to isolate the more dense mitochondria from the rest of the cellular components. First, freeze-thawed guinea pig liver homogenate was centrifuged at a low speed for 3 minutes, to remove cell debris (such as nuclei, broken cells and red blood cells). This was followed by a second centrifugation at a higher speed for either 10 min or a series of 3 min centrifugations, which they claim reduced the loss of mitochondria at this stage. They state that a "considerable loss" of mitochondria occurs whilst removing the cell debris. The final supernatant, containing the mitochondria as well as connective tissue, fat, soluble proteins and glycogen, was centrifuged at a high speed for a longer period. The resulting precipitate contained the mitochondria, albeit they admit to contamination from fat, cell fragments and connective tissue. They washed the mitochondrial pellet with 0.85 % NaCl solution followed by centrifugation, which they stated caused some mitochondrial swelling. A caveat to this method is the use of freeze-thawed tissue homogenate because the process of freeze-thaw lyses membranes, including mitochondrial membranes. Therefore, this method is not compatible for metabolomic studies as the mitochondrial metabolites will not be contained in the mitochondria and compartmentalisation is lost before the extraction. Furthermore, the speed and temperature of the centrifugation steps were not recorded in the paper.

Pallade and Hogeboom were concerned that the use of saline or water in the Bensley method was generating artefacts due to the rupturing of cellular membranes. They addressed this by the use of a hypertonic sucrose solution to homogenise the tissue (Hogeboom et al., 1947, 1948). They worked with rat liver and used both nearly isotonic levels of sucrose (250 mM) and hypertonic sucrose solutions (880 mM sucrose). They found the use of 250 mM sucrose for homogenisation did not result in agglutination and allowed separation of the mitochondria from nuclei. The hypertonic sucrose solution was found to be protective for mitochondria. They also observed that the use of saline resulted in agglutination of mitochondria and firm attachments to nuclei. KCl, K_2SO_4 and phosphate buffers were also found to cause agglutination. They used EM studies to investigate the structure of mitochondria isolated

in increasing concentrations of sucrose, and decided on 880 mM sucrose as the optimal homogenisation buffer concentration in terms of osmotic support as this had a high proportion of rod-like mitochondria, which they used as an indicator of healthy mitochondria. Their procedure was as follows: rat livers were forced through a tissue masher with a mesh screen of 1 mm. 5 g of the resulting "pulp" was homogenised in a Potter-Elvehjem tissue grinder in 50 mL of 880 mM sucrose. 40 mL (4 x 10 mL in 15 mL tubes) of the homogenate was centrifuged 3 times for 10 min at 600 x g. In the first of these centrifugations the homogenate was placed on a 1 mL cushion of high density sucrose. This formed a 2-phase system in which nuclei and cell debris entered the denser sucrose phase. The supernatants were then centrifuged for 20 min at 24,000 x g and the resulting mitochondrial pellet was resuspended in 35-40 mL of 880 mM sucrose before a final centrifugation at 24,000 x g to remove any soluble substances from the mitochondria. They used a 30° angle type centrifuge, refrigerated at 4°C.

Weinbach (1961) et al. devised a similar method for rat liver and kidney mitochondria but reduced the sucrose content to 250 mM, close to isotonic levels. The tissue was homogenised in a nine-volume ratio using a Delepine Press motorised homogeniser (1,000 rpm for 1 min), kept at 4^oC. They also reduced the time and speed of the centrifugation steps to 600 x g for 10 min followed by 8,500 x g for 10 min (reduced from 3 x 600 x g for 10 min then 24,000 x g for 20 min). The mitochondrial pellet was resuspended such that 2 mL of 250 mM sucrose was added per g of liver tissue. This was recentrifuged at 8,500 x g for 10 min and the final mitochondrial pellet resuspended in 250 mM sucrose at 1 mg wet weight/mL. Weinbach et al. highlighted the importance that "meticulous attention" must be given to the "minutiae" of the isolation procedure, such as keeping all equipment and isolation components cold by storing on ice and performing as many steps as possible in the cold room.

Corcelli et al. (2010) argue that isoosmotic sucrose/mannitol buffers, such as those used in the methods of Bensley, Hoerr (1934), Hogeboom et al. (1948) and Weinbach (1961) above, are not isotonic or physiological. Corcelli argues these osmolytes can lead to changes in the mitochondrial matrix composition due to abnormal movement of ions and water across the membrane. This in turn could alter matrix metabolism and therefore mitochondria isolated in this way are not suitable for metabolomic analysis. They were able to isolate coupled and functionally active mitochondria using a more physiological KCl buffer (180 mM KCl, 1 mM EDTA, 5 mM 3-(N-morpholino)propanesulfonic acid (MOPS), pH 7.25), despite the general perception that KCl isolation buffer results in the formation of mitoplasts (mitochondria whose outer membrane has been removed) and agglutination (Hogeboom et al., 1947, 1948).

Corcelli et al. (2010) homogenised rat livers in either mannitol buffer (220 mM mannitol, 75 mM sucrose, 1 mM EDTA, 10 mM HEPES, pH 7.4) or the KCl buffer listed above. The homogenate was centrifuged at 500 x g for 10 min and the supernatant was centrifuged for a further 10 min at 5,000 x g. They state that they were able to obtain active mitochondria, but that they were less pure than those isolated using the sucrose/mannitol buffer. They also found a lower cardiolipin content in mitochondria isolated in KCl buffer. As cardiolipin is a phospholipid found almost exclusively in the MIM, this could perhaps indicate that the method is altering or damaging the mitochondria. It can be seen that although Corcelli made efforts to make the mitochondrial isolation process more physiological, they introduced additional problems, and sacrificed the purity of the mitochondria for physiological relevance. For some applications this compromise may be acceptable, but for mitochondrial metabolite localisation studies this is not practical.

Isolated mitochondria are contaminated with organelles such as lysosomes and ER fragments (microsomes), either due to their similar densities causing them to co-pellet or due to physical interactions with the mitochondria. There are various methods to purify these crude mitochondrial fractions. One common technique is purification by a discontinuous Percoll gradient. Percoll is a mixture of colloidal silica particles coated with polyvinylpyrrolidone (Pertoft et al., 1978). It has a low osmolality and is non-toxic. It is diluted to generate layers with densities between 1.00 g/mL and 1.2 g/mL and layered in centrifuge tubes to form a discontinuous gradient. The advantage of a discontinuous gradient is the formation of a distinct band of mitochondria, facilitating their retrieval. The method of Wettmarshausen, Perocchi (2017) describes layering 80%, 52% and 26% Percoll in an ultracentrifuge tube. A diluted crude mitochondrial fraction, isolated in 220 mM mannitol, 70 mM sucrose, 5 mM HEPES-KOH pH 7.4, 1 mM EGTA-KOH, pH 7.4, is placed at the top of the Percoll gradient and centrifuged at 44,000 x g for 45 min at 4°C. The mitochondria settle at the interface of 26% and 52% Percoll, so these two layers are removed, diluted ten-fold and moved to a fresh tube. This is centrifuged at 8,000 x g for 10 min at 4°C to obtain a purified mitochondrial pellet.

Another method of purifying crude mitochondrial fractions is the use of a sucrose gradient. A method described by Colbeau et al. (1971) involves centrifugation of crude mitochondria, isolated by classical differential centrifugation in 0.27 M sucrose buffered by 2 mM Tris-HCl, pH 7.6, through a 2-layer sucrose gradient of 41.4% (w/v) and 39.3% (w/v) sucrose (buffered by 2 mM Tris-HCl, pH 7.6) and centrifuging at 55,000 x g for 2 hours. The mitochondria form a pellet at the bottom of the tube. In this case, the lysosomes were removed by pre-

treatment with Triton WR-1339, which is taken up by lysosomes and reduces their density, causing them to stay at the top of the sucrose gradient whilst the mitochondria enter the bottom.

The Percoll and sucrose gradient purification methods both add significant time to an already long extraction protocol. All of the isolation methods from tissue described above require significant time, have impure mitochondrial pellets, or both. For many applications, such as functional studies, this is a reasonable compromise but for metabolomic studies this additional time is not an option. Ideally, the method of mitochondrial isolation for metabolomic studies should concomitantly isolate and purify the mitochondria away from cellular contaminants, saving valuable time.

1.7.2 Isolation of mitochondria from mammalian cells in culture

In the 1970s and early 1980s many new methods for isolating mitochondria from mammalian cells in culture were published, some of which were also based on differential centrifugation. The method of Zuurendonk, Tager (1974) did not use differential centrifugation; instead, their method relied on the distinct cholesterol content of mitochondrial membranes. They added digitonin to their isolation buffer, which binds to cholesterol and forms pores in membranes. Because the MIM contains no cholesterol, and the plasma membrane (PM) and membranes of other organelles do (Colbeau et al., 1971), by adding the correct amount of digitonin the mitochondria can be selectively retained and contaminating organelles are destroyed by membrane lysis, increasing the yield and purity of the mitochondrial pellet. Zuurendonk and Tager used the method of Berry, Friend (1969) to isolate liver cells, whereby the liver is perfused with a buffer containing the enzymes collagenase and hyaluronidase. They then isolated the mitochondria from these liver cells by mixing 1.5 mL of the cell suspension with 5 mL of a buffer containing 250 mM sucrose, 20 mM MOPS, 3 mM EDTA and 0.5 or 1 mg/mL digitonin. After incubation for 10, 20 or 40 s the suspension was centrifuged for 20 s at 3,000 x g using a swing-out rotor, pre-cooled to 0^{o}C. The mitochondrial pellet was found to contain 90 % of total adenylate kinase and glutamate dehydrogenase activity (both mitochondrial enzymes), and the supernatant contained 80 % of the lactate dehydrogenase activity (a cytosolic enzyme), indicating good separation of mitochondria from the cytosol.

Siess, Wieland (1975) then built on the method of Zuurendonk and Tager and combined the use of digitonin and differential centrifugation. They incubated 0.1 mL rat liver cells

(corresponding to 35-40 mg fresh liver, in calcium-free Krebs-Henseleit bicarbonate buffer + 1.5 % gelatin, 80 mM $CaCl_2$) in 1 mL of 250 mM sucrose, 20 mM MOPS, 3 mM EDTA and 4 mg/mL digitonin. This was mixed for 15 sec, before 1 mL was placed on top of 0.5 mL of a silicone oil mixture (AR200:AR20, 1:1) layered above 0.12 mL of 12 % perchloric acid (PCA). 30 sec after digitonin was added, the tube was centrifuged for 10 sec, allowing the denser mitochondria to pass through the oil and enter the acid. To perform analyses on the mitochondrial pellet the oil phase was removed by suction and the pellet was resuspended in a total of 0.312 mL of PCA. This was important work which combined the benefits of both density centrifugation and digitonin addition.

Wiesner et al. (1988) used a similar method to isolate mitochondria from mammalian cells in culture to look at the distribution of metabolites from the MAS, but used a layer of bromododecane instead of silicone oil. Rat myocytes were isolated from heart tissue by Langendorff perfusion with collagenase, and then separated from the isolation medium by injection into 250 mM sucrose buffered with 20 mM MOPS and 2 mM Tris-EGTA. This was layered on 350 µL bromododecane above 100 µL of 2 M PCA. Mitochondria were subsequently isolated from the cells by adding the cell suspension to the buffered 250 mM sucrose solution with the addition of 0.6 mg/ mL digitonin, which was then layered on 350 µL bromododecane above a layer 100 µL of 2 M PCA and centrifuged. As they have not published the length or speed of this centrifugation step it is difficult to analyse whether this method is suitable for metabolomics.

However, the addition of digitonin was considered controversial by some, with Soboll et al. (1978) proposing that phosphorylation of mitochondrial ADP may occur during isolation if digitonin is used, generating artificially high mitochondrial ATP/ADP ratios. Brocks et al. (1980) investigated this by studying metabolic stability during mitochondrial isolation from rat liver cells. They followed the general procedure of Zuurendonk, Tager (1974), except they lowered the temperature of the whole isolation process to -5°C, and increased the digitonin concentration from 4 mg/mL to 15 mg/mL. They performed the whole experiment in the cold room and added 0.2 mL of cell suspension to 1 mL of digitonin medium (15 mg/mL digitonin, 3 mM EDTA and 0.1 mL toluene), pre-cooled to -12 °C. After shaking, the mixture was layered on 0.5 mL silicone oil mix (AR200/AR20 2:1 w/w) above 0.12 mL of 12 % PCA and centrifuged in an Eppendorf centrifuge for 10-15 sec. They found that mitochondrial levels of aspartate and malate were twice as high when mitochondria were isolated at -5°C than 4°C. However, at -5°C there would be some shearing of the mitochondrial membranes

due to ice crystal formation, so the metabolite compartmentation may well have been lost during this isolation procedure.

Others argued that the incubation time needed for the digitonin to work was sufficient for spontaneous metabolic reactions to occur and consequently the use of digitonin was redundant. Based on this argument, the method of Tischler et al. (1977) for isolating mitochondria from rat liver cells made use of centrifugation through silicone oil but did not use digitonin. Instead, they disrupted the cell membrane by forcing the cells through a small diameter needle (needle gauge ranged from 22 to 25) under high pressure, generated by the addition of a three-way valve. The turbulent flow of a solution through a narrow aperture generates shearing forces sufficient to break the plasma membrane, but was optimised such that minimal mitochondrial shearing was caused. 100 µL of the broken cell suspension was then layered on 350 µL silicone oil (a mixture of 500 and 200 silicone oil from Dow Corning, 4:1 ratio, density 1.029 g/mL) into 100 µL of 21% (w/v) PCA. This was centrifuged at 12,000 x g for 10 sec to isolate mitochondria. They were able to measure mitochondrial and cytosolic metabolite pools but acknowledge that there is some "uncertainty" about how closely these measured values reflect actual values in the intact cell.

A different approach for mitochondrial isolation from cells is to use magnetic sorting. Hornig-Do et al. (2009) adapted a protocol previously used to separate cells – magnetic cell separation (MACS), incorporated in Miltenyi kits (Miltenyi Biotec, Bergisch Gladbach, Germany). Superparamagnetic beads are conjugated to an anti-TOM22 antibody, which binds to the mitochondria and isolates them in a gradient magnetic field. They report that the quality, enrichment and purity is comparable to standard isolation procedures. However, the whole process takes 1-2 hours, rendering it irrelevant for metabolomic studies. Similar to this method is the use of immunopurification. This was used in the method of Chen et al. (2016a), in which an epitope-tagged recombinant protein expressed on the MOM binds to magnetic beads. This work is discussed in greater detail in **Section 1.7.3**.

All of the above methods have attempted to overcome the challenge of achieving speed and high quality mitochondria, but have compromised in either speed or quality.

1.7.3 Metabolomic studies on isolated mitochondria

As written by Van Vranken, Rutter (2016), "the whole (cell) is less than the sum of its parts". Many metabolomic studies have been performed on isolated mitochondria with a view to study mitochondrial metabolism, with varying levels of success. Below, I describe the methods and findings of some of these studies.

Siess, Wieland (1975) isolated rat hepatocytes via a modified digitonin method. They measured the subcellular distribution of a range of metabolites and reported the mitochondrial/cytosolic concentration gradients for malate (1.0); citrate (8.8); 2-oxoglutarate (1.6); glutamate (2.2); aspartate (0.5); oxaloacetate (0.7), acetyl-CoA (13) and CoASH (40). This is in contradiction to the studies of Chen et al. (2016a) which suggested that all metabolites had a higher concentration in the cytosol than the mitochondria.

Ross-Inta et al. (2008) used isolated mitochondria to study the mitochondrial pool of free amino acids. Rat liver mitochondria were isolated by a Percoll method and the amino acids were measured using a commercially available kit. They found that the mitochondrial pool of free amino acids is significantly higher than that of the cytosol, except for citrulline, glutamic acid, hydroxyPro, 1-methyl- histidine, proline, sarcosine, and Tau.

Roede et al. (2012) used a metabolomic approach to study isolated mice liver mitochondria. They were able to distinguish male from female and WT from mutant thioredoxin-2 transgenic (TG) mice based purely on their mitochondrial metabolite signature.

The work of Matuszczyk et al. (2015) measured metabolites of whole Chinese hamster ovary (CHO) cells and "cytosol-depleted" CHO cells, which they claimed were equivalent to the mitochondrial fraction. To obtain this fraction they used digitonin as a lysis detergent and then filtered the CHO cells to remove the cytosol. This method has the major disadvantage of "lumping together" all organelles except the nucleus, meaning that the mitochondrial fraction is actually just a non-cytosolic fraction. They based this technique on the assumption that central metabolites will be either in the mitochondria or the cytosol, and disregard the fact that metabolites are present in other organelles such as ER, peroxisomes and lysosomes. The fractions were analysed by liquid chromatography-isotope dilution mass spectrometry. They reported that the ATP pool was significantly lower in the mitochondria than the cytosol. This is an expected and logical result as the mitochondria exports the majority of its ATP to the cytosol for use in various cellular processes.

Pan et al. (2018) performed a gas-chromatography mass spectrometry (GC-MS) study on isolated mitochondria from yeast. They were able to distinguish WT from mutant-complex II and complex IV by principal component analysis, with altered TCA cycle-related metabolites, amino acids, fatty acids, purine and pyrimidine intermediates and others.

To date, the quickest method of isolating mitochondria from cells for metabolomic analysis was published by Chen et al. (Chen et al., 2017, 2016a). They devised a new isolation buffer from KCl, based on work by Corcelli, which contains only KCl and KH_2PO_4 and is therefore compatible with LC-MS analysis. They developed an immunopurification (IP) strategy to capture HA-tagged mitochondria from HeLa cells in 12 min. They report good integrity of mitochondria, based on the mitochondria retaining MitoTracker Deep Red dye, with less contamination from other organelles than conventional differential centrifugation methods, based on immunoblot analyses of subcellular compartments.

They used their method to investigate the subcellular location of polar mitochondrial metabolites and state that they can distinguish between cytosolic and mitochondrial pools of metabolites. However, their total extraction time of 12 min is still slow relative to metabolism and allows plenty of time for dismutation, although they claim that their results between their normal workflow and one lengthened by 4 min are similar. They point out that they do not know the behaviour of the mitochondria at time points less than 12 min, which I would argue is a fundamental flaw with their method as there could be a large amount of metabolism occurring in these initial 12 min.

Chen et al. found the expected cofactors and redox pairs NAD, NADH, FAD, NADP, GSH, GSSG and SAM in the mitochondria, as well as other known mitochondrial metabolites involved in the TCA cycle, energy production and fatty acid metabolism. They report a lack of cytosolic metabolites such as fructose 1,6-bisphosphate and the lysosomal metabolite cystine in their mitochondrial samples, which does indicate good separation of mitochondria from the rest of the cell. When measuring metabolism at the whole cell level, ETC inhibition caused little perturbation to NADH/NAD^+ and GSH/GSSG ratios. When ETC inhibition was repeated on mitochondria isolated via their method, these ratios were markedly changed. However, the major issue I find with their results is most metabolites have a lower concentration in the matrix than the cytosol. Although the concentration of matrix metabolites is not known, it seems logical that the concentration of some of them should be higher than in the cytosol: for example, fumarate plays a major role in the mitochondria-specific TCA cycle and has no specific fumarate transporter. The consistently lower mitochondrial

concentrations signal many possibilities. It could be that their isolation procedure damaged many mitochondria, which became leaky and lost their metabolites, or their mitochondrial yield was much lower than they expected. Alternatively, in the 12 min of the isolation procedure the metabolites may have reacted with each other, degraded or were transported out of the mitochondria and distributed throughout the cell.

1.8 Methods to measure metabolites

The study of metabolism is inherently challenging because metabolites are a broad range of molecules, with different reactivities, structural diversity and broad concentration ranges (Lu et al., 2017). This diversity has led to the development of many ways to measure cellular metabolites, with each method generally more suited to measuring a particular metabolic subtype. Therefore, to measure all groups of metabolites accurately, multiple analytical tools must be used. Mass spectrometry (MS) is a popular way to measure metabolites, and LC-MS is the most popular MS technique for metabolomics.

1.8.1 LC-MS

LC-MS combines two analytical techniques: physical separation by liquid chromatography (LC) and mass analysis by mass spectrometry (MS). During the LC stage, the sample is separated by distribution between a stationary and a mobile phase. Effective separation at this stage is important because it reduces ion suppression, which is often an issue when analysing metabolites from tissue. Ion suppression occurs when a highly abundant ion blocks the electrospray of other metabolites in the MS and hence suppresses their detection (see below). This can be a major issue in biological samples due to the presence of highly abundant metabolites and salts, such as NaCl and KH_2PO_4.

After the sample has been separated by LC, it is passed to the MS, which measures the mass-to-charge ratio (m/z) of charged molecules. To be detected by the MS, the sample must be ionised. In the commonly used technique of electrospray ionisation (ESI), a high voltage is applied to the liquid sample to create an aerosol of charged droplets (Jang et al., 2018). ESI often produces multiple-charged ions and results in very little fragmentation (Pitt, 2009). These ions are then sent to the mass analyser, such as an Orbitrap or a quadrupole. An

Orbitrap mass analyser detects the oscillations of the ions around a spindle-shaped electrode, in which the electrostatic attraction is balanced by centripetal force around the spindle (Jang et al., 2018). The frequency of the oscillations is dependent on the m/z. The m/z and the retention time can together be used to identify the analyte.

Multiple LC approaches must be employed to analyse all metabolites classes, due to their distinct chemical and physical properties. For example, the study of lipids is termed lipidomics, emphasising the different analytical approaches they require compared to water-soluble metabolites (Jang et al., 2018).

There are a variety of approaches to study metabolism by LC-MS. These are steady state, flux or stable isotope tracing analysis. Metabolite concentration and pathway flux are two distinct parameters, and information on both is necessary to be able to draw strong conclusions (Jang et al., 2018). Metabolomic MS methods can be either targeted or non-targeted. A targeted MS study is one in which a select group of metabolites are quantified, whereas a non-targeted approach will study the global metabolome, and is typically not quantitative.

1.8.2 Other metabolite analysis techniques

LC-MS is not appropriate for all metabolites. GC-MS is a technique commonly used for low molecular weight and volatile metabolites and uncharged species that do not ionise under electrospray.

For some metabolites and experimental conditions, no MS method is appropriate. For example, glycogen cannot be measured by MS due to its heterogeneity. Instead, glycogen and other metabolites are often measured by enzymatic assays, in which the accumulation of a product, such as NADH, is followed on a spectrophotometer. There are many commercially available kits which claim to perform these assays. However, these should be approached with caution in an *in vivo* setting because they are often dependent on H_2O_2, which can confound quantification due to the multitude of enzymes and other components present in tissue that can react with H_2O_2. Genetically encoded sensors can be designed which fluoresce upon binding to certain metabolites, such as NADH (Zhao et al., 2011) or glucose (Hou et al., 2011). Although these techniques have the advantage of being able to dynamically follow metabolic changes in real time, their use is limited to cultured cells.

The other leading approach for metabolomics in tissue and cells is nuclear magnetic resonance (NMR) spectroscopy. This has a lower sensitivity than MS (Markley et al., 2017) but does not need such extensive sample preparation. It is also better at detecting metabolites that do not ionise easily and can distinguish between metabolites of the same mass, which is an issue with MS. By using stable isotope labels, NMR is often employed for studying metabolic flux and can even be used in living organisms (Markley et al., 2017).

1.9 Metabolism during ischaemia reperfusion injury

Ischaemia reperfusion injury (IRI) occurs when the blood supply to an organ is blocked (ischaemia) and then restored (reperfusion). It occurs during heart attack, stroke and many types of surgery. Whilst there is no blood flow during ischaemia there is a lack of oxygen and nutrients. However, the return of blood flow is paradoxically more damaging to the tissue because early upon reperfusion there is a burst of ROS production from mitochondria (Loor et al., 2011; Zweier et al., 1987). This can cause direct damage to the mitochondria, causing calcium dysregulation and further disruption to ATP production (Murphy, Steenbergen, 2008) which was already in deficit because of the previous lack of oxygen.

1.9.1 Ischaemia

During ischaemia, both cellular and mitochondrial metabolism are remodelled in an attempt to keep the cell alive without oxygen and maintain energy homeostasis, ion homeostasis and pH. During early ischaemia, intracellular acidosis and breakdown of nucleotides occurs, which accumulates P_i and reduces pH. The low pH and high P_i stop contraction of the ischaemic zone, which is protective in the short-term. The cell is also forced to break down nucleotides, leading to accumulation of nucleotide breakdown products such as xanthine and hypoxanthine (Chouchani et al., 2014; Harmsen et al., 1981; Pacher et al., 2006). These are metabolised by xanthine oxidase (XO) in the cytosol and are thus not involved in mitochondrial metabolism (**Figure 1.19**).

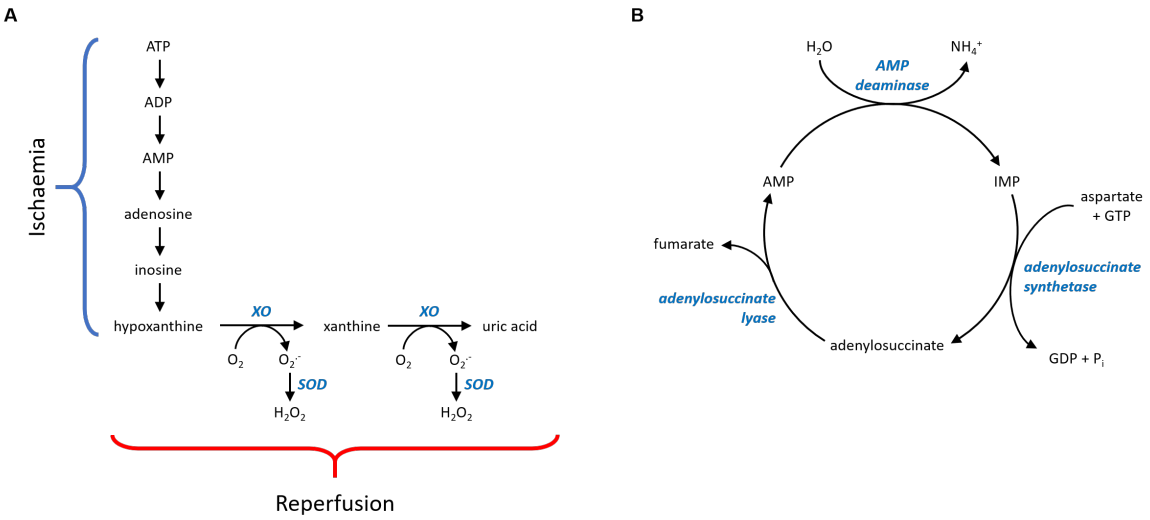

Fig. 1.19 Purine catabolism. ***A)*** Adenine nucleotide depletion in ischaemia and action of xanthine oxidase to generate ROS in reperfusion. During ischaemia cellular ATP is catabolised in multiple steps to hypoxanthine. During reperfusion the accumulated hypoxanthine is metabolised to xanthine by xanthine oxidase (XO) which can further metabolise xanthine to uric acid. XO uses oxygen for catalysis and can generate the superoxide radical ($O_2^{\cdot -}$) which is metabolised to H_2O_2 by superoxide dismutase (SOD). Scheme from Pacher et al. (2006). ***B)*** The purine nucleotide cycle. AMP is deaminated to IMP. The synthesis of AMP from IMP yields fumarate.

1.9.1.1 Glycolysis in ischaemia

A protective mechanism employed in early ischaemia is anaerobic metabolism via glycolysis. This allows the cell to generate ATP in the absence of oxygen (**Figure 1.5**). As glycolysis continues, lactate accumulates and is not removed due to the lack of blood flow. It was previously thought that the accumulation of lactate was deleterious due to increased H^+, but there is evidence that lactate has more direct damaging effects, for example in influencing ion homeostasis and ROS production (Cross et al., 1995; Lin, Suleiman, 2003). In aerobic conditions, lactate is a respiratory substrate for the heart and is imported into cardiac myocytes via a specific monocarboxylate/proton cotransporter (MCT) on the cardiac sarcolemmal membrane. However, during ischaemia, lactate is exported from the cell along with H^+ in an attempt to limit intracellular acidosis associated with lactate accumulation (Halestrap et al., 1997). Thus the MCT can be seen to play a crucial role in maintaining intracellular pH. However, glycolysis is blocked after a time due to a high NADH/NAD^+ ratio.

1.9.1.2 Mitochondrial responses to ischaemia

Numerous studies have found succinate to be increased during ischaemia (Chouchani et al., 2014; Hochachka, Dressendorfer, 1976; Taegtmeyer, 1978). Further work by Chouchani et al. (2014) reported succinate to be a universal metabolic signature of ischaemia. Succinate was found to accumulate 3-19-fold across a range of tissues exposed to IRI. Its accumulation during ischaemia was driven by reversal of Complex II (succinate dehydrogenase), caused by excess fumarate. The fumarate is thought to be generated by 2 sources. One is the increased uptake of malate (from aspartate and oxaloacetate) which is converted to fumarate in the mitochondria. The second source of fumarate is thought to be from increased AMP breakdown by the purine nucleotide cycle (PNC), generating adenylosuccinate, which is metabolised to fumarate by adenylosuccinate lyase (**Figures 1.19 and 1.20**). The proposal of the PNC as a source of fumarate is supported by the finding that inhibition of adenylosuccinate lyase by AICAR (5-Aminoimidazole-4-carboxamide ribonucleotide) limits succinate accumulation (Chouchani et al., 2014). As there is no fumarate transporter in the MIM, fumarate is thought to enter the mitochondria via partial reversal of the MAS, and in exchange for succinate by the DIC (**Figure 1.20**). Transamination of aspartate to oxaloacetate could also contribute to succinate accumulation and feeds in by conversion to malate driven by high NADH levels. This is supported by the transaminase inhibitor aminooxyacetate (AOA) reducing ischaemic succinate accumulation (Chouchani et al., 2016). However, this model is not fully accepted in the field yet. Zhang et al. (2018) propose that reversal of complex II plays only a minor role in succinate accumulation in ischaemia. Instead, they postulate that canonical function of the TCA cycle generates the remainder of the succinate. However, they used a hypoxic cardiomyocyte model and a different ischaemic model to that used in Chouchani et al. (2014).

1.9.1.3 Fatty acids in ischaemia

In aerobic conditions, the heart is dependent on fatty acid oxidation as its main fuel source, by mitochondrial β-oxidation. This is not possible during ischaemia due to the lack of oxygen. As well as a reduction in fatty acid oxidation, cellular uptake of fatty acids is reduced, with FAT/CD36 (a fatty acid translocase) expression reduced by 32% in the sarcolemma during ischaemia (Heather et al., 2013). In contrast, the expression of the glucose transporter

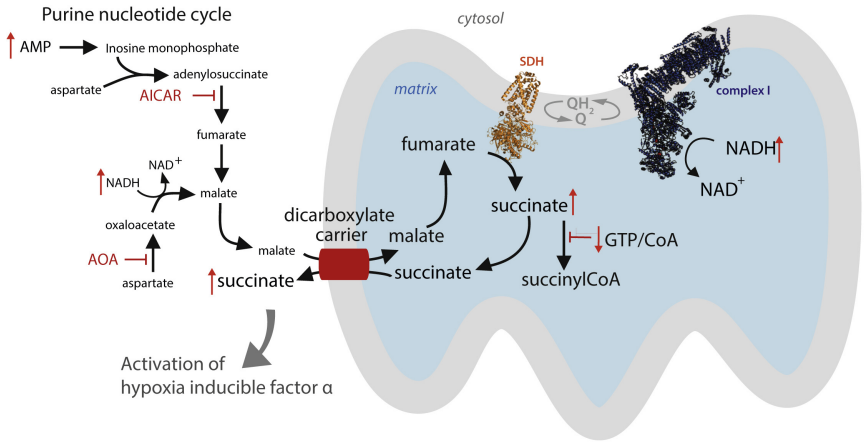

Fig. 1.20 Proposed mechanisms of succinate accumulation in ischaemia. The mechanisms that generate the fumarate that drives reversal of SDH are shown. NADH accumulates during ischaemia and passes its electrons to the CoQ pool via complex I. Fumarate is generated during ischaemia by the breakdown of accumulated AMP by the purine nucleotide cycle (PNC) in the cytosol. Fumarate can then be metabolised to malate by cytosolic fumarate hydratase. Malate is also generated in the cytosol from oxaloacetate. Malate then enters the mitochondria in exchange for succinate by the action of the dicarboxylate carrier (DIC). Once in the mitochondrial matrix malate is converted to fumarate. AOA: Aminooxyacetate. From Chouchani et al. (2016).

GLUT4 is increased during ischaemia by 90% in the sarcolemma, allowing glucose uptake for glycolysis.

In the first hour of ischaemia free fatty acids increase due to catecholamine stimulation of adipose tissue lipolysis. The accumulation of free fatty acids during ischaemia is damaging for a number of reasons. Fatty acid oxidation consumes more O_2 than glucose oxidation, leading to oxygen wasting. Fatty acids can bind to albumin, increasing the uptake into the ischaemic myocardium which can lead to ventricular fibrillation. Fatty acids inhibit PDH, which stops glucose oxidation, and blocks β-oxidation. This leads to accumulation of long chain acylcarnitines and acyl-CoAs. Fatty acids inhibit Na^+K^+-ATPase pump, leading to high intracellular Na^+ and Ca^{2+}, contributing to Ca^{2+} overload and arrhythmia (Oliver, 2015). The sequestration of fatty acids into the TAG pool is cardioprotective (Kolwicz et al., 2015).

Adenosine is protective in ischaemia. It is thought to be protective by partially inhibiting glycolysis, limiting glycolytic ATP production, and therefore proton production. This is proposed to be how adenosine stops intracellular acidosis during ischaemia, and less H^+ produced also means Na^+/H^+ exchange is limited, preventing Na^+ and Ca^{2+} overload (Fraser et al., 1999).

1.9.2 Reperfusion

1.9.2.1 Mitochondrial responses to reperfusion

Upon reperfusion, Complex II reoxidises succinate back to normoxic levels within 5 min (Chouchani et al., 2014), the same time frame that mitochondrial ROS are generated during IRI. Therefore, Chouchani et al. proposed that succinate was responsible for mitochondrial ROS generation during IRI. In this way, succinate acts as an electron sink in the absence of oxygen, and is then used to drive ROS by RET upon reperfusion (Murphy, 2016).

It was previously thought that the ROS produced during reperfusion was non-specific, but it has been recently proposed that there are widely conserved metabolic pathways that generate the ROS (Chouchani et al., 2016). During ischaemia, the lack of the terminal electron acceptor oxygen cause the ETC, enzymes and electron carrier pools (NADH and CoQ) to become reduced. Concomitantly ATP depletion, lack of ion homeostasis, pH changes and calcium overload lead to non-functioning mitochondria (Burwell et al., 2009). The large amount of electrons close to the ETC led to the assumption that mitochondrial ROS production was an inevitable and nonspecific response, with electrons uncontrollably spilling onto various sites to form $O_2^{\cdot -}$. However, there is evidence that Complex I is the major site of mitochondrial ROS production upon reperfusion, mostly from studies using selective pharmacological inhibition (Chen et al., 2006; Lesnefsky et al., 2004; Niatsetskaya et al., 2012). These studies also hint to the specific mechanism of $O_2^{\cdot -}$ production by Complex I because rotenone reduces $O_2^{\cdot -}$ production, indicating that forward electron transfer is unlikely to play a role (Chen et al., 2006; Lesnefsky et al., 2004). RET is the proposed method of ROS production at Complex I as the ΔP is high and the CoQ pool is reduced ($4\Delta P > 2\Delta E_h$) (**Figure 1.21**). RET is most likely as it requires a reduced CoQ pool and a high PMF, both of which occur physiologically during IRI. For RET to occur, mechanisms of ΔP dissipation must be inhibited, such as ATP synthesis and proton leak. This occurs in IRI because the adenine nucleotide pools are depleted by metabolism to inosine and hypoxanthine (**Figure 1.19**) (Grover et al., 2004). They can also be further metabolised by the PNC.

The high levels of ROS generated upon reperfusion can lead to opening of the MPTP (Bernardi et al., 2015; Burwell et al., 2009; Halestrap, 2005). This dysregulation of calcium levels, prevention of ATP synthesis and MPTP opening leads to both necrotic and

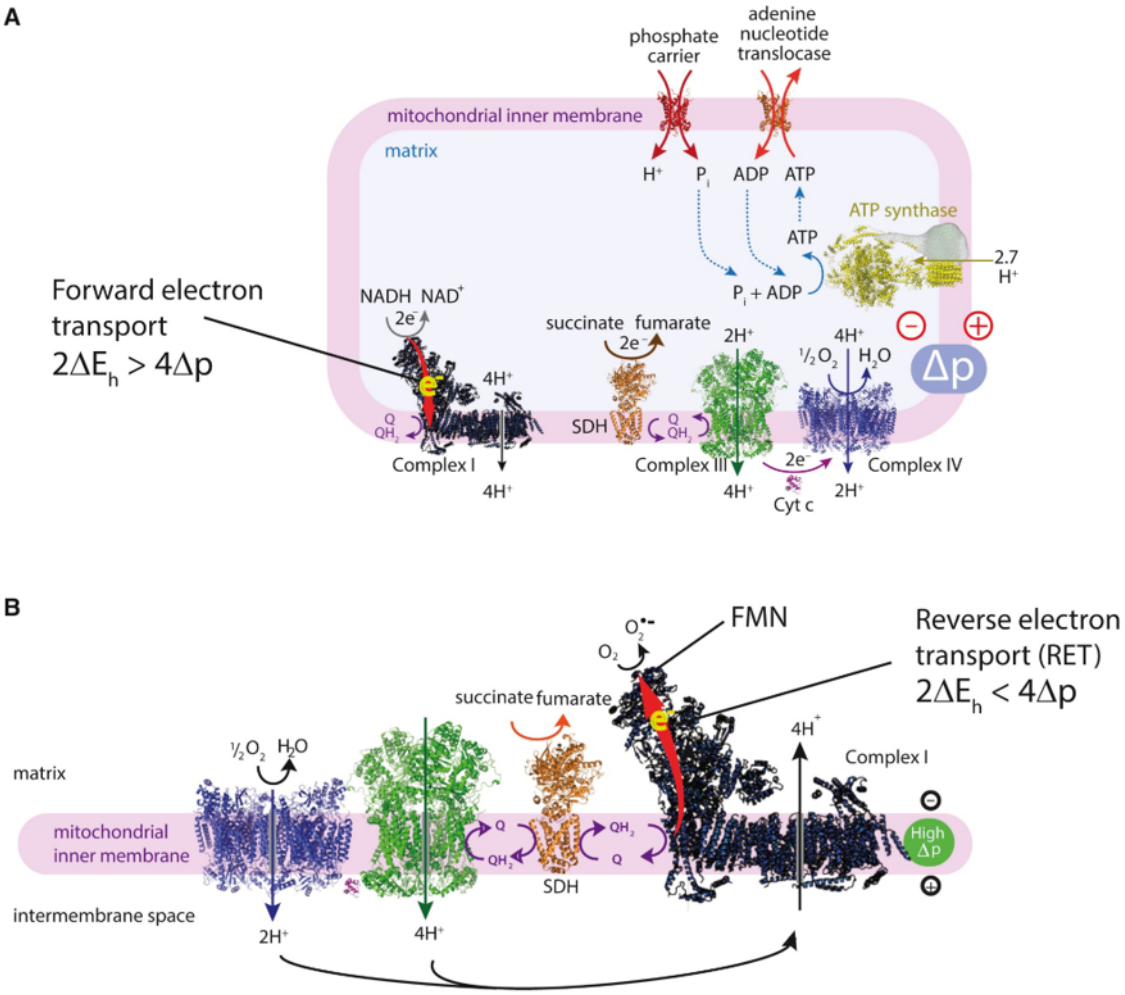

Fig. 1.21 Proposed mechanisms of superoxide production in ischaemia-reperfusion injury. ***A)*** During forward electron transfer 2 electrons are donated to complex I from NADH. These pass along a series of Fe-S clusters to Q, reducing it to QH_2. A high NADH/NAD^+ ratio or blockage of the ETC cause electrons to back up and hyper-reduce the FMN of complex I, leading to reduction of O_2 to superoxide. The ΔE_h between NADH/NAD^+ and Q/QH_2 drives the pumping of four protons across the MIM, maintaining the proton motive force (Δp), which allows ATP synthesis to continue. For forward electron transfer to occur, the ΔE_h must be greater than the energy required to pump four protons against the Δp: $2\Delta E_h > 4\Delta p$. **B)** Reverse electron transport can occur when the Δp is high and/or the CoQ pool is reduced, such that $4\Delta p > 2\Delta E_h$ (opposite to forward electron transfer). This allows electrons to flow backwards through complex I onto the FMN. Here, they can reduce NAD^+ to NADH, or O_2 to superoxide. The red arrows in complex I indicate the direction of electron transfer. Cyt c: Cytochrome c; FMN: flavin mononucleotide; SDH: succinate dehydrogenase. From Chouchani et al. (2016).

programmed cell death (apoptosis) upon reperfusion (Loor et al., 2011). Damaged mitochondria release damage-associated molecular pattern molecules (DAMPs) which trigger the inflammatory response, leading to longer-term damage to the organ (Arslan et al., 2011; Mills, O'Neill, 2014; Mills et al., 2017).

1.9.3 Succinate signaling in IRI

Succinate leaves the mitochondria by the DIC in exchange for cytosolic malate and enters the cytosol, where it can regulate the transcription factors hypoxia inducible factor 1 and 2 (HIF-1 and HIF-2) (Tannahill et al., 2013). HIFs are heterodimers of HIFα and HIFβ proteins. Under normoxic conditions prolyl hydroxylase (PHD) hydroxylates HIFα, which directs HIFα for degradation. Under ischaemic conditions succinate enters the cytosol and inhibits PHD, leading to stabilisation of HIF-1α (Tannahill et al., 2013; Tormos, Chandel, 2010). HIF-1α is then able to induce the cytokine IL-1β, involved in the inflammatory response (Mills, O'Neill, 2014; Mills et al., 2016; Tannahill et al., 2013). Thus, succinate can act as a pro-inflammatory signal.

Extracellular succinate binds and activates its G protein-coupled receptor GPR91 (He et al., 2004), renamed SUCNR1 after its ligand was discovered. This receptor is found in many tissues and cell types, including cardiomyocytes, hepatocytes and dendritic cells (Tretter et al., 2016). SUCNR1 stimulation caused IP_3 signalling and calcium mobilisation (Sundström et al., 2013), with transient phosphorylation of extracellular regulated kinase (ERK)1/2 (Tretter et al., 2016). Activation of SUCNR1 leads to hypertension by release of renin, involved in the renin-angiotensin system (He et al., 2004). The receptor provides another mechanism for succinate involvement in immunity, as its activation on dendritic cells triggers pro-inflammatory cytokines and T helper cell activation (Rubic et al., 2008).

An interesting avenue of future research in this area is to investigate what proportion of the accumulated succinate leaves the cell compared to what proportion is oxidised, where exactly the succinate signal goes to and any organ-specific responses.

1.9.4 Metabolite compartmentalisation in IRI

The above sections demonstrate that compartmentalisation of metabolism plays a role in the pathology of ischaemia. The small mitochondrial compartment allows succinate to increase to a certain concentration (yet to be exactly quantified) such that upon reperfusion the mitochondria produce the burst of ROS which causes much of the damage of IRI. The accumulated succinate is also important in the initiation of the immune response, causing inflammation that can persist for days after the initial injury and contributes to IRI (Arslan et al., 2011). The Δp that is necessary for RET to occur accumulates because the mitochondrial adenine nucleotide pools are depleted, meaning ATP synthase cannot function and the Δp is not consumed. The adenine nucleotide pools can not be regenerated by the action of the P_iC and APC.

1.10 Summary and Aims

Above, I have outlined the key ways in which mitochondria contribute to the general workings of the cell, in particular to metabolism. Mitochondria synthesise various important biomolecules, e.g. haem, and are involved in the production of fatty acids. They are important in various metabolic pathways, including the TCA cycle, amino acid metabolism, fatty acid oxidation and the urea cycle. Besides this, they also have other diverse roles in apoptosis and necrosis, Fe-S centre assembly, calcium storage and signalling. The recently reported phenomenon of mitochondrial signalling was introduced, whereby the mitochondria relay information to the rest of the cell. This signalling can be through ROS, which are mostly generated at complex I of the ETC (Murphy, 2009). The importance of compartmentalisation of metabolism was discussed, including how this enables mitochondria to perform their functions. The role of mitochondrial metabolism in IRI was discussed, which highlighted the gaps in our understanding of mitochondrial metabolism in this and other disease states. In order to understand further what is occurring in mitochondria during IRI (and other diseases) we need a robust method to isolate mitochondria rapidly and in such a way that the information obtained is accurate.

Aim 1. Fundamental to this project was the development of a method that could isolate mitochondria from mouse tissue rapidly and coolly enough such that the mitochondrial metabolites from the isolated mitochondria could be analysed by LC-MS. In **Chapter 3**, I

describe the approach taken to develop such a method. The chapter describes the optimisation of each step of a method, based on some aspects of various mitochondrial isolation methods, described in **Section 1.7**. The initial development of the method was performed in rat, before progressing to mouse tissue. In **Chapter 4**, I then describe the analysis of isolated mitochondria using this method, confirming that the method yields functional, coupled, pure mitochondria.

Aim 2. The second aim of this thesis was to employ the method to elucidate and understand the differences between cytosolic and mitochondrial metabolite pools in mouse heart and liver, under control conditions. In order to do so, an LC-MS approach had to be developed. In **Chapter 5**, I describe the development and rationale of the LC-MS approach used and some preliminary results. The use of metabolic and transport inhibitors to prevent metabolite distribution is explored. In **Chapter 6**, I present the LC-MS metabolomic data from control mouse heart and liver, examining the differences between the cytosolic and the mitochondrial compartments.

Aim 3. The third aim of this thesis was to use the results of the control cytosolic and mitochondrial pools described in **Chapter 6** to understand differences in the metabolic behaviours between these two compartments in disease conditions. Our lab is particularly interested in ischaemia-reperfusion injury (IRI) which occurs during heart attack, stroke and many surgical procedures such as organ transplant. **Chapter 6** outlines the results obtained from ischaemic mouse heart and liver, and explores how mitochondrial metabolism differs to the cytosol, and how this compares to normoxic metabolism.

Chapter 2

Materials and Methods

2.1 General materials and methods

2.1.1 Chemicals and consumables

All chemicals and consumables were obtained from Merck (previously Sigma-Aldrich), UK unless otherwise stated.

2.1.2 Animals

Rat tissue was harvested from female Wistar rats (Charles River Laboratories, UK) at 8-12 weeks of age. Mice tissue was harvested from female C57BL/6 mice (Charles River Laboratories, UK) at 6-8 weeks of age. Animals were kept on 12 h light/dark cycles in specific pathogen-free animal facilities with *ad libitum* access to food and water. Animals were culled within the same 3 h window of the day. All animal experiments were approved by the UK Home Office under the Animals (Scientific Procedures) Act 1986 and the University of Cambridge Animal Welfare Policy. For rapid mitochondrial extraction experiments, mice were culled by cervical dislocation. For glycogen assays mice were culled by exsanguination under anaesthesia by Jack L. Martin (see **Section 2.4.1.2**).

2.1.3 Quantitative and qualitative protein assays and reagents

2.1.3.1 Antibodies

Primary antibodies

All primary antibodies were monoclonal and were raised in either rabbit or mouse.

- ***rabbit-glyceraldehyde 3-phosphate dehydrogenase (GAPDH):*** (Sigma, G9545) 1:10,000
- ***mouse- pyruvate dehydrogenase (PDH):*** (Abcam, UK, ab110333) 1:1,000
- ***mouse-Ndufb8:*** (Abcam, UK, ab110242) 1:2,000
- ***mouse-Ndufs3:*** (Abcam, UK, ab14711) 1:2,000
- ***rabbit-inositol trisphosphate receptor (IP3R):*** (Cell Signaling Technology, USA, D53A5) 1:500
- ***mouse-GM130:*** (BD Biosciences, 610822) 1:500
- ***rabbit-lysosomal-associated membrane protein 1 (LAMP1):*** (Abcam, UK, ab24170) 1:1,000
- ***rabbit-peroxisomal biogenesis factor 14 (Pex14):*** (Proteintech, USA, 10594-1-AP) 1:750
- ***rabbit-Lamin B1:*** (Proteintech, USA, 12987-1-AP) 1:500

Secondary antibodies

All secondary antibodies were raised in goat and were specific for either rabbit or mouse IgG.

- ***IRDye® 680RD goat anti-mouse IgG (H+L):*** (LI-COR Biosciences: 926-68070) 1:10,000
- ***IRDye® 800CW goat anti-rabbit IgG (H+L):*** (LI-COR Biosciences: 926-32211) 1:20,000

2.1.3.2 Bicinchoninic acid (BCA) assay

Protein concentration of tissue fraction lysates and mitochondrial pellets were determined using a Pierce BCA Protein Assay Kit (ThermoScientific, UK) for use with 96-well microplates (Corning®, Costar®) and a microplate reader (SpectraMax® Plus 384 Microplate Reader, Molecular Devices, UK). Samples were measured against a 7-part Bovine Serum Albumin (BSA) standard curve (0 – 2 mg/mL). Samples and standard curve were diluted in appropriate buffer and measured in triplicate. Reagent A (1 % (w/v) BCA, 2% (w/v) Na_2CO_3, 0.16% (w/v) $Na_2C_4H_4O_6$, 0.4% (w/v) NaOH and 0.95% (w/v) $NaHCO_3$, pH 11.25) was mixed with reagent B (4% (w/v) $CuSO_4.5H_2O$) in a 50:1 ratio. 200 µL of reagent A:B mix was added to 10 µL of samples and standards and incubated at 37°C for 30 min. Absorbance was measured at 562 nm.

2.1.3.3 SDS-polyacrylamide gel electrophoresis (SDS-PAGE)

Lysates of isolation fractions were heated in an appropriate volume of 4X Laemmli sample buffer (125 mM Tris (pH 6.8), 4% (w/v) sodium dodecyl sulphate (SDS), 40% (v/v) glycerol, 25 mg/mL bromophenol blue and freshly added reducing agent (5% (v/v) β-Mercaptoethanol (BME)) for 5 min at 95°C. 10 µg protein was loaded per lane of mini-PROTEAN® TGX™ Precast 4-20% gradient gels (BIO-RAD). Proteins were electrophoresed at 100 V (until the loading dye ran off the gel) in running buffer (25 mM Tris (pH 8.3), 192 mM glycine, 0.1% (w/v) SDS). Precision Plus Protein Dual Color standards (BIO-RAD) or MagicMark™ XP Western Protein Standard (ThermoFisher) was loaded on all gels.

2.1.3.4 Western blotting

Electrophoresed proteins were transferred onto polyvinylidene difluoride (PVDF) membranes using either a wet or semi-dry transfer method. For wet transfer the proteins were transferred to Immobilon®-FL PVDF membranes (Merck Millipore: IPFL00010) for 1 h at 100 V, 4°C. The PVDF membranes were activated in methanol for 15 s before pre-equilibration of the membranes, gels, filter papers and fiber pads in pre-chilled transfer buffer (25 mM Tris, 192 mM glycine, 20% (v/v) methanol, pH 8.4 (unadjusted) at 4°C). For semi-dry transfer the membranes were transferred using Trans-Blot® Turbo™ Transfer packs (BIO-RAD: 1704157) at 2.5 A (constant), 25 V (max) for 7 min. Post-transfer, the membranes were

blocked for 1 hour at RT in Odyssey® Blocking Buffer (PBS) (LI-COR Biosciences: 927-40000) with gentle shaking (Bibby Stuart Platform Rocker STR6 at 30 revolutions/min (rpm)). The membranes were then incubated with primary antibodies overnight at 4°C in 4 % (v/v) blocking buffer in PBST (137 mM NaCl, 2.7 mM KCl, 10 mM Na_2HPO_4, 1.8 mM KH_2PO_4, 0.05 % (v/v) Tween-20). The membranes were incubated in secondary antibodies in 4 % (v/v) blocking buffer/PBST for 1 hour at RT with shaking, protected from light. Dilutions of primary and secondary antibody used were specific for the antibody (see **Section 2.1.3.1**). Excess primary and secondary antibodies were removed from the membrane by washing in PBST (4 buffer changes in 1 hour) with gentle shaking (30 rpm). Final washes were performed in the absence of Tween-20 (PBS only). The signal intensities of the target bands were measured as fluorescence emission at 680 nm or 800 nm (depending on the secondary antibody used) with the Odyssey® CLx Infrared Imaging System (LI-COR Biosciences). The signal intensities of target bands were normalised against control bands using Image Studio™ Lite software (LI-COR Biosciences).

2.1.3.5 Coomassie protein stain

Coomassie Brilliant Blue R-250 (BIO-RAD: 161-0436) was used to visualise protein separation on SDS-PAGE gels, according to the manufacturer's guidelines. Gels were scanned using an Epson perfection V750 Pro scanner.

2.2 Mitochondrial Isolations

2.2.1 Conventional isolation methods

2.2.1.1 Isolation of rat liver mitochondria

This procedure was adapted from work by Chappell, Hansford (1972). In preparation, all equipment was washed in deionised water and then STE buffer (250 mM sucrose, 5 mM Tris, 1 mM EGTA, pH 7.4) and kept at 4°C. After culling the rat by stunning and cervical dislocation the liver was removed and placed in ice-cold STE buffer. From this point onwards the whole experiment was performed on ice. The liver was rinsed in STE

to remove blood, and clots and connective tissue were removed. The liver was chopped and washed 3 times in fresh STE. Approximately 40 mL of STE was added and transferred to a 55 mL Potter-Elvehjem tissue grinder (Wheaton, USA). The liver was homogenised gently with 3 strokes of a loose-fitting PTFE pestle (Wheaton, USA) followed by 8 strokes of a tight-fitting PTFE pestle (Wheaton, USA). The homogenate was transferred to a 50 mL centrifuge tube. Unbroken cells were pelleted by centrifuging at 1,000 x g for 3 min at 4°C in a Sorval RC-5B centrifuge using the Sorval SS-34 rotor. The supernatant was transferred to a fresh centrifuge tube and centrifuged at 10,000 x g for 10 min at 4°C to pellet the mitochondria. The supernatant was discarded and a small amount of STE buffer added to resuspend the mitochondrial pellet using a glass rod, leaving the central pellet of blood behind. The mitochondria were transferred to a fresh centrifuge tube, topped up with fresh, cold STE and centrifuged at 10,000 x g for 10 min at 4°C. The final mitochondrial pellet was resuspended in 5 mL STE and transferred to a Falcon tube.

2.2.1.2 Isolation of rat heart mitochondria

This procedure was adapted from work by Tyler, Gonze (1967). Rat hearts with aortas removed were washed in ice cold STEB buffer (STE buffer with 0.1 % (w/v) fatty acid-free BSA) to remove atrial and ventricular blood. The tissue was chopped and rinsed thoroughly with STEB. The tissue was homogenised in a 55 mL Potter-Elvehjem tissue grinder (Wheaton, USA) in 40 mL STEB with 10 strokes of a loose-fitting PTFE pestle (Wheaton, USA) followed by 8 strokes of a tight-fitting PTFE pestle (Wheaton, USA). The homogenate was split between two 50 mL centrifuge tubes and centrifuged at 1,000 x g, 5 min at 4°C to pellet blood and cell debris. The supernatant was filtered through two layers of pre-wetted muslin into fresh 50 mL centrifuge tubes and centrifuged at 10,000 x g for 10 min at 4°C to pellet mitochondria. The supernatants were discarded and each mitochondrial pellet was resuspended in 20 mL STEB buffer, avoiding any pelleted blood. The resuspended mitochondria were combined and placed in a fresh 50 mL centrifuge tube and fully resuspended using 3 strokes of the loose-fitting PTFE pestle. This was centrifuged at 10,000 x g for 10 min at 4°C, supernatant was removed and pellet resuspended in fresh STEB an re-centrifuged. The resulting final mitochondrial pellet was resuspended in 400 µL STE buffer (no BSA) and kept on ice.

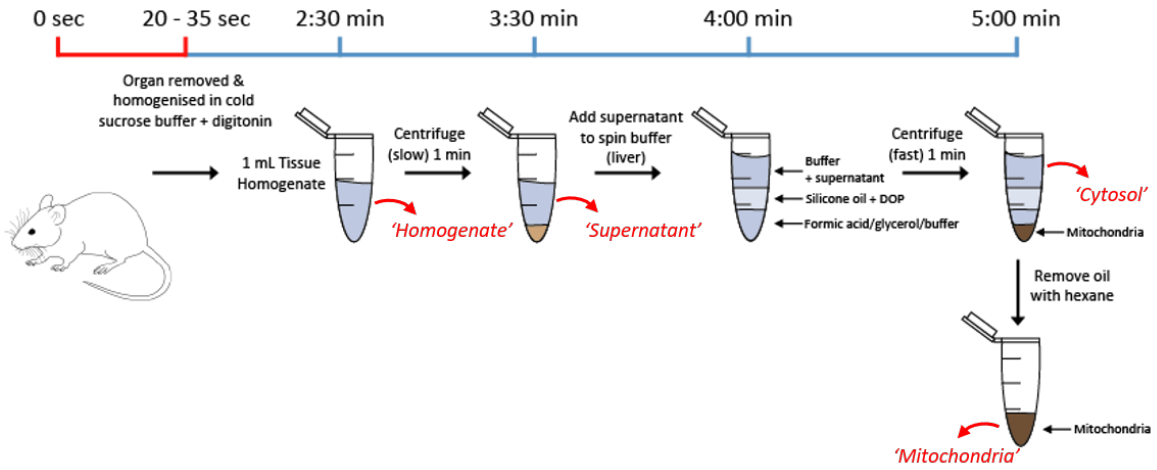

Fig. 2.1 Schematic of method to rapidly isolate mitochondria from mouse heart and liver. The main steps to isolate mitochondria are shown against an approximate timeline. The red line depicts the initial period of warm ischaemia before the organ is placed into cold buffer, and the blue line depicts steps performed at 4°C. The range of options for the lower layer are shown, highlighting the method can be used for LC-MS, protein analysis and enzymatic assays. The red arrows and text indicate when each fraction is obtained and the nomenclature of each fraction.

2.2.2 Rapid isolation of mitochondria from mouse tissue

2.2.2.1 Ischaemic mouse model for rapid extraction followed by LC-MS analysis

Liver and heart were rapidly extracted (20-35 secs) from female C57/Bl6 mice and placed into 2 mL Eppendorf tubes containing 500 µL phosphate buffered saline (PBS; 137 mM $NaCl_2$, 2.7 mM KCl, 10 mM Na_2HPO_4, 1.8 mM KH_2PO_4 (pH 7.4)) and a cut pipette tip (to suspend the tissue above the liquid), pre-warmed in a heat block at 37°C. Tubes were incubated at 37°C for 6, 12, and 30 min before organ was removed and mitochondria isolated according to the protocols described below.

2.2.2.2 Rapid isolation of mouse liver mitochondria

This protocol describes the final optimised method for isolating mitochondria from mouse liver, and the main steps, common to mouse liver and mouse heart, are depicted in **Figure 2.1**. All work involving dioctyl phthalate (DOP) must be performed in the fume cupboard. In preparation, all equipment was washed in deionised water and then in 200 mM sucrose STE buffer. All equipment and reagents were kept on ice until needed. Before culling the

animal, 4 separate 1.5 mL Eppendorf tubes were prepared by layering 300 µL Liver Oil Mix (60:40 silicone oil:dioctyl phthalate; density: 1.066 g/mL at RT), above 100 µL of either: 23 % glycerol (density: 1.0598 g/mL at RT; for WB), 25 % formic acid (density: 1.055 g/mL; for LC-MS) or heavy Seahorse assay buffer (HSAB, density: 1.049 g/mL; for Seahorse). These tubes were kept on ice in a metal heat-block until required. The liver was then rapidly extracted from a female C57/Bl6 mouse (within 30-35 secs of culling the animal) and placed into ice-cold 'Liver Homogenisation Buffer' (200 mM sucrose, 5 mM Tris, 1 mM EGTA, 100 µg/mL digitonin, pH 7.4; density: 1.0248 g/mL at RT) to remove excess blood. The whole liver was then placed in a 7 mL glass tissue grinder (Kimble Chase, UK, 885300-0007) containing 5 mL 'Liver Homogenisation Buffer' pre-cooled on ice to 4°C. From this point onwards the whole experiment was performed on ice. The tissue was homogenised by 3 strokes using pestle A (loose fitting) followed by 3 strokes of pestle B (tight fitting). A fraction of this homogenate was retained for analysis and termed "Homogenate". 1 mL aliquots of the homogenate were placed in 2 mL Eppendorf tubes and 4 of these tubes were centrifuged in parallel at 1,000 x g for 1 min at 4°C to pellet cell debris. A fraction of this supernatant was retained for analysis and termed "Supernatant". 4 aliquots of 200 µL of the resulting supernatant was mixed with ice-cold 500 µL 'Spin Buffer' (150 mM sucrose, 5 mM Tris, 1 mM EGTA, 25 mM ammonium bicarbonate, pH 7.4; density: 1.0200 g/mL at RT) to reduce the density of the suspension. 700 µL of each of these 4 aliquots were carefully layered above the oil in the 4 1.5 mL Eppendorf tubes that were prepared in advance. These were centrifuged for 1 min at 9,727 x g at 4°C in a swing out rotor (Heraeus, #75007592) fitted in a Heraeus Biofuge Primo R centrifuge (Thermo Scientific). The layer above the oil, termed the "Cytosolic" layer, and the majority of the oil were aspirated off and the tip of the tube was placed in a dry ice and ethanol bath. Once the lower layer had frozen solid, the remaining oil (which does not freeze solid) was washed off using dry ice-cold hexane. The 4 mitochondrial pellets were then pooled to obtain the final mitochondrial pellet.

2.2.2.3 Rapid isolation of mouse heart mitochondria

This protocol describes the final optimised method for isolating mitochondria from mouse heart, and the main steps that are common to the mouse heart and mouse liver protocol are depicted in **Figure 2.1**. All work involving DOP must be performed in the fume cupboard. In preparation, all equipment was washed in deionised water and then in 150 mM sucrose STE buffer. All equipment and reagents were kept on ice until needed. Before culling the

animal, 4 separate 1.5 mL Eppendorf tubes were prepared by layering 300 µL Heart Oil Mix (38:62 silicone oil:dioctyl phthalate; density: 1.0158 g/mL at RT), above 100 µL of either: 15 % glycerol (density: 1.0390 g/mL at RT; for WB), 15 % formic acid (density: 1.033 g/mL; for LC-MS) or heavy Seahorse assay buffer (HSAB, density: 1.049 g/mL; for Seahorse). These tubes were kept on ice in a metal heat-block until required. The heart was then rapidly extracted (within 20-25 secs of culling the animal) from a female C57/Bl6 mouse and placed into cold 'Heart Homogenisation Buffer' (25 mM sucrose, 5 mM Tris, 1 mM EGTA, 87.5 mM ammonium bicarbonate, 100 µg/mL digitonin, pH 7.4; density: 1.0075 g/mL at RT) to remove excess blood. The heart was rapidly chopped with scissors into a 7 mL glass tissue grinder (Kimble Chase, UK, 885300-0007) containing 3 mL 'Heart Homogenisation Buffer', pre-cooled on ice to 4°C. From this point onwards the whole experiment was performed on ice. The tissue was homogenised by 3 strokes using pestle A (loose fitting) and 3 strokes of pestle B (tight fitting). A fraction of this homogenate was retained for analysis and termed "Homogenate". 1 mL aliquots of the homogenate were placed in 2 mL Eppendorf tubes and 4 of these tubes were centrifuged in parallel at 1,000 x g for 1 min at 4°C to pellet cell debris. A fraction of this supernatant was retained for analysis and termed "Supernatant". 650 µL of this supernatant was carefully layered on to the Heart Oil Mix in the 4 1.5 mL Eppendorf tubes that were prepared in advance. These were centrifuged for 1 min at 9,727 x g at 4°C in a swing out rotor (Heraeus, #75007592) fitted in a Heraeus Biofuge Primo R centrifuge (Thermo Scientific). The layer above the oil, termed the "Cytosolic" layer, and the majority of the oil were aspirated off and the tip of the tube was placed in a dry ice and ethanol bath. Once the lower layer had frozen solid, the remaining oil (which does not freeze solid) was washed off using dry ice-cold hexane. The 4 mitochondrial pellets were then pooled to obtain the final mitochondrial pellet.

2.3 LC-MS

2.3.1 Preparation of samples

As soon as each fraction was obtained, 40 µL of homogenate, supernatant and top fractions were added to 400 µL of 25 % formic acid (liver samples) or 15 % formic acid (heart samples). After obtaining a mitochondrial pellet by centrifugation through oil into either 25% (liver) or 18% (heart) formic acid (see **Section 2.2.2**) the pellets were vortexed. All samples were

then centrifuged for 10 min at 17,000 x g. Supernatants of quadruplicate mitochondrial samples were pooled and dried under vacuum (miVac Quattro concentrator, Genevac) along with homogenate, supernatant and top fractions for 4 hours, with temperature capped at 40^oC. Dried samples were resuspended in 75 µL of H_2O, agitated for 10 min at 4°C to resuspend metabolites. A final centrifugation for 1 min at 17,000 x g, 4^oC was run to remove any remaining particulates. The supernatants were transferred to high recovery vials (9512S-3MP-RS or Low adsorption vials, 29659-U, Sigma) and stored at -80°C until LC-MS analysis.

2.3.2 Liquid Chromatography-Mass Spectrometry

LC-MS analyses were performed by Ana S. H. Costa, Efterpi Nikitopolou and Laura Tronci (MRC Cancer Unit, University of Cambridge, Hutchison/MRC Research Centre, University of Cambridge, UK) on a Q Exactive Orbitrap (Thermo Fisher Scientific) mass spectrometer coupled to an Ultimate 3000 RSLC system (Dionex). The liquid chromatography system was fitted with either a ZIC-HILIC column (150 mm × 4.6 mm) or a ZIC-pHILIC column (150 mm × 2.1 mm) (both described in further detail in **Section 5.1.1**) and respective guard columns (20 mm × 2.1 mm) (all Merck, Germany). The ZIC-HILIC column mobile phase was: 0.1 % formic acid in water (aqueous) and 0.1 % formic acid in acetonitrile (organic). The ZIC-pHILIC column mobile phase was: 20 mM ammonium carbonate + 0.1 % ammonium hydroxide (aqueous) and acetonitrile (organic). The mass spectrometer was operated in full MS and polarity switching mode. Samples were randomised in order to avoid bias due to machine drift and processed blindly. The acquired spectra were analysed using XCalibur Qual Browser and XCalibur Quan Browser software (Thermo Fisher Scientific) by referencing to an internal library of compounds.

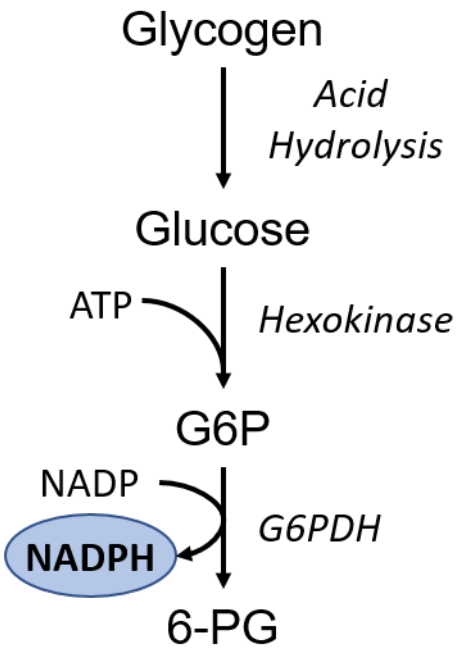

Fig. 2.2 Schematic of glycogen assay G6P: Glucose-6-phosphate; G6PDH: Glucose-6-phosphate dehydrogenase; 6PG: 6-Phosphogluconic acid.

2.4 Assays

2.4.1 Measuring glycogen in tissue samples

2.4.1.1 Background

The protocol was adapted from Zhang (2012), to be suitable for 96-well plate format. Glycogen is acid hydrolysed to glucose. As glycogen is not base hydrolysed, background glucose is measured by incubating the tissue in NaOH. Hexokinase phosphorylates glucose to glucose-6-phosphate (G6P). Glucose-6-phosphate dehydrogenase (G6PDH) oxidises G6P to 6-phosphogluconic acid (6PG), generating NADPH. The accumulation of NADPH is measured at 340 nm using a SpectraMax® Plus 384 Microplate Reader (see **Figure 2.2**).

2.4.1.2 Ischaemic mouse model for glycogen analysis

The following procedure was performed by Jack L. Martin. Female C57BL/6 mice were anaesthetised with isoflurane (Abbott Laboratories, US) and O_2 at 2 L/min. Heparin (100 µL bolus (25 iU); Leo Pharma A/S, Denmark) was administered intravenously into the inferior vena cava (IVC) 5 min prior to exsanguination by division of the IVC and aorta. Hearts were excised by division of the major vessels and the still-beating heart was rapidly frozen using Wollenberger clamps at liquid nitrogen temperature, taking <5 s to go from beating heart to frozen. For cold ischemia (CI), the heart was placed directly in PBS at 4°C. For warm ischaemia (WI), the excised heart was placed into 2 mL Eppendorf tubes containing 500 µL PBS and a cut pipette tip (to suspend the tissue above the liquid), pre-warmed in a heat block at 37°C. For analysis at various times, ∼20 mg sections were cut off the heart and clamped at liquid nitrogen temperature as above. Tissues were stored at -80°C until analysis.

2.4.1.3 Assay method

5-10 mg of frozen tissue was added to 1.5 mL Eppendorf tubes containing 250 µL of either 2 M NaOH or 2 M HCl (both pre-heated to 100°C) and minced with scissors. The weight of tissue added to each tube was recorded. The tubes were incubated at 100°C for 1 hour, with vigorous shaking every 10 min. After incubation the tubes were left to cool to RT and neutralised with 250 µL of 2 M HCl or 2 M NaOH and 500 µL of 400 mM TRIS, pH 7.4. The pH was adjusted to pH 7 using HCl or NaOH, and the volume added was recorded. The samples were vortexed and centrifuged at 17,000 x g for 10 min. Glucose standards (0, 0.01, 0.02, 0.04, 0.08 and 0.16 mg/mL glucose) were made up in H_2O by serial dilution. 60 µL standard and samples were added in duplicate to a 96-well plate. 200 µL Glucose Assay Reagent (G3293, Sigma) was added to each well, incubated at RT for 5 min and absorbance at 340 nm was measured. The average absorbance of each sample was interpolated using the standard curve and multiplied by the final volume after pH adjustment to give µg of glycogen (or glucose for NaOH control) in original sample. This was divided by the weight of tissue added and the NaOH control was subtracted from the HCl sample to give µg glycogen per mg of frozen tissue.

2.4.2 GSH Recycling Assay

2.4.2.1 Sample preparation

The GSH recycling assay was used to measure total GSH (**Figure 2.3**) (Griffith, 1980; Tietze, 1969). Mitochondrial samples were obtained by following **Section 2.2.2** with either 100 µL of 15 % (w/v) 5-sulfosalicylic acid (SSA; density: 1.07995 g/mL) or 15 % (heart) or 23 % (liver) glycerol as the bottom layer (glycerol was used when WB analysis was run in parallel). Isolated mitochondria from duplicate tubes were combined and pellets were resuspended. For 15 % SSA samples, 400 µL of H_2O was added to dilute SSA to 5 % (w/v). For glycerol samples, 40 µL of mitochondria were added to 40 µL of 10 % SSA to achieve a final concentration of 5 % SSA.

2.4.2.2 Assay method

10 µL of homogenate, supernatant and top fractions were placed in 90 µL of 5 % (w/v) SSA immediately and placed in dry ice while the mitochondrial fraction was obtained. Mitochondria, homogenate, supernatant and top fractions were vortexed to ensure maximal extraction of GSH and GSSG and then centrifuged at 16,000 x g for 10 min at 4°. 10 µL of supernatant was analysed in triplicate on a 96-well plate. A standard curve of 0, 5, 10, 25, 50 and 100 µM GSH was made in 5 % (w/v) SSA. Samples were incubated in 0.5 mM NADPH, 0.5 mM 5,5'-dithio-bis-[2-nitrobenzoic acid] (DTNB) and 4 U/mL glutathione reductase (GR) from bakers yeast in NaE buffer (143 mM sodium phosphate, 6.3 mM EDTA, pH 7.5). Production of 2-nitro-5-thiobenzoic acid (TNB) was followed by measuring absorbance at 412 nm using a 96-well plate spectrophotometer (Molecular Devices, USA) for 10 min at 25°C. Kinetic rates of samples were compared to standard curve to determine µM of GSH in the sample.

2.4.3 ATP/ADP Ratio Assay

This assay was performed by Anja V. Gruszczyk at the MRC Mitochondrial Biology Unit. ATP and ADP levels were measured by detecting luciferase/luciferin bioluminescence using an AutoLumat LB-953-Plus multi-tube luminometer (Berthold), fitted with an autoinjector,

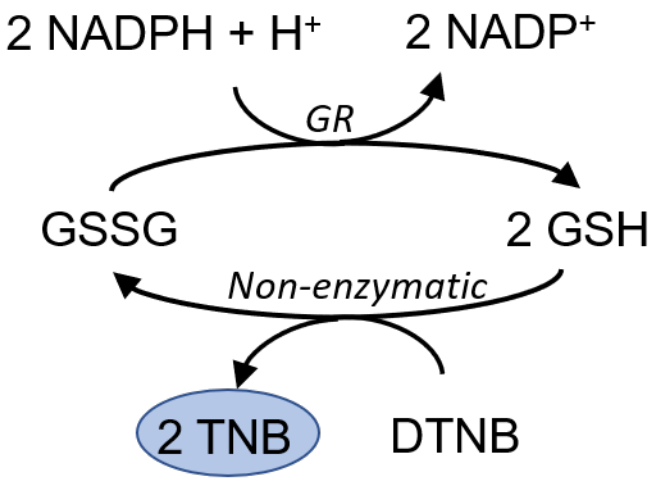

Fig. 2.3 Schematic of GSH recycling assay. GR: Glutathione reductase; DTNB: 5,5'-dithio-bis-[2-nitrobenzoic acid]; TNB: 2-nitro-5-thiobenzoic acid.

and quantified against standard curves of purified ATP and ADP. Mitochondrial fractions were spun into PCA ($HClO_4$ (4.2 % (v/v))) and pooled to a total volume of 400 µL. Cytosolic fractions were diluted 2:1 (133 µL: 266 µL) with PCA to a final concentration of 2% PCA. The mitochondrial and cytosolic fractions were pH neutralised with KOH immediately before use. For ATP measurements, 100 µL of sample was added to 400 µL Tris-acetate (TA) buffer (100 mM Tris, 2 mM Na_2EDTA, 50 mM $MgCl_2$, pH 7.75 with glacial acetic acid) in luminometer tubes. Luciferase/luciferin solution (DTT (7.5 mM), BSA (0.4 mg/mL), firefly luciferase (1.92 µg protein/mL), D-luciferin (120 µM)) was made up immediately prior to use, protected from light, and 100 µl was added to each sample tube via auto injection. Reactions were performed at 30°C and light emission (RLU) was recorded 30 s post injection. ADP was measured by first degrading endogenous ATP with 2X ATP sulfurylase solution, followed by incubation at 30°C for 30 min with agitation (500 rpm) before heat inactivation. 200 µL of each ATP sulfurylase-treated sample was added to 400 µL TA buffer in luminometer tubes (in duplicate). To convert endogenous ADP to ATP, 10 µl pyruvate kinase/ phospho(enoyl)pyruvate solution (type II PK from rabbit muscle (5 U), PEP (100 mM)) was added to one of the duplicate tubes (and to all ADP standards) and incubated at 30°C for 30 min prior to ATP measurement. The PK/PEP-blank tubes served as blanks for quantification. Quantification was performed with GraphPad Prism 7.0. ATP and ADP values (nmol/µL) were expressed as ATP/ADP ratios.

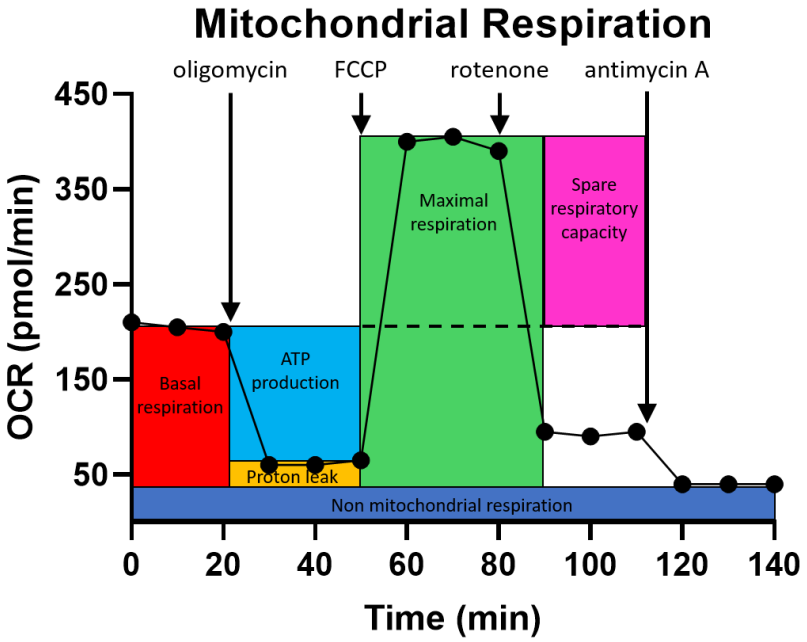

Fig. 2.4 A typical trace from a Seahorse XF96 Analyser depicting mitochondrial respiration. Basal respiration, ATP production, proton leak, maximal respiration and spare respiratory capacity can all be measured by the Seahorse XF96 Analyser.

2.5 Mitochondrial Respiration and Function Assays

2.5.1 Seahorse XF96 respirometry

2.5.1.1 Background

The Seahorse XF96 Analyser allows the real-time measurement of respiration in live cells. Respiration (measured as Oxygen Consumption Rate (OCR)) is measured by adding sequential injections of selective respiratory chain and F_1F_o-ATP synthase inhibitors to measure key parameters of respiration (see **Figure 2.4**). In this work, CII-driven respiration was measured by the use of the SDH substrate succinate. CI-mediated respiration was blocked by the addition of rotenone.

2.5.1.2 Buffers and reagents

- ***Seahorse Assay Buffer (SAB):*** sucrose (300 mM), mannitol (220 mM), KH_2PO_4 (10 mM), $MgCl_2$ (5 mM), HEPES (2 mM), EGTA (1 mM), 0.2 % (w/v) fatty acid-free BSA, pH 7.2, density 1.015 g/mL
- ***Heavy Seahorse Assay Buffer (HSAB):*** sucrose (700 mM), mannitol (220 mM), KH_2PO_4 (10 mM), $MgCl_2$ (5 mM), HEPES (2 mM), EGTA (1 mM), 0.2 % (w/v) fatty acid-free BSA, pH 7.2, density 1.049 g/mL
- ***Seahorse XF96 well culture plates (Agilent)***
- ***Seahorse XF96 sensor cartridges (Agilent)***
- ***Calibrant solution (Agilent)***
- ***Stock solutions:*** Rotenone (4 mg/mL), FCCP (10 mM), antimycin A (5 mM) (all made in EtOH)

2.5.1.3 Preparation of mitochondria

To measure respiration in isolated mitochondria instead of cells, the XF96 protocol was adapted using changes described in Iuso et al. (2017). Mitochondria were isolated from mouse and rat heart and liver using the rapid method outlined in **Section 2.2.2**. The lower layer was HSAB so that the buffer was dense enough (1.049 vs. 1.015 g/mL) to sit beneath the oil. After isolation the mitochondria were resuspended in SAB and protein content was quantified. Mitochondria were then diluted to 100 µg/mL in cold SAB supplemented with 4 µg/mL rotenone and 5 mM succinate. 2 µg of mitochondria was added to each well of the 96-well Seahorse plate, leaving the outside wells as blank. The plate was centrifuged for 20 min at 2,000 x g at 4°C to attach the mitochondria to the bottom of the plate. The wells were made up to 180 µL with pre-warmed SAB supplemented with rotenone and succinate.

2.5.1.4 Seahorse XF96 analyser preparation and running

The XF96 sensor cartridge was hydrated with 200 µL of Seahorse calibrant solution and incubated in a CO_2-free incubator at 37°C overnight. Port additions were added to the

cartridge at 10X final concentration (**Table 2.1**). The XF96 sensor cartridge was placed in the XF96 analyser and calibrated (∼30 min). Assays were performed at 37°C according to the manufacturer's guidelines: https://www.agilent.com/en/products/cell-analysis/how-to-run-an-assay.

Table 2.1 Seahorse XF96 port injections

Port	Compound	Conc. (10X)	Injection vol. (µL) (10% of well vol.)
A	FCCP	40 µM	20
B	Antimycin	30 µM	22

2.5.2 Oroboros Respirometry

2.5.2.1 Background

The respiration of isolated mitochondria was assessed by the Oroboros Oxygraph-2K (O2K) high resolution respirometer (Oroboros Instruments, Austria). The Oroboros is suitable for small amounts of a broad range of biological samples, such as isolated mitochondria, permeabilised tissues and intact cells. It measures dissolved oxygen (O_2) gas in an aqueous buffer solution. By following oxygen flux in the experimental chamber, respiration can be measured. The addition of specific respiratory inhibitors enables analysis of OXPHOS and whether respiration is coupled.

2.5.2.2 Oroboros preparation and running

Isolated mouse heart or rat liver mitochondria were measured whilst respiring with complex II-mediated respiration. Prior to isolation of mitochondria 2 mL of pre-warmed SAB buffer was added to the stirred (200 rpm), temperature-controlled (37°C) chambers and the top completely closed before opening to the height set by the Oroboros equilibration guide. The buffer within the chamber was left to equilibrate for approximately 2 hours. The Oroboros was calibrated to the stable oxygen concentration achieved.

Rat liver mitochondria (0.5 mg protein/mL) or mouse heart mitochondria were added in 2 mL of pre-warmed SAB buffer containing 4 µg/mL rotenone to a chamber of the O2K

respirometer. Respiration was assessed in the presence of succinate (1 mM). Uncoupled respiration was assessed by the addition of 1 µM FCCP.

All compounds were injected into the chamber using gastight syringes (Hamilton Robotics, UK), in a total volume of 2 µL.

2.5.3 Citrate Synthase Assay

The method was adapted from Srere (1969) to be suitable for a 96-well plate format. The assay reactions are shown in **Figure 2.5**. Briefly, oxaloacetate (OAA) and acetyl-CoA are converted to citrate and CoA by citrate synthase (CS). 5,5'-dithio-bis-[2-nitrobenzoic acid] (DTNB) is used to convert CoA to CoA-SS-TNB. Production of TNB is monitored at 412 nm. 80 µL assay buffer (100 µM DTNB, 300 µM AcCoA in KPi buffer (25 mM KH_2PO_4)) was added to each well. 8 µg of homogenate, supernatant or mitochondrial protein in 100 µL KPi buffer was added and the reaction was started by the addition of 20 µL of 500 µM OAA and mixed. Background activity was measured by replacing sample with KPi buffer. To correct for any endogenous substances that could provide the thiol necessary to split the DTNB a no-OAA control was also run. Absorbance at 412 nm was measured for 10 min at 30°C. ε_{412} = 13,600 $M^{-1}cm^{-1}$.

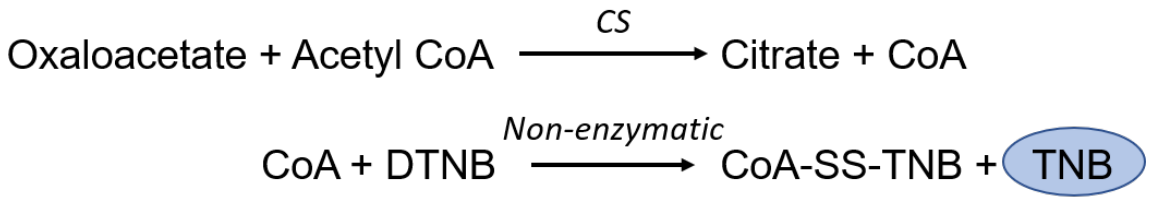

Fig. 2.5 Schematic of citrate synthase assay. Oxaloacetate and acetyl-CoA are converted to citrate and CoA by citrate synthase (CS). 5,5'-dithio-bis-[2-nitrobenzoic acid] (DTNB) is used to convert CoA to CoA-SS-TNB. Production of TNB is monitored at 412 nm.

2.6 Statistical Analysis

Data analysis was performed with GraphPad Prism 7.0. Results were expressed as mean ± standard error of the mean (SEM). Results of the control vs. 30 min WI experiment were analysed by two-way analysis of variance (ANOVA) and expressed as mean ± SEM.

P-values < 0.0032 were considered statistically significant. For heat maps, metabolites were normalised to taurine and the mean of 6 biological replicates was taken.

2.7 Collaborations

Collaborators were from the MRC Mitochondrial Biology Unit, University of Cambridge, UK, unless otherwise stated. Mouse surgery for tissue glycogen analysis was performed by Jack L. Martin (Department of Surgery and Cambridge NIHR Biomedical Research Centre, University of Cambridge, UK). Human heart retrievals were performed by Jack L. Martin and Kourosh Saeb-Parsy (Department of Surgery and Cambridge NIHR Biomedical Research Centre, University of Cambridge, UK), with assistance from Anja V. Gruszczyk and Timothy E. Beach (Department of Surgery and Cambridge NIHR Biomedical Research Centre, University of Cambridge, Cambridge, UK). Pig surgery for glycogen analysis was performed by Kourosh Saeb-Parsy, Timothy E. Beach, Jack L. Martin and Mazin Hamed (Department of Surgery and Cambridge NIHR Biomedical Research Centre, University of Cambridge, UK). LC-MS metabolomics and analysis was performed by Ana S. H. Costa, Efterpi Nikitopolou and Laura Tronci (at MRC Cancer Unit, University of Cambridge, Hutchison/MRC Research Centre, University of Cambridge, UK). Mice for rapid mitochondrial isolations were provided by Carlo Viscomi. Georgina Bates and Thomas Bright assisted with rapid mitochondrial isolations in mouse.

Chapter 3

Development of a rapid method for isolating mitochondria from tissue

3.1 Introduction

Metabolites are spread across the cell in different organelles, forming distinct pools. These pools can change independently of each other, which confounds metabolomic analysis, as this is often performed at the whole cell or tissue level. Cytosolic pools of metabolites can be larger than the mitochondrial pool, meaning the cytosolic pools can mask any changes that are occurring specifically in the mitochondria because the overall cellular pool size may not change. Also, if mitochondrial metabolite pools are bigger than the other pools they could over-represent the pool and lead to conclusions that the whole cell is changing its levels of that metabolite, whereas it is actually just the mitochondrial pool that is changing. This separation must be performed as quickly as possible to limit the effect of spontaneous and enzyme-catalysed metabolic reactions and their distribution throughout the cell. Therefore, a reliable method of separating mitochondria as quickly as possible from the rest of the cell is key to elucidating the metabolism of mitochondria.

Mitochondria form physical connections with the plasma membrane and other organelles, such as the ER (Lebiedzinska et al., 2009). It is thought that these interactions are important for facilitating transport of molecules, particularly phospholipids and other lipids needed for membrane structure (Szymański et al., 2017). These close interactions also enable

communication between the mitochondria and other organelles, helping to maintain calcium homeostasis and other important functions like apoptosis (Giorgi et al., 2009; Raturi, Simmen, 2013). These physical interactions are an important factor to consider when isolating mitochondria from tissue or cells, as the mitochondria must be purified away from the rest of the cell, as far as this is possible, to reduce contamination from other subcellular organelles. Contamination can confound metabolomic analysis as it would lead to erroneous conclusions that some metabolites are present in the mitochondria, and also dilutes the signal from truly mitochondrial metabolites. The strength of these interactions will vary with cell type.

A further consideration when isolating mitochondria from tissue is subpopulations of mitochondria in different regions of the same cell, which have distinct morphologies and different interactions with other organelles (Kuznetsov, Margreiter, 2009). These mitochondria can also have different biochemical properties, with varying membrane potential, volume and uncoupling responses (Saunders et al., 2013). It is thought that these mitochondrial subpopulations serve a physiological role. For example, muscle subsarcolemmal mitochondria were found to have a more oxidised state of mitochondrial flavoproteins than the intermyofibrillar mitochondria (Kuznetsov et al., 2006). This was hypothesised to be due to the subsarcolemmal mitochondria being nearer the periphery of the cell and thus exposed to a higher level of oxygen. This may even act as a protective barrier to decrease oxidative damage, maintaining a lower oxygen level in the rest of the cell. Importantly, subpopulations of mitochondria may also reflect a metabolic heterogeneity of mitochondria, caused by specific microenvironments or pools of metabolites. It is possible that subpopulations of mitochondria have different densities and behave differently during the extraction process, particularly centrifugation through oil. This may lead to only certain subpopulations of mitochondria being obtained and analysed in the final mitochondrial pellet.

Linked to the issue of density is the fact that some mitochondria within the tissue will be already damaged. This damage may be due to inherent "wear and tear" damage or due to factors the sample is exposed to, such as ischaemia or DNA mutations. Furthermore, the isolation process itself may damage the mitochondria (Picard et al., 2011). Mitochondrial damage may also impact what groups of mitochondria, and therefore what metabolites, are obtained in the final mitochondrial pellet. This idea is explored further in **Section 4.5**.

The method used to isolate mitochondria from tissue, or cells, is critical in determining the value of the information that can be obtained from studies of the isolated mitochondria. Metabolism requires the action of enzymes and metabolite transporters whose activity can be

limited by low temperature, but some activity persists even at temperatures below 4°C (Chen et al., 2017). The speed of the isolation is thus paramount to limit enzyme-mediated and spontaneous metabolic reactions and redistribution, so that a true picture of mitochondrial and whole cell metabolism as it exists in the organism can be obtained. There are two major challenges to isolating mitochondria from tissue so that they can be used for metabolomic analysis: the first is to purify the mitochondria away from other cellular components and the second is to quench metabolism and redistribution of metabolites. This is achieved by performing the isolation quickly and at a low temperature (4°C).

Section 1.7 of the Introduction described the various approaches to isolate mitochondria from tissue and cultured mammalian cells. The general architecture of most of these methods is based on various differential centrifugation steps, with or without the addition of digitonin. All isolation methods face the same two major challenges: achieving satisfactory fractionation (high as possible yields of enriched mitochondria, with no major contamination from other organelles) and completing the fractionation as quickly as possible to limit the effect of metabolic activity and redistribution of metabolites during the fractionation. In this section, the development of a method that encompasses all of these requirements is described. Components of previously published protocols were incorporated into the method, namely the use of differential centrifugation to remove cell debris, followed by centrifugation through a silicone oil layer into an acid layer. This acid serves to stabilise the mitochondrial metabolites, and renders them suitable for analysis by LC-MS.

All mitochondrial isolation buffers require pH buffering, osmotic support and metal ion buffering. In the case of STE buffer, the pH buffering is performed by 5 mM Tris. This pH buffer has a pKa of 8.1 at 25°C, and so is an effective buffer between pH 7 and pH 9 at room temperature. STE also contains 1 mM EGTA. This chelating agent binds metal ions and has a higher affinity for Ca^{2+} than Mg^{2+}. Sequestering these ions helps the mitochondria maintain their osmolarity, and also prevents the degradation of DNA and RNA by metal-dependent nucleases.

The osmotic balance between the cytosol and the mitochondria regulates mitochondrial matrix volume. Imbalances in the flux of ions, such as K^{+}, Ca^{2+} and Na^{+}, will lead to the movement of water between the two compartments, changing the matrix volume (Kaasik et al., 2006). In this way, mitochondria act as an osmometer (Devin et al., 1997), responding to changes in cell osmolarity. Mitochondrial matrix volume has affects on cellular metabolism: Halestrap (1989) showed that increased volume stimulated respiratory rate, pyruvate metabolism and

fatty acid oxidation. This must be considered when choosing mitochondrial isolation buffers. The external conditions should be kept such that they limit changes to mitochondrial volume, which affect metabolite levels. Many studies have shown that in hypoosmotic sucrose medium, the matrix volume and state 3 respiration increase in isolated mitochondria (Devin et al., 1997; Halestrap, 1989; Halestrap et al., 1990). Conversely, in hyperosmotic medium, the AAC is inhibited, leading to a decrease in OXPHOS (Devin et al., 1996). However, how these affect the isolation of the mitochondria and their metabolite pools is unclear.

The first step of isolating mitochondria from tissue is the homogenisation of the tissue. This is often performed by placing the tissue in a 1:10 w/v of tissue:buffer (Pallotti, Lenaz, 2001) and using a manual plunger to break up the tissue into a homogeneous mix in which the cells are ruptured. This step is important as a homogeneous mixture in which as much tissue as possible is broken up will maximise the yield of mitochondria. For softer tissues such as liver and kidney, this manual process is often sufficient, but for "tough", fibrous tissues, such as heart and skeletal muscle, mechanical disruption using a motorised homogeniser, such as an Ultra-Turrax disperser, is often used to further enhance tissue homogenisation. This helps to obtain a homogenous mix by breaking down the muscle fibres and connective tissue, whilst reducing the time and variability of the homogenisation step. In comparison, the brain is a soft, heterogeneous organ but poses a challenge due to its high lipid content, which make the tissue much less dense (**Table 3.8**). This means that the method of isolating brain mitochondria must be different to the methods for other organs. Wettmarshausen, Perocchi (2017) describes a method for isolating mitochondria from mouse brain using the same differential centrifugation approach as for kidney and liver, but the centrifugation steps are at a higher speed and for longer periods than for kidney and liver.

There are also additional challenges specific to metabolomic analysis of isolated mitochondria by LC-MS. Sucrose is added to many mitochondrial isolation buffers to maintain the osmolarity of the mitochondria, in concentrations upwards of 250 mM. It is also beneficial for differential centrifugation as changing its concentration can increase the density of the media with few side effects. However, sucrose cannot be used at such a high concentration for MS studies as it disrupts analysis, so in the development of this rapid method for LC-MS analysis, other components were required to be incorporated into the buffer to contribute to the osmotic support and to provide density.

3.2 Aim

The aim of this section was to develop a method of rapidly isolating mitochondria and cytosol from rat and mouse liver and heart so that LC-MS could be used to analyse their different metabolite pools. The overall goal was to understand the differences between mitochondrial and whole cell metabolism, with enhanced accuracy compared to established methods.

3.3 Strategy

To explore mitochondrial metabolism, the method of mitochondrial isolation must be performed in such a way that cell metabolism is quenched as rapidly as possible, preventing interconversion and distribution of metabolites throughout the cell. To do this, I aimed to cool and isolate the mitochondria as quickly as possible, to keep all components cold and to transfer the isolated mitochondria into an acid that would stop metabolic reactions and stabilise the metabolites for subsequent analysis. The strategy was to build on the previously used method of centrifuging small batches of tissue homogenate through silicone oil in an Eppendorf tube, as described in Burns, Murphy (1997); Siess, Wieland (1975); Smith et al. (1999); Tischler et al. (1977), as the short path length for centrifugation and small volumes allow the steps to be performed quicker than larger volumes of homogenate. The general set up from these methods was adopted, with 100 µL of acid forming the lowest layer in a 1.5 mL Eppendorf tube, beneath 300 µL of silicone oil. 700 µL of diluted tissue homogenate was then placed on top of the oil before centrifugation. Each step of this process (displayed in **Figure 3.1**) was systematically optimised for use with LC-MS. The strategy was to first

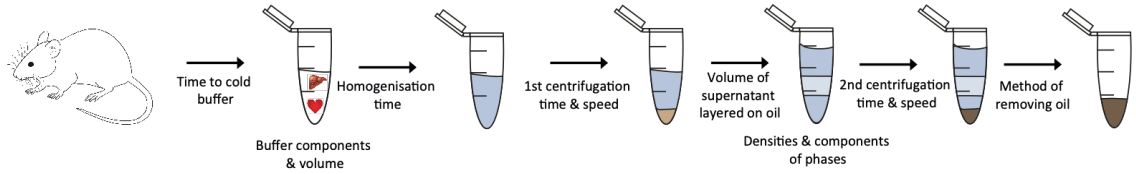

Fig. 3.1 Simplified schematic of rapid isolation method. Each step of the rapid isolation procedure is displayed. The text depicts the components that require optimising for tailoring the method for use with LC-MS analysis.

identify suitable components for the lower layer and for the buffer that the organs would be homogenised in, or transferred to, prior to centrifugation through oil. Acid was chosen as the

lower layer for metabolomic analysis so that when the mitochondria entered this layer they would burst and release their metabolites, which would then be stabilised by the acid. The main requirement of this acid layer was to be compatible with LC-MS and to have a density higher than the oil phase and close to 1.1 g/mL (the density of mitochondria). Identifying the correct homogenisation buffer to use was more complicated because it needed to maintain the osmolarity of the mitochondria, have a density less than the silicone oil layer to prevent inversion of the layers upon centrifugation, and be compatible with LC-MS. The buffer needed to be LC-MS compatible because although the mitochondria would end up in the acid layer, it was unknown how much of the buffer would be brought into the lower layer with the mitochondria. Also, it would be beneficial to be able to analyse cytosolic metabolism by analysing the whole homogenate, the supernatant of the whole homogenate (from the first centrifugation) and the "cytosolic" fraction (the layer left above the silicone oil after the second centrifugation step, see **Figure 3.1**), without further processing. Based on the acid and buffer densities the silicone oil layer was adapted to the correct density. Initial optimisation experiments were performed on rat liver, due to the large amount of tissue and mitochondria available. After the method was optimised in rat liver the conditions were applied to rat heart and then translated to mouse heart and liver, which required only minimal changes, highlighting the robustness of the method. The separation of mitochondria from cytosolic components was assessed by western blot and the function of mitochondria was assessed by various respiratory and enzymatic assays to establish whether any part of the extraction process was damaging to the mitochondria. For some optimisation experiments 3 µM tetramethylrhodamine, methyl ester (TMRM) was added to the mitochondria with 1 mM succinate before centrifugation through the oil. TMRM is a red dye that is taken up by active mitochondria, and so helped visualise the mitochondria.

3.4 Initial optimisation experiments in rat liver

The following experiments outline how each step of the isolation process (displayed in **Figure 3.1**) was optimised in rat liver for LC-MS metabolite analysis.

3.4.1 Acid phase

The first part of the extraction method explored was the choice of acid to form the lowest layer. Volatile ions should be used for MS, so the use of non-volatile ions and salts such as phosphate should be reduced. These leave a residue in the capillary and the mass spectrometer, which can reduce sensitivity and limit the function of the machine. 18 % perchloric acid (PCA), 20 % trichloroacetic acid (TClA) or 50 % formic acid (FA) were chosen due to being inert, compatible with LC-MS analysis and, at the concentrations listed in **Table 3.1**, their densities fit the criteria of being close to the density of mitochondria (1.1 g/mL) (Rickwood, Birnie, 1978). Perchloric acid was a potential candidate because when it is neutralised with KOH it forms the precipitate potassium perchlorate ($KClO_4$). This can be easily removed by centrifugation, leaving the metabolites in solution, which can then be analysed by a number of techniques. However, the KOH and PCA must be carefully balanced to avoid KOH or PCA remaining in solution. This is achieved by addition of a pH buffer, such as MOPS. TClA is an acid commonly used in LC-MS for protein removal by precipitation and has been found to increase retention times and MS signals of polar metabolites (Cheng et al., 2010; Huang et al., 2018). Formic acid was chosen because it is a weak acid that does not cause ion suppression in MS.

	Acid		
	18% PCA	**20% TClA**	**50% FA**
Density (g/mL)	1.166	1.126	1.11

Table 3.1 Densities of initial acids trialled. The initial acids tested were 18% PCA, 20% TClA and 50% FA. The concentrations were chosen based on their densities. Densities listed were calculated at RT (20-24°C) by weighing 1 mL of each acid. PCA: perchloric acid; TClA: trichloroacetic acid; FA: formic acid.

3.4.2 Homogenisation buffer

The next step was to look at the buffer the tissue would be homogenised in. The standard STE buffer used for mitochondrial isolations contains 250 mM sucrose. This level of sucrose is incompatible with LC-MS analysis because it is "sticky", meaning it can form particulates which can block the LC columns and lead to high back pressures, which can damage the machine. It can also form background peaks, which can interfere with the visualisation of

	Buffer			
	AB (50 mM)	**HEPES (50 mM)**	**KCl***	**STE****
Density (g/mL)	1.066	1.011	1.023	1.032

Table 3.2 Densities of initial buffers trialled. The initial buffers tested were 50 mM ammonium bicarbonate (AB), 50 mM HEPES, KCl and STE. The concentrations were chosen based on their densities and the molarity. Densities listed were calculated at RT (20-24°C) by weighing 1 mL of each buffer. Densities listed were calculated at RT (20-24°C). *KCl: 120 mM KCl, 10 mM HEPES, 1 mM EGTA; **STE: 250 mM sucrose, 5 mM Tris, 1 mM EGTA.

other metabolite peaks. As it was unknown how much of the homogenisation buffer would come through the oil layer with the mitochondria, a new buffer was sought. This buffer must have no (or low) sucrose but must maintain the osmolarity of the mitochondria, be compatible with LC-MS and be less dense than the acid layer to prevent inversion. 50 mM ammonium bicarbonate (AB) buffer and 50 mM HEPES buffer were chosen as they were estimated to match this criteria (densities listed in **Table 3.2**).

3.4.3 Silicone oil

Previous work by Burns, Murphy (1997) and Smith et al. (1999) used an oil with density 1.07 g/mL (Dow Corning 550) for the middle oil phase. The Poly(methylphenylsiloxane) oil (MPS) (Sigma 378496, viscosity 450-550 cSt) had a density similar to this (1.102 g/mL at RT) and was available. This was trialled for initial experiments as its density was compatible for the acids and buffers used in **Tables 3.1 and 3.2**.

3.4.4 Interaction between phases

The interaction between the acid layer, silicone oil and the homogenisation buffer was then tested at RT. 100 µL of each acid was placed in the bottom of a 1.5 mL Eppendorf tube, being careful not to let any acid touch the sides of the tube as this could allow a path for the layers to mix, leading to inversion. 300 µL of MPS silicone oil was placed carefully on top of the acid. 700 µL of each buffer (supplemented with 40 µM Phenol Red) was placed carefully on top. Phenol Red was added to help identify whether there was any mixing between the buffer layer and the oil or acid layer. The tube was centrifuged in a swing rotor centrifuge (Heraeus Biofuge Primo R with swing out rotor Heraeus, #7592) at

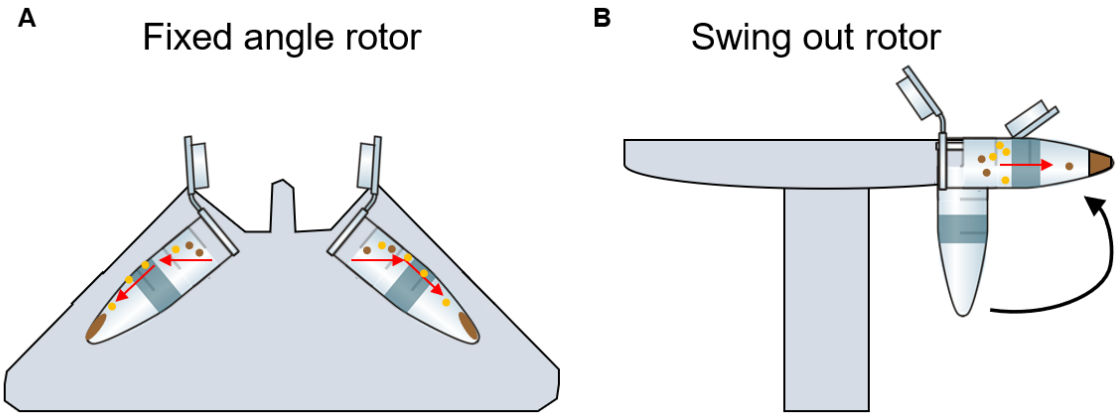

Fig. 3.2 Schematic of direction of force in angled and swing out rotors. A) In a fixed angle rotor the direction of force causes cytosolic contaminants (orange circles) to hit the side of the tube and then slide through the oil into the lower layer down the side of the tube, contaminating the mitochondrial pellet (brown circles). **B)** In a swing out rotor the direction of force is horizontal, meaning that the only path to the lower layer is directly through the oil. This means that cytosolic contaminants are trapped in the top phase and only mitochondria can enter the lower layer.

9,727 x g (10,000 min^{-1}) for 1 min. A swing rotor centrifuge must be used because the direction of the force is vertically down the tube, as opposed to angled (**Figure 3.2**). If the direction of force is angled then non-mitochondrial components from the cytosolic layer may hit the wall of the tube and begin to slide down the wall into the phases below, thus contaminating the final mitochondrial pellet. This can also lead to inversion of the layers due to inconsistent densities spread across a cross-section of the tube. A standard angled rotor centrifuge consistently resulted in inversion of the layers. The pH of the cytosolic fraction was measured (in triplicate) after centrifugation following 0, 5 and 10 min of resting to determine whether any seepage would occur between the layers. The pH of the cytosolic fraction remained stable after centrifugation (AB: pH 7.5, HEPES: pH 7) for all acids used over 10 min. This demonstrated that there is no leakage between the layers.

3.4.5 Addition of homogenate and mitochondria

After determining that the layers did not acidify, rat liver mitochondria (RLM) were added to identify if mitochondria are able to pass through the oil layer. Mitochondria were isolated in KCl buffer (120 mM KCl, 10 mM HEPES, 1 mM EGTA) as it was hypothesised this could maintain the osmolarity of the mitochondria for the entire duration of the prep, whilst also being compatible with LC-MS. 100 µg (11.1 µL) or 1 mg (111 µL) of mitochondrial protein

was made up to 700 µL with KCl buffer, layered on top of 300 µL of oil above 100 µL of each acid (18% PCA, 20% TClA and 50% FA) and centrifuged in a swing rotor centrifuge at 9,727 x g for 1 min. A layer of brown sediment was seen at the buffer:oil interface but it was difficult to determine if the mitochondria had entered the acid phase. To determine whether mitochondria would be visible in the acid phase, 100 µg of mitochondrial protein was layered directly onto 100 µL of acid and centrifuged. A pellet was seen in the acid layer, showing that a mitochondrial pellet would indeed be visible if the mitochondria were able to pass through the oil.

After these experiments, it was unclear what was the cause of the failure to obtain a mitochondrial pellet after centrifugation through oil. It could have been because the KCl buffer that the mitochondria were isolated in was not able to maintain the osmolarity of the mitochondria. To establish whether a mitochondrial pellet could be obtained at all in the silicone oil system, for the following preliminary experiments the mitochondria were isolated in the standard STE buffer and then diluted into KCl buffer.

3.4.6 Further silicone oil phase optimisation

As initial attempts to get mitochondria to pass through the a single component oil phase were unsuccessful, dioctyl phthalate (DOP) (density 0.985 g/mL at RT) was added to the silicone oil. This was based on previous work by Scarlett et al. (1996) who mixed DOP with the silicone oil in a ratio of 58:42 (v/v) silicone oil:DOP. They added the acid and oil mix to the tubes and centrifuged briefly to ensure separation of the layers. After centrifugation, the tubes were left on ice until the sample was ready. This technique was adopted into the method. Smith et al. (1999) also used silicone oil mixed with DOP to purify isolated mitochondria but in a ratio of 66:34 and Burns, Murphy (1997) used a ratio of 70:30 to purify hepatocytes.

To investigate whether the addition of DOP to the silicone oil phase would facilitate the movement of mitochondria into the lower phase, a ratio of 60:40 MPS:DOP was used initially, due to its density of 1.052 g/mL at RT. It was thought that this would be dense enough to form distinct layers but not too dense that the movement of mitochondria through the oil is inhibited. Mitochondria were isolated from mouse liver in STE using the standard method of isolation (isolation performed by Lee Booty) and the mitochondrial pellet was diluted in KCl buffer (120 mM KCl, 50 mM HEPES, pH 7.4) to 15 mg mitochondrial protein/mL. Various stages of the fractionation were layered on the mix of 60:40 MPS:DOP and centrifuged, to

assess the procedure. The experimental procedure and the results are displayed in **Table 3.3** and explained below.

100 µL of the supernatant of homogenate was layered on 300 µL 60:40 MPS:DOP (density: 1.055 g/mL) above 100 µL 18% PCA and centrifuged. This resulted in a layer of beige protein forming on top of the oil phase, possibly because there was too much protein. To reduce the amount of protein 1 mg of mouse liver mitochondria (MLM) (66 µL in 700 µL of KCl buffer) was added to 2 tubes with 60:40 MPS:DOP and centrifuged. Some mitochondria were seen in the oil layer. It was hypothesised that the interface between the top phase and the oil phase may have been blocking the passage of mitochondrial protein through the oil into the acid. To investigate this further 250 µg (16.5 µL) of mitochondrial protein was added directly into the oil layer of 60:40 MPS:DOP above 100 µL 18 % perchloric acid. Before centrifugation the mitochondria formed a sphere in the middle of the oil layer but after centrifugation at 16,250 x g the mitochondria were sat above the oil layer in the buffer. This showed that the oil phase was too dense for the mitochondria to pass through. Therefore, it was decided to make the oil layer less dense. The density of mitochondria is $\sim$1.1 g/cm^3 (Rickwood, Birnie, 1978), so the lower density Poly(dimethylsiloxane-co-methyl-phenyl siloxane) oil (DSMPS) (Sigma 378488, viscosity: 125 cSt) was chosen due to its density of 1.066 g/mL at RT, compared to 1.102 g/mL for MPS. When used to make up the 60:40 oil:DOP mix, DSMPS lowered the density of the mix to 1.034 g/mL from 1.052 g/mL. To ascertain whether lowering the density to this value was sufficient to obtain a mitochondrial pellet, 16.5 µL of homogenate of supernatant (250 µg protein) was added onto this oil layer and centrifuged. A protein pellet was seen at the bottom of the acid layer and a beige sphere was seen suspended in the oil layer, which was hypothesised to be mitochondrial protein. This was repeated except the 16.5 µL of supernatant was made up to 700 µL with KCl buffer and the same result was seen. The results of these experiments are displayed in **Table 3.3**.

Oil mix	Oil mix density at RT (g/mL)	Addition	Result	Implication
60:40 MPS:DOP	1.052	100 µL of supernatant of homogenate	Layer of beige protein formed on top of oil	Too much protein, blocked access
60:40 MPS:DOP	1.052	1 mg of MLM (66 µL in 700 µL of KCl buffer)	Mitochondria in oil phase	Oil too dense or too much mitochondria
60:40 MOS:DOP	1.052	250 µg of MLM (16.5 µL directly into oil phase)	Mitochondria moved from middle to top of oil	Oil too dense
60:40 DSMPS:DOP	1.034	16.5 µL of supernatant of homogenate (directly into oil phase)	Pellet in acid layer, sphere in oil	Mitochondria able to separate from cytosol and pass through oil, some trapped
60:40 DSMPS:DOP	1.034	16.5 µL of supernatant of homogenate (in 700 µL of KCl buffer)	Pellet in acid layer, sphere in oil	Mitochondria able to separate from cytosol and pass through oil, some trapped

Table 3.3 Oil optimisation experiments. A mouse liver of weight ∼1.5 g was homogenised in STE buffer and mitochondria were isolated via the standard method. At each stage a fraction was reserved for layering on a mix of silicone oil:DOP. The final mitochondrial pellet was diluted in KCl buffer (120 mM KCl, 50 mM HEPES, pH 7.4) to 15 mg/mL. The reserved crude tissue homogenate was centrifuged for 1.5 min at 1,000 x g to generate the supernatant of homogenate. 100 µL of this supernatant of homogenate (made up to 700 µL with KCl buffer) or 1 mg mouse liver mitochondria (MLM) (66 µL, made up to 700 µL with KCl buffer) were layered on 300 µL of 60:40 MPS:DOP above 100 µL of 18 % perchloric acid (PCA) and centrifuged at 9,727 x g for 1 min. No pellet was obtained in either condition, so the amount of protein was reduced by loading 250 µg of MLM (16.5 µL) undiluted onto the oil. No pellet was seen so the density of the oil:DOP layer was changed by replacing MPS with DSMPS, a lower density silicone oil. A pellet was seen in the acid layer when 16.5 µL of supernatant of homogenate was layered directly onto the oil and when it was made up to 700 µL with KCl buffer. RT: 20-24°C. MPS: Poly(methylphenylsiloxane) oil; DSMPS: Poly(dimethylsiloxane-co-methyl-phenyl siloxane) oil; DOP: dioctyl phthalate; MLM: mouse liver mitochondria.

Based on these experiments it can be concluded that DOP is beneficial and necessary for the mitochondria to pass through the oil, although the reason for this is unclear. It can also be seen how sensitive the system is to the density of the oil phase: the difference of only 0.018 g/mL between 60:40 MPS:DOP and 60:40 DSMPS:DOP allowed the mitochondria to enter the acid phase.

The beige spheres often seen floating in or just above the oil layer were a concern as this means they are the same density of the oil, and therefore slight fluctuations in the preparation of the oil could cause them to enter the acid layer and contaminate it. What they contain was not investigated at this stage but they may contain broken mitochondria and/or microsomes. Investigations into the contents of the interface are described in **Section 3.4.9**.

3.4.7 Inversion of layers

Using silicone oil to isolate mitochondria, both with and without the addition of DOP, has been attempted in several iterations in this lab (Burns, Murphy, 1997; Smith et al., 1999). Despite different conditions being trialled there were often variable results: many attempts resulted in inversion of the layers upon centrifugation or did not generate a mitochondrial pellet. I also encountered these issues, and it occurred when using the same batches of reagents that had previously not inverted and had resulted in mitochondrial pellets. It was found that when reagents were weighed out and their densities were checked after mixing, the density changed after being left for even short periods of time (5-10 min). It was hypothesized that the phases were inverting because the heavier components of each mix sink to the bottom of the layer over time. Therefore, if the tubes are made up too far in advance there will be a density gradient within each layer (see **Figure 3.3**). This would also explain why sometimes no mitochondria were able to pass through the oil, as the bottom of the oil layer was too close in density to the mitochondria. This is in contradiction to Scarlett et al. (1996) who leave their tubes (on ice) for some time before the experiment. To help prevent inversion the reagents were made up in bulk to reduce any impact of minor errors in weighing out the oil, DOP, and homogenisation buffer components. To investigate this hypothesis, all reagents were thoroughly mixed before use and layered in the Eppendorf tubes less than 5 min prior to use. This prevented inversion occurring. This showed that the success of this technique is heavily dependent on the components being mixed well and that the density of the layers must be correctly balanced. Speed and cold temperature are necessary for metabolomic

studies, but were also shown to have important effects on the density of the oil and acid phases.

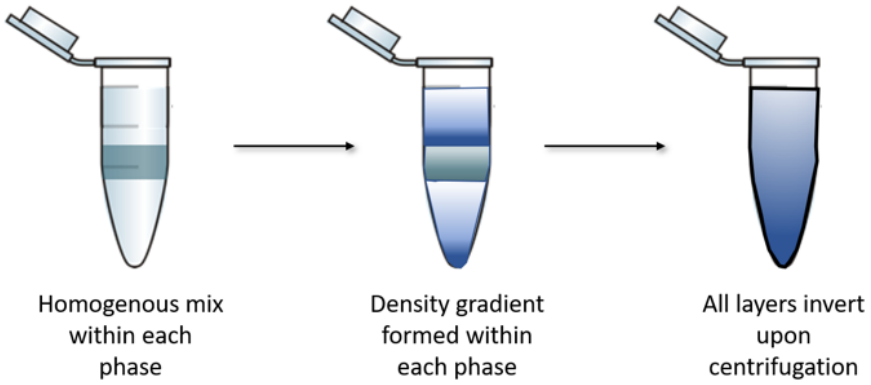

Fig. 3.3 Density gradients form within each phase over time. Schematic of how density gradients formed within each phase cause inversion upon centrifugation.

3.4.8 Further homogenisation buffer optimisation

3.4.8.1 STE vs. KCl buffer

In the experiments described in **Table 3.3**, mitochondria were isolated in standard STE buffer and diluted in KCl buffer (120 mM KCl, 50 mM HEPES, pH 7.4). Subsequent attempts to repeat the experiment using mitochondria isolated wholly in KCl buffer were unsuccessful, with no mitochondrial pellets obtained. The lack of a pellet suggests that the KCl buffer used was not able to sustain the osmolarity of the mitochondria for the duration of the isolation process. Imbalances in osmolarity cause the mitochondria to swell and change density, which could be what is preventing them passing through the oil. The ability to use KCl as a homogenisation buffer would be beneficial due to its compatibility with LC-MS analysis. Therefore, 2 different KCl buffers were trialled and compared to the standard STE buffer. One of the KCl buffers was the same used in the method of Corcelli et al. (2010) (described in more detail in **Section 1.7.1**), who were able to isolate coupled mitochondria using this buffer. The buffer from Corcelli was used to directly compare how their buffer behaved in my system, and KME2 was devised to have a lower KCl concentration and a higher buffering capacity (50 mM MOPS compared to 5 mM). It was hypothesised that these three buffers may be better able to buffer and sustain the osmolarity of the mitochondria compared to the

initial KCl buffer used (120 mM KCl, 50 mM HEPES, pH 7.4). The buffer components are listed below:

- ***KME1:*** 180 mM KCl, 5 mM MOPS, 1 mM EGTA, 0.1 % BSA, pH 7.25 (from Corcelli et al. (2010))
- ***KME2:*** 100 mM KCl, 50 mM MOPS, 0.5 mM EGTA, 0.1 % BSA, pH 7.4
- ***STE:*** 250 mM sucrose, 5 mM Tris, 1 mM EGTA, pH 7.4

A rat liver was homogenised in STE using the conventional method (**Section 2.2.1.1**), except the supernatant from the first fast centrifugation (at 10,000 x g) was split into 3 centrifuge tubes (containing ∼10 mL each) and each was run in parallel to generate 3 separate mitochondrial pellets. These were resuspended in 5 mL of either KME1, KME2 or STE buffer (for detailed protocol see **Table 3.4**). These mitochondria were then centrifuged through oil. The general procedure was 300 µL oil (DSMPS:DOP 60:40 (1.034 g/mL at RT) or 65:35 (1.013 g/mL at RT)) was placed on 100 µL 18 % perchloric acid and left on ice until required as described in Scarlett et al. (1996). After addition of either the supernatant, isolated mitochondria or the white layer containing broken mitochondria, the tubes were centrifuged at 9,727 x g for 1 min at 4°C. The results of these experiments are displayed in **Table 3.4**. Experiments 1-3 show that only when STE buffer was used were mitochondria able to pass through the oil. The KCl buffers may have failed to do this due to altered mitochondrial density due to swelling. It was hypothesised that too much mitochondrial protein was added, but this was determined to not be the problem, because a trial with reduced mitochondrial protein (1 mg and 0.5 mg) also had no pellet in the acid for KME buffers but consistently showed pellets in the acid layer for STE samples.

Experiment 4 investigated whether broken mitochondria and microsomes pass through the oil. A fraction of the white layer which forms above the supernatant of the final 10,000 x g centrifugation of a standard mitochondrial isolation, and is known to contain broken mitochondria and microsomes, was collected. This was placed above the oil and centrifuged to see where these fragments would migrate to in the prep. No pellet was obtained, which is encouraging as it indicates that the oil phase will block broken mitochondria and endosomes from entering the acid. Further investigations into damaged mitochondria are described in **Section 4.5**.

Experiment 5 shows that the system is capable of separating mitochondria from homogenate, as a pellet was obtained when 70 µL of supernatant of homogenate (made up to 700 µL in STE) was layered on the oil mix.

Experiment	Top Layer	Buffer	Observations
1	1.5 mg MLM	STE	A pellet was seen in the acid for both oil mixes, but was larger for 60:40. A small pellet was suspended in the oil.
2	1.5 mg MLM	KME1	Nothing visible in oil or acid for either oil mix
3	1.5 mg MLM	KME2	Nothing visible in oil or acid for either oil mix
4	700 µL of white layer (broken mitochondria)	STE	Nothing visible in oil or acid for either oil mix
5	70 µL of supernatant of homogenate (made up to 700 µL in STE buffer)	STE	Both oil mixes had a pellet in acid layer, some beige droplets seen in oil

Table 3.4 Results of buffer trial experiments. A standard mitochondrial isolation from rat liver was performed in STE buffer (**Section 2.2.1.1**), with the following modifications. The supernatant from the first fast centrifugation (at 10,000 x g) was split into 3 tubes and each was run in parallel to generate 3 separate mitochondrial pellets. After being split into 3 each tube was centrifuged at 10,000 x g for 10 min before being resuspended in 5 mL of either KME1, KME2 or STE buffer. The protein concentration of each pellet was assessed by BCA: KME1: 27 mg/mL, KME2: 27 mg/mL, STE: 17.7 mg/mL. Isolated mitochondria, supernatant or the white layer containing broken mitochondria, was then layered on pre-prepared tubes. These had 300 µL oil mix (DSMPS:DOP 60:40 (1.0336 g/mL at RT) or 65:35 (1.01335 g/mL at RT)) layered above 100 µL of 18 % perchloric acid, and were centrifuged at 9,727 x g for 30 sec and left on ice until required. After addition of the top layer the tubes were centrifuged at 9,727 x g for 1 min at 4°C. **Experiments 1-3:** 1.5 mg of mitochondrial protein (KME1 and KME2: 55.5 µL, STE: 84.7 µL) was made up to 700 µL in each buffer and centrifuged for 1 min at 9,727 x g through 300 µL of either 60:40 or 65:35 DSMPS:DOP. A mitochondrial pellet was obtained from the tubes containing mitochondria isolated in STE, from both oils, but no mitochondrial pellets were obtained from mitochondria isolated in either KME1 or KME2 buffers. **Experiment 4:** 700 µL of the white layer (obtained from supernatant of the final 10,000 x g centrifugation step of the STE mitochondria) was centrifuged through 60:40 and 65:35 DSMPS:DOP. No pellet was seen in the oil or acid using either oil mix. **Experiment 5:** 70 µL of supernatant of homogenate (made up to 700 µL with STE) was layered on 60:40 and 65:35 DSMPS:DOP. A pellet was seen in the acid layer after centrifugation through both oil mixes. KME1: 100 mM KCl, 50 mM MOPS, 0.5 mM EGTA, 0.1 % BSA, pH 7.4; KME2: 180 mM KCl, 5 mM MOPS, 1 mM EGTA, 0.1 % BSA, pH 7.25; STE: 250 mM sucrose, 5 mM Tris, 1 mM EGTA, pH 7.4. MLM: Mouse liver mitochondria. DSMPS: Poly(dimethylsiloxane-co-methyl-phenyl siloxane) oil; DOP: dioctyl phthalate.

3.4.8.2 Addition of digitonin to homogenisation buffer

An opportunity for further optimisation during initial experiments was that pellets obtained from centrifuging the supernatant of homogenate through oil were not purely mitochondrial. They may have contained peroxisomes, which have a density of $\sim$1.2 g/mL and so may sediment with mitochondria (Wilcke et al., 1995). Microsomes, 100-300 nm vesicles composed of ER and plasma membrane formed artefactually during cell homogenisation, may also co-migrate due to their similar density to mitochondria (within the range of 1.1-1.25 g/mL, Norseth et al. (1982)). However, due to their smaller size (100-300 nm vs. 0.5-10 µM for mitochondria), the microsomes should take longer to move down during centrifugation. Therefore, the time of centrifugation should be optimised such that it is long enough for the mitochondria to enter the acid phase but short enough to limit microsomes contaminating the mitochondrial pellet. To further reduce the risk of contamination from microsomes and other organelles, digitonin was added.

Digitonin is a non-ionic detergent which causes membrane permeabilisation by binding to membrane cholesterol and forming permanent pores. It has been proposed that it functions by binding to cholesterol in the inner leaflet of membranes and moving as a bound complex to the outer leaflet (Frenkel et al., 2014). This can cause changes to the membrane curvature, thus forming pores of 8-10 nm (Olofsson et al., 2009) which allow the passage of metabolites and ions across the membrane. At high enough concentrations the addition of digitonin can cause complete lysis of cholesterol-rich membranes. Because digitonin requires cholesterol to act (Sudji et al., 2015), it can be exploited experimentally to selectively lyse cholesterol-rich membranes. The MIM contains negligible levels of cholesterol (Colbeau et al., 1971), compared to the PM, microsomes (18.4%; (Cheng, Kimura, 1983)) and ER membranes (3-6 % of total lipid (Ridsdale et al., 2006)). The MOM contains more cholesterol than the MIM (8.3% vs. 2.8%; Cheng, Kimura (1983)), but due to the short time frame that the supernatant is exposed to digitonin, it is likely that the digitonin will mainly affect the PM. Digitonin also aids the homogenisation process: by breaking the PM membrane the mitochondria are more easily released from the cytosol. Therefore, it was hypothesised that by optimising the amount of digitonin added microsomes and other organelles could be selectively removed, whilst keeping the mitochondria intact. The digitonin was sourced from Sigma which cites a 73.5% purity (based on TLC area %).

To investigate if digitonin could be beneficial in rapidly isolating mitochondria from rat liver, 200 µg/mL of digitonin was added to the homogenisation buffer, along with TMRM

and succinate for visualisation of the mitochondria. The addition of digitonin resulted in a compact pellet in the lower layer, shown in **Figure 3.4B**, compared to no pellet when digitonin was not added (**Figure 3.4A**). Therefore, digitonin was necessary to consistently obtain mitochondrial pellets.

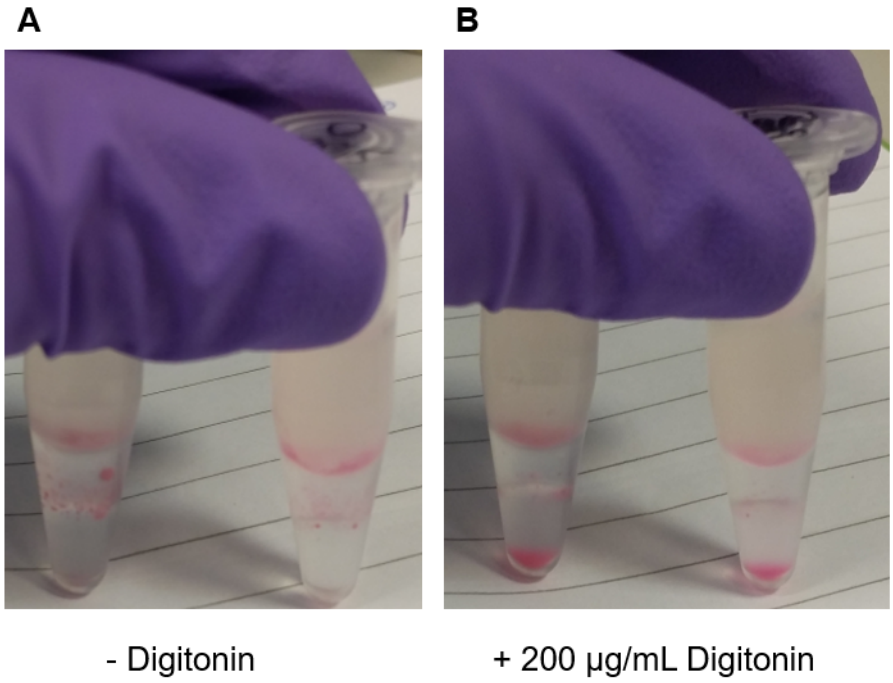

Fig. 3.4 Addition of Digitonin ***A)*** - Digitonin. ***B)*** + 200 µg/mL Digitonin. A rat liver was homogenised in 40 mL STE as described in Section 2.2.1.1. 1 mL aliquots were centrifuged at 1,000 x g for 1.5 min. 2 mg of homogenate protein (41 µL) was added to a tube containing 3 µM TMRM and 1 mM succinate in STE buffer ± 200 µg/mL digitonin, to a total volume of 700 µL. Upon addition of digitonin the tubes were incubated at RT for 5 min, shaking gently. This suspension was then layered on 300 µL of 60:40 DSMPS:DOP above 100 µL 23 % glycerol. The tubes were centrifuged at 9,727 x g for 1 min.

After this preliminary experiment, a range of digitonin concentrations in rat liver were trialled to determine if there was an optimum digitonin concentration to use. The protein composition of the pellets obtained from 0, 20, 50, 100, 200, 400 and 800 µg/ml digitonin was assessed by WB. The extent of mitochondrial enrichment and cytosolic contaminants appeared the same across all concentrations of digitonin. Therefore, 100 µg/mL digitonin was chosen for subsequent experiments, as it is in the mid-range of the concentrations tested. This meant that slight fluctuations in the weight of tissue homogenised would not lead to artefactual variability due to digitonin levels, increasing the robustness of the method. 100

µg/mL digitonin is also equivalent to values cited in the literature: James et al. (1996) found 30 µg digitonin/mg protein to permeabilise the PM of fibroblasts without damaging the mitochondria. In my system, 2 mg of protein was added to the 700 µL loaded on top of the oil. For the 100 µg/mL digitonin sample, this equates to 35 µg digitonin/mg protein.

3.4.8.3 Addition of ammonium bicarbonate to homogenisation buffer

The high sucrose concentration in STE buffer makes it incompatible with LC-MS. However, as the sucrose concentration is diluted during the process of the isolation, this may improve the compatibility. A calculation of the maximal possible amount of sucrose that could enter the acid phase with the mitochondria was performed. This is the maximal possible value because whilst passing through the oil a large proportion of the extracellular volume is likely to be lost. If 1.5 mg of enriched mitochondrial protein in 200 mM sucrose STE is pelleted by centrifugation then there is approximately 1.5 µL matrix and 1.5 µL extracellular space, based on the frequently used approximate values of 1 µL of matrix and extracellular space volumes per mg protein (Woelders et al., 1985). If all of these mitochondria pass through the oil into 100 µL acid with the same amount of sucrose then the sucrose concentration would be 3-4 mM. It was then decided to trial lower sucrose concentration STE buffers as the buffer for the top layer, termed the "spin buffer" that the supernatant of homogenate is diluted into. The Tris and EGTA concentrations were kept constant at 5 mM and 1 mM, respectively. The sucrose was substituted with ammonium bicarbonate (AB) to maintain the osmotic support that is lost with reduced sucrose concentrations, and to maintain the molarity at 200 mM. AB was chosen as it is volatile and is often a component of the mobile phase for MS. STE buffers with increasing concentrations of sucrose and decreasing concentrations of AB were trialled for isolating mitochondria from rat liver. The buffer components and photographs of the tubes after centrifugation through oil are shown in **Figure 3.5A**. Buffer 6 was the only buffer to produce a large mitochondrial pellet upon centrifugation through oil. Although the protein content of this pellet was unknown, it can be assumed to contain a sizeable amount of mitochondrial protein due to the bright pink TMRM staining. To investigate the protein composition of the pellets, the lower layers and the cytosolic fractions of each buffer were analysed by WB (**Figure 3.5B and D**). This showed Buffer 6 to generate pellets with maximal enrichment of mitochondrial protein, with no detectable cytosolic contamination. Combined, these results clearly showed Buffer 6 (150 mM sucrose STE + 25 mM AB) to be the best buffer.

A

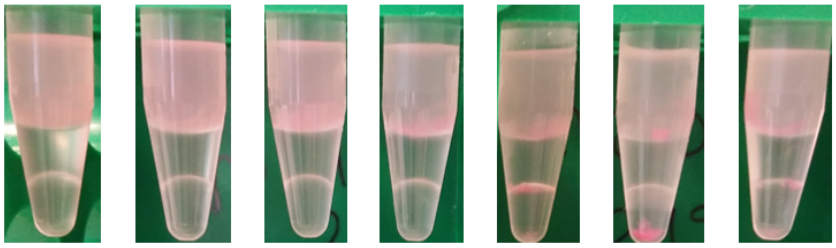

Buffer	1	2	3	4	5	6	7
[Sucrose] (mM)	0	25	50	75	100	150	200
[AB] (mM)	120	87.5	75	62.5	50	25	0

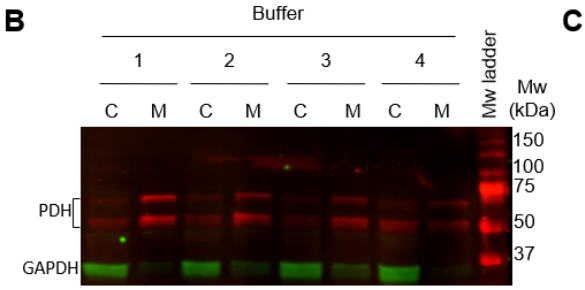

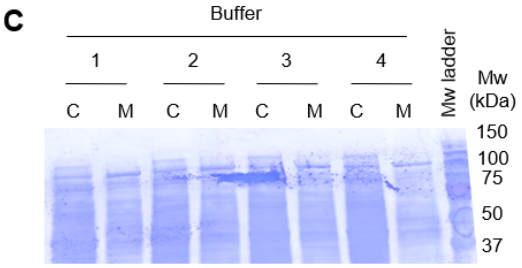

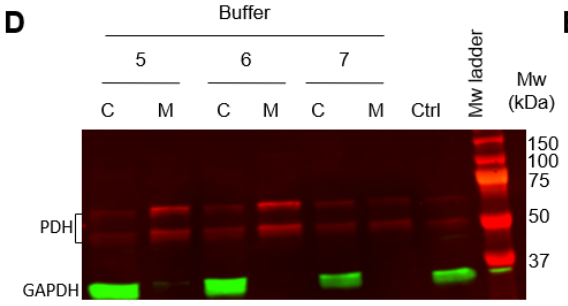

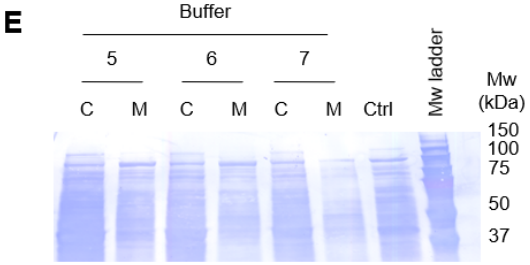

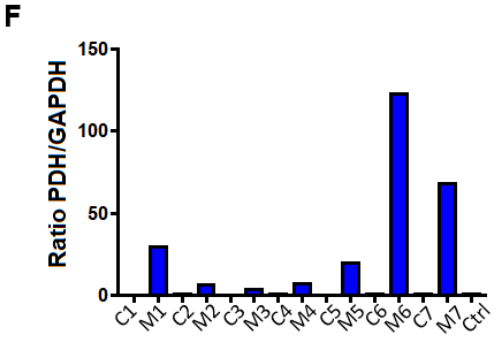

Fig. 3.5 Investigating sucrose:AB ratio in homogenisation buffer for rat liver. A rat liver was homogenised in STE buffer and 1 mL portions of the homogenate were centrifuged at 1,000 x g for 1 min. The supernatants were combined and the protein concentration was assessed by BCA as 32.2 mg/mL. 2 mg (62 µL) of this supernatant was added to tubes containing 140 µL of digitonin to a final concentration of 100 µg/mL and STE/AB buffer 1-7 (described in table) to a total volume of 700 µL. Upon addition of digitonin, 3 µM TMRM and 1 mM succinate the tubes were incubated at RT for 2 min, shaking gently. All 700 µL of this suspension was layered on 300 µL 60:40 DSMPS:DOP above 100 µL 23 % glycerol. This was centrifuged at 9,727 x g for 1 min. 100 µL of the cytosolic fraction from each tube was removed and lysed with 75 µL lysis buffer. The oil mix and the majority of the glycerol was removed before the mitochondrial pellet was lysed with 50 µL NP40 lysis buffer (10 min on ice followed by 10 min centrifugation at max speed). Protein was quantified in all samples before dilution to 10 µg in 40 µL lysis buffer and Laemmli loading buffer + 5 % BME. ***A)*** Photographs of tubes after final centrifugation, with sucrose and AB concentrations displayed in corresponding column in table underneath. Western blots. ***B and D)*** Western blots. 10 µg of protein was loaded per lane. Marker: Protein Plus Dual Color standard. Mitochondrial marker: PDH (red bands, 54 + 69 kDa), cytosolic marker: GAPDH (green band, 37 kDa). Mitochondrial Control: RLM isolated by conventional method. Homogenate Control: supernatant of homogenate of rat liver from a conventional isolation. C: Cytosolic fraction, M: Mitochondrial fraction. ***C and E)*** Coomassie stains of membranes. ***F)*** Ratio of PDH/GAPDH band intensities.

3.4.8.4 LC-MS sucrose trial

To determine whether the use of these sucrose concentrations was compatible with LC-MS analysis, a preliminary LC-MS analysis was run. Rat liver mitochondria were isolated in 250 mM sucrose STE with 100 µg/mL of digitonin, and the pellets were diluted in either Buffer 4 (75 mM sucrose STE + 62.5 mM AB) , Buffer 5 (100 mM sucrose STE + 50 mM AB) or Buffer 6 (150 mM sucrose STE + 25 mM AB) before centrifugation through oil into 25 % formic acid. 75 µL of the formic acid layer was removed and analysed by LC-MS. **Figure 3.6** shows the LC-MS signal was not dependent on the amount of sucrose and AB. This confirms it is not necessary to remove all of the sucrose from the STE buffer. The first graph suggests that sucrose is present at mM levels but does not interfere with the analysis of other metabolites. 150 mM STE + 25 mM AB gave the most consistent results, and 75mM STE + 62.5 mM AB the least successful. This is beneficial for the extraction as a higher amount of sucrose will maintain the osmolarity of the mitochondria. This prevents them from swelling or bursting, changing their density and preventing them passing through the oil to be captured in the acid phase.

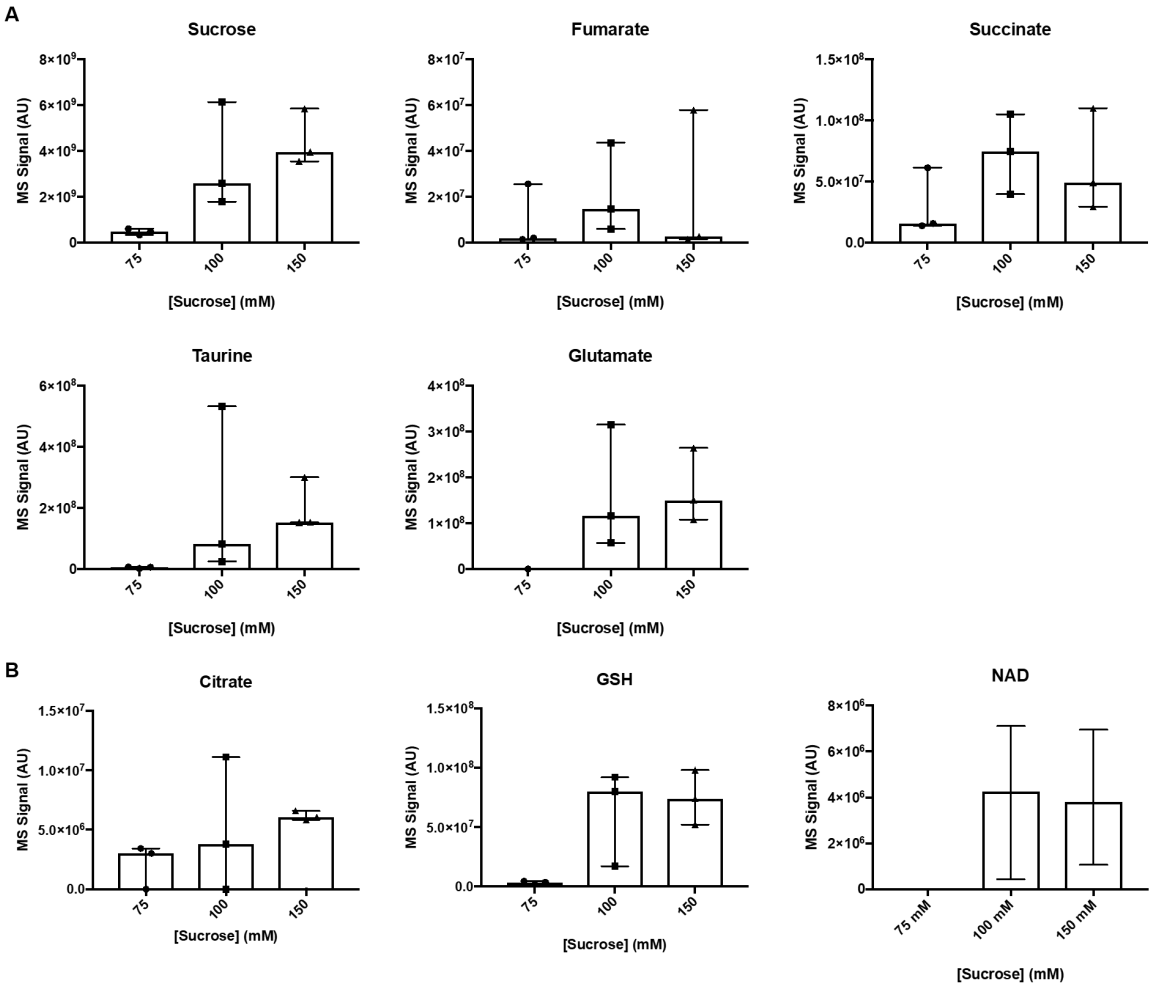

Fig. 3.6 Preliminary LC-MS analysis of rat liver mitochondrial pellets diluted in 75, 100 and 150 mM sucrose STE buffer before centrifugation through oil. ***A)*** MS signal (AU) from metabolites analysed on ZIC-HILIC column. ***B)*** MS signal (AU) from metabolites analysed on ZIC-pHILIC column. A rat liver was homogenised in STE in the presence of 100 µg/mL of digitonin. 2 mg of homogenate was added to either 150 mM sucrose STE + 25 mM AB, 100 mM sucrose STE + 50 mM AB or 75mM STE + 62.5 mM AB and centrifuged through 60:40 DSMPS:DOP on top of 100 µL of 25 % formic acid. n=3 biological replicates, data is mean ±SEM.

3.4.9 Interface protein

To determine whether mitochondria or other material become stuck at the interface between the oil and the top phase, thus reducing the overall yield, the protein at this interface was removed and analysed by WB to determine its composition. A rat liver was processed as described in **Figure 3.5** and after centrifugation through oil the protein left at the interface was stained pink with TMRM, suggesting it contained mitochondrial protein (**Figure 3.7**). WB analysis was performed as a secondary method of protein identification. This showed that a mixture of mitochondrial and cytosolic protein is present at the interface (**Figure 3.8**). This suggests that the method does not yield 100 % of the mitochondria from the homogenate. Another possibility is that the mitochondrial protein seen at the interface is from broken mitochondria, an idea discussed further in **Section 4.5**. The photographs of the tubes stained with TMRM and centrifuged through oil (**Figure 3.7**) show the amount of protein at the interface is greatly reduced with Buffer 6, as is the cytosolic contamination (**Figure 3.8**). More protein is seen at the interface in lower sucrose concentration buffers (**Figure 3.7**). This could be due to mitochondrial swelling preventing them passing through the oil. It is possible that there is simply too much homogenate added and the entire surface of the oil is covered with protein that will not pass through the oil, blocking the passage of intact mitochondria. However, this is unlikely as there is a pellet seen when using Buffer 6 with the same amount of protein. Therefore, I conclude Buffers 1-5 cause mitochondrial swelling and limit their passage through the oil.

3.4.10 Effect of exogenous succinate on isolation of mitochondria

The maintenance of mitochondrial volume is an energy-dependent process, in which Na^+ and K^+ are exchanged for H^+. Healthy, energised mitochondria are more compact than damaged, uncoupled mitochondria. Therefore, it could be that the succinate added in conjunction with the TMRM in order to aid visualisation of the mitochondrial pellets was changing the shape and/or density of the mitochondria. Furthermore, in physiological conditions exogenous succinate will not be present. It is possible that in the absence of succinate the mitochondria do not pass through the oil. To test this hypothesis, the extraction was trialled in rat liver $\pm$succinate and $\pm$TMRM to ascertain whether the mitochondria still pass through the oil. Photographs of the mitochondrial pellets after centrifugation through oil are shown in **Figure 3.9**. Protein analysis by WB was also run to look at whether the level of mitochondrial

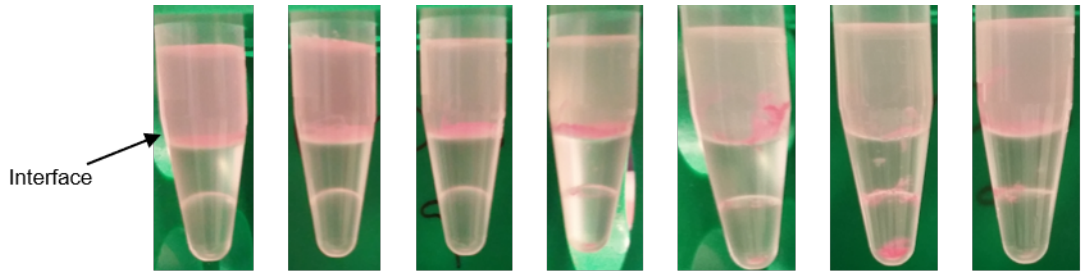

Buffer	1	2	3	4	5	6	7
[Sucrose] (mM)	0	25	50	75	100	150	200
[AB] (mM)	120	87.5	75	62.5	50	25	0

Fig. 3.7 Analysis of protein at buffer:oil interface in rat liver mitochondrial isolations. A rat liver was processed as described in Figure 3.5. The protein concentration of the supernatant of homogenate was 40.3 mg/mL, and 2 mg (49.6 µL) of protein was used. Photographs are displayed of tubes after centrifugation through oil, with sucrose and AB concentrations depicted in corresponding column in the table underneath. The location of the protein that was removed from the buffer:oil interface is depicted by the arrow. 1 mM succinate and 3 µM TMRM were added for visualisation of mitochondria.

protein in the pellets was changed ± succinate and ± TMRM. These results are displayed in **Figure 3.10** and show that the absence of added succinate (or TMRM) does not impact on the mitochondria passing through the oil, as the level of enrichment of mitochondrial protein is the same in the presence or absence of succinate.

3.4.11 General optimisation of the procedure

3.4.11.1 Centrifugation steps

The first centrifugation step at 1,000 x g to remove cell debris was trialled at 30 sec, 1 min and 1.5 min. The 1.5 min centrifugation step did not result in a significantly larger cell debris pellet, whereas 30 sec generated a very small pellet, so 1 min was decided as the optimum time for this step. Also, performing 2 spins before the final centrifugation through oil was trialled, to mimic the conventional method of mitochondrial isolation and to reduce cytosolic contamination (as it was hypothesised that more cell debris would be removed). The first spin was at 1,000 x g for 1 min, followed by centrifuging this supernatant at 2,500 x g for

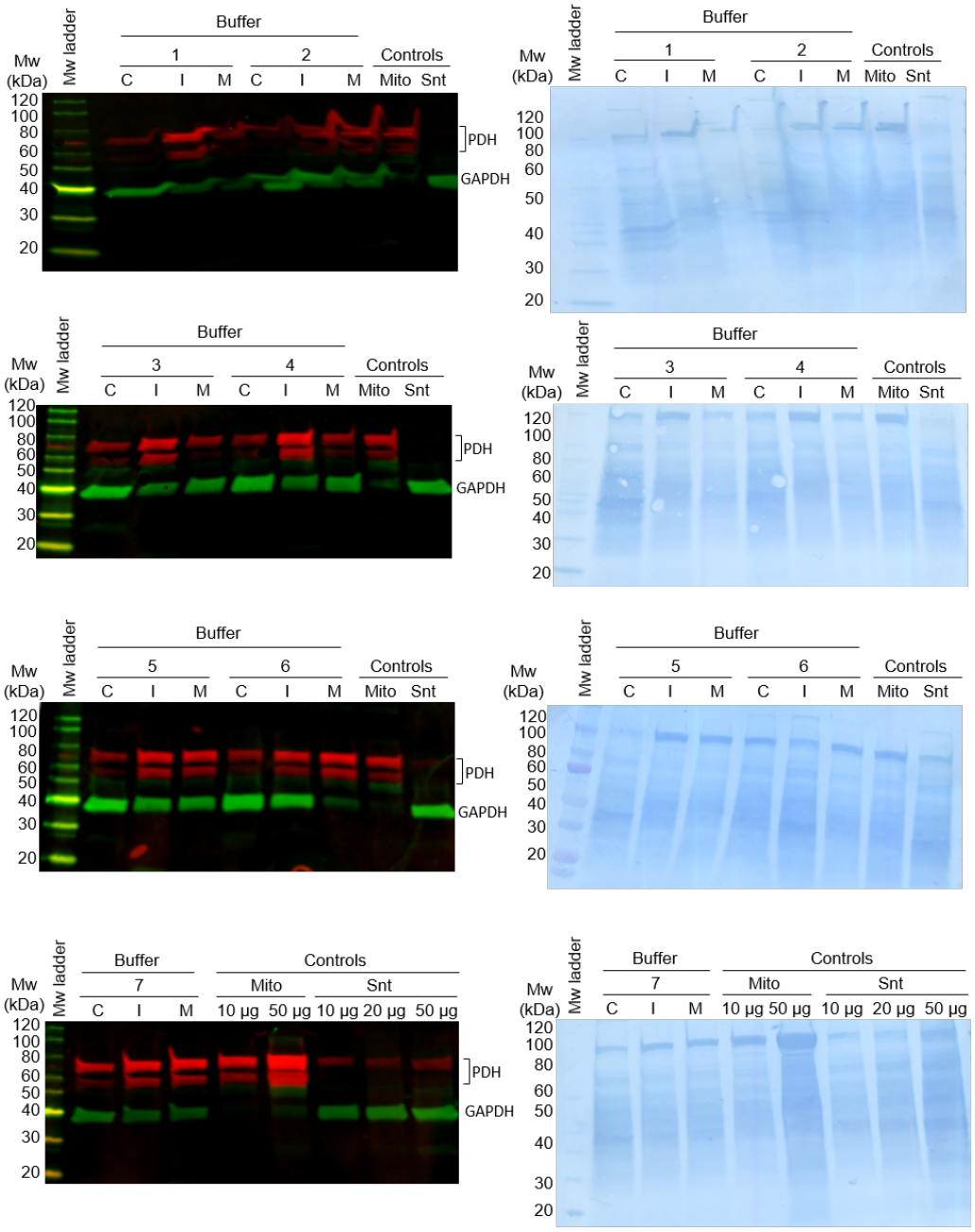

Fig. 3.8 Analysis of protein at buffer:oil interface in rat liver isolations by WB. The samples from Figure 3.7 were processed for WB analysis as described in Figure 3.5. Components of buffers 1-7 are described in Figure 3.7. ***Left)*** Western blots. Mitochondrial marker: PDH (red bands, 54 and 69 kDa), cytosolic marker: GAPDH (green band, 37 kDa). C: Cytosolic fraction; I: interface fraction; M: Mitochondrial fraction. Mito control: RLM isolated by conventional method; Snt control: supernatant of rat liver homogenate isolated by conventional method. Marker: Protein Plus Dual Color standard. ***Right)*** Coomassie stains of membranes.

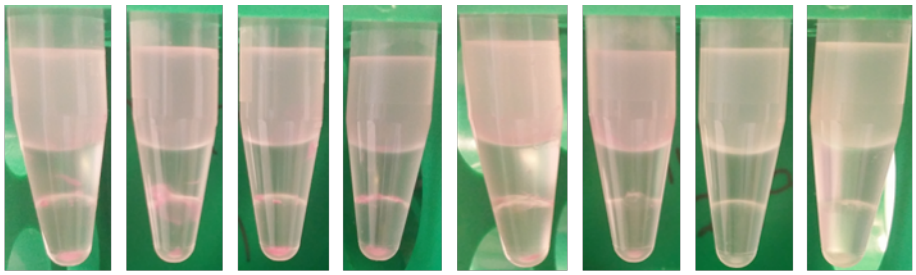

Condition	1	2	3	4	5	6	7	8
[Sucrose] (mM)	100	100	150	150	200	200	100	100
[AB] (mM)	50	50	25	25	0	0	50	50
Succinate	+	-	+	-	+	-	+	-
TMRM	+	+	+	+	+	+	-	-

Fig. 3.9 Effect of Succinate and TMRM on mitochondrial isolation from rat liver. A rat liver was processed as described in Figure 3.5 using the buffers described in the table. The protein concentration of the supernatant of homogenate was 38.1 mg/mL, and 2 mg (52.5 µL) of protein was used. ***Top:*** Photographs of tubes after centrifugation through oil, with sucrose and AB concentrations displayed in corresponding column in table underneath, indicating presence or absence of 1 mM succinate and 3 µM TMRM.

30 sec. However, this was not beneficial in that the mitochondrial pellets obtained were not larger than when one centrifugation step was used and only added more time to the extraction process. The centrifugation steps were optimised to be 1 min at 1,000 x g to remove cell debris, followed by 1 min at 9,727 x g through the oil. The centrifugation step in the swing rotor centrifuge takes 25 sec to attain 9,727 x g. After 35 sec at full speed (1 min from starting) it takes a further 35 sec to completely stop.

3.4.11.2 Weighed Tissue

At this stage, the protocol had been optimised to begin with a BCA assay to determine the protein concentration of the supernatant of rat liver homogenate, and thus how much volume to layer on the oil so that 2 mg of protein was used. This prolonged the isolation process by 30 min, which is not appropriate for the intended application of the method for metabolomic analysis of tissues, as this needs to be performed as quickly as possible. To remove this step

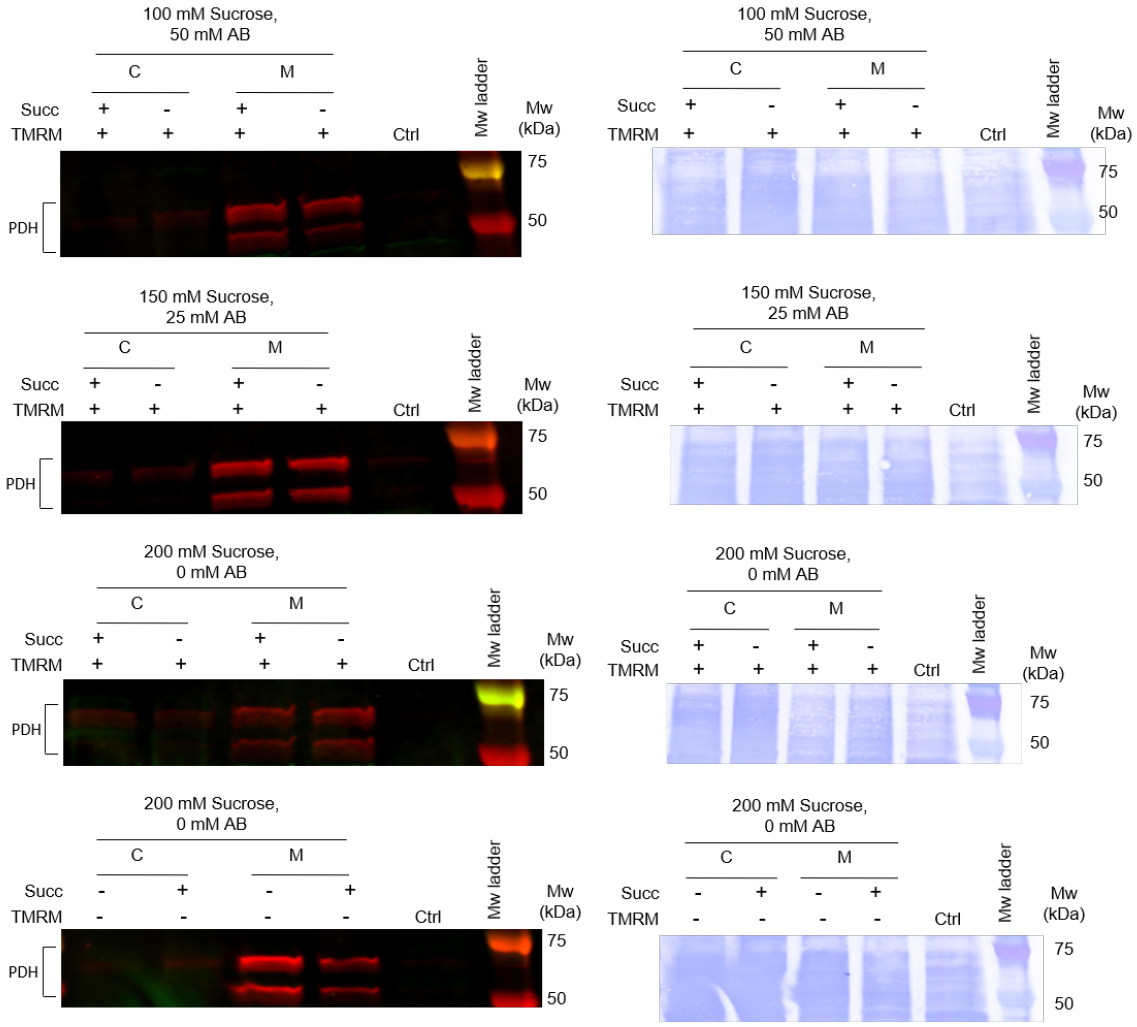

Fig. 3.10 Effect of Succinate and TMRM on mitochondrial isolation in rat liver. The samples from Figure 3.9 were processed for WB analysis as described in Figure 3.5. ***Left)*** Western blots. Mitochondrial marker: PDH (red bands, 54 and 69 kDa). C: Cytosolic fraction, M: Mitochondrial fraction. Ctrl: RLM isolated by conventional method. Marker: Protein Plus Dual Color standard. ***Right)*** Coomassie stains of membranes.

the homogenisation step was scaled down by homogenising known weights of tissue pieces in smaller volumes.

A female Wistar rat liver harvested at 8-12 weeks of age typically weighs 15 g. For standard mitochondrial isolations this is normally homogenised in 25 mL of STE buffer. In order to scale down the homogenisation step, smaller glass Potter-Elvehjem tissue grinders were chosen, which have a maximum volume of 7 mL (as opposed to the 55 mL Potter-Elvehjem tissue grinders used for a standard rat liver isolation). 5 mL of buffer was chosen as a suitable volume that would fit in the grinder and give enough volume of homogenate to use. To scale down tissue at the same proportion it was hypothesised 3 g (wet weight) of tissue in 5 mL should be used (25 mL/5 mL = 5, 15 g/5 = 3 g). 2 and 5 g of tissue were also trialled. The rat liver pieces (2, 3 and 5 g) were homogenised in triplicate in 5 mL STE buffer. 5 g of tissue was too dense to produce a supernatant after the 1 min spin at 1,000 x g and was not used. The protein concentration of the homogenate supernatant for the 2 g sample was 41.9 mg/mL and for the 3 g sample 48.4 mg/mL. 2 mg of protein from these samples is the equivalent of 47.7 µL and 41.3 µL respectively, which are similar volumes to what was used in previous experiments. If the isolation is proportionate to tissue amount, then 2 g and 3 g of tissue in 5 mL should yield 400 mg/mL and 600 mg/mL respectively. However, it is unlikely to be exactly proportional as a large amount of protein is lost to the cell debris pellet during the first centrifugation step. The fact that the 3 g sample only generated a slightly higher protein concentration in the homogenate supernatant than the 2 g sample shows that proportionally more protein is lost to the cell debris pellet from the 3 g sample, suggesting that there is incomplete homogenisation with this amount of tissue. It is also possible that a larger proportion of mitochondria became trapped in the cell debris pellet of the 3 g sample.

Figure 3.11 shows the mitochondrial pellets generated by 2 g and 3 g of tissue. Each generated similar sized mitochondrial pellets, but the 3 g samples had more protein in the oil and left in the top phase, further suggesting that there is incomplete tissue homogenisation with this amount of tissue. 2 g of tissue appears to be the optimum total amount of liver tissue. The whole rapid extraction method in rat liver was thus able to be scaled down in volume and the total extraction time reduced by over 30 min.

In an attempt to further reduce the time and variability of the homogenisation step, mechanical homogenisation using the Bullet Blender was trialled, instead of the manual method of a Potter-Elvehjem tissue grinder. 200 mg (wet weight) of rat liver tissue was placed in a 2 mL Eppendorf tube containing 1.5 mL of STE buffer and 0.5 mm ceria-stabilised zirconium

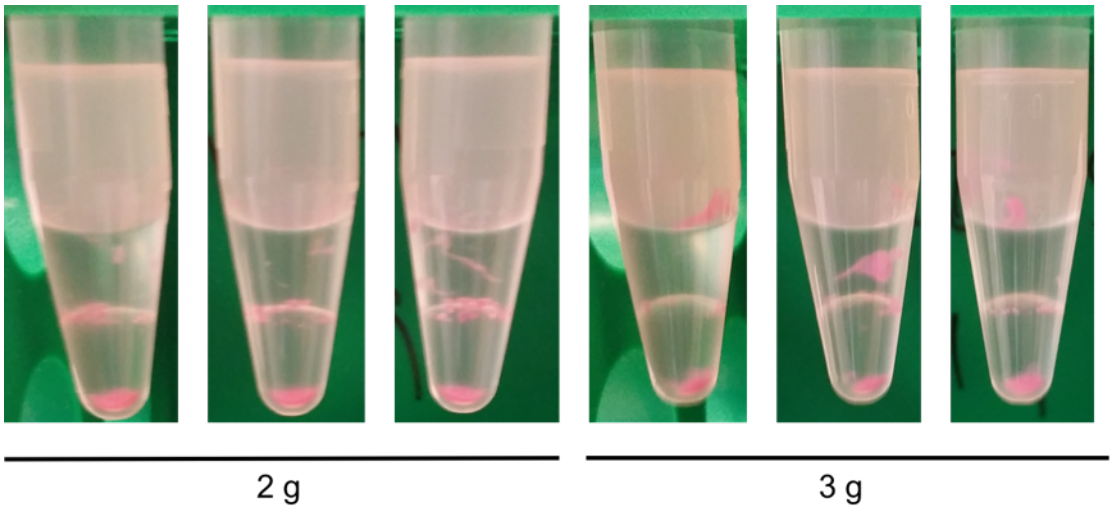

Fig. 3.11 Mitochondrial pellets from 2 and 3 g of rat liver. 2 and 3 g of rat liver were homogenised in 5 mL of STE buffer. 5 x 1 mL portions were centrifuged at 1,000 x g for 1 min. 55 µL of supernatant was added to a tube containing 100 µg/mL of digitonin (140 µL) in Buffer 6 (150 mM sucrose STE + 25 mM AB) to a total volume of 700 µL. 3 µM TMRM and 1 mM succinate was added. This suspension was layered on 300 µL of 60:40 DSMPS:DOP above 100 µL of 23 % glycerol before centrifugation at 9,727 x g for 1 min.

oxide beads (ZrOB05, Next Advance). This was homogenised in the Bullet Blender Storm24 machine (Next Advance) on speed setting 8 for 4 min. 1 mL of the homogenate was removed and centrifuged for 1 min at 1,000 x g. 55 µL of the supernatant was added to 150 mM sucrose STE + 25 mM AB buffer + 100 µg/mL digitonin to a total of 700 µL, and layered on 300 µL of 60:40 DSMPS:DOP above 100 µL 23 % glycerol. This was centrifuged at 9,727 x g for 1 min. However, no mitochondrial pellets were seen. This could be because the Bullet Blender was too harsh and lysed the mitochondria. Therefore, mechanical homogenisation using the Bullet Blender was not pursued further.

3.4.11.3 Pellet extraction

Once the method was successfully optimised to consistently produce a mitochondrial pellet, a way of extracting the pellet from underneath the oil mix was required. However, it proved challenging to remove all trace of the silicone oil and DOP from the pellet. Attempts to wash the oil away with 1 mL of 23 % glycerol or STE buffer followed by a 1 min centrifugation at 9,727 x g were unsuccessful, as relatively large amounts of the oil mix were still visible. As DOP is miscible with hexane, the most effective method attempted was to remove the

cytosolic fraction and the majority of the oil, freeze the pellet and wash the oil off with dry ice-cold hexane in a dry ice and ethanol bath (-72°C, see **Section 2.2.2**). However, this procedure is not suitable for most enzymatic assays and assays requiring intact mitochondria (as freeze-thaw damages mitochondrial membranes). For these applications the mitochondrial pellet was not frozen, and was removed from under the oil using a P1000 pipette tip after the majority of the oil was removed by pipette. However, this retrieval method results in a lower recovery of the mitochondrial pellet because some of the pellet is unavoidably lost. This is because as more of the lower layer (generally glycerol) is removed, the remnants of the oil phase become closer to the pipette tip. A compromise of lower mitochondrial yield with no contamination from the oil/DOP phase must be taken in this situation, as the oil and DOP may have adverse effects on enzymatic activity.

3.5 Rapid isolation of rat heart mitochondria

Initial attempts to isolate mitochondria from rat heart using the same conditions optimised for rat liver were unsuccessful. It was hypothesised this was due to heart mitochondria having a different density to liver mitochondria. To test this hypothesis, the density of the oil layer was reduced and homogenisation buffers 2-7 were trialled. 50:50 DSMPS:DOP oil was trialled initially due to its lower density of 1.026 g/mL compared to 1.034 g/mL of 60:40 DSMPS:DOP.

A rat heart was homogenised in 200 mM sucrose STE + 100 µg/mL digitonin. 180 µL of supernatant of homogenate (∼2 mg) was added to 520 µL of buffers 2-7 with 1 mM succinate and 3 µM TMRM. This was layered on 300 µL of 50:50 DSMPS:DOP oil above 100 µL of 23 % glycerol and centrifuged at 9,727 x g for 1 min. No pellets were seen in the oil using any of the buffers. As these conditions were unsuccessful, the density of the oil was reduced even further to 1.016 g/mL (38:62 DSMPS:DOP), as was the density of the glycerol (reduced to 10% glycerol, density 1.026 g/mL) (see **Table 3.5**). Another rat heart was homogenised as above and the protein concentration of the supernatant of homogenate was measured as 4.2 mg/mL. When 2 mg of protein (476 µL in 700 µL) was layered on 10 % glycerol and 38:62 DSMPS:DOP oil the lower phases inverted. After reviewing the densities of the components used (displayed in **Table 3.5** and **Table 3.6**), it was hypothesised that the inversion occurred because the densities were too close together (38:62 DSMPS:DOP = 1.016 g/mL and 10 % glycerol = 1.026 g/mL). Therefore, the glycerol concentration was

Buffer	[Sucrose] (mM)	[AB] (mM)	Density at RT (g/mL)
2	25	87.5	**1.008**
3	50	75	**1.008**
4	75	62.5	**1.012**
5	100	50	1.015
6	150	25	1.020
7	200	0	1.025

Table 3.5 Densities of buffers 2-7. Densities compatible with 38:62 DSMPS:DOP and 10 % glycerol are highlighted in blue. Densities were determined by weighing 1 mL of each buffer at RT (20-24^{o}C) and taking an average of 3 readings.

DSMPS:DOP	Density at RT (g/mL)	Glycerol	Density at RT (g/ml)
60:40	1.034	23%	1.060
50:50	1.026	**15%**	**1.039**
40:60	1.017	10%	1.026
38:62	**1.016**		
35:65	1.014		

Table 3.6 Densities of different DSMPS:DOP ratio mixes and glycerol mixes. Compatible density combinations are highlighted in blue. Densities were determined by weighing 1 mL of each buffer at RT (20-24^{o}C) and taking an average of 3 readings.

increased to 15 % (v/v, 1.039 g/mL) and the oil was kept at 38:62 DSMPS:DOP. Buffers 2, 3 and 4 (with 100 µg/mL digitonin) were trialled under these conditions (as the densities of these buffers are compatible with 38:62 oil and Buffers 5-7 are not) and this resulted in pink pellets in the glycerol layer and the layers consistently did not invert.

15 % glycerol, 38:62 oil and 25 mM sucrose STE + 87.5 mM AB (Buffer 2) were selected as the optimal combination for rat heart, based on density compatibility and WB analysis (**Figure 3.12**). A digitonin trial in rat heart showed that above 200 µg/mL digitonin the mitochondrial enrichment becomes reduced and cytosolic contamination increases (**Figure 3.13A**). 100 µg/mL digitonin was chosen to match the concentration used for liver, and because it showed a good enrichment of mitochondrial protein, based on the ratio of PDH:GAPDH of mitochondrial pellet:cytosolic fraction (**Figure 3.13B**). The digitonin-induced permeabilisation is known to differ between cell types (Olofsson et al., 2009), which may explain why digitonin had a different effect compared to rat liver.

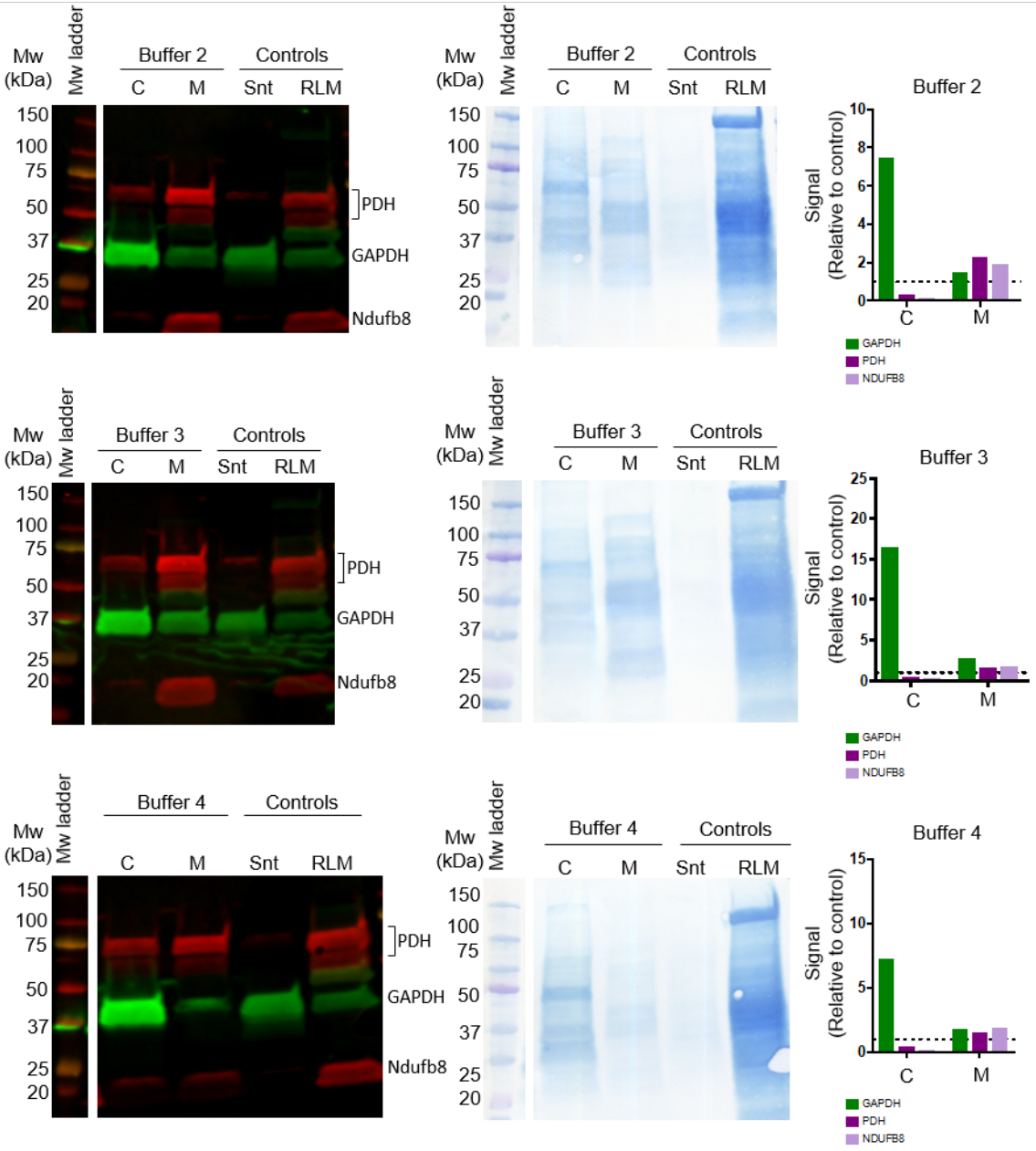

Fig. 3.12 Mitochondrial isolation from rat heart using homogenisation buffers 2, 3 and 4. A rat heart was homogenised in 5 mL of STE buffer. 1 mL aliquots were centrifuged at 1,000 x g for 1 min and the supernatants were combined. The protein concentration of the supernatant was assessed as 6.9 mg/mL. 2 mg of supernatant (290 µL) was added to 410 µL of buffer 2, 3 or 4, ± 100 µg/mL digitonin. This was layered on 300 µL of 38:62 DSMPS:DOP above 100 µL of 15% glycerol and centrifuged at 9,727 x g for 1 min. ***Left)*** Western blots. ***Middle)*** Coomassie stains of membranes. Marker: Protein Plus Dual Color standard. Primary antibodies: anti-PDH mouse, 1 in 2,000; anti-GAPDH rabbit, 1 in 10,000; anti-Ndufb8 mouse, 1 in 2,000. ***Right)*** Band intensities normalised to RLM control. C: Cytosolic fraction, M: Mitochondrial fraction. Controls - Snt: Supernatant of homogenate from a standard rat liver mitochondria isolation; RLM: rat liver mitochondria isolated by a standard isolation method.

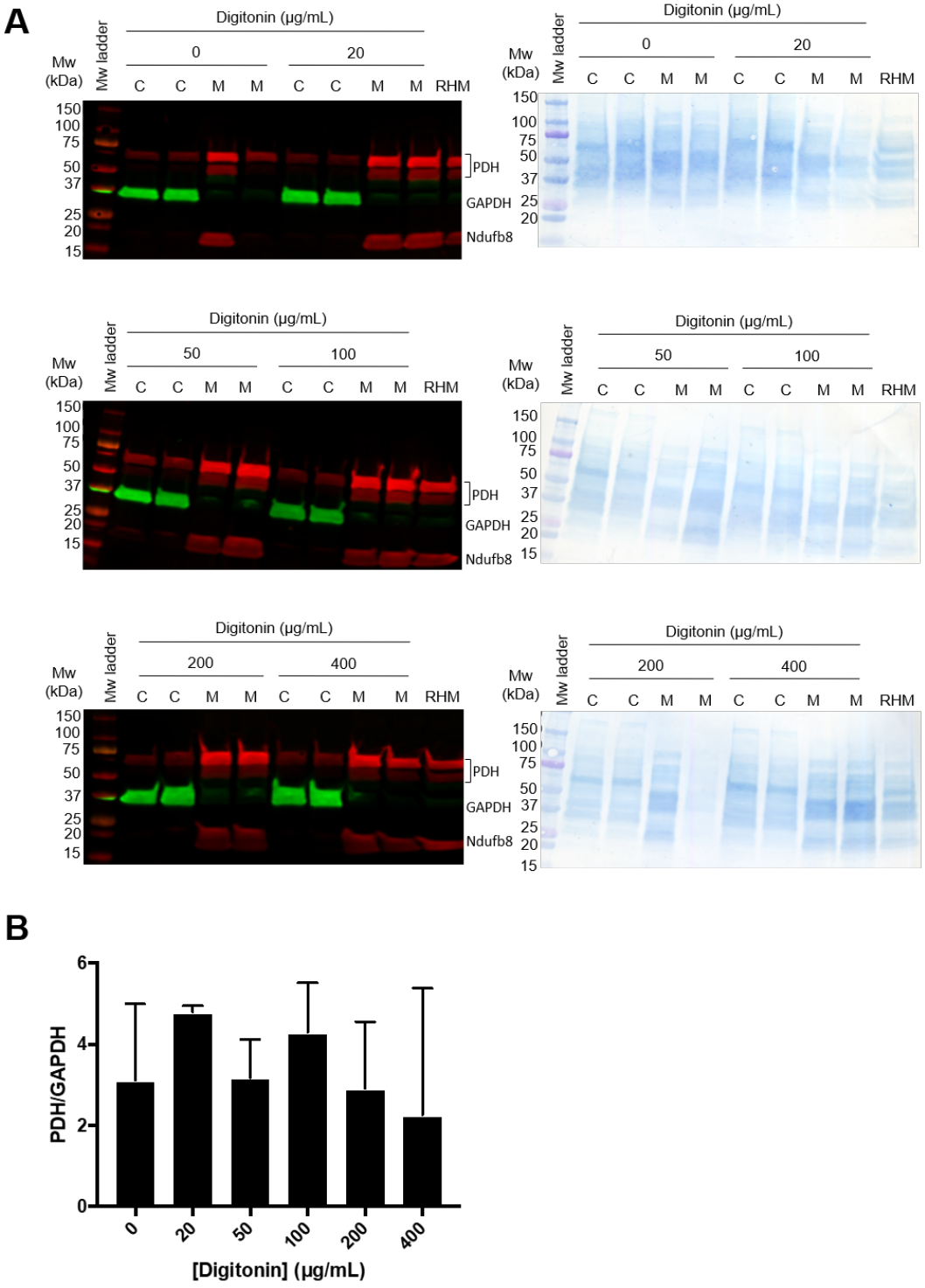

Fig. 3.13 Digitonin titration in rat heart. A rat heart was homogenised in 5 mL of 25 mM sucrose STE + 87.5 mM AB. 1 mL aliquots were centrifuged at 1,000 x g for 1 min and the protein concentration of the pooled supernatants was 7.8 mg/mL. 2 mg of supernatant (256 µL) was added to a tube with 0, 20, 50, 100, 200 or 400 µg/mL digitonin to a total of 700 µL. This was layered on 300 µL DSMPS:DOP above 100 µL of 15% glycerol and centrifuged for 1 min at 9,727 x g. **A)** Western blots and Coomassie stains of membranes. Marker: Protein Plus Dual Color standard. Primary antibodies (anti-GAPDH rabbit, 1 in 10,000; anti-PDH mouse, 1 in 2,000; anti-Ndufb8 mouse, 1 in 2,000). C: Cytosolic fraction, M: Mitochondrial fraction. **B)** Ratio of intensity of bands of PDH of mitochondrial pellet:GAPDH of cytosolic fraction. Data is mean ±SD.

3.6 Rapid isolation of mouse liver mitochondria

Minimal changes to the protocol optimised for rat liver were required to isolate mitochondria from mouse liver. A female C57BL/6 mouse liver harvested at 6-8 weeks of age is approximately 2-3 g (wet weight). As described in **Section 3.4.11.2**, 5 mL of buffer is a suitable volume to homogenise 2 or 3 g of rat liver tissue to generate a homogenate supernatant such that adding ∼50 µL of the supernatant of homogenate loads ∼2 mg of protein into the system. In rat liver isolations ∼50 µL of this homogenate supernatant is made up to 700 µL with STE buffer + 100 µg/mL digitonin. When repeated in mouse liver it was found that a larger and more consistent mitochondrial pellet is obtained when 200 µL of homogenate supernatant is made up to 700 µL with 150 mM sucrose STE + 25 mM AB.

The optimised protocol for mouse liver mitochondria isolation was to homogenise the whole mouse liver in 5 mL of "Homogenisation" buffer (200 mM sucrose STE + 100 µg/mL digitonin), centrifuge 1 mL portions at 1,000 x g for 1 min, take 200 µL of the supernatant and mix with 500 µL of "Spin" buffer (150 mM sucrose STE + 25 mM AB) before layering on 60:40 DSMPS:DOP and centrifuging for 1 min at 9,727 x g.

3.7 Rapid isolation of mouse heart mitochondria

Preliminary experiments to optimise rapid extraction of mitochondria from rat heart used ∼200 µL (2 mg protein) of supernatant of the homogenate. When attempted in mice, this amount of supernatant did not yield mitochondrial pellets. Increasing the volume of supernatant loaded resulted in inversion of the layers upon centrifugation due to the higher proportion of heavier 200 mM sucrose STE used for homogenisation. Therefore, instead of homogenising the heart in 200 mM sucrose STE and diluting in Buffer 2 (25 mM sucrose STE + 87.5 mM AB), the heart was homogenised directly in 3 mL of Buffer 2 + 100 µg/mL digitonin and 650 µL of supernatant was layered undiluted above the oil phase. This consistently resulted in mitochondrial pellets and stopped inversion of the layers. Unlike in the liver extraction method no separate ‘Spin Buffer’ is used: the homogenisation buffer with ammonium bicarbonate is used throughout the whole experiment. This method could also be used for the extraction from liver but it is was decided to maximise the sucrose concentration when possible, to maintain the mitochondria in an optimum state.

	Liver	Heart
Homogenising volume	5 mL	3 mL
Homogenising buffer	200 mM sucrose STE + 100 µg/mL digitonin	25 mM sucrose STE + 87.5 mM AB + 100 µg/mL digitonin
Loaded on oil	100 µL supernatant + 600 µL Spin Buffer*	650 µL supernatant
Oil ratio (DSMPS:DOP)	60:40	38:62
Lower layer	25% formic acid or 23% glycerol	15% formic acid or 15% glycerol

Table 3.7 Details of isolation protocols for mouse liver and heart. *Spin buffer: 150 mM sucrose STE + 25 mM AB.

3.8 Discussion

The above experiments describe the approach to develop a rationally-designed method to isolate mitochondria from tissue within 5 min of culling the animal, to optimise the analysis of mitochondrial and whole cell metabolites by LC-MS. The method was optimised in rat liver, rat heart, mouse liver and mouse heart. The details of the optimised protocols for mouse liver and heart are displayed in **Figure 3.14**. The mitochondrial preps are suitable for metabolic analysis by LC-MS.

The optimised conditions were to homogenise 2 g of rat liver in 5 mL of STE + 100 µg/mL digitonin. 1 mL aliquots of the homogenate are centrifuged for 1 min at 1,000 x g at 4°C, and ∼50 µL of supernatant are made up to 700 µL with 150 mM sucrose STE + 50 mM AB. This is layered on 300 µL of 60:40 DSMPS:DOP above 100 µL 23 % glycerol. This is centrifuged at 9,727 x g for 1 min.

As with all experiments involving animals, steps are required to be taken to minimise the numbers of animals used where possible. Thus, optimisation decisions were made logically, based on data and observations sometimes from individual experiments. However, the robustness of these decisions was confirmed in sequential optimisation steps.

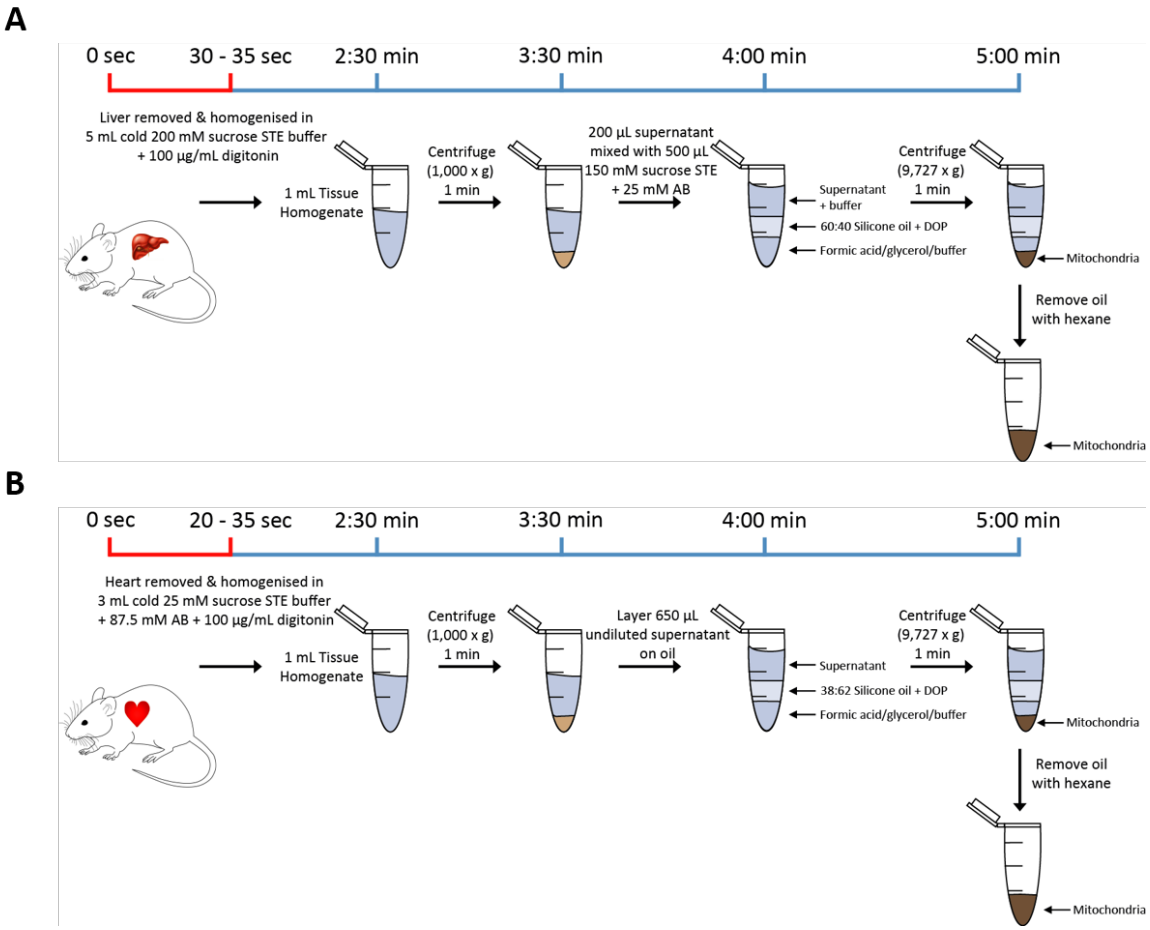

Fig. 3.14 Mitochondrial isolation protocol from mouse liver and heart. **A)** A mouse liver is removed and homogenised in 5 mL of "Homogenisation Buffer": 200 mM sucrose STE + 100 µg/mL digitonin. 1 mL portions are centrifuged at 1,000 x g for 1 min, and 200 µL of the supernatant is mixed with 500 µL of "Spin Buffer": 150 mM sucrose STE + 25 mM AB. 700 µL of this mixture is layered on 300 µL of 60:40 DSMPS:DOP and centrifuged for 1 min at 9,727 x g. For LC-MS analysis the lower layer is 23% FA, and for protein analysis 23% glycerol is used. **B)** A mouse heart is removed and homogenised in 3 mL of 25 mM sucrose STE + 87.5 mM AB + 100 µg/mL digitonin. 1 mL portions are centrifuged at 1,000 x g for 1 min and 650 µL of supernatant is layered on 300 µL of 38:62 DSMPS:DOP and centrifuged for 1 min at 9,727 x g. For LC-MS analysis the lower layer is 15% FA, and for protein analysis 15% glycerol is used.

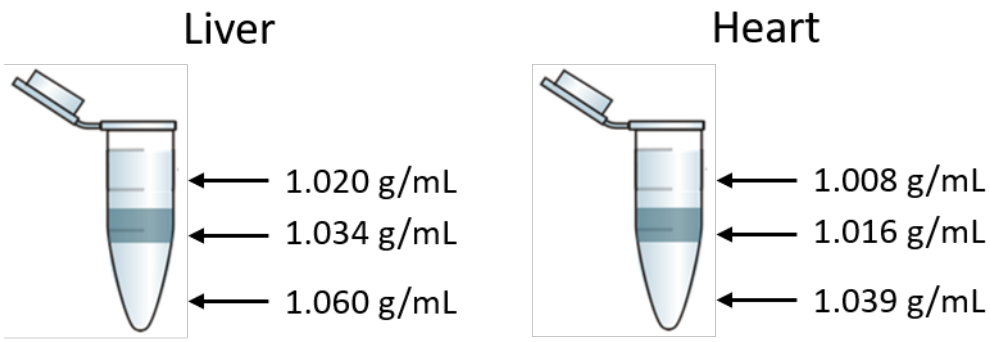

Fig. 3.15 Densities of the phases for mouse liver and heart mitochondrial isolations.

In developing and optimising the method I discovered there are certain points that are necessary and important for the successful isolation of mitochondria. The system is extremely sensitive to density, both within and between the phases. When designing the three different layers the densities must fall within the narrow window of being sufficiently distinct to prevent inversion and mixing, yet not too separate that the mitochondria cannot pass between the phases. The densities of each phase in a liver and heart mitochondrial isolation are displayed in **Figure 3.15**. Furthermore, thoroughly mixing all reagents (buffers, oil mixes, acids and glycerol) immediately (< 2 min) prior to use is extremely important and appears to be the main reason behind limited success with this method in the past. Despite there being no visible interface between the phases, even in the DSMPS:DOP mixes, density gradients are present.

The speed at which the whole procedure is performed is also important, particularly for metabolomic analysis. The most crucial step to perform quickly is the removal of the organ from the animal, to limit the time the organ is subjected to WI. With extensive practice I am able to remove the heart within 20 s of culling the animal, and the liver within 30 s. The rest of the procedure is also performed as quickly as possible by placing all equipment (centrifuges, fume cupboards and tissue grinders etc.) close together and having assistance from another person. This was found to reduce the total time by up to 2 min, which is significant in the timeline of this experiment.

The addition of digitonin was beneficial to the purity and yield of the mitochondrial pellet. Contrary to reports from Tischler et al. (1977) that the incubation needed for digitonin to act was long enough to allow metabolite dismutation, digitonin was able to act in the time frame of the isolation procedure.

DOP was seen to be necessary for generating a mitochondrial pellet. It is unclear what the mechanism of this is but is more complex than simply reducing the density as a less dense silicone oil with no DOP did not generate a pellet.

It is interesting that heart mitochondria require a much less dense oil than liver mitochondria (1.0158 g/mL for heart compared to 1.0336 g/mL for liver). This implies that heart mitochondria are less dense than liver mitochondria. **Table 3.8** lists the densities of various biological components. It shows that DNA and RNA are twice as dense as water. Starch granules, which are abundant in liver, have a high relative density of 1.5, whereas lipids and fatty acids have a lower relative density of 0.85. The heart relies heavily on fatty acid oxidation in the mitochondria for energy generation. Therefore, heart mitochondria contain a higher amount of less dense fatty acids and lipids, leading to less dense mitochondria. In contrast, liver mitochondria contain denser starch granules, increasing the overall density of liver mitochondria. Furthermore, liver mitochondria are more metabolically active than heart mitochondria and contain more enzymes and protein-rich electron transport chain complexes. The next step for the development of the method was to analyse the purity and function of the isolated mitochondria, and this is picked up in **Chapter 4**.

Component	Density (rel. to H_2O)
DNA	2.0
RNA	2.0
Starch granules	1.5
Chromatin	1.4
Proteins	1.2-1.4
Mitochondria	1.05-1.2
Hepatocyte	1.05-1.15
Erythrocyte	1.1
Skeletal muscle	1.06
Fibroblast	1.03-1.05
Membrane (including proteins)	1.02-1.18
Phospholipid (+ cholesterol)	1.01
Adipocyte	0.92
Palmitic acid	0.85

Table 3.8 Densities of various biological components in cells. The densities of biological components relative to the density of H_2O are listed. Table adapted from CellBiology Numbers website (Milo, Phillips, 2016).

Chapter 4

Analysis of rapidly isolated mouse liver and heart mitochondria

4.1 Introduction and aims

Chapter 3 described the approach to develop and optimise a method to rapidly isolate mitochondria from tissue and focused on the densities and solute molarity of the phases used. The success of the method was assessed by the visualisation of a mitochondrial pellet in the lower layer after centrifugation, facilitated by staining the pellet pink with TMRM, and also by western blot analysis. This chapter describes the assessment of the quality and purity of the mitochondria isolated by this method in more detailed ways, to ascertain whether the isolated mitochondria obtained could indeed be used for metabolomic analysis.

How well the mitochondria are separated from cytosolic contaminants is an important question to address for this project. If there is a lot of cytosolic contamination then it will not be possible to distinguish whether any given metabolite analysed is localised to the mitochondria, cytosol or both. The level of cytosolic and mitochondrial protein in the mitochondrial pellet was assessed by western blot. The level of contamination of other organelles in the mitochondrial pellet was also assessed by western blotting.

Intact mitochondria are more likely to retain their metabolites as they pass through the oil into the acid layer than damaged mitochondria. To assess whether the rapidly isolated mitochondria are intact, respiratory assays were performed using the Seahorse and Oroboros

systems. The hypothesis here was that if the mitochondria are capable of coupled respiration then this indicates that they are able to generate a membrane potential, which requires an intact inner membrane. If respiration rates increase upon uncoupling with FCCP this is a further indication that the mitochondrial membrane is intact. It could be that there are only small holes in the membrane, which would allow small metabolites to leave the mitochondria. However, protons are smaller than metabolites, so if protons are unable to pass through the holes then metabolites will also be trapped. In addition, ATP and ADP were measured in the mitochondrial pellet to determine whether the mitochondria are able to bring their metabolites through the oil.

Different mitochondrial isolation techniques will give different yields of mitochondria. Ideally, the yield will be high but a higher yield can often mean a compromise in purity. Hence, a low yield of mitochondria would not necessarily render the rapid isolation procedure obsolete, especially if it as a result of enhanced purity. Furthermore, LC-MS is a sensitive technique that does not require a large amount of material. Therefore, the isolation procedure only needs to generate a high enough amount of mitochondria for the LC-MS to detect any low abundance metabolites and that is representative of the endogenous mitochondrial population. Conversely, a low yield may mean that only a specific subset of more stable mitochondria are obtained in the final mitochondrial pellet, which may distort the outcome. Mitochondrial recovery was assessed by the proportion of citrate synthase activity in the mitochondrial pellet compared to the activity in the fraction that was layered onto the oil.

As discussed in **Section 3.1**, mitochondria can be damaged by the isolation process or other factors. This damage can result in the loss of membrane potential whilst maintaining intact mitochondria or it may break the mitochondrial membranes. Whether damaged mitochondria pass through the oil into the final mitochondrial pellet is not necessarily an indicator of the success of the isolation procedure. However, it is important to establish if the pellet contains damaged mitochondria, as this has implications for the interpretation and normalisation of the MS results. Damaged mitochondria lose their membrane potential, leading to swelling from the movement of water due to osmotic imbalances between the mitochondria and the cytosol. This swelling can reduce the density of mitochondria, preventing them passing through the oil and from being incorporated into the final mitochondrial pellet. Furthermore, more extensive or prolonged damage can cause the mitochondria to burst. This generates dense membrane fragments and clumps, which may also be able to pass through the oil. In this case, the protein from these damaged mitochondria will be detected in the pellet, but the metabolites will (probably) have been released into the top layer before centrifugation

through the oil. To investigate this, mitochondria were damaged by the addition of the pore-forming antibiotic alamethicin before centrifugation through oil. This is assuming that damaged mitochondria will lose their metabolites before passing through the oil, but it could be that they retain larger metabolites if only small holes are made in the membrane.

The digitonin will act mostly on the MOM, thus releasing any metabolites in the IMS. However, as the MOM is permeable to small metabolites, these pools are likely to be very similar to cytosolic pools and therefore of less interest for this project.

Metabolites are involved in metabolic reactions but can also act as signals. One way in which they do this is by interacting with proteins. Metabolites are known to bind to enzymes, either in the active site as substrates or cofactors, or allosterically to modify protein activity (Chandel, 2015; Piazza et al., 2018). They can also bind non-enzymatic proteins such as transporters, transmembrane receptors and transcription factors (Evans, 1988; Li et al., 2010; Piazza et al., 2018). In order to incorporate these metabolites into the analysis, the LC-MS extraction method will release any metabolites bound to protein (discussed in **Section 5.1.2**).

4.1.1 Aim

The aim of this Chapter was to assess whether the procedure was suitable for use with metabolomic analysis. To do this, 4 main questions were addressed. 1) Are the mitochondria sufficiently separated from the cytosol? - analysed by western blotting; 2) Are the mitochondria intact? - analysed by Seahorse and Oroboros respirometry; 3) What is the recovery of mitochondria in the extraction? - analysed by citrate synthase activity; and 4) Do damaged mitochondria pass through the oil? - analysed by GSH and protein assays on alamethicin-treated mitochondria. These questions are addressed in the following sections.

4.2 Are the mitochondria sufficiently separated from the cytosol?

The overarching aim of this project was to elucidate the metabolic differences between the mitochondria and the rest of the cell under various conditions in tissue. Therefore, it was important that the method resulted in enrichment of mitochondria in the pellet whilst also

purifying them away from the cytosol and other cellular organelles (discussed in **Section 3.1**).

4.2.1 Protein composition analysis of mitochondrial pellets

The separation of mitochondria and cytosol was assessed via WB. The level of cytosolic contamination in the mitochondrial pellets was measured by probing for the abundant cytosolic protein GAPDH. The extent of mitochondrial enrichment was assessed by probing for the mitochondrial matrix protein PDH. **Figure 4.1** shows that the level of mitochondrial protein is greatly enriched in the rapidly isolated mitochondrial pellets, with largely reduced levels of cytosolic protein. This indicates the mitochondria are removed from the cytosol by the procedure.

4.2.2 Contamination from other organelles

Mouse liver and mouse heart mitochondria isolated by the rapid method were analysed by WB to determine the purity of the mitochondria and the level of contamination from other cellular organelles. Rat heart and liver mitochondria isolated by the conventional method were included on the blot as a comparison of the two methods. **Figure 4.2** shows that, in general, the rapidly isolated mitochondria have qualitatively similar levels of other organelle contamination compared to standard isolated mitochondria. An exception was that heart mitochondria isolated by the standard method have less peroxisome contamination than rapidly isolated heart mitochondria (no Pex14 band in control heart). Overall, liver mitochondria have lower levels of contamination from other organelles than heart mitochondria.

4.2.3 Detection of mitochondrial and cytosolic metabolite pools

A preliminary LC-MS experiment in mouse heart was run to determine if distinct metabolite pools could be detected from the different fractions collected during the isolation procedure. The data shown in **Figure 4.3** are non-normalised ion intensities for a range of metabolites whose distribution in the cell is known. Although the intensities are not normalised, they clearly show that distinct metabolite pools can be detected, and reflect what is known about

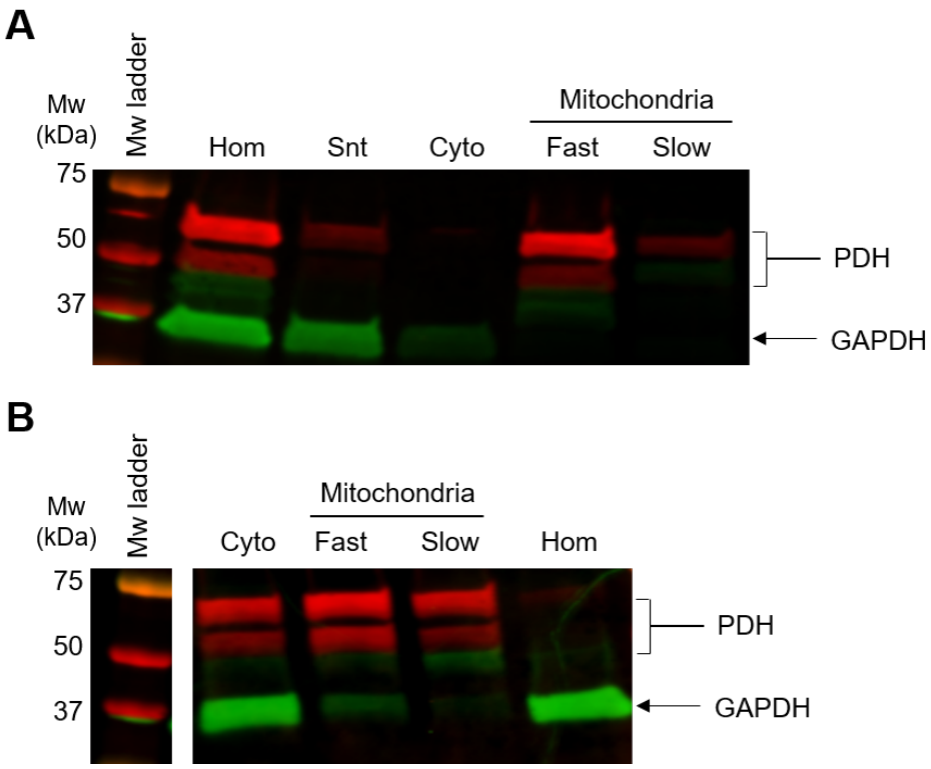

Fig. 4.1 Protein composition of mitochondrial isolation fractions. The amount of mitochondrial (PDH) and cytosolic (GAPDH) protein was assessed in fractions from rapid isolations of mouse heart ***(A)*** and liver ***(B)***. Electrophoresed proteins were transferred using the semi-dry transfer method. Hom: Homogenate of tissue; Snt: supernatant of tissue homogenate; Cyto: cytosolic fraction; Fast: rapidly isolated mitochondria; Slow: control mitochondria isolated via the standard method.

the cellular distribution of these metabolite pools. For example, a higher aconitate signal is detected in the mitochondrial fraction compared to all other fractions, whereas the lactate signal in the mitochondrial fraction was lower than all other compartments. Importantly, very little of the cytosolic metabolite fructose-6-phosphate was detected in the mitochondrial fraction but was abundant in all other fractions. Succinate is known to be distributed

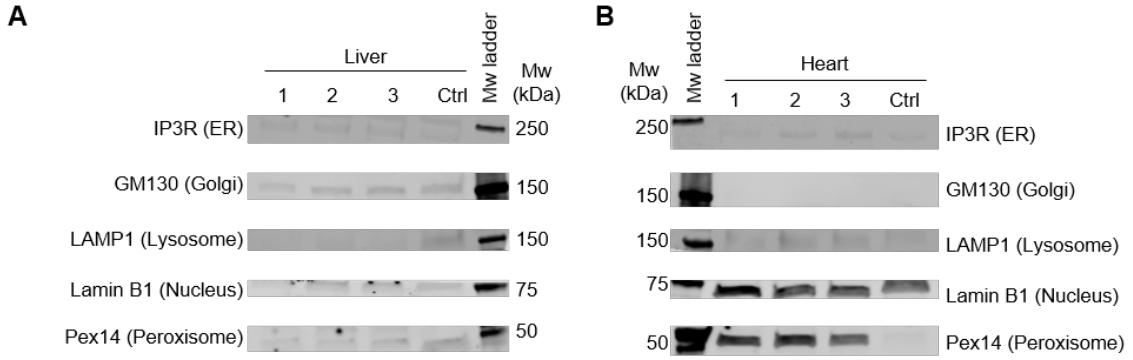

Fig. 4.2 Western blot of cellular organelles in rapidly isolated mouse heart and liver mitochondria. ***A)*** Liver mitochondria; ***B)*** Heart mitochondria. Proteins: IP3R (ER); GM130 (Golgi apparatus); LAMP1 (Lysosome); Nucleus Lamin B1 (Nucleus) and Pex14 (Peroxisome). Electrophoresed proteins were transferred using the wet transfer method. Controls: rat heart and liver mitochondria isolated by the standard method.

across the cell, which is reflected in the broadly similar signals across all fractions. This indicates that the isolation procedure is capable of separating different cellular metabolite pools. Nevertheless, this data is preliminary and requires normalisation to make any further inferences and to reduce variability.

4.3 What is the recovery of mitochondria?

The mitochondrial yield of an isolation procedure is an important measurement, but is not the only indication of its success. Here, a balance must be found between recovery of mitochondria and purity, as a high recovery is often at the expense of a lower purity mitochondrial sample, and vice versa. The recovery of mitochondria can be measured in a variety of ways. Chen et al. (2017) use the combined abundance of GSH and GSSG as a proxy for mitochondrial yield. However, this does not take into account damaged mitochondria which may lose their metabolites, and in **Section 4.5** I explain why this is not appropriate here. In addition, GSH is also found in the cytosol which makes the recovery hard to quantify. Instead, I have calculated the mitochondrial recovery using the activity of the mitochondrial citrate synthase enzyme.

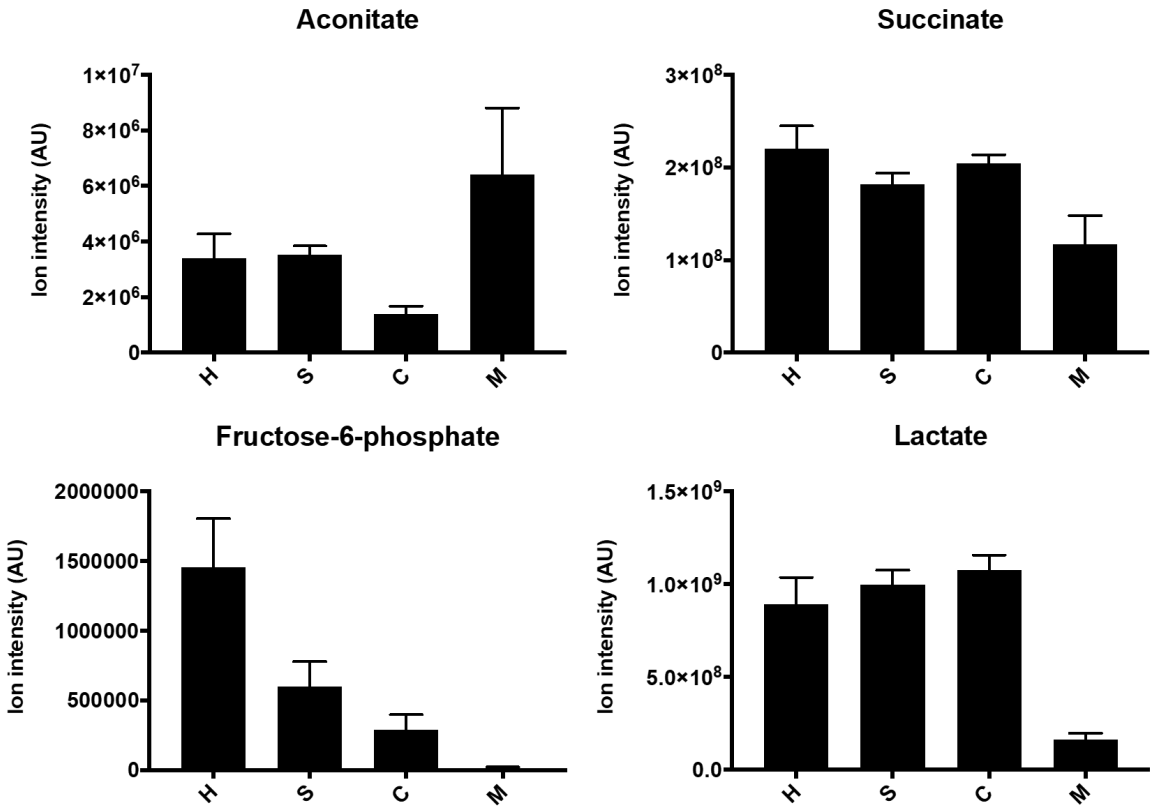

Fig. 4.3 Preliminary LC-MS signals of cellular metabolite pools in mouse heart. Mitochondria were rapidly isolated from mouse hearts into 100 µL 15% formic acid and analysed by LC-MS. The graphs show raw LC-MS signals of aconitate, succinate, fructose-6-phosphate and lactate in mouse heart fractions from the ZIC-pHILIC column analysis. Data is mean ±SEM, n=6. H: Homogenate; S: Supernatant; C: Cytosol; M: Mitochondria.

4.3.1 Citrate synthase activity

Citrate synthase (CS) is a mitochondrial matrix enzyme and its activity is therefore a useful and widely used measure of the amount of mitochondria in a sample (Kudin et al., 2004). Here, the CS activity was measured in each fraction of mouse liver and heart mitochondrial isolations to determine both the mitochondrial enrichment and recovery. **Figure 4.4A** demonstrates that the highest amount of CS activity in a rapid liver mitochondria isolation is in the mitochondrial fraction, at 220 µM TNB/min/µg protein, with very low activity recorded in all other fractions. Based on this experiment, **Table 4.1** shows that there is an 8.8-fold higher rate of CS activity in the liver mitochondrial pellet and a 86.0% recovery of CS activity from the liver isolation. In comparison, although heart mitochondria did display the highest CS activity of all fractions (**Figure 4.4B**), the CS activity was only increased by 1.2-fold (**Table 4.1**), whereas the CS activity recovery was 47.2%. These results are similar to values obtained in this lab for rat heart mitochondria. These experiments also indicate the mitochondria are not grossly damaged by passing through the oil or by other steps of the extraction method, as the CS enzyme is still functional.

4.4 Are the mitochondria intact?

The CS assays in **Section 4.3.1** demonstrate the mitochondrial enzyme CS is retained after passing through the oil. However, they did not identify whether the mitochondrial inner membrane is intact, as a low level of damage could lead to the loss of small metabolites whilst retaining CS activity. The mitochondria could be damaged by the digitonin or by shearing during homogenising and pipetting. To assess this, respiratory assays of the mitochondrial pellet were performed.

4.4.1 Seahorse analysis of mitochondrial respiration

Measuring mitochondrial respiration and coupling would identify whether the mitochondria are intact because complete, non-leaky membranes are required to generate a membrane potential and drive coupled respiration. One method to assess this was if there was a stimulation of OCR upon addition of FCCP. The Seahorse was chosen as a method to

Liver			
	Volume (mL)	**CS Activity (µM TNB/min/µg protein)**	**Total CS (nmol TNB/min)**
Homogenate	0.2*	0.025	1.57
Mitochondria	0.1	0.220	1.83
		8.8-fold enrichment	*86.0% recovery*
Heart			
	Volume (mL)	**CS Activity (µM TNB/min/µg protein)**	**Total CS (nmol TNB/min)**
Homogenate	0.65**	0.144	6.93
Mitochondria	0.1	0.177	3.27
		1.2-fold enrichment	*47.2% recovery*

Table 4.1 Calculations of purity and recovery of CS activity in mouse liver and heart mitochondrial isolations. The purity of the mitochondrial pellet can be inferred from the enrichment of CS activity, which is calculated by taking the CS activity (µM TNB/min/µg protein) of the mitochondrial pellet as a fraction of the CS activity in the homogenate. The mitochondrial recovery is calculated by taking the total CS activity (nmol TNB/min) of the mitochondrial pellets in 100 µL as a fraction of the total CS activity in the 200 µL of liver homogenate or 650 µL of heart homogenate that was used in the experiment. *0.2 mL: 200 µL of supernatant of liver homogenate was centrifuged through the oil (diluted with 500 µL of buffer). **0.65 mL: 650 µL of supernatant of heart homogenate was centrifuged through the oil.

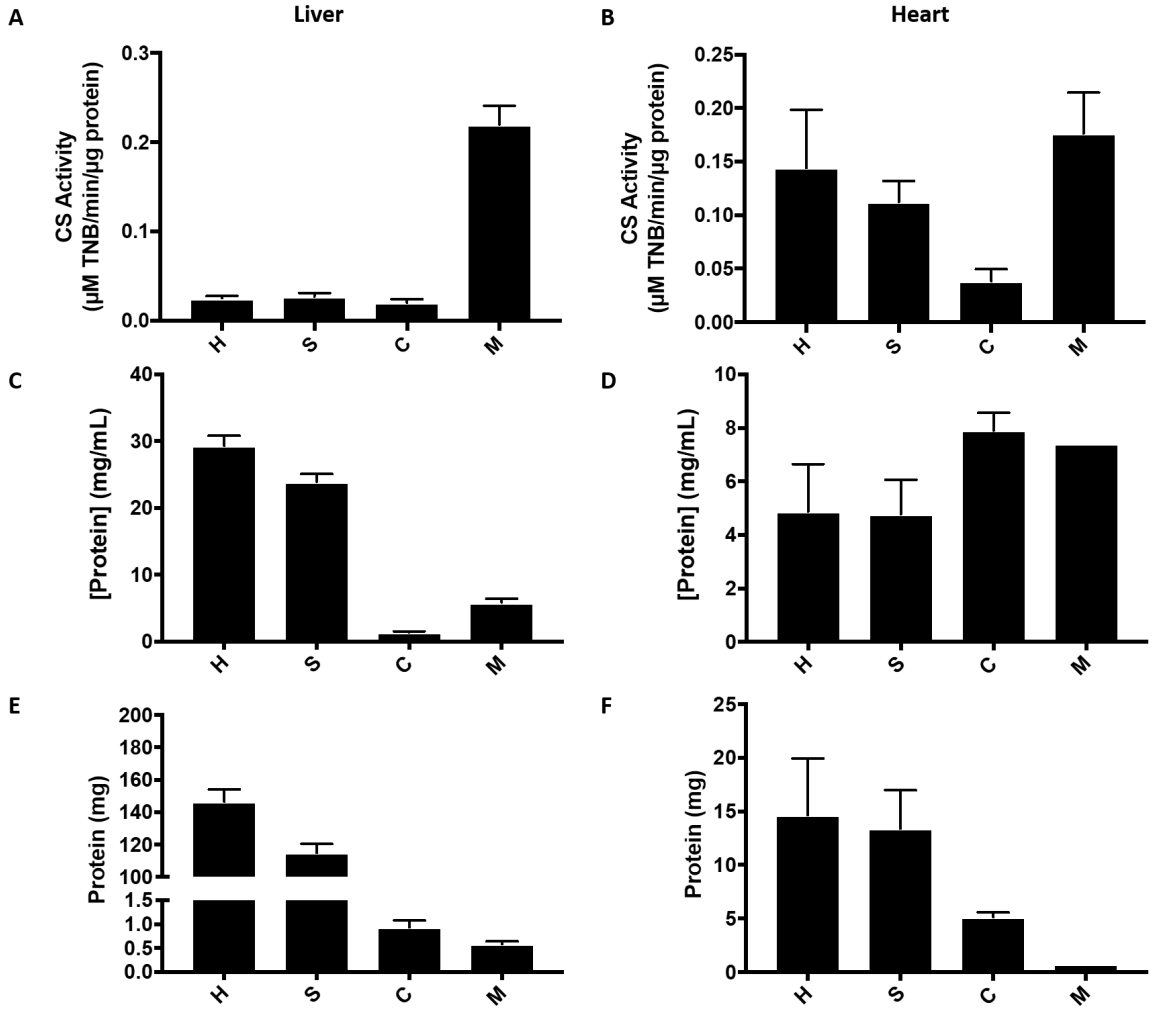

Fig. 4.4 CS activities and yields in mouse heart and liver mitochondrial isolations. ***A)*** CS activity in mouse liver. Mitochondria were rapidly isolated from 4 mouse livers, as described in Section 2.2.2.2. 100 µL fractions of homogenate, supernatant and top were retained for analysis. The mitochondrial pellet was obtained by removing the majority of the oil by pipette and then retrieving the pellet by pipette. A BCA assay was performed on all fractions before dilution to 8 µg in 100 µL total volume in 25 mM KPi buffer. The CS assay was performed as described in Section 2.5.3. ***B)*** CS activity in mouse heart. Mitochondria were rapidly isolated from 3 mouse hearts, as described in Section 2.2.2.3. ***C)*** Protein concentrations of liver fractions from ***(A)***; ***(D)*** protein concentrations of heart fractions from ***(B)***. Mitochondria were diluted into 150 mM sucrose STE. Homogenate and supernatant samples were diluted 1 in 50 and cytosolic and mitochondrial samples were diluted 1 in 10. Protein concentration was then assessed by the BCA assay. All data is mean ±SEM, n=4 for liver experiments, n=3 for heart experiments. H: Homogenate; S: Supernatant; C: Cytosol; M: Mitochondria.

measure mitochondrial respiration due to its capability of measuring microgram quantities of mitochondria in multiple conditions at the same time (Iuso et al., 2017; Rogers et al., 2011).

Approximately 1/3 of a rat liver was used to isolate mitochondria via the standard method (**Section 2.2.1.1**) as a control and the remaining 2/3 of the liver was used to isolate mitochondria via the rapid method (**Section 2.2.2**) with the following adaptations. The supernatants of the first spin were pooled and either 100 µL or 400 µL were made up to 700 µL with spin buffer (5 of each condition). The total 700 µL was placed on 300 µL of 60:40 DSMPS:DOP above 100 µL of either heavy seahorse assay buffer (HSAB: 700 mM sucrose, 220 mM mannitol, 10 mM KH_2PO_4, 5 mM $MgCl_2$, 2 mM HEPES, 1 mM EGTA, 0.2 % (w/v) fatty acid-free BSA, pH 7.2, density 1.049 g/mL, **Section 2.5.1**) or KHS buffer (120 mM KCl, 10 mM HEPES, 325 mM sucrose, density 1.044 g/mL). HSAB is a modified, more dense version of the standard seahorse assay buffer (SAB), so that the buffer was dense enough to form the lower layer underneath the oil. After centrifugation through oil, the mitochondria from each condition were pooled and resuspended in SAB buffer for protein quantification, as outlined in **Section 2.5.1**. The OCR traces are shown in **Figure 4.5**.

After optimising the conditions with rat liver mitochondria, the respiration of mouse liver mitochondria was assessed using the Seahorse. The respiratory traces (**Figure 4.6A**) show minimal differences between mouse liver mitochondria isolated by the rapid or standard method and **Figure 4.6B** shows that both exhibit strong stimulation upon addition of FCCP. Therefore, mitochondria rapidly isolated from mouse liver are intact and capable of coupled respiration.

Attempts to analyse mouse heart mitochondria respiration using Seahorse respirometry were unsuccessful. Mouse heart mitochondria isolated using the rapid method are hard to resuspend (without further damaging them), possibly due to the lower sucrose concentration of the heart isolation buffer. This makes quantification of mitochondrial protein more difficult as it is not a homogenous mixture. This also means that each well of the Seahorse plate may contain different amounts of mitochondria, leading to inconsistent readings. It could also be that the mitochondria in this suspension do not attach to the Seahorse plate. To overcome these issues, the respiration of mouse heart mitochondria was assessed using the Oroboros system.

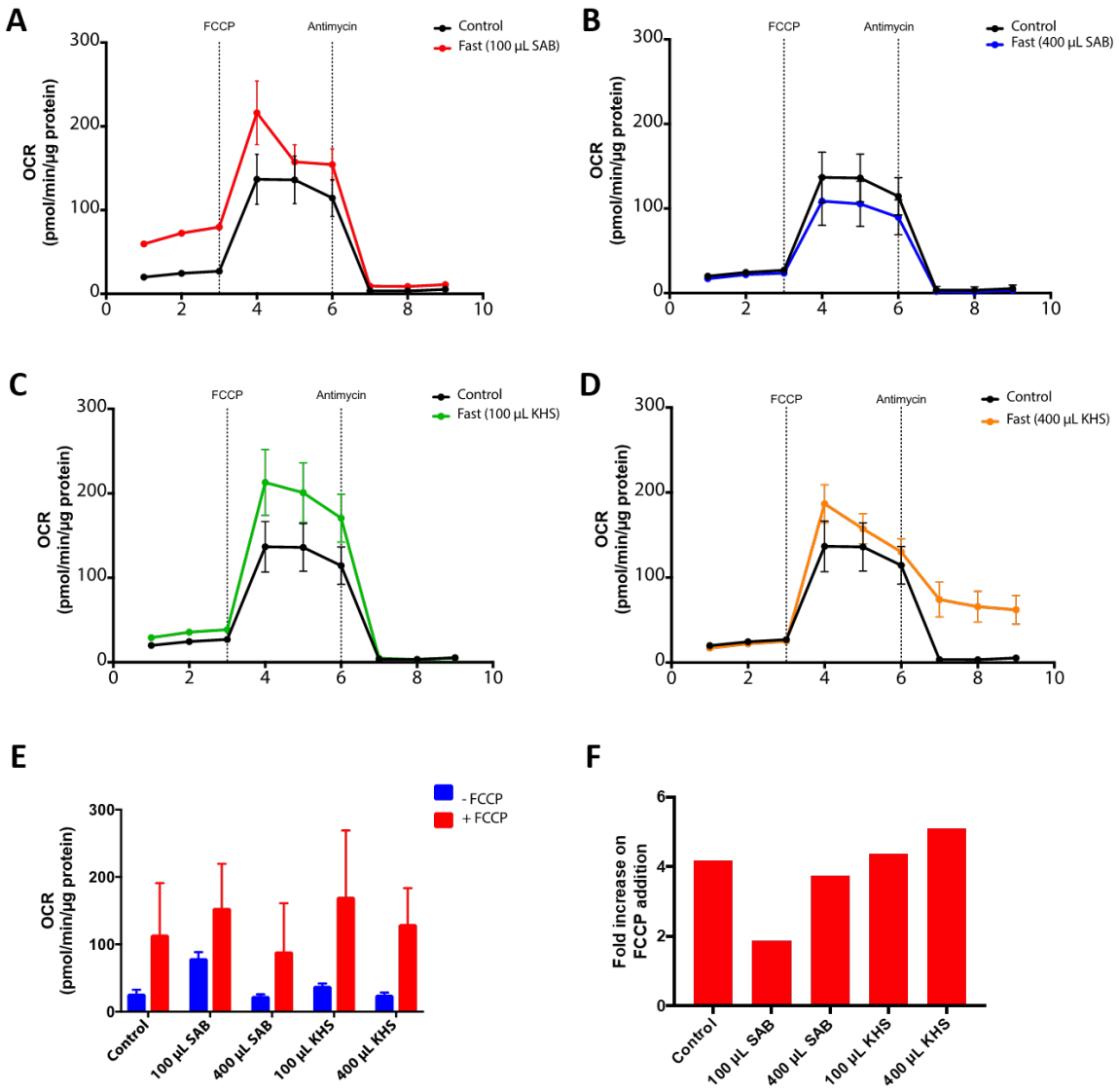

Fig. 4.5 Seahorse analysis of respiration in rat liver isolated by different buffers. Control mitochondria were isolated via the standard method from 1/3 of a rat liver and the remaining 2/3 was used to rapidy isolate mitochondria as described in Section 2.2.2 with the following adaptations. The supernatants of the first spin were pooled and 100 µL or 400 µL were made up to 700 µL with spin buffer (5 of each condition). The total 700 µL was placed on 300 µL of 60:40 DSMPS:DOP above 100 µL of either: 23 % glycerol, HSAB (700 mM sucrose, 220 mM mannitol, 10 mM KH_2PO_4, 5 mM $MgCl_2$, 2 mM HEPES, 1 mM EGTA, 0.2 % (w/v) fatty acid-free BSA, pH 7.2, density 1.049 g/mL) or KHS buffer (120 mM KCl, 10 mM HEPES, 325 mM sucrose, density 1.044 g/mL). After centrifugation through oil the mitochondria from each condition were pooled and resuspended in STE for protein quantification, before resuspension in SAB buffer as outlined in (**Section 2.5.1**). OCR traces for rat liver mitochondria isolated using SAB (***A*** and ***B***) or KHS buffer (***C*** and ***D***). ***A*** and ***C*** contained 100 µL of supernatant and ***B*** and ***D*** contained 400 µL of supernatant. ***E)*** shows the OCR of the time point immediately before FCCP addition and immediately after FCCP addition. Control was rat liver mitochondria isolated via the standard method (Section 2.2.1.1) Succinate: 5mM; FCCP: 4 µM; Antimycin: 3 µM.

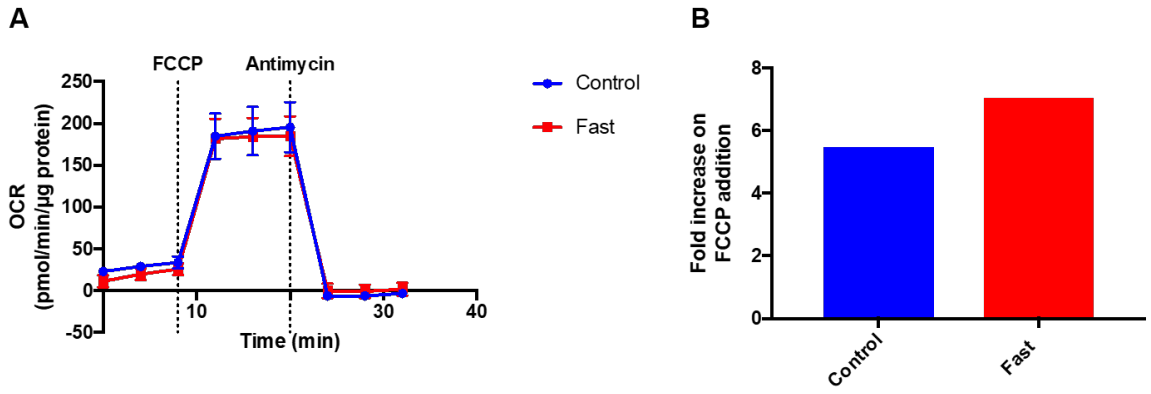

Fig. 4.6 Seahorse analysis of respiration in mouse liver. A mouse liver was homogenised in 5 mL of 200 mM sucrose STE + 100 µg/mL digitonin. 1 mL aliquots were centrifuged at 1,000 x g for 1 min. 100 µL of supernatant was mixed with 600 µL of spin buffer (150 mM sucrose STE + 25 mM AB) and layered on 300 µL of 60:40 DSMPS:DOP above 100 µL of HSAB (300 mM sucrose, 220 mM mannitol, 10 mM KH_2PO_4, 5 mM $MgCl_2$, 2 mM HEPES, 1 mM EGTA, 0.2 % (w/v) fatty acid-free BSA, pH 7.2). This was centrifuged at 9,727 x g for 1 min. The top and oil layers were removed and the mitochondrial pellet was gently resuspended in the HSAB. The protein content was assessed as 9.7 mg/mL for the control (mitochondria isolated from a whole mouse liver by the standard method on the same day as the rapid method) and 3.8 mg/mL for the rapid sample. The control and rapid mitochondria were then diluted in SAB and run on the Seahorse as described in Section 2.5.1. ***A)*** Respiratory trace (OCR) of control and rapidly isolated liver mitochondria. ***B)*** Ratio of OCR immediately after:before addition of FCCP. Succinate: 5mM; FCCP: 4 µM; Antimycin: 3 µM.

4.4.2 Oroboros analysis of mouse heart and liver mitochondrial respiration

Mouse heart mitochondria were analysed by Oroboros respirometry, which overcame the issues encountered when attempting to measure mouse heart mitochondrial respiration using the Seahorse. The Seahorse relies on the mitochondria sticking to the bottom of the wells because the oxygen probes are lowered to within ∼200 nm of the bottom of the well and only measure the O_2 concentration in that area. Therefore, any mitochondria that are above the probes will not contribute to the O_2 measurement. In contrast, the Oroboros measures the O_2 content of the whole chamber in which the mitochondria are kept in suspension, and therefore does not require the mitochondria to adhere and gives more consistent readings.

The OCR responded to the addition of succinate, and increased ∼2-fold on addition of FCCP (**Figure 4.7B and C**). Rat liver mitochondria were also analysed by the Oroboros (**Figure 4.7A**) and also showed good response to FCCP (**Figure 4.7C**). The above experiments demonstrate that both mouse heart and liver mitochondria isolated by the rapid method have intact membranes and are capable of coupled respiration. This indicates that the mitochondria have retained their metabolites during their movement through the oil into the lower layer.

4.4.3 Adenine nucleotide retention by rapidly isolated mitochondria

The ATP and ADP levels were assayed in rapidly isolated mitochondria. In tissue, the assay is often used to calculate the ATP/ADP ratio. This is an accurate readout of mitochondrial energy status and function. A high ATP/ADP ratio (typically 5-10 in tissue and up to 20 in cultured cells) is required for cells to perform essential energy-requiring processes (Hardie, Hawley, 2001). Therefore, if cells perform more work than they can sustain they will deplete their ATP/ADP ratio. However, rather than looking at energy metabolism, the ATP/ADP assay was used on rapidly isolated mitochondria and cytosolic fractions to identify whether the isolation was performed such that nucleotide exchange was limited. The total pools of ATP and ADP were measured, as this gives an indication of the ability of the mitochondria to retain metabolites.

The assays were performed in collaboration with Anja Gruszczyk at the MRC MBU. The ATP and ADP assay had to be adapted and optimised for use with liquid samples (mitochondrial

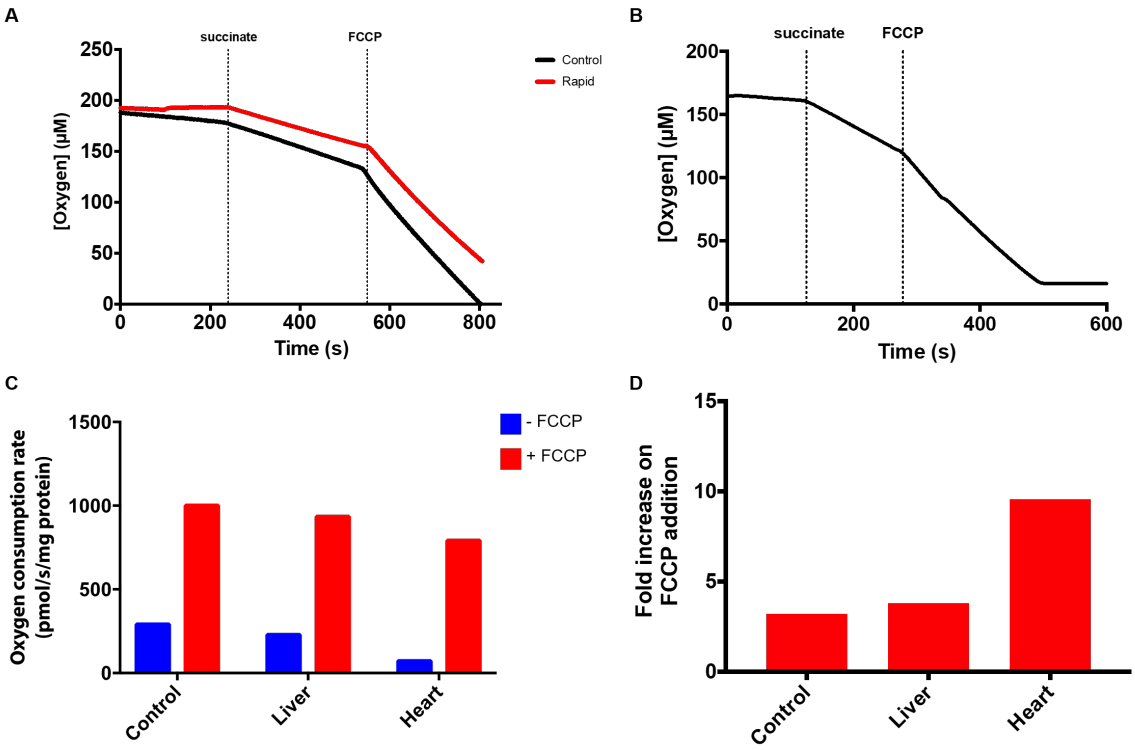

Fig. 4.7 Oroboros analysis of respiration. Mouse liver (***A***) and heart (***B***) mitochondria were isolated via the rapid method as described in 2.2.2, except they were centrifuged into 100 µL HSAB before dilution to 0.5 mg/mL mitochondrial protein in SAB and placed in the Oroboros chamber with 4 µg/mL rotenone before the addition of 1 mM succinate and 1 µM FCCP. The control liver trace is from a whole mouse liver isolated by the standard method on the same day as the rapid method. ***C)*** Oxygen consumption rate (OCR) before and after addition of FCCP. ***D)*** Fold increase of OCR after addition of FCCP.

pellet in FA), as it had previously only been used on solid tissue samples. For optimisation experiments, rat heart mitochondria were rapidly isolated, spun into 4.2% PCA and made up to 400 µL with Tris-acetate (TA) buffer (100 mM Tris, 2 mM Na_2EDTA, 50 mM $MgCl_2$, pH 7.75; **Section 2.4.3**). Homogenate, supernatant and cytosolic fractions were diluted 2:1 (2% PCA final concentration) in TA buffer and ATP and ADP was assayed. Other concentrations of PCA were also trialled for these fractions but 2% was shown to be optimal. **Figure 4.8** shows the total pool of adenine nucleotides and the proportion of ATP and ADP in the pools. The lower ATP/ADP ratio in the cytosol compared to the supernatant could reflect some adenine nucleotide degradation during the isolation procedure, as the cytosolic fraction is obtained after the supernatant fraction.

After establishing that the assay works on liquid samples in rat tissue, the retention of adenine nucleotides was tested in rapidly isolated mouse heart mitochondria and cytosol (**Figure 4.9**). As expected, the cytosolic adenine nucleotide pool was larger than the mitochondrial pool and had a high level of ADP, possibly suggesting that some breakdown has occurred. The mitochondrial pool has a high proportion of ADP (approximately 2:1 ADP:ATP), which is expected as this drives ATP synthase to make more ATP. On average, $\sim$1 mg of protein is obtained in per rapid mitochondrial isolation. Therefore, approximately 3 nmol AMP + ADP/mg protein was detected in the assay. This is comparable to the value of 5 nmol total adenine nucleotides (including AMP)/mg protein reported by Geisbuhler et al. (1984). This indicates that the rapidly isolated mitochondria are able to retain a sizeable proportion of their adenine nucleotides.

4.5 Do damaged mitochondria pass through the oil?

After confirming that functional mitochondria pass through the oil, the next step was to identify to what level (if at all) damaged mitochondria pass through the oil phase into the lower layer along with healthy mitochondria. Damaged mitochondria lose their membrane potential, rendering them unable to maintain their ion gradients and osmolarity. This can lead to swelling and changes in density, preventing them passing through the oil. If the damage is extensive then the mitochondria may burst, generating fragments of mitochondrial membrane. As membranes are protein-dense, these fragments may be able to pass through the oil into the lower layer. This has implications for the LC-MS analysis and the method of normalisation of metabolite levels. Ideally, to normalise to protein the metabolites should be normalised

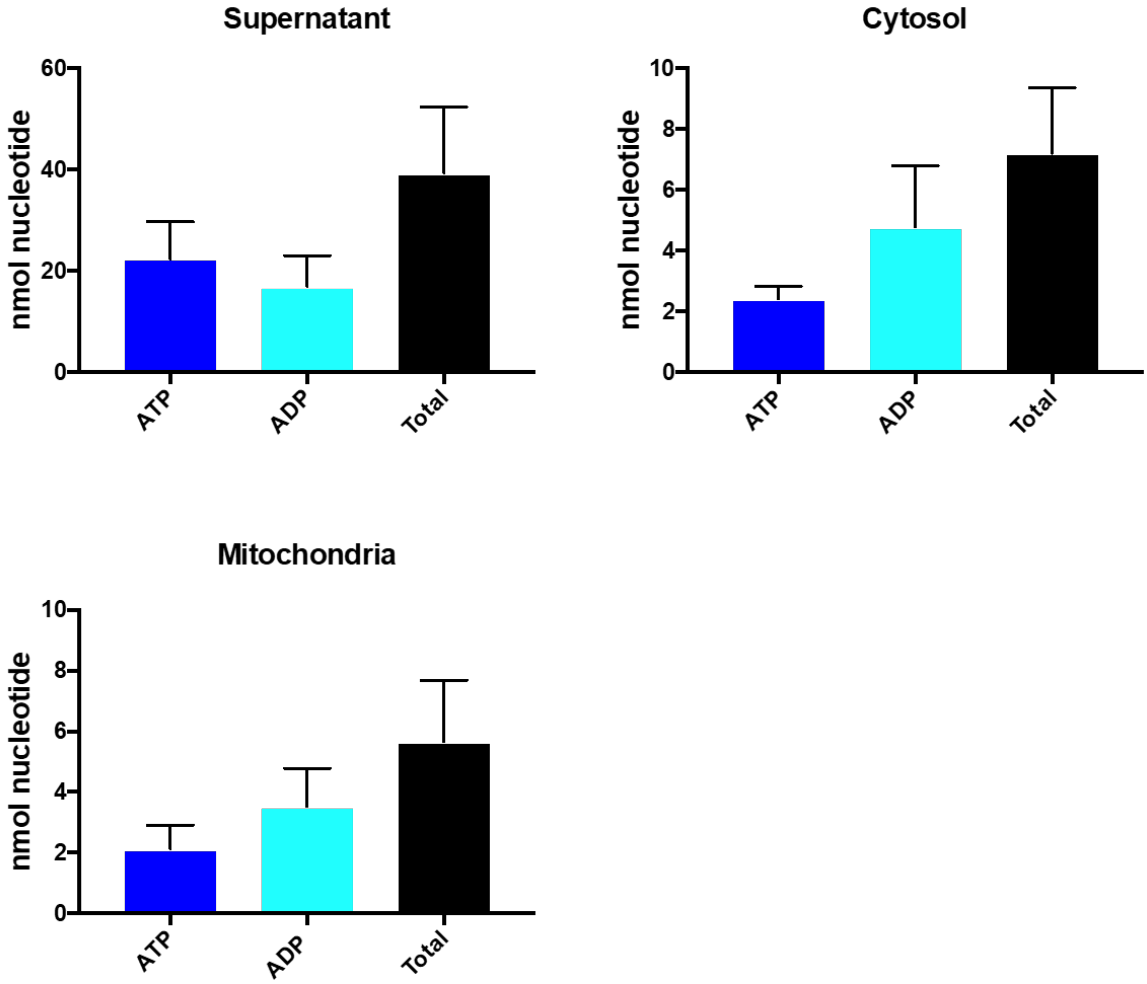

Fig. 4.8 ATP and ADP analysis in rapidly isolated rat heart mitochondria and other fractions. Absolute amounts of ATP and ADP in rat heart supernatant, cytosolic fraction and mitochondria. Supernatant and cytosolic fractions were prepared by adding 133 µL to 267 µL of TA buffer (2:1) to give a final concentration of 2% PCA. Mitochondrial fractions were prepared by centrifuging through 38:62 DSMPS:DOP oil into 4.2% PCA. ATP and ADP levels were assayed by the ATP and ADP assay. Data is mean ±SEM, n=3 biological replicates.

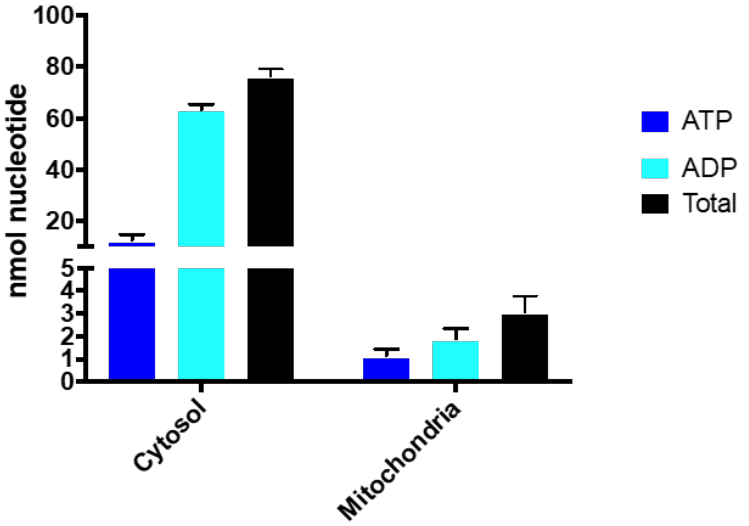

Fig. 4.9 ATP and ADP pools in rapidly isolated mouse heart cytosolic and mitochondrial fractions. Mitochondria were rapidly isolated from mouse heart by centrifuging through 38:62 DSMPS:DOP oil into 4.2% PCA. Cytosolic fraction was prepared by adding 133 µL to 267 µL of TA buffer. ATP and ADP levels were measured and extrapolated to calculate the total nmol of adenine nucleotides in the original cytosolic (layered on oil) and mitochondrial fractions (in 100 µL of mitochondria obtained after centrifugation). Data is mean ±SEM, n=3.

only to the amount of intact mitochondrial protein. However, if damaged mitochondria pass through the oil the ratio of mitochondrial metabolites to mitochondrial protein would be artificially decreased by the presence of mitochondrial membrane fragments. **Figure 4.10** depicts the possible fates of damaged mitochondria in rapid isolations.

4.5.1 GSH quantification in rapidly isolated mitochondria

GSH was measured in rapidly isolated mitochondria to investigate whether they are able to retain their metabolites during the rapid isolation procedure. It was decided to measure GSH because it is an abundant metabolite with slow transport mechanisms (Booty et al., 2015), with a robust, quantitative assay. GSH was detected at ∼2 mM in both mouse heart and liver mitochondria (**Figure 4.11**). Although this is within the range of 1-5 mM reported in the literature (Booty et al., 2015; Scarlett et al., 1996; Smith et al., 1996), it is towards the lower end of the range and liver mitochondria are thought to have more GSH than heart mitochondria. Unpublished work from this lab has reported GSH concentrations of 12 mM in fed mouse liver tissue, which dropped to 5 mM in starved mouse liver tissue. Mouse heart tissue GSH was calculated as 2 mM. These concentrations are higher than those obtained

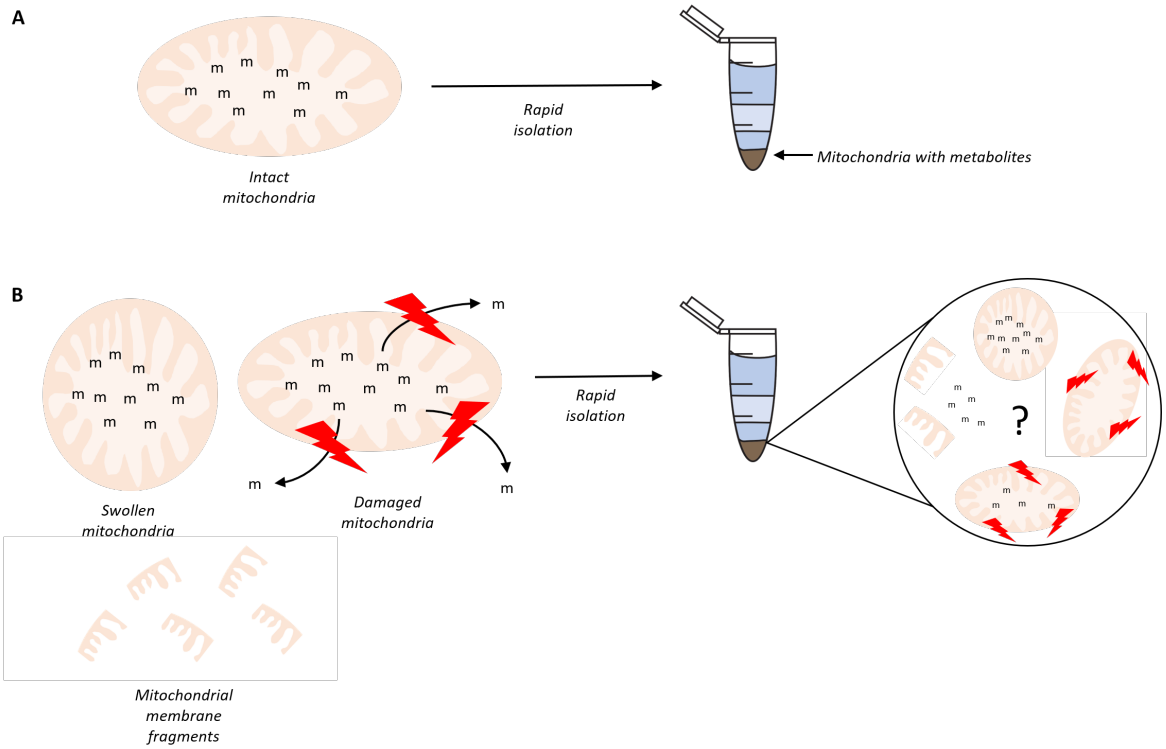

Fig. 4.10 Schematic of the possible fates of damaged mitochondria in rapid mitochondrial isolations. A) Rapidly isolating intact mitochondria generates a mitochondrial pellet containing mitochondrial metabolites (Section 4.4). **B)** Damage to mitochondria can result in swollen mitochondria, mitochondria with holes in their membrane (signified by red shapes) either losing some of their metabolites or cause the mitochondria to burst, losing all their metabolites and forming mitochondrial membrane fragments. It was not known how these damaged mitochondria would behave upon rapid isolation or whether mitochondrial metabolites would be brought through the oil. To investigate, mitochondrial damage was simulated by treatment with alamethicin. m: mitochondrial metabolite.

in **Figure 4.11**, suggesting that damaged mitochondrial protein (with no GSH) is able to pass through the oil, along with the intact mitochondria which have retained their GSH. The damaged mitochondrial protein then artificially decreases the calculated GSH concentration due to the protein component of the volume correction (∼0.6 µL/mg mitochondrial protein (Ross et al., 2006)).

4.5.2 Use of alamethicin to damage mitochondria

To investigate further, mitochondria were damaged by the addition of increasing amounts of alamethicin (AlaM), a pore-forming antibiotic that permeabilises mitochondrial membranes (Gostimskaya et al., 2003). After adding AlaM to the supernatant of the mouse liver ho-

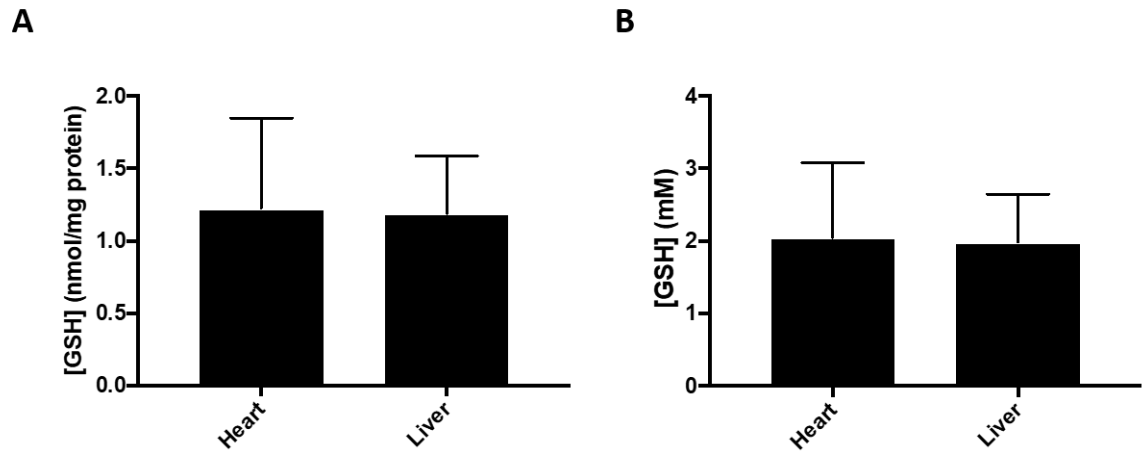

Fig. 4.11 Detection of GSH in mitochondrial pellets. Mouse heart and liver mitochondria were isolated via the rapid method as described in Section 2.2.2. After resuspension in glycerol, 40 µL of isolated mitochondria was added to 40 µL of 10% SSA, and GSH concentration was assessed by the GSH recycling assay, as described in Section 2.4.2. ***A)*** GSH concentration displayed relative to amount of protein in assay; ***B)*** GSH concentration displayed as mM. This was calculated based on the approximate value of 0.6 µL/mg mitochondrial protein (Ross et al., 2006). n=3, data is mean ±SEM.

mogenate (see legend to **Figure 4.12**), the suspension was layered above 60:40 DSMPS:DOP and centrifuged into 23% glycerol. Portions of the cytosolic fraction and mitochondrial fraction were retained for GSH and protein quantification as described in the legend of **Figure 4.12**. **Figure 4.12** shows that within individual biological experiments there is poor correlation between protein and GSH levels in the mitochondrial pellet. **Figure 4.13** shows that plotting µmol GSH against µg protein exhibits some correlation, but the correlation is offset: even when there is no GSH detected (at 40 µg/mL AlaM, red dots in **Figure 4.13**) there is protein in the pellet. This indicates that damaged mitochondria, which have lost their metabolites, are able to pass through the oil. Therefore, normalising metabolites, such as GSH, to protein concentration is not appropriate as there is no fixed ratio between metabolite and protein levels.

The increase in both protein and GSH concentrations between 0 and 5-10 µg/mL AlaM was unexpected. It may be that at low concentrations of AlaM the pores formed facilitate the release of GSH for analysis, similar to the action of digitonin. The concentrations of protein and GSH may then decline at higher AlaM concentrations as it becomes more damaging: by forming more pores more GSH is released in the layer above the oil before centrifugation. Similarly, the mitochondrial protein concentration decreases at higher AlaM concentrations as more mitochondria are severely damaged and are not able to pass through the oil.

Freeze-thaw was also trialled as a method to damage the mitochondria by placing the supernatant of homogenate into a dry ice and ethanol bath followed by thawing in a 37°C heat block for up to 5 cycles. However, no differences were seen, which could have been due to the sucrose in the buffer acting as a cryopreservant.

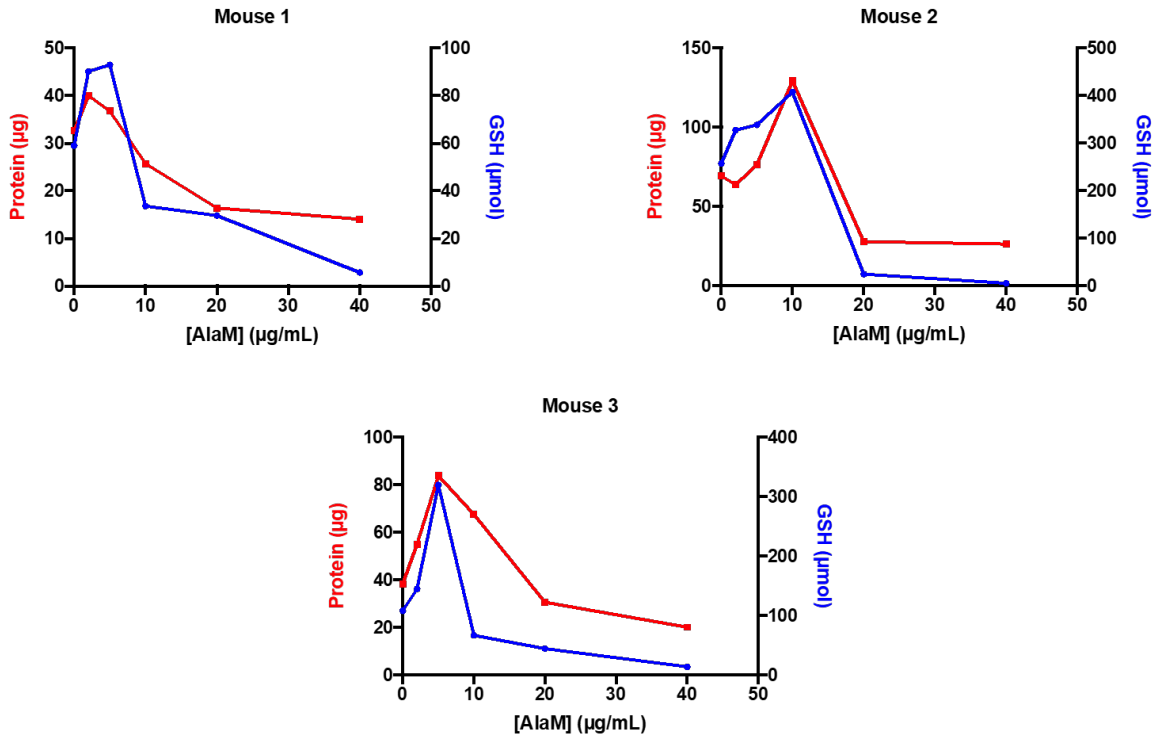

Fig. 4.12 Correlation of protein and GSH in mouse liver isolations. A mouse liver was homogenised as described in Section 2.2.2. After the first centrifugation step, 200 µL aliquots of the supernatant were added to 500 µL of buffer with alamethicin to a final concentration of 0, 2, 5, 10, 20 or 40 µg/mL, with a total volume of 700 µL. Each concentration of alamethicin was run in duplicate. The 700 µL was layered on 300 µL of 60:40 DSMPS:DOP and centrifuged into 100 µL of 23% glycerol. 10 µL of the cytosolic fraction was removed and added to 90 µL of 5% SSA for analysis of GSH concentration, 500 µL was retained for protein quantification, and the rest was removed, along with the oil:DOP layer. The mitochondrial pellet was resuspended in the glycerol and 40 µL was added to 40 µL of 10% SSA for analysis of GSH concentration, and the rest was retained for protein quantification. The protein and GSH concentrations of the cytosolic and mitochondrial fractions was assessed. Protein and GSH absolute amounts at increasing alamethicin concentrations for each mouse. AlaM: alamethicin.

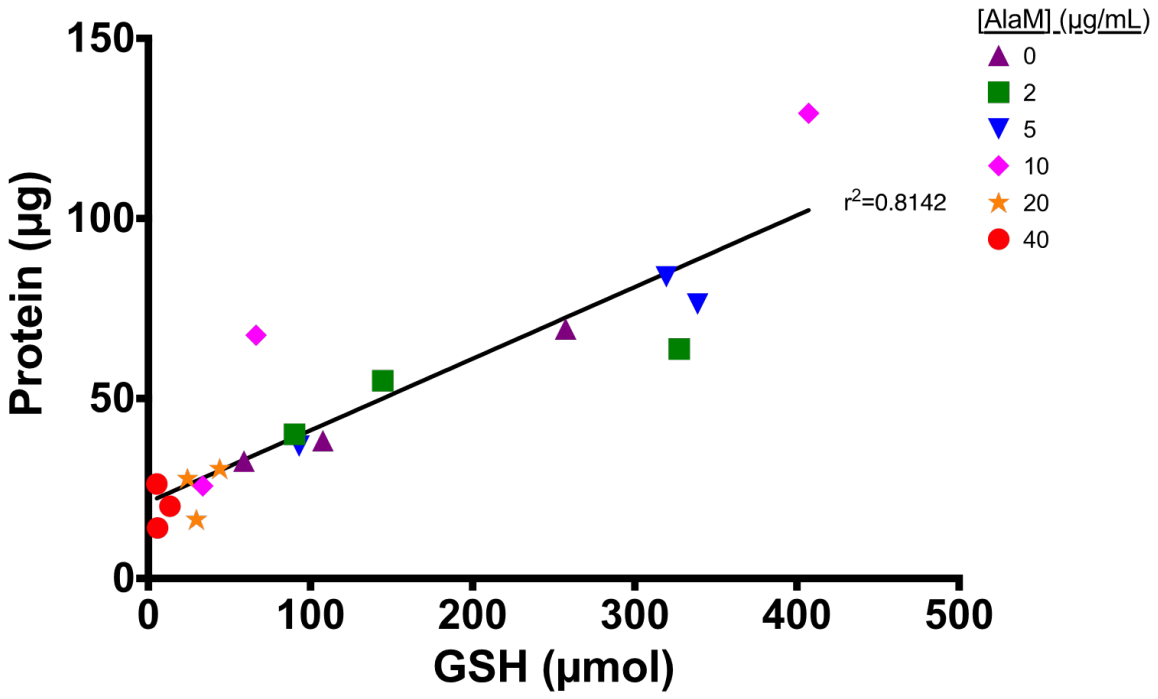

Fig. 4.13 Correlation of protein and GSH in mouse liver isolations. A mouse liver was homogenised as described in Section 2.2.2. After the first centrifugation step, 200 µL aliquots of the supernatant were added to 500 µL of buffer with alamethicin to a final concentration of 0, 2, 5, 10, 20 or 40 µg/mL, with a total volume of 700 µL. Each concentration of alamethicin was run in duplicate. The 700 µL was layered on 300 µL of 60:40 DSMPS:DOP and centrifuged into 100 µL of 23% glycerol. 10 µL of the cytosolic fraction was removed and added to 90 µL of 5% SSA for analysis of GSH concentration, 500 µL was retained for protein quantification, and the rest was removed, along with the oil:DOP layer. The mitochondrial pellet was resuspended in the glycerol and 40 µL was added to 40 µL of 10% SSA for analysis of GSH concentration, and the rest was retained for protein quantification. The protein and GSH concentrations of the cytosolic and mitochondrial fractions was assessed. Correlation between GSH and protein levels in the mitochondrial pellet, colour coded by alamethicin concentration. AlaM: alamethicin.

4.6 Discussion

The WBs in **Section 4.2** show that the mitochondria are well separated from the cytosol and that there is a comparable level of organelle contaminants to a standard mitochondrial prep. The preliminary LC-MS graphs in **Figure 4.3** show that the procedure is capable of distinguishing mitochondrial and cytosolic pools, and excludes cytosolic metabolites such as the glycolytic intermediate fructose-6-phosphate from the mitochondrial metabolite pools. Thus, the mitochondria are successfully separated from the cytosol by the procedure.

The purity of the mitochondrial pellet was further examined using the enrichment of CS activity in the mitochondrial pellet. **Table 4.1** shows that CS activity is enriched by ∼8.8-fold and ∼1.2-fold in liver and heart mitochondria respectively. The recovery of mitochondria from this procedure is 86.0% from liver and 47.2% from heart. For metabolomic analysis speed is paramount, so to reduce the processing time not all of the tissue homogenate is used. For example, 5 mL of tissue homogenate is produced during a liver mitochondria isolation: 1 mL of this centrifuged slowly and of this, only 200 µL of supernatant (liver) and 650 µL (heart) per isolation is centrifuged through the oil (with 4 isolations performed per mouse for LC-MS samples). This is to reduce the time of the isolation procedure as it would take more time to layer the supernatant on the oil for more than 4 separate isolations and to pool all of the mitochondrial pellets after the final centrifugation. Using all of the tissue homogenate would easily increase the absolute amount of mitochondria obtained, and the overall yield from the tissue, but would require the assistance of another person and additional centrifuges to maintain the speed required for the isolation. If the isolated mitochondria are to be used for an application that is not dependent on the speed of the isolation then the amount of mitochondria obtained could be increased easily. Alternatively, the procedure could be modified to be performed in a larger tube, so that more supernatant could be centrifuged through the oil at once, but this would require a longer centrifugation time and possibly further optimisation.

The mitochondrial respiration assays demonstrate that the mitochondrial membranes remain intact during the isolation process. This means that any matrix metabolites will be brought through the oil into the lower layer, and can therefore be analysed by LC-MS. The preliminary LC-MS data displayed in **Figure 3.6** also confirmed that a range of metabolites can be detected in the isolated mitochondria.

The experiments with alamethicin to damage the mitochondria strongly indicate that mitochondrial protein can be detected in the lower layer even when no metabolites can be detected. This demonstrates that damaged mitochondria are able to pass through the oil, either as semi-intact mitochondria with many holes that have lost all matrix metabolites, or as fragments of mitochondrial protein, formed when extensively damaged mitochondria have burst or been sheared. Regardless of the form in which the mitochondrial protein passes into the lower layer, these experiments show that there is no correlation between mitochondrial metabolites and mitochondrial protein. Therefore, the metabolites cannot be quantified by normalisation to protein. A caveat to consider here is that the use of alamethicin is inducing

artificial damage and may not truly mimic the damage that may occur during the isolation process.

Overall, the above experiments highlight that a proportion of the mitochondria remain intact during the rapid isolation procedure and are suitable for their intended application of metabolomic analysis by LC-MS. They also indicate that the method is adaptable and the mitochondria can be used in different applications.

Chapter 5

Optimisation of LC-MS analysis of rapidly isolated mitochondria

5.1 Introduction

Chapter 4 described the testing and confirmation of the rapid mitochondrial isolation procedure, which is to be coupled with an LC-MS analysis. In this chapter, the development and optimisation of the LC-MS protocol and analysis is described. Below I outline important factors that I considered when designing the metabolomic approach and cover the main aspects involved: the extraction method, LC columns used, the normalisation technique and the caveats to consider. I then present results of the optimisation of these factors. Next, I investigate whether the use of transport and respiratory inhibitors are necessary to quench metabolism, or whether performing the isolation procedure quickly and at low temperature is sufficient.

5.1.1 Metabolite analysis by LC-MS

To analyse metabolites, this project used LC-MS for a range of reasons: it has very high sensitivity (limit of detection of 0.5 nM compared to 0.5 µM for GC-MS); requires only small sample volumes (10 - 100 µL); can detect a wide range of organic molecules (Lu et al., 2017) and can analyse complex mixtures (Mackay et al., 2015). Compared to NMR, separation on

the LC column provides an extra parameter for distinguishing metabolites: metabolites are retained on the column for different amounts of time (based on their chemical characteristics, such as hydrophobicity and charge), meaning they enter the MS at different times. However, using LC has limitations, as it cannot detect all metabolites and is not ideal for the detection of lipids. Therefore, it was decided to focus on the detection of polar metabolites such as TCA cycle intermediates, amino acids and nucleotide breakdown products, as previous work from this lab (Chouchani et al., 2014; Martin et al., 2019) has suggested that these are the most important and relevant for studying mitochondrial metabolism during IRI. Furthermore, the use of positive/negative polarity switching allows the detection of a range of metabolite classes to be analysed in a single run (Mackay et al., 2015).

This project employed hydrophilic interaction liquid chromatography (HILIC). In this chromatographic method, only water-miscible solvents are used and small polar metabolites are separated on polar stationary phases and eluted using a gradient of increasing water content (Buszewski, Noga, 2012; Lu et al., 2017). In HILIC, water is the strongest solvent, which eliminates the issue of low aqueous solubility and increases MS sensitivity (Guo, Gaiki, 2005). The zwitterionic ZIC-HILIC and ZIC-pHILIC columns were used, which are both packed with a stationary phase with a zwitterionic sulfobetaine group. This sulfobetaine group is covalently bonded to porous silica in the ZIC-HILIC column, and to porous polymer beads in the ZIC-pHILIC column (Lu et al., 2017; Mackay et al., 2015). The permanent zwitterion enhances the retention of polar metabolites to the column. Due to the nature of the polymeric beads, the ZIC-pHILIC column is used at a high pH (pH 9.2, maximum pH 10), whereas the ZIC-HILIC column is used at a much lower pH (pH 2.8, maximum pH 8).

The mobile phase used for the ZIC-pHILIC column was A) (aqueous) 20 mM ammonium carbonate and 0.05% ammonium hydroxide and B) (organic) 100% acetonitrile and for the ZIC-HILIC column was A) 0.01% formic acid in H_2O and B) 0.01% formic acid in acetonitrile. The gradients used for separation are shown in **Figure 5.1**. The LC-MS metabolomic analysis conditions chosen for this project have been used in many projects (Chouchani et al., 2014; Mills et al., 2016; Tannahill et al., 2013).

The ZIC-pHILIC column has the broadest coverage of metabolites, and performs better in terms of least variability in retention time and peak areas, as well as peak shape (Zhang, 2012). In particular, amino acids, nucleosides, phosphates, organic acids and sugars perform better on the ZIC-pHILIC column. This is because organic acids and phosphates ionise better in negative ion mode on the MS and as the high pH of the ZIC-pHILIC column is above

A

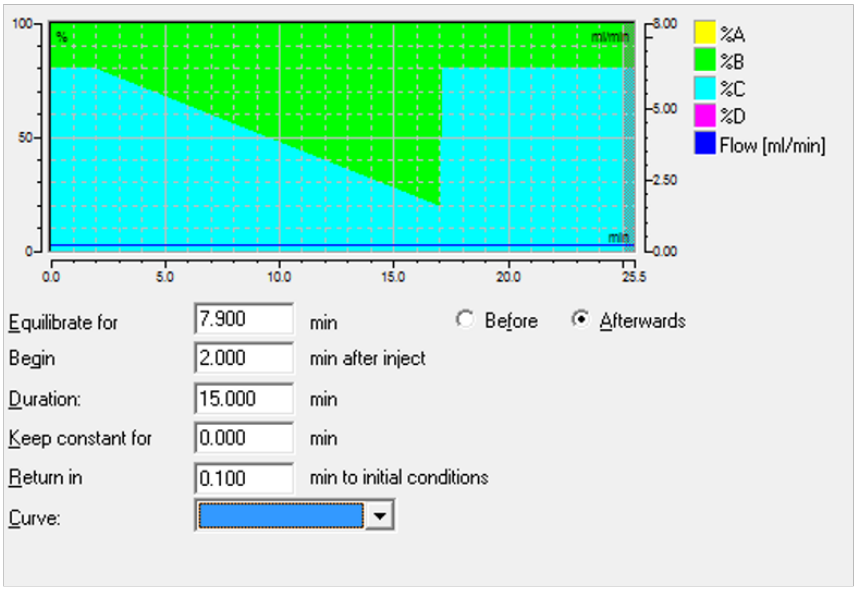

B

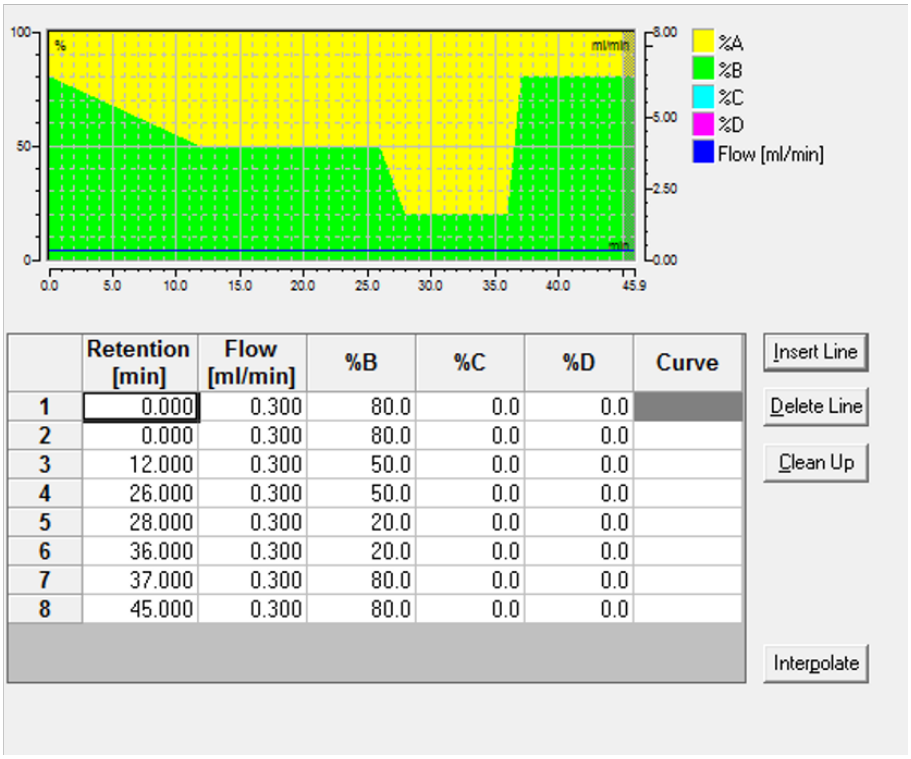

	Retention [min]	Flow [ml/min]	%B	%C	%D	Curve
1	0.000	0.300	80.0	0.0	0.0	
2	0.000	0.300	80.0	0.0	0.0	
3	12.000	0.300	50.0	0.0	0.0	
4	26.000	0.300	50.0	0.0	0.0	
5	28.000	0.300	20.0	0.0	0.0	
6	36.000	0.300	20.0	0.0	0.0	
7	37.000	0.300	80.0	0.0	0.0	
8	45.000	0.300	80.0	0.0	0.0	

Fig. 5.1 Mobile phase gradients for HILIC columns. ***A)*** Mobile phase gradient for ZIC-pHILIC column. B (green): 20 mM ammonium carbonate and 0.05% ammonium hydroxide; C (blue): Acetonitrile. ***B)*** Mobile phase gradient for ZIC-HILIC column. A (yellow): 0.01% formic acid in water; B (green): 0.01% formic acid in acetonitrile.

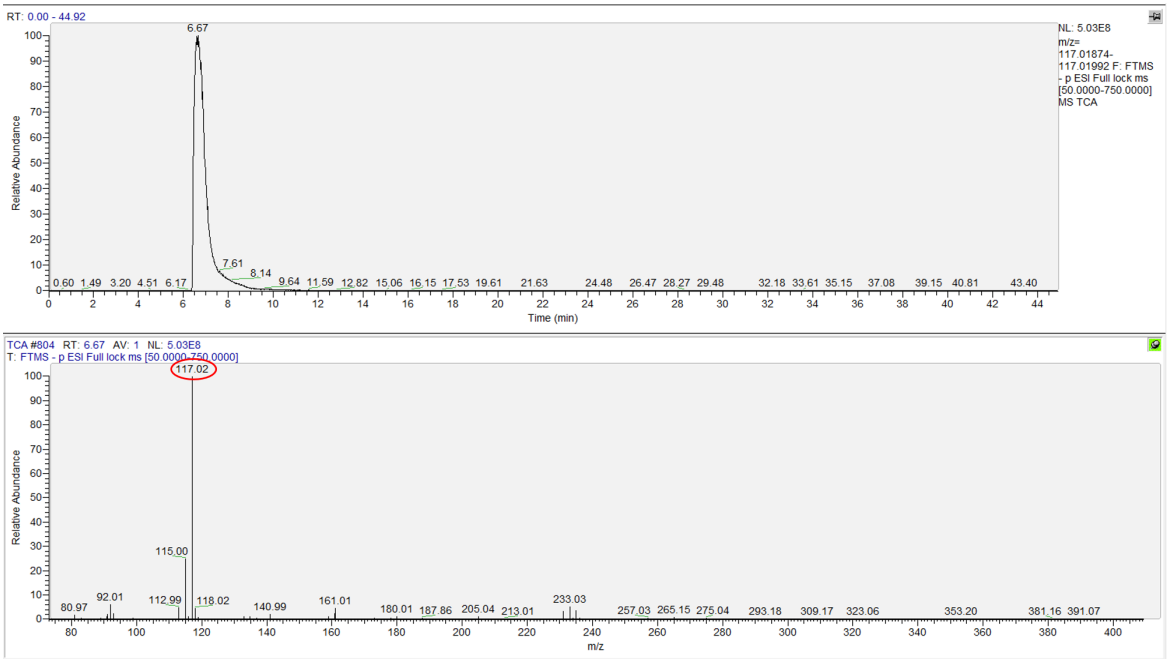

Fig. 5.2 Succinate LC-MS analysis using the ZIC-HILIC column. ***A)*** Chromatogram of peaks with mass:charge ratios (m/z) of 117.01874-117.01992 (m/z of succinate). A peak is seen at retention time (RT) 6.67 min, which is the retention time of succinate on the ZIC-HILIC column. ***B)*** Mass spectra of peaks with RT of 6.67 min. The main ion for succinate is at m/z 117.02 (circled in red). The chromatogram and mass spectra are from a 200 µM succinate standard.

the pKa of these acids and phosphates, negative ions are more easily generated. More basic amino acids and amines perform better on the lower pH of the ZIC-HILIC column (Zhang, 2012). The ZIC-HILIC column is also better for cysteine, cystine, GSH and succinate. Cysteine and GSH are less reactive at the lower pH of the ZIC-HILIC column due to their free thiol groups (Mackay et al., 2015). Fumarate is a difficult metabolite to quantify, as although the peak shape is better on the ZIC-pHILIC column, the high pH of the mobile phase can cause ∼10% of malate to be converted to fumarate (Zhang, 2012), artificially elevating the fumarate signal and depressing the malate signal. To ensure that conversion from malate is not artificially elevating the fumarate signal, the normalised ion intensities for fumarate from both columns are presented to check that they show the same trend. The chromatogram and mass spectrum from a succinate standard are shown in **Figure 5.2**.

This project used the Thermo Q Exactive mass spectrometer with Orbitrap technology, which is a high-resolution mass analyser (>100,000) with accurate mass analysis (<2 ppm) (Mackay et al., 2015). The mass spectrometer was operated in full MS and polarity switching mode, to improve the overall ionisation response for the full range of metabolites to be analysed: amino

acids have a better response in positive ion mode, whereas organic acids and phosphates ionise better in negative ion mode (Mackay et al., 2015). The following sections describe the relevant factors to consider when designing an LC-MS metabolomics experiment.

5.1.2 Metabolite quenching and extraction

Quenching of further metabolism is an important step in any metabolomic study and aims to generate a stable sample that contains an accurate representation of the metabolites in the cell or tissue that is being studied (Dettmer et al., 2007; Jang et al., 2018). Quenching is one of the most crucial steps of a metabolomic analysis to perform correctly, as inefficient quenching can lead to artefactual levels of metabolites and incorrect conclusions. The main challenges are to not perturb metabolite levels and to terminate enzyme activity fast. This can be very difficult in practice as enzymes that have ATP and glucose-6-phosphate as substrates can have extremely high turnover numbers (Lu et al., 2017; Matuszczyk et al., 2015). To successfully quench enzymatic activity, organic solvent, cold, heat, acid or base can be used, alone or in combination (Lu et al., 2017; Zhou et al., 2012). When measuring whole tissue, the tissue sample is rapidly frozen using Wollenberger clamps pre-cooled in liquid nitrogen to increase heat transfer. When working with cells, organic solvent is added directly to the tissue culture plate. Boiling ethanol is another approach and denatures enzymes, but is problematic due to the increased risk of thermal degradation of metabolites. The use of an acidic solvent, such as formic acid or PCA, is a common extraction method to stabilise metabolites and to precipitate protein (Lu et al., 2017).

Once the metabolic activity has been quenched, the metabolites are extracted. The extraction step aims to generate a sample with the representative amounts of metabolites as well as releasing metabolites bound to protein, such as $NADP^+$(Dettmer et al., 2007). Degradation products can be formed if the extraction is performed slowly or not at low enough temperatures, such as adenosine formation from AMP breakdown. Organic solvent mixtures are commonly used as extractants, such as 40:40:20 acetonitrile:methanol:water with 0.1 M formic acid (Lu et al., 2017). The solvent mixture used must often be adapted for the specific metabolites of interest, as no single solvent is efficient at extracting all metabolites. For tissue experiments the frozen tissue can be ground to a powder before addition of the extractant, or can be lysed directly in the extractant.

For extractions using acid, the sample is often neutralised after extraction because some metabolites are prone to acid-catalysed degradation. However, this is not the case for all metabolites and many metabolites are more stable in acidic conditions than basic or neutral conditions, due to the base lability of esters and thioesters. Therefore, to achieve stability for the majority of metabolites, this project used formic acid for quenching and extraction. The volatile formic acid was then evaporated and the dried metabolites were resuspended in water before storage at -80°C (**Section 5.3.2**). After removing the formic acid, the samples retained an acidic pH and were not neutralised as the acidic matrix was thought to be beneficial for stabilising the metabolites during storage. Water-soluble and insoluble metabolites require different solvents for optimal extraction. Therefore, water-insoluble metabolites, such as lipids, will be under-represented in this project due to the single extraction approach. A further consideration for extraction is that redox-active metabolites, such as NADPH and GSH, can be oxidised during the drying step (discussed in **Section 5.3.2**).

5.1.3 Missing value imputation

In large metabolomic datasets, there are often missing values. These can occur for a number of reasons, such as the metabolite is present but at a concentration less than the limit of detection of the method, or because the data processing software did not detect and report the metabolite (Di Guida et al., 2016). It is important to understand the reason behind the missing values, which can be grouped into 3 categories: missing completely at random (MCAR); missing at random (MAR); and missing not at random (MNAR). MCAR occurs when the missing value is not related to any variable or response, MAR is related to one or more variables and MNAR refers to when the missing value is related to the response itself (Di Guida et al., 2016). As such, missing values can be due to biological or technical causes. In order to correct for these values, missing value imputation (MVI) is often applied. This aims to logically replace the missing values with a non-zero value, which will maintain the data structure and allows statistical analyses to be performed (Di Guida et al., 2016). There are several MVI methods, including small value replacement (SV), mean replacement (MN) and median replacement (MD). This project used the SV method, and assigned the smallest detected value of 0.0002% of taurine signal to the missing values.

5.1.4 Normalisation

Ion intensities alone are not sufficient to quantify metabolites, because different metabolites ionise with different efficiencies. This means that the same ion intensity for two different metabolites could represent millimolar and nanomolar concentrations. Furthermore, there is significant variation between different MS runs and detector responses, even on the same machine. Therefore, to quantify metabolites either quantified standards must be added (enabling absolute quantification) or the ion intensities must be normalised to an independent factor, such as protein or another metabolite (termed relative quantification). Absolute values for metabolites can be acquired by comparing the MS signals to internal standards, such as ^{13}C-labelled or deuterated standards, which are added externally to the sample. This must be done before the extraction step to account for losses during the extraction and matrix effects, which occur when the matrix (e.g. the tissue) that is co-extracted with the metabolites interfere with the signal response (Cappiello et al., 2008). Internal standards are not available for all metabolites. As this project aimed to study a very wide range of metabolites and to explore differences between cytosolic and mitochondrial pools, a relative quantification strategy was chosen.

5.2 Aims and Strategy

The first aim of this section was to identify the LC-MS conditions that would yield accurate metabolomic data, such that comparisons and deductions could be drawn on mitochondrial and cytosolic metabolism in tissues. The second aim was to identify if the procedure is performed sufficiently quickly or whether transport inhibitors are required to prevent metabolite distribution. The strategy employed to optimise the sample preparation, LC-MS analysis protocol and the normalisation method was to focus on a selected group of specific metabolites to assess how well the procedure was working. These metabolites were taurine, GSH and succinate. All of these metabolites are abundant and are either relevant for normalisation purposes (taurine), susceptible to oxidation and are thus an insightful readout on the speed of the method (GSH and succinate) or relevant to the goal of studying mitochondrial metabolism (succinate). Other metabolites were also studied further, depending on the preliminary experimental aim. To address the second aim, the metabolite transport inhibitors pyridoxal phosphate (PRP), N-ethylmaleimide (NEM), butylmalonate (BTM) and respiratory

inhibitors oligomycin and carboxyatractyloside (CATR) were added to the homogenisation buffer of mouse heart and liver and the metabolites were measured by LC-MS, or via the ATP and ADP assay for oligomycin and CATR.

5.3 Metabolomic analysis

5.3.1 Sample analysis & data normalisation

Often, in metabolomic LC-MS analysis, either a standard curve of metabolites is run to enable metabolite quantification or the data is normalised to protein concentration. Using the rapid isolation procedure means it is not possible to normalise to protein because the amount of mitochondria that pass through the oil is variable, and damaged mitochondria (which may have lost their metabolites) also pass through the oil (described in **Section 4.5**). Therefore, the metabolites must be normalised to a parameter that will behave in the same way to them, i.e. another metabolite. This metabolite should be relatively metabolically inactive; abundant for ease of LC-MS measurement; have similar concentrations in the mitochondria and the cytosol and/or have a slow transport system between these compartments. Metabolite candidates that fit this description include GSH and taurine. These metabolites should also remain stable during conditions such as ischaemia, thus enabling changes in other metabolites to be attributed to ischaemia alone.

GSH is an important antioxidant in mitochondria, but is synthesised in the cytosol, leading to both mitochondrial and cytosolic pools of GSH. Therefore, to enter the mitochondria there must be a transport system. The OGC and DIC were thought to transport GSH, but this has been disproved and the identity of the GSH transporter remains unknown (Booty et al., 2015). Previous work in this lab has calculated the mitochondrial GSH concentration is in the range of 1-5 mM (Booty et al., 2019), which is abundant enough to be easily measured by LC-MS under most conditions. 95-99% of the glutathione pool is in the reduced GSH form (Booty et al., 2015), with the rest as glutathione disulphide (GSSG). The cytosolic GSH concentration is thought to be similar to the mitochondrial concentration, between 1-10 mM (Mari et al., 2009; Ribas et al., 2014; Smith et al., 1996). However, normalising to GSH gave inconsistent results, possibly due to oxidation to GSSG and therefore it was not used here.

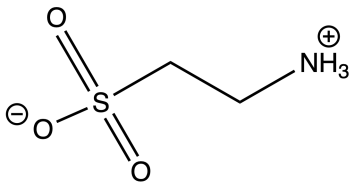

Fig. 5.3 The structure of taurine. Taurine is a sulphur-containing amino acid.

Taurine is an appealing candidate for normalisation, even though the metabolic role of taurine is not well established. Taurine is a sulphur-containing amino acid (**Figure 5.3**) which is known to be present in mammalian cells at high concentrations, up to 20-50 mM in leukocytes (Schuller-Levis, Park, 2003) and in heart tissue it has been reported at levels of 6.5 mmol/kg wet weight in human and 33.9 mmol/kg wet weight in mouse (Chapman et al., 1993). Its zwitterionic nature prevents it crossing lipid membranes and necessitates its specific transporter (TauT) to cross the PM (Lambert, 2004; Ripps, Shen, 2012; Warskulat et al., 2004). Taurine is known to be present at high concentrations inside the mitochondria, despite the fact that the mitochondrial taurine transporter has not been identified yet (Hansen et al., 2010). It is an important osmolyte (Lambert, 2004) and antioxidant (Jong et al., 2012), with a role in oxidative tissues (Hansen et al., 2010).

Succinate is known to be distributed across the cell in both the mitochondria and the cytosol, and to be transported out of the mitochondria via the DIC (Murphy, O'Neill, 2018), (**Section 1.5.2.4**). It is thought to act as an electron sink during ischaemia (Chouchani et al., 2014). It is known to have a role in the HIF-1α pathway by inhibiting PHD activity, stabilising and activating HIF-1α (Tannahill et al., 2013). It has also been implicated in inflammation (Mills, O'Neill, 2014). Studies into the behaviour of succinate would aid understanding of its involvement in these areas.

Figure 5.4 displays the raw ion intensities of taurine in the heart and liver, from both column analyses. It shows that in the heart, the taurine signal is significantly lower in the normoxic and ischaemic mitochondrial fractions than the other fractions. As taurine is relatively stable, this implies that there was less sample loaded onto the MS for these samples, further emphasising the need for normalisation. In the liver, this difference is less pronounced.

To ensure that any trends that were inferred from this normalisation were not merely due to changes in the taurine pool, the raw ion intensities of the metabolites were also analysed. As an example, the raw and normalised signals of succinate (ZIC-HILIC column) and malate (ZIC-pHILIC column) from the heart and liver are displayed in **Figures 5.5 and 5.6**. In

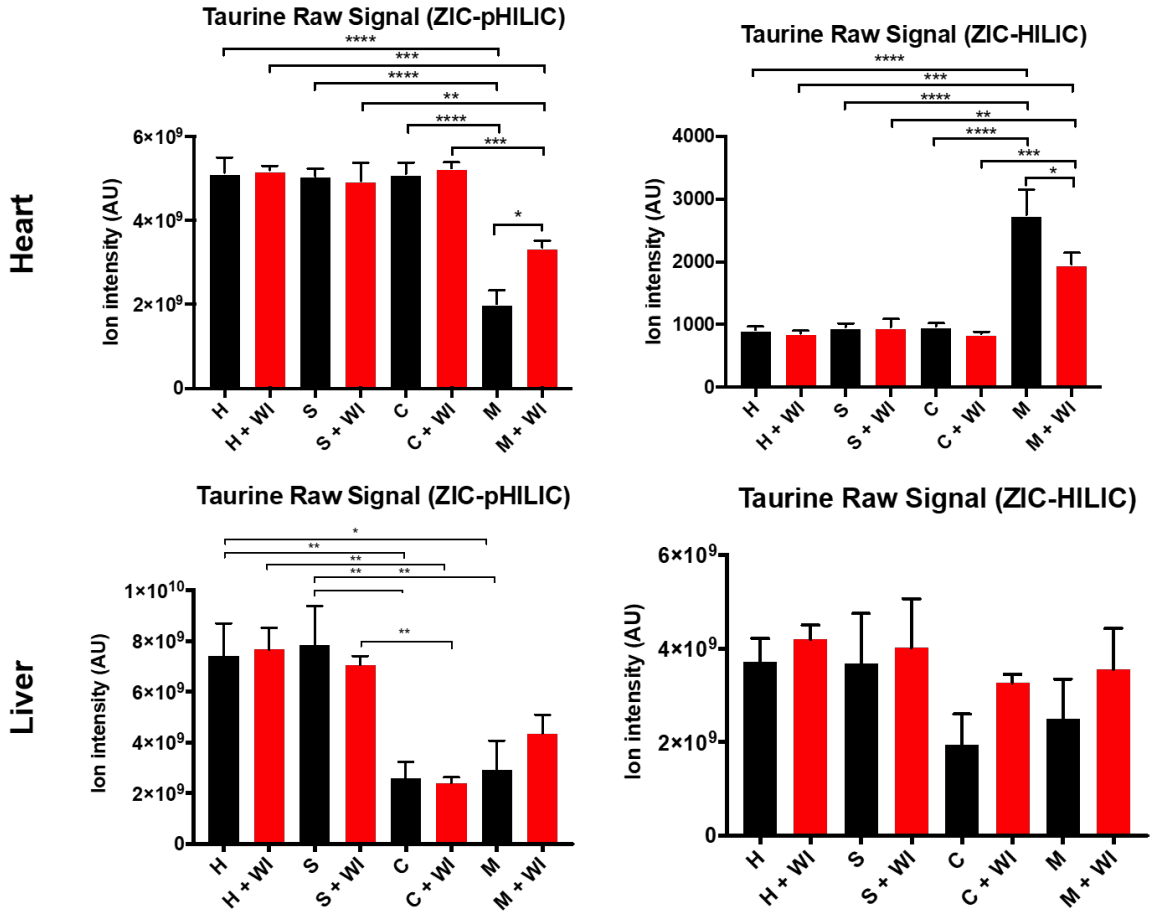

Fig. 5.4 Ion intensities of taurine from both column analyses in heart and liver. The ion intensities of taurine from heart (top) and liver (bottom) datasets in all fractions. For heart, data is average of 6 biological replicates, displayed as mean ±SEM and for liver, data is average of 3 biological replicates, displayed as mean ±SEM. The statistical differences between the fractions were analysed by a two-way ANOVA. H: Homogenate; S: Supernatant; C: Cytosolic fraction; M: Mitochondrial fraction; WI: Warm ischaemia.

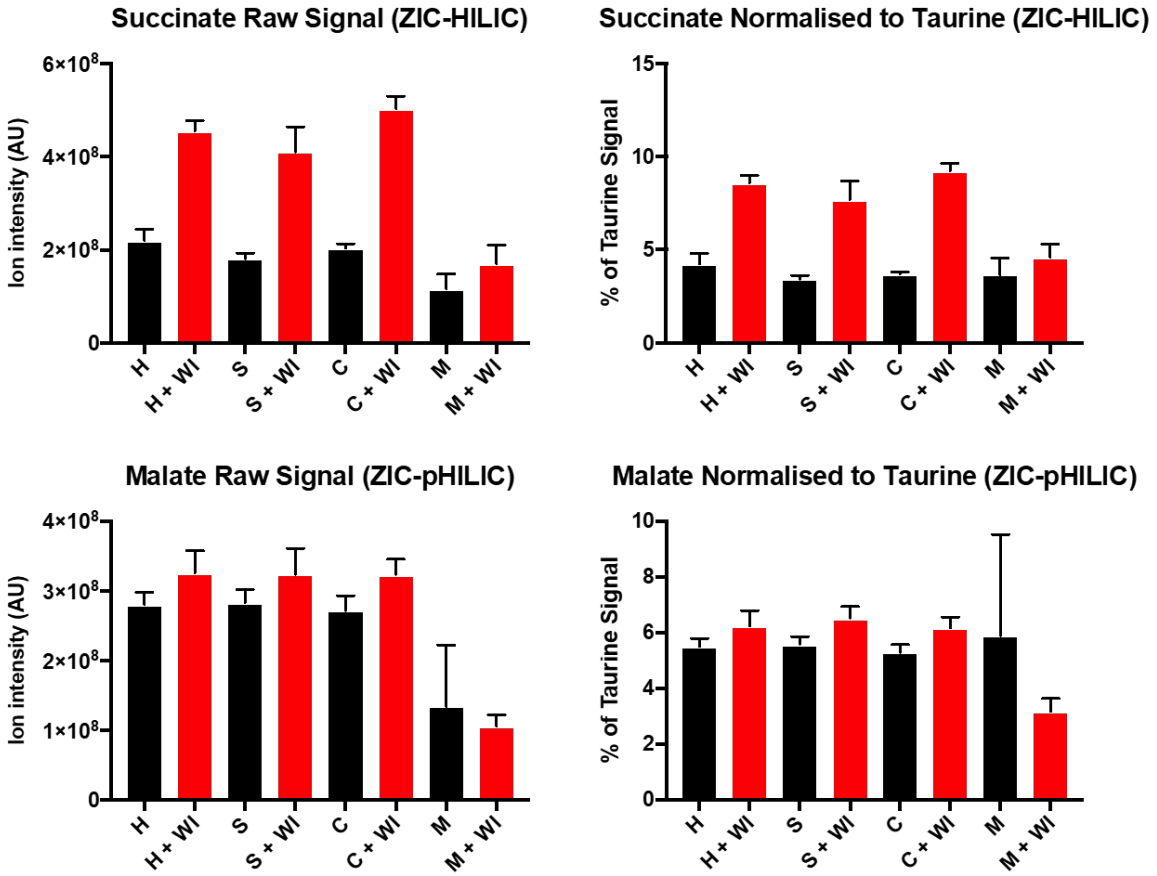

Fig. 5.5 Comparison of raw and taurine-normalised ion intensities in heart. The raw and taurine-normalised ion intensity of a metabolite from each column was compared to ensure normalisation to taurine does not alter the trend. Data is average of 6 biological replicates, presented as mean ±SEM. H: Homogenate; S: Supernatant; C: Cytosolic fraction; M: Mitochondrial fraction; WI: Warm ischaemia.

applying these analytical approaches, I had to be very cautious about interpretation because if a metabolite has a higher ion intensity than taurine or another metabolite, it does not necessarily mean that it is present at a higher concentration, but may merely indicate that it ionises or is detected by the MS more efficiently than the other metabolite. Taurine levels may be different between the heart and the liver. This means that to make comparisons between these tissues only the trends, and not the percentage of the taurine signal, can be compared.

Both the ZIC-HILIC and ZIC-pHILIC columns were used to increase the range of metabolite classes that could be analysed (discussed in **Section 5.1.1**). Initial work was performed by normalising metabolites from either the ZIC-pHILIC or ZIC-HILIC column to taurine on

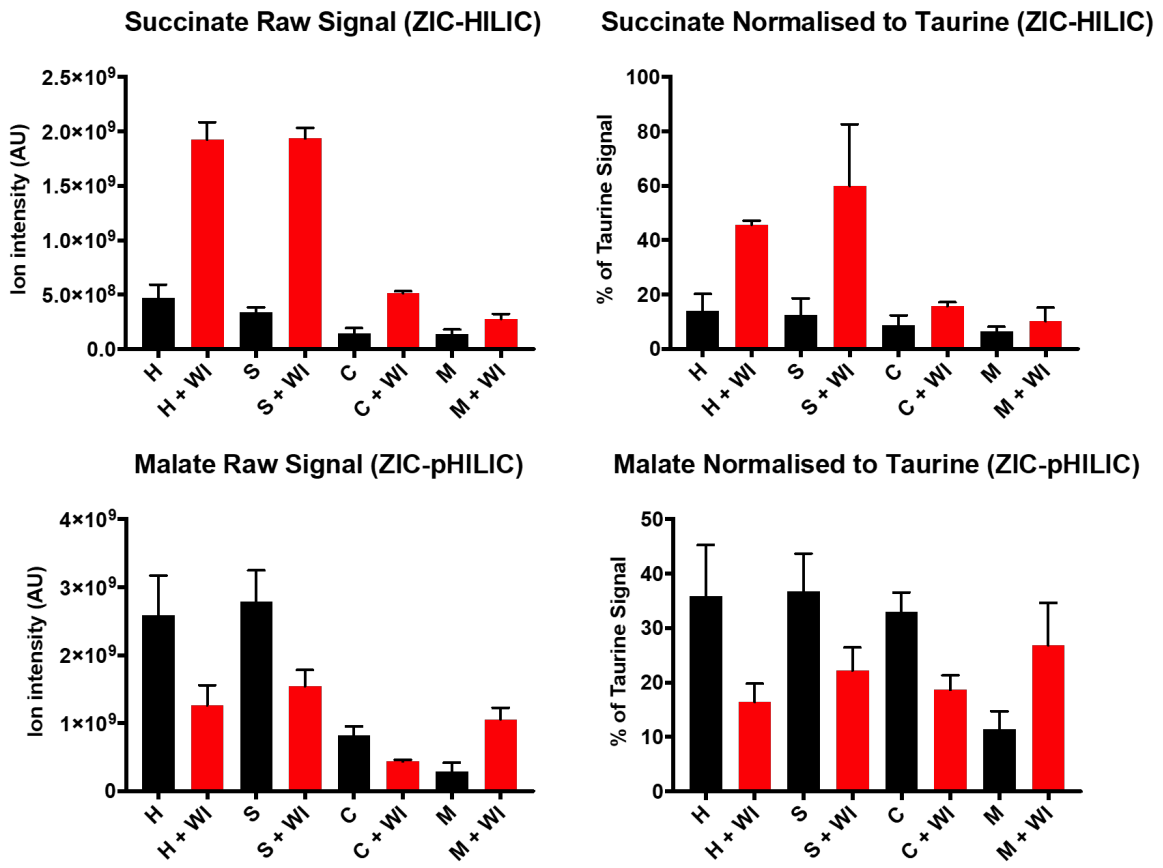

Fig. 5.6 Comparison of raw and taurine-normalised ion intensities in liver. The raw and taurine-normalised ion intensity of a metabolite from each column was compared to ensure normalisation to taurine does not alter the trend. Data is average of 3 biological replicates, presented as mean ±SEM. H: Homogenate; S: Supernatant; C: Cytosolic fraction; M: Mitochondrial fraction; WI: Warm ischaemia.

one column only. To investigate if this was appropriate, the raw ion intensities from the ZIC-HILIC column were plotted against the raw ion intensities from the ZIC-pHILIC column for GSH, taurine, succinate, glutamate and lactate. Glutamate was included in the select group of metabolites due to its abundance and involvement in mitochondrial metabolism (Frigerio et al., 2008). Lactate was informative as it accumulates during hypoxia and ischaemia and so was an indicator of the speed of the extraction, and should not accumulate to high levels inside the mitochondria (Chen et al., 2016a). However, **Figure 5.7** shows there is limited correlation between ion intensities between the ZIC-pHILIC and ZIC-HILIC columns. Some metabolites exhibited a strong correlation between the columns, e.g. lactate had an r^2 value of 0.9542 and the r^2 value for succinate was 0.9126. However, other metabolites showed very poor correlation, such as GSH (r^2 = 0.1854). This poor correlation means normalising across the columns is not appropriate. Instead, metabolites should be normalised to a metabolite from the same column. The ZIC-pHILIC column demonstrated the most consistent data and covers a broad range of metabolites, so the majority of metabolites were analysed using data from the ZIC-pHILIC column only. There are two main differences between the columns: the mobile phase pH and the internal diameter of the column. The mobile phase for the ZIC-pHILIC column was pH 9.5, whereas the ZIC-HILIC column mobile phase was only pH 2.6. It may be that some precipitation occurs at the extreme pH level of the ZIC-HILIC which interferes with the detection of certain metabolites. The internal diameter of the ZIC-HILIC is 4.6 mm, whereas the ZIC-pHILIC is 2.1 mm. The larger diameter results in more sample dispersion which is not good for low abundance compounds, which could be why the ZIC-pHILIC produced better signals overall. Therefore, the majority of metabolites were analysed from the ZIC-pHILIC column, with the exception of individual metabolites of importance that performed better on the ZIC-HILIC column, such as succinate.

5.3.2 Optimisation of LC-MS sample preparation

LC-MS experiments were performed in collaboration with Ana S. H. Costa and Efterpi Nikitopolou (MRC Cancer Unit, University of Cambridge). Preliminary mitochondrial samples for LC-MS were prepared by centrifuging the mitochondria through oil into formic acid (23% for liver and 15% for heart), removing the oil and briefly centrifuging the resulting formic acid extract (1 min, 10,000 x g, 4°C) to remove particulates. Similarly, homogenate, supernatant and cytosolic samples were prepared by placing 10 µL of each fraction into 100 µL of formic acid (23% for liver and 15% for heart) and centrifuging. These samples had

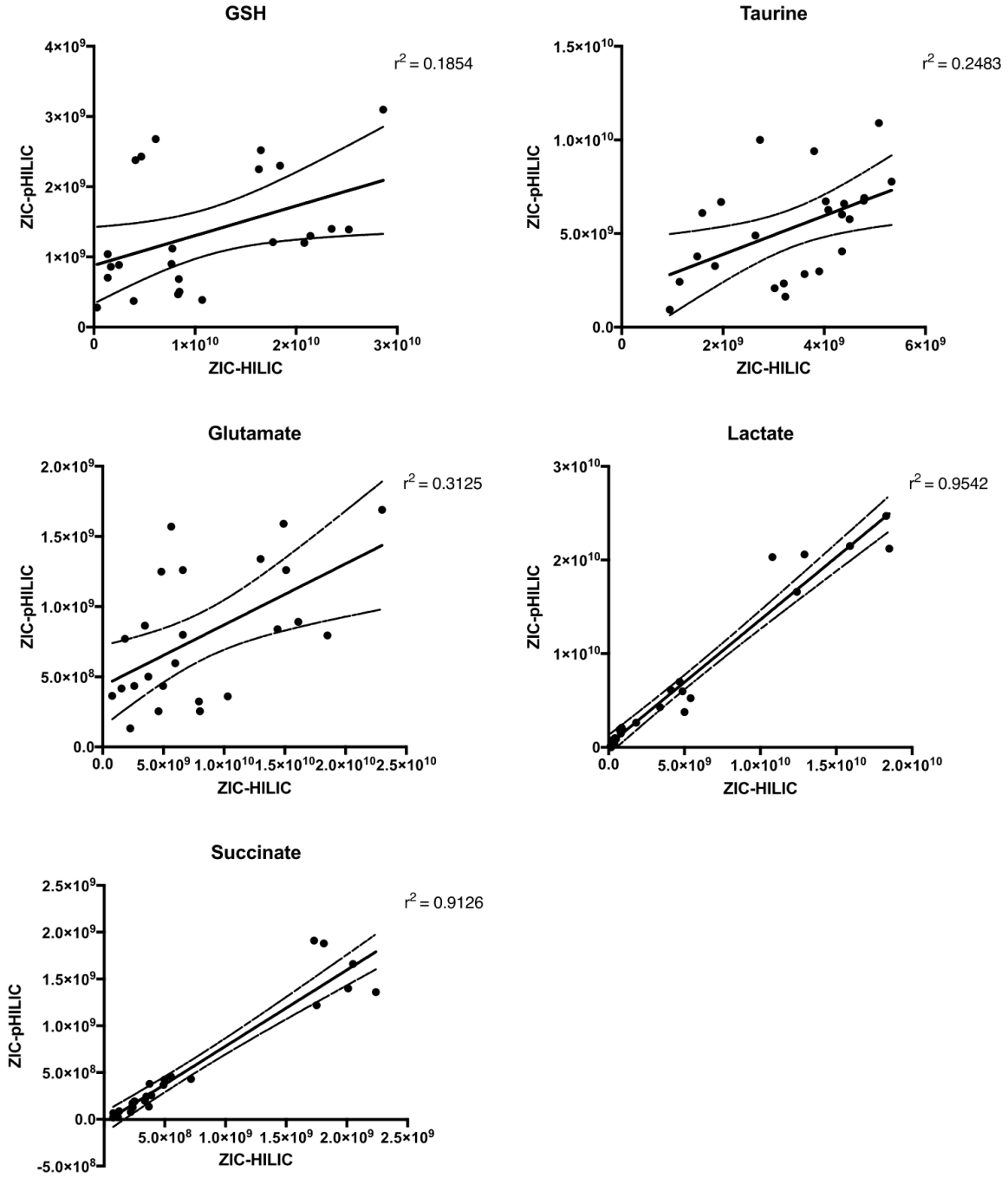

Fig. 5.7 Correlation of ion intensities between ZIC-pHILIC and ZIC-HILIC columns. Raw ion intensities (AU) for GSH, taurine, glutamate, lactate and succinate across all 4 fractions of 6 mouse liver mitochondria isolations from the ZIC-HILIC column were plotted against raw ion intensities for the ZIC-pHILIC column. Lines of 95% confidence intervals are shown, n= 6 biological replicates.

different retention times to the standards run in parallel, as well as variable and low MS signals for many metabolites. This made analysis and quantification difficult and produced variable results. It was hypothesised that the different retention times could have been due to differences in pH, caused by the formic acid in the samples. The experiment was repeated and the formic acid was evaporated from the samples under vacuum (4 hours, ∼40°C) before resuspension in 75 µL ultrapure H_2O to increase the pH. This resolved the retention times of the metabolites to match the standards, but low metabolite yields and MS signals remained an issue.

It was hypothesised that using a different extraction approach may increase metabolite yields and MS signals. To investigate, a rapid mouse liver isolation was performed, with 4 isolation experiments run per mouse. Of these 4 isolations, 2 of them had their mitochondrial fractions pooled prior to the drying step, and after evaporation of the formic acid they were resuspended in 75 µL ultrapure H_2O. The remaining 2 isolations were not pooled, and after evaporation of the formic acid 1 was resuspended in 75 µL ultrapure H_2O and the other was resuspended in 75 µL MS extraction solution (50 % methanol, 30 % acetonitrile, 20 % ultrapure H_2O, 100 ng/mL HEPES). This is a commonly used extraction solution, in which HEPES is added as an internal standard and was used by this lab in Chouchani et al. (2014). **Figure 5.8** shows unexpectedly that using the MS extraction solution does not seem beneficial and for some metabolites it reduces the signal, particularly in mitochondrial samples. Therefore, all subsequent samples were resuspended in water after evaporation of the formic acid. Although this experiment was performed on only 1 biological replicate, pooling the mitochondrial samples increased the signal for taurine and glutamate (**Figure 5.8**) and other metabolites, so subsequently 4 mitochondrial isolations per mouse were run in parallel and pooled to increase the signal for mitochondrial metabolites. 4 isolations was chosen because it was the maximum amount of isolations that could be run in parallel without impacting too much on the speed of the procedure. Accordingly, the amount of homogenate and supernatant signal was increased by adding 40 µL of homogenate or supernatant to 400 µL of formic acid, before vortexing and drying, then resuspending in 75 µL of H_2O. The samples were kept in agitation for 10 min at 4°C to aid metabolite resuspension, before a 1 min centrifugation at 17,000 x g to remove any remaining particulates. The supernatants were transferred to MS vials and stored at -80°C until analysis by LC-MS.

When evaporating the formic acid, a balance must be obtained between time and temperature, especially considering that the vacuum concentrator is not a perfect vacuum and so some oxygen is present. A higher temperature means the sample will dry quicker and be

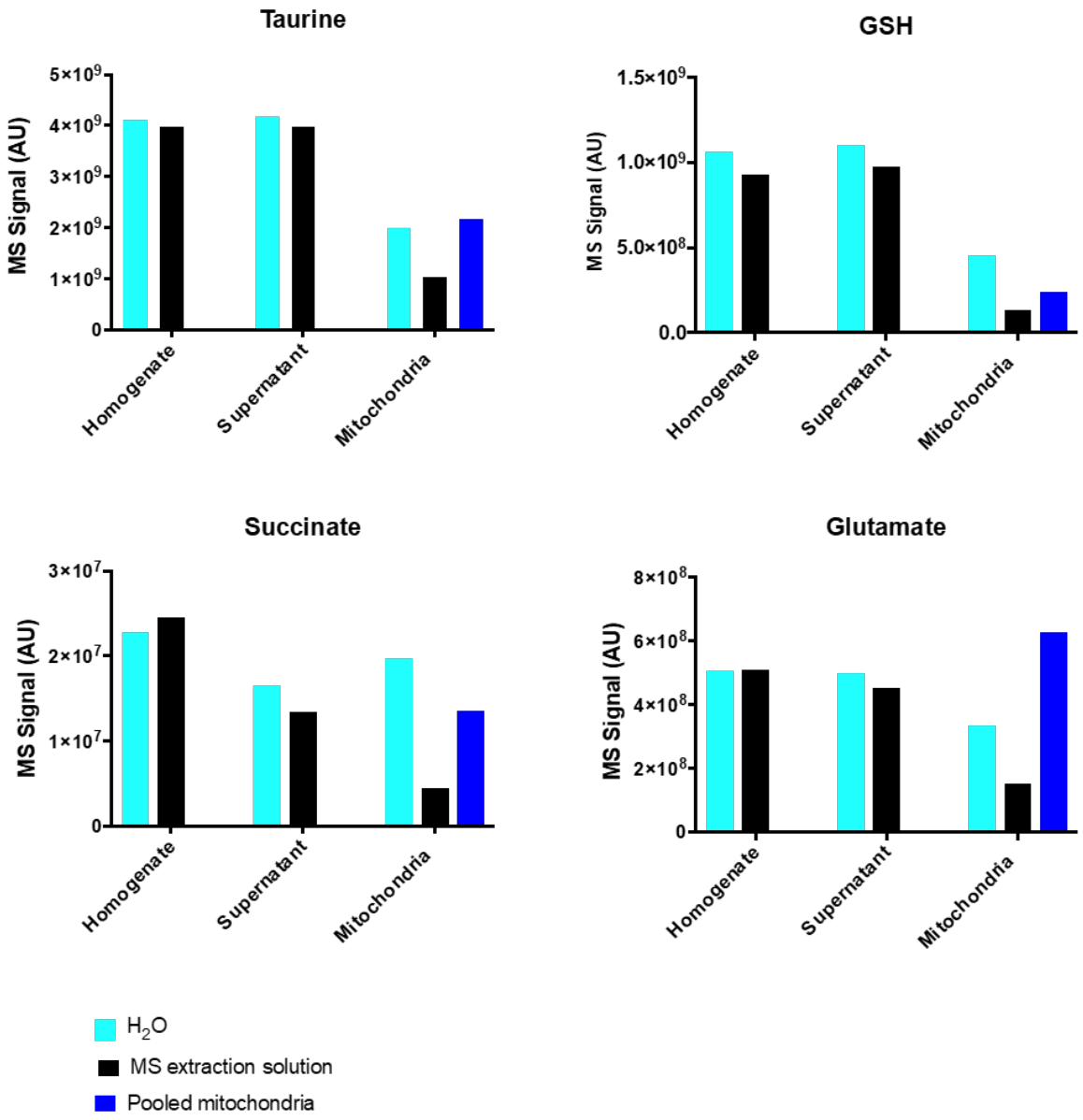

Fig. 5.8 Use of MS extraction solution to resuspend dried metabolites. Mitochondria were rapidly isolated from mouse liver. 10 µL of homogenate and homogenate supernatant were placed in 100 µL of 25 % formic acid. All fractions were centrifuged at maximum speed for 10 min before the supernatant was removed and dried under vacuum. For the pooled mitochondrial sample 2 mitochondrial samples were pooled before the drying step. Dried samples were either resuspended in 75 µL of H_2O or 75 µL of MS extraction solution (50% methanol, 30% acetonitrile, 20% ultrapure water, 100 ng/mL HEPES) and sent for MS analysis. Samples extracted with MS extraction solution were centrifuged for 10 min at full speed before incubation at -20°C for 1 hour. The pooled mitochondria were resuspended in 75 µL H_2O. All samples were kept in agitation for 15 min at 4°C then centrifuged for 10 min to remove debris. The supernatants were transferred to MS vials and analysed by LC-MS. n=1 biological replicate.

exposed to oxygen for a shorter period but the higher temperature makes it more likely for reactions to occur within the sample, especially as they become more concentrated. Using a lower temperature would reduce the rate of reaction but would increase the time it takes to evaporate and therefore time exposed to oxygen. Drying the metabolites for 4 hours, with the temperature capped at 40°C, was found to dry the metabolites completely without excess metabolic activity (confirmed by the lack of adenine nucleotide breakdown products such as xanthine and hypoxanthine).

5.3.3 Optimised sample preparation and analysis protocol

Based on the above experiments the isolation procedure was adapted so that 4 isolation experiments were run in parallel per mouse. The optimised protocol for LC-MS sample preparation is shown in **Figure 5.9**. Mitochondria were centrifuged into 100 µL of 25% (liver) or 15% (heart) formic acid, to quench and extract the metabolites. To match the mitochondrial volume, 40 µL of homogenate, supernatant and cytosolic fractions were added to 400 µL of 25% (liver) or 15% (heart) formic acid. All fractions were centrifuged for 10 min at 17,000 x g at 4°C to remove any particulates that may block the LC column. The supernatants from the homogenate, supernatant and cytosolic fractions were removed into fresh Eppendorf tubes, and the supernatants from the 4 mitochondrial samples were pooled into the same tube. After drying under vacuum for 4 hours at ∼40°C, the metabolites were resuspended in 75 µL of H_2O. The samples were kept in agitation for 10 min at 4°C, centrifuged for 1 min at 17,000 x g, 4°C and the supernatants were transferred to MS vials.

The raw ion intensities for metabolites were normalised to both taurine and GSH ion intensities from the same column (i.e. the ion intensity for succinate from the ZIC-HILIC column was normalised to the taurine and GSH ion intensity from the ZIC-HILIC column, and the ion intensity for succinate from the ZIC-pHILIC column was normalised to the taurine and GSH ion intensity from the ZIC-pHILIC column). In general, most metabolites were analysed using data from the ZIC-pHILIC column. However, for some metabolites, such as succinate and fumarate, the ZIC-HILIC column data was also used as this column is preferable for some metabolites (discussed in **Section 5.3.1**).

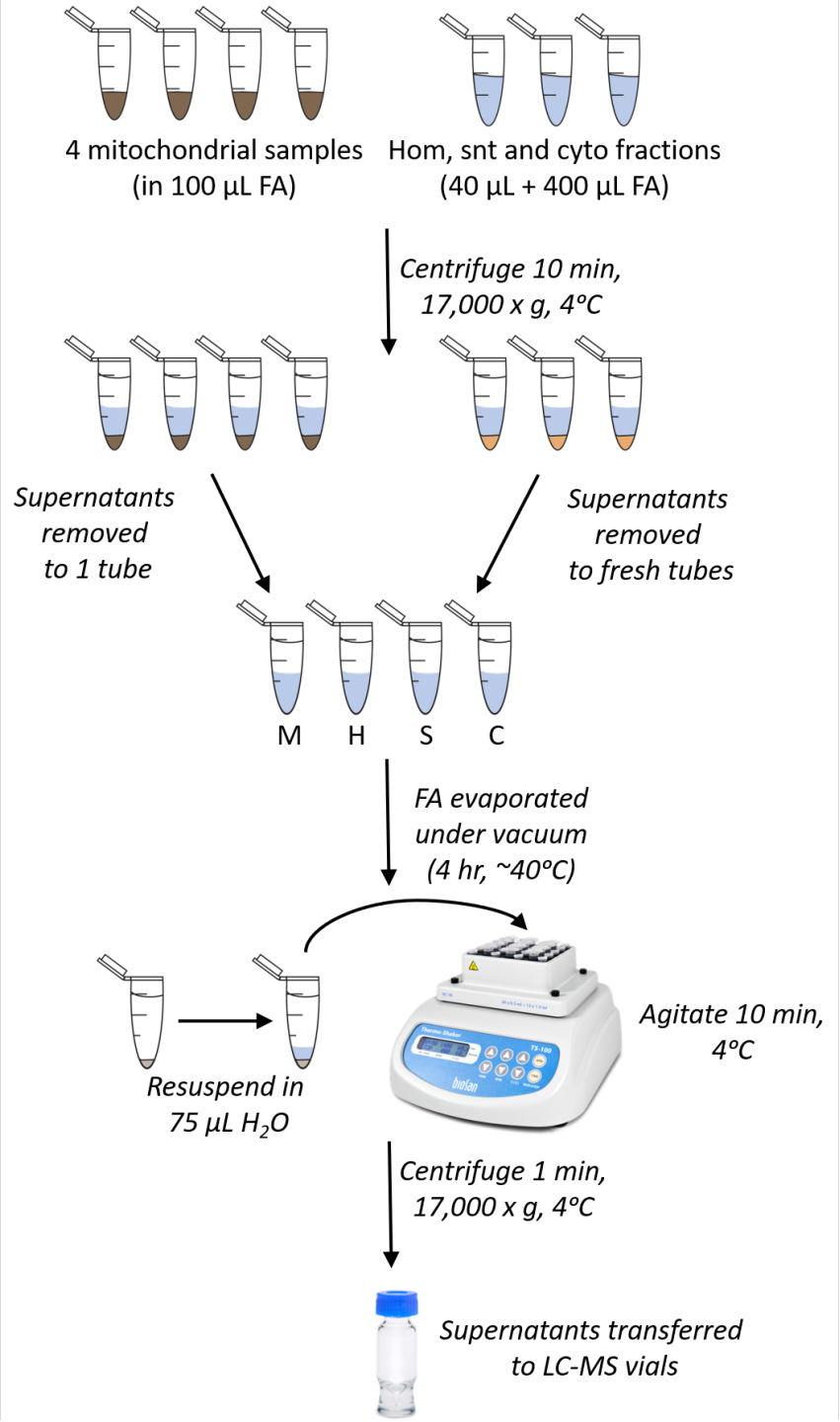

Fig. 5.9 LC-MS sample preparation protocol. 4 isolation experiments per animal were run in parallel. 40 µL of homogenate, supernatant and cytosolic fraction was added to 400 µL of 25% (liver) or 15% (heart) to extract the metabolites. All 4 mitochondrial samples as well as the homogenate, supernatant and cytosolic extracted samples were centrifuged for 10 min at 17,000 x g, 4°C. The supernatants from the mitochondrial samples were pooled into the same fresh 1.5 mL Eppendorf tube, and the supernatants from the other fractions were removed into fresh tubes. The FA was evaporated under vacuum (4 hr, 40°C) and the dried metabolites were resuspended in 75 µL of H_2O under agitation for 10 min at 4°C. After a 1 min centrifuge at 17,000 x g, 4°C the supernatants were transferred to LC-MS vials and stored at -80°C until LC-MS analysis. FA: formic acid; M: mitochondria; H: homogenate; S: supernatant; C: cytosol.

5.4 Effect of transport and respiratory inhibitors on metabolite retention

Attempts were made to carry out the mitochondrial isolation from tissue as quickly as possible with rapid cooling in order to quench metabolism. The heart is placed in ice-cold buffer within 25 sec and the liver within 30 sec of culling the animal, and both are fully homogenised in ice-cold buffer within 1.5 min of culling. However, it could be that this is not sufficient to quench metabolism or limit metabolite distribution. To identify whether metabolism is indeed quenched by rapid cooling, a range of respiratory and transport inhibitors were added to the homogenisation buffer prior to homogenisation to see if they further affected metabolite distribution in addition to cooling. The results were assessed by LC-MS with a focus on succinate. This is a metabolite of interest because it is known to be distributed between the mitochondria and the cytosol and is elevated during ischaemia. The hypothesis was that if the procedure is successfully quenching metabolism and limiting the exchange of metabolites across the MIM, then there should be no difference between the relative amounts of metabolites between samples that contained inhibitors and control samples (**Figure 5.10**).

5.4.1 Time dependence of extraction

To determine the extent of the time dependence of the isolation procedure, homogenised mouse liver was left for 10 min on ice before continuing with the rapid mitochondrial isolation procedure. The results are shown in **Figure 5.11** and show that in general, after 10 min left on ice the level of metabolites are very similar to those processed immediately, or are only slightly lower. Therefore, the most time-sensitive step of the procedure is to get the tissue homogenised because this speeds up the cooling of the whole organ, similar to freeze-clamping the organ with Wollenberger clamps.

The cooling that occurs during homogenisation slows metabolism and helps prevent metabolite distribution by reducing the activity of metabolite transporters. Homogenising also prevents metabolite distribution by limiting the exchange of metabolites across the MIM because the concentration of metabolites outside the mitochondria is diluted in the large volume of buffer, reducing the driving force of these exchangers. Thus, mitochondrial metabolites

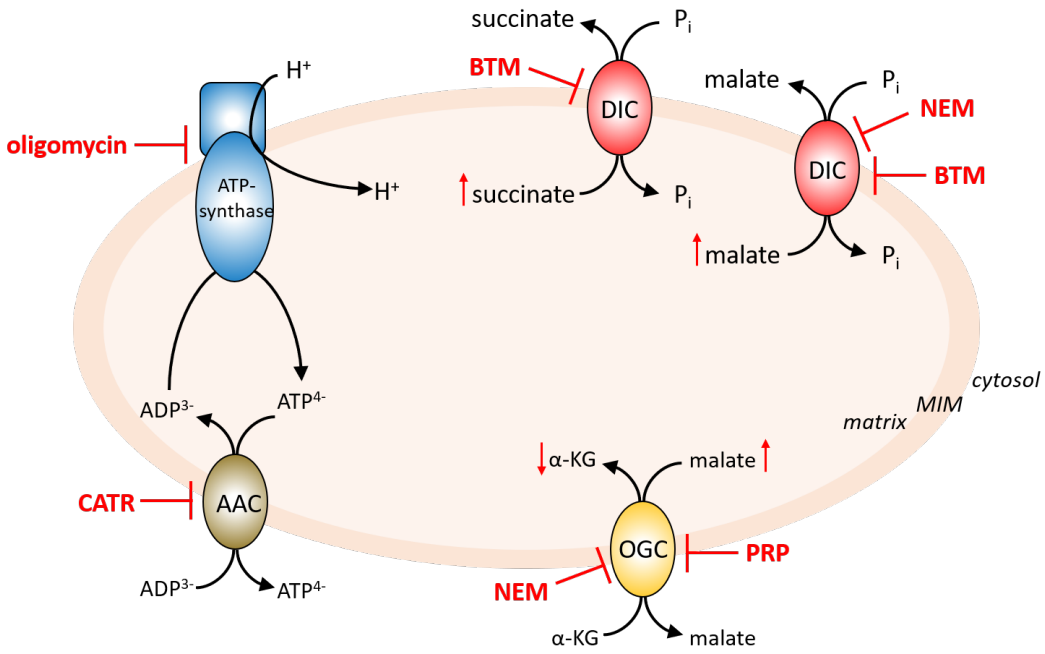

Fig. 5.10 Schematic of transport inhibitors used. Butylmalonate (BTM) inhibits the dicarboxylate carrier (DIC), which transports succinate and malate in exchange for P_i. Pyridoxal 5'-phosphate (PRP) inhibits transporters containing lysine residues, such as the oxoglutarate carrier (OGC). Carboxyatractyloside (CATR) inhibits the ATP/ADP carrier (AAC). Oligomycin inhibits ATP-synthase. N-ethylmaleimide (NEM) is a general transport inhibitor and will affect many transporters, either through direct inhibition or indirectly affecting ion transporters which influence their activity. If the rapid isolation procedure is not quenching metabolism then adding the inhibitors should have the following effects in the mitochondria - BTM: elevated succinate and malate; PRP: reduced α-ketoglutarate (αKG) and increased malate; CATR and oligomycin: increased adenine nucleotide pools.

should remain trapped inside the matrix. To investigate the activity of these transporters further, various transport and respiratory inhibitors were added to the homogenisation buffer.

5.4.2 Butylmalonate

Butylmalonate (BTM) is an inhibitor of the DIC. It was added to the homogenisation buffer to determine whether dicarboxylates (i.e. succinate and malate) are lost during the mitochondrial isolation procedure. It was hypothesised that if the DIC is exchanging dicarboxylates across the MIM during the procedure, leading to loss of some metabolites, then adding BTM should increase the amount seen in the mitochondrial fraction. By blocking mitochondrial

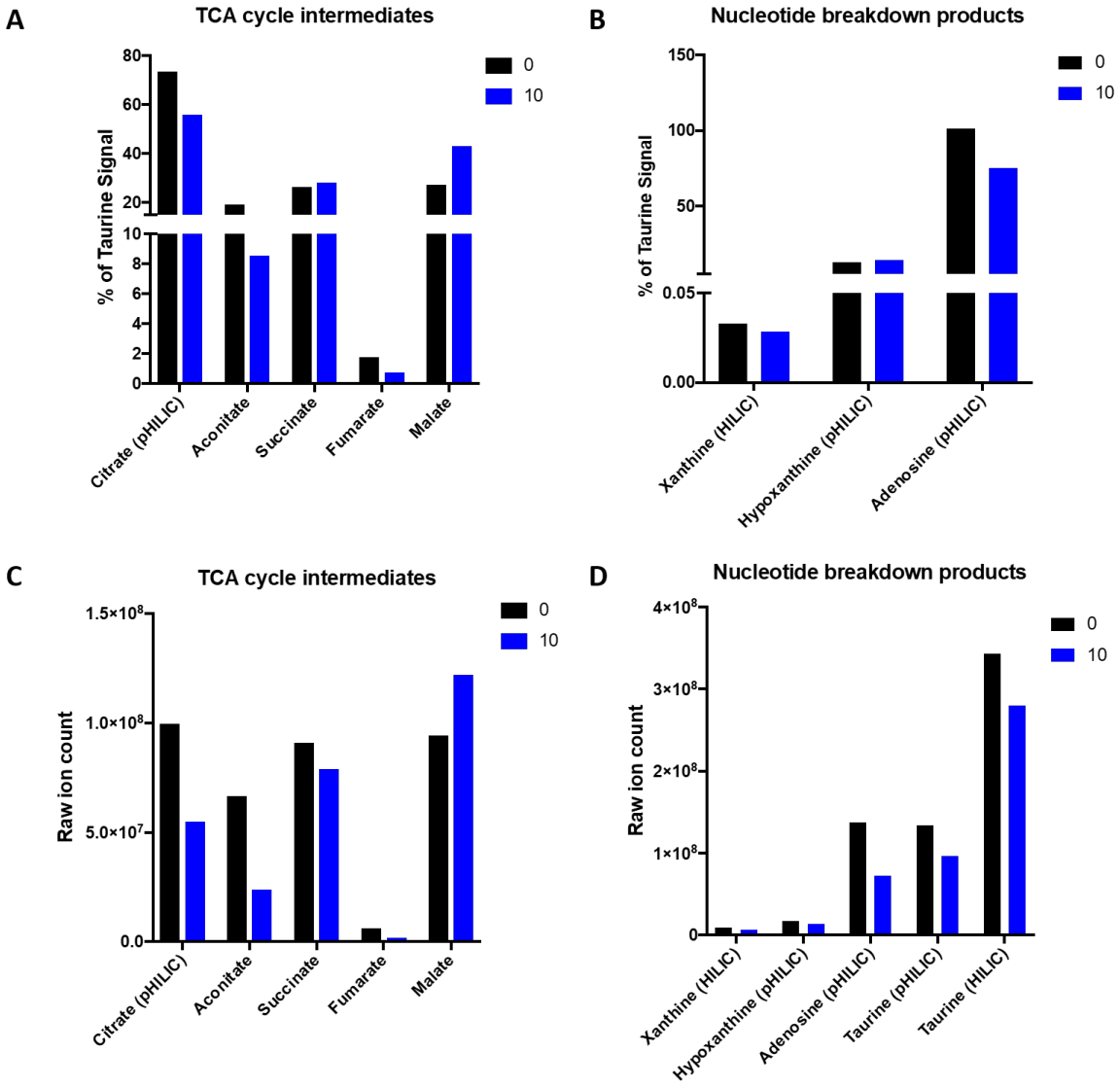

Fig. 5.11 LC-MS analysis of TCA cycle intermediates and nucleotide breakdown products after 10 min on ice. Mouse liver mitochondria were rapidly isolated from 2 mice, except one was processed immediately and for the other the homogenate was left on ice for 10 min before isolating the mitochondria. The metabolites were analysed by LC-MS and normalised to taurine. ***A)*** TCA cycle intermediates normalised to taurine; ***B)*** Nucleotide breakdown products normalised to taurine; ***C)*** raw ion intensities of TCA cycle intermediates; ***D)*** Raw ion intensities of nucleotide breakdown products. Unless otherwise specified data is from the ZIC-HILIC column. n=1.

dicarboxylate transport, the exchange of some metabolites between the mitochondria and the cytosol is slowed down.

As a mouse heart weighs ∼200 mg (Wettmarshausen, Perocchi, 2017) it was estimated there are 40 nmol of succinate in a mouse heart. This was based on the approximate value of 1 mg

tissue equating to ∼1 µL volume and the published value of 200 µmol/L succinate in whole tissue (Martin et al., 2019). As a whole heart is placed in 3 mL of homogenisation buffer the succinate concentration in the homogenate is estimated as 13.3 nmol/mL succinate (13 µM). 500 µM butylmalonate was added (a 50 X excess over succinate). This concentration was chosen as the IC50 of BTM is 0.99 mM at 1 mM succinate (in rat liver mitochondria) (Hiran Prag, unpublished work), therefore 500 µM BTM should be sufficient to block the DIC.

As a mouse liver weighs ∼1 g (Wettmarshausen, Perocchi, 2017) it was estimated there are 200 nmol of succinate in a mouse liver. This calculation was based on the same values as used for the heart calculations: 200 µmol/L succinate in whole tissue, 1 mL volume in mouse liver = 200 nmol. As a whole liver is placed in 5 mL of homogenisation buffer there was an estimated 40 nmol/mL succinate (40 µM) in the whole liver homogenate. 500 µM of BTM (∼10 X excess over succinate) was hypothesised to be a large enough excess to inhibit the carrier.

Figure 5.12 demonstrates that the addition of BTM does not significantly increase the amount of succinate inside the mitochondria, indicating there is minimal dicarboxylate loss during the extraction process. This is probably due to the temperature being suitably low and the lack of substrates available for exchange on the other side of the membrane (phosphate, sulphate and thiosulphate, **Table 1.2**). Across other metabolites there is no effect from the addition of BTM.

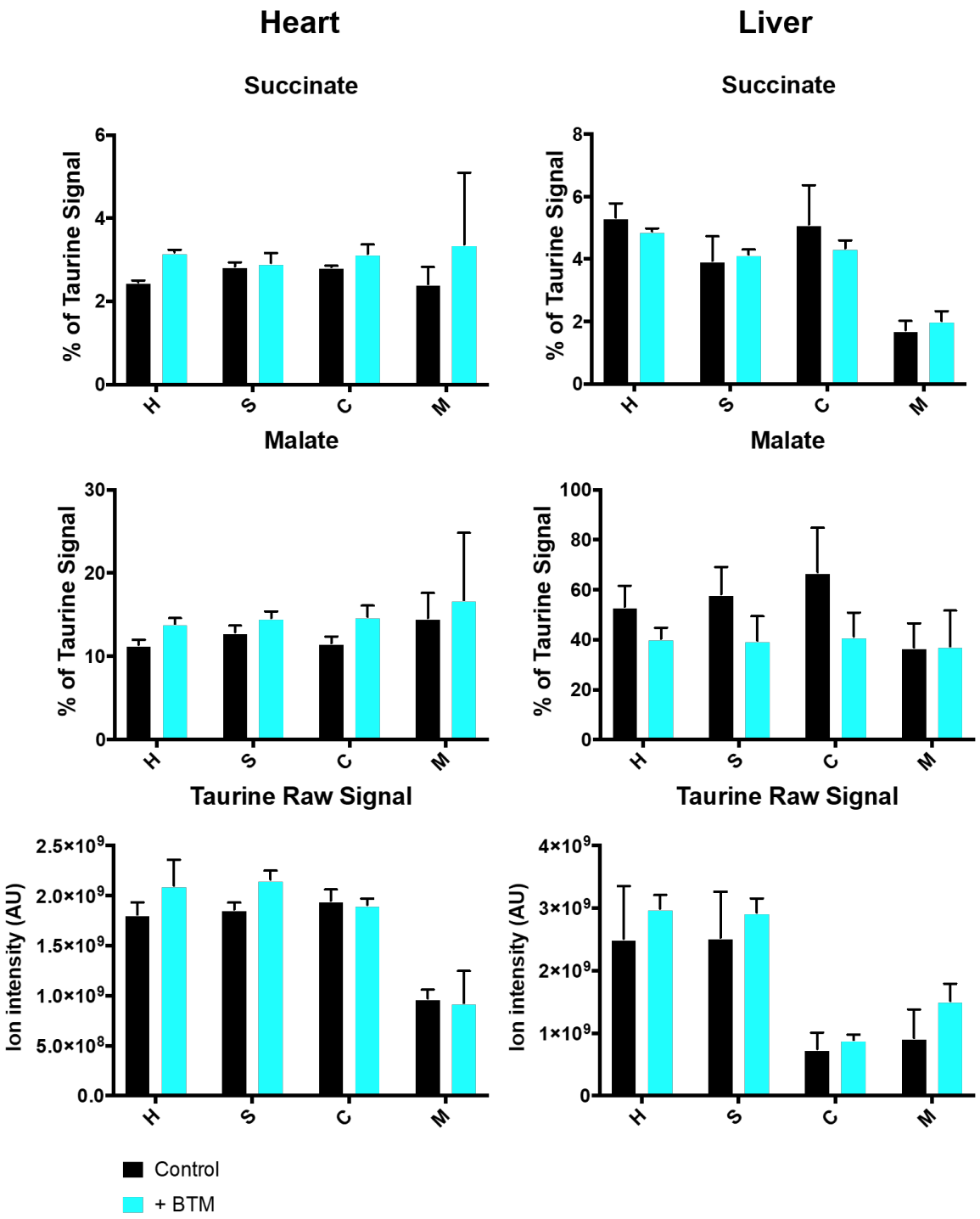

Fig. 5.12 Effect of butylmalonate inhibition on metabolite levels. Left: Mouse heart metabolites. Right: Mouse liver metabolites. Mouse heart and liver mitochondria were isolated in the presence of 500 µM butylmalonate. Control: n=2, BTM: n=3 biological replicates. Data is range for control samples and mean ±SEM for BTM samples. BTM: Butylmalonate; H: Homogenate; S: Supernatant; C: Cytosol; M: Mitochondria.

5.4.3 NEM and PRP

N-ethylmaleimide (NEM) modifies cysteine residues in proteins and is reactive to thiols. It is known to be a potent inhibitor of many transporters that have an exposed cysteine residue, such as the carnitine/acylcarnitine carrier (CAC) (Tonazzi et al., 2017). Pyridoxal 5'-phosphate (PRP) is a lysine reagent (Lundblad, 1991) and has been shown to inhibit transporters containing a lysine residue in the binding site, such as the oxoglutarate carrier (Natuzzi et al., 1999), the tricarboxylate carrier (Gremse et al., 1995), the yeast citrate carrier (Remani et al., 2008) and the yeast dicarboxylate carrier (Kakhniashvili et al., 1997).

A caveat to using these inhibitors is that any metabolite with a thiol, e.g. GSH, will be labelled by NEM and any metabolites with lysines will be labelled by PRP, which generates problems for normalisation. These labelled metabolites will still be present in the sample, but the analysis methods must be changed as the metabolites will be labelled with one or two NEM molecules, and therefore will have a higher mass.

To investigate the effect of these inhibitors, 3 mouse livers were isolated with 200 μM PRP or 500 μM NEM added to the homogenisation buffer. The taurine ion intensities and a selection of metabolites from the LC-MS analysis are shown in **Figure 5.13**. Neither homocysteine or cysteine were detected in the samples with inhibitor added, which suggests that their thiol groups were labelled and their detection was prevented. Many of the samples with NEM and PRP had particulates present, which affected the detection method and blocked the MS columns. These particulates may have been caused by NEM and PRP altering the hydrophobicity of the metabolites and causing aggregation. The particulates may also have been due to trace remnants of the oil, DOP or hexane. Hexane must be completely removed, as although most metabolites shouldn't enter hexane due to its negative charge, some metabolites may move into it, such as acyl carnitines. This could be why there is a low amount of palmitoylcarnitine and oleylcarnitine, and fatty acids such as linoleic acid and oleic acid seen in the samples, although the analysis conditions are not optimal for these metabolites anyway. In general, the presence of NEM or PRP led to a reduction in the amount of metabolites detected, possibly for reasons explained above.

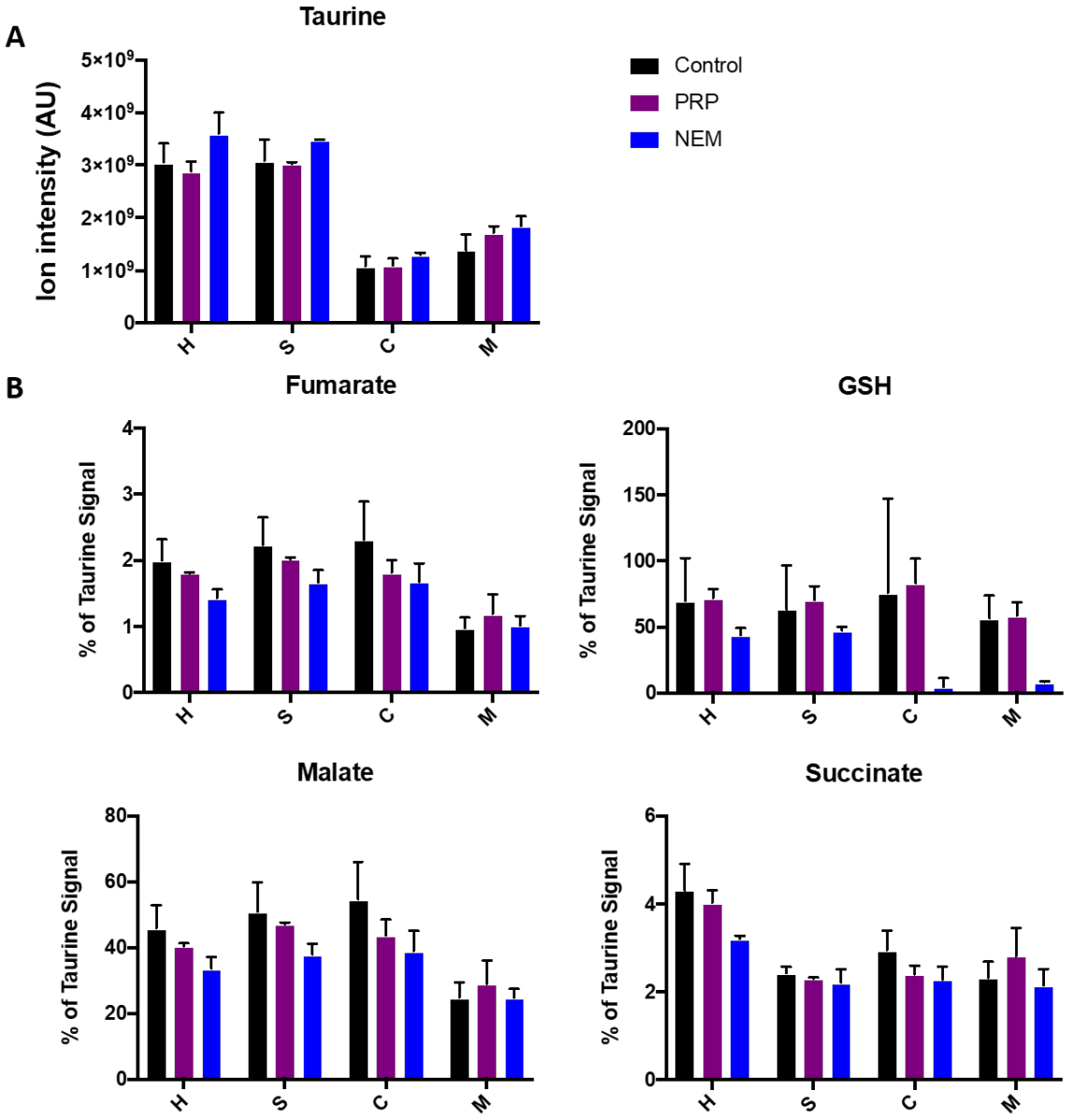

Fig. 5.13 LC-MS analysis of metabolites in the presence of the inhibitors PRP and NEM in mouse liver fractions. A) Ion intensities of taurine. **B)** Metabolite levels normalised to taurine. n=3 biological replicates, data is mean ±SEM. Data was analysed by 2-way ANOVA as not significant. H: Homogenate; S: Supernatant; C: Cytosol; M: Mitochondria.

5.4.4 Oligomycin and CATR

The inhibitors carboxyatractyloside (CATR) and oligomycin were added to the homogenisation buffer to investigate whether the isolation is performed sufficiently quickly such that

mitochondrial adenine nucleotides are maintained. CATR is a selective inhibitor of the AAC and stabilising a specific conformation of the carrier. Oligomycin inhibits ATP synthase, blocking oxidative phosphorylation and the ETC. The results are displayed in **Figure 5.14**.

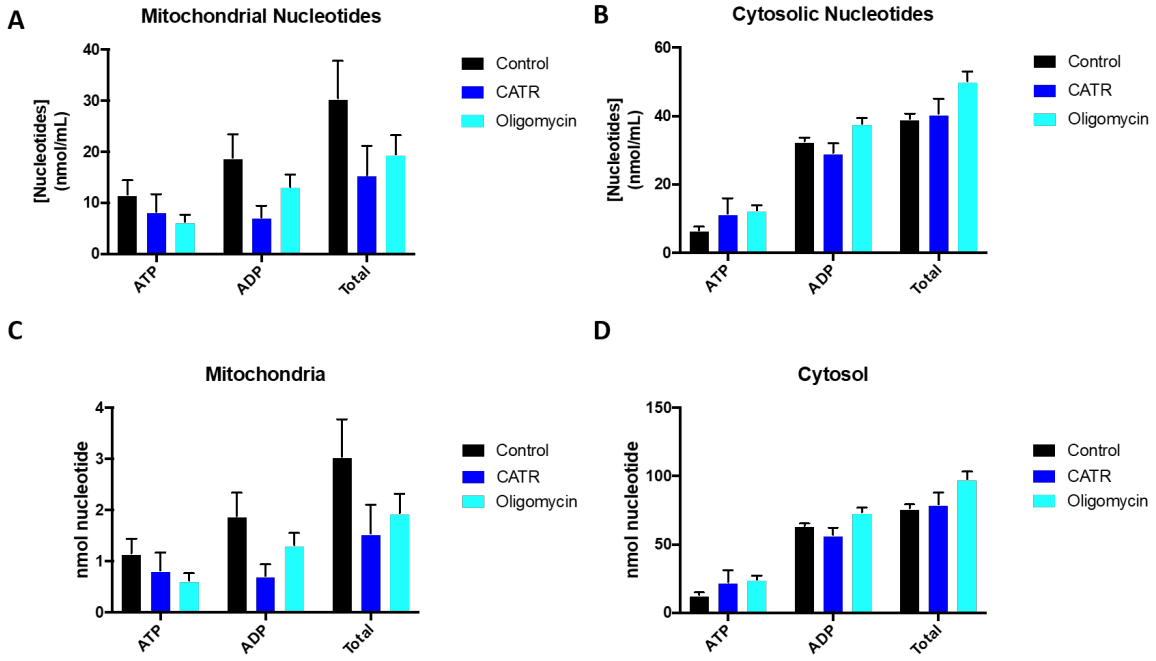

Fig. 5.14 ATP/ADP analysis in rapidly isolated mouse heart mitochondria. Mitochondria were rapidly isolated from mouse hearts with either no inhibitor, 20 µM CATR or 5 µM oligomycin in the homogenisation buffer. ATP and ADP levels were measured and extrapolated to calculate the total nmol of adenine nucleotides in the original cytosolic (650 µL layered on oil) and final mitochondrial fractions (100 µL of mitochondria obtained after centrifugation). ***A)*** Mitochondrial nucleotide concentrations; ***B)*** Cytosolic nucleotide concentrations; ***C)*** Total mitochondrial nucleotide pools; ***D)*** Total cytosolic nucleotide pools. Differences in ATP and ADP between control and CATR and oligomycin in ***A*** and ***B*** were analysed by 2-way ANOVA as not significant. Data is mean ±SEM, n=3. CATR: carboxyatractyloside.

Figure 5.14 shows that the cytosolic pools of adenine nucleotides were only mildly affected by the addition of either inhibitor, with a slight increase in the level of ATP. In contrast, the total mitochondrial adenine nucleotide pool was reduced by both inhibitors, although neither inhibitor caused a statistically significant change. CATR caused a large reduction in the level of ADP, with a smaller reduction in ATP. CATR inhibits the AAC, preventing the import of ADP into the mitochondria in exchange for ATP. Conversely, oligomycin caused a larger reduction in ATP levels than ADP levels. This could be due to oligomycin inhibiting ATP synthase and preventing ATP production.

5.5 Discussion

5.5.1 LC-MS analysis technique

The optimised LC-MS sample preparation was to quench and extract the metabolites in either 15% (heart) or 23% (liver) formic acid. It was found that pooling 4 mitochondrial isolations increased the LC-MS signal. The acidic extracts were dried under vacuum and resuspended in water to increase the pH, as a low pH was found to alter retention times. Taurine was chosen as the best metabolite for normalisation of metabolite ion intensities. Although normalisation has some caveats, it is the best approach for this technique as it enables a wide range of metabolites to be quantified. To achieve absolute quantification of metabolites, multiple metabolite isotopes would have to be added as standards.

HILIC was chosen as the chromatographic method for this project. The 2 columns (ZIC-pHILIC and ZIC-HILIC) are optimised for polar metabolites, such as TCA cycle intermediates. The relative quantification of polar metabolites is of potential interest to this lab in the context of IRI. Other metabolites, such as positively charged fatty acids and carnitines, will not be ionised as efficiently and will therefore not be detected as accurately. Therefore, only tentative conclusions can be drawn on the behaviour of these non-polar metabolites using HILIC.

5.5.2 Transport inhibitors

Neither BTM, PRP or NEM resulted in any statistically significant change in the levels of metabolites detected in any fraction. This supports the view that the use of these inhibitors is not necessary because the procedure is performed quickly and with rapid cooling such that metabolism and distribution is quenched successfully. It could also be that the time frame for the inhibitors to have an effect is longer than the time they are exposed to the mitochondria (i.e. the time from the homogenisation of the tissue to the time the mitochondria pass through the oil into the acid), although this is unlikely as they are very fast-acting. The cold temperature could also inhibit their efficacy. If any of these reasons is correct then the use of inhibitors is limited. Alternatively, it is possible that the concentration of inhibitor used was not optimal, or that the metabolites are switching to transport through other carriers.

In this case, adding a targeted cocktail of different inhibitors may be beneficial. However, the exchange of metabolites across the MIM will be limited during homogenisation due to dilution of external metabolites in the large volume of homogenisation buffer, so the activity of most carriers will be reduced after homogenisation.

The addition of oligomycin and CATR did not generate any statistically significant changes in the cytosolic or mitochondrial total adenine nucleotide pools. Again, this indicates that the extraction is performed quickly enough that metabolite degradation does not occur, or that it is performed quicker than the inhibitors can have an effect.

The use of inhibitors may be suitable for a more targeted approach, such as looking at a particular metabolite like succinate, but does not seem necessary or helpful for looking at a range of metabolites. Using a combination of different inhibitors, targeted to specific transporters, may aid understanding of mitochondrial metabolite pools. Nevertheless, the use of pharmacological inhibition is challenging, because the inhibitors may well have effects on other transporters, causing complex downstream effects on multiple metabolite pools.

Chapter 6

Metabolic characteristics of normoxic and ischaemic mitochondria and cytosol

6.1 Introduction

Chapters 3 to 5 developed and optimised the rapid mitochondrial isolation procedure from tissues. This section describes the results of the application of this method to study the metabolism of control and ischaemic mouse heart and liver. This builds upon previous studies which looked at whole cell metabolomics in mouse heart subjected to cold and warm ischaemia (Chouchani et al., 2014; Martin et al., 2019).

It was hoped that measuring metabolites in rapidly isolated cytosolic and mitochondrial fractions would expose any metabolic changes that may have been masked by whole cell analyses. Control, normoxic tissue was measured first to get an understanding of how normoxic metabolite pools in the cytosol and mitochondria behave and therefore provide a baseline to help understand more about those changes that occur during ischaemia.

Although the distribution and transport of some metabolites is well known, the behaviour of others in both normoxia and ischaemia is less well-established. For example, TCA cycle intermediates are known to be present in the mitochondria, but some are also thought to be distributed throughout the cell by transporters on the MIM. Therefore, it was of potential interest to determine how the distribution of these metabolites was altered during ischaemia. It was also of interest to establish those metabolite pools that did not change during ischaemia.

6.2 Aims

Chapter 4 described the development of the rapid mitochondrial isolation procedure and **Chapter 5** described the optimisation of the procedure for metabolite analysis by LC-MS. In this Chapter, the second aim of the project was addressed: to use the method to elucidate and understand the differences between cytosolic and mitochondrial metabolite pools in mouse heart and liver, during normoxia and ischaemia. The optimised rapid mitochondrial isolation procedure generates homogenate, supernatant, cytosolic and mitochondrial fractions sequentially. The LC-MS analysis aimed to examine how the metabolic profile of each of these fractions differs.

6.3 Strategy

The strategy was to generate a control data set for the cytosol and mitochondria of mouse heart and liver. After this, an ischaemic data set was generated for both organs by subjecting them to 30 min warm ischaemia (WI), which is a duration we routinely use in mouse studies of IRI before reperfusion, hence these changes are pathologically relevant. As 30 min is late-stage ischaemia, a more detailed viewpoint of relative changes to metabolite pools was also obtained by performing a time course of WI at earlier time points. To quantify the metabolites, the ion intensities were normalised to taurine, as described in **Section 5.1.4**. The data was displayed as bar graphs showing the taurine-normalised ion intensity in each fraction. To help understand differences between the mitochondrial and cytosolic pools, the ratio of mitochondrial:cytosolic normalised ion intensities in normoxia and ischaemia was displayed as heat maps.

To facilitate analysis, the metabolites were divided into metabolic pathways and metabolite types. This gave information on how particular pathways were behaving during normoxic and ischaemic conditions in both compartments. As the cellular localisation of some metabolites is well known, this grouping also served as a marker for how well the isolation procedure had worked in separating the mitochondria and cytosol. For example, phosphorylated glycolytic intermediates, such as 3-phosphoglycerate and fructose-6-phosphate, are not able to enter the mitochondria and, therefore, should only be detected at low levels (or not at all) in the mitochondrial fraction. Similarly, the nucleotide breakdown products xanthine and

hypoxanthine are established markers of ischaemia, so the presence of these metabolites were good indicators of the success of the ischaemic protocol.

6.4 Data analysis

The metabolites were generally normalised to taurine. The rationale for normalisation to taurine is discussed in detail in **Section 5.3.1**. The normoxic datasets for heart and liver are displayed as bar graphs of taurine-normalised ion intensities. To elucidate how the distribution of these metabolites differs between the mitochondria and the cytosol, this data was also presented as heat maps of mitochondrial:cytosolic taurine-normalised ion intensities. These heat maps clearly show which metabolites are compartmentalised to the mitochondria or the cytosol (at the extreme ends of the heat maps) and which metabolites are distributed throughout the cell. Heat maps were also made to explore how these distributions changed following 30 min WI by comparing the normoxic mitochondria:normoxic cytosol and ischaemic mitochondria:ischaemic cytosol ratios.

As is often the case with LC-MS analyses, there were some missing values in the datasets. For metabolites that were present in only one fraction, MVI was applied and they were assigned an "adjusted zero" value of 0.0002% of taurine (the smallest detected value), so that a virtual ratio could be calculated for comparison with the other data (see **Section 5.1.3**). These metabolites are included on the heat maps, but are separated from the other metabolites as the ratio will be artificially increased (for metabolites not detected in the cytosol) or decreased (for metabolites not detected in the mitochondria) by the adjusted zero value. Metabolites that were expected, but nevertheless not detected in either fraction, either due to column suitability, or for unknown reasons, were excluded.

Although data for all 4 fractions (homogenate, supernatant, cytosol and mitochondria) was collected, the differences between the cytosolic and mitochondrial fractions were of particular interest for this project and so were the focus of this section. **Figure 6.1** shows two examples of metabolites, fumarate and glutamate, showing that the signal for the homogenate, supernatant and cytosolic fractions are broadly similar. The signals for all fractions are displayed in **Appendix C**. Most analyses and interpretations were based on taurine-normalised ion intensities, unless otherwise indicated.

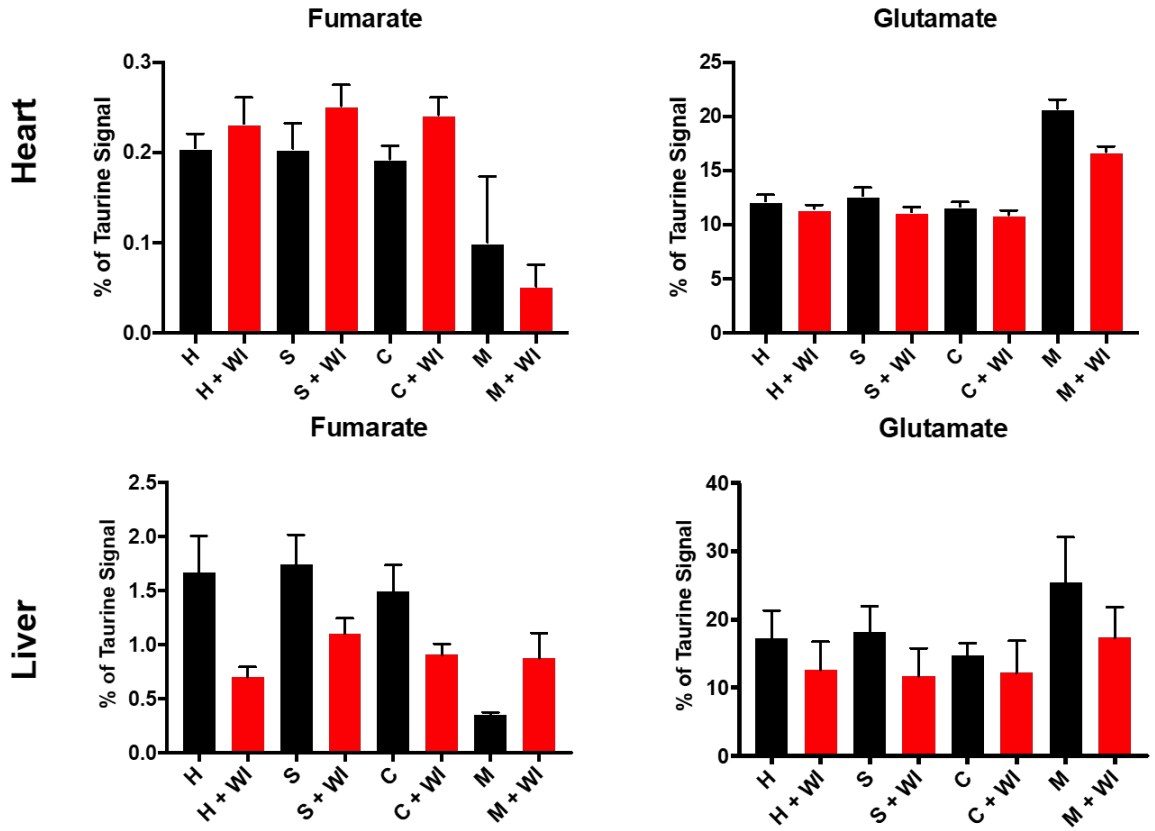

Fig. 6.1 The normalised ion intensities for the homogenate, supernatant and cytosolic fractions are broadly similar. The taurine-normalised ion intensities from the heart (top) and liver (bottom) datasets are displayed to demonstrate that the signals from the homogenate, supernatant and cytosolic fractions are similar. Data is average of 6 biological replicates, presented as mean ±SEM. H: Homogenate; S: Supernatant; C: Cytosolic fraction; M: Mitochondrial fraction; WI: Warm ischaemia.

The majority of metabolites for this project were analysed using the ZIC-pHILIC column because it detects the broadest range of metabolites (**Section 5.1.1**). Some metabolites are detected better under the conditions of the ZIC-HILIC column, and so were analysed on both columns, where this was possible. These metabolites were: arginine, cysteine, cystine, GSH, histidine, lysine and succinate. In addition, the ZIC-HILIC column was used to supplement any gaps in the data set from metabolites that were not detected by the ZIC-pHILIC column, which are listed in the relevant sections.

6.5 Normoxic metabolism

First, the distribution of metabolites of control mice under normoxia was studied. The control data set was compiled from 6 WT C57/BL6 mouse hearts and 3 WT C57/BL6 mouse livers which were kept under normoxic conditions. The control distribution of metabolites was studied by an initial screen of raw ion intensities (displayed in **Appendix A**). Next, the data was analysed by normalisation to taurine (values displayed in **Appendix B**) and displayed in bar graphs. In the following section, the bar graphs for TCA cycle intermediates, glycolytic intermediates and nucleotides and breakdown products are displayed. The bar graphs for amino acids and peptides, fatty acids and carnitines and any ungrouped metabolites are displayed in **Appendix C.1 and C.2** alongside the 30 min WI data. To aid in identifying the relative distribution of metabolites across the cytosolic and mitochondrial compartment, the data was then collated into heat maps of mitochondrial:cytosolic taurine-normalised ion intensities.

6.5.1 Metabolite analysis in the control heart

The ZIC-HILIC column was used to increase metabolite coverage, as the following metabolites were not detected on the ZIC-pHILIC column in the control heart dataset: allantoin, dihydrothymine, GABA, leucine, N-acetylaspartate, nicotinamide, tyrosine, uracil, uric acid, uridine and xanthine.

The levels of taurine-normalised TCA cycle intermediates across all fractions are shown in **Figure 6.2**. Relative to taurine, aconitate, αKG and citrate are compartmentalised to the mitochondria, whereas malate and succinate are seen to be more distributed across

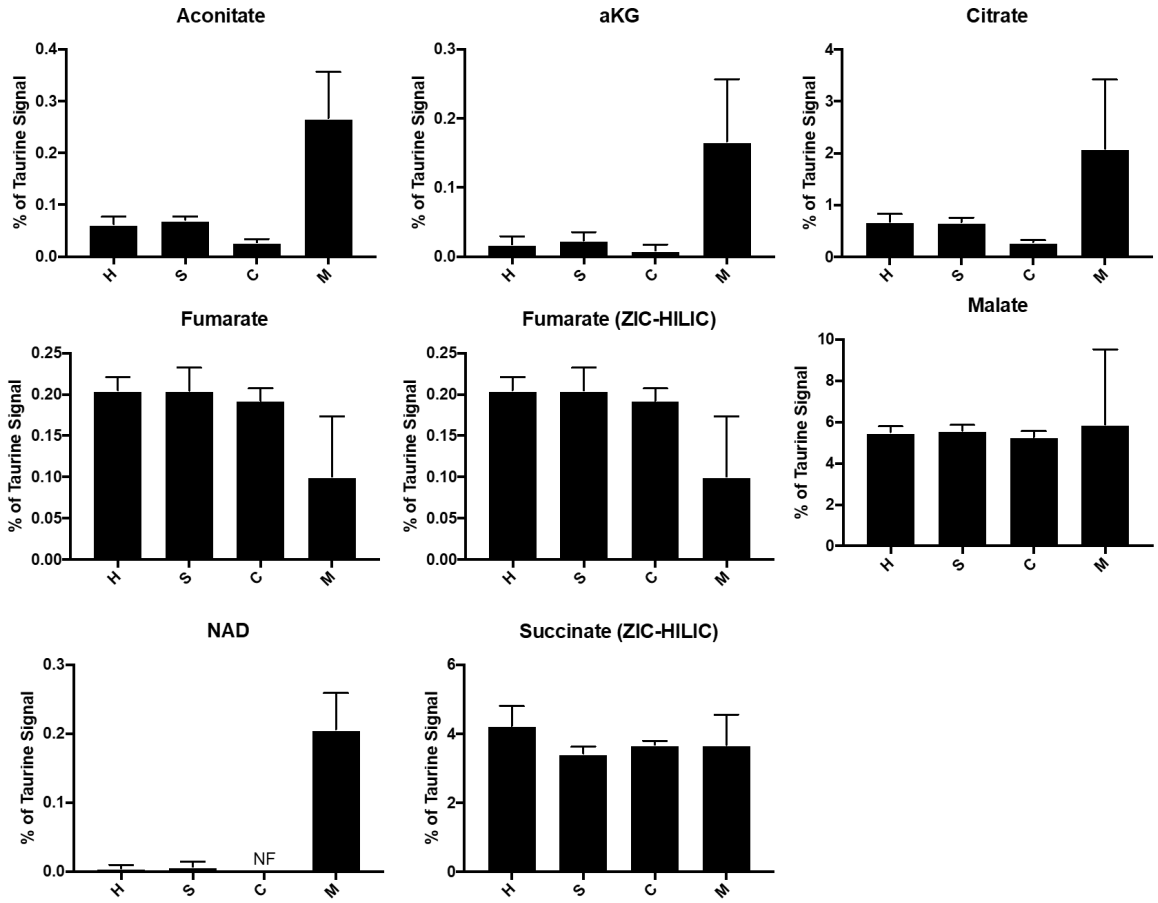

Fig. 6.2 TCA cycle intermediates in control mouse heart homogenate, supernatant, cytosol and mitochondria. Metabolite ion intensities from the control heart data set were normalised to taurine. Data is from ZIC-pHILIC column unless otherwise stated as from ZIC-HILIC column. Data is average of 6 biological replicates, presented as mean ±SEM. H: Homogenate; S: Supernatant; C: Cytosolic fraction; M: Mitochondrial fraction. NF: Not found.

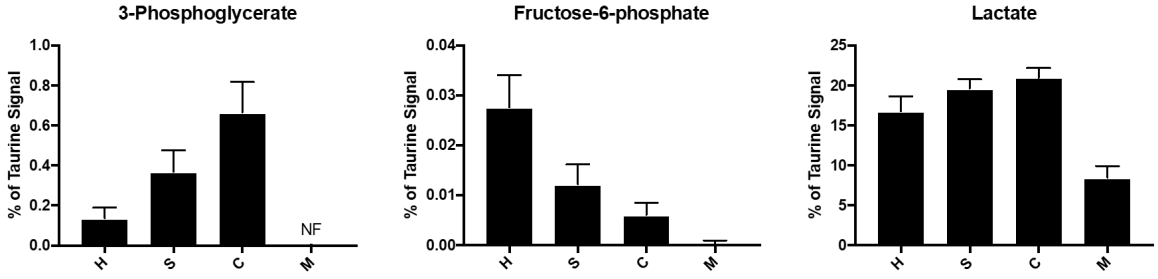

Fig. 6.3 Glycolytic intermediates in control mouse heart homogenate, supernatant, cytosol and mitochondria. Metabolite ion intensities from the control heart data set were normalised to taurine. Data is from ZIC-pHILIC column unless otherwise stated as from ZIC-HILIC column. Data is average of 6 biological replicates, presented as mean ±SEM. H: Homogenate; S: Supernatant; C: Cytosolic fraction; M: Mitochondrial fraction. NF: Not found.

the cellular fractions. NAD^+ was only detected at very low levels in the homogenate and supernatant fractions, and was not seen at all in the cytosolic fraction, whereas it was seen in the mitochondrial fraction. The glycolytic intermediates 3-phosphoglycerate and fructose-6-phosphate were not detected or were at very low levels relative to taurine in the mitochondrial fraction, whereas lactate was distributed across the cell (**Figure 6.3**).

Nucleotides and their breakdown products were generally evenly distributed across the two compartments (**Figures 6.4 and 6.5**), except for kynurenic acid and guanosine which were not detected in the cytosol and were abundant in the mitochondria. Conversely, CDP, hypotaurine, uracil, uric acid and uridine were not detected in the mitochondria.

Figures C.1 and C.2 shows that amino acids are evenly distributed across the cell, except for asparagine and glycine which were higher in the mitochondria relative to taurine. On the ZIC-pHILIC column GSH is shown to be evenly distributed across the all fractions, whereas on the ZIC-HILIC column analysis, GSH is lower in the mitochondrial fraction. GSSG was also seen distributed across all fractions.

Figure C.3 lists the fatty acids and carnitines that were detected in the control heart. Other fatty acids and carnitines were looked for, but were excluded from this analysis due to having less than 3 values per fraction above zero. These are listed in the legend of **Figure C.3**. Acetylcarnitine, butyrylcarnitine, carnitine and propionylcarnitine were relatively evenly distributed across the cell, with slightly lower levels in the mitochondrial fraction.

The high level of sucrose seen in both compartments (**Figure C.5**) is due to contamination carried through from the sucrose-based homogenisation buffers.

Figure 6.6 shows the ratio of mitochondrial:cytosolic metabolites. The data show which metabolites are accumulated in the mitochondria and which are depleted compared to the cytosol, relative to taurine. TCA cycle intermediates αKG, aconitate and citrate are seen at a higher level in the mitochondria, with phosphorylated glycolytic intermediates fructose-6-phosphate and 3-phosphoglycerate not detected in the mitochondria. Kynurenic acid, NAD^+, guanosine, palmitic acid and oleic acid were increased relative to taurine more in the mitochondria. However, none of these were found in the cytosol and were therefore assigned a low virtual ratio value. Furthermore, fatty acids and their derivatives are poorly detected in this system, which was mainly optimised for the TCA cycle, and had low ion intensities (in the range of 10^5 - 10^6, **Figure A.2**). Succinate is shown to be lower in the mitochondrial fraction compared to the cytosolic fraction, relative to taurine. Further, on the ZIC-HILIC

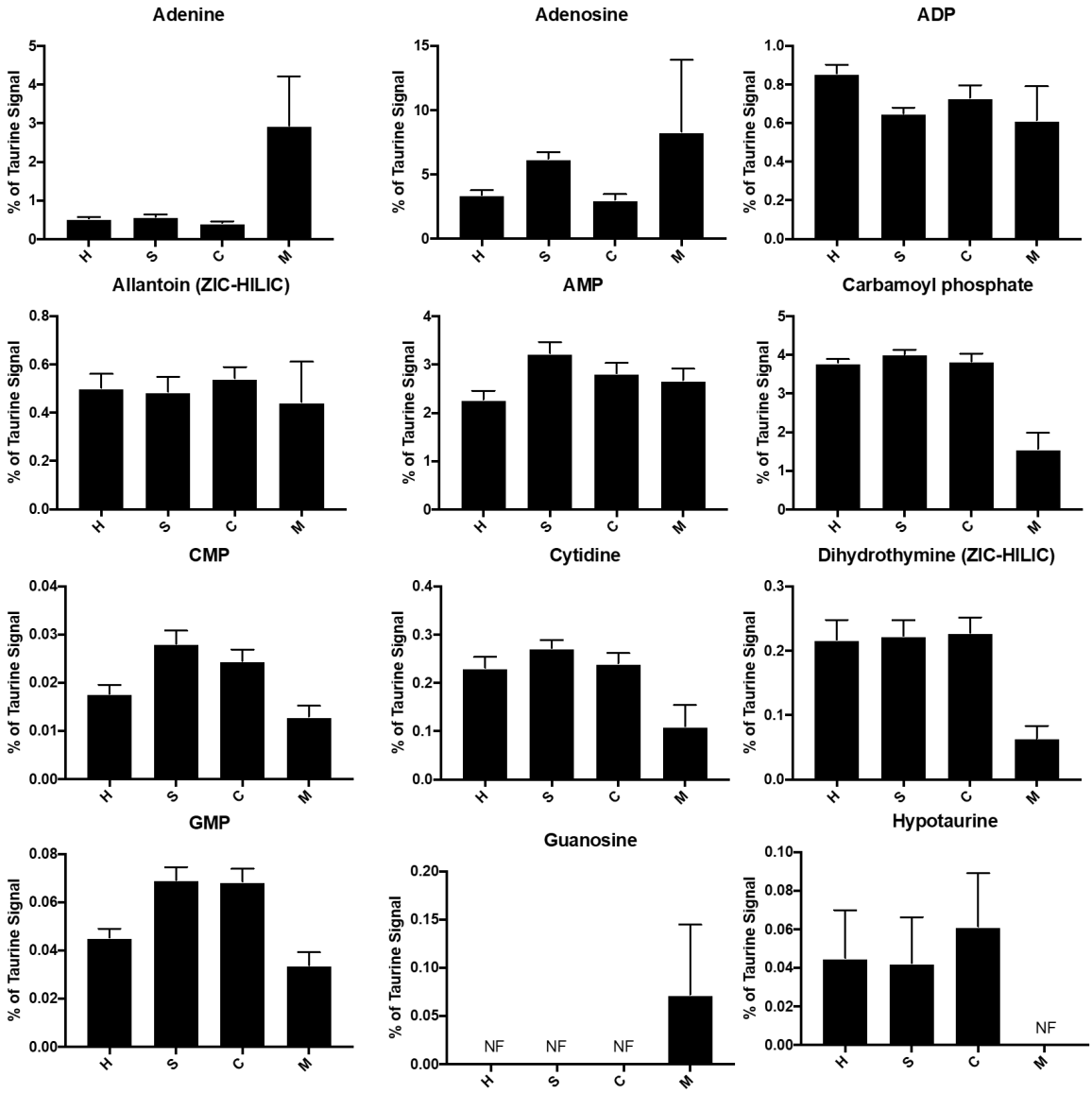

Fig. 6.4 Nucleotides and breakdown products in control mouse heart homogenate, supernatant, cytosol and mitochondria. Metabolite ion intensities from the control heart data set were normalised to taurine. Data is from ZIC-pHILIC column unless otherwise stated as from ZIC-HILIC column. Data is average of 6 biological replicates, presented as mean ±SEM. H: Homogenate; S: Supernatant; C: Cytosolic fraction; M: Mitochondrial fraction. NF: Not found.

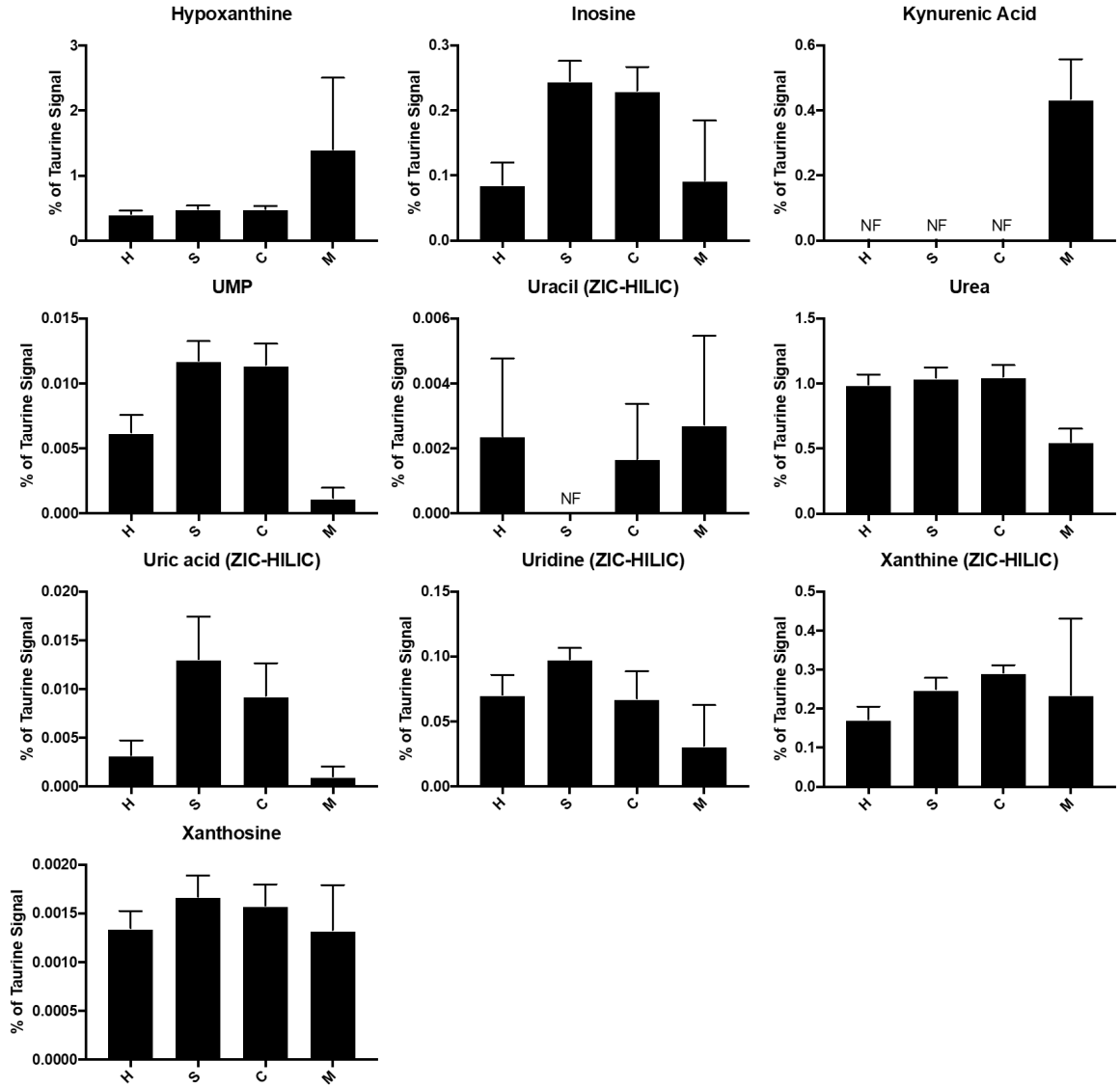

Fig. 6.5 Nucleotides and breakdown products in control mouse heart homogenate, supernatant, cytosol and mitochondria (ctd.). Metabolite ion intensities from the control heart data set were normalised to taurine. Data is from ZIC-pHILIC column unless otherwise stated as from ZIC-HILIC column. Data is average of 6 biological replicates, presented as mean ±SEM. H: Homogenate; S: Supernatant; C: Cytosolic fraction; M: Mitochondrial fraction. NF: Not found.

column fumarate is higher than succinate, relative to taurine. Hypoxanthine was high in the mitochondria (ZIC-pHILIC) but xanthine was low in the mitochondria on the ZIC-HILIC column analysis.

6.5.2 Metabolite analysis in the control liver

As was the case for the control heart data set, the majority of metabolites for the control liver data set were analysed using the ZIC-pHILIC column. The ZIC-HILIC column was used to improve metabolite coverage, as asparagine, cytidine, dihydrothymine, GABA, homocysteine, hypotaurine, leucine, nicotinamide, uracil, uric acid, uridine, valine and xanthine were not detected by the ZIC-pHILIC column analysis.

Compared to control heart, TCA cycle intermediates in the control liver appear more evenly distributed across the cell (**Figure 6.7**). As for the heart, glycolytic intermediates are much lower or are not detected in the mitochondria (**Figure 6.8**).

Figures 6.9 and 6.10 indicate that there are more nucleotide breakdown products detected in the mitochondria relative to the cytosol. In particular, hypoxanthine, inosine and xanthine were not detected or were very low in the cytosol but were relatively high in the mitochondria.

In general, amino acids were distributed across the compartments (**Figures C.6 and C.7**), except for citrulline which was much higher in the mitochondrial fraction. Similarly to the control heart data, GSH was seen to be slightly lower in the mitochondria on the ZIC-HILIC column analysis.

The fatty acids and carnitines that were detected are displayed in **Figure C.8**, and the excluded metabolites are listed in the legend. Acetylcarnitine, butyrylcarnitine, carnitine and propionylcarnitine are evenly distributed, whereas all other fatty acids and acylcarnitines that were detected are compartmentalised, mostly in the cytosol.

Figure C.11 indicates the liver also has some sucrose contamination from the homogenisation buffers in both compartments.

Figure 6.11 shows that, relative to taurine, succinate is evenly distributed between the mitochondria and the cytosol, whereas in the control heart it was lower in the mitochondrial fraction. The accumulation of hypoxanthine in the mitochondria suggests that there was ATP

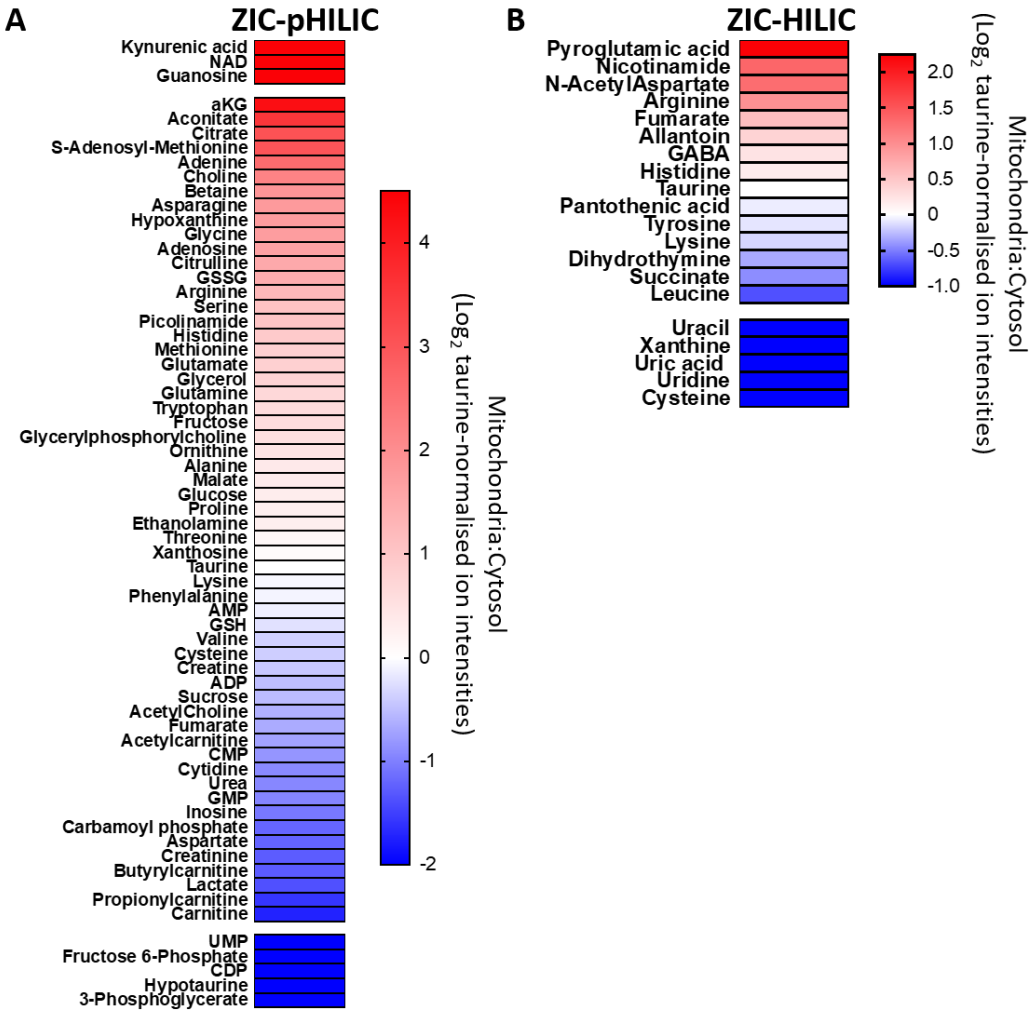

Fig. 6.6 Metabolite enrichment in control mouse heart mitochondria. Metabolites from the control heart data set were normalised to taurine and presented as a ratio of mitochondrial:cytosolic relative amounts ($\log_2$ of the values), arranged in order of accumulation in the mitochondria. **A)** Metabolites analysed on the ZIC-pHILIC column; **B)** metabolites analysed on the ZIC-HILIC column. Data is average of 6 biological replicates. Metabolites which were assigned an adjusted zero value, due to no detection in the cytosolic or mitochondrial fraction, are placed above (cytosolic adjusted zero) or below (mitochondrial adjusted zero) the gaps in the heat map.

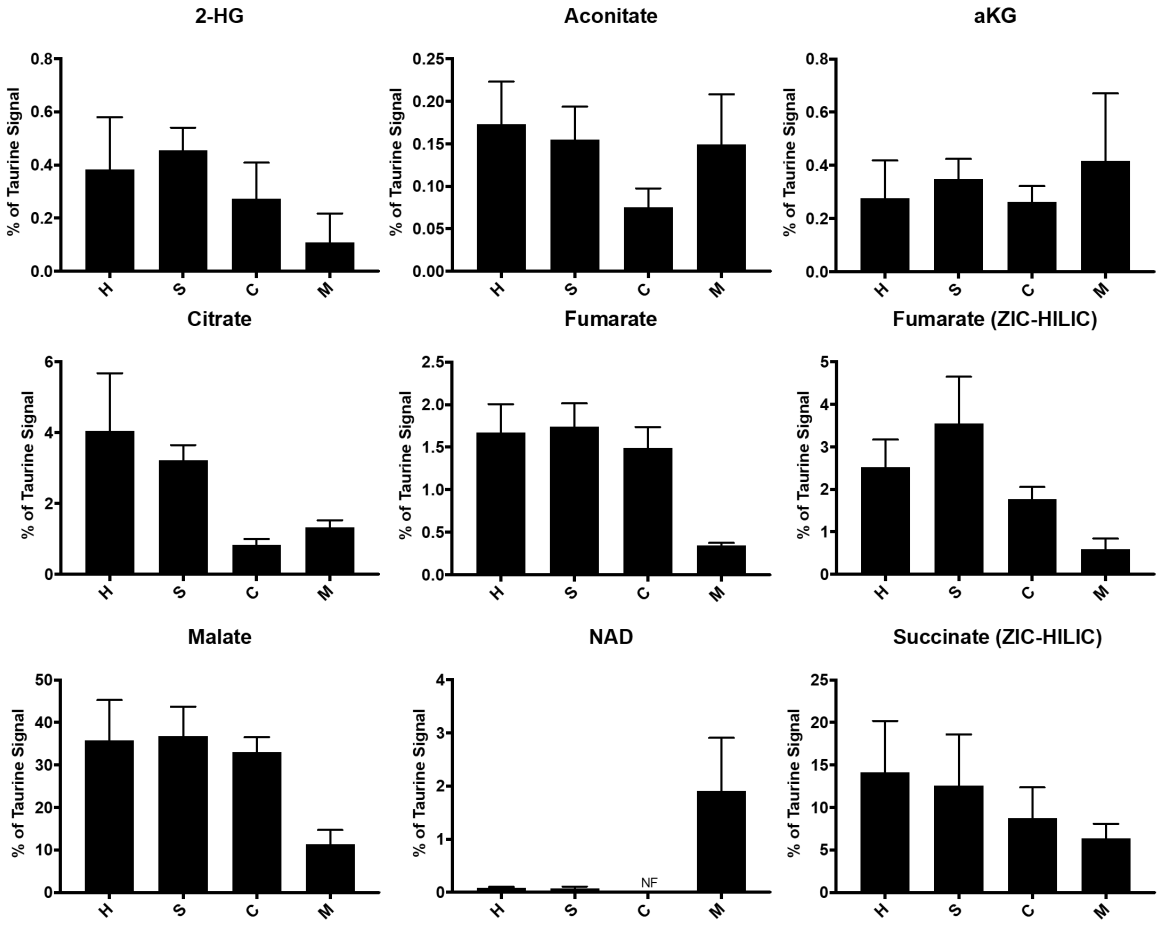

Fig. 6.7 TCA cycle intermediates in control mouse liver homogenate, supernatant, cytosol and mitochondria. Metabolite ion intensities from the control liver data set were normalised to taurine. Data is from ZIC-pHILIC column unless otherwise stated as from ZIC-HILIC column. Data is average of 3 biological replicates, presented as mean ±SEM. H: Homogenate; S: Supernatant; C: Cytosolic fraction; M: Mitochondrial fraction. NF: Not found.

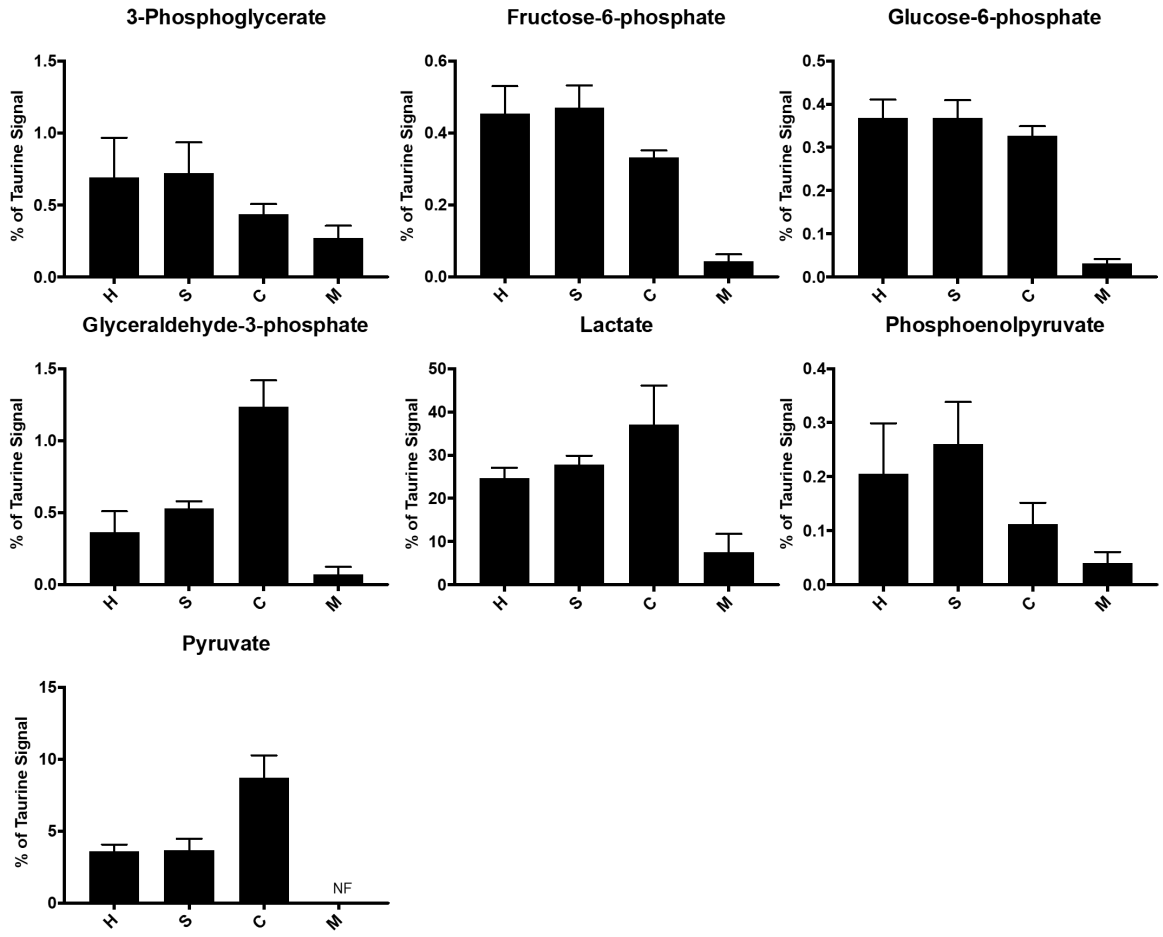

Fig. 6.8 Glycolytic intermediates in control mouse liver homogenate, supernatant, cytosol and mitochondria. Metabolite ion intensities from the control liver data set were normalised to taurine. Data is from ZIC-pHILIC column unless otherwise stated as from ZIC-HILIC column. Data is average of 3 biological replicates, presented as mean ±SEM. H: Homogenate; S: Supernatant; C: Cytosolic fraction; M: Mitochondrial fraction. NF: Not found.

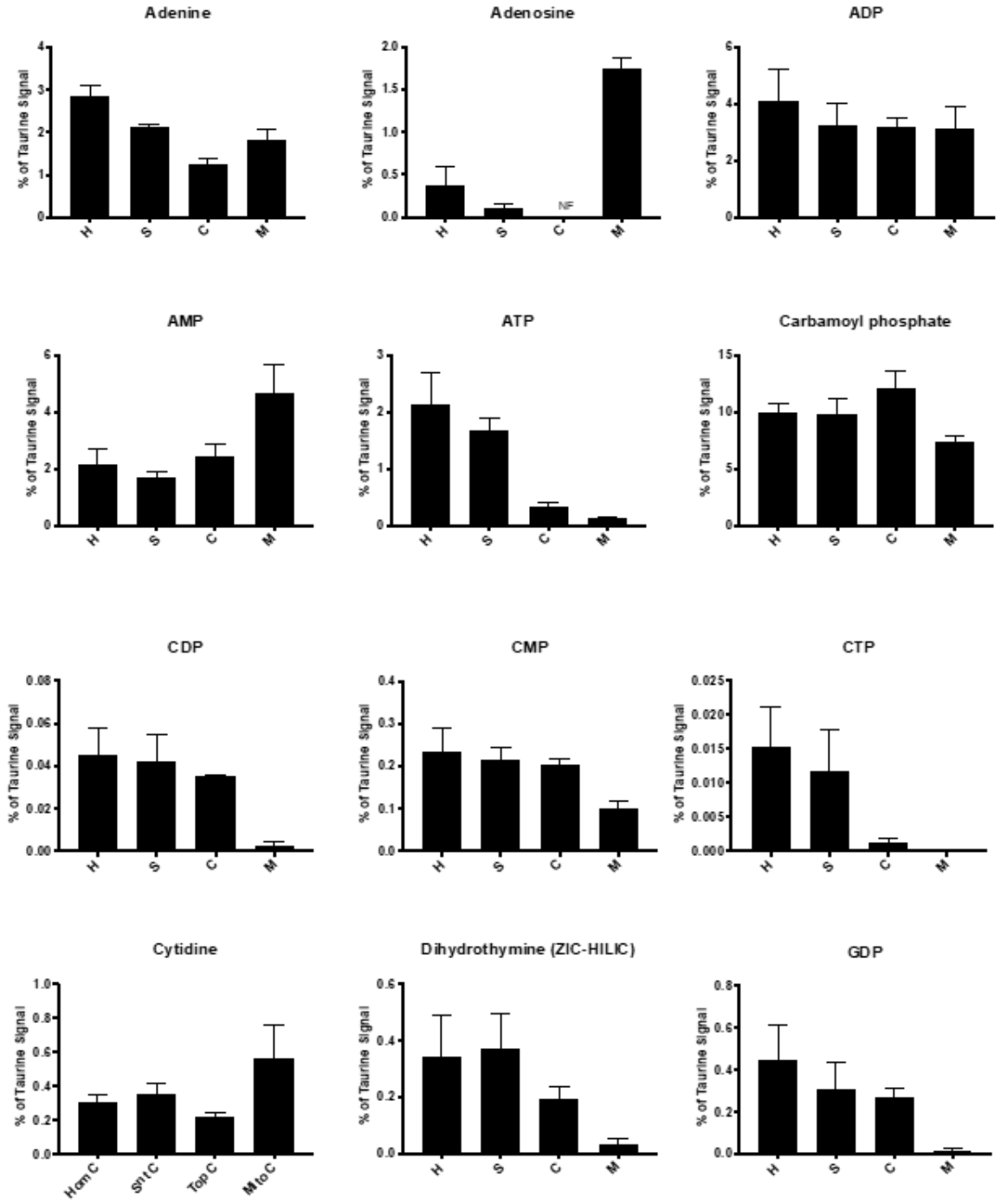

Fig. 6.9 Nucleotides and breakdown products in control mouse liver homogenate, supernatant, cytosol and mitochondria. Metabolite ion intensities from the control liver data set were normalised to taurine. Data is from ZIC-pHILIC column unless otherwise stated as from ZIC-HILIC column. Data is average of 3 biological replicates, presented as mean ±SEM. H: Homogenate; S: Supernatant; C: Cytosolic fraction; M: Mitochondrial fraction. NF: Not found.

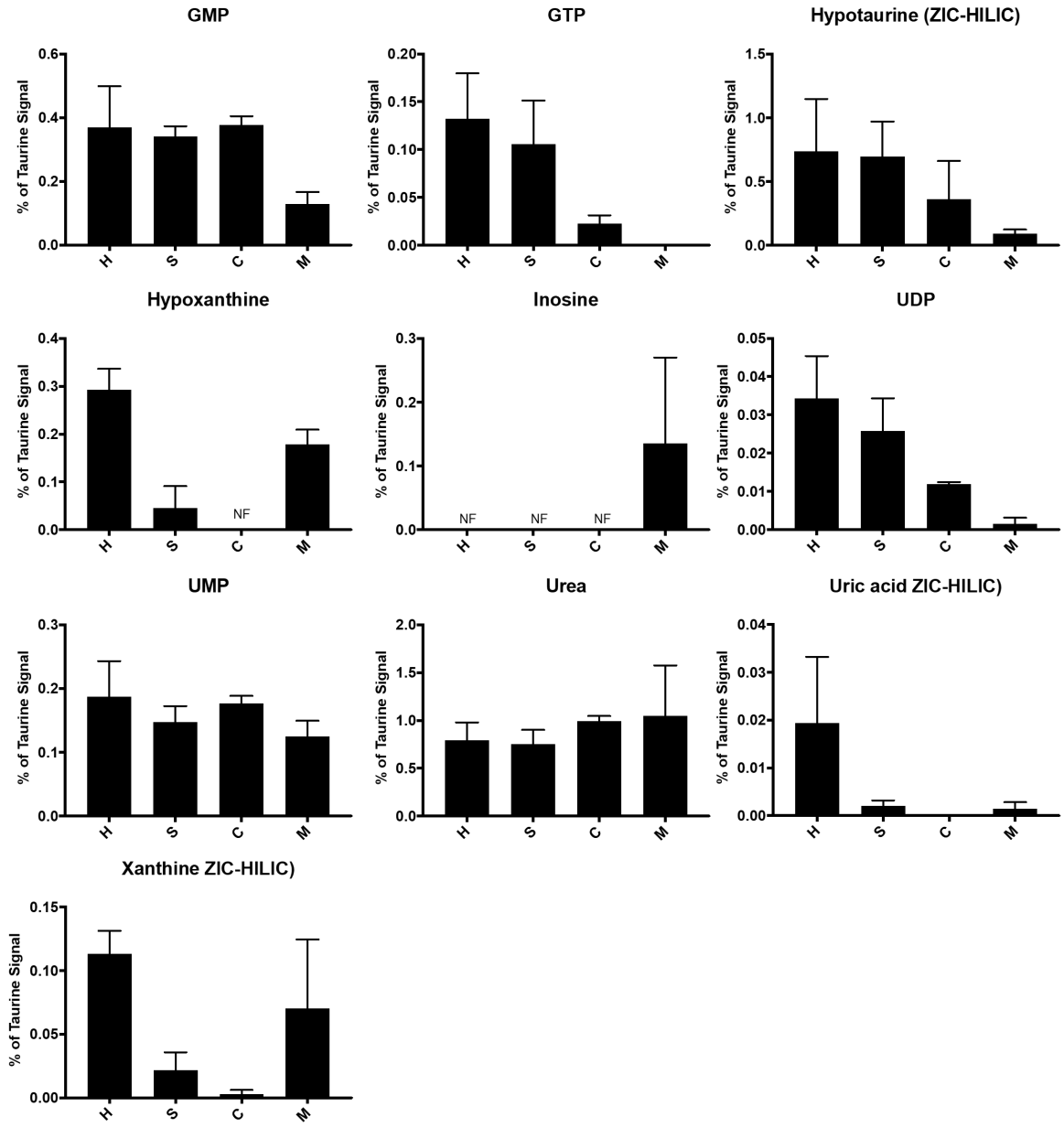

Fig. 6.10 Nucleotides and breakdown products in control mouse liver homogenate, supernatant, cytosol and mitochondria (ctd.). Metabolite ion intensities from the control liver data set were normalised to taurine. Data is from ZIC-pHILIC column unless otherwise stated as from ZIC-HILIC column. Data is average of 3 biological replicates, presented as mean ±SEM. H: Homogenate; S: Supernatant; C: Cytosolic fraction; M: Mitochondrial fraction. NF: Not found.

breakdown, but there was none in the cytosol where ATP breakdown occurs. As was found in the heart, the TCA cycle intermediates aconitate, αKG and citrate were accumulated in the mitochondria relative to the cytosol. Phosphorylated glycolytic intermediates (fructose-6-phosphate, glucose-6-phosphate and glyceraldehyde-3-phosphate) were depleted in the mitochondria. Unlike in the heart, succinate was found to be more accumulated in the mitochondria than fumarate.

6.6 Ischaemic metabolism

6.6.1 Glycolysis and energy storage during ischaemia

During ischaemia, the lack of oxygen causes the cessation of oxidative phosphorylation, and the lack of blood flow means that glucose is no longer delivered to tissue from the blood. This forces the cell to switch to glycogen-fuelled glycolysis to maintain the ATP/ADP ratio in order to supply the energetic demands of the cell and also supplies many of the precursors for ischaemic metabolites. To investigate how energy stores change during both cold and warm ischaemia, glycogen was measured in various tissues that had been subjected to ischaemia by the model described in **Section 2.4.1.2**, using the assay described in **Section 2.4.1**. Glycogen was measured via this assay instead of LC-MS because it is a large, heterogeneous molecule. Where possible, human heart samples were also analysed, but supply was limited. Pig heart was also used as this is very similar in terms of size, blood-flow and metabolism to human heart. The limited amount of human heart samples available meant that only WI experiments were performed in human. Glycogen was found to deplete rapidly in mouse and pig heart during WI (**Figure 6.12A** and **B**) and plateaued after approximately 1 hour, despite 20-25% of the glycogen remaining. When subjected to CI, glycogen stores in mouse and pig heart decreased in a slower, more steady manner and did not reach a plateau after 1 hour but continued to decrease for up to 120 min. Glycogen stores in human heart subjected to WI also plateaued after approximately 1 hour (**Figure 6.12C**), but did not decrease as rapidly during early WI compared to mouse and pig. However, due to the nature of the collection procedure of the human heart tissue, the tissue is not frozen as rapidly as the mouse tissues. Therefore, it is possible that previous episodes of WI during acquisition may have depleted some of the glycogen prior to the freezing of the tissue, meaning that the control value has artificially low glycogen values.

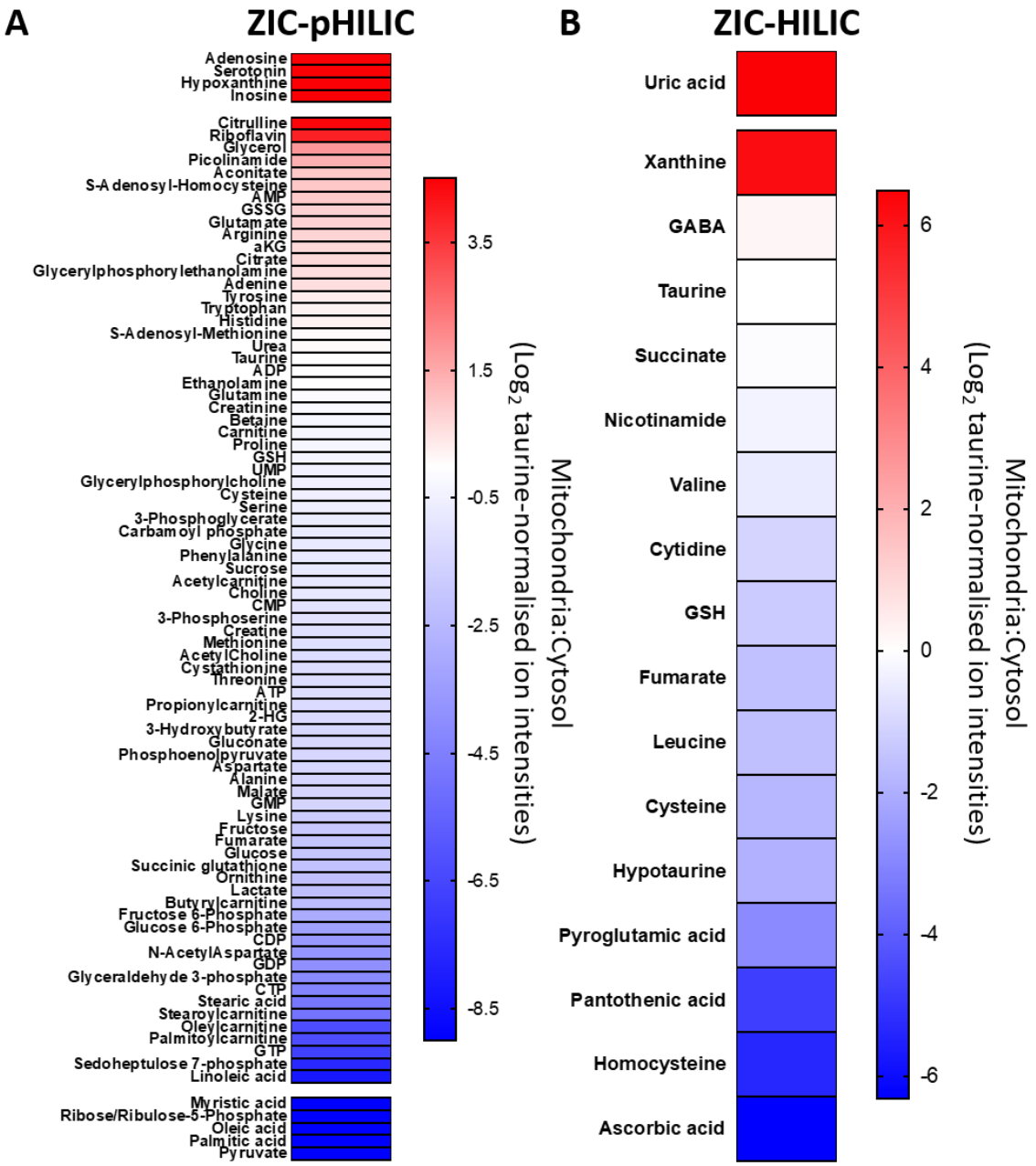

Fig. 6.11 Metabolite enrichment in control mouse liver mitochondria. Metabolites from the control liver data set were normalised to taurine and presented as a ratio of mitochondrial:cytosolic relative amounts ($\log_2$ of the values), arranged in order of accumulation in the mitochondria. **A)** Metabolites analysed on the ZIC-pHILIC column; **B)** metabolites analysed on the ZIC-HILIC column. Data is average of 6 biological replicates. Metabolites which were assigned an adjusted zero value, due to no detection in the cytosolic or mitochondrial fraction, are placed above (cytosolic adjusted zero) or below (mitochondrial adjusted zero) the gaps in the heat map.

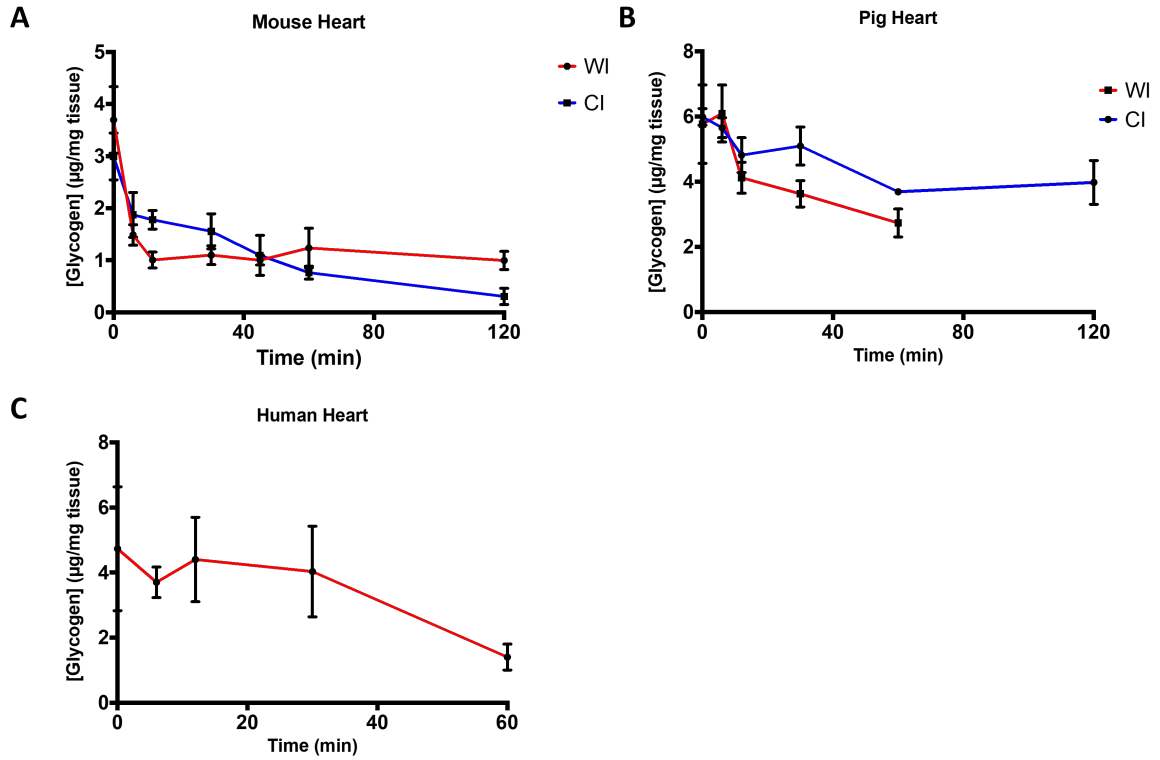

Fig. 6.12 Glycogen in mouse, pig and human heart during warm and cold ischaemia. ***A)*** Glycogen in ischaemic mouse heart. n=5 for time points 0 to 30 min and n=4 for time points 45 to 120 min. ***B)*** Glycogen in ischaemic pig heart. n=3. ***C)*** Glycogen in warm ischaemic human heart. n=3 for time points 0 to 30 min and n=2 for 60 min. Data is mean ±SEM, and range for 60 min values, for all graphs.

The ischaemic metabolism of the kidney was of interest to this lab, as it can also be subjected to both WI and CI during surgery. To investigate this in parallel, the glycogen stores of WI mouse kidney were measured. The kidney displayed a similar trend to mouse heart in that the glycogen stores of WI tissue were depleted rapidly and plateaued after approximately 45 min, whereas in CI tissue glycogen levels were reduced more slowly (**Figure 6.13**).

6.6.2 Metabolite analysis of rapidly isolated ischaemic mitochondria and cytosol

The above experiments shed light on glycolysis, which is an important metabolic pathway during ischaemia that helps to maintain the energy requirements of the cell. The glycogen assay was used to investigate the behaviour of glycolysis during ischaemia. To investigate

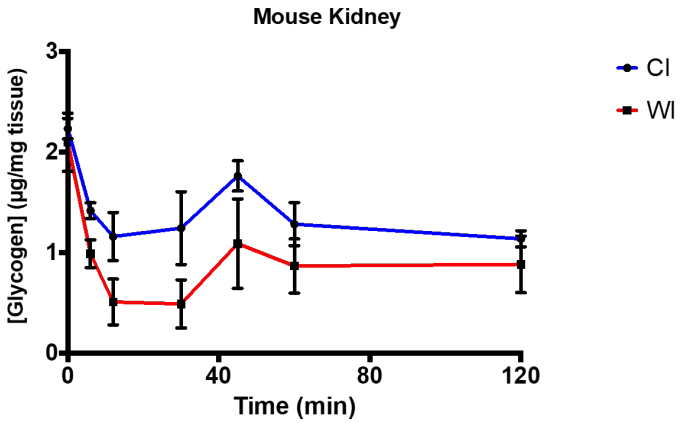

Fig. 6.13 Glycogen in mouse kidney during warm and cold ischaemia. Glycogen in ischaemic mouse kidney. n=4. Data is mean ±SEM.

how other glycolytic intermediates, and other metabolites, behave during ischaemia, the mitochondrial and cytosolic fractions from ischaemic mouse heart and liver were rapidly isolated, their metabolites measured by LC-MS and the relative enrichment of metabolites in the cytosol and mitochondria were calculated. To do this, whole mouse hearts and livers were rapidly removed and placed in a heat block at 37°C for 30 min before homogenisation and mitochondrial isolation (described in further detail in **Section 2.2.2.1**). These data were collected in parallel to the control heart and liver data sets. To understand how the distribution of metabolites in the cytosolic and mitochondrial pools change due to warm ischaemia, the ion intensities were normalised to taurine and presented as bar graphs. To improve the strength of any conclusions, two-way ANOVAs were performed, comparing the normoxic cytosol to ischaemic cytosol, normoxic cytosol to normoxic mitochondria, ischaemic cytosol to ischaemic mitochondria and normoxic mitochondria to ischaemic mitochondria. The data was also presented in heat maps comparing the mitochondrial:cytosolic ratio of taurine-normalised ion intensities in normoxia and after 30 min WI.

6.6.2.1 Metabolite analysis in the ischaemic heart

To identify ischaemic trends in metabolic groups, the metabolic intermediates of the TCA cycle and glycolysis and nucleotides and their breakdown products are displayed below. To simplify statistical analysis, only the cytosolic and mitochondrial fractions are displayed. Amino acids and peptides, fatty acids and carnitines and all other metabolites are displayed in **Appendix C.1**.

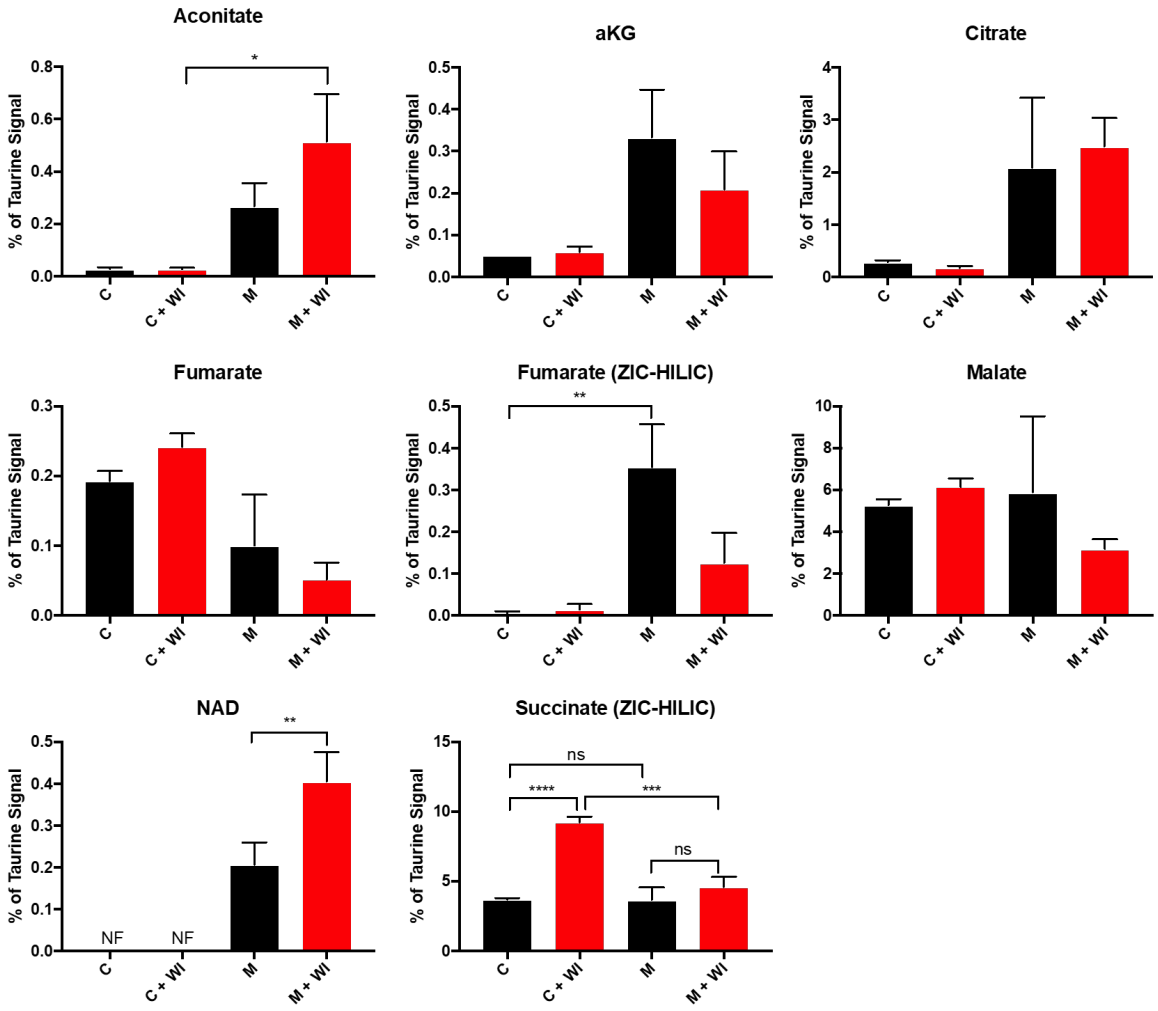

Fig. 6.14 TCA cycle intermediates in control and 30 min WI mouse heart homogenate, supernatant, cytosol and mitochondria. Metabolite ion intensities from the control and 30 min WI heart data sets were normalised to taurine. Data is from ZIC-pHILIC column unless otherwise stated as from ZIC-HILIC column. Data is average of 6 biological replicates, presented as mean ±SEM. H: Homogenate; S: Supernatant; C: Cytosolic fraction; M: Mitochondrial fraction. NF: Not found. Statistical analysis was performed by a two-way ANOVA. Means were considered statistically significant when ****$p < 0.0001$; ***$p < 0.0002$; **$p < 0.0021$; *$p < 0.0032$.

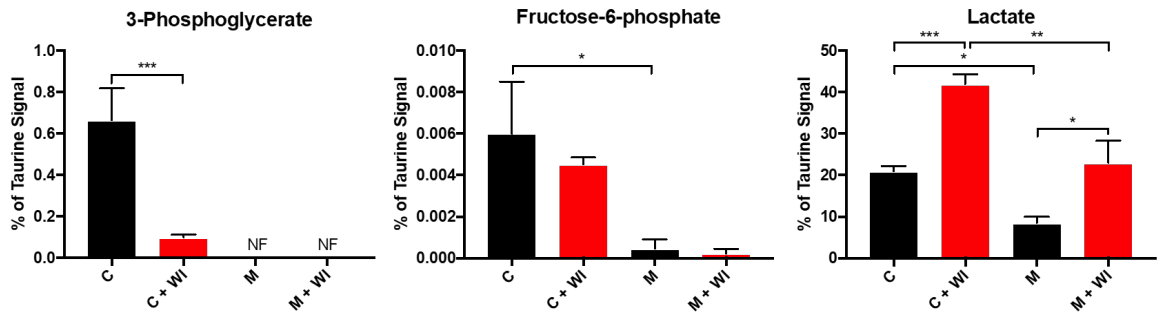

Fig. 6.15 Glycolytic intermediates in control and 30 min WI mouse heart homogenate, supernatant, cytosol and mitochondria. Metabolite ion intensities from the control and 30 min WI heart data sets were normalised to taurine. Data is from ZIC-pHILIC column unless otherwise stated as from ZIC-HILIC column. Data is average of 6 biological replicates, presented as mean ±SEM. H: Homogenate; S: Supernatant; C: Cytosolic fraction; M: Mitochondrial fraction. NF: Not found. Statistical analysis was performed by a two-way ANOVA. Means were considered statistically significant when ****$p < 0.0001$; ***$p < 0.0002$; **$p < 0.0021$; *$p < 0.0032$.

Succinate was seen to increase significantly in the cytosolic fraction following WI (**Figure 6.14**). A slight increase was seen in the mitochondrial fraction but this change was not statistically significant. Fumarate decreased in the mitochondrial fraction on both column analyses following ischaemia (although not significantly). In the ZIC-pHILIC column analysis, fumarate increased in the cytosolic fraction after ischaemia but this change was not significant. Fumarate was barely detected in the cytosol on the ZIC-HILIC analysis.

The phosphorylated glycolytic intermediates 3-phosphoglycerate and fructose-6-phosphate decreased in the cytosol following ischaemia (**Figure 6.15**). 3-phosphoglycerate was not detected in normoxic or ischaemic mitochondria, and fructose-6-phosphate was only seen at very low levels. Lactate was seen to accumulate in both fractions following ischaemia.

As expected, there was a general decrease in nucleotides and an increase in nucleotide breakdown products in both compartments following ischaemia (**Figures 6.16 and 6.17**). There were some discrepancies seen between the two compartments, with adenine and adenosine increasing in the cytosol and remaining stable in the mitochondria and the accumulation of kynurenic acid exclusively in the mitochondria. Conversely, ADP, CMP and hypotaurine decreased in the cytosol following ischaemia but remained stable, or were not detected in the case of hypotaurine, in the mitochondrial fraction. Interestingly, GMP decreased in the cytosolic fraction following ischaemia but increased in the mitochondrial fraction.

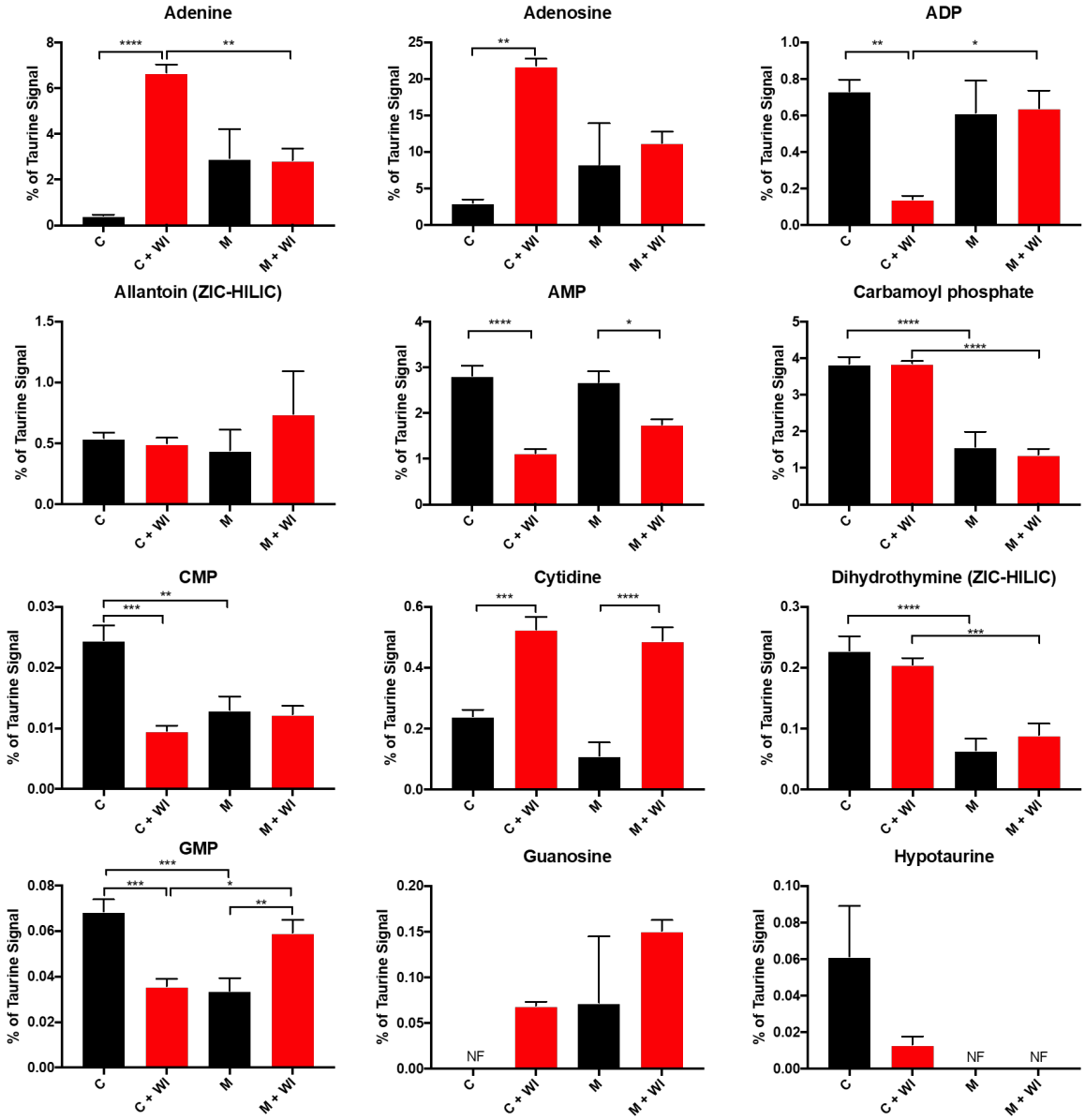

Fig. 6.16 Nucleotides and breakdown products in control and 30 min WI mouse heart homogenate, supernatant, cytosol and mitochondria. Metabolite ion intensities from the control and 30 min WI heart data sets were normalised to taurine. Data is from ZIC-pHILIC column unless otherwise stated as from ZIC-HILIC column. Data is average of 6 biological replicates, presented as mean ±SEM. H: Homogenate; S: Supernatant; C: Cytosolic fraction; M: Mitochondrial fraction. NF: Not found. Statistical analysis was performed by a two-way ANOVA. Means were considered statistically significant when ****$p < 0.0001$; ***$p < 0.0002$; **$p < 0.0021$; *$p < 0.0032$.

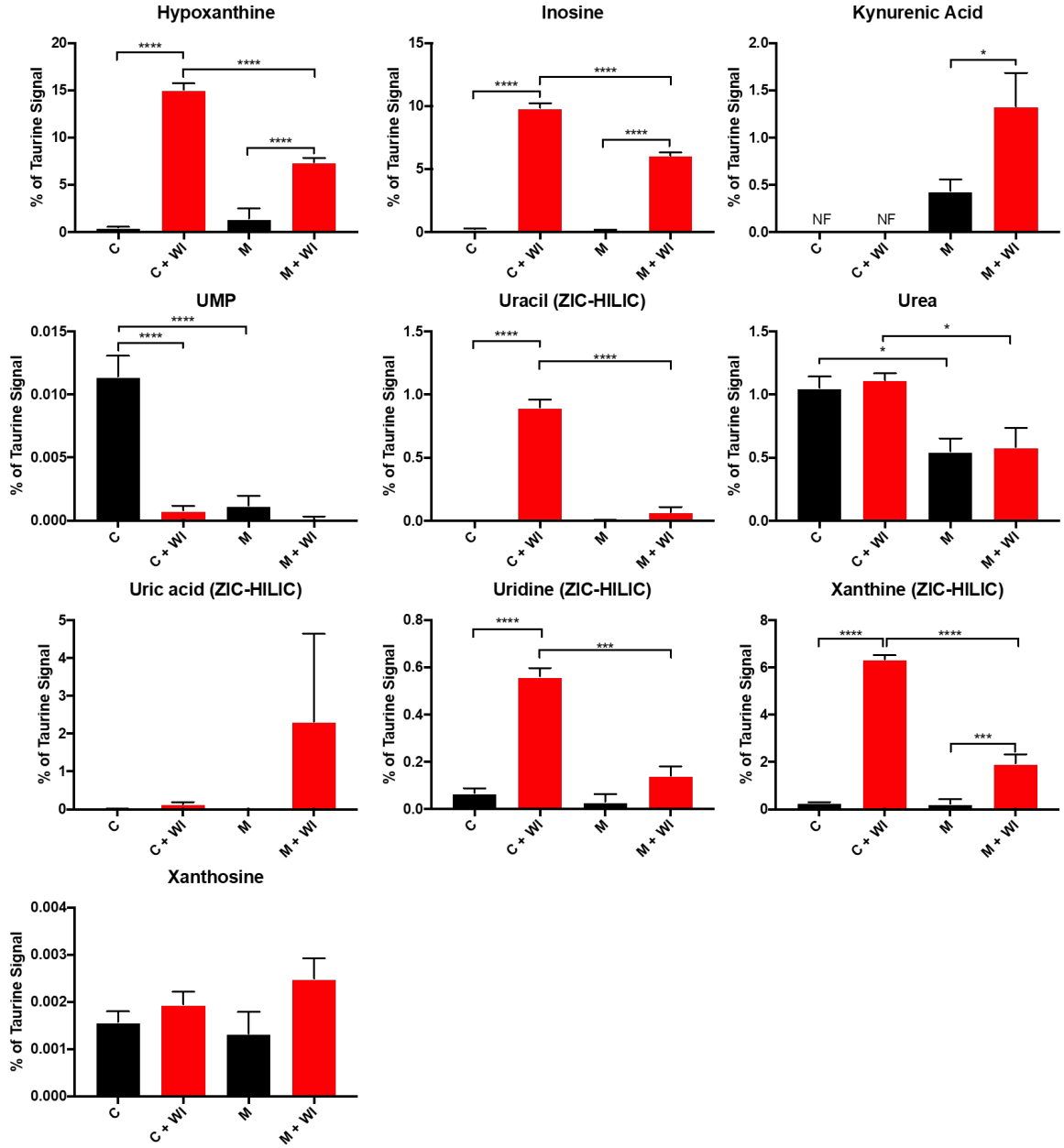

Fig. 6.17 Nucleotides and breakdown products in control and 30 min WI mouse heart homogenate, supernatant, cytosol and mitochondria (ctd.). Metabolite ion intensities from the control and 30 min WI heart data sets were normalised to taurine. Data is from ZIC-pHILIC column unless otherwise stated as from ZIC-HILIC column. Data is average of 6 biological replicates, presented as mean ±SEM. H: Homogenate; S: Supernatant; C: Cytosolic fraction; M: Mitochondrial fraction. NF: Not found. Statistical analysis was performed by a two-way ANOVA. Means were considered statistically significant when ****p < 0.0001; ***p < 0.0002; **p < 0.0021; *p < 0.0032.

There is little change in most amino acids between normoxia and ischaemia in the heart (**Figures C.1 and C.2**), with some exceptions. Namely, aspartate was seen to decrease in all fractions, and asparagine and citrulline (both higher in the mitochondrial fraction relative to taurine), decreased in the mitochondrial fraction after ischaemia but remained stable in all other fractions. Interestingly, on the ZIC-HILIC analysis, cysteine was seen to increase after ischaemia in all compartments, except the mitochondrial fraction. On both column analyses, GSH remained stable across all fractions. Some increase in GSSG levels were seen after ischaemia.

Of the carnitines that were detected, the trends following ischaemia were the same across the compartments for carnitine and propionylcarnitine (both increased following ischaemia) and butyrylcarnitine (decreased following ischaemia) (**Figure C.3**). In contrast, acetylcarnitine decreased in the cytosolic fraction but increased in the mitochondrial fraction after ischaemia.

Figure 6.18 uncovers metabolites whose cellular distribution is altered by 30 min WI, by comparing the mitochondrial:cytosolic ratio of taurine-normalised ion intensities in normoxia and after 30 min WI. Adenine, hypoxanthine, adenosine and methionine were more accumulated in the mitochondria relative to taurine under normoxic conditions, but were higher in the cytosol relative to taurine after ischaemia. In contrast, ADP, acetylcarnitine and GMP were lower in the mitochondria under normoxia but higher after ischaemia. The ZIC-HILIC column data shows that fumarate accumulates in the mitochondria after ischaemia, whereas the mitochondria:cytosol ratio for succinate decreases after ischaemia, suggesting that succinate leaves the mitochondria.

After looking at late stage-ischaemic metabolism, the metabolic changes of ischaemia were investigated in more detail by measuring metabolites at the earlier time points of 6 and 12 min WI. Mouse hearts were removed and either processed immediately (0 min WI control) or incubated at 37°C in a heat block for 6 or 12 min before homogenisation and rapid isolation of mitochondria. These data are displayed in bar graphs in **Appendix C.3**.

These data show that for the majority of metabolites, any increase or decrease has already occurred after 6 min of WI. Some metabolites, such as glycolytic intermediates (**Figure C.13**) and nucleotide breakdown products (**Figure C.14 and C.15**) continue to accumulate or deplete to 12 min, suggesting that glycolysis and nucleotide breakdown are continuing over this time frame. Fatty acids and carnitines and amino acids do not exhibit much change during the time course (**Figure C.18**).

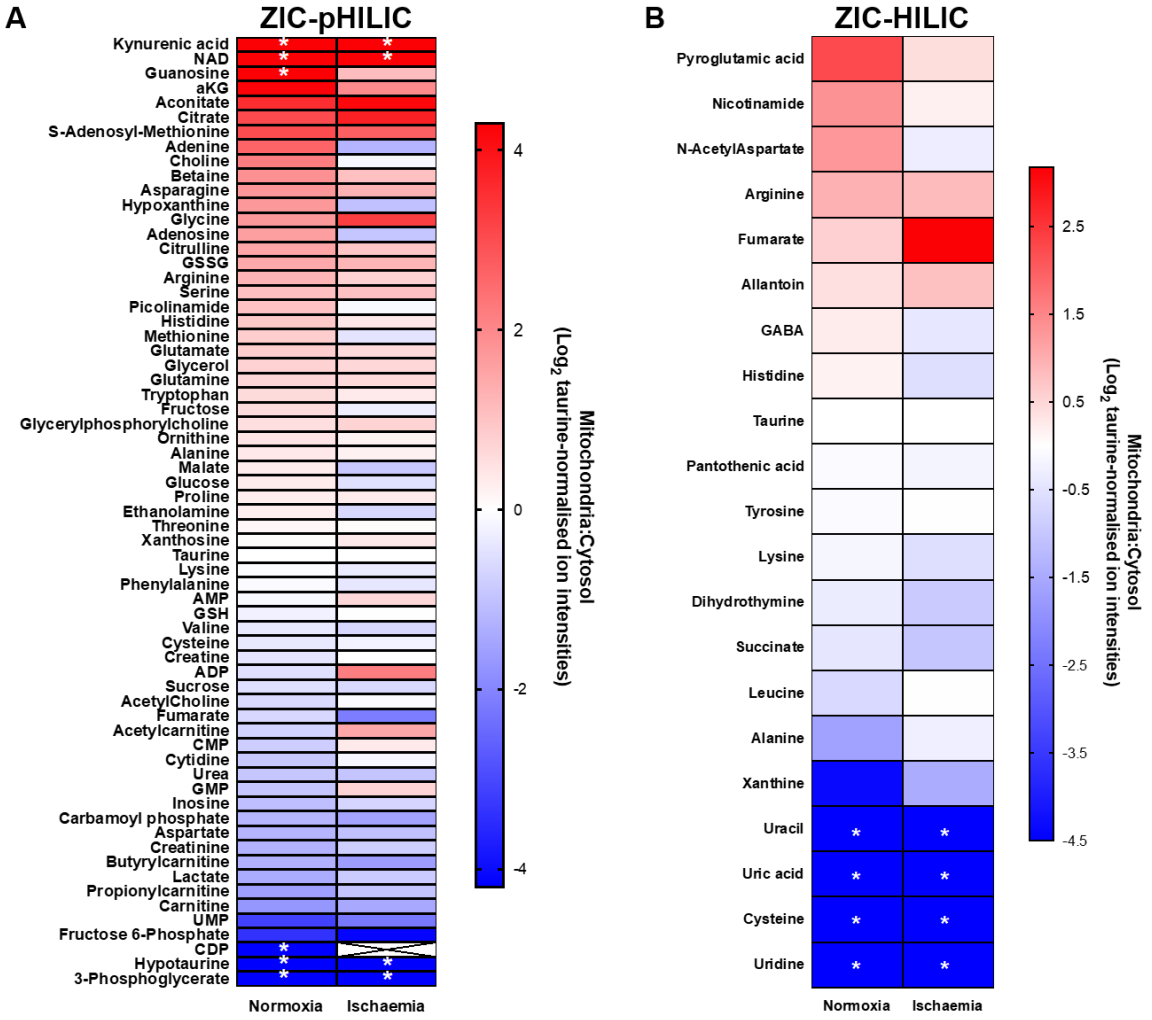

Fig. 6.18 Metabolite enrichment in normoxic and ischaemic mouse heart mitochondria. Metabolites from the control and ischaemic heart data sets were normalised to taurine and are presented as a ratio of mitochondrial:cytosolic relative amounts ($\log_2$ of the values), arranged in order of accumulation in the mitochondria. **A)** Metabolites analysed on the ZIC-pHILIC column; **B)** metabolites analysed on the ZIC-HILIC column. * - Metabolites that were not detected in the cytosolic (red) or mitochondrial (blue) fraction and were assigned an adjusted zero value. Crosses: blank values in both ischaemia and normoxia. Data are average of 6 biological replicates.

6.6.2.2 Metabolite analysis in the ischaemic liver

The ischaemic metabolism of liver was then investigated. As was done for the heart, the metabolic intermediates of the TCA cycle, glycolysis and nucleotides and their breakdown products are displayed below. Again, only the cytosolic and mitochondrial fractions are displayed. Amino acids and peptides, fatty acids and carnitines and all other metabolites are displayed in **Appendix C.2**.

Figure 6.19 shows the TCA cycle intermediates in control and ischaemic liver. Although it is hard to draw strong conclusions from these data due to the lack of statistical significance, succinate and 2-HG, a derivative of αKG, are seen to increase in both fractions following ischaemia, whereas aconitate, αKG, citrate and fumarate decrease. Malate was seen to decrease in the cytosolic fraction but increase in the mitochondrial fraction after ischaemia.

Figure 6.20 shows that the glycolytic intermediates 3-PG, glyceraldehyde-3-phosphate and PEP all decrease in ischaemic cytosol, with fructose-6-phosphate and glucose-6-phosphate remaining stable. The end products of glycolysis lactate and pyruvate are seen to increase in both the cytosolic and mitochondrial fractions following ischaemia.

In general, nucleotides, such as ADP and CTP decreased in both fractions during ischaemia and breakdown products, such as hypoxanthine and xanthine increased (**Figure 6.21 and 6.22**).

As for the heart, the majority of amino acids show the same trend across all fractions in the liver during ischaemia (**Figure C.6** and **C.7**). Many amino acids remain stable during ischaemia but some, such as asparagine, cysteine, phenylalanine, proline and tyrosine increased following ischaemia. Others, such as serine decreased after ischaemia. Aspartate was seen to decrease in all fractions after ischaemia, except in the mitochondria where it remained stable.

The normoxic and ischaemic levels of fatty acids and carnitines detected are displayed in **Figure C.8**. Carnitine and propionylcarnitine increased in all fractions following ischaemia. Acetylcarnitine decreased in all fractions except the mitochondria, where it increased slightly. Similarly, butyrylcarnitine decreased in all fractions except the mitochondria, where it remained stable.

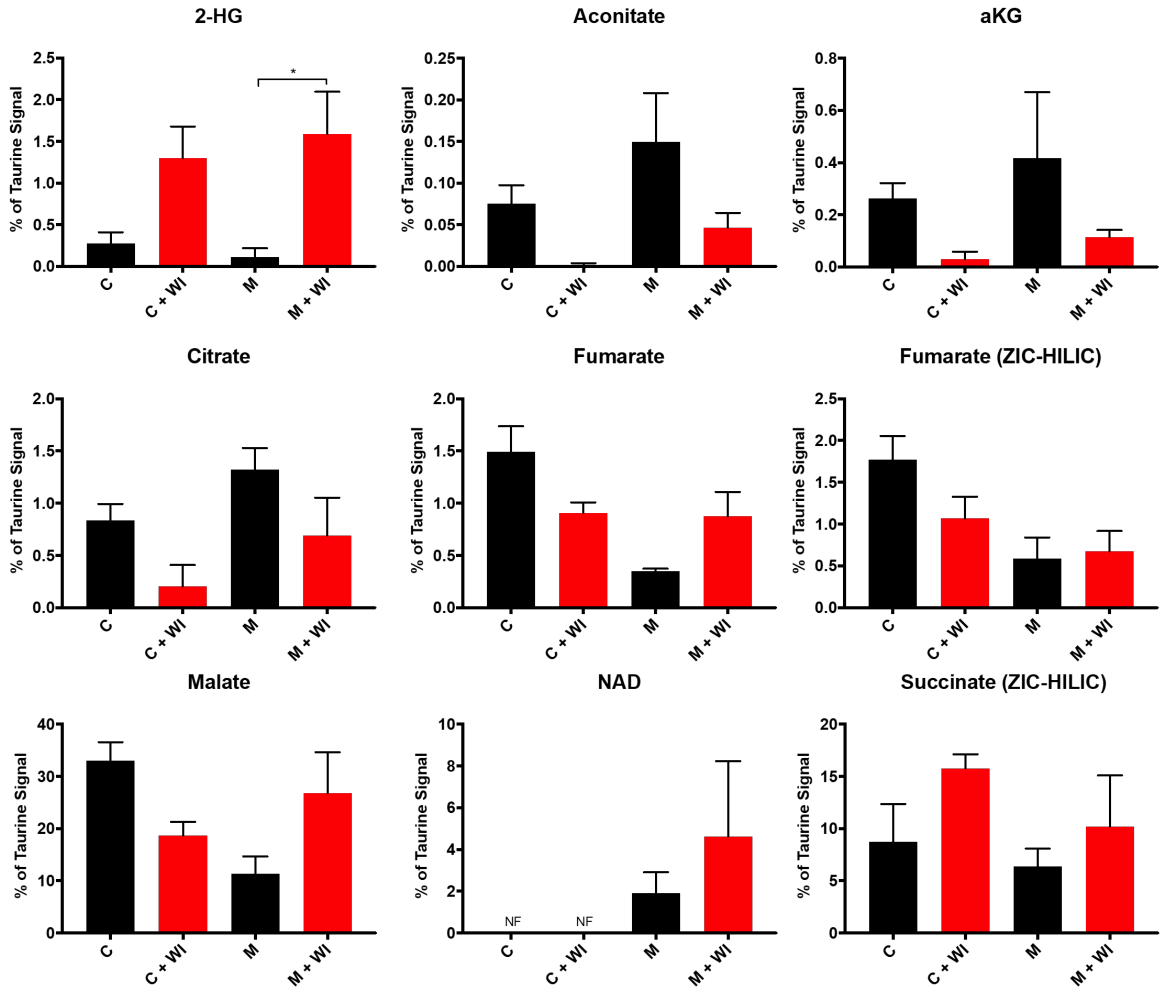

Fig. 6.19 TCA cycle intermediates in control and 30 min WI mouse liver homogenate, supernatant, cytosol and mitochondria. Metabolite ion intensities from the control and 30 min WI liver data sets were normalised to taurine. Data is from ZIC-pHILIC column unless otherwise stated as from ZIC-HILIC column. Data is average of 3 biological replicates, presented as mean ±SEM. H: Homogenate; S: Supernatant; C: Cytosolic fraction; M: Mitochondrial fraction; WI: Warm ischaemia. NF: Not found. Statistical analysis was performed by a two-way ANOVA. Means were considered statistically significant when ****$p < 0.0001$; ***$p < 0.0002$; **$p < 0.0021$; *$p < 0.0032$.

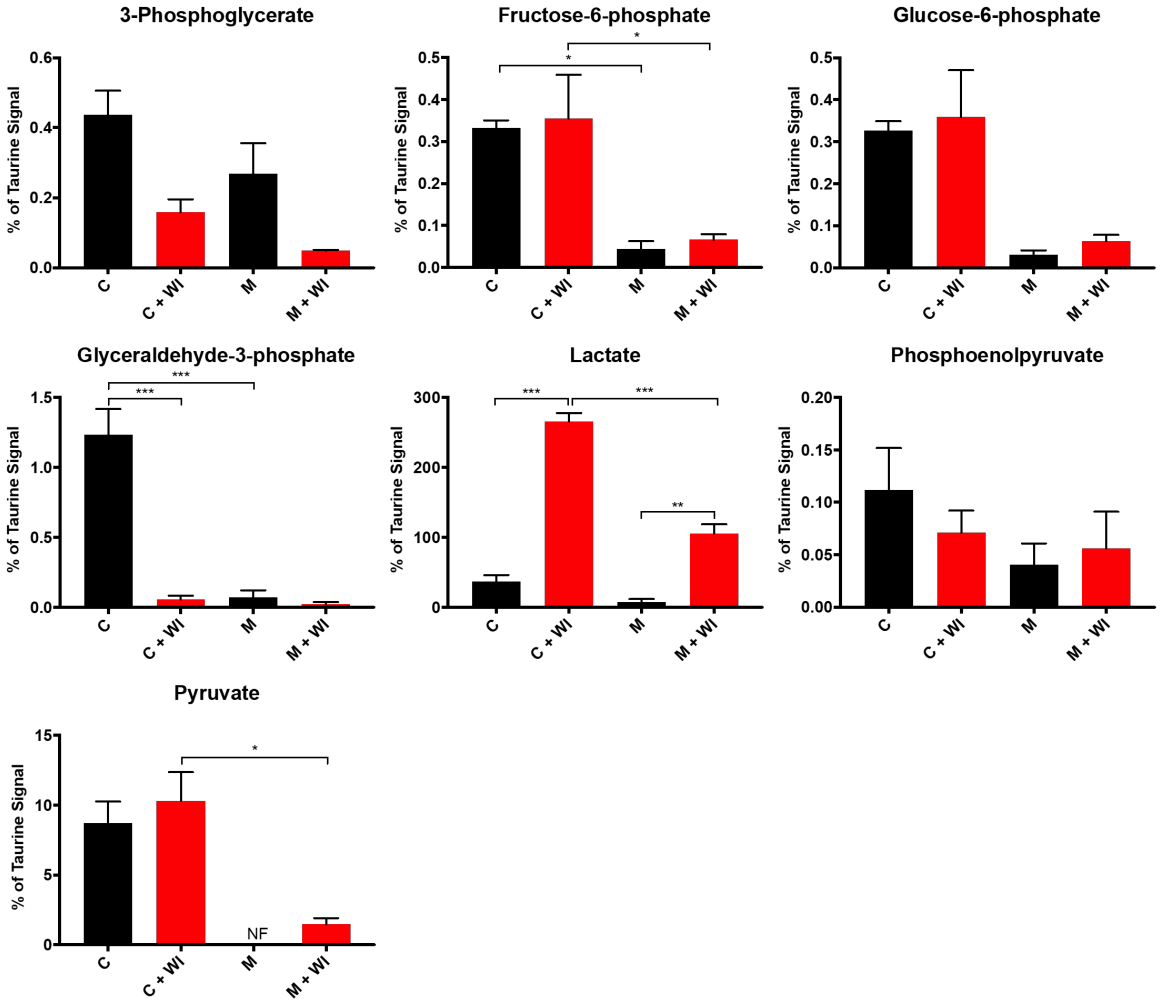

Fig. 6.20 Glycolytic intermediates in control and 30 min WI mouse liver homogenate, supernatant, cytosol and mitochondria. Metabolite ion intensities from the control and 30 min WI liver data sets were normalised to taurine. Data is from ZIC-pHILIC column unless otherwise stated as from ZIC-HILIC column. Data is average of 3 biological replicates, presented as mean ±SEM. H: Homogenate; S: Supernatant; C: Cytosolic fraction; M: Mitochondrial fraction; WI: Warm ischaemia. NF: Not found. Statistical analysis was performed by a two-way ANOVA. Means were considered statistically significant when ****$p < 0.0001$; ***$p < 0.0002$; **$p < 0.0021$; *$p < 0.0032$.

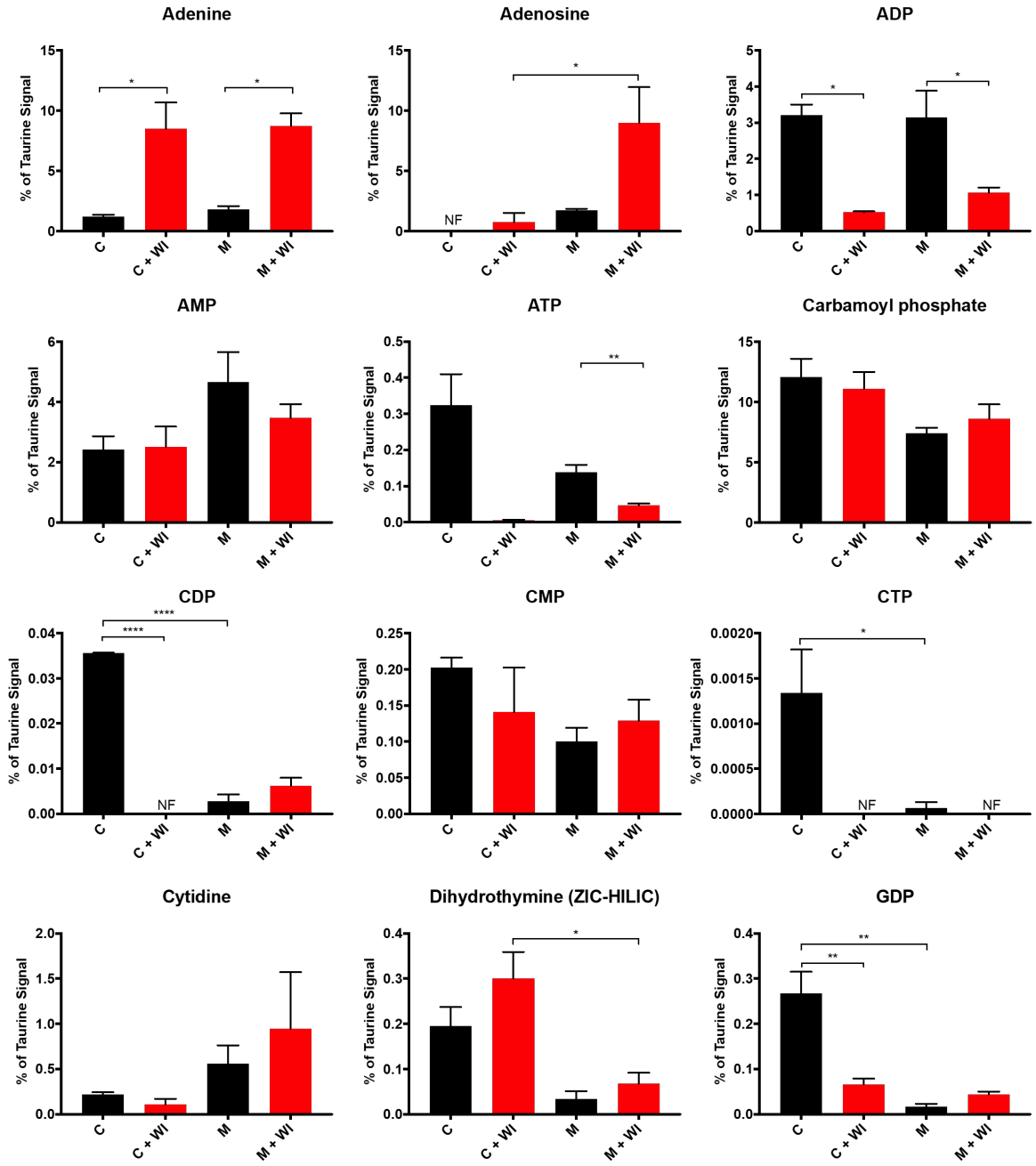

Fig. 6.21 Nucleotides & breakdown products in control and 30 min WI mouse liver homogenate, supernatant, cytosol and mitochondria. Metabolite ion intensities from the control and 30 min WI liver data sets were normalised to taurine. Data is from ZIC-pHILIC column unless otherwise stated as from ZIC-HILIC column. Data is average of 3 biological replicates, presented as mean ±SEM. H: Homogenate; S: Supernatant; C: Cytosolic fraction; M: Mitochondrial fraction; WI: Warm ischaemia. NF: Not found. Statistical analysis was performed by a two-way ANOVA. Means were considered statistically significant when ****$p < 0.0001$; ***$p < 0.0002$; **$p < 0.0021$; *$p < 0.0032$.

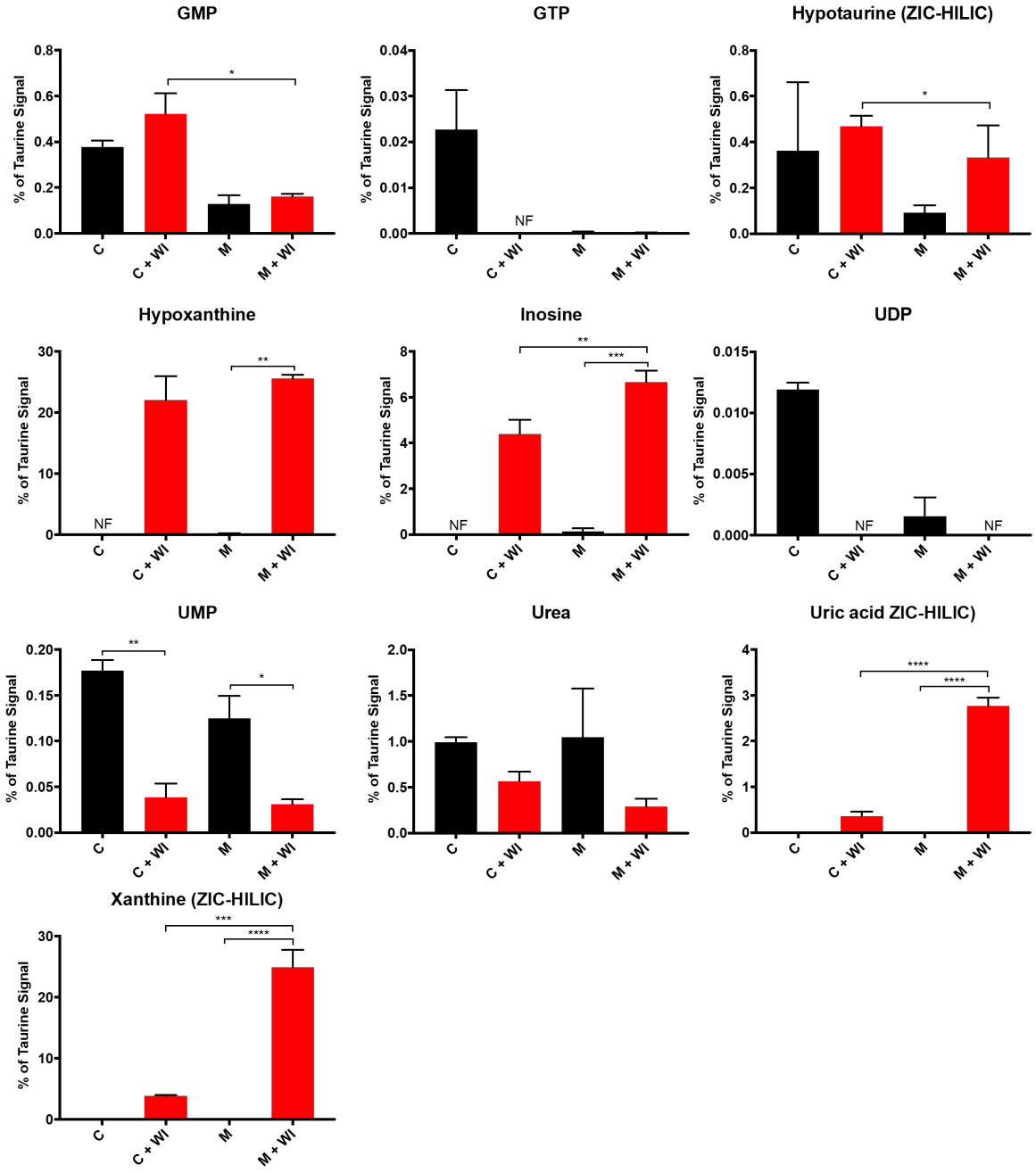

Fig. 6.22 Nucleotides & breakdown products in control and 30 min WI mouse liver homogenate, supernatant, cytosol and mitochondria (ctd.). Metabolite ion intensities from the control and 30 min WI liver data sets were normalised to taurine. Data is from ZIC-pHILIC column unless otherwise stated as from ZIC-HILIC column. Data is average of 3 biological replicates, presented as mean ±SEM. H: Homogenate; S: Supernatant; C: Cytosolic fraction; M: Mitochondrial fraction; WI: Warm ischaemia. NF: Not found. Statistical analysis was performed by a two-way ANOVA. Means were considered statistically significant when ****$p < 0.0001$; ***$p < 0.0002$; **$p < 0.0021$; *$p < 0.0032$.

Figure 6.23 examines how ischaemia alters the cellular distribution of metabolites, as was presented in **Figure 6.18** for the heart. It shows that succinic glutathione, ATP and acetylcarnitine are more accumulated in the mitochondria after ischaemia. The ZIC-HILIC column analysis (right) shows that succinate is consistently lower in the mitochondria than the cytosol (relative to taurine) in normoxia and ischaemia, as was fumarate. Cytidine was seen to become higher in the mitochondria than the cytosol after ischaemia.

As was done for the heart, a more detailed exploration of ischaemic changes in liver metabolism was performed by measuring metabolites at 0, 6, 12 and 30 min WI (**Appendix C.4**). Similar to the situation in the heart, a lot of ischaemic metabolism appears to have already occurred by 6 min WI in the liver. However, one difference from the heart was that αKG decreases over the time course of WI in liver but increases in the heart (**Figure C.21**). Amino acids and peptides generally remained stable across all fractions (**Figure C.25 and C.26**). Nucleotides decreased over the time course of ischaemia and their breakdown products increased (**Figure C.23 and C.24**).

6.7 Summary & Discussion

6.7.1 Data analysis

The data displayed here were analysed by a two-way ANOVA to investigate the statistical relationships between all fractions. However, this may not be the most appropriate method of analysis. Going forward, the data may be reanalysed using a different statistical analysis, such as a one-way ANOVA. Importantly, this may alter the statistical significance of the changes between the normoxic and ischaemic fractions and allow us to draw more confident conclusions from the data.

6.7.2 Normoxic metabolism

Analysis of the control heart showed that TCA cycle intermediates and associated metabolites aconitate, αKG and citrate were compartmentalised to the mitochondria, and the other TCA intermediates that were detected were distributed across the cell, including succinate. NAD^+ was detected in the mitochondria but not the cytosol. This is consistent with the finding that

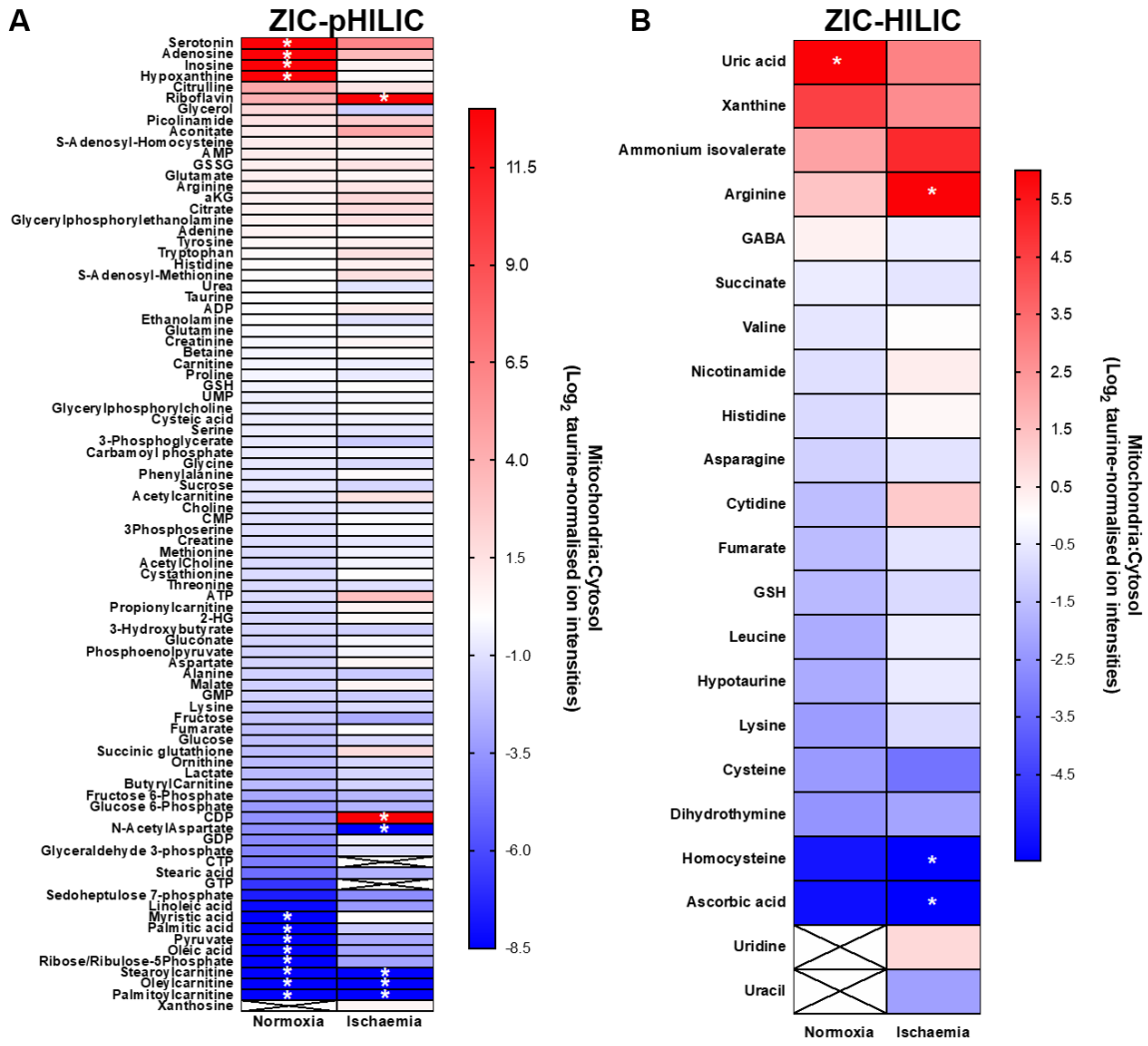

Fig. 6.23 Metabolite enrichment in normoxic and ischaemic mouse liver mitochondria. Metabolites from the control and ischaemic liver data sets were normalised to taurine and are presented as a ratio of mitochondrial:cytosolic relative amounts ($\log_2$ of the values), arranged in order of accumulation in the mitochondria. **A)** Metabolites analysed on the ZIC-pHILIC column; **B)** metabolites analysed on the ZIC-HILIC column. * - Metabolites that were not detected in the cytosolic (red) or mitochondrial (blue) fraction and were assigned an adjusted zero value. Crosses: blank values in both ischaemia and normoxia. Data is average of 3 biological replicates.

up to 70% of cellular NAD^+ is in the mitochondria (VanLinden et al., 2015). However, why NAD^+ was not detected in the cytosol is unclear. In comparison, the control liver TCA cycle intermediates were all more evenly distributed throughout the cell. Phosphorylated glycolytic intermediates were either not detected or were only seen at low levels relative to taurine in both heart and liver mitochondria, which was anticipated because these metabolites do not have carriers on the MIM. These results indicate that the method is capable of showing the correct locations of metabolites whose distribution is already known, suggesting that it can be used to determine the distribution of metabolites with unknown cellular distributions.

The breakdown of nucleotides occurs when there are excess nitrogenous compounds or when the cell is deprived of oxygen and needs an alternative energy source. Therefore, it was not expected to see a high level of breakdown products in the control data set. **Figures 6.4, 6.5, 6.9 and 6.10** show that some are seen in both control heart and liver in all fractions, and that, overall, they are evenly distributed between the mitochondria and cytosol, although there are some differences. Namely, hypotaurine was not detected in heart mitochondria and was very low in liver mitochondria, but was high relative to taurine in the cytosol. Kynurenic acid and guanosine were only found in heart mitochondria (they were not present in the liver dataset). In the heart, hypoxanthine was highest in the mitochondrial fraction, with xanthine distributed across all fractions, whereas in the liver hypoxanthine and xanthine were detected in the mitochondrial fraction but were very low in the cytosolic fraction.

In the heart, the amino acids that were analysed were evenly distributed between the mitochondria and the cytosol. In comparison, in the liver, many amino acids were seen to increase after ischaemia. In both tissues, GSSG was very low relative to taurine, indicating very little oxidation of GSH had occurred during the isolation procedure.

The conditions of the LC-MS method are not optimal for fatty acids and carnitines, so it is difficult to draw strong conclusions from the data obtained for these metabolites. Carnitine was shown to increase after 30 min WI in all fractions of heart and liver, and acetylcarnitine was shown to increase in the mitochondria of both tissues but decrease in all other fractions after ischaemia. However, for the technical reasons given above, this needs to be assessed further before we can draw any conclusions.

6.7.3 Ischaemic metabolism

Glycogen is an important energy storage molecule, which releases glucose that can enter glycolysis to generate energy under conditions such as ischaemia. The levels of glycogen were measured over a time course of both warm and cold ischaemia in heart tissue of mouse, pig and human (**Figure 6.12**). During WI, all animals showed a rapid drop in the levels of glycogen in the early stages of WI, as the cell shifts to glycolysis to survive the ischaemic insult. This decrease then plateaus, despite some glycogen remaining. In contrast, the depletion of glycogen levels is much more steady during CI, and does not reach a plateau but continues to decrease for the full time course of ischaemia measured in the experiment. This suggests that cooling the tissue is a protective mechanism that slows down metabolism and may enable the tissue to withstand longer periods of ischaemia and, in addition, to more fully utilise its glycogen stores to supply energy to the tissue.

A caveat to the ischaemic experiments is that during ischaemia, and other insults, the mitochondria will become damaged, potentially affecting the isolation yield. The mitochondrial density may change due to swelling and could even burst, so it may be that a greater proportion of "healthy" mitochondrial metabolites is obtained in the mitochondrial pellet, because the very "unhealthy" mitochondria will have not passed through the oil and are thus excluded from the mitochondrial pellet. In this case it may be that we see a higher level of mitochondrial metabolites in the cytosolic fraction.

Citrate was seen to be compartmentalised to the mitochondria in heart, which confirms the robustness of the method as the CIC has low activity in heart tissue (Palmieri, 2004). In contrast, in the liver, which has much higher CIC activity, citrate was more distributed throughout the cell, consistent with its role in fatty acid synthesis.

Lactate was seen to accumulate in both the cytosol and the mitochondria after ischaemia in the heart and the liver (**Figures 6.15 and 6.20**). Lactate accumulates during ischaemia when the end-product of glycolysis, pyruvate, is converted to lactate. Lactate can then enter gluconeogenesis to regenerate glucose. Traditionally, it was assumed that lactate was converted back to pyruvate in the cytosol, with pyruvate entering the mitochondria and the TCA cycle via AcCoA. However, recent evidence has suggested that lactate also enters the mitochondria and is there converted to pyruvate (Chen et al., 2016b). This theory is reinforced by the detection of lactate in rapidly isolated mitochondria.

A summary of the normoxic and ischaemic distributions of metabolites in heart and liver are shown in **Figures 6.18 and 6.23**, respectively. Due to the high number of metabolites on these heat maps, the scale is very large and thus they should only be used as a qualitative tool to determine which metabolites are abundant in the mitochondria and which are more abundant in the cytosol. They show that in both the heart and the liver, succinate is more accumulated in the cytosol during normoxia and ischaemia. Further exploration into this area is needed, but this could reflect one of a number of possibilities. One interesting scenario is that the succinate that accumulates during ischaemia is exported to the cytosol, potentially via an exchange mechanism through the DIC in exchange for malate. However, the precise mechanism of how succinate enters the cytosol during ischaemia is not known. It is unlikely that the succinate enters the cytosol as a result of rupturing of the mitochondria, as other metabolites are retained, hence the low amounts of succinate in the rapidly isolated mitochondria suggest that it is selectively exported to the cytosol. Another potential reason for the low amount of succinate in the mitochondria is that the speed of cooling and homogenising the organ is not sufficient to prevent the oxidation of mitochondrial succinate. Taken in the context of the behaviour of other metabolites during ischaemia, the data is consistent with the model depicted in **Figure 6.24**. In this model of heart ischaemia, fumarate is decreased in the mitochondria following WI, due to conversion to succinate by reversal of CII. The succinate is exported to the cytosol via the DIC, in exchange for cytosolic malate. Once in the mitochondria, malate is converted to fumarate (by fumarate hydratase), which is itself metabolised to succinate by reversal of SDH. The export of succinate leads to the accumulation of cytosolic succinate following ischaemia. Succinate is known to activate its receptor SUCNR1 on the PM, and as such is expected to be present in the cytosol (Gilissen et al., 2016; He et al., 2004; Peti-Peterdi et al., 2013). Despite these expectations, this has not been directly demonstrated to my knowledge and thus this project is the first time succinate has been shown to accumulate in the cytosol of an ischaemic tissue. The succinate that is transported to the cytosol acts as a signal, relaying the ischaemic stress signal to the rest of the cell. For example, succinate is known to be involved in the activation of the HIF-1α pathway, by inhibiting the PHD enzyme in the cytosol (Tannahill et al., 2013).

Upon reperfusion, there are two possible fates for the succinate that accumulated during WI (**Figure 6.24**). The first is that it is reoxidised to fumarate by the forward activity of SDH. While we did not show that the succinate that was exported to the cytosol is then imported back into the mitochondria upon reperfusion, this seems likely because the succinate decreases back to baseline levels in tissues upon reperfusion (Chouchani et al., 2014). In

addition, a second fate for the succinate is that it can be released from the cell. There is mounting evidence that succinate may act as a paracrine signal to activate SUCNR1 on neighbouring cells (Murphy, O'Neill, 2018). Thus, the discovery of succinate accumulating in the cytosol during WI lends credence to the hypothesis of succinate efflux from the cell during reperfusion.

Figure 6.25 displays the two fates of the succinate that accumulates during WI. The line graph depicts the amount of succinate detected in the perfusate over 6 min of reperfusion following 20 min of WI. The grey bar on the right shows the amount of succinate in heart tissue at the end of the 20 min WI period and the blue bar on the left shows the amount of succinate in heart tissue after 6 min of reperfusion (following 20 min WI). Thus, the difference between these 2 bars (red arrow) is the amount of succinate that is oxidised during reperfusion. It can be seen that a significant proportion of succinate is released from the cell into the perfusate and the remainder is reoxidised. Important future experiments would be to explore the fate of the succinate once in the cytosol. It may activate cytosolic signalling pathways such as the HIF pathway. There is evidence for succinate efflux from the cell after periods of ischaemia (**Figure 6.25**), where it may then signal to other cells via activating the G-coupled receptor SUCNR1. This receptor is expressed in many organs (heart, liver, kidney and retina) and different cell types, including cardiomyocytes and immune cells. (Sundström et al., 2013).

In conclusion, I have shown by applying this technique that succinate distributes during ischaemia, leading to discrete pools in the cytosol and the mitochondria. The project has also elucidated the cellular distribution of a wide range of other metabolites and highlighted some differences between heart and liver tissue. Thus, the rapid isolation procedure is capable of studying compartmentalisation of metabolism in tissue.

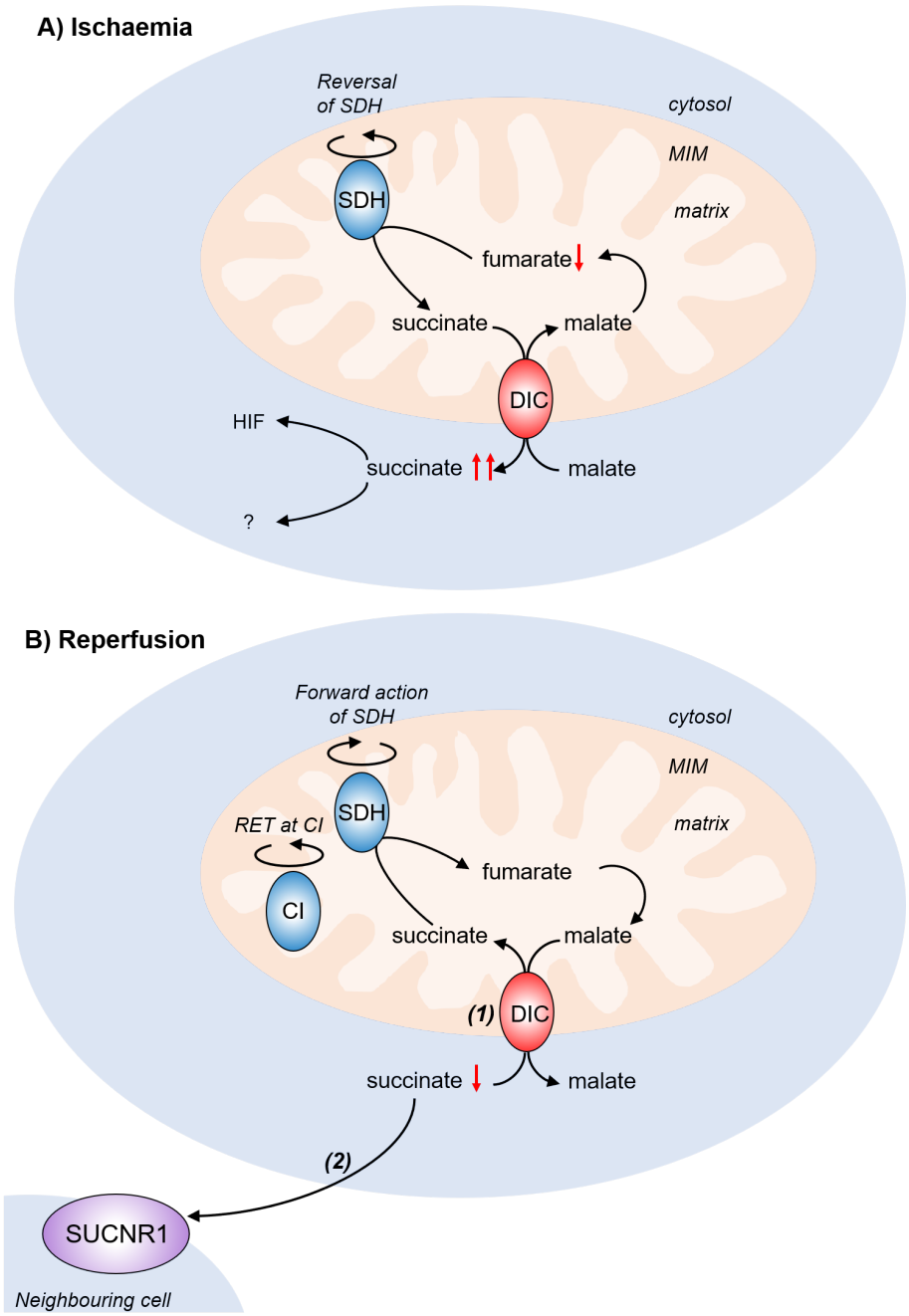

Fig. 6.24 Schematic depicting proposed model of metabolism in the cytosolic and mitochondrial compartments of the heart during ischaemia and reperfusion. **A)** During ischaemia, succinate accumulates due to the reversal of SDH. Succinate is then exported to the cytosol through the DIC, in exchange for cytosolic malate. Once in the cytosol, succinate is known to be involved in the activation of the HIF-1α pathway. Investigation into other signalling roles of cytosolic succinate is an interesting area for research. **B)** Upon reperfusion, succinate may either be imported back into the mitochondria for oxidation by the forward action of SDH (1), or it may be exported from the cell (2) and act as a paracrine signal by activating the succinate receptor, SUCNR1, on neighbouring cells.

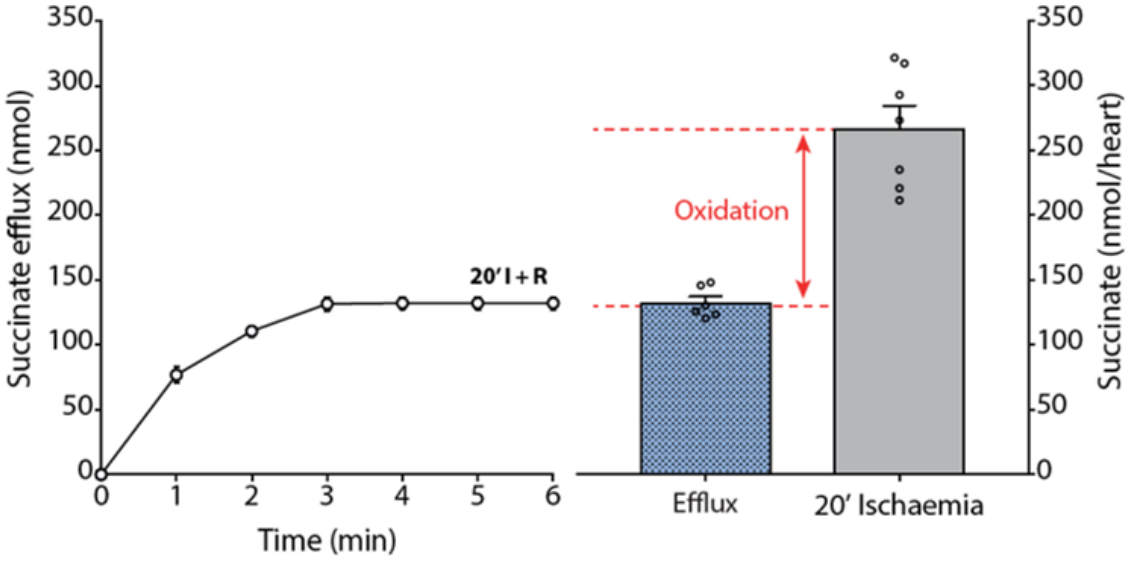

Fig. 6.25 Succinate accumulation and efflux during ischaemia and reperfusion in the isolated Langendorff mouse heart. Isolated Langendorff mouse hearts were subjected to 20 min WI before reperfusion. Succinate levels were measured in the heart and in the perfusate. Experiments performed and data provided by Dunja Aksentijević and Hiran Prag.

Chapter 7

General discussion & future directions

Detailed discussions of the method development and findings have been outlined at the end of each chapter. In this section, the limitations of the isolation procedure, the major implications of the findings and future experiments will be discussed. The focus of this thesis has been to develop a rapid method of isolating mitochondria from tissue, such that information can be obtained on the differences in metabolism between the mitochondrial and the cytosolic compartments. This was of interest to our lab because previous studies have shown specific metabolic changes during disease states, such as ischaemia-reperfusion injury (Chouchani et al., 2014; Ferrari, 1995; Heather et al., 2013; Martin et al., 2019), but were not able to identify where in the cell these metabolic changes were occurring. To do so, a new mitochondrial isolation procedure was necessary because at the start of this project there was no mitochondrial isolation method that was compatible with LC-MS metabolomic studies. Furthermore, the rapid redistribution of metabolites from mitochondria to the rest of the cell was thought to be important in pathology and signalling, but the existing mitochondrial isolation methods were not fast enough to prevent artefactual metabolite distribution and metabolism during isolation. The best method at the time was that of Chen et al. (2016a), but even this took 12 min and required HA-tagging of mitochondria in cultured cells prior to isolation. As we were interested in metabolism in tissue during normoxia and ischaemia, this method was not suitable and we required a new isolation procedure. The major stipulations of this new method were that it should be able to be performed extremely quickly and at a low temperature to prevent metabolite distribution and dismutation, and that it should sufficiently separate the mitochondria from the cytosol. The most important step to prevent metabolism is to get the organ into the cold homogenisation buffer and fully homogenised as quickly

as possible, because low temperature is an extremely effective way of limiting metabolite transporter and enzymatic activities.

The first sections of the thesis addressed the development of the rapid mitochondrial isolation procedure, first in rat heart and liver and then in mouse heart and liver. The last section used the method to analyse metabolic differences between the mitochondria and the cytosol under normoxic conditions in both mouse heart and liver tissue and how these change under ischaemic conditions. The rapid isolation procedure was based on a range of previous isolation methods and adopted the use of a tripartite layering system: the tissue homogenate is layered on a silicone oil layer mixed with DOP, above an acidic layer at the bottom of the tube. Whilst optimising the conditions, I discovered that the technique is extremely sensitive to the density, and thus the temperature and methods of preparation, of the three layers. This discovery allowed me to develop the method much further and more successfully than previous attempts by this lab and others.

After optimising the technique to rapidly isolate mitochondria from tissue, the first objective was to characterise the function and purity of the isolated mitochondria. The experiments described in **Chapter 4** demonstrate that the mitochondria are separated from the cytosol and other organelles to a level similar to a standard "slow" mitochondrial isolation. The absolute amounts of mitochondria obtained using this method from heart and liver is lower than a standard mitochondrial isolation, but for the intended application of LC-MS this is not an issue, as only a small amount of sample material is necessary to detect metabolites using this sensitive method. Indeed, preliminary LC-MS data indicated that the method can detect mitochondrial metabolites and can distinguish both mitochondrial and cytosolic metabolite pools. The mitochondria were shown to remain intact, allowing them to perform coupled respiration and, fundamentally, to retain their metabolites. An important finding of **Chapter 4** was that damaged mitochondria are able to pass through the silicone oil into the acidic layer. This has implications for the normalisation and analysis of the metabolomic data and dictated that the metabolite ion intensities cannot be normalised to protein.

Building on this information, the LC-MS analytical approach was developed. To improve the MS signal, it was found that the optimum procedure was to pool 4 mitochondrial isolations together, before evaporating the formic acid and resuspending the dried metabolites in water. The LC-MS method that was used was designed to focus on polar metabolites, meaning that fatty acids and other non-polar metabolites are not measured as effectively. However, by using

a different LC-MS method, such as different extraction conditions and LC columns, these metabolites could easily be detected more reliably from the rapidly isolated mitochondria.

For this project, a relative quantification approach was taken, to facilitate the measurement of a broad range of metabolites (>100), as opposed to the absolute quantification of a small selection of metabolites. However, in future work we can use this system to analyse and quantify the absolute distribution of certain key metabolites, such as succinate, by the use of internal standards. For relative quantification to be performed, the metabolite ion intensities must be normalised. The experiments with alamethicin to damage the mitochondria in **Chapter 4** demonstrated that damaged mitochondrial protein is able to pass through the silicone oil layer. This meant that the ion intensities cannot be normalised to protein and must be normalised to another, stable metabolite, as it will behave in the same way to themselves. The requirements of this metabolite were that it must be: relatively evenly distributed across the cytosolic and mitochondrial compartments, with either no or slow transport systems between them; relatively metabolically inactive during the conditions the organ is experimentally exposed to, and abundant enough to be easily detected on the LC-MS. Both GSH and taurine were considered, but due to the inconsistent results when normalising to GSH, taurine was chosen. Preliminary experiments comparing taurine-normalised and raw ion intensities showed that normalising to taurine did not skew any trends. However, there is evidence that taurine is not as metabolically inactive as we would wish, especially in the ischaemic myocardium (Venturini et al., 2009). Nevertheless, its metabolism is slow so it is unlikely to be affected in the time frames of these experiments. Indeed, the raw ion intensities of taurine in the ischaemic heart suggest it is not affected. In the future, normalisation to other metabolites should be trialled. For more targeted analyses, it would be possible to quantify the metabolites by adding a stable isotope but this was not suitable for the global metabolomic analysis performed here because of the large number of metabolites analysed simultaneously. While developing the normalisation approach, it was found that the correlation between the ZIC-pHILIC and the ZIC-HILIC column was not as strong as expected, which meant that the metabolites must be normalised to the taurine ion intensity from the same column. In the future, absolute quantification techniques will be used by others in the lab to obtain a more accurate picture of metabolism. For example, isotope labelling, internal standard and pulse chase could be used to quantify succinate accumulation and distribution during ischaemia and its oxidation during reperfusion.

The use of transport and respiratory inhibitors was explored to identify whether they could limit distribution and interconversion of metabolites within the rapid time frame of the

isolation procedure. The preliminary data obtained shows that none of the inhibitors trialled (BTM, NEM and PRP) had a significant effect on metabolite levels and distribution. This probably indicates that the extraction is performed quickly enough that metabolism is quenched sufficiently by the cold temperature and acid. However, we cannot entirely eliminate the possibility that the concentration of inhibitor added was not high enough. Further experiments are required here to understand the implications of these results, such as with genetic knock-out (KO) mice or by pre-infusing with inhibitors. Nevertheless, the addition of transport and respiratory inhibitors should be carefully considered and may be more useful when looking at a specific area of metabolism rather than a global metabolic overview, because the downstream and off-target metabolic effects of these inhibitors is unknown. For example, they may also inhibit other transporters and affect other metabolite pools, leading to erroneous conclusions that certain metabolic pathways are connected or affected in specific conditions.

Once the isolation procedure had been fully optimised, it was used to explore the important question of what happens to the metabolite pools in the cytosolic and mitochondrial compartments, in particular succinate, during ischaemia. It is of interest to determine whether the succinate that accumulates during ischaemia remains in the mitochondria or is transported to the cytosol, and, if so, how much succinate is transported and at what stage during ischaemia. Understanding the behaviour of these pools would aid in the identification of therapeutic targets to limit damage during IRI. To this end, a metabolomic analysis was performed on ischaemic mouse heart and liver. As discussed in **Section 6.7.3**, the data obtained from this analysis suggests that the succinate that accumulates during WI is exported to the cytosol. In the ischaemic model used, some primary WI inevitably occurs between the moment of breaking the neck and extracting the organ from the animal and placing it into cold sucrose buffer. To avoid this, anaesthesia could be applied before opening the chest cavity and removing the heart, reducing the time of WI to 5 sec, as in the ischaemic model used for glycogen measurements. However, there is evidence that anaesthetic may affect cellular metabolism (Overmyer et al., 2015). The use of inhibitors to minimise the effect of this primary WI was explored, but again the interpretation of the results is complicated, because it is unknown what effect blocking some of these transporters would have on downstream metabolism, and also whether they would target other transporters.

This method has prepared the groundwork that will enable my lab and others to perform many potentially insightful experiments in the future. An interesting avenue would be to perform a metabolomic analysis on tissue that has been reperfused after a period of WI. For the heart,

this should be done using the Langendorff model, in which the whole heart is removed from the animal and retrogradely perfused *ex vivo* (Bell et al., 2011). The Langendorff model of global organ ischaemia via cessation of perfusate flow would be preferable to regional ischaemia via occlusion of the left anterior descending artery (LAD) in this case, because it would be difficult to quickly cut out the ischaemic zone after LAD occlusion, and this delay could lead to metabolite distribution and degradation. This would further our understanding of how the cytosolic and mitochondrial metabolite pools behave during the full course of IRI, and how therapeutic treatments, such as dimethyl malonate (Chouchani et al., 2014), alter these changes. This should also be performed in other organs, such as the liver and kidney, to aid understanding of the different metabolic responses to ischaemic insults in these organs. The isolation procedure could also be used to examine the metabolism of animals with genetic KO of metabolically relevant genes, offering insight into the role of particular steps in metabolism in health and disease.

Together, this work has contributed to the field a method that can be used to obtain more information on many aspects of mitochondrial biology. The isolation procedure is relatively simple to perform and does not require the use of specialised equipment or reagents. The total time from mouse to mitochondria is under 5 min, which is much shorter than other methods currently used. Importantly, the organ is removed from the animal within 25-30 sec and immediately placed in ice-cold buffer, and fully homogenised within 1.5 min. The method uses whole tissue not cultured cells, meaning that the metabolic information obtained is much more physiologically relevant. The isolation procedure has been shown to generate comparatively pure mitochondria which are capable of coupled respiration and can be used for a wide range of applications to study mitochondria. The metabolomic study on these rapidly isolated mitochondria has shown that succinate accumulates in the cytosol during ischaemia, and highlights this as an interesting avenue for future study.

References

Acín-Pérez Rebeca, Carrascoso Isabel, Baixauli Francesc, Roche-Molina Marta, Latorre-Pellicer Ana, Fernández-Silva Patricio, Mittelbrunn María, Sanchez-Madrid Francisco, Pérez-Martos Acisclo, Lowell Clifford A., Manfredi Giovanni, Enríquez José Antonio. ROS-Triggered Phosphorylation of Complex II by Fgr Kinase Regulates Cellular Adaptation to Fuel Use // Cell Metabolism. 2014. 19, 6. 1020–1033.

Adeva-Andany María M, Carneiro-Freire Natalia, Seco-Filgueira Mónica, Fernández-Fernández Carlos, Mouriño-Bayolo David. Mitochondrial β -oxidation of saturated fatty acids in humans // Mitochondrion. 2019. 46, October 2017. 73–90.

Akram Muhammad. Citric Acid Cycle and Role of its Intermediates in Metabolism // Cell Biochem Biophys. 2014. 68. 475–478.

Arnoult Damien, Soares Fraser, Tattoli Ivan, Girardin Stephen E. Mitochondria in innate immunity // EMBO Rep. 2011. 12, 9. 901–910.

Arslan Fatih, De Kleijn Dominique P., Pasterkamp Gerard. Innate immune signaling in cardiac ischemia // Nature Reviews Cardiology. 2011. 8, 5. 292–300.

Bar-Even Arren, Flamholz Avi, Noor Elad, Milo Ron. Rethinking glycolysis: on the biochemical logic of metabolic pathways // Nature Chemical Biology. 2012. 8, 6. 509–517.

Barron John T, Gu Liping, Parrillo Joseph E. Malate-Aspartate Shuttle, Cytoplasmic NADH Redox Potential, and Energetics in Vascular Smooth Muscle // Journal of Molecular and Cellular Cardiology. 1998. 30. 1571–1579.

Bell Robert M, Mocanu Mihaela M, Yellon Derek M. Retrograde heart perfusion: The Langendorff technique of isolated heart perfusion // Journal of Molecular and Cellular Cardiology. 2011. 50, 6. 940–950.

Bender Tom, Martinou Jean-claude. The mitochondrial pyruvate carrier in health and disease: To carry or not to carry ? // Biochimica et biophysica acta. 2016. 1863, 10. 2436–2442.

Bensley R. R., Hoerr N. L. Studies on cell structure by the freezing-drying method VI. The preparation and properties of mitochondria // The Anatomical Record. 1934. 60, 4. 449–455.

Bernardi Paolo, Rasola Andrea, Forte Michael, Lippe Giovanna. The Mitochondrial Permeability Transition Pore: Channel Formation by F-ATP Synthase, Integration in Signal

Transduction, and Role in Pathophysiology // Physiological Reviews. 2015. 95, 4. 1111–1155.

Berry M N, Friend D S. High-yield preparation of isolated rat liver parenchymal cells // The Journal of Cell Biology. 1969. 43.

Blaza James N., Serreli Riccardo, Jones Andrew J. Y., Mohammed Khairunnisa, Hirst Judy. Kinetic evidence against partitioning of the ubiquinone pool and the catalytic relevance of respiratory-chain supercomplexes. // Proceedings of the National Academy of Sciences of the United States of America. 2014. 111, 44. 15735–40.

Booty Lee M, Gawel Justyna M, Cvetko Filip, Caldwell Stuart T, Hall Andrew R, Mulvey John F, James Andrew M, Hinchy Elizabeth C, Prime Tracy A, Arndt Sabine, Beninca Cristiane, Bright Thomas P, Clatworthy Menna R, Ferdinand John R, Prag Hiran A, Logan Angela, Prudent Julien, Krieg Thomas, Hartley Richard C, Murphy Michael P. Selective Disruption of Mitochondrial Thiol Redox State in Cells and In Vivo // Cell Chemical Biology. 2019. 26, 3. 449–461.

Booty Lee M., King Martin S., Thangaratnarajah Chancievan, Majd Homa, James Andrew M., Kunji Edmund R S, Murphy Michael P. The mitochondrial dicarboxylate and 2-oxoglutarate carriers do not transport glutathione // FEBS Letters. 2015. 589, 5. 621–628.

Brand Martin D., Esteves Telma C. Physiological functions of the mitochondrial uncoupling proteins UCP2 and UCP3 // Cell Metabolism. 2005. 2, 8. 85–93.

Brand Martin D., Murphy Michael P. Control of electron flux through the respiratory chain in mitochondria and cells // Biol. Rev. 1987. 62. 141–193.

Brandt Ulrich. Energy Converting NADH:Quinone Oxidoreductase (Complex I) // Annual Review of Biochemistry. 2006. 75. 69–92.

Bricker Daniel K., Taylor Eric B., Schell John C., Orsak Thomas, Boutron Audrey, Chen Yu-Chan, Cox James E., Cardon Caleb M., G. Van Vranken. Jonathan, Dephoure Noah, Redin Claire, Boudina Sihem, Gygi Steven P., Brivet Michele, Thummel Carl S., Rutter Jared. A Mitochondrial Pyruvate Carrier Required for Pyruvate Uptake in Yeast, Drosophila, and Humans // Science. 2012. 337, 6090. 96–100.

Brocks D G, Siess E a, Wieland O H. Validity of the digitonin method for metabolite compartmentation in isolated hepatocytes. // The Biochemical journal. 1980. 188, 1. 207–12.

Brown Guy C. Control of respiration and ATP synthesis in mammalian mitochondria and cells // Biochemical Journal. 1992. 284. 1–13.

Burns Rhys J., Murphy Michael P. Labeling of mitochondrial proteins in living cells by the thiol probe thiobutyltriphenylphosphonium bromide // Archives of Biochemistry and Biophysics. 1997. 339, 1. 33–39.

Burwell Lindsay S., Nadtochiy Sergiy M., Brookes Paul S. Cardioprotection by metabolic shut-down and gradual wake-up // Journal of Molecular and Cellular Cardiology. 2009. 46, 6. 804–810.

Busiello Rosa A., Savarese Sabrina, Lombardi Assunta. Mitochondrial uncoupling proteins and energy metabolism // Frontiers in Physiology. 2015. 6, 2. 36.

Buskiewicz Iwona A, Montgomery Theresa, Yasewicz Elizabeth C, Huber Sally A, Murphy Michael P, Hartley Richard C, Kelly Ryan, Crow Mary K, Perl Andras, Budd Ralph C, Koenig Andreas. Reactive oxygen species induce virus-independent MAVS oligomerization in systemic lupus erythematosus // Science Signaling. 2016. 9, 115. 1–18.

Buszewski Boguslaw, Noga Sylwia. Hydrophilic interaction liquid chromatography (HILIC) — a powerful separation technique // Anal Bioanal Chem. 2012. 402. 231–247.

Cappiello Achille, Famiglini Giorgio, Palma Pierangela, Pierini Elisabetta, Termopoli Veronica, Trufelli Helga. Overcoming Matrix Effects in Liquid Chromatography - Mass Spectrometry // Analytical Chemistry. 2008. 80, 23. 9343–9348.

Carling David, Mayer Faith V, Sanders Matthew J, Gamblin Steven J. AMP-activated protein kinase: nature's energy sensor // Nature Chemical Biology. 2011. 7, 8. 512–518.

Cavalier-Smith Thomas. Origin of mitochondria by intracellular enslavement of a photosynthetic purple bacterium // Proc Biol Sci. 2006. 273, April. 1943–1952.

Chae Ho Zoon, Robison Keith, Poole Leslie B., Church George, Storz Gisela, Rhee S. G. Cloning and sequencing of thiol-specific antioxidant from mammalian brain : Alkyl hydroperoxide reductase and thiol-specific antioxidant define a large family of antioxidant enzymes // Proceedings of the National Academy of Sciences of the United States of America. 1994. 91, July. 7017–7021.

Chance Britton, Williams G R. The Respiratory Chain and Oxidative Phosphorylation // Advances in Enzymology and Related Areas of Molecular Biology. 1956. 17.

Chandel Navdeep S. Navigating Metabolism. 2015. 1.

Chapman R A, Suleiman M_S, Earm Y E. Taurine and the heart // Cardiovascular Research. 1993. 27. 358–363.

Preparation of mitochondria from animal tissues and yeasts. // . 12 1972. 77–91.

Chen Qun, Moghaddas Shadi, Hoppel Charles L., Lesnefsky Edward J. Modulation of electron transport protects cardiac mitochondria and decreases myocardial injury during ischemia and reperfusion // The Journal of Pharmacology and Experimental Therapeutics. 2006. 319, 3. 1405–1412.

Chen Walter W, Freinkman Elizaveta, Sabatini David M. Rapid immunopurification of mitochondria for metabolite profiling and absolute quantification of matrix metabolites // Nature Protocols. 2017. 12, 10. 2215–2231.

Chen Walter W., Freinkman Elizaveta, Wang Tim, Birsoy Kıvanç, Sabatini David M., Berry M.N., Barritt G.J., Edwards A.M., Burdon R.H., Berthet J., Baudhuin P., Bestwick R.K., Moffett G.L., Mathews C.K., Birsoy K., Wang T., Chen W.W., Freinkman E., Abu-Remaileh M., Sabatini D.M., Bogenhagen D., Clayton D.A., Bowsher C.G., Tobin A.K., Cacciatore S., Loda M., Cardaci S., Zheng L., MacKay G., Broek N.J.F. van den, MacKenzie E.D., Nixon C., Stevenson D., Tumanov S., Bulusu V., Kamphorst J.J., Al. Et, Chantranupong L.,

Wolfson R.L., Orozco J.M., Saxton R.A., Scaria S.M., Bar-Peled L., Spooner E., Isasa M., Gygi S.P., Sabatini D.M., Chen W.W., Birsoy K., Mihaylova M.M., Snitkin H., Stasinski I., Yucel B., Bayraktar E.C., Carette J.E., Clish C.B., Brummelkamp T.R., Al. Et, Corcelli A., Saponetti M.S., Zaccagnino P., Lopalco P., Mastrodonato M., Liquori G.E., Lorusso M., Elo J.M., Yadavalli S.S., Euro L., Isohanni P., Götz A., Carroll C.J., Valanne L., Alkuraya F.S., Uusimaa J., Paetau A., Al. Et, Erecińska M., Wilson D.F., Nishiki K., Fly R., Lloyd J., Krueger S., Fernie A., Merwe M.J., Gerencser A.A., Chinopoulos C., Birket M.J., Jastroch M., Vitelli C., Nicholls D.G., Brand M.D., Harris M., Idell-Wenger J.A., Grotyohann L.W., Neely J.R., Kanehisa M., Goto S., Ke H., Lewis I.A., Morrisey J.M., McLean K.J., Ganesan S.M., Painter H.J., Mather M.W., Jacobs-Lorena M., Llinás M., Vaidya A.B., King M.P., Attardi G., Linskens H.F., Anderson J.M., Anderson B., Jackson J.F., Berkowitz G.A., Cline K., Gibbs M., Goldberg R., Hirokawa T., Huang A.H.C., Markovitz P.J., Chuang D.T., Cox R.P., Matuszczyk J.-C., Teleki A., Pfizenmaier J., Takors R., Messmer M., Blais S.P., Balg C., Chênevert R., Grenier L., Lagüe P., Sauter C., Sissler M., Giegé R., Lapointe J., Florentz C., Mullen A.R., Wheaton W.W., Jin E.S., Chen P.-H., Sullivan L.B., Cheng T., Yang Y., Linehan W.M., Chandel N.S., DeBerardinis R.J., Nemoto Y., Camilli P. De, Nishiki K., Erecińska M., Wilson D.F., Pagliarini D.J., Calvo S.E., Chang B., Sheth S.A., Vafai S.B., Ong S.-E., Walford G.A., Sugiana C., Boneh A., Chen W.K., Al. Et, Palmieri F., Roede J.R., Park Y., Li S., Strobel F.H., Jones D.P., Ross-Inta C., Tsai C.-Y., Giulivi C., Safer B., Saldanha A.J., Scovassi A.I., Shaham O., Slate N.G., Goldberger O., Xu Q., Ramanathan A., Souza A.L., Clish C.B., Sims K.B., Mootha V.K., Srere P.A., Sumegi B., Stark R., Pasquel F., Turcu A., Pongratz R.L., Roden M., Cline G.W., Shulman G.I., Kibbey R.G., Stark R., Guebre-Egziabher F., Zhao X., Feriod C., Dong J., Alves T.C., Ioja S., Pongratz R.L., Bhanot S., Roden M., Al. Et, Sullivan L.B., Gui D.Y., Hosios A.M., Bush L.N., Freinkman E., Heiden M.G. Vander, Tischler M.E., Hecht P., Williamson J.R., Vranken J.G. Van, Rutter J., Vianey-Liaud C., Divry P., Gregersen N., Mathieu M., Wagner G.R., Payne R.M., Wallace D.C., Wheaton W.W., Weinberg S.E., Hamanaka R.B., Soberanes S., Sullivan L.B., Anso E., Glasauer A., Dufour E., Mutlu G.M., Budigner G.S., Chandel N.S., Wiegand G., Remington S.J., Williamson J.R., Corkey B.E., Yoshii S.R., Kishi C., Ishihara N., Mizushima N. Absolute Quantification of Matrix Metabolites Reveals the Dynamics of Mitochondrial Metabolism // Cell. 2016a. 166, 5. 1324–1337.e11.

Chen Ying-Jr, Mahieu Nathaniel G, Huang Xiaojing, Singh Manmilan, Crawford Peter A, Johnson Stephen L, Gross Richard W, Schaefer Jacob, Patti Gary J. Lactate metabolism is associated with mammalian mitochondria // Nature Chemical Biology. 2016b. 12, 11. 937–943.

Cheng Behling, Kimura Tokuji. The distribution of cholesterol and phospholipid composition in submitochondrial membranes from bovine adrenal cortex: Fundamental studies of steroidogenic mitochondria // Lipids. Sep 1983. 18, 9. 577–584.

Cheng Chang, Liu Shaorong, Xiao Deqing, Hansel Steven. The Application of Trichloroacetic Acid as an Ion Pairing Reagent in LC–MS–MS Method Development for Highly Polar Aminoglycoside Compounds // Chromatographia. 2010. 72, 1/2. 133–139.

Chouchani Edward T., Kazak Lawrence, Spiegelman Bruce M. New Advances in Adaptive Thermogenesis: UCP1 and Beyond // Cell Metabolism. 2019. 29, 1. 27–37.

Chouchani Edward T., Pell Victoria R., Gaude Edoardo, Aksentijević Dunja, Sundier Stephanie Y., Robb Ellen L., Logan Angela, Nadtochiy Sergiy M., Ord Emily N. J., Smith

Anthony C., Eyassu Filmon, Shirley Rachel, Hu Chou-Hui, Dare Anna J., James Andrew M., Rogatti Sebastian, Hartley Richard C., Eaton Simon, Costa Ana S. H., Brookes Paul S., Davidson Sean M., Duchen Michael R., Saeb-Parsy Kourosh, Shattock Michael J., Robinson Alan J., Work Lorraine M., Frezza Christian, Krieg Thomas, Murphy Michael P. Ischaemic accumulation of succinate controls reperfusion injury through mitochondrial ROS // Nature. 2014. 515, V. 431–435.

Chouchani Edward T., Pell Victoria R., James Andrew M., Work Lorraine M., Saeb-Parsy Kourosh, Frezza Christian, Krieg Thomas, Murphy Michael P. A Unifying Mechanism for Mitochondrial Superoxide Production during Ischemia-Reperfusion Injury // Cell Metabolism. 2016. 23, 2. 254–263.

Civitarese Anthony E, Carling Stacy, Heilbronn Leonie K, Hulver Mathew H, Ukropcova Barbara, Deutsch Walter A, Smith Steven R, Ravussin Eric. Calorie Restriction Increases Muscle Mitochondrial Biogenesis in Healthy Humans // PLoS Med. 2007. 4, 3. e76.

Colbeau A., Nachbaur J., Vignais P. M. Enzymac characterization and lipid composition of rat liver subcellular membranes // BBA - Biomembranes. 1971. 249, 2. 462–492.

Corcelli Angela, Sublimi Matilde, Zaccagnino Patrizia, Lopalco Patrizia, Mastrodonato Maria, Liquori Giuseppa E, Lorusso Michele. Mitochondria isolated in nearly isotonic KCl buffer : Focus on cardiolipin and organelle morphology // BBA - Biomembranes. 2010. 1798, 3. 681–687.

Covian Raul, Balaban Robert S. Cardiac mitochondrial matrix and respiratory complex protein phosphorylation // American Journal of Physiology-Heart and Circulatory Physiology. 2012. 303, 8. H940–H966.

Cox Andrew G, Winterbourn Christine C, Hampton Mark B. Mitochondrial peroxiredoxin involvement in antioxidant defence and redox signalling // Biochemical Journal. 2010. 425. 313–325.

Crofts Antony R. The Cytochrome bc1 Complex: Function in the Context of Structure // Annual Review of Physiology. 2004. 66. 689–733.

Cross Heather R, Clarke Kieran, Opie Lionel H, Radda George K. Is Lactate-induced Myocardial Ischaemic Injury Mediated by Decreased pH or Increased Intracellular Lactate ? // Journal of Molecular and Cellular Cardiology. 1995. 27. 1369–1381.

Czibik Gabor, Steeples Violetta, Yavari Arash, Ashrafian Houman. Citric acid cycle intermediates in cardioprotection // Circulation: Cardiovascular Genetics. 2014. 7, 5. 711–719.

Dettmer Katja, Aronov Pavel A, Hammock Bruce D. Mass spectrometry-based metabolomics // Mass Spectrometry Reviews. 2007. 26. 51–78.

Devin Anne, Guerin Bernard, Rigoulet Michel. Dependence of flux size and efficiency of oxidative phosphorylation on external osmolarity in isolated rat liver mitochondria: role of adenine nucleotide carrier // BBA. 1996. 1273, 1. 13–20.

Devin Anne, Guerin Bernard, Rigoulet Michel. Response of Isolated Rat Liver Mitochondria to Variation of External Osmolarity in KCl Medium: Regulation of Matrix Volume and Oxidative Phosphorylation // Journal of Bioenergetics and Biomembranes. 1997. 29, 6. 579–590.

Di Guida Riccardo, Engel Jasper, Allwood J William, Weber Ralf J M, Jones Martin R, Sommer Ulf, Viant Mark R, Dunn Warwick B. Non-targeted UHPLC-MS metabolomic data processing methods: a comparative investigation of normalisation, missing value imputation, transformation and scaling // Metabolomics. 2016. 12, 5. 1–14.

Diaz Francisca, Moraes Carlos T. Mitochondrial biogenesis and turnover // Cell Calcium. 2008. 44, 1. 24–35.

Dolce Vincenza, Cappello Anna Rita, Capobianco Loredana. Mitochondrial Tricarboxylate and Dicarboxylate – Tricarboxylate Carriers : From Animals to Plants // International Union of Biochemistry and Molecular Biology. 2014. 66, 7. 462–471.

Drake K J, Sidorov V Y, McGuinness O P, Wasserman D H, Wikswo John P. Amino Acids as Metabolic Substrates during Cardiac Ischaemia // Experimental Biology and Medicine. 2012. 237, 12.

Dwyer Barney E, Smith Mark A, Richardson Sandy L, Perry George, Zhu Xiongwei. Down-regulation of aminolevulinate synthase, the rate-limiting enzyme for heme biosynthesis in Alzheimer's disease // Neuroscience Letters. 2009. 460. 180–184.

Evans Ronald M. The Steroid and Thyroid Hormone Receptor Superfamily // Science. 1988. 240, 4854. 889–895.

Ferrari Roberto. Metabolic Disturbances During Myocardial lschemia and Reperfusion // The American Journal of Cardiology. 1995. 76.

Finkel Toren. Signal Transduction by Mitochondrial Oxidants // The Journal of Biological Chemistry. 2012. 287, 7. 4434–4440.

Fraser Heather, Lopaschuk Gary D, Clanachan Alexander S. Alteration of glycogen and glucose metabolism in ischaemic and post-ischaemic working rat hearts by adenosine A 1 receptor stimulation // British Journal of Pharmacology. 1999. 128. 197–205.

Frenkel Nataliya, Makky Ali, Sudji Ikhwan Resmala, Wink Michael, Tanaka Motomu. Mechanistic Investigation of Interactions between Steroidal Saponin Digitonin and Cell Membrane Models // The Journal of Physical Chemistry. 2014. 118. 14632–14639.

Frey Terrence G, Mannella Carmen A. The internal structure of mitochondria // TIBS. 2000. 25, July. 319–324.

Friedman Jonathan R, Nunnari Jodi. Mitochondrial form and function // Nature. 2014. 505. 335–343.

Frigerio Francesca, Casimir Marina, Carobbio Stefania, Maechler Pierre. Tissue specificity of mitochondrial glutamate pathways and the control of metabolic homeostasis // Biochimica et Biophysica Acta. 2008. 1777. 965–972.

Garcia Daniel, Shaw Reuben J. AMPK: Mechanisms of Cellular Energy Sensing and Restoration of Metabolic Balance // Molecular Cell. 2017. 66, 6. 789–800.

Geisbuhler Timothy, Altschuld Ruth A, Trewyn Ronald W, Ansel Ann Z, Lamka Karla, Brierley Gerald P. Adenine Nucleotide Metabolism and Compartmentalization in Isolated Adult Rat Heart Cells // Circulation Research. 1984. 54, 5. 536–546.

Gilissen Julie, Jouret François, Pirotte Bernard, Hanson Julien. Insight into SUCNR1 (GPR91) structure and function // Pharmacology and Therapeutics. 2016. 159. 56–65.

Giorgi Carlotta, De Stefani Diego, Bononi Angela, Rizzuto Rosario, Pinton Paolo. Structural and functional link between the mitochondrial network and the endoplasmic reticulum // International Journal of Biochemistry and Cell Biology. 2009. 41, 10. 1817–1827.

Gorenkova Natalia, Robinson Emma, Grieve David J, Galkin Alexander. Conformational Change of Mitochondrial Complex I Increases ROS Sensitivity During Ischemia // Antioxidants & Redox Signaling. 2013. 19, 13. 1459–1466.

Gostimskaya Irina S., Grivennikova Vera G., Zharova Tatyana V., Bakeeva Lora E., Vinogradov Andrei D. In situ assay of the intramitochondrial enzymes: Use of alamethicin for permeabilization of mitochondria // Analytical Biochemistry. 2003. 313, 1. 46–52.

Gottlieb Roberta A., Gustafsson Åsa B. Mitochondrial turnover in the heart // Biochimica et Biophysica Acta - Molecular Cell Research. 2011. 1813, 7. 1295–1301.

Gray Michael W. Mitochondrial Evolution // Cold Spring Harb Perspect Biol. 2012. 4. a011403.

Gremse D A, Dean B, Kaplan R S. Effect of pyridoxal 5'-phosphate on the function of the purified mitochondrial tricarboxylate transport protein. 1995. 215–9.

Griffith Owen W. Determination of Glutathione and Glutathione Disulfide Using Glutathione Reductase and 2-Vinylpyridine // Analytical Biochemistry. 1980. 106. 207–212.

Grover Gary J., Atwal Karnail S., Sleph Paul G., Wang Feng-Li, Monshizadegan Hossain, Monticello Thomas, Green David W. Excessive ATP hydrolysis in ischemic myocardium by mitochondrial F1F0-ATPase: effect of selective pharmacological inhibition of mitochondrial ATPase hydrolase activity // American Journal of Physiology-Heart and Circulatory Physiology. 2004. 287, 4. H1747–H1755.

Grynberg Alain, Demaison Luc. Fatty Acid Oxidation in the Heart // Journal of Cardiovascular Pharmacology. 1996. 28. 11–17.

Guo Yong, Gaiki Sheetal. Retention behavior of small polar compounds on polar stationary phases in hydrophilic interaction chromatography // Journal of Chromatography. 2005. 1074. 71–80.

Gustafsson Claes M, Falkenberg Maria, Larsson Nils-Goran. Maintenance and Expression of Mammalian Mitochondrial DNA // Annual Rev Biochem. 2016. 85. 133–160.

Halestrap Andrew. A pore way to die // Biochemistry. 2005. 434, March. 578–579.

Halestrap Andrew P. The regulation of the matrix volume of mammalian mitochondria in vivo and in vitro and its role in the control of mitochondrial metabolism // BBA - Bioenergetics. 1989. 973, 3. 355–382.

Halestrap Andrew P., Davidson Anne M., Potter W. D. Mechanisms involved in the hormonal regulation of mitochondrial function through changes in the matrix volume // BBA - Bioenergetics. 1990. 1018, 2-3. 278–281.

Halestrap Andrew P, Wang Xuemin, Poole Robert C, Jackson Vicky N, Price Nigel T. Lactate Transport in Heart in Relation to Myocardial Ischemia // American Journal of Cardiology. 1997. 80, 3. 17–25.

Hansen Svend Høime, Andersen Mogens Larsen, Cornett Claus, Gradinaru Robert, Grunnet Niels. A role for taurine in mitochondrial function // Journal of Biomedical Science. 2010. 17, SUPPL. 1. 1–8.

Hardie D. Grahame, Hawley Simon A. AMP-activated protein kinase: The energy charge hypothesis revisited // BioEssays. 2001. 23, 12. 1112–1119.

Hardie D Grahame, Ross Fiona A, Hawley Simon A. AMPK: a nutrient and energy sensor that maintains energy homeostasis // Nature Publishing Group. 2012. 13, 4. 251–262.

Harmsen E., Jong J. W. de, Serruys P. W. Hypoxanthine production by ischemic heart demonstrated by high pressure liquid chromatography of blood purine nucleosides and oxypurines // Clinica Chimica Acta. 1981. 115, 1. 73–84.

He Welhal, Miao Frederick J.P., Lin Daniel C.H., Schwandner Ralf T., Wang Zhulun, Gao Jinhal, Chen Jin Long, Tlan Hui, Ling Lei. Citric acid cycle intermediates as ligands for orphan G-protein-coupled receptors // Nature. 2004. 429, 6988. 188–193.

Heather Lisa C., Pates Katharine M., Atherton Helen J., Cole Mark A., Ball Daniel R., Evans Rhys D., Glatz Jan F., Luiken Joost J., Griffin Julian L., Clarke Kieran. Differential translocation of the fatty acid transporter, FAT/CD36, and the glucose transporter, GLUT4, coordinates changes in cardiac substrate metabolism during ischemia and reperfusion // Circulation: Heart Failure. 2013. 6, 5. 1058–1066.

Herzig Sébastien, Raemy Etienne, Montessuit Sylvie, Veuthey Jean-Luc, Zamboni Nicola, Westermann Benedikt, Kunji Edmund R S, Martinou Jean-claude. Identification and Functional Expression of the Mitochondrial Pyruvate Carrier // Science. 2012. 337, 6090. 93–96.

Hochachka Peter W, Dressendorfer Rudolph H. Succinate Accumulation in Man during Exercise // European Journal of Applied Physiology. 1976. 35. 235–242.

Hogeboom G H, Schneider W C, Pallade G E. The Isolation of Morphologically Intact Mitochondria from Rat Liver // Experimental Biology and Medicine. 1947. 65, 2. 320–321.

Hogeboom G H, Schneider W C, Pallade G E. Cytochemical studies of mammalian tissues // Journal of Biological Chemistry. 1948. 172, 2. 619–635.

Holmström Kira M, Finkel Toren. Cellular mechanisms and physiological consequences of redox-dependent signalling // Nat Rev Mol Cell Biol. 2014. 15, 6. 411–421.

Hornig-Do Hue Tran, Günther Gritt, Bust Maria, Lehnartz Patricia, Bosio Andreas, Wiesner Rudolf J. Isolation of functional pure mitochondria by superparamagnetic microbeads // Analytical Biochemistry. 2009. 389, 1. 1–5.

Hosler Jonathan P, Ferguson-Miller Shelagh, Mills Denise A. Energy Transduction: Proton Transfer Through the Respiratory Complexes // Annual Review of Biochemistry. 2006. 75. 165–187.

Hou Bi-Huei, Takanaga Hitomi, Grossmann Guido, Chen Li-Qing, Qu Xiao-Qing, Jones Alexander M., Lalonde Sylvie, Schweissgut Oliver, Wiechert Wolfgan, Frommer Wolf B. Optical sensors for monitoring dynamic changes of intracellular metabolite levels in mammalian cells // Nature Protocols. 2011. 6, 11. 1818–1833.

Houten Sander M, Violante Sara, Ventura Fatima V, Wanders Ronald J A. The Biochemistry and Physiology of Mitochondrial Fatty Acid β-Oxidation and Its Genetic Disorders // Annual Review of Physiology. 2016. 78. 23–44.

Huang Liusheng, Haagensen Janus Anders Juul, Verotta Davide, Cheah Vincent, Spormann Alfred M., Aweeka Francesca, Yang Katherine. Determination of Tobramycin in M9 Medium by LC-MS/MS: Signal Enhancement by Trichloroacetic Acid // Journal of Analytical Methods in Chemistry. 2018. 2018. 1–8.

Iuso Arcangela, Repp Birgit, Biagosch Caroline, Terrile Caterina, Prokisch Holger. Assessing Mitochondrial Bioenergetics in Isolated Mitochondria from Various Mouse Tissues Using Seahorse XF96 Analyzer // Mitochondria: Practical Protocols. 1567. 2017. 13, 217–230.

Iverson T M. Catalytic mechanisms of complex II enzymes: A structural perspective // BBA - Bioenergetics. 2013. 1827, 5. 648–657.

James Andrew M, Wei Yau-Huei, Pang Cheng-Yoong, Murphy Michael P. Altered mitochondrial function in fibroblasts containing MELAS or MERRF mitochondrial DNA mutations // Biochemical Journal. 1996. 318. 401–407.

Jang Cholsoon, Chen Li, Rabinowitz Joshua D. Metabolomics and Isotope Tracing // Cell. 2018. 173, 4. 822–837.

Janssen-Heininger Yvonne M W, Mossman Brooke T, Heintz Nicholas H, Forman Henry J, Kalyanaraman Balaraman, Finkel Toren, Stamler Jonathan S, Rhee Sue Goo, Vliet Albert van der. Redox-based regulation of signal transduction: Principles, pitfalls, and promises // Free Radical Biology & Medicine. 2008. 45, 1. 1–17.

Jong Chian Ju, Azuma Junichi, Schaffer Stephen. Mechanism underlying the antioxidant activity of taurine: Prevention of mitochondrial oxidant production // Amino Acids. 2012. 42, 6. 2223–2232.

Jornayvaz François R., Shulman Gerald I. Regulation of mitochondrial biogenesis // Essays in Biochemistry. 2010. 47. 69–84.

Kaasik Allen, Safiulina Dzhamilja, Zharkovsky Alexander, Veksler Vladimir. Regulation of mitochondrial matrix volume // American Journal of Physiology-Cell Physiology. 2006. 292, 1. C157–C163.

Kaila Ville R. I., Verkhovsky Michael I., Wikström Mårten. Proton-Coupled Electron Transfer in Cytochrome Oxidase // Chemical Reviews. 2010. 110, 12. 7062–7081.

Kakhniashvili D, Mayor J A, Gremse D A, Xu Y, Kaplan R S. Identification of a novel gene encoding the yeast mitochondrial dicarboxylate transport protein via overexpression, purification, and characterization of its protein product // J Biol Chem. 1997. 272, 7. 4516–4521.

Kastaniotis Alexander J, Autio Kaija J, Kerätär Juha M, Monteuuis Geoffray, Mäkelä Anne M, Nair Remya R, Pietikäinen Laura P, Shvetsova Antonina, Chen Zhijun, Hiltunen J Kalervo. Mitochondrial fatty acid synthesis, fatty acids and mitochondrial physiology // BBA - Molecular and Cell Biology of Lipids. 2017. 1862, 1. 39–48.

Kerner Janos, Hoppel Charles. Fatty acid import into mitochondria // BBA. 2000. 1486. 1–17.

Kim Insil, Rodriguez-Enriquez Sara, Lemasters John J. Selective degradation of mitochondria by mitophagy // Archives of Biochemistry and Biophysics. 2007. 462, 2. 245–253.

King A., Selak M. A., Gottlieb E. Succinate dehydrogenase and fumarate hydratase: Linking mitochondrial dysfunction and cancer // Oncogene. 2006. 25, 34. 4675–4682.

Klingenberg Martin. The ADP and ATP transport in mitochondria and its carrier // BBA. 2008. 1778. 1978–2021.

Kolwicz Stephen C., Liu Li, Goldberg Ira J., Tian Rong. Enhancing Cardiac Triacylglycerol Metabolism Improves Recovery From Ischemic Stress // Diabetes. 2015. 64, 8.

Kudin Alexei P, Bimpong-Buta Nana Yaw-B, Vielhaber Stefan, Elger Christian E, Kunz Wolfram S. Characterization of Superoxide-producing Sites in Isolated Brain Mitochondria // Journal of Biological Chemistry. 2004. 279, 6. 4127–4135.

Kuehl Frederick A, Egan Robert W. Prostaglandins, Arachidonic Acid, and Inflammation // Science. 1980. 210, November.

Kunji Edmund R.S., Robinson Alan J. Coupling of proton and substrate translocation in the transport cycle of mitochondrial carriers // Current Opinion in Structural Biology. 2010. 20, 4. 440–447.

Kuznetsov Andrey V., Margreiter Raimund. Heterogeneity of mitochondria and mitochondrial function within cells as another level of mitochondrial complexity // International Journal of Molecular Sciences. 2009. 10, 4. 1911–1929.

Kuznetsov Andrey V., Troppmair Jakob, Sucher Robert, Hermann Martin, Saks Valdur, Margreiter Raimund. Mitochondrial subpopulations and heterogeneity revealed by confocal imaging: Possible physiological role? // Biochimica et Biophysica Acta - Bioenergetics. 2006. 1757, 5-6. 686–691.

Lambert Ian Henry. Regulation of the Cellular Content of the Organic Osmolyte Taurine in Mammalian Cells // Neurochemical Research. 2004. 29, 1. 27–63.

Lane Nick, Martin William. The energetics of genome complexity // Nature. 2010. 467, 7318. 929–934.

Lebiedzinska Magdalena, Szabadkai György, Jones Aleck W.E., Duszynski Jerzy, Wieckowski Mariusz R. Interactions between the endoplasmic reticulum, mitochondria, plasma membrane and other subcellular organelles // International Journal of Biochemistry and Cell Biology. 2009. 41, 10. 1805–1816.

Lee Hakjoo, Yoon Yisang. Mitochondrial fission and fusion // Biochemical Society Transactions. 2016. 44, May. 1725–1735.

Lee Jisun, Giordano Samantha, Zhang Jianhua. Autophagy, mitochondria and oxidative stress: cross-talk and redox signalling // Biochemical Journal. 2012. 441, 2. 523–540.

Lesnefsky Edward J., Chen Qun, Moghaddas Shadi, Hassan Medhat O., Tandler Bernard, Hoppel Charles L. Blockade of Electron Transport during Ischemia Protects Cardiac Mitochondria // The Journal of Biological Chemistry. 2004. 279, 46. 47961–47967.

Li Xiyan, Gianoulis Tara A., Yip Kevin Y., Gerstein Mark, Snyder Michael. Extensive in vivo metabolite-protein interactions revealed by large-scale systematic analyses // Cell. 2010. 143, 4. 639–650.

Lill Roland, Kispal Gyula. Mitochondrial ABC transporters // Research in Microbiology. 2001. 152, 3. 331–340.

Lin H., Suleiman M. S. Cariporide enhances lactate clearance upon reperfusion but does not alter lactate accumulation during global ischaemia // European Journal of Physiology. 2003. 447. 8–13.

Locher Kaspar P. Mechanistic diversity in ATP-binding cassette (ABC) transporters // Nature Structural and Molecular Biology. 2016. 23, 6. 487–493.

Lodish Harvey, Berk Arnold, Kaiser Chris A. Molecular Cell Biology. 2007. 6.

Loor Gabriel, Kondapalli Jyothisri, Iwase Hirotaro, Chandel Navdeep S., Waypa Gregory B., Guzy Robert D., Vanden Hoek Terry L., Schumacker Paul T. Mitochondrial oxidant stress triggers cell death in simulated ischemia-reperfusion // Biochimica et Biophysica Acta - Molecular Cell Research. 2011. 1813, 7. 1382–1394.

Lopez-Fabuel Irene, Le Douce Juliette, Logan Angela, James Andrew M, Bonvento Gilles, Murphy Michael P, Almeida Angeles, Bolaños Juan P. Complex I assembly into supercomplexes determines differential mitochondrial ROS production in neurons and astrocytes // PNAS. 2016. 113, 46. 13063–13068.

Lu Wenyun, Su Xiaoyang, Klein Matthias S., Lewis Ian A., Fiehn Oliver, Rabinowitz Joshua D. Metabolite Measurement: Pitfalls to Avoid and Practices to Follow // Annual Review of Biochemistry. 2017. 86, 1. 277–304.

Lundblad R. L. Chemical Reagents for Protein Modification. 1991.

Mackay Gillian M, Zheng Liang, Broek Niels J F van den, Gottlieb Eyal. Analysis of Cell Metabolism Using LC-MS and Isotope Tracers. 561. 2015. 1. 171–196.

Mammucari Cristina, Patron Maria, Granatiero Veronica, Rizzuto Rosario. Molecules and roles of mitochondrial calcium signaling // Biofactors. 2011. 37. 219–227.

Mannella Carmen A. The 'ins' and 'outs' of mitochondrial membrane channels // Trends Biochem Sci. 1992. 17, August. 315–320.

Margulis Lynn. Symbiosis In Cell Evolution: Life and Its Environment On the Early Earth. 1981.

Mari Montserrat, Morales Albert, Colell Anna, Garcia-Ruiz Carmen, Fernandez-Checa Jose. Mitochondrial Glutathione, a Key Survival Antioxidant // Antioxidants & Redox Signaling. 2009. 11, 11. 2685–2700.

Markley John L., Brüschweiler Rafael, Edison Arthur S., Eghbalnia Hamid R., Powers Robert, Raftery Daniel, Wishart David S. The future of NMR-based metabolomics // Current Opinion in Biotechnology. 2017. 43. 34–40.

Martin Jack L., Costa Ana S. H., Gruszczyk Anja V., Beach Timothy B., Allen Fay M., Prag Hiran A., Hinchy Elizabeth C., Mahbubani Krishnaa, Hamed Mazin, Tronci Laura, Nikitopoulou Efterpi, James Andrew M., Krieg Thomas, Robinson Alan J., Huang Margaret H., Caldwell Stuart T., Logan Angela, Pala Laura, Hartley Richard C., Frezza Christian, Saeb-Parsy Kourosh, Murphy Michael P. Succinate accumulation drives ischaemia-reperfusion injury during organ transplantation // Nature Metabolism. 2019. (In press).

Matuszczyk Jens Christoph, Teleki Attila, Pfizenmaier Jennifer, Takors Ralf. Compartment-specific metabolomics for CHO reveals that ATP pools in mitochondria are much lower than in cytosol // Biotechnology Journal. 2015. 10, 10. 1639–1650.

McCormack J. G., Halestrap Andrew P., Denton R. M. Role of calcium ions in regulation of mammalian intramitochondrial metabolism. // Physiological Reviews. 1990. 70, 2. 391–425.

Meng T. C., Fukada T., Tonks N. K. Reversible oxidation and inactivation of protein tyrosine phosphatases in vivo. // Molecular Cell. 2002. 9. 387–399.

Menger Katja E, James Andrew M, Cocheme Helena M, Harbour Michael E, Chouchani Edward T, Ding Shujing, Fearnley Ian M, Partridge Linda, Murphy Michael P. Fasting, but Not Aging , Dramatically Alters the Redox Status of Cysteine Residues on Proteins in Drosophila melanogaster // Cell Reports. 2015. 11, 6. 1856–1865.

Menzies Robert A., Gold Philip H. The Turnover of Mitochondria in a Variety of Tissues of Young Adult and Aged Rats // The Journal of Biological Chemistry. 1971. 246, 8. 2425–2429.

Mills Evanna, O'Neill Luke A J. Succinate: A metabolic signal in inflammation // Trends in Cell Biology. 2014. 24, 5. 313–320.

Mills Evanna L, Kelly Beth, Logan Angela, Costa Ana S H, Varma Mukund, Bryant Clare E, Frezza Christian, Murphy Michael P, O'Neill Luke A. Succinate Dehydrogenase Supports Metabolic Repurposing of Mitochondria to Drive Inflammatory Macrophages // Cell. 2016. 167. 457–470.

Mills Evanna L, Kelly Beth, O'Neill Luke A J. Mitochondria are the powerhouses of immunity // Nature Immunology. 2017. 18, 5. 488–498.

Milo Ron, Phillips Rob. What is the density of cells? 2016.

Mitchell Peter. Coupling of phosphorylation to electron and hydrogen transfer by a chemi-osmotic type of mechanism // Nature. 1961. 191, 4784. 144–148.

Moreno-Loshuertos Raquel, Enríquez José Antonio. Respiratory supercomplexes and the functional segmentation of the CoQ pool // Free Radical Biology and Medicine. 2016. 100. 5–13.

Morris Sidney M. Regulation of Enzymes of the Urea Cycle and Arginine Metabolism // Annu Rev Nutr. 2002. 22, 58. 87–105.

Mráček Tomáš, Drahota Zdeněk, Houštěk Josef. The function and the role of the mitochondrial glycerol-3-phosphate dehydrogenase in mammalian tissues // Biochimica et Biophysica Acta - Bioenergetics. 2013. 1827, 3. 401–410.

Murley Andrew, Nunnari Jodi. The Emerging Network of Mitochondria-Organelle Contacts // Molecular Cell. 2016. 61, 5. 648–653.

Murphy Elizabeth, Steenbergen Charles. Mechanisms Underlying Acute Protection from Cardiac Ischemia-Reperfusion Injury // Physiological Reviews. 2008. 88, 2. 581–609.

Murphy Michael P. How mitochondria produce reactive oxygen species // Biochemical Journal. 2009. 13. 1–13.

Murphy Michael P. Mitochondrial Thiols in Antioxidant Protection and Redox Signaling: Distinct Roles for Glutathionylation and Other Thiol Modifications // Antioxidants & Redox Signaling. 2012. 16, 6. 476–495.

Murphy Michael P. Understanding and preventing mitochondrial oxidative damage // Biochemical Society Transactions. 2016. 44. 1219–1226.

Murphy Michael P, Brand Martin D. The control of electron flux through cytochrome oxidase // Biochemical Journal. 1987. 243. 499–505.

Murphy Michael P., O'Neill Luke A.J. Krebs Cycle Reimagined: The Emerging Roles of Succinate and Itaconate as Signal Transducers // Cell. 2018. 174, 4. 780–784.

Natuzzi D, Daddabbo L, Stipani V, Cappello A R, Miniero D V, Capobianco L, Stipani I. Inactivation of the reconstituted oxoglutarate carrier from bovine heart mitochondria by pyridoxal 5'-phosphate. // Journal of bioenergetics and biomembranes. 1999. 31, 6. 535–41.

Niatsetskaya Z. V., Sosunov S. A., Matsiukevich D., Utkina-Sosunova I. V., Ratner V. I., Starkov A. A., Ten V. S. The Oxygen Free Radicals Originating from Mitochondrial Complex I Contribute to Oxidative Brain Injury Following Hypoxia-Ischemia in Neonatal Mice // Journal of Neuroscience. 2012. 32, 9. 3235–3244.

Nicholls David G., Ferguson Stuart J. Bioenergetics. 2013. 4.

Norseth Jon, Normann Per T, Flatmark Torgeir. Hydrodynamic parameters and isolation of mitochondria, microperoxisomes and microsomes of rat heart // Biochimica et Biophysica Acta. 1982. 719. 569–579.

Oliver Michael F. Fatty acids and the risk of death during acute myocardial ischaemia // Clinical Science. mar 2015. 128, 6. 349–355.

Olofsson Jessica, Bridle Helen, Jesorka Aldo, Isaksson Ida, Weber Stephen, Orwar Owe. Direct access and control of the intracellular solution environment in single cells // Analytical Chemistry. 2009. 81, 5. 1810–1818.

Overmyer Katherine A, Thonusin Chanisa, Qi Nathan R, Burant Charles F, Evans Charles R. Impact of Anesthesia and Euthanasia on Metabolomics of Mammalian Tissues: Studies in a C57BL/6J Mouse Model // PLoS ONE. 2015. 10, 2. 1–19.

Pacher Pal, Nivorozhkin Alex, Szabo Csaba. Therapeutic Effects of Xanthine Oxidase Inhibitors: Renaissance Half a Century after the Discovery of Allopurinol // Pharmacological Reviews. 2006. 58, 1. 87–114.

Pallotti Francesco, Lenaz Giorgio. Isolation and subfractionation of mitochondria from animal cells and tissue culture lines // Methods in Cell Biology. 2001. 1, 1–35.

Palmieri Ferdinando. The mitochondrial transporter family (SLC25): physiological and pathological implications // Pflügers Archiv: European Journal of Physiology. 2004. 447. 689–709.

Palmieri Ferdinando. Diseases caused by defects of mitochondrial carriers : A review // Biochimica et Biophysica Acta. 2008. 1777. 564–578.

Palmieri Ferdinando. Mitochondrial transporters of the SLC25 family and associated diseases: a review // Journal of Inherited Metabolic Disease. 2014. 37. 565–575.

Pan Daqiang, Lindau Caroline, Lagies Simon, Wiedemann Nils, Kammerer Bernd. Metabolic profiling of isolated mitochondria and cytoplasm reveals compartment-specific metabolic responses // Metabolomics. 2018. 14, 5. 59.

Paul Viktoria Desiree, Lill Roland. Biogenesis of cytosolic and nuclear iron – sulfur proteins and their role in genome stability // BBA - Molecular Cell Research. 2015. 1853, 6. 1528–1539.

Paulsen Candice E, Carroll Kate S. Cysteine-Mediated Redox Signaling: Chemistry, Biology, and Tools for Discovery // Chemical Reviews. 2013. 113. 4633–4679.

Pertoft Hakan, Laurent Torvard C., Laas Torgny, Kagedal Lennart. Density Gradients Prepared from Colloidal Silica Particles Coated by Polyvinylpyrrolidone (Percoll) // Analytical Biochemistry. 1978. 282, 88. 271–282.

Peti-Peterdi Janos, Gevorgyan Haykanush, Lam Lisa, Riquier-Brison Anne. Metabolic control of renin secretion // Pflugers Arch. 2013. 465, 1. 53–58.

Piazza Ilaria, Kochanowski Karl, Cappelletti Valentina, Fuhrer Tobias, Noor Elad, Sauer Uwe, Picotti Paola. A Map of Protein-Metabolite Interactions Reveals Principles of Chemical Communication // Cell. 2018. 172, 1-2. 358–372.e23.

Picard Martin, Taivassalo Tanja, Ritchie Darmyn, Wright Kathryn J., Thomas Melissa M., Romestaing Caroline, Hepple Russell T. Mitochondrial structure and function are disrupted by standard Isolation methods // PLoS ONE. 2011. 6, 3. 1–12.

Pitt James J. Principles and Applications of Liquid Chromatography-Mass Spectrometry in Clinical Biochemistry // Clinical Biochemistry Review. 2009. 30, 2. 19–34.

Pryde Kenneth R, Hirst Judy. Superoxide Is Produced by the Reduced Flavin in Mitochondrial Complex I: a single, unified mechanism that applies during both forward and reverse electron transfer // Journal of Biological Chemistry. 2011. 286, 20. 18056–18065.

Quinlan Casey L, Gerencser Akos A, Treberg Jason R, Brand Martin D. The Mechanism of Superoxide Production by the Antimycin-inhibited Miotchondrial Q-cycle // The Journal of Biological Chemistry. 2011. 286, 36. 31361–31372.

Rasola Andrea, Bernardi Paolo. Mitochondrial permeability transition in Ca2+-dependent apoptosis and necrosis // Cell Calcium. 2011. 50, 3. 222–233.

Raturi Arun, Simmen Thomas. Where the endoplasmic reticulum and the mitochondrion tie the knot: The mitochondria-associated membrane (MAM) // Biochimica et Biophysica Acta - Molecular Cell Research. 2013. 1833, 1. 213–224.

Remani Sreevidya, Sun Jiakang, Kotaria Rusudan, Mayor June A., Brownlee June M., Harrison David H.T., Walters D. Eric, Kaplan Ronald S. The yeast mitochondrial citrate transport protein: Identification of the Lysine residues responsible for inhibition mediated by Pyridoxal 5-phosphate // Journal of Bioenergetics and Biomembranes. 2008. 40, 6. 577–585.

Ribas Vicent, García-Ruiz Carmen, Fernández-Checa José C. Glutathione and mitochondria // Frontiers in Pharmacology. 2014. 5, July. 1–19.

Rich Peter R, Maréchal Amandine. The mitochondrial respiratory chain // Essays Biochem. 2010. 47. 1–23.

Rickwood D, Birnie G D. Fractionations in Zonal Rotors // Centrifugal Separations in Molecular and Cell Biology. 1978.

Ridsdale Andrew, Denis Maxime, Gougeon Pierre-Yves, Ngsee Johnny K., Presley John F., Zha Xiaohui. Cholesterol Is Required for Efficient Endoplasmic Reticulum-to-Golgi Transport of Secretory Membrane Proteins // Molecular Biology of the Cell. 2006. 17. 1593–1605.

Ripps Harris, Shen Wen. Taurine: A “very essential” amino acid" // Molecular vision. 2012. 18, November. 2673–2686.

Roede James R., Park Youngja, Li Shuzhao, Strobel Frederick H., Jones Dean P. Detailed mitochondrial phenotyping by high resolution metabolomics // PLoS ONE. 2012. 7, 3. 1–8.

Rogers George W., Brand Martin D., Petrosyan Susanna, Ashok Deepthi, Elorza Alvaro A., Ferrick David A., Murphy Anne N. High throughput microplate respiratory measurements using minimal quantities of isolated mitochondria // PLoS ONE. 2011. 6, 7.

Röhrig Florian, Schulze Almut. The multifaceted roles of fatty acid synthesis in cancer // Nature Publishing Group. 2016. 16, 11. 732–749.

Ross-Inta Catherine, Tsai Chern-Yi, Giulivi Cecilia. The mitochondrial pool of free amino acids reflects the composition of mitochondrial-DNA encoded proteins // Bioscience Reports. 2008. 28, 5. 239–249.

Ross Meredith F, Ros Tatiana D A, Blaikie Frances H, Prime Tracy A, Porteous Carolyn M, Severina Inna I, Skulachev Vladimir P, Kjaergaard Henrik G, Smith Robin A J, Murphy Michael P. Accumulation of lipophilic dications by mitochondria and cells // Biochemical Journal. 2006. 400, 1. 199–208.

Rubic Tina, Lametschwandtner Gunther, Jost Sandra, Hinteregger Sonja, Kund Julia, Carballido-Perrig Nicole, Schwarzler Christoph, Junt Tobias, Voshol Hans, Meingassner Josef G, Mao Xiaohong, Werner Gudrun, Rot Antal, Carballido Jose M. Triggering the succinate receptor GPR91 on dendritic cells enhances immunity // Nature Immunology. 2008. 9, 11. 1261–1269.

Saunders Janet E., Beeson Craig C., Schnellmann Rick G. Characterization of functionally distinct mitochondrial subpopulations // Journal of Bioenergetics and Biomembranes. 2013. 45, 1-2. 87–99.

Sazanov Leonid A. A giant molecular proton pump: structure and mechanism of respiratory complex I // Nature Reviews Molecular Cell Biology. 2015. 16, 6. 375–388.

Scarlett Jared L., Packer Michael A., Porteous Carolyn M., Murphy Michael P. Alterations to Glutathione and Nicotinamide Nucleotides During the Mitochondrial Permeability Transition Induced by Peroxynitrite // Biochemical Pharmacology. 1996. 52. 1047–1055.

Scarpulla Richard C. Transcriptional activators and coactivators in the nuclear control of mitochondrial function in mammalian cells // Gene. 2002. 286, 1. 81–89.

Schmidt Oliver, Pfanner Nikolaus, Meisinger Chris. Mitochondrial protein import: from proteomics to functional mechanisms. // Nature reviews. Molecular cell biology. 2010. 11, 9. 655–667.

Schuller-Levis Georgia B., Park Eunkyue. Taurine: new implications for an old amino acid // FEMS Microbiology Letters. 2003. 226. 195–202.

Scialo Filippo, Sriram Ashwin, Fernandez-Ayala , Gubina Nina, Lohmus Madis, Nelson Glyn, Logan Angela, Cooper Helen M, Navas Placido, Enrıquez Jose Antonio, Murphy Michael P, Sanz Alberto. Mitochondrial ROS Produced via Reverse Electron Transport Extend Animal Lifespan // Cell Metabolism. 2016. 23. 725–734.

Siess E A, Wieland O H. Regulation of pyruvate dehydrogenase interconversion in isolated hepatocytes by the mitochondrial ATP/ADP ratio // FEBS Letters. 1975. 52, 2. 226–230.

Smith Charles V., Jones Dean P., Guenthner Thomas M., Lash Lawrence H., Lauterburg Bernhard H. Compartmentation of glutathione: Implications for the study of toxicity and disease // Toxicology and Applied Pharmacology. 1996. 140, 1. 1–12.

Smith Robin A J, Hartley Richard C, Cocheme Helena M, Murphy Michael P. Mitochondrial pharmacology // Trends in Pharmaceutical Sciences. 2012. 33, 6. 341–352.

Smith Robin A.J., Porteous Carolyn M., Coulter Carolyn V., Murphy Michael P. Selective targeting of an antioxidant to mitochondria // European Journal of Biochemistry. 1999. 263, 3. 709–716.

Soboll S, Scholz R, Heldt H W. Subcellular metabolite concentrations. Dependence of mitochondrial and cytosolic ATP systems on the metabolic state of perfused rat liver. // European journal of biochemistry / FEBS. 1978. 87, 2. 377–390.

Srere P. A. Citrate Synthase: [EC 4.1.3.7. Citrate oxaloacetate-lyase (CoA-acetylating)] // Methods in Enzymology. 1969. 13, 7. 3–11.

Sudji Ikhwan Resmala, Subburaj Yamunadevi, Frenkel Nataliya, García-Sáez Ana J, Wink Michael. Membrane Disintegration Caused by the Steroid Saponin Digitonin Is Related to the Presence of Cholesterol // Molecules. 2015. 20. 20146–20160.

Sundström Linda, Greasley Peter J., Engberg Susanna, Wallander Malin, Ryberg Erik. Succinate receptor GPR91, a Gai coupled receptor that increases intracellular calcium concentrations through PLCB // FEBS Letters. 2013. 587, 15. 2399–2404.

Szymański Jędrzej, Janikiewicz Justyna, Michalska Bernadeta, Patalas-Krawczyk Paulina, Perrone Mariasole, Ziółkowski Wiesław, Duszyński Jerzy, Pinton Paolo, Dobrzyń Agnieszka, Więckowski Mariusz R. Interaction of mitochondria with the endoplasmic reticulum and plasma membrane in calcium homeostasis, lipid trafficking and mitochondrial structure // International Journal of Molecular Sciences. 2017. 18, 7. 1–24.

Taegtmeyer Heinrich. Metabolic Responses to Cardiac Hypoxia Increased Production of Succinate by Rabbit Papillary Muscles // Circulation Research. 1978. 43.

Tait S. W G, Green Douglas R. Mitochondria and cell death: Outer membrane permeabilization and beyond // Nature Reviews Molecular Cell Biology. 2010. 11, 9. 621–632.

Tannahill G. M., Curtis A. M., Adamik J., Palsson-McDermott E. M., McGettrick A. F., Goel G., Frezza C., Bernard N. J., Kelly B., Foley N. H., Zheng L., Gardet A., Tong Z., Jany S. S., Corr S. C., Haneklaus M., Caffrey B. E., Pierce K., Walmsley S., Beasley F. C., Cummins E., Nizet V., Whyte M., Taylor C. T., Lin H., Masters S. L., Gottlieb E., Kelly V. P., Clish C., Auron P. E., Xavier R. J., O'Neill L. A. J. Succinate is an inflammatory signal that induces IL-1β through HIF-1α // Nature. 2013. 496. 238–242.

Tietze Frank. Enzymic Method for Quantitative Nanogram Amounts of Total Glutathione // Analytical Biochemistry. 1969. 27. 502–522.

Tischler M E, Hecht P, Williamson J R. Determination of mitochondrial/cytosolic metabolite gradients in isolated rat liver cells by cell disruption. // Archives of biochemistry and biophysics. 1977. 181, 1. 278–93.

Tonazzi Annamaria, Giangregorio Nicola, Console Lara, De Palma Annalisa, Indiveri Cesare. Nitric oxide inhibits the mitochondrial carnitine / acylcarnitine carrier through reversible S -nitrosylation of cysteine 136 // BBA - Bioenergetics. 2017. 1858, 7. 475–482.

Tormos Kathryn V, Anso Elena, Hamanaka Robert B, Eisenbart James, Joseph Joy, Kalyanaraman Balaraman, Chandel Navdeep S. Mitochondrial Complex III ROS Regulate Adipocyte Differentiation // Cell Metabolism. 2011. 14, 4. 537–544.

Tormos Kathryn V, Chandel Navdeep S. Inter-connection between mitochondria and HIFs // Journal of Cellular and Molecular Medicine. 2010. 14, 4. 795–804.

Tretter Laszlo, Patocs Attila, Chinopoulos Christos. Succinate, an intermediate in metabolism, signal transduction, ROS, hypoxia, and tumorigenesis // BBA - Bioenergetics. 2016.

Twig Gilad, Elorza Alvaro, Molina Anthony J A, Mohamed Hibo, Wikstrom Jakob D, Walzer Gil, Stiles Linsey, Haigh Sarah E, Katz Steve, Las Guy, Alroy Joseph, Wu Min, Py Benedicte F, Yuan Junying, Deeney Jude T, Corkey Barbara E, Shirihai Orian S. Fission and selective fusion govern mitochondrial segregation and elimination by autophagy // EMBO Journal. 2008. 27, 11. 433–446.

Preparation of heart mitochondria from laboratory animals. // . 10. 12 1967. 75–77.

Van Vranken Jonathan G., Rutter Jared. The Whole (Cell) Is Less Than the Sum of Its Parts // Cell. 2016. 166, 5. 1078–1079.

VanLinden Magali R., Dölle Christian, Pettersen Ina K.N., Kulikova Veronika A., Niere Marc, Agrimi Gennaro, Dyrstad Sissel E., Palmieri Ferdinando, Nikiforov Andrey A., Tronstad Karl Johan, Ziegler Mathias. Subcellular distribution of NAD+ between cytosol and mitochondria determines the metabolic profile of human cells // Journal of Biological Chemistry. 2015. 290, 46. 27644–27659.

Vanderperre Benoit, Bender Tom, Kunji Edmund R S, Martinou Jean-claude. Mitochondrial pyruvate import and its effects on homeostasis // Current Opinion in Cell Biology. 2015. 33. 35–41.

Venturini A, Ascione R, Lin H., Polesel E, Angelini G D, Suleiman M S. The importance of myocardial amino acids during ischemia and reperfusion in dilated left ventricle of patients with degenerative mitral valve disease // Molecular and Cellular Biochemistry. 2009. 330. 63–70.

Virbasius C. M.A., Virbasius J. V., Scarpulla R. C. NRF-1, an activator involved in nuclear-mitochondrial interactions, utilizes a new DNA-binding domain conserved in a family of developmental regulators // Genes and Development. 1993a. 7, 12. 2431–2445.

Virbasius J. V., Virbasius C. A., Scarpulla R. C. Identity of GABP with NRF-2, a multisubunit activator of cytochrome oxidase expression, reveals a cellular role for and ETS domain activator of viral promoters // Genes and Development. 1993b. 7, 3. 380–392.

Voet Donald, Voet Judith G. Biochemistry. 2011. 4.

Walker John. The ATP synthase: The understood, the uncertain and the unknown // Biochemical Society transactions. 02 2013. 41. 1–16.

Warskulat Ulrich, Flögel Ulrich, Jacoby Christoph, Hartwig Hans-Georg, Merx Marc W, Molojavyi Andrej, Heller-stilb Birgit, Schrader Jürgen, Haussinger Dieter. Taurine transporter knockout depletes muscle taurine levels and results in severe skeletal muscle impairment but leaves cardiac function uncompromised // FASEB Journal. 2004. 18, 3. 577–9.

Watmough Nicholas J., Frerman Frank E. The electron transfer flavoprotein: Ubiquinone oxidoreductases // Biochimica et Biophysica Acta - Bioenergetics. 2010. 1797, 12. 1910–1916.

Watt Ian N, Montgomery Martin G, Runswick Michael J, Leslie Andrew G W, Walker John E. Bioenergetic cost of making an adenosine triphosphate molecule in animal mitochondria // PNAS. 2010. 107, 39. 16823–16827.

Weinbach E. C. A Procedure for Isolating Stable Mitochondria from Rat Liver and Kidney // Analytical Biochemistry. 1961. 2. 335–343.

Westermann Benedikt. Merging mitochondria matters. Cellular role and molecular machinery of mitochondrial fusion // EMBO Reports. 2002. 3, 6. 527–531.

Wettmarshausen Jennifer, Perocchi Fabiana. Isolation of Functional Mitochondria from Cultured Cells and Mouse Tissues // Mitochondria: Practical Protocols. 1567. 2017. 2, 15–32.

Wiedemann Nils, Pfanner Nikolaus. Mitochondrial Machineries for Protein Import and Assembly // Annual Rev Biochem. 2017. 86. 685–714.

Wiesner Rudolf J., Kreutzer Ulrike, Rösen Peter, Grieshaber Manfred K. Subcellular distribution of malate-aspartate cycle intermediates during normoxia and anoxia in the heart // BBA - Bioenergetics. 1988. 936, 1. 114–123.

Wilcke Mona, Hultenby Kjell, Alexson Stefan E. H. Novel Peroxisomal Populations in Subcellular Fractions from Rat Liver // Journal of Biological Chemistry. 1995. 270, 12. 6949–6958.

Wilson David F. Oxidative phosphorylation: regulation and role in cellular and tissue metabolism // The Journal of Physiology. 2017. 595, 23. 7023–7038.

Winterbourn Christine C. The Biological Chemistry of Hydrogen Peroxide. 528. 2013. 1. 3–25.

Woelders Henri, Zande Wim J van der, Colen Anne-marie A F, Dam Karel van. The phosphate potential maintained by mitochondria in State 4 is proportional to the proton-motive force // FEBS. 1985. 179, 2.

Xu Yan, Tao Yuyong, Cheung Lily S, Fan Chao, Chen Li-Qing, Xu Sophia, Perry Kay, Frommer Wolf B, Feng Liang. Structures of bacterial homologues of SWEET transporters in two distinct conformations // Nature. 2014. 515, 7527. 448–452.

Ye Hong, Rouault Tracey A. Human Iron-Sulfur Cluster Assembly, Cellular Iron Homeostasis, and Disease // Biochemistry. 2010. 49, 24. 4945–4956.

Zecchin Annalisa, Stapor Peter C., Goveia Jermaine, Carmeliet Peter. Metabolic pathway compartmentalization: An underappreciated opportunity? // Current Opinion in Biotechnology. 2015. 34. 73–81.

Zhang Jimmy, Wang Yves T., Miller James H., Day Mary M., Munger Joshua C., Brookes Paul S. Accumulation of Succinate in Cardiac Ischemia Primarily Occurs via Canonical Krebs Cycle Activity // Cell Reports. 2018. 23, 9. 2617–2628.

Zhang P. Analysis of Mouse Liver Glycogen Content // Bio-Protocol. 2012. 2, 10. 3–6.

Zhang Xueping, Yang Shanshan, Chen Jinglu, Su Zhiguang. Unraveling the Regulation of Hepatic Gluconeogenesis // Frontiers in Endocrinology. 2019. 9, January. 1–17.

Zhao Yuzheng, Jin Jing, Hu Qingxun, Zhou Hai Meng, Yi Jing, Yu Zhenhang, Xu Lei, Wang Xue, Yang Yi, Loscalzo Joseph. Genetically encoded fluorescent sensors for intracellular NADH detection // Cell Metabolism. 2011. 14, 4. 555–566.

Zhou Bin, Xiao Jun Feng, Tuli Leepika, Ressom Habtom W. LC-MS-based metabolomics // Molecular Biosystems. 2012. 8. 470–481.

Zuurendonk P. F., Tager J. M. Rapid separation of particulate components and soluble cytoplasm of isolated rat-liver cells // BBA - Bioenergetics. 1974. 333, 2. 393–399.

Zweier J. L., Flaherty J. T., Weisfeldt M. L. Direct measurement of free radical generation following reperfusion of ischemic myocardium // Proceedings of the National Academy of Sciences of the United States of America. 1987. 84, 5. 1404–7.

Appendix A

LC-MS data tables - raw ion intensities

Metabolite	Hom	SEM	n	Hom + WI	SEM	n	Snt	SEM	n	Snt + WI	SEM	n	Cyto	SEM	n	Cyto + WI	SEM	n	Mito	SEM	n	Mito + WI	SEM	n
2-HG	4.11E+06	1.85E+06	3	2.97E+06	1.95E+06	2	3.09E+06	1.47E+06	3	1.02E+06	1.02E+06	1	4.61E+06	2.15E+06	3	2.78E+06	1.27E+06	3	2.21E+06	2.21E+06	1	0.00E+00	0.00E+00	0
3-Phosphoglycerate	7.90E+06	3.32E+06	6	5.85E+05	3.71E+05	2	1.93E+07	6.17E+06	6	1.55E+06	5.67E+05	4	3.59E+07	9.88E+06	6	5.25E+06	5.91E+05	6	0.00E+00	0.00E+00	0	0.00E+00	0.00E+00	0
Acetylcarnitine	5.06E+09	6.20E+08	6	1.73E+09	1.56E+08	6	6.11E+09	5.09E+08	6	2.37E+09	1.88E+08	6	5.27E+09	5.30E+08	6	1.54E+09	7.56E+07	6	1.24E+09	2.56E+08	6	2.78E+09	3.33E+08	6
AcetylCholine	2.68E+08	5.08E+07	6	2.08E+08	1.00E+07	6	2.71E+08	3.61E+07	6	1.99E+08	2.34E+07	6	2.63E+08	3.99E+07	6	2.11E+08	9.23E+06	6	6.73E+07	1.82E+07	6	1.30E+08	1.24E+07	6
Aconitate	3.40E+06	8.81E+05	6	1.86E+06	3.81E+05	6	3.54E+06	2.97E+05	6	3.52E+06	6.68E+05	6	1.40E+06	2.74E+05	6	1.40E+06	2.89E+05	6	6.41E+06	2.40E+06	6	1.75E+07	6.25E+06	6
Adenine	2.71E+07	1.71E+06	6	3.39E+08	2.11E+07	6	2.94E+07	2.26E+06	6	3.07E+08	3.22E+07	6	2.17E+07	1.63E+06	6	3.52E+08	2.26E+07	6	5.22E+07	1.71E+07	6	9.43E+07	1.43E+07	6
Adenosine	1.74E+08	1.76E+07	6	1.13E+09	6.99E+07	6	3.17E+08	2.78E+07	6	1.25E+09	9.49E+07	6	1.54E+08	2.09E+07	6	1.14E+09	5.35E+07	6	1.87E+08	1.36E+08	6	3.78E+08	5.18E+07	6
ADP	4.45E+07	4.31E+06	6	1.08E+07	1.43E+06	6	3.29E+07	1.94E+06	6	1.01E+07	1.60E+06	6	3.73E+07	2.94E+06	6	7.33E+06	8.87E+05	6	1.02E+07	2.08E+06	6	2.20E+07	4.13E+06	6
aKG	1.11E+06	7.10E+05	2	2.15E+06	8.36E+05	4	1.16E+06	5.75E+05	3	1.07E+07	1.95E+06	6	5.04E+05	5.04E+05	1	2.14E+06	7.97E+05	4	3.80E+06	2.07E+06	3	5.95E+06	2.75E+06	5
Alanine	1.43E+08	8.05E+06	6	2.24E+08	1.12E+07	6	1.47E+08	7.61E+06	6	2.17E+08	1.65E+07	6	1.46E+08	6.35E+06	6	2.24E+08	3.50E+06	6	7.41E+07	1.55E+07	6	1.68E+08	1.10E+07	6
AMP	1.19E+08	1.58E+07	6	5.89E+07	5.45E+06	6	1.65E+08	1.65E+07	6	5.86E+07	6.69E+06	6	1.47E+08	1.82E+07	6	5.89E+07	4.73E+06	6	5.30E+07	9.39E+06	6	5.92E+07	5.68E+06	6
Arginine	3.26E+07	2.51E+06	6	4.42E+07	2.16E+06	6	3.32E+07	3.06E+06	6	4.12E+07	5.42E+06	6	2.92E+07	2.29E+06	6	4.69E+07	2.27E+06	6	2.72E+07	8.49E+06	6	5.67E+07	3.31E+07	6
Asparagine	1.00E+07	1.17E+06	6	8.79E+06	4.00E+05	6	9.72E+06	1.08E+06	6	8.67E+06	5.40E+05	6	9.22E+06	1.19E+06	6	7.63E+06	5.35E+05	6	1.24E+07	4.17E+06	6	1.21E+07	1.18E+06	6
Aspartate	1.44E+08	1.33E+07	6	9.65E+07	8.83E+06	6	1.62E+08	1.91E+07	6	8.97E+07	1.17E+07	6	1.53E+08	2.02E+07	6	9.55E+07	8.85E+06	6	2.56E+07	8.58E+06	6	2.96E+07	2.61E+06	6
Betaine	6.73E+08	1.84E+08	6	5.34E+08	3.87E+07	6	6.78E+08	1.50E+08	6	4.67E+08	6.84E+07	6	6.72E+08	1.58E+08	6	5.18E+08	3.36E+07	6	9.67E+08	8.16E+08	6	7.83E+08	5.52E+08	6
Butyrylcarnitine	1.31E+08	1.84E+07	6	9.36E+07	6.42E+06	6	1.36E+08	1.21E+07	6	8.15E+07	1.31E+07	6	1.38E+08	1.42E+07	6	9.75E+07	6.22E+06	6	2.20E+07	4.20E+06	6	2.00E+07	2.97E+06	6
Carbamoyl phosphate	1.96E+08	1.57E+07	6	2.00E+08	8.20E+06	6	2.04E+08	1.05E+07	6	1.85E+08	1.91E+07	6	1.98E+08	1.73E+07	6	2.03E+08	4.84E+06	6	3.37E+07	1.15E+07	6	4.59E+07	5.70E+06	6
Carnitine	2.85E+09	5.34E+08	6	8.34E+09	2.58E+08	6	2.82E+09	4.09E+08	6	7.11E+09	8.60E+08	6	2.92E+09	4.44E+08	6	8.76E+09	3.42E+08	6	3.44E+08	1.13E+08	6	2.07E+09	1.29E+08	6
CDP	2.15E+05	4.64E+04	6	3.46E+03	3.46E+03	1	9.31E+04	2.80E+04	5	0.00E+00	0.00E+00	0	1.40E+05	2.59E+04	6	0.00E+00	0.00E+00	0	0.00E+00	0.00E+00	0	0.00E+00	0.00E+00	0
Choline	7.69E+08	2.08E+08	6	1.41E+09	1.05E+08	6	7.75E+08	1.66E+08	6	1.26E+09	1.57E+08	6	7.74E+08	1.84E+08	6	1.42E+09	1.32E+08	6	1.38E+09	1.16E+09	6	8.88E+08	3.24E+08	6
Citrate	3.67E+07	9.26E+06	6	2.09E+07	4.33E+06	6	3.49E+07	5.29E+06	6	3.70E+07	6.24E+06	6	1.54E+07	2.44E+06	6	9.48E+06	2.12E+06	5	5.01E+07	3.19E+07	5	8.54E+07	2.06E+07	6
Citrulline	4.46E+07	3.31E+06	6	4.30E+07	2.30E+06	6	4.98E+07	5.93E+06	6	4.00E+07	3.95E+06	6	4.05E+07	2.09E+06	6	4.26E+07	4.39E+06	6	4.52E+07	8.94E+06	6	5.22E+07	2.78E+06	6
CMP	9.45E+05	1.59E+05	6	4.63E+05	7.35E+04	6	1.43E+06	1.62E+05	6	6.12E+05	6.81E+04	6	1.29E+06	1.88E+05	6	5.02E+05	4.37E+04	6	2.82E+05	7.25E+04	6	4.23E+05	6.03E+04	6
Creatine	2.82E+10	1.45E+09	6	2.78E+10	6.32E+08	6	2.82E+10	9.18E+08	6	2.61E+10	2.05E+09	6	2.80E+10	1.46E+09	6	2.76E+10	8.55E+08	6	8.09E+09	1.71E+09	6	1.75E+10	5.73E+08	6
Creatinine	3.91E+09	3.75E+08	6	3.90E+09	1.95E+08	6	4.22E+09	3.05E+08	6	3.38E+09	4.02E+08	6	4.41E+09	2.70E+08	6	4.16E+09	1.88E+08	6	7.11E+08	2.24E+08	6	1.50E+09	2.70E+08	6
Cysteic acid	4.59E+08	4.10E+07	6	4.55E+08	1.42E+07	6	4.58E+08	1.99E+07	6	4.31E+08	4.44E+07	6	4.67E+08	2.85E+07	6	4.73E+08	1.23E+07	6	1.40E+08	2.49E+07	6	2.62E+08	1.65E+07	6
Cytidine	1.17E+07	9.28E+05	6	2.82E+07	2.33E+06	6	1.37E+07	7.48E+05	6	2.64E+07	2.60E+06	6	1.22E+07	9.19E+05	6	2.76E+07	2.22E+06	6	2.52E+06	1.15E+06	6	1.66E+07	2.04E+06	6
Ethanolamine	1.07E+07	1.94E+06	6	1.61E+07	7.87E+05	6	1.08E+07	1.71E+06	6	1.38E+07	1.20E+06	6	1.01E+07	1.48E+06	6	1.68E+07	1.02E+06	6	4.80E+06	1.73E+06	6	7.23E+06	2.38E+06	6
Fructose	7.05E+08	2.30E+07	6	6.61E+08	3.02E+07	6	7.27E+08	3.62E+07	6	6.61E+08	6.11E+07	6	7.16E+08	3.49E+07	6	7.01E+08	5.01E+07	6	4.24E+08	1.40E+08	6	3.63E+08	1.12E+08	6
Fructose 6-Phosphate	1.46E+06	3.48E+05	6	4.23E+05	9.35E+04	6	5.99E+05	1.78E+05	6	2.26E+05	3.63E+04	6	2.88E+05	1.10E+05	5	2.36E+05	1.65E+04	6	1.08E+04	1.08E+04	1	8.02E+03	8.02E+03	1
Fumarate	1.05E+07	9.70E+05	6	1.21E+07	1.58E+06	6	1.04E+07	1.58E+06	6	1.25E+07	1.54E+06	6	1.00E+07	1.13E+06	6	1.27E+07	1.03E+06	6	2.48E+06	1.74E+06	3	1.83E+06	8.47E+05	3
Glucose	4.45E+08	3.14E+07	6	3.98E+08	1.99E+07	6	4.42E+08	3.02E+07	6	3.50E+08	3.40E+07	6	4.77E+08	2.11E+07	6	4.19E+08	1.37E+07	6	2.33E+08	7.60E+07	6	1.83E+08	5.58E+07	6
Glucose 6-Phosphate	8.17E+05	2.55E+05	6	2.86E+04	2.86E+04	1	7.18E+04	5.15E+04	2	0.00E+00	0.00E+00	0	0.00E+00	0.00E+00	0	0.00E+00	0.00E+00	0	0.00E+00	0.00E+00	0	1.10E+04	7.10E+03	2
Glutamate	6.24E+08	4.67E+07	6	5.96E+08	1.16E+07	6	6.41E+08	4.19E+07	6	5.46E+08	3.90E+07	6	5.99E+08	3.48E+07	6	5.73E+08	2.63E+07	6	4.13E+08	6.50E+07	6	5.65E+08	4.05E+07	6
Glutamine	1.67E+09	2.08E+08	6	1.51E+09	5.32E+07	6	1.66E+09	1.67E+08	6	1.44E+09	9.64E+07	6	1.62E+09	1.90E+08	6	1.45E+09	6.16E+07	6	1.02E+09	2.04E+08	6	1.41E+09	6.77E+07	6

Fig. A.1 Control and 30 min WI heart metabolite ion intensities, ZIC-pHILIC column. 1 of 2.

Metabolite	Hom	SEM	n	Hom + WI	SEM	n	Snt	SEM	n	Snt + WI	SEM	n	Cyto	SEM	n	Cyto + WI	SEM	n	Mito	SEM	n	Mito + WI	SEM	n
Glycerol	3.47E+07	2.78E+06	6	6.58E+07	6.11E+06	6	3.39E+07	3.95E+06	6	6.25E+07	8.66E+06	6	3.79E+07	3.89E+06	6	6.58E+07	6.61E+06	6	2.54E+07	8.59E+06	6	7.33E+07	4.71E+07	6
Glycerylphosphorylcholine	1.15E+08	6.07E+06	6	6.67E+07	5.56E+06	6	1.30E+08	6.38E+06	6	7.23E+07	5.59E+06	6	1.09E+08	5.08E+06	6	6.73E+07	3.29E+06	6	6.24E+07	3.06E+07	6	7.86E+07	4.27E+07	6
Glycine	3.38E+06	3.28E+05	6	4.34E+06	2.73E+05	6	3.27E+06	3.40E+05	6	3.94E+06	3.79E+05	6	4.57E+06	1.22E+06	6	4.25E+06	4.45E+05	6	5.93E+06	2.87E+06	6	3.00E+07	2.36E+07	6
GMP	2.38E+06	3.27E+05	6	1.71E+06	1.91E+05	6	3.55E+06	3.94E+05	6	2.06E+06	2.67E+05	6	3.59E+06	4.39E+05	6	1.87E+06	1.54E+05	6	7.22E+05	1.88E+05	6	2.02E+06	2.62E+05	6
GSH	6.72E+07	4.60E+06	6	7.21E+07	3.04E+06	6	6.97E+07	4.69E+06	6	6.38E+07	6.19E+06	6	6.70E+07	4.90E+06	6	7.01E+07	2.01E+06	6	2.23E+07	4.20E+06	6	4.45E+07	3.65E+06	6
GSSG	2.33E+05	3.74E+04	6	3.85E+05	4.08E+04	6	1.57E+05	3.77E+04	6	3.27E+05	4.85E+04	6	2.13E+05	2.12E+04	6	3.82E+05	2.61E+04	6	2.30E+05	6.55E+04	6	5.76E+05	5.56E+04	6
Guanosine	0.00E+00	0.00E+00	0	4.06E+06	1.59E+05	6	0.00E+00	0.00E+00	0	5.12E+06	4.61E+05	6	0.00E+00	0.00E+00	0	3.64E+06	2.31E+05	6	1.72E+06	1.72E+06	1	5.15E+06	6.05E+05	6
Histidine	8.83E+07	1.16E+07	6	8.12E+07	2.13E+06	6	8.56E+07	9.17E+06	6	7.68E+07	4.90E+06	6	8.68E+07	1.10E+07	6	8.07E+07	2.86E+06	6	6.46E+07	1.24E+07	6	6.91E+07	9.27E+06	6
Hypotaurine	2.73E+06	1.52E+06	4	2.30E+05	1.50E+05	2	2.26E+06	1.28E+06	4	0.00E+00	0.00E+00	0	3.45E+06	1.64E+06	6	7.19E+05	2.44E+05	5	0.00E+00	0.00E+00	0	0.00E+00	0.00E+00	0
Hypoxanthine	2.12E+07	2.98E+06	6	7.63E+08	3.49E+07	6	2.46E+07	2.47E+06	6	7.67E+08	6.74E+07	6	2.47E+07	1.90E+06	6	7.93E+08	4.45E+07	6	3.24E+07	2.64E+07	6	2.48E+08	1.83E+07	6
Inosine	4.64E+06	1.71E+06	4	4.84E+08	1.73E+07	6	1.24E+07	1.49E+06	6	5.05E+08	3.98E+07	6	1.17E+07	1.74E+06	6	5.18E+08	2.39E+07	6	2.20E+06	2.20E+06	1	2.05E+08	1.53E+07	6
Kynurenic acid	0.00E+00	0.00E+00	0	0.00E+00	0.00E+00	0	0.00E+00	0.00E+00	0	0.00E+00	0.00E+00	0	0.00E+00	0.00E+00	0	0.00E+00	0.00E+00	0	7.12E+06	1.11E+06	6	4.58E+07	1.30E+07	6
Lactate	8.93E+08	1.43E+08	6	1.80E+09	1.72E+08	6	9.97E+08	7.97E+07	6	1.69E+09	3.80E+08	6	1.08E+09	8.06E+07	6	2.19E+09	7.46E+07	6	1.62E+08	3.53E+07	6	7.90E+08	1.87E+08	6
Lysine	3.22E+07	1.42E+06	6	4.00E+07	2.42E+06	6	3.44E+07	4.54E+06	6	3.77E+07	5.54E+06	6	3.35E+07	3.60E+06	6	4.08E+07	2.70E+06	6	1.26E+07	3.30E+06	6	2.15E+07	3.62E+06	6
Malate	2.81E+08	1.75E+07	6	3.26E+08	3.18E+07	6	2.83E+08	1.90E+07	6	3.24E+08	3.70E+07	6	2.72E+08	2.12E+07	6	3.24E+08	2.19E+07	6	1.35E+08	8.81E+07	6	1.06E+08	1.60E+07	6
Methionine	6.97E+07	7.40E+06	6	8.73E+07	6.88E+06	6	7.37E+07	8.55E+06	6	8.00E+07	1.13E+07	6	7.44E+07	8.36E+06	6	8.76E+07	7.71E+06	6	5.15E+07	3.68E+07	6	4.17E+07	4.51E+06	6
Myristic acid	5.30E+05	5.30E+05	1	2.09E+05	2.09E+05	1	8.97E+05	6.39E+05	2	3.31E+06	1.75E+06	3	0.00E+00	0.00E+00	0	0.00E+00	0.00E+00	0	0.00E+00	0.00E+00	0	9.94E+06	3.31E+06	4
Myristoylcarnitine	1.01E+05	2.44E+04	5	0.00E+00	0.00E+00	0	2.25E+05	1.30E+05	4	0.00E+00	0.00E+00	0	5.68E+04	4.66E+04	2	0.00E+00	0.00E+00	0	0.00E+00	0.00E+00	0	0.00E+00	0.00E+00	0
NAD	2.98E+05	2.98E+05	1	0.00E+00	0.00E+00	0	3.38E+05	3.38E+05	1	0.00E+00	0.00E+00	0	0.00E+00	0.00E+00	0	0.00E+00	0.00E+00	0	4.94E+06	1.56E+06	5	1.37E+07	2.59E+06	6
Oleic acid	2.44E+05	2.44E+05	1	0.00E+00	0.00E+00	0	0.00E+00	0.00E+00	0	2.23E+06	1.55E+06	3	0.00E+00	0.00E+00	0	2.44E+04	2.44E+04	1	2.31E+05	2.31E+05	1	3.92E+06	1.35E+06	4
Oleylcarnitine	1.08E+05	1.08E+05	1	0.00E+00	0.00E+00	0	2.09E+05	2.09E+05	1	0.00E+00	0.00E+00	0	0.00E+00	0.00E+00	0	0.00E+00	0.00E+00	0	0.00E+00	0.00E+00	0	0.00E+00	0.00E+00	0
Ornithine	3.10E+06	5.51E+05	6	3.07E+06	1.76E+05	6	3.06E+06	4.45E+05	6	2.74E+06	4.36E+05	6	3.16E+06	5.54E+05	6	2.91E+06	2.38E+05	6	1.70E+06	4.84E+05	6	2.32E+06	8.61E+05	6
Palmitic acid	2.78E+06	2.78E+06	1	1.86E+06	1.18E+06	2	3.10E+06	2.09E+06	2	1.08E+07	5.84E+06	3	0.00E+00	0.00E+00	0	0.00E+00	0.00E+00	0	1.41E+06	8.97E+05	2	1.54E+07	4.99E+06	4
Palmitoylcarnitine	1.54E+05	1.34E+05	2	0.00E+00	0.00E+00	0	4.07E+05	3.62E+05	3	0.00E+00	0.00E+00	0	2.00E+04	2.00E+04	1	0.00E+00	0.00E+00	0	0.00E+00	0.00E+00	0	0.00E+00	0.00E+00	0
Phenylalanine	5.50E+07	8.62E+06	6	6.58E+07	2.21E+06	6	5.92E+07	6.28E+06	6	6.25E+07	6.78E+06	6	5.70E+07	7.14E+06	6	6.87E+07	2.78E+06	6	2.10E+07	8.81E+06	6	3.39E+07	4.61E+06	6
Picolinamide	3.85E+08	5.51E+07	6	6.00E+08	3.16E+07	6	4.68E+08	4.35E+07	6	7.53E+08	7.52E+07	6	3.18E+08	4.36E+07	6	5.16E+08	1.89E+07	6	2.53E+08	2.66E+07	6	3.00E+08	8.36E+07	6
Proline	3.63E+08	5.62E+07	6	5.41E+08	5.03E+07	6	3.67E+08	5.88E+07	6	4.98E+08	7.41E+07	6	3.53E+08	5.46E+07	6	5.21E+08	5.63E+07	6	1.68E+08	8.16E+07	6	4.39E+08	1.59E+08	6
Propionylcarnitine	5.41E+07	7.62E+06	6	8.76E+07	9.28E+06	6	5.70E+07	7.35E+06	6	7.39E+07	9.07E+06	6	5.77E+07	7.37E+06	6	8.65E+07	7.03E+06	6	7.51E+06	2.14E+06	6	2.76E+07	4.70E+06	6
S-Adenosyl-Methionine	6.28E+05	1.09E+05	6	6.17E+05	1.09E+05	6	7.77E+05	5.22E+04	6	6.30E+05	5.67E+04	6	5.78E+05	8.94E+04	6	5.04E+05	6.61E+04	6	1.83E+06	3.92E+05	6	2.11E+06	3.88E+05	6
Serine	8.92E+06	7.13E+05	6	1.00E+07	6.49E+05	6	9.02E+06	6.44E+05	6	9.19E+06	1.04E+06	6	8.69E+06	4.66E+05	6	9.39E+06	8.76E+05	6	7.12E+06	1.05E+06	6	1.31E+07	3.56E+06	6
Stearic acid	3.77E+05	3.77E+05	1	4.10E+05	4.10E+05	1	5.19E+05	5.19E+05	1	4.57E+06	2.44E+06	3	0.00E+00	0.00E+00	0	0.00E+00	0.00E+00	0	0.00E+00	0.00E+00	0	8.85E+06	2.85E+06	4
Stearoyl carnitine	8.98E+03	8.98E+03	1	4.49E+03	2.89E+03	2	5.48E+04	5.48E+04	1	5.43E+04	5.43E+04	1	0.00E+00	0.00E+00	0	0.00E+00	0.00E+00	0	0.00E+00	0.00E+00	0	0.00E+00	0.00E+00	0
Succinate	1.05E+08	9.00E+06	6	2.41E+08	1.13E+07	6	1.01E+08	5.57E+06	6	2.10E+08	3.30E+07	6	1.18E+08	4.73E+06	6	2.70E+08	1.32E+07	6	1.39E+07	5.50E+06	4	5.12E+07	6.04E+06	6
Sucrose	1.48E+10	4.63E+08	6	1.45E+10	2.49E+08	6	1.53E+10	1.70E+08	6	1.41E+10	9.55E+08	6	1.56E+10	1.00E+08	6	1.54E+10	1.27E+08	6	4.23E+09	8.95E+08	6	6.23E+09	4.28E+08	6
Taurine	5.15E+09	3.67E+08	6	5.20E+09	1.06E+08	6	5.06E+09	1.80E+08	6	4.94E+09	4.34E+08	6	5.13E+09	2.61E+08	6	5.26E+09	1.41E+08	6	2.01E+09	3.27E+08	6	3.36E+09	1.58E+08	6
Threonine	5.05E+07	1.41E+06	6	6.84E+07	2.94E+06	6	5.41E+07	4.66E+06	6	6.41E+07	5.04E+06	6	5.51E+07	4.29E+06	6	6.95E+07	4.33E+06	6	2.37E+07	5.53E+06	6	4.75E+07	5.73E+06	6
Tryptophan	2.13E+07	2.54E+06	6	2.36E+07	9.30E+05	6	2.31E+07	3.35E+06	6	2.16E+07	2.64E+06	6	2.22E+07	3.03E+06	6	2.37E+07	1.27E+06	6	1.32E+07	8.22E+06	6	2.08E+07	9.06E+06	6
UMP	3.43E+05	9.71E+04	6	3.49E+04	2.29E+04	2	6.04E+05	9.03E+04	6	0.00E+00	0.00E+00	0	6.04E+05	1.13E+05	6	4.37E+04	1.82E+04	4	2.70E+04	1.71E+04	2	5.02E+03	5.02E+03	1
Urea	5.00E+07	2.19E+06	6	6.11E+07	2.87E+06	6	5.31E+07	5.21E+06	6	4.77E+07	5.60E+06	6	5.38E+07	4.89E+06	6	5.83E+07	1.80E+06	6	1.10E+07	2.76E+06	6	1.94E+07	5.12E+06	6
Valine	1.23E+08	1.15E+07	6	1.59E+08	5.54E+06	6	1.23E+08	1.47E+07	6	1.39E+08	1.22E+07	6	1.26E+08	1.76E+07	6	1.62E+08	8.57E+06	6	3.80E+07	1.06E+07	6	6.67E+07	8.36E+06	6
Xanthosine	6.93E+04	8.99E+03	6	9.47E+04	1.11E+04	6	8.37E+04	9.75E+03	6	1.12E+05	2.10E+04	6	8.15E+04	1.30E+04	6	1.02E+05	1.40E+04	6	3.32E+04	1.17E+04	4	8.40E+04	1.44E+04	6

Fig. A.2 Control and 30 min WI heart metabolite ion intensities, ZIC-pHILIC column. 2 of 2.

Metabolite	Hom	SEM	n	Hom + WI	SEM	n	Snt	SEM	n	Snt + WI	SEM	n	Cyto	SEM	n	Cyto + WI	SEM	n	Mito	SEM	n	Mito + WI	SEM	n
Acetylcarnitine	3.57E+09	3.39E+08	6	1.50E+09	1.41E+08	6	4.13E+09	2.54E+08	6	1.95E+09	1.08E+08	6	3.86E+09	3.43E+08	6	1.28E+09	9.15E+07	6	1.13E+09	1.91E+08	6	1.80E+09	4.11E+08	6
AcetylCholine	2.25E+08	4.72E+07	6	1.67E+08	9.81E+06	6	2.25E+08	3.57E+07	6	1.64E+08	1.83E+07	6	2.39E+08	4.65E+07	6	1.72E+08	7.15E+06	6	4.97E+07	1.46E+07	6	6.87E+07	1.62E+07	6
Adenine	1.76E+07	1.46E+06	6	2.80E+08	1.83E+07	6	1.46E+07	1.92E+06	6	2.86E+08	3.51E+07	6	1.32E+07	1.88E+06	6	3.22E+08	1.80E+07	6	4.68E+07	1.90E+07	6	9.95E+07	2.44E+07	6
Adenosine	2.02E+08	1.98E+07	6	1.29E+09	1.38E+08	6	3.57E+08	3.43E+07	6	1.31E+09	1.09E+08	6	1.82E+08	1.77E+07	6	1.22E+09	1.03E+08	6	1.89E+08	1.19E+08	6	4.89E+08	1.18E+08	6
Alanine	1.24E+09	8.06E+07	6	2.05E+09	2.56E+08	6	1.15E+09	5.12E+07	6	2.32E+09	2.80E+08	6	1.53E+09	7.66E+07	6	2.13E+09	2.10E+08	6	4.69E+08	1.02E+08	6	1.19E+09	2.61E+08	6
Allantoin	2.66E+07	3.45E+06	6	2.69E+07	2.32E+06	6	2.57E+07	3.26E+06	6	2.74E+07	3.98E+06	6	2.98E+07	2.16E+06	6	2.73E+07	2.90E+06	6	1.41E+07	5.67E+06	6	3.18E+07	1.45E+07	5
AMP	7.87E+08	1.19E+08	6	4.17E+08	3.80E+07	6	1.13E+09	1.18E+08	6	4.31E+08	6.24E+07	6	1.11E+09	1.30E+08	6	4.60E+08	3.69E+07	6	1.88E+08	3.93E+07	6	1.75E+08	3.92E+07	6
Arginine	1.13E+08	8.51E+06	6	1.52E+08	6.39E+06	6	1.14E+08	9.42E+06	6	1.49E+08	1.85E+07	6	1.02E+08	5.07E+06	6	1.60E+08	9.43E+06	6	9.48E+07	2.70E+07	6	1.96E+08	1.28E+08	5
Asparagine	6.27E+07	8.73E+06	6	5.36E+07	2.84E+06	6	6.17E+07	6.01E+06	6	5.23E+07	7.19E+06	6	6.60E+07	7.58E+06	6	5.51E+07	3.51E+06	6	2.89E+07	1.17E+07	6	2.64E+07	6.58E+06	5
Aspartate	6.71E+08	7.55E+07	6	4.49E+08	3.64E+07	6	7.42E+08	9.00E+07	6	4.61E+08	6.76E+07	6	7.84E+08	1.01E+08	6	4.95E+08	5.37E+07	6	1.08E+08	3.54E+07	6	1.01E+08	2.34E+07	6
Betaine	7.18E+08	1.42E+08	6	6.15E+08	3.91E+07	6	6.96E+08	1.10E+08	6	5.75E+08	7.76E+07	6	7.59E+08	1.33E+08	6	6.66E+08	2.94E+07	6	7.80E+08	5.29E+08	6	6.48E+08	3.84E+08	6
Butyrylcarnitine	1.65E+08	1.91E+07	6	1.08E+08	7.63E+06	6	1.59E+08	1.03E+07	6	8.64E+07	2.35E+07	6	1.74E+08	2.06E+07	6	1.14E+08	4.19E+06	6	1.58E+07	9.99E+06	2	5.62E+06	3.57E+06	2
Carnitine	1.50E+09	1.87E+08	6	3.25E+09	1.79E+08	6	1.30E+09	1.33E+08	6	3.00E+09	2.46E+08	6	1.39E+09	2.11E+08	6	3.14E+09	1.18E+08	6	2.64E+08	7.36E+07	6	1.04E+09	2.17E+08	6
Choline	1.26E+09	3.26E+08	6	2.22E+09	8.87E+07	6	1.17E+09	2.64E+08	6	2.28E+09	2.17E+08	6	1.34E+09	3.27E+08	6	2.30E+09	2.01E+08	6	1.63E+09	1.23E+09	6	1.41E+09	5.23E+08	6
Citrulline	2.16E+08	1.96E+07	6	2.14E+08	1.51E+07	6	2.22E+08	1.28E+07	6	2.13E+08	3.01E+07	6	2.31E+08	1.00E+07	6	2.32E+08	1.59E+07	6	8.29E+07	1.54E+07	6	1.03E+08	2.32E+07	6
Creatinine	2.17E+09	1.90E+08	6	2.06E+09	1.75E+08	6	2.14E+09	1.85E+08	6	2.02E+09	2.50E+08	6	2.61E+09	1.77E+08	6	2.31E+09	2.20E+08	6	4.27E+08	1.43E+08	6	8.78E+08	2.37E+08	6
Cysteine	2.02E+06	6.80E+05	6	9.50E+06	1.18E+06	6	1.47E+06	7.78E+05	6	1.08E+07	2.36E+06	6	1.16E+06	3.66E+05	6	8.75E+06	1.47E+06	6	2.41E+05	2.41E+05	1	2.59E+05	9.71E+04	4
Cytidine	5.12E+06	1.04E+06	6	2.00E+07	1.81E+06	6	6.89E+06	8.99E+05	6	1.92E+07	3.00E+06	6	6.97E+06	1.11E+06	6	2.14E+07	2.21E+06	6	2.97E+05	2.97E+05	1	7.39E+06	2.52E+06	5
Dihydrothymine	1.17E+07	1.96E+06	6	9.79E+06	6.85E+05	6	1.19E+07	1.49E+06	6	1.06E+07	1.42E+06	6	1.27E+07	1.59E+06	6	1.12E+07	6.38E+05	6	2.28E+06	7.44E+05	6	3.95E+06	9.41E+05	5
Fructose	2.85E+09	1.34E+08	6	2.85E+09	1.20E+08	6	2.90E+09	1.56E+08	6	2.75E+09	2.23E+08	6	3.07E+09	1.15E+08	6	2.97E+09	1.13E+08	6	1.40E+09	3.93E+08	6	1.22E+09	3.62E+08	6
Fumarate	6.61E+05	4.27E+05	2	1.73E+06	1.18E+06	2	0.00E+00	0.00E+00	0	1.21E+06	7.63E+05	2	2.91E+05	2.91E+05	1	7.57E+05	7.57E+05	1	1.01E+07	2.86E+06	5	4.65E+06	3.34E+06	3
GABA	2.20E+07	2.24E+06	6	1.94E+07	6.63E+05	6	2.12E+07	1.24E+06	6	1.95E+07	1.90E+06	6	2.24E+07	1.60E+06	6	2.14E+07	5.09E+05	6	7.97E+06	1.73E+06	6	1.09E+07	2.44E+06	5
Glucose	1.61E+09	2.81E+08	6	1.36E+09	2.28E+08	6	1.44E+09	1.94E+08	6	1.66E+09	2.30E+08	6	1.90E+09	1.64E+08	6	1.67E+09	3.32E+08	6	6.06E+08	1.78E+08	6	6.59E+08	2.11E+08	6
Glutamate	6.67E+09	6.84E+08	6	6.00E+09	2.53E+08	6	6.47E+09	3.54E+08	6	6.00E+09	5.90E+08	6	6.79E+09	4.06E+08	6	6.43E+09	1.49E+08	6	2.52E+09	4.08E+08	6	3.32E+09	7.18E+08	6
Glutamine	7.70E+09	1.25E+09	6	6.85E+09	3.54E+08	6	7.75E+09	9.93E+08	6	6.70E+09	8.82E+08	6	8.30E+09	1.09E+09	6	7.08E+09	4.33E+08	6	2.18E+09	4.77E+08	6	3.14E+09	7.14E+08	6
Glycerylphosphorylcholine	5.14E+07	2.93E+06	6	3.10E+07	2.47E+06	6	6.15E+07	5.30E+06	6	3.22E+07	3.87E+06	6	5.55E+07	4.80E+06	6	3.27E+07	2.85E+06	6	1.68E+07	1.08E+07	6	2.78E+07	2.01E+07	5
Glycine	3.53E+08	3.43E+07	6	4.10E+08	2.86E+07	6	3.42E+08	1.72E+07	6	3.74E+08	5.22E+07	6	4.71E+08	1.21E+08	6	4.31E+08	2.39E+07	6	2.19E+08	9.90E+07	6	1.23E+09	9.75E+08	6
GSH	5.85E+08	4.53E+07	6	6.29E+08	3.83E+07	6	5.62E+08	4.27E+07	6	6.10E+08	8.84E+07	6	5.77E+08	3.54E+07	6	6.48E+08	3.63E+07	6	1.32E+08	2.55E+07	6	1.95E+08	4.65E+07	6
Histidine	6.12E+07	1.13E+07	6	5.37E+07	2.46E+06	6	6.06E+07	8.16E+06	6	5.09E+07	5.08E+06	6	6.50E+07	1.01E+07	6	5.62E+07	2.23E+06	6	1.79E+07	4.93E+06	6	2.57E+07	6.85E+06	6

Fig. A.3 Control and 30 min WI heart metabolite ion intensities, ZIC-HILIC column. 1 of 2.

Metabolite	Hom	SEM	n	Hom + WI	SEM	n	Snt	SEM	n	Snt + WI	SEM	n	Cyto	SEM	n	Cyto + WI	SEM	n	Mito	SEM	n	Mito + WI	SEM	n
Hypotaurine	6.05E+07	1.90E+07	6	3.32E+07	1.04E+06	6	5.71E+07	1.67E+07	6	3.12E+07	3.90E+06	6	6.21E+07	1.78E+07	6	3.60E+07	1.38E+06	6	1.28E+07	4.61E+06	6	1.06E+07	2.67E+06	5
Hypoxanthine	5.34E+07	8.83E+06	6	1.97E+09	1.12E+08	6	5.27E+07	6.19E+06	6	1.98E+09	2.21E+08	6	5.28E+07	5.12E+06	6	2.19E+09	1.61E+08	6	7.19E+07	6.46E+07	6	3.94E+08	8.97E+07	6
Inosine	3.34E+07	6.74E+06	6	1.67E+09	6.58E+07	6	5.56E+07	5.24E+06	6	1.81E+09	1.53E+08	6	5.73E+07	5.23E+06	6	1.88E+09	7.22E+07	6	1.11E+07	9.04E+06	6	5.73E+08	1.29E+08	6
Lactate	7.83E+08	9.12E+07	6	1.51E+09	1.30E+08	6	8.55E+08	3.10E+07	6	1.39E+09	2.91E+08	6	9.22E+08	4.04E+07	6	1.78E+09	1.44E+08	6	1.92E+08	3.83E+07	6	6.49E+08	2.23E+08	6
Leucine	4.16E+08	8.14E+07	6	6.94E+08	9.41E+07	6	4.30E+08	9.85E+07	6	5.02E+08	5.28E+07	6	3.83E+08	1.06E+08	6	5.78E+08	9.89E+07	6	2.72E+08	1.45E+08	6	3.99E+08	9.02E+07	6
Lysine	1.96E+08	5.47E+06	6	2.30E+08	1.10E+07	6	2.11E+08	2.48E+07	6	2.30E+08	3.13E+07	6	2.10E+08	1.67E+07	6	2.58E+08	1.71E+07	6	7.61E+07	1.89E+07	6	1.17E+08	3.35E+07	6
Methionine	1.85E+08	2.07E+07	6	2.47E+08	2.07E+07	6	1.95E+08	2.42E+07	6	2.36E+08	3.66E+07	6	2.10E+08	2.57E+07	6	2.54E+08	2.03E+07	6	1.17E+08	7.79E+07	6	1.10E+08	2.83E+07	6
N-AcetylAspartate	7.61E+07	4.67E+06	6	7.92E+07	9.80E+06	6	7.90E+07	7.51E+06	6	7.41E+07	1.57E+07	6	8.54E+07	7.05E+06	6	8.48E+07	1.25E+07	6	2.89E+07	9.01E+06	6	4.60E+07	1.26E+07	6
Nicotinamide	1.24E+09	1.98E+08	6	1.82E+09	1.63E+08	6	1.53E+09	1.62E+08	6	2.80E+09	3.70E+08	6	1.12E+09	1.62E+08	6	1.88E+09	1.27E+08	6	8.77E+08	1.31E+08	6	1.46E+09	4.12E+08	6
Ornithine	2.41E+07	5.31E+06	6	2.33E+07	1.46E+06	6	2.38E+07	5.47E+06	6	2.54E+07	5.54E+06	6	2.68E+07	5.93E+06	6	2.37E+07	2.29E+06	6	1.04E+07	4.60E+06	6	2.21E+07	1.42E+07	5
Pantothenic_acid	4.89E+07	5.58E+06	6	5.37E+07	4.71E+06	6	4.76E+07	4.84E+06	6	5.35E+07	8.09E+06	6	4.85E+07	5.87E+06	6	5.72E+07	4.35E+06	6	2.00E+07	6.70E+06	6	3.40E+07	7.73E+06	5
Phenylalanine	1.32E+08	2.30E+07	6	1.48E+08	6.88E+06	6	1.27E+08	1.92E+07	6	1.48E+08	2.50E+07	6	1.27E+08	1.48E+07	6	1.66E+08	2.04E+07	6	7.52E+07	3.79E+07	6	6.97E+07	1.48E+07	6
Proline	3.38E+08	5.78E+07	6	4.72E+08	8.06E+07	6	3.16E+08	5.48E+07	6	5.25E+08	8.46E+07	6	3.74E+08	4.75E+07	6	5.20E+08	4.92E+07	6	1.33E+08	5.91E+07	6	3.58E+08	1.53E+08	6
Propionylcarnitine	6.42E+07	7.75E+06	6	1.21E+08	1.19E+07	6	7.06E+07	9.32E+06	6	9.88E+07	1.12E+07	6	7.35E+07	1.14E+07	6	1.15E+08	1.07E+07	6	8.92E+06	2.96E+06	6	2.71E+07	6.14E+06	6
Pyroglutamic acid	1.84E+08	2.04E+07	6	1.84E+08	1.26E+07	6	1.91E+08	2.05E+07	6	1.77E+08	2.44E+07	6	2.23E+08	2.32E+07	6	2.05E+08	1.93E+07	6	1.16E+08	4.72E+07	6	1.88E+08	6.05E+07	6
Serine	4.55E+08	4.67E+07	6	4.71E+08	3.90E+07	6	4.42E+08	2.54E+07	6	4.74E+08	6.67E+07	6	4.76E+08	2.72E+07	6	4.93E+08	3.83E+07	6	1.53E+08	2.94E+07	6	2.88E+08	9.41E+07	6
Succinate	2.21E+08	2.41E+07	6	4.56E+08	2.17E+07	6	1.81E+08	1.22E+07	6	4.11E+08	5.43E+07	6	2.04E+08	9.64E+06	6	5.03E+08	2.68E+07	6	1.17E+08	3.11E+07	6	1.71E+08	3.96E+07	6
Sucrose	2.66E+08	1.98E+07	6	2.57E+08	1.29E+07	6	2.57E+08	1.13E+07	6	2.84E+08	1.92E+07	6	2.87E+08	1.13E+07	6	2.89E+08	2.34E+07	6	1.46E+08	7.28E+06	6	1.55E+08	1.86E+07	6
Taurine	5.27E+09	1.48E+08	6	5.30E+09	8.54E+07	6	5.28E+09	9.31E+07	6	5.33E+09	2.04E+08	6	5.52E+09	1.21E+08	6	5.44E+09	7.93E+07	6	3.14E+09	3.20E+08	6	3.72E+09	6.74E+08	6
Threonine	3.62E+08	5.80E+06	6	4.77E+08	2.47E+07	6	3.75E+08	3.77E+07	6	4.59E+08	4.60E+07	6	4.03E+08	3.01E+07	6	4.96E+08	2.58E+07	6	1.26E+08	3.00E+07	6	2.34E+08	5.86E+07	6
Tryptophan	4.92E+07	6.09E+06	6	6.25E+07	3.49E+06	6	5.68E+07	9.16E+06	6	5.66E+07	5.74E+06	6	5.33E+07	1.04E+07	6	6.11E+07	3.64E+06	6	3.63E+07	2.36E+07	6	5.46E+07	2.59E+07	5
Tyrosine	7.65E+07	1.10E+07	6	8.42E+07	9.95E+06	6	8.17E+07	1.56E+07	6	8.84E+07	1.45E+07	6	7.07E+07	1.03E+07	6	7.44E+07	8.77E+06	6	2.78E+07	8.53E+06	6	5.12E+07	1.43E+07	6
Uracil	1.37E+05	1.37E+05	1	4.51E+07	3.33E+06	6	0.00E+00	0.00E+00	0	4.10E+07	6.90E+06	6	9.94E+04	9.94E+04	1	4.89E+07	3.37E+06	6	8.99E+04	8.99E+04	1	3.02E+06	1.71E+06	3
Urea	3.08E+09	9.78E+07	6	3.33E+09	1.67E+08	6	3.12E+09	2.48E+08	6	3.05E+09	3.05E+08	6	3.52E+09	1.90E+08	6	3.60E+09	1.46E+08	6	7.74E+08	1.81E+08	6	1.29E+09	4.05E+08	5
Uric acid	1.70E+05	7.96E+04	3	5.58E+06	2.07E+06	6	6.97E+05	2.37E+05	5	5.60E+06	2.67E+06	6	5.26E+05	1.97E+05	4	7.43E+06	2.89E+06	6	3.72E+04	3.72E+04	1	9.62E+07	9.59E+07	3
Uridine	3.74E+06	8.13E+05	6	2.79E+07	2.22E+06	6	5.16E+06	4.46E+05	6	3.00E+07	4.05E+06	6	3.76E+06	1.13E+06	5	3.06E+07	2.21E+06	6	1.03E+06	1.03E+06	1	6.34E+06	1.83E+06	5
Valine	7.20E+08	1.43E+08	6	6.11E+08	3.79E+07	6	6.93E+08	1.07E+08	6	5.82E+08	7.25E+07	6	7.48E+08	1.29E+08	6	6.60E+08	2.89E+07	6	7.30E+08	5.25E+08	6	6.48E+08	3.77E+08	6
Xanthine	9.17E+06	1.77E+06	6	3.18E+08	1.99E+07	6	1.32E+07	1.61E+06	6	3.12E+08	2.71E+07	6	1.62E+07	1.21E+06	6	3.45E+08	1.18E+07	6	7.85E+06	6.43E+06	4	8.51E+07	1.97E+07	6
Xanthosine	0.00E+00	0.00E+00	0	2.16E+06	5.61E+05	6	0.00E+00	0.00E+00	0	2.49E+06	5.41E+05	6	0.00E+00	0.00E+00	0	3.24E+06	3.95E+05	6	0.00E+00	0.00E+00	0	5.08E+04	5.08E+04	1

Fig. A.4 Control and 30 min WI heart metabolite ion intensities, ZIC-HILIC column. 2 of 2.

Metabolite	Hom	SEM	n	Hom + WI	SEM	n	Snt	SEM	n	Snt + WI	SEM	n	Cyto	SEM	n	Cyto + WI	SEM	n	Mito	SEM	n	Mito + WI	SEM	n
2-HG	3.05E+07	1.56E+07	2	1.10E+08	3.71E+07	3	3.44E+07	5.26E+06	3	8.97E+07	2.83E+07	3	8.44E+06	4.51E+06	2	2.98E+07	6.29E+06	3	5.33E+06	5.33E+06	1	6.18E+07	1.25E+07	3
3-Hydroxybutyrate	4.91E+08	1.48E+08	3	6.58E+08	6.09E+07	3	6.27E+08	2.33E+08	3	8.60E+08	7.30E+07	3	1.44E+08	2.50E+07	3	2.33E+08	1.24E+07	3	7.01E+07	3.00E+07	3	1.39E+08	4.66E+06	3
3-Phosphoglycerate	5.06E+07	1.78E+07	3	1.31E+07	5.05E+06	3	5.58E+07	1.65E+07	3	2.22E+07	6.92E+06	3	1.12E+07	3.11E+06	3	3.68E+06	6.41E+05	3	9.42E+06	6.11E+06	3	2.09E+06	2.70E+05	3
3Phosphoserine	3.72E+06	1.30E+06	3	8.81E+05	1.86E+05	3	4.73E+06	1.35E+06	3	1.54E+06	1.61E+05	3	1.07E+06	1.80E+05	3	6.31E+05	8.00E+04	3	6.40E+05	3.72E+05	3	9.40E+05	2.02E+05	3
Acetylcarnitine	6.28E+09	1.06E+09	3	1.59E+09	5.53E+08	3	7.02E+09	1.47E+09	3	1.77E+09	4.96E+08	3	2.08E+09	4.86E+08	3	5.37E+08	1.33E+08	3	1.26E+09	6.21E+08	3	2.53E+09	3.28E+08	3
AcetylCholine	4.16E+08	1.05E+08	3	4.56E+08	1.43E+08	3	3.84E+08	8.27E+07	3	3.93E+08	8.35E+07	3	1.08E+08	2.49E+07	3	1.10E+08	2.44E+07	3	5.81E+07	3.77E+07	3	1.51E+08	3.35E+07	3
Aconitate	1.20E+07	2.43E+06	3	1.76E+05	8.85E+04	2	1.14E+07	1.74E+06	3	4.61E+04	4.61E+04	1	1.79E+06	3.63E+05	3	4.69E+04	4.69E+04	1	3.40E+06	1.12E+06	3	1.92E+06	6.36E+05	3
Adenine	2.09E+08	3.51E+07	3	7.76E+08	1.53E+08	3	1.68E+08	3.81E+07	3	5.70E+08	9.07E+07	3	3.29E+07	9.27E+06	3	1.98E+08	3.47E+07	3	5.28E+07	2.35E+07	3	3.68E+08	2.51E+07	3
Adenosine	2.76E+07	1.42E+07	2	1.98E+08	7.22E+07	3	9.58E+06	5.19E+06	2	5.87E+07	3.03E+07	3	0.00E+00	0.00E+00	0	1.59E+07	1.59E+07	1	5.13E+07	1.87E+07	3	3.54E+08	6.30E+07	3
adenylosuccinate	2.80E+06	8.72E+05	3	1.91E+05	9.58E+04	2	2.16E+06	6.36E+05	3	2.40E+05	9.18E+04	3	2.31E+05	6.70E+04	3	0.00E+00	0.00E+00	0	0.00E+00	0.00E+00	0	0.00E+00	0.00E+00	0
ADP	3.01E+08	7.36E+07	3	5.81E+07	9.67E+06	3	2.45E+08	5.09E+07	3	4.26E+07	3.80E+06	3	8.15E+07	1.62E+07	3	1.25E+07	7.99E+05	3	8.33E+07	3.45E+07	3	4.43E+07	2.90E+06	3
aKG	2.17E+07	1.10E+07	2	0.00E+00	0.00E+00	0	2.70E+07	6.13E+06	3	8.11E+05	8.11E+05	1	6.91E+06	2.59E+06	3	6.07E+05	6.07E+05	1	8.82E+06	5.27E+06	2	4.58E+06	4.29E+05	3
Alanine	5.57E+08	1.39E+08	3	1.97E+09	3.17E+08	3	6.04E+08	1.62E+08	3	1.67E+09	2.19E+08	3	2.33E+08	6.87E+07	3	6.92E+08	8.02E+07	3	8.62E+07	5.10E+07	3	3.60E+08	3.61E+07	3
Allantoin	4.66E+05	2.34E+05	2	3.72E+06	1.08E+06	3	0.00E+00	0.00E+00	0	4.52E+06	3.09E+05	3	0.00E+00	0.00E+00	0	0.00E+00	0.00E+00	0	0.00E+00	0.00E+00	0	1.29E+05	1.29E+05	1
AMP	1.50E+08	3.00E+07	3	2.11E+08	4.46E+07	3	1.27E+08	1.38E+07	3	1.75E+08	4.75E+07	3	6.26E+07	1.53E+07	3	5.85E+07	1.10E+07	3	1.18E+08	3.64E+07	3	1.48E+08	2.12E+07	3
Arginine	1.72E+07	3.76E+06	3	1.51E+07	1.42E+06	3	1.28E+07	3.95E+06	3	1.02E+07	2.79E+06	3	1.71E+06	4.57E+05	3	6.83E+05	7.20E+04	3	3.08E+06	1.38E+06	3	3.14E+06	7.29E+05	3
Argininosuccinate	2.45E+05	1.12E+05	3	1.25E+05	2.94E+04	3	1.42E+05	5.92E+04	3	6.57E+04	1.30E+04	3	9.37E+03	5.25E+03	2	0.00E+00	0.00E+00	0	6.66E+04	5.90E+04	2	2.25E+05	5.95E+04	3
Aspartate	2.45E+08	4.40E+07	3	8.95E+07	1.22E+07	3	2.83E+08	4.76E+07	3	7.87E+07	8.57E+06	3	8.20E+07	7.14E+06	3	2.33E+07	1.64E+06	3	2.90E+07	1.12E+07	3	4.90E+07	1.26E+07	3
ATP	9.61E+07	3.12E+07	3	3.84E+06	1.04E+06	3	7.57E+07	2.67E+07	3	2.89E+06	7.61E+05	3	7.91E+06	1.93E+06	3	1.33E+05	5.89E+04	3	4.42E+06	2.24E+06	3	1.99E+06	1.60E+05	3
Betaine	3.21E+10	9.34E+09	3	5.55E+10	1.90E+10	3	3.30E+10	9.50E+09	3	4.73E+10	1.54E+10	3	1.08E+10	3.20E+09	3	2.08E+10	7.29E+09	3	9.97E+09	5.82E+09	3	4.00E+10	8.97E+09	3
Butyryl(Carnitine	4.11E+08	1.55E+08	3	2.92E+08	8.18E+07	3	4.77E+08	1.96E+08	3	2.32E+08	5.13E+07	3	1.31E+08	6.09E+07	3	5.88E+07	1.15E+07	3	2.84E+07	2.03E+07	3	3.69E+07	2.62E+06	3
Carbamoyl phosphate	7.34E+08	1.01E+08	3	6.85E+08	7.81E+07	3	7.32E+08	4.37E+07	3	6.88E+08	4.93E+07	3	3.00E+08	4.64E+07	3	2.62E+08	1.06E+07	3	2.17E+08	9.01E+07	3	3.60E+08	1.98E+07	3
Carnitine	7.41E+09	2.45E+09	3	1.26E+10	3.54E+09	3	7.13E+09	2.25E+09	3	1.00E+10	2.41E+09	3	2.04E+09	6.97E+08	3	2.95E+09	6.19E+08	3	1.93E+09	1.26E+09	3	3.57E+09	5.08E+08	3
CDP	3.36E+06	9.02E+05	3	2.58E+05	1.01E+05	3	3.25E+06	8.48E+05	3	9.36E+04	2.85E+04	3	9.30E+05	2.27E+05	3	0.00E+00	0.00E+00	0	1.05E+05	8.52E+04	3	2.82E+05	1.12E+05	3
Choline	1.93E+09	4.35E+08	3	6.33E+09	1.08E+09	3	1.94E+09	5.68E+08	3	6.01E+09	9.03E+08	3	6.59E+08	2.49E+08	3	1.71E+09	3.67E+08	3	4.60E+08	3.36E+08	3	1.83E+09	4.78E+08	3
Citrate	2.83E+08	9.20E+07	3	1.83E+07	3.52E+06	3	2.52E+08	5.16E+07	3	1.16E+07	5.34E+06	3	1.99E+07	1.25E+06	3	4.76E+06	4.76E+06	1	4.18E+07	2.16E+07	3	2.58E+07	1.00E+07	3
Citrulline	4.48E+07	2.26E+07	3	2.19E+07	4.92E+06	3	5.73E+07	2.40E+07	3	1.70E+07	4.94E+06	3	6.65E+06	1.71E+06	3	5.35E+06	2.43E+06	3	1.54E+08	7.58E+07	3	2.39E+07	2.80E+06	3
CMP	1.68E+07	3.54E+06	3	1.27E+07	4.19E+06	3	1.65E+07	2.52E+06	3	1.06E+07	3.94E+06	3	5.11E+06	9.03E+05	3	3.18E+06	1.16E+06	3	2.76E+06	1.18E+06	3	5.25E+06	4.72E+05	3
Creatine	3.20E+09	6.00E+08	3	6.36E+09	2.54E+09	3	3.39E+09	7.82E+08	3	5.37E+09	2.49E+09	3	1.20E+09	2.79E+08	3	1.99E+09	8.68E+08	3	5.86E+08	2.56E+08	3	2.05E+09	3.46E+08	3
Creatinine	4.89E+08	1.13E+08	3	2.40E+08	6.37E+07	3	4.41E+08	1.02E+08	3	2.18E+08	7.63E+07	3	1.45E+08	4.27E+07	3	7.62E+07	2.32E+07	3	1.21E+08	5.63E+07	3	1.89E+08	1.04E+07	3
CTP	1.18E+06	4.64E+05	3	0.00E+00	0.00E+00	0	9.21E+05	4.35E+05	3	0.00E+00	0.00E+00	0	3.63E+04	1.83E+04	3	0.00E+00	0.00E+00	0	3.18E+03	3.18E+03	1	0.00E+00	0.00E+00	0
Cystathionine	3.62E+06	1.24E+06	3	2.32E+06	3.02E+05	3	3.70E+06	1.27E+06	3	2.30E+06	6.70E+05	3	7.22E+05	3.66E+05	3	5.18E+05	2.73E+05	3	4.26E+05	3.54E+05	3	1.00E+06	5.33E+05	3
Cysteine	9.97E+08	1.72E+08	3	1.04E+09	1.18E+08	3	1.10E+09	2.19E+08	3	1.05E+09	1.01E+08	3	3.03E+08	6.91E+07	3	3.06E+08	2.91E+07	3	2.43E+08	1.04E+08	3	4.16E+08	8.94E+07	3
Ethanolamine	8.59E+06	1.87E+06	3	3.53E+07	5.44E+06	3	9.18E+06	1.64E+06	3	3.03E+07	2.85E+06	3	4.91E+06	1.03E+06	3	1.33E+07	5.44E+05	3	4.32E+06	1.25E+06	3	1.18E+07	1.00E+06	3
Fructose	8.55E+09	2.07E+08	3	8.67E+09	5.66E+08	3	9.21E+09	5.04E+08	3	8.71E+09	7.27E+08	3	7.86E+09	2.88E+08	3	7.74E+09	4.18E+08	3	1.72E+09	5.00E+08	3	1.97E+09	2.90E+08	3
Fructose 6-Phosphate	3.34E+07	6.79E+06	3	3.17E+07	7.15E+06	3	3.64E+07	6.79E+06	3	2.90E+07	6.73E+06	3	8.56E+06	1.80E+06	3	8.19E+06	1.75E+06	3	1.02E+06	4.54E+05	3	2.79E+06	4.62E+05	3
Fumarate	1.20E+08	1.87E+07	3	5.37E+07	9.31E+06	3	1.32E+08	1.52E+07	3	7.68E+07	6.72E+06	3	3.66E+07	5.96E+06	3	2.16E+07	1.44E+06	3	1.06E+07	4.72E+06	3	3.48E+07	4.75E+06	3
GDP	3.27E+07	1.07E+07	3	8.94E+06	2.07E+06	3	2.30E+07	7.37E+06	3	7.49E+06	2.11E+06	3	6.46E+06	7.19E+05	3	1.55E+06	1.58E+05	3	4.73E+05	2.77E+05	3	1.84E+06	4.94E+04	3
Gluconate	1.37E+08	3.27E+07	3	2.21E+08	3.39E+07	3	1.54E+08	3.60E+07	3	1.94E+08	3.31E+07	3	3.88E+07	1.10E+07	3	5.12E+07	6.63E+06	3	1.89E+07	1.23E+07	3	7.70E+07	1.42E+07	3
Gluconate 6-phosphate	1.69E+06	8.30E+05	3	5.49E+05	4.04E+05	2	1.88E+06	1.05E+06	3	1.52E+06	3.58E+05	3	0.00E+00	0.00E+00	0	1.61E+05	1.61E+05	1	0.00E+00	0.00E+00	0	0.00E+00	0.00E+00	0
Glucose	9.20E+09	4.02E+08	3	1.59E+10	1.70E+09	3	1.00E+10	3.79E+08	3	1.57E+10	8.02E+08	3	7.85E+09	9.18E+07	3	9.43E+09	5.56E+08	3	1.62E+09	4.99E+08	3	6.82E+09	5.80E+08	3
Glucose 6-Phosphate	2.75E+07	5.80E+06	3	2.31E+07	5.85E+06	3	2.88E+07	6.00E+06	3	2.80E+07	7.93E+06	3	8.62E+06	2.22E+06	3	8.25E+06	1.91E+06	3	8.33E+05	4.29E+05	3	2.63E+06	4.56E+05	3
Glutamate	1.23E+09	2.18E+08	3	9.77E+08	3.28E+08	3	1.38E+09	2.49E+08	3	8.03E+08	2.57E+08	3	3.69E+08	5.73E+07	3	2.74E+08	8.78E+07	3	6.08E+08	1.44E+08	3	6.91E+08	9.50E+07	3
Glutamine	2.94E+09	3.81E+08	3	2.56E+09	3.68E+08	3	3.09E+09	4.96E+08	3	2.11E+09	1.86E+08	3	1.02E+09	2.10E+08	3	7.67E+08	7.74E+07	3	7.91E+08	1.95E+08	3	1.14E+09	2.39E+08	3
Glyceraldehyde 3-phosphate	2.57E+07	8.41E+06	3	1.85E+07	2.81E+06	3	4.10E+07	7.07E+06	3	2.18E+07	7.84E+05	3	3.05E+07	4.97E+06	3	1.22E+06	6.39E+05	2	3.00E+06	2.71E+06	3	1.20E+06	9.08E+05	3
Glycerol	3.02E+07	1.99E+07	2	3.35E+08	2.19E+07	3	2.72E+07	7.41E+06	3	3.64E+08	6.90E+06	3	1.49E+07	1.49E+07	1	9.93E+07	3.37E+06	3	4.50E+07	1.75E+07	3	5.72E+07	2.72E+06	3
Glycerylphosphorylcholine	3.00E+09	8.45E+08	3	1.49E+09	9.73E+07	3	2.93E+09	9.32E+08	3	1.22E+09	2.03E+08	3	1.05E+09	3.60E+08	3	4.70E+08	8.31E+07	3	8.06E+08	5.08E+08	3	9.22E+08	2.67E+08	3
Glycerylphosphorylethanolamine	1.81E+07	4.97E+06	3	1.12E+07	6.86E+05	3	1.80E+07	5.88E+06	3	1.08E+07	1.12E+06	3	1.62E+06	8.61E+05	3	9.36E+05	2.42E+05	3	2.49E+06	1.09E+06	3	4.89E+06	1.06E+06	3
Glycine	2.95E+07	8.13E+06	3	4.09E+07	7.05E+06	3	3.37E+07	9.41E+06	3	3.17E+07	5.28E+06	3	7.66E+06	1.99E+06	3	9.87E+06	1.62E+06	3	3.88E+06	1.48E+06	3	7.88E+06	1.53E+06	3

Fig. A.5 Control and 30 min WI liver metabolite ion intensities, ZIC-pHILIC column. 1 of 2.

Metabolite	Hom	SEM	n	Hom + WI	SEM	n	Snt	SEM	n	Snt + WI	SEM	n	Cyto	SEM	n	Cyto + WI	SEM	n	Mito	SEM	n	Mito + WI	SEM	n
GMP	2.60E+07	7.23E+06	3	4.42E+07	5.73E+06	3	2.59E+07	2.83E+06	3	4.09E+07	6.42E+06	3	9.57E+06	1.72E+06	3	1.23E+07	1.24E+06	3	4.00E+06	2.42E+06	3	7.00E+06	1.29E+06	3
GSH	2.05E+09	4.36E+08	3	2.00E+09	4.08E+08	3	2.27E+09	5.25E+08	3	1.72E+09	3.30E+08	3	6.60E+08	1.46E+08	3	5.53E+08	6.75E+07	3	5.05E+08	1.80E+08	3	1.02E+09	6.49E+07	3
GSSG	1.91E+07	7.46E+06	3	2.69E+07	4.11E+06	3	1.30E+07	3.79E+06	3	1.50E+07	1.72E+06	3	1.60E+06	9.34E+05	3	2.28E+06	7.16E+05	3	2.90E+06	1.38E+06	3	1.13E+07	2.75E+06	3
GTP	9.90E+06	3.45E+06	3	5.32E+05	3.01E+05	3	8.25E+06	3.29E+06	3	2.76E+05	1.15E+05	3	5.32E+05	1.51E+05	3	0.00E+00	0.00E+00	0	1.02E+04	1.02E+04	1	4.27E+03	4.27E+03	1
Histidine	8.78E+08	1.79E+08	3	9.59E+08	1.76E+08	3	8.87E+08	1.92E+08	3	7.85E+08	5.79E+07	3	3.66E+08	9.31E+07	3	3.12E+08	2.74E+07	3	4.62E+08	1.73E+08	3	8.87E+08	6.58E+07	3
Hypoxanthine	2.08E+07	1.68E+06	3	1.60E+09	1.98E+08	3	3.01E+06	3.01E+06	1	1.39E+09	1.18E+08	3	0.00E+00	0.00E+00	0	5.18E+08	4.80E+07	3	5.65E+06	2.99E+06	3	1.11E+09	1.67E+08	3
Inosine	0.00E+00	0.00E+00	0	4.21E+08	4.55E+07	3	0.00E+00	0.00E+00	0	4.03E+08	4.30E+07	3	0.00E+00	0.00E+00	0	1.04E+08	6.90E+06	3	4.03E+06	4.03E+06	1	2.83E+08	2.65E+07	3
Lactate	1.79E+09	1.73E+08	3	1.94E+10	1.42E+09	3	2.13E+09	2.50E+08	3	2.22E+10	1.30E+09	3	8.71E+08	6.63E+07	3	6.37E+09	3.18E+08	3	1.81E+08	1.20E+08	2	4.44E+09	4.29E+08	3
Linoleic acid	1.85E+08	4.90E+07	3	1.78E+08	7.45E+07	3	2.05E+08	4.34E+07	3	2.27E+08	1.57E+08	3	9.16E+06	1.72E+06	3	7.07E+06	2.83E+06	3	6.20E+04	6.20E+04	1	1.22E+06	3.28E+05	3
Lysine	3.91E+08	9.72E+07	3	4.46E+08	4.65E+07	3	4.23E+08	1.39E+08	3	4.02E+08	4.06E+07	3	9.91E+07	3.70E+07	3	9.83E+07	1.33E+07	3	3.36E+07	2.13E+07	3	8.15E+07	3.09E+07	3
Malate	2.59E+09	5.82E+08	3	1.27E+09	2.91E+08	3	2.79E+09	4.57E+08	3	1.55E+09	2.36E+08	3	8.24E+08	1.33E+08	3	4.40E+08	2.48E+07	3	2.95E+08	1.27E+08	3	1.06E+09	1.67E+08	3
Mannitol/Sorbitol	0.00E+00	0.00E+00	0	7.93E+06	2.43E+06	3	0.00E+00	0.00E+00	0	6.61E+06	2.57E+06	3	0.00E+00	0.00E+00	0	1.72E+05	8.91E+04	2	0.00E+00	0.00E+00	0	5.76E+05	2.13E+05	3
Methionine	1.73E+08	3.53E+07	3	2.31E+08	1.26E+07	3	1.63E+08	3.39E+07	3	1.98E+08	3.58E+07	3	6.75E+07	1.94E+07	3	8.07E+07	1.41E+07	3	3.31E+07	1.89E+07	3	9.81E+07	3.38E+07	3
Myristic acid	8.02E+07	9.78E+06	3	6.39E+07	9.31E+06	3	7.09E+07	1.24E+07	3	7.06E+07	3.39E+07	3	4.54E+06	9.12E+05	3	3.65E+06	7.72E+05	3	0.00E+00	0.00E+00	0	7.59E+06	2.16E+06	3
Myristoylcarnitine	5.82E+06	1.19E+06	3	2.20E+05	1.32E+05	2	1.75E+06	6.44E+05	3	1.66E+05	1.66E+05	1	0.00E+00	0.00E+00	0	0.00E+00	0.00E+00	0	0.00E+00	0.00E+00	0	0.00E+00	0.00E+00	0
N-AcetylAspartate	1.12E+07	2.06E+06	3	5.42E+06	2.76E+06	2	1.21E+07	2.65E+06	3	4.28E+06	2.78E+06	2	1.74E+06	1.60E+05	3	1.03E+06	5.34E+05	2	2.68E+05	2.68E+05	1	0.00E+00	0.00E+00	0
Oleic acid	1.77E+08	4.40E+07	3	3.15E+08	1.42E+08	3	1.97E+08	4.96E+07	3	4.12E+08	2.95E+08	3	1.38E+07	3.24E+06	3	1.94E+07	6.94E+06	3	0.00E+00	0.00E+00	0	3.98E+06	2.31E+06	2
Oleylcarnitine	1.77E+07	3.78E+06	3	6.76E+06	2.07E+06	3	7.17E+06	2.30E+06	3	3.18E+06	2.31E+06	3	3.70E+05	1.15E+05	3	3.46E+04	1.78E+04	2	0.00E+00	0.00E+00	0	0.00E+00	0.00E+00	0
Ornithine	1.22E+08	2.68E+07	3	2.12E+08	3.13E+07	3	1.36E+08	3.03E+07	3	1.87E+08	2.45E+07	3	4.11E+07	9.61E+06	3	5.68E+07	5.60E+06	3	8.87E+06	3.32E+06	3	4.15E+07	9.57E+06	3
Palmitic acid	4.41E+08	1.03E+08	3	4.68E+08	1.35E+08	3	3.83E+08	7.52E+07	3	5.14E+08	2.96E+08	3	3.81E+07	2.22E+06	3	4.15E+07	5.28E+06	3	0.00E+00	0.00E+00	0	2.32E+07	2.47E+06	3
Palmitoleic acid	3.10E+07	9.18E+06	3	5.86E+07	3.44E+07	3	3.46E+07	1.09E+07	3	8.19E+07	6.49E+07	3	0.00E+00	0.00E+00	0	8.14E+05	8.14E+05	1	0.00E+00	0.00E+00	0	0.00E+00	0.00E+00	0
Palmitoylcarnitine	1.48E+07	2.61E+06	3	4.81E+06	1.47E+06	3	6.92E+06	1.43E+06	3	2.23E+06	1.84E+06	3	3.40E+05	9.34E+04	3	1.76E+04	1.76E+04	1	0.00E+00	0.00E+00	0	0.00E+00	0.00E+00	0
Phenylalanine	3.56E+08	6.20E+07	3	7.32E+08	6.18E+07	3	3.76E+08	7.53E+07	3	6.64E+08	1.37E+08	3	1.40E+08	4.05E+07	3	2.64E+08	5.03E+07	3	9.35E+07	5.08E+07	3	5.59E+08	1.46E+08	3
Phosphoenolpyruvate	1.51E+07	6.03E+06	3	2.30E+06	1.00E+06	3	2.02E+07	5.92E+06	3	5.74E+06	1.17E+06	3	2.57E+06	5.14E+05	3	1.63E+06	3.59E+05	3	1.61E+06	1.19E+06	3	2.46E+06	1.39E+06	3
Picolinamide	2.19E+09	6.84E+08	3	1.47E+09	3.53E+08	3	2.00E+09	7.15E+08	3	1.15E+09	3.61E+08	3	6.87E+08	2.72E+08	3	3.33E+08	1.08E+08	3	1.87E+09	1.08E+09	3	3.70E+09	7.93E+08	3
Proline	4.58E+08	8.41E+07	3	1.86E+09	7.66E+07	3	5.52E+08	1.37E+08	3	1.56E+09	2.11E+08	3	1.34E+08	3.41E+07	3	4.89E+08	8.00E+07	3	1.13E+08	5.42E+07	3	5.63E+08	1.63E+08	3
Propionylcarnitine	1.99E+08	6.57E+07	3	8.34E+08	2.98E+08	3	2.16E+08	7.13E+07	3	7.18E+08	2.32E+08	3	5.46E+07	1.87E+07	3	1.42E+08	4.77E+07	3	2.47E+07	1.54E+07	3	3.56E+08	1.10E+08	3
Pyruvate	2.58E+08	9.42E+06	3	4.03E+08	3.77E+07	3	2.74E+08	3.29E+07	3	3.84E+08	6.56E+07	3	2.10E+08	2.76E+07	3	2.43E+08	3.13E+07	3	0.00E+00	0.00E+00	0	6.06E+07	1.30E+07	3
Riboflavin	1.49E+06	5.75E+05	3	2.53E+06	3.38E+05	3	8.09E+05	2.84E+05	3	1.40E+06	2.58E+05	3	2.35E+05	2.35E+05	1	0.00E+00	0.00E+00	0	3.42E+06	2.14E+06	3	1.61E+07	2.30E+06	3
Ribose/Ribulose-5Phosphate	1.41E+07	3.63E+06	3	2.95E+07	3.88E+06	3	2.03E+07	3.30E+06	3	3.35E+07	3.50E+06	3	5.75E+06	1.95E+06	3	7.99E+06	1.19E+06	3	0.00E+00	0.00E+00	0	1.79E+06	4.06E+05	3
S-Adenosyl-Homocysteine	2.57E+07	5.54E+06	3	1.00E+08	1.84E+07	3	1.84E+07	5.40E+06	3	7.53E+07	1.55E+07	3	2.76E+06	9.02E+05	3	1.90E+07	4.59E+06	3	6.37E+06	3.28E+06	3	7.35E+07	3.23E+06	3
S-Adenosyl-Methionine	1.87E+07	5.59E+06	3	6.45E+06	2.02E+06	3	1.89E+07	6.58E+06	3	4.68E+06	1.59E+06	3	4.44E+06	1.32E+06	3	9.95E+05	5.90E+05	3	4.79E+06	2.00E+06	3	5.64E+06	7.96E+05	3
Sedoheptulose 7-phosphate	2.91E+07	5.93E+06	3	7.29E+07	9.01E+06	3	3.22E+07	6.20E+06	3	6.83E+07	7.43E+06	3	6.76E+06	1.94E+06	3	1.95E+07	3.12E+06	3	6.52E+04	6.52E+04	1	2.63E+06	9.52E+05	3
Serine	1.87E+07	4.64E+06	3	6.41E+06	9.03E+05	3	2.08E+07	6.33E+06	3	4.83E+06	1.30E+06	3	4.53E+06	1.04E+06	3	1.30E+06	2.90E+05	3	2.96E+06	9.05E+05	3	1.38E+06	3.63E+05	3
Serotonin	1.65E+06	1.37E+06	3	1.95E+05	1.06E+05	2	2.64E+06	4.97E+05	3	4.06E+05	1.63E+05	3	0.00E+00	0.00E+00	0	5.49E+04	2.93E+04	2	6.57E+06	2.76E+06	3	6.65E+06	9.41E+05	3
Stearic acid	2.17E+08	5.76E+07	3	1.56E+08	1.26E+07	3	1.73E+08	3.99E+07	3	1.52E+08	6.26E+07	3	1.37E+07	1.00E+06	3	1.58E+07	8.07E+05	3	9.83E+05	9.83E+05	1	5.43E+06	2.81E+06	2
Stearoycarnitine	5.34E+06	1.11E+06	3	3.71E+06	1.38E+06	3	3.78E+06	8.66E+05	3	2.41E+06	1.75E+06	3	1.24E+05	4.57E+04	3	1.28E+04	1.28E+04	1	0.00E+00	0.00E+00	0	0.00E+00	0.00E+00	0
Succinate	2.91E+08	7.15E+07	3	1.72E+09	1.80E+08	3	2.76E+08	5.46E+07	3	1.43E+09	1.27E+08	3	9.50E+07	1.79E+07	3	4.16E+08	2.61E+07	3	4.01E+07	1.93E+07	3	1.49E+08	1.23E+07	3
Succinic glutathione	8.97E+05	3.28E+05	3	4.50E+05	1.56E+05	3	8.43E+05	2.63E+05	3	3.99E+05	1.20E+05	3	3.40E+04	2.35E+04	2	1.32E+04	1.32E+04	1	1.27E+04	1.27E+04	1	8.75E+04	4.40E+03	3
Sucrose	4.40E+10	4.40E+09	3	5.26E+10	7.49E+09	3	5.10E+10	2.45E+09	3	4.54E+10	3.68E+09	3	4.37E+10	3.63E+09	3	4.01E+10	2.95E+09	3	2.19E+10	5.65E+09	3	2.80E+10	2.59E+09	3
Taurine	7.43E+09	1.29E+09	3	7.67E+09	8.63E+08	3	7.88E+09	1.54E+09	3	7.07E+09	3.51E+08	3	2.61E+09	6.31E+08	3	2.42E+09	2.24E+08	3	2.94E+09	1.14E+09	3	4.36E+09	7.41E+08	3
Threonine	1.61E+08	3.95E+07	3	2.56E+08	3.04E+06	3	1.72E+08	4.25E+07	3	2.24E+08	4.22E+07	3	5.53E+07	1.35E+07	3	7.10E+07	1.39E+07	3	2.48E+07	1.17E+07	3	6.16E+07	1.77E+07	3
Tryptophan	4.75E+07	1.33E+07	3	8.01E+07	9.09E+06	3	3.94E+07	1.06E+07	3	7.81E+07	1.79E+07	3	1.49E+07	4.57E+06	3	2.32E+07	4.73E+06	3	1.98E+07	9.11E+06	3	1.16E+08	2.22E+07	3
Tyrosine	5.02E+07	7.37E+06	3	1.42E+08	1.46E+07	3	4.76E+07	8.99E+06	3	1.32E+08	2.66E+07	3	8.74E+06	3.21E+06	3	3.08E+07	7.39E+06	3	1.10E+07	3.67E+06	3	9.75E+07	2.42E+07	3
UDP	2.54E+06	7.89E+05	3	1.94E+04	1.94E+04	1	1.97E+06	5.65E+05	3	0.00E+00	0.00E+00	0	3.12E+05	8.37E+04	3	0.00E+00	0.00E+00	0	7.60E+04	7.60E+04	1	0.00E+00	0.00E+00	0
UMP	1.34E+07	3.26E+06	3	4.34E+06	7.67E+05	3	1.13E+07	1.94E+06	3	3.48E+06	6.67E+05	3	4.60E+06	1.06E+06	3	8.82E+05	2.82E+05	3	3.58E+06	1.71E+06	3	1.29E+06	1.12E+05	3
Urea	5.85E+07	1.40E+07	3	3.89E+07	5.21E+06	3	5.77E+07	1.16E+07	3	3.78E+07	7.21E+06	3	2.64E+07	7.68E+06	3	1.35E+07	2.34E+06	3	2.32E+07	1.10E+07	3	1.37E+07	6.03E+06	3
UTP	4.38E+05	2.04E+05	3	0.00E+00	0.00E+00	0	4.31E+05	2.06E+05	3	0.00E+00	0.00E+00	0	2.60E+03	2.60E+03	1	0.00E+00	0.00E+00	0	0.00E+00	0.00E+00	0	0.00E+00	0.00E+00	0
Xanthosine	0.00E+00	0.00E+00	0	1.30E+08	1.96E+07	3	0.00E+00	0.00E+00	0	1.06E+08	1.26E+07	3	0.00E+00	0.00E+00	0	2.49E+07	2.25E+06	3	0.00E+00	0.00E+00	0	5.87E+07	6.62E+06	3

Fig. A.6 Control and 30 min WI liver metabolite ion intensities, ZIC-pHILIC column. 2 of 2.

Metabolite	Hom	SEM	n	Hom + WI	SEM	n	Snt	SEM	n	Snt + WI	SEM	n	Cyto	SEM	n	Cyto + WI	SEM	n	Mito	SEM	n	Mito + WI	SEM	n
2-HG	3.52E+07	3.52E+06	3	9.19E+07	2.03E+07	3	5.14E+07	1.10E+07	3	1.36E+08	1.67E+07	3	1.42E+07	1.42E+07	1	4.48E+07	1.13E+07	3	2.67E+07	1.34E+07	2	8.37E+07	5.33E+07	2
3-hydroxybutyrate	7.61E+07	4.16E+07	2	2.07E+08	2.07E+07	3	1.20E+08	1.96E+07	3	2.78E+08	3.42E+07	3	9.53E+06	9.53E+06	1	1.38E+07	1.38E+07	1	2.02E+07	1.32E+07	2	1.12E+07	1.12E+07	1
Acetylcarnitine	3.94E+09	2.17E+08	3	1.28E+09	1.39E+08	3	4.76E+09	1.05E+08	3	1.93E+09	5.13E+08	3	1.84E+09	2.62E+08	3	6.51E+08	9.89E+07	3	1.09E+09	4.64E+08	3	1.59E+09	3.20E+08	3
AcetylCholine	2.84E+08	2.20E+07	3	4.73E+08	7.96E+07	3	3.81E+08	9.85E+07	3	5.48E+08	1.79E+08	3	1.16E+08	3.49E+07	3	1.74E+08	3.84E+07	3	4.26E+07	1.82E+07	3	1.48E+08	6.01E+07	3
Adenine	1.58E+08	3.28E+07	3	6.73E+08	1.19E+08	3	1.38E+08	5.08E+07	3	7.08E+08	1.69E+08	3	2.58E+07	7.69E+06	3	2.98E+08	1.18E+07	3	2.58E+07	6.45E+06	3	1.39E+08	2.80E+07	3
Adenosine	3.44E+07	1.35E+07	3	2.49E+08	8.29E+07	3	1.72E+07	1.07E+07	2	6.64E+07	8.45E+06	3	2.15E+05	2.15E+05	1	3.98E+07	1.91E+07	3	3.16E+07	1.78E+07	3	2.52E+08	3.64E+07	3
Alanine	3.81E+09	2.89E+08	3	1.82E+10	1.67E+09	3	5.45E+09	2.25E+09	3	1.95E+10	4.34E+09	3	1.50E+09	6.54E+08	3	7.23E+09	4.08E+08	3	2.94E+08	1.24E+08	3	1.97E+09	7.14E+08	3
Allantoin	8.41E+07	2.62E+07	3	2.45E+08	2.64E+07	3	1.25E+08	6.23E+07	3	3.03E+08	1.02E+08	3	1.85E+07	1.21E+07	3	9.17E+07	6.57E+06	3	2.05E+07	9.29E+06	3	1.71E+08	6.33E+07	3
AMP	1.27E+09	2.63E+08	3	2.50E+09	3.96E+08	3	1.42E+09	4.86E+08	3	2.66E+09	7.64E+08	3	5.79E+08	1.36E+08	3	8.06E+08	7.87E+07	3	4.43E+08	1.69E+08	3	6.94E+08	1.84E+08	3
Arginine	3.46E+07	1.58E+06	3	4.65E+07	8.95E+06	3	3.55E+07	1.81E+07	3	4.08E+07	1.83E+07	3	1.79E+06	1.07E+06	3	0.00E+00	0.00E+00	0	5.62E+06	3.73E+06	2	3.83E+06	1.82E+06	3
Ascorbic acid	2.34E+08	1.64E+08	2	0.00E+00	0.00E+00	0	9.18E+08	3.22E+08	3	0.00E+00	0.00E+00	0	2.68E+08	1.77E+08	3	3.70E+07	2.11E+07	2	3.36E+06	1.68E+06	2	0.00E+00	0.00E+00	0
Asparagine	5.17E+07	2.03E+07	3	1.18E+08	3.91E+07	3	6.51E+07	2.71E+07	3	1.33E+08	6.16E+07	3	1.37E+07	5.69E+06	3	6.48E+07	1.05E+07	3	8.47E+06	3.51E+06	3	4.74E+07	1.75E+07	3
Aspartate	7.54E+08	3.02E+08	3	4.78E+08	6.94E+07	3	8.19E+08	2.98E+08	3	5.02E+08	2.23E+08	3	2.67E+08	1.78E+08	3	1.76E+08	7.92E+06	3	1.31E+08	3.63E+07	3	2.18E+08	4.42E+07	3
Betaine	9.67E+09	4.41E+09	3	2.88E+10	3.36E+09	3	1.24E+10	6.45E+09	3	2.54E+10	1.29E+10	3	4.12E+09	3.71E+09	3	1.48E+10	2.98E+09	3	1.41E+09	1.27E+09	3	9.79E+09	5.71E+09	3
ButyrylCarnitine	3.50E+08	7.87E+07	3	3.45E+08	7.11E+07	3	6.40E+08	3.25E+08	3	3.75E+08	5.53E+07	3	1.70E+08	5.71E+07	3	8.63E+07	1.29E+07	3	2.56E+07	1.99E+07	3	3.59E+07	6.65E+06	3
Carnitine	4.94E+09	1.49E+09	3	8.15E+09	8.50E+08	3	6.22E+09	1.45E+09	3	1.01E+10	8.21E+08	3	2.13E+09	5.36E+08	3	3.20E+09	5.42E+08	3	1.42E+09	8.42E+08	3	2.45E+09	3.26E+08	3
Choline	2.72E+09	5.73E+08	3	8.23E+09	1.64E+09	3	3.52E+09	1.21E+09	3	9.93E+09	2.33E+09	3	1.14E+09	2.89E+08	3	2.96E+09	4.00E+08	3	5.22E+08	3.60E+08	3	2.02E+09	6.41E+08	3
Citrulline	1.44E+08	5.69E+07	3	8.85E+07	1.55E+07	3	2.15E+08	1.24E+08	3	9.38E+07	2.91E+07	3	4.03E+07	2.28E+07	3	2.94E+07	2.71E+06	3	2.07E+08	9.17E+07	3	4.27E+07	1.44E+07	3
Creatinine	3.34E+08	8.44E+06	3	2.67E+08	6.09E+07	3	4.07E+08	1.34E+08	3	2.24E+08	4.30E+07	3	1.45E+08	2.74E+07	3	8.22E+07	1.75E+07	3	5.16E+07	8.58E+06	3	6.93E+07	1.80E+07	3
Cysteine	1.29E+08	3.24E+07	3	5.77E+08	1.08E+08	3	2.16E+08	9.75E+07	3	6.63E+08	3.11E+08	3	3.93E+07	1.88E+07	3	2.71E+08	3.55E+07	3	1.14E+07	6.38E+06	3	3.32E+07	1.44E+07	3
Cytidine	1.47E+07	1.59E+06	3	6.45E+06	2.26E+06	3	2.29E+07	8.99E+06	3	7.28E+06	1.83E+06	3	2.33E+06	5.86E+05	3	4.57E+05	4.89E+04	3	1.11E+06	7.67E+05	3	1.04E+06	2.45E+05	3
Dihydrothymine	1.42E+07	6.65E+06	3	1.28E+07	6.65E+06	3	1.51E+07	6.79E+06	3	2.01E+07	9.26E+06	3	4.22E+06	2.17E+06	3	9.99E+06	2.27E+06	3	1.13E+06	6.23E+05	2	2.81E+06	1.27E+06	3
Fructose	4.19E+09	2.44E+09	2	1.29E+10	2.36E+09	3	9.14E+09	4.62E+09	3	1.19E+10	6.00E+09	2	5.70E+09	5.54E+09	3	1.43E+10	1.12E+09	3	2.77E+08	2.77E+08	1	6.93E+08	2.10E+08	3
Fumarate	1.00E+08	3.39E+07	3	4.41E+07	8.06E+06	3	1.11E+08	3.21E+07	3	7.20E+07	2.66E+07	3	3.15E+07	5.65E+06	3	3.49E+07	8.27E+06	3	1.08E+07	9.36E+05	3	2.14E+07	8.13E+06	3
GABA	2.12E+07	1.05E+07	3	2.69E+07	3.36E+06	3	2.22E+07	1.07E+07	3	2.01E+07	1.03E+07	3	6.12E+06	5.70E+06	3	9.42E+06	1.68E+06	3	7.16E+06	4.62E+06	3	8.24E+06	4.43E+06	3
Glucose	1.65E+10	2.06E+09	3	2.24E+10	4.03E+09	3	1.76E+10	1.30E+09	3	3.40E+10	4.99E+09	3	1.69E+10	3.11E+09	3	1.98E+10	1.52E+09	3	6.73E+09	1.09E+09	3	1.41E+10	2.07E+09	3
Glutamate	1.20E+10	2.70E+09	3	1.20E+10	2.12E+09	3	1.49E+10	5.04E+09	3	1.12E+10	3.97E+09	3	4.05E+09	2.00E+09	3	3.95E+09	8.46E+08	3	3.42E+09	1.50E+09	3	4.07E+09	1.39E+09	3
Glutamine	2.03E+10	2.28E+09	3	2.42E+10	3.06E+09	3	2.70E+10	7.68E+09	3	2.67E+10	8.25E+09	3	7.56E+09	1.65E+09	3	9.05E+09	1.04E+09	3	1.98E+09	6.05E+08	3	3.61E+09	1.36E+09	3
Glycerylphosphorylcholine	7.83E+08	6.31E+07	3	5.07E+08	1.87E+08	3	9.39E+08	8.17E+07	3	8.35E+08	1.85E+08	3	3.11E+08	9.11E+07	3	1.40E+08	2.88E+07	3	9.77E+07	5.02E+07	3	1.40E+08	4.32E+07	3
Glycine	2.30E+09	2.42E+08	3	4.28E+09	4.77E+08	3	3.41E+09	1.31E+09	3	4.55E+09	1.33E+09	3	8.61E+08	3.36E+08	3	1.62E+09	6.80E+07	3	1.84E+08	6.51E+07	3	4.97E+08	1.86E+08	3
GMP	3.75E+07	1.92E+07	2	1.15E+08	3.57E+07	3	4.79E+07	1.78E+07	3	1.57E+08	4.04E+07	3	3.45E+06	3.45E+06	1	3.03E+07	4.05E+06	3	2.78E+05	1.64E+05	2	6.83E+06	1.48E+06	3

Fig. A.7 Control and 30 min WI liver metabolite ion intensities, ZIC-HILIC column. 1 of 2.

Metabolite	Hom	SEM	n	Hom + WI	SEM	n	Snt	SEM	n	Snt + WI	SEM	n	Cyto	SEM	n	Cyto + WI	SEM	n	Mito	SEM	n	Mito + WI	SEM	n
GSH	1.34E+10	3.65E+09	3	1.86E+10	1.25E+09	3	1.82E+10	7.08E+09	3	1.76E+10	6.78E+09	3	4.85E+09	2.95E+09	3	8.39E+09	3.41E+07	3	1.96E+09	1.05E+09	3	5.59E+09	2.12E+09	3
GSSG	4.79E+06	3.81E+06	3	7.35E+06	4.15E+06	3	1.76E+06	9.87E+05	2	1.47E+07	9.46E+06	3	0.00E+00	0.00E+00	0	1.97E+05	1.12E+05	2	3.52E+06	3.42E+06	2	7.76E+06	8.36E+05	3
Histidine	4.32E+08	1.70E+07	3	5.51E+08	4.48E+07	3	5.94E+08	1.33E+08	3	7.05E+08	1.33E+08	3	1.63E+08	3.36E+07	3	2.06E+08	8.23E+06	3	1.32E+08	5.33E+07	3	2.47E+08	4.92E+07	3
Homocysteine	3.42E+06	2.54E+06	2	1.76E+06	8.83E+05	2	1.01E+07	5.19E+06	3	9.95E+06	3.88E+06	3	6.42E+06	3.87E+06	3	9.05E+06	3.27E+06	3	1.53E+05	1.53E+05	1	0.00E+00	0.00E+00	0
Hypotaurine	3.03E+07	1.72E+07	3	2.95E+07	2.17E+06	3	3.06E+07	1.67E+07	3	3.06E+07	1.51E+07	3	1.10E+07	9.98E+06	2	1.54E+07	1.88E+06	3	2.83E+06	1.61E+06	3	1.42E+07	6.70E+06	3
Hypoxanthine	2.18E+07	4.56E+06	3	2.59E+09	4.12E+07	3	5.68E+06	3.98E+06	2	2.59E+09	8.05E+08	3	0.00E+00	0.00E+00	0	9.13E+08	1.43E+07	3	2.55E+06	1.30E+06	2	1.32E+09	4.59E+08	3
Inosine	1.56E+07	5.62E+06	3	2.27E+09	1.25E+08	3	2.19E+06	2.19E+06	1	2.49E+09	7.42E+08	3	0.00E+00	0.00E+00	0	7.10E+08	3.53E+07	3	4.97E+05	2.70E+05	2	8.35E+08	2.28E+08	3
Lactate	8.49E+08	2.57E+07	3	1.46E+10	1.94E+09	3	1.15E+09	3.36E+08	3	1.50E+10	2.19E+09	3	3.68E+08	9.25E+07	3	4.55E+09	2.30E+08	3	2.25E+08	7.48E+07	3	4.60E+09	6.20E+08	3
Leucine	1.20E+09	1.01E+08	3	5.65E+09	1.16E+09	3	2.63E+09	1.57E+09	3	5.35E+09	2.25E+09	3	5.30E+08	1.25E+08	3	1.30E+09	2.73E+08	3	1.78E+08	8.63E+07	3	1.15E+09	7.37E+08	3
Lysine	1.52E+09	1.56E+08	3	2.53E+09	4.33E+08	3	2.39E+09	1.13E+09	3	3.26E+09	1.18E+09	3	4.69E+08	1.28E+08	3	6.11E+08	8.21E+07	3	1.39E+08	8.00E+07	3	3.95E+08	1.79E+08	3
Methionine	2.17E+08	4.81E+07	3	4.81E+08	1.45E+08	3	2.67E+08	5.27E+07	3	4.31E+08	6.42E+07	3	9.02E+07	2.53E+07	3	1.35E+08	2.76E+07	3	3.78E+07	2.22E+07	3	7.44E+07	2.54E+07	3
N-AcetylAspartate	5.91E+07	1.36E+07	3	6.66E+07	4.31E+06	3	6.54E+07	1.92E+07	3	5.69E+07	1.66E+07	3	1.53E+07	5.22E+06	3	2.26E+07	1.50E+06	3	2.13E+07	1.19E+06	3	2.34E+07	2.45E+06	3
Nicotinamide	7.12E+09	1.15E+09	3	8.51E+09	9.47E+08	3	9.09E+09	3.18E+09	3	1.04E+10	2.47E+09	3	2.51E+09	6.70E+08	3	3.20E+09	2.49E+08	3	2.03E+09	7.96E+08	3	5.06E+09	2.11E+09	3
Ornithine	9.29E+08	1.17E+08	3	1.99E+09	1.81E+08	3	1.26E+09	5.03E+08	3	2.35E+09	7.11E+08	3	3.12E+08	1.31E+08	3	5.38E+08	5.86E+07	3	4.93E+07	2.47E+07	2	3.31E+08	1.47E+08	3
Pantothenic acid	5.17E+06	1.01E+06	3	4.86E+07	1.38E+07	3	1.36E+07	9.32E+06	3	5.27E+07	1.24E+07	3	1.39E+06	6.98E+05	2	2.39E+07	1.06E+07	3	5.04E+04	5.04E+04	1	1.09E+07	3.27E+06	3
Phenylalanine	6.53E+08	1.41E+08	3	2.17E+09	2.43E+08	3	9.97E+08	5.80E+08	3	2.30E+09	6.87E+08	3	2.18E+08	5.55E+07	3	5.38E+08	8.35E+07	3	1.37E+08	6.03E+07	3	1.43E+09	6.45E+08	3
Proline	5.62E+08	5.50E+07	3	2.42E+09	7.86E+08	3	6.95E+08	1.86E+08	3	2.90E+09	1.04E+09	3	2.56E+08	8.02E+07	3	1.25E+09	2.95E+08	3	7.20E+07	2.87E+07	3	3.09E+08	1.37E+08	3
Propionylcarnitine	1.60E+08	2.50E+07	3	1.00E+09	2.47E+08	3	2.39E+08	1.04E+08	3	1.04E+09	2.42E+08	3	5.86E+07	2.44E+07	3	2.72E+08	6.50E+07	3	1.89E+07	1.29E+07	3	4.28E+08	1.16E+08	3
Pyroglutamic acid	6.28E+08	1.09E+08	3	1.17E+09	4.84E+07	3	9.46E+08	3.57E+08	3	1.45E+09	5.11E+08	3	3.02E+08	9.04E+07	3	4.62E+08	2.55E+07	3	4.09E+07	1.66E+07	3	1.45E+08	5.19E+07	3
Serine	8.62E+08	1.21E+08	3	5.36E+08	1.06E+08	3	1.35E+09	5.68E+08	3	5.35E+08	1.85E+08	3	3.87E+08	2.03E+08	3	2.04E+08	2.30E+07	3	9.35E+07	4.08E+07	3	1.73E+08	1.20E+08	3
Succinate	4.67E+08	1.24E+08	3	1.92E+09	1.57E+08	3	3.38E+08	4.37E+07	3	1.94E+09	9.53E+07	3	1.45E+08	4.74E+07	3	5.13E+08	1.93E+07	3	1.36E+08	4.33E+07	3	2.79E+08	4.50E+07	3
Sucrose	6.28E+09	3.01E+09	3	7.33E+09	2.68E+09	3	7.31E+09	2.99E+09	3	9.65E+09	2.46E+09	3	6.01E+09	6.71E+08	3	3.54E+09	1.63E+09	3	2.58E+09	1.51E+09	3	4.54E+09	1.31E+09	3
Taurine	3.72E+09	5.01E+08	3	4.20E+09	3.00E+08	3	3.69E+09	1.07E+09	3	4.02E+09	1.04E+09	3	1.96E+09	6.47E+08	3	3.28E+09	1.73E+08	3	2.50E+09	8.56E+08	3	3.56E+09	8.61E+08	3
Threonine	5.89E+08	8.72E+07	3	1.23E+09	3.41E+08	3	8.01E+08	2.99E+08	3	1.34E+09	5.58E+08	3	2.30E+08	1.06E+08	3	4.80E+08	1.10E+08	3	5.75E+07	1.80E+07	3	2.04E+08	1.14E+08	3
Tryptophan	9.03E+07	2.87E+06	3	3.80E+08	9.33E+07	3	1.59E+08	7.84E+07	3	3.34E+08	1.09E+08	3	2.65E+07	8.36E+06	3	9.49E+07	1.53E+07	3	1.93E+07	8.32E+06	3	1.86E+08	8.81E+07	3
Tyrosine	1.84E+08	4.03E+07	3	6.77E+08	2.13E+08	3	2.05E+08	6.73E+07	3	8.41E+08	3.12E+08	3	5.33E+07	2.63E+07	3	2.62E+08	4.39E+07	3	3.71E+07	1.72E+07	3	3.03E+08	1.18E+08	3
Uracil	0.00E+00	0.00E+00	0	1.32E+08	2.39E+07	3	0.00E+00	0.00E+00	0	1.65E+08	7.71E+07	3	0.00E+00	0.00E+00	0	4.57E+07	1.06E+07	3	0.00E+00	0.00E+00	0	1.22E+07	7.17E+06	3
Urea	4.38E+09	4.27E+08	3	6.39E+09	4.37E+08	3	5.71E+09	1.77E+09	3	7.11E+09	2.03E+09	3	1.99E+09	9.88E+08	3	2.88E+09	1.52E+08	3	5.09E+08	1.89E+08	3	9.83E+08	3.93E+08	3
Uric acid	5.85E+05	3.51E+05	3	5.84E+07	1.55E+06	3	9.83E+04	5.01E+04	2	4.48E+07	5.95E+06	3	0.00E+00	0.00E+00	0	1.21E+07	4.04E+06	3	3.73E+04	3.73E+04	1	9.55E+07	1.94E+07	3
Uridine	1.17E+06	1.17E+06	1	1.99E+08	4.72E+07	3	1.96E+06	9.83E+05	2	2.42E+08	4.21E+07	3	0.00E+00	0.00E+00	0	5.91E+07	1.18E+07	3	0.00E+00	0.00E+00	0	1.20E+08	4.06E+07	3
Valine	1.50E+10	1.81E+09	3	2.89E+10	3.50E+09	3	1.80E+10	2.94E+09	3	3.75E+10	5.31E+09	3	6.83E+09	2.62E+09	3	1.49E+10	2.97E+09	3	4.76E+09	1.62E+09	3	1.45E+10	3.02E+09	3
Xanthine	4.06E+06	4.11E+05	3	5.17E+08	8.41E+06	3	9.91E+05	6.11E+05	2	5.17E+08	5.79E+07	3	3.53E+04	3.53E+04	1	1.26E+08	6.76E+06	3	2.60E+06	2.17E+06	2	9.36E+08	2.93E+08	3
Xanthosine	0.00E+00	0.00E+00	0	6.47E+08	2.94E+07	3	1.43E+05	1.43E+05	1	6.73E+08	2.31E+08	3	0.00E+00	0.00E+00	0	2.06E+08	7.19E+06	3	0.00E+00	0.00E+00	0	2.74E+08	8.26E+07	3

Fig. A.8 Control and 30 min WI liver metabolite ion intensities, ZIC-HILIC column. 2 of 2.

Appendix B

LC-MS data tables - taurine-normalised ion intensities

Metabolite	Hom	SEM	n	Hom + WI	SEM	n	Snt	SEM	n	Snt + WI	SEM	n	Cyto	SEM	n	Cyto + WI	SEM	n	Mito	SEM	n	Mito + WI	SEM	n
2-HG	7.77E-02	3.57E-02	3	5.61E-02	3.73E-02	2	6.45E-02	3.01E-02	3	1.73E-02	1.73E-02	1	8.73E-02	3.99E-02	3	5.13E-02	2.37E-02	3	9.29E-02	9.29E-02	1	0.00E+00	0.00E+00	0
3-Phosphoglycerate	1.37E-01	5.25E-02	6	1.11E-02	7.00E-03	2	3.69E-01	1.08E-01	6	2.75E-02	1.00E-02	4	6.66E-01	1.53E-01	6	1.00E-01	1.10E-02	6	0.00E+00	0.00E+00	0	0.00E+00	0.00E+00	0
Acetylcarnitine	9.68E+01	5.55E+00	6	3.30E+01	2.41E+00	6	1.20E+02	6.63E+00	6	4.82E+01	1.82E+00	6	1.01E+02	5.34E+00	6	2.93E+01	1.30E+00	6	5.85E+01	6.02E+00	6	8.21E+01	8.26E+00	6
AcetylCholine	5.03E+00	6.30E-01	6	3.99E+00	1.45E-01	6	5.31E+00	6.04E-01	6	3.98E+00	1.97E-01	6	5.02E+00	5.34E-01	6	4.02E+00	1.73E-01	6	3.04E+00	6.58E-01	6	3.83E+00	2.33E-01	6
Aconitate	6.29E-02	1.41E-02	6	3.52E-02	6.69E-03	6	7.07E-02	6.95E-03	6	6.98E-02	9.88E-03	6	2.79E-02	5.97E-03	6	2.69E-02	5.57E-03	6	2.68E-01	8.87E-02	6	5.15E-01	1.81E-01	6
Adenine	5.36E-01	4.15E-02	6	6.51E+00	3.83E-01	6	5.86E-01	5.64E-02	6	6.18E+00	2.87E-01	6	4.29E-01	4.11E-02	6	6.68E+00	3.55E-01	6	2.94E+00	1.27E+00	6	2.86E+00	5.03E-01	6
Adenosine	3.42E+00	3.59E-01	6	2.18E+01	9.98E-01	6	6.24E+00	5.03E-01	6	2.56E+01	1.23E+00	6	3.04E+00	4.50E-01	6	2.18E+01	9.55E-01	6	8.33E+00	5.60E+00	6	1.12E+01	1.50E+00	6
ADP	8.58E-01	4.48E-02	6	2.07E-01	2.72E-02	6	6.50E-01	3.04E-02	6	2.02E-01	2.17E-02	6	7.33E-01	6.34E-02	6	1.41E-01	1.98E-02	6	6.16E-01	1.75E-01	6	6.38E-01	9.70E-02	6
aKG	1.80E-02	1.14E-02	2	4.12E-02	1.56E-02	4	2.34E-02	1.19E-02	3	2.36E-01	6.63E-02	6	8.80E-03	8.80E-03	1	3.98E-02	1.49E-02	4	1.67E-01	9.01E-02	3	1.74E-01	8.14E-02	5
Alanine	2.82E+00	1.58E-01	6	4.30E+00	1.93E-01	6	2.92E+00	1.62E-01	6	4.41E+00	1.33E-01	6	2.87E+00	1.84E-01	6	4.29E+00	1.68E-01	6	3.77E+00	4.98E-01	6	5.01E+00	2.19E-01	6
AMP	2.28E+00	1.78E-01	6	1.13E+00	9.86E-02	6	3.24E+00	2.34E-01	6	1.18E+00	9.00E-02	6	2.82E+00	2.14E-01	6	1.12E+00	9.24E-02	6	2.68E+00	2.34E-01	6	1.75E+00	1.16E-01	6
Arginine	6.35E-01	3.29E-02	6	8.49E-01	3.49E-02	6	6.57E-01	5.44E-02	6	8.18E-01	5.11E-02	6	5.71E-01	3.96E-02	6	8.92E-01	3.31E-02	6	1.26E+00	2.97E-01	6	1.67E+00	9.76E-01	6
Asparagine	1.94E-01	1.62E-02	6	1.69E-01	7.38E-03	6	1.90E-01	1.74E-02	6	1.78E-01	8.04E-03	6	1.76E-01	1.43E-02	6	1.45E-01	8.91E-03	6	5.88E-01	1.54E-01	6	3.58E-01	2.42E-02	6
Aspartate	2.92E+00	4.02E-01	6	1.86E+00	1.73E-01	6	3.21E+00	3.77E-01	6	1.82E+00	1.66E-01	6	3.02E+00	4.12E-01	6	1.82E+00	1.60E-01	6	1.22E+00	3.11E-01	6	8.82E-01	6.87E-02	6
Betaine	1.23E+01	2.58E+00	6	1.03E+01	6.46E-01	6	1.32E+01	2.63E+00	6	9.19E+00	7.16E-01	6	1.26E+01	2.40E+00	6	9.84E+00	5.39E-01	6	4.14E+01	3.41E+01	6	2.31E+01	1.63E+01	6
Butyrylcarnitine	2.49E+00	2.06E-01	6	1.80E+00	1.10E-01	6	2.67E+00	1.65E-01	6	1.61E+00	1.54E-01	6	2.66E+00	1.72E-01	6	1.86E+00	1.07E-01	6	1.05E+00	7.06E-02	6	5.97E-01	9.66E-02	6
Carbamoyl phosphate	3.80E+00	9.08E-02	6	3.85E+00	1.08E-01	6	4.02E+00	1.17E-01	6	3.73E+00	1.62E-01	6	3.84E+00	1.97E-01	6	3.87E+00	5.68E-02	6	1.58E+00	4.13E-01	6	1.37E+00	1.54E-01	6
Carnitine	5.41E+01	7.89E+00	6	1.61E+02	5.04E+00	6	5.57E+01	7.76E+00	6	1.42E+02	6.72E+00	6	5.62E+01	7.21E+00	6	1.67E+02	3.37E+00	6	1.57E+01	4.11E+00	6	6.16E+01	2.88E+00	6
CDP	4.01E-03	6.80E-04	6	6.68E-05	6.68E-05	1	1.78E-03	4.94E-04	5	0.00E+00	0.00E+00	0	2.76E-03	5.69E-04	6	0.00E+00	0.00E+00	0	0.00E+00	0.00E+00	0	0.00E+00	0.00E+00	0
Choline	1.42E+01	2.95E+00	6	2.72E+01	2.02E+00	6	1.51E+01	2.98E+00	6	2.54E+01	2.04E+00	6	1.45E+01	2.82E+00	6	2.69E+01	2.22E+00	6	5.91E+01	4.87E+01	6	2.62E+01	9.49E+00	6
Citrate	6.79E-01	1.48E-01	6	3.97E-01	7.81E-02	6	6.75E-01	8.06E-02	6	7.29E-01	8.40E-02	6	2.92E-01	3.27E-02	6	1.77E-01	4.05E-02	5	2.09E+00	1.33E+00	5	2.49E+00	5.40E-01	6
Citrulline	8.72E-01	5.30E-02	6	8.28E-01	4.48E-02	6	9.83E-01	1.02E-01	6	8.13E-01	4.83E-02	6	7.91E-01	2.55E-02	6	8.10E-01	7.65E-02	6	2.16E+00	1.25E-01	6	1.55E+00	4.08E-02	6
CMP	1.77E-02	1.81E-03	6	8.79E-03	1.28E-03	6	2.81E-02	2.71E-03	6	1.23E-02	6.95E-04	6	2.45E-02	2.42E-03	6	9.58E-03	8.49E-04	6	1.30E-02	2.22E-03	6	1.23E-02	1.41E-03	6
Creatine	5.53E+02	2.04E+01	6	5.35E+02	1.03E+01	6	5.57E+02	1.27E+01	6	5.32E+02	1.03E+01	6	5.46E+02	9.06E+00	6	5.26E+02	6.96E+00	6	3.91E+02	4.12E+01	6	5.25E+02	1.62E+01	6
Creatinine	7.55E+01	2.84E+00	6	7.50E+01	3.31E+00	6	8.35E+01	5.39E+00	6	6.75E+01	3.58E+00	6	8.59E+01	2.50E+00	6	7.96E+01	4.58E+00	6	3.37E+01	8.12E+00	6	4.47E+01	8.44E+00	6
Cysteic acid	8.86E+00	1.64E-01	6	8.74E+00	1.00E-01	6	9.05E+00	1.41E-01	6	8.66E+00	2.09E-01	6	9.09E+00	1.14E-01	6	9.02E+00	1.74E-01	6	6.83E+00	1.96E-01	6	7.78E+00	1.78E-01	6
Cytidine	2.32E-01	2.22E-02	6	5.43E-01	4.63E-02	6	2.73E-01	1.64E-02	6	5.41E-01	4.50E-02	6	2.41E-01	2.16E-02	6	5.26E-01	4.10E-02	6	1.10E-01	4.42E-02	6	4.89E-01	4.45E-02	6
Ethanolamine	2.00E-01	2.23E-02	6	3.10E-01	1.38E-02	6	2.11E-01	2.84E-02	6	2.79E-01	7.50E-03	6	1.94E-01	1.96E-02	6	3.19E-01	1.55E-02	6	2.35E-01	6.61E-02	6	2.16E-01	6.97E-02	6
Fructose	1.41E+01	1.23E+00	6	1.27E+01	5.05E-01	6	1.45E+01	1.09E+00	6	1.36E+01	1.03E+00	6	1.43E+01	1.33E+00	6	1.34E+01	1.17E+00	6	2.28E+01	7.88E+00	6	1.09E+01	3.39E+00	6
Fructose 6-Phosphate	2.76E-02	6.40E-03	6	8.15E-03	1.81E-03	6	1.22E-02	3.96E-03	6	4.41E-03	4.94E-04	6	6.00E-03	2.49E-03	5	4.51E-03	3.40E-04	6	4.54E-04	4.54E-04	1	2.21E-04	2.21E-04	1
Fumarate	2.05E-01	1.57E-02	6	2.32E-01	2.91E-02	6	2.05E-01	2.79E-02	6	2.52E-01	2.33E-02	6	1.93E-01	1.47E-02	6	2.42E-01	1.94E-02	6	1.00E-01	7.32E-02	3	5.20E-02	2.36E-02	3
Glucose	8.86E+00	8.66E-01	6	7.65E+00	3.72E-01	6	8.81E+00	7.00E-01	6	7.19E+00	6.41E-01	6	9.48E+00	7.37E-01	6	7.99E+00	3.06E-01	6	1.26E+01	4.25E+00	6	5.52E+00	1.69E+00	6
Glucose 6-Phosphate	1.60E-02	5.64E-03	6	5.52E-04	5.52E-04	1	1.51E-03	1.13E-03	2	0.00E+00	0.00E+00	0	0.00E+00	0.00E+00	0	0.00E+00	0.00E+00	0	0.00E+00	0.00E+00	0	3.10E-04	2.02E-04	2
Glutamate	1.22E+01	5.98E-01	6	1.15E+01	3.18E-01	6	1.27E+01	7.51E-01	6	1.12E+01	4.50E-01	6	1.17E+01	4.07E-01	6	1.09E+01	3.86E-01	6	2.07E+01	8.14E-01	6	1.67E+01	5.00E-01	6
Glutamine	3.20E+01	2.24E+00	6	2.91E+01	1.04E+00	6	3.26E+01	2.74E+00	6	2.95E+01	1.19E+00	6	3.12E+01	2.26E+00	6	2.76E+01	1.12E+00	6	5.01E+01	3.97E+00	6	4.21E+01	7.62E-01	6

Fig. B.1 Control and 30 min WI heart taurine-normalised ion intensities, ZIC-pHILIC column. 1 of 2.

Metabolite	Hom	SEM	n	Hom + WI	SEM	n	Snt	SEM	n	Snt + WI	SEM	n	Cyto	SEM	n	Cyto + WI	SEM	n	Mito	SEM	n	Mito + WI	SEM	n
Glycerol	7.01E-01	9.07E-02	6	1.26E+00	1.01E-01	6	6.73E-01	7.73E-02	6	1.25E+00	1.07E-01	6	7.50E-01	8.72E-02	6	1.25E+00	1.29E-01	6	1.33E+00	3.44E-01	6	2.18E+00	1.38E+00	6
Glycerylphosphorylcholine	2.28E+00	1.99E-01	6	1.28E+00	9.10E-02	6	2.59E+00	1.42E-01	6	1.48E+00	8.12E-02	6	2.15E+00	1.45E-01	6	1.29E+00	8.54E-02	6	2.87E+00	1.22E+00	6	2.32E+00	1.25E+00	6
Glycine	6.52E-02	2.65E-03	6	8.34E-02	4.72E-03	6	6.43E-02	6.09E-03	6	8.07E-02	7.14E-03	6	8.70E-02	1.99E-02	6	8.09E-02	8.23E-03	6	3.10E-01	1.45E-01	6	8.89E-01	6.95E-01	6
GMP	4.54E-02	3.66E-03	6	3.28E-02	3.27E-03	6	6.93E-02	5.37E-03	6	4.10E-02	2.75E-03	6	6.87E-02	5.23E-03	6	3.58E-02	3.19E-03	6	3.38E-02	5.49E-03	6	5.93E-02	5.69E-03	6
GSH	1.31E+00	5.94E-02	6	1.39E+00	4.87E-02	6	1.37E+00	5.64E-02	6	1.29E+00	5.43E-02	6	1.30E+00	4.25E-02	6	1.34E+00	3.45E-02	6	1.09E+00	4.46E-02	6	1.32E+00	6.71E-02	6
GSSG	4.46E-03	4.86E-04	6	7.41E-03	7.85E-04	6	3.04E-03	6.47E-04	6	6.59E-03	9.23E-04	6	4.18E-03	4.13E-04	6	7.33E-03	6.44E-04	6	9.94E-03	2.08E-03	6	1.71E-02	1.29E-03	6
Guanosine	0.00E+00	0.00E+00	0	7.81E-02	2.50E-03	6	0.00E+00	0.00E+00	0	1.07E-01	1.20E-02	6	0.00E+00	0.00E+00	0	6.92E-02	3.97E-03	6	7.24E-02	7.24E-02	1	1.51E-01	1.18E-02	6
Histidine	1.70E+00	1.35E-01	6	1.57E+00	5.82E-02	6	1.68E+00	1.39E-01	6	1.58E+00	6.33E-02	6	1.66E+00	1.34E-01	6	1.54E+00	4.22E-02	6	3.17E+00	2.64E-01	6	2.06E+00	2.56E-01	6
Hypotaurine	4.52E-02	2.47E-02	4	4.32E-03	2.78E-03	2	4.24E-02	2.38E-02	4	0.00E+00	0.00E+00	0	6.15E-02	2.76E-02	6	1.33E-02	4.34E-03	5	0.00E+00	0.00E+00	0	0.00E+00	0.00E+00	0
Hypoxanthine	4.11E-01	5.36E-02	6	1.47E+01	7.41E-01	6	4.89E-01	5.33E-02	6	1.56E+01	9.82E-01	6	4.89E-01	4.84E-02	6	1.51E+01	6.87E-01	6	1.41E+00	1.10E+00	6	7.39E+00	4.50E-01	6
Inosine	8.59E-02	3.40E-02	4	9.31E+00	3.28E-01	6	2.46E-01	3.04E-02	6	1.03E+01	4.59E-01	6	2.31E-01	3.65E-02	6	9.86E+00	3.55E-01	6	9.23E-02	9.23E-02	1	6.09E+00	2.31E-01	6
Kynurenic acid	0.00E+00	0.00E+00	0	0.00E+00	0.00E+00	0	0.00E+00	0.00E+00	0	0.00E+00	0.00E+00	0	0.00E+00	0.00E+00	0	0.00E+00	0.00E+00	0	4.35E-01	1.23E-01	6	1.33E+00	3.53E-01	6
Lactate	1.68E+01	1.83E+00	6	3.45E+01	2.82E+00	6	1.96E+01	1.15E+00	6	3.18E+01	5.80E+00	6	2.10E+01	1.18E+00	6	4.19E+01	2.34E+00	6	8.50E+00	1.42E+00	6	2.30E+01	5.28E+00	6
Lysine	6.34E-01	3.20E-02	6	7.69E-01	3.98E-02	6	6.76E-01	7.38E-02	6	7.49E-01	6.02E-02	6	6.54E-01	6.03E-02	6	7.75E-01	4.33E-02	6	5.85E-01	9.99E-02	6	6.32E-01	9.93E-02	6
Malate	5.51E+00	2.85E-01	6	6.24E+00	5.63E-01	6	5.59E+00	2.71E-01	6	6.52E+00	4.21E-01	6	5.29E+00	2.73E-01	6	6.16E+00	3.94E-01	6	5.89E+00	3.63E+00	6	3.18E+00	4.56E-01	6
Methionine	1.37E+00	1.50E-01	6	1.68E+00	1.35E-01	6	1.45E+00	1.47E-01	6	1.60E+00	1.37E-01	6	1.46E+00	1.70E-01	6	1.67E+00	1.47E-01	6	2.29E+00	1.52E+00	6	1.23E+00	1.12E-01	6
Myristic acid	1.01E-02	1.01E-02	1	3.82E-03	3.82E-03	1	1.70E-02	1.17E-02	2	6.39E-02	3.12E-02	3	0.00E+00	0.00E+00	0	0.00E+00	0.00E+00	0	0.00E+00	0.00E+00	0	3.01E-01	1.08E-01	4
Myristoylcarnitine	1.93E-03	4.74E-04	5	0.00E+00	0.00E+00	0	4.37E-03	2.35E-03	4	0.00E+00	0.00E+00	0	1.07E-03	8.59E-04	2	0.00E+00	0.00E+00	0	0.00E+00	0.00E+00	0	0.00E+00	0.00E+00	0
NAD	4.70E-03	4.70E-03	1	0.00E+00	0.00E+00	0	7.23E-03	7.23E-03	1	0.00E+00	0.00E+00	0	0.00E+00	0.00E+00	0	0.00E+00	0.00E+00	0	2.06E-01	5.29E-02	5	4.06E-01	6.99E-02	6
Oleic acid	4.63E-03	4.63E-03	1	0.00E+00	0.00E+00	0	0.00E+00	0.00E+00	0	4.06E-02	2.77E-02	3	0.00E+00	0.00E+00	0	4.56E-04	4.56E-04	1	9.72E-03	9.72E-03	1	1.15E-01	3.88E-02	4
Oleylcarnitine	2.05E-03	2.05E-03	1	0.00E+00	0.00E+00	0	3.77E-03	3.77E-03	1	0.00E+00	0.00E+00	0	0.00E+00	0.00E+00	0	0.00E+00	0.00E+00	0	0.00E+00	0.00E+00	0	0.00E+00	0.00E+00	0
Ornithine	6.07E-02	9.90E-03	6	5.92E-02	3.87E-03	6	6.03E-02	7.85E-03	6	5.52E-02	6.76E-03	6	6.08E-02	8.99E-03	6	5.52E-02	3.82E-03	6	8.66E-02	1.78E-02	6	6.86E-02	2.52E-02	6
Palmitic acid	5.27E-02	5.27E-02	1	3.50E-02	2.22E-02	2	5.96E-02	3.90E-02	2	2.09E-01	1.05E-01	3	0.00E+00	0.00E+00	0	0.00E+00	0.00E+00	0	5.38E-02	3.40E-02	2	4.57E-01	1.52E-01	4
Palmitoylcarnitine	2.98E-03	2.54E-03	2	0.00E+00	0.00E+00	0	7.48E-03	6.51E-03	3	0.00E+00	0.00E+00	0	3.69E-04	3.69E-04	1	0.00E+00	0.00E+00	0	0.00E+00	0.00E+00	0	0.00E+00	0.00E+00	0
Phenylalanine	1.05E+00	1.16E-01	6	1.27E+00	3.91E-02	6	1.16E+00	1.04E-01	6	1.25E+00	4.68E-02	6	1.10E+00	1.04E-01	6	1.31E+00	4.43E-02	6	9.86E-01	3.43E-01	6	1.01E+00	1.28E-01	6
Picolinamide	7.29E+00	6.53E-01	6	1.15E+01	4.39E-01	6	9.17E+00	6.35E-01	6	1.52E+01	5.07E-01	6	6.08E+00	6.07E-01	6	9.82E+00	3.28E-01	6	1.46E+01	2.79E+00	6	8.93E+00	2.45E+00	6
Proline	7.18E+00	1.16E+00	6	1.04E+01	1.03E+00	6	7.27E+00	1.19E+00	6	1.00E+01	1.01E+00	6	6.95E+00	1.15E+00	6	9.93E+00	1.01E+00	6	7.96E+00	3.21E+00	6	1.31E+01	4.67E+00	6
Propionylcarnitine	1.05E+00	1.23E-01	6	1.68E+00	1.74E-01	6	1.13E+00	1.50E-01	6	1.49E+00	1.39E-01	6	1.11E+00	1.20E-01	6	1.66E+00	1.65E-01	6	3.41E-01	7.69E-02	6	8.17E-01	1.25E-01	6
S-Adenosyl-Methionine	1.18E-02	1.33E-03	6	1.18E-02	2.09E-03	6	1.54E-02	1.07E-03	6	1.29E-02	1.02E-03	6	1.11E-02	1.31E-03	6	9.76E-03	1.49E-03	6	8.78E-02	8.49E-03	6	6.28E-02	1.16E-02	6
Serine	1.73E-01	5.01E-03	6	1.93E-01	1.35E-02	6	1.78E-01	1.09E-02	6	1.88E-01	2.02E-02	6	1.70E-01	6.08E-03	6	1.78E-01	1.49E-02	6	3.69E-01	3.06E-02	6	3.86E-01	1.03E-01	6
Stearic acid	7.15E-03	7.15E-03	1	7.92E-03	7.92E-03	1	9.35E-03	9.35E-03	1	8.76E-02	4.35E-02	3	0.00E+00	0.00E+00	0	0.00E+00	0.00E+00	0	0.00E+00	0.00E+00	0	2.61E-01	8.46E-02	4
Stearoyl carnitine	1.42E-04	1.42E-04	1	8.87E-05	5.82E-05	2	9.87E-04	9.87E-04	1	9.78E-04	9.78E-04	1	0.00E+00	0.00E+00	0	0.00E+00	0.00E+00	0	0.00E+00	0.00E+00	0	0.00E+00	0.00E+00	0
Succinate	2.03E+00	9.87E-02	6	4.64E+00	1.62E-01	6	1.99E+00	7.14E-02	6	4.12E+00	3.87E-01	6	2.32E+00	5.63E-02	6	5.15E+00	2.58E-01	6	5.76E-01	2.34E-01	4	1.52E+00	1.70E-01	6
Sucrose	2.93E+02	1.48E+01	6	2.79E+02	3.79E+00	6	3.03E+02	1.03E+01	6	2.89E+02	9.30E+00	6	3.08E+02	1.56E+01	6	2.93E+02	7.75E+00	6	2.17E+02	2.98E+01	6	1.88E+02	1.57E+01	6
Taurine	1.00E+02	0.00E+00	6	1.00E+02	0.00E+00	6	1.00E+02	0.00E+00	6	1.00E+02	0.00E+00	6	1.00E+02	0.00E+00	6	1.00E+02	0.00E+00	6	1.00E+02	0.00E+00	6	1.00E+02	0.00E+00	6
Threonine	1.00E+00	7.62E-02	6	1.32E+00	6.70E-02	6	1.07E+00	7.58E-02	6	1.31E+00	6.79E-02	6	1.08E+00	8.23E-02	6	1.33E+00	7.85E-02	6	1.16E+00	1.57E-01	6	1.41E+00	1.48E-01	6
Tryptophan	4.16E-01	4.55E-02	6	4.54E-01	1.26E-02	6	4.51E-01	5.36E-02	6	4.31E-01	2.37E-02	6	4.29E-01	4.69E-02	6	4.50E-01	2.19E-02	6	5.90E-01	3.37E-01	6	6.14E-01	2.66E-01	6
UMP	6.22E-03	1.36E-03	6	6.79E-04	4.44E-04	2	1.18E-02	1.50E-03	6	0.00E+00	0.00E+00	0	1.14E-02	1.62E-03	6	8.21E-04	3.42E-04	4	1.20E-03	7.76E-04	2	1.66E-04	1.66E-04	1
Urea	9.92E-01	7.69E-02	6	1.17E+00	4.75E-02	6	1.04E+00	7.88E-02	6	9.54E-01	5.79E-02	6	1.05E+00	8.78E-02	6	1.12E+00	5.28E-02	6	5.51E-01	1.00E-01	6	5.83E-01	1.53E-01	6
Valine	2.49E+00	3.69E-01	6	3.07E+00	1.29E-01	6	2.43E+00	2.81E-01	6	2.83E+00	1.22E-01	6	2.46E+00	3.37E-01	6	3.09E+00	1.60E-01	6	1.80E+00	3.33E-01	6	1.97E+00	2.27E-01	6
Xanthosine	1.35E-03	1.76E-04	6	1.84E-03	2.35E-04	6	1.67E-03	2.17E-04	6	2.23E-03	3.07E-04	6	1.58E-03	2.20E-04	6	1.95E-03	2.69E-04	6	1.33E-03	4.60E-04	4	2.50E-03	4.27E-04	6

Fig. B.2 Control and 30 min WI heart taurine-normalised ion intensities, ZIC-pHILIC column. 2 of 2.

Metabolite	Hom	SEM	n	Hom + WI	SEM	n	Snt	SEM	n	Snt + WI	SEM	n	Cyto	SEM	n	Cyto + WI	SEM	n	Mito	SEM	n	Mito + WI	SEM	n
Acetylcarnitine	6.71E+01	4.61E+00	6	2.82E+01	2.25E+00	6	7.81E+01	3.94E+00	6	3.67E+01	2.06E+00	6	6.95E+01	5.08E+00	6	2.35E+01	1.73E+00	6	3.46E+01	3.41E+00	6	4.36E+01	5.80E+00	6
AcetylCholine	4.19E+00	7.64E-01	6	3.14E+00	1.41E-01	6	4.22E+00	5.93E-01	6	3.02E+00	2.45E-01	6	4.25E+00	7.29E-01	6	3.15E+00	9.76E-02	6	1.46E+00	4.14E-01	6	1.57E+00	3.37E-01	6
Adenine	3.34E-01	2.72E-02	6	5.28E+00	3.09E-01	6	2.79E-01	4.05E-02	6	5.29E+00	5.03E-01	6	2.39E-01	3.45E-02	6	5.93E+00	3.14E-01	6	1.50E+00	6.71E-01	6	2.31E+00	4.64E-01	6
Adenosine	3.86E+00	3.87E-01	6	2.43E+01	2.52E+00	6	6.78E+00	6.81E-01	6	2.43E+01	1.40E+00	6	3.31E+00	3.44E-01	6	2.25E+01	2.04E+00	6	5.85E+00	3.59E+00	6	1.16E+01	1.84E+00	6
Alanine	2.34E+01	1.28E+00	6	3.84E+01	4.30E+00	6	2.18E+01	8.67E-01	6	4.30E+01	3.82E+00	6	2.77E+01	1.49E+00	6	3.90E+01	3.37E+00	6	1.46E+01	2.61E+00	6	2.89E+01	4.24E+00	6
Allantoin	5.03E-01	5.83E-02	6	5.07E-01	4.24E-02	6	4.87E-01	6.19E-02	6	5.06E-01	6.02E-02	6	5.43E-01	4.60E-02	6	5.00E-01	4.73E-02	6	4.43E-01	1.67E-01	6	7.40E-01	3.51E-01	5
AMP	1.47E+01	1.84E+00	6	7.84E+00	6.34E-01	6	2.13E+01	1.89E+00	6	7.93E+00	9.56E-01	6	2.00E+01	2.00E+00	6	8.44E+00	6.22E-01	6	5.74E+00	9.44E-01	6	4.03E+00	7.63E-01	6
Arginine	2.14E+00	1.52E-01	6	2.87E+00	9.47E-02	6	2.16E+00	1.86E-01	6	2.74E+00	2.58E-01	6	1.86E+00	1.15E-01	6	2.94E+00	1.48E-01	6	2.85E+00	7.65E-01	6	4.63E+00	3.11E+00	5
Asparagine	1.17E+00	1.31E-01	6	1.01E+00	4.62E-02	6	1.16E+00	9.39E-02	6	9.62E-01	1.04E-01	6	1.18E+00	1.13E-01	6	1.01E+00	5.49E-02	6	8.60E-01	3.51E-01	6	5.97E-01	1.36E-01	5
Aspartate	1.28E+01	1.50E+00	6	8.49E+00	7.30E-01	6	1.41E+01	1.74E+00	6	8.53E+00	1.01E+00	6	1.43E+01	1.93E+00	6	9.08E+00	9.41E-01	6	3.32E+00	1.00E+00	6	2.40E+00	4.24E-01	6
Betaine	1.33E+01	2.29E+00	6	1.16E+01	6.67E-01	6	1.30E+01	1.84E+00	6	1.06E+01	1.15E+00	6	1.35E+01	2.06E+00	6	1.22E+01	4.44E-01	6	2.39E+01	1.60E+01	6	1.61E+01	9.09E+00	6
Butyrylcarnitine	3.11E+00	2.89E-01	6	2.03E+00	1.24E-01	6	3.01E+00	1.59E-01	6	1.55E+00	4.03E-01	6	3.12E+00	3.13E-01	6	2.10E+00	6.74E-02	6	4.60E-01	2.92E-01	2	1.44E-01	9.25E-02	2
Carnitine	2.83E+01	3.15E+00	6	6.12E+01	3.15E+00	6	2.46E+01	2.27E+00	6	5.58E+01	2.75E+00	6	2.48E+01	3.31E+00	6	5.78E+01	2.48E+00	6	7.90E+00	2.05E+00	6	2.53E+01	3.18E+00	6
Choline	2.32E+01	5.39E+00	6	4.18E+01	1.33E+00	6	2.19E+01	4.57E+00	6	4.24E+01	2.95E+00	6	2.37E+01	5.25E+00	6	4.22E+01	3.59E+00	6	4.94E+01	3.75E+01	6	3.33E+01	1.21E+01	6
Citrulline	4.06E+00	2.77E-01	6	4.04E+00	2.93E-01	6	4.19E+00	1.88E-01	6	3.92E+00	4.35E-01	6	4.18E+00	1.47E-01	6	4.26E+00	2.60E-01	6	2.51E+00	2.98E-01	6	2.39E+00	4.54E-01	6
Creatinine	4.09E+01	2.47E+00	6	3.88E+01	2.99E+00	6	4.03E+01	2.86E+00	6	3.72E+01	3.49E+00	6	4.70E+01	2.38E+00	6	4.23E+01	3.56E+00	6	1.31E+01	4.18E+00	6	2.09E+01	4.19E+00	6
Cysteine	3.87E-02	1.30E-02	6	1.78E-01	2.00E-02	6	2.77E-02	1.47E-02	6	1.97E-01	3.82E-02	6	2.12E-02	7.00E-03	6	1.61E-01	2.57E-02	6	7.34E-03	7.34E-03	1	5.88E-03	2.09E-03	4
Cytidine	9.65E-02	1.90E-02	6	3.78E-01	3.28E-02	6	1.31E-01	1.73E-02	6	3.54E-01	4.76E-02	6	1.26E-01	2.06E-02	6	3.92E-01	3.80E-02	6	9.05E-03	9.05E-03	1	1.65E-01	5.31E-02	5
Dihydrothymine	2.17E-01	3.08E-02	6	1.84E-01	1.10E-02	6	2.23E-01	2.42E-02	6	1.95E-01	2.08E-02	6	2.28E-01	2.37E-02	6	2.05E-01	1.06E-02	6	6.45E-02	1.89E-02	6	8.93E-02	1.91E-02	5
Fructose	5.45E+01	3.58E+00	6	5.38E+01	2.32E+00	6	5.52E+01	3.54E+00	6	5.14E+01	3.14E+00	6	5.59E+01	2.91E+00	6	5.45E+01	1.83E+00	6	4.46E+01	1.18E+01	6	2.82E+01	7.71E+00	6
Fumarate	1.35E-02	8.69E-03	2	3.28E-02	2.22E-02	2	0.00E+00	0.00E+00	0	2.11E-02	1.34E-02	2	4.98E-03	4.98E-03	1	1.36E-02	1.36E-02	1	3.55E-01	1.02E-01	5	1.26E-01	7.13E-02	3
GABA	4.14E-01	3.32E-02	6	3.66E-01	1.15E-02	6	4.02E-01	1.94E-02	6	3.62E-01	2.33E-02	6	4.04E-01	2.23E-02	6	3.95E-01	1.23E-02	6	2.38E-01	4.20E-02	6	2.49E-01	5.23E-02	5
Glucose	3.02E+01	4.70E+00	6	2.56E+01	4.12E+00	6	2.73E+01	3.45E+00	6	3.09E+01	3.66E+00	6	3.45E+01	3.33E+00	6	3.04E+01	5.64E+00	6	1.91E+01	5.16E+00	6	1.51E+01	4.53E+00	6
Glutamate	1.25E+02	9.63E+00	6	1.13E+02	3.62E+00	6	1.22E+02	5.21E+00	6	1.11E+02	7.18E+00	6	1.23E+02	5.20E+00	6	1.18E+02	3.34E+00	6	7.76E+01	7.77E+00	6	7.97E+01	1.11E+01	6
Glutamine	1.44E+02	1.94E+01	6	1.29E+02	6.13E+00	6	1.46E+02	1.61E+01	6	1.24E+02	1.25E+01	6	1.49E+02	1.63E+01	6	1.30E+02	6.41E+00	6	6.53E+01	9.83E+00	6	7.54E+01	1.07E+01	6
Glycerylphosphorylcholine	9.77E-01	5.75E-02	6	5.84E-01	4.24E-02	6	1.17E+00	1.01E-01	6	5.96E-01	5.58E-02	6	1.01E+00	9.09E-02	6	5.99E-01	4.62E-02	6	5.07E-01	3.29E-01	6	6.56E-01	4.88E-01	5
Glycine	6.63E+00	4.63E-01	6	7.71E+00	4.54E-01	6	6.47E+00	2.39E-01	6	6.91E+00	8.15E-01	6	8.37E+00	1.95E+00	6	7.93E+00	4.50E-01	6	6.61E+00	2.81E+00	6	2.96E+01	2.36E+01	6
GSH	1.10E+01	5.84E-01	6	1.18E+01	6.07E-01	6	1.06E+01	6.87E-01	6	1.12E+01	1.31E+00	6	1.04E+01	5.61E-01	6	1.19E+01	5.34E-01	6	4.00E+00	5.10E-01	6	4.48E+00	9.19E-01	6
Histidine	1.14E+00	1.79E-01	6	1.01E+00	3.74E-02	6	1.14E+00	1.34E-01	6	9.44E-01	6.35E-02	6	1.16E+00	1.59E-01	6	1.03E+00	3.80E-02	6	5.15E-01	1.35E-01	6	5.91E-01	1.54E-01	6

Fig. B.3 Control and 30 min WI heart taurine-normalised ion intensities, ZIC-HILIC column. 1 of 2.

Metabolite	Hom	SEM	n	Hom + WI	SEM	n	Snt	SEM	n	Snt + WI	SEM	n	Cyto	SEM	n	Cyto + WI	SEM	n	Mito	SEM	n	Mito + WI	SEM	n
Hypotaurine	1.11E+00	3.23E-01	6	6.25E-01	1.12E-02	6	1.06E+00	2.91E-01	6	5.75E-01	5.47E-02	6	1.09E+00	2.90E-01	6	6.62E-01	2.58E-02	6	3.62E-01	1.21E-01	6	2.39E-01	5.48E-02	5
Hypoxanthine	1.01E+00	1.64E-01	6	3.72E+01	2.11E+00	6	1.00E+00	1.25E-01	6	3.66E+01	3.14E+00	6	9.61E-01	1.03E-01	6	4.03E+01	2.85E+00	6	2.18E+00	1.97E+00	6	9.20E+00	1.55E+00	6
Inosine	6.28E-01	1.24E-01	6	3.15E+01	9.58E-01	6	1.05E+00	9.78E-02	6	3.37E+01	1.85E+00	6	1.04E+00	9.16E-02	6	3.45E+01	1.27E+00	6	3.36E-01	2.76E-01	6	1.37E+01	1.95E+00	6
Lactate	1.47E+01	1.51E+00	6	2.85E+01	2.31E+00	6	1.62E+01	4.58E-01	6	2.52E+01	4.74E+00	6	1.67E+01	7.54E-01	6	3.26E+01	2.37E+00	6	6.19E+00	1.07E+00	6	1.54E+01	4.37E+00	6
Leucine	8.07E+00	1.74E+00	6	1.32E+01	1.90E+00	6	8.23E+00	1.92E+00	6	9.41E+00	8.66E-01	6	7.06E+00	2.05E+00	6	1.07E+01	1.87E+00	6	8.42E+00	4.36E+00	6	9.56E+00	1.50E+00	6
Lysine	3.71E+00	7.97E-02	6	4.34E+00	1.76E-01	6	4.00E+00	4.56E-01	6	4.24E+00	4.58E-01	6	3.81E+00	3.36E-01	6	4.74E+00	2.93E-01	6	2.26E+00	5.12E-01	6	2.66E+00	7.66E-01	6
Methionine	3.52E+00	4.01E-01	6	4.66E+00	4.04E-01	6	3.70E+00	4.72E-01	6	4.36E+00	5.54E-01	6	3.84E+00	5.29E-01	6	4.66E+00	3.39E-01	6	3.59E+00	2.36E+00	6	2.57E+00	5.84E-01	6
N-AcetylAspartate	1.44E+00	8.51E-02	6	1.50E+00	1.93E-01	6	1.50E+00	1.46E-01	6	1.37E+00	2.56E-01	6	1.56E+00	1.44E-01	6	1.55E+00	2.18E-01	6	8.81E-01	2.57E-01	6	1.05E+00	2.68E-01	6
Nicotinamide	2.31E+01	3.20E+00	6	3.42E+01	2.60E+00	6	2.88E+01	2.75E+00	6	5.18E+01	5.46E+00	6	2.01E+01	2.55E+00	6	3.46E+01	2.10E+00	6	2.88E+01	3.84E+00	6	3.66E+01	6.03E+00	6
Ornithine	4.53E-01	9.24E-02	6	4.40E-01	2.82E-02	6	4.49E-01	1.01E-01	6	4.66E-01	9.72E-02	6	4.84E-01	1.04E-01	6	4.36E-01	4.24E-02	6	3.16E-01	1.36E-01	6	5.18E-01	3.43E-01	5
Pantothenic_acid	9.19E-01	8.39E-02	6	1.01E+00	7.68E-02	6	8.96E-01	7.51E-02	6	9.84E-01	1.23E-01	6	8.70E-01	8.94E-02	6	1.05E+00	7.38E-02	6	5.84E-01	1.95E-01	6	7.75E-01	1.66E-01	5
Phenylalanine	2.49E+00	3.80E-01	6	2.78E+00	1.10E-01	6	2.41E+00	3.56E-01	6	2.71E+00	3.80E-01	6	2.30E+00	2.42E-01	6	3.04E+00	3.55E-01	6	2.32E+00	1.14E+00	6	1.68E+00	2.85E-01	6
Proline	6.41E+00	1.09E+00	6	8.91E+00	1.58E+00	6	6.01E+00	1.05E+00	6	9.70E+00	1.29E+00	6	6.81E+00	9.37E-01	6	9.55E+00	8.69E-01	6	4.17E+00	1.76E+00	6	8.67E+00	3.62E+00	6
Propionylcarnitine	1.22E+00	1.52E-01	6	2.27E+00	2.09E-01	6	1.34E+00	1.81E-01	6	1.84E+00	1.80E-01	6	1.33E+00	2.08E-01	6	2.12E+00	1.96E-01	6	2.60E-01	8.59E-02	6	6.30E-01	1.20E-01	6
Pyroglutamic_Acid	3.46E+00	2.93E-01	6	3.48E+00	2.34E-01	6	3.59E+00	3.26E-01	6	3.26E+00	3.57E-01	6	4.01E+00	3.38E-01	6	3.76E+00	3.21E-01	6	3.54E+00	1.35E+00	6	4.41E+00	1.30E+00	6
Serine	8.55E+00	6.54E-01	6	8.87E+00	6.65E-01	6	8.36E+00	3.36E-01	6	8.78E+00	1.07E+00	6	8.58E+00	2.98E-01	6	9.07E+00	6.98E-01	6	4.76E+00	7.25E-01	6	6.79E+00	2.10E+00	6
Succinate	4.24E+00	5.67E-01	6	8.60E+00	3.85E-01	6	3.43E+00	2.00E-01	6	7.68E+00	1.02E+00	6	3.69E+00	1.09E-01	6	9.24E+00	3.85E-01	6	3.68E+00	8.75E-01	6	4.60E+00	7.02E-01	6
Sucrose	5.03E+00	3.06E-01	6	4.84E+00	2.08E-01	6	4.87E+00	1.89E-01	6	5.33E+00	2.93E-01	6	5.21E+00	2.51E-01	6	5.30E+00	3.59E-01	6	4.85E+00	4.45E-01	6	5.90E+00	1.99E+00	6
Taurine	1.00E+02	0.00E+00	6	1.00E+02	0.00E+00	6	1.00E+02	0.00E+00	6	1.00E+02	0.00E+00	6	1.00E+02	0.00E+00	6	1.00E+02	0.00E+00	6	1.00E+02	0.00E+00	6	1.00E+02	0.00E+00	6
Threonine	6.88E+00	1.14E-01	6	9.00E+00	4.62E-01	6	7.11E+00	7.05E-01	6	8.53E+00	6.18E-01	6	7.32E+00	6.11E-01	6	9.14E+00	5.14E-01	6	3.88E+00	8.01E-01	6	5.58E+00	1.14E+00	6
Tryptophan	9.41E-01	1.31E-01	6	1.18E+00	6.71E-02	6	1.08E+00	1.72E-01	6	1.05E+00	7.41E-02	6	9.73E-01	2.01E-01	6	1.12E+00	6.61E-02	6	1.09E+00	7.19E-01	6	1.27E+00	6.28E-01	5
Tyrosine	1.46E+00	2.15E-01	6	1.60E+00	1.99E-01	6	1.55E+00	2.93E-01	6	1.64E+00	2.34E-01	6	1.28E+00	1.94E-01	6	1.36E+00	1.52E-01	6	8.42E-01	2.43E-01	6	1.19E+00	3.32E-01	6
Uracil	2.38E-03	2.38E-03	1	8.50E-01	5.67E-02	6	0.00E+00	0.00E+00	0	7.51E-01	1.08E-01	6	1.68E-03	1.68E-03	1	8.99E-01	5.96E-02	6	2.74E-03	2.74E-03	1	6.89E-02	4.08E-02	3
Urea	5.85E+01	1.51E+00	6	6.27E+01	2.56E+00	6	5.92E+01	4.47E+00	6	5.66E+01	3.93E+00	6	6.39E+01	3.98E+00	6	6.61E+01	1.75E+00	6	2.45E+01	4.93E+00	6	2.99E+01	9.68E+00	5
Uric_acid	3.23E-03	1.52E-03	3	1.04E-01	3.84E-02	6	1.31E-02	4.35E-03	5	1.02E-01	4.67E-02	6	9.32E-03	3.36E-03	4	1.34E-01	4.98E-02	6	1.03E-03	1.03E-03	1	2.32E+00	2.32E+00	3
Uridine	7.06E-02	1.51E-02	6	5.26E-01	4.01E-02	6	9.80E-02	8.72E-03	6	5.55E-01	5.98E-02	6	6.77E-02	2.08E-02	5	5.62E-01	3.53E-02	6	3.13E-02	3.13E-02	1	1.42E-01	3.83E-02	5
Valine	1.34E+01	2.30E+00	6	1.15E+01	6.32E-01	6	1.30E+01	1.79E+00	6	1.08E+01	1.07E+00	6	1.33E+01	2.00E+00	6	1.21E+01	4.45E-01	6	2.24E+01	1.59E+01	6	1.61E+01	8.92E+00	6
Xanthine	1.73E-01	3.27E-02	6	5.99E+00	3.05E-01	6	2.50E-01	2.86E-02	6	5.80E+00	3.35E-01	6	2.92E-01	1.96E-02	6	6.35E+00	1.70E-01	6	2.36E-01	1.96E-01	4	1.94E+00	3.91E-01	6
Xanthosine	0.00E+00	0.00E+00	0	4.04E-02	1.04E-02	6	0.00E+00	0.00E+00	0	4.55E-02	9.03E-03	6	0.00E+00	0.00E+00	0	5.92E-02	6.65E-03	6	0.00E+00	0.00E+00	0	1.23E-03	1.23E-03	1

Fig. B.4 Control and 30 min WI heart taurine-normalised ion intensities, ZIC-HILIC column. 2 of 2.

Metabolite	Hom	SEM	n	Hom + WI	SEM	n	Snt	SEM	n	Snt + WI	SEM	n	Cyto	SEM	n	Cyto + WI	SEM	n	Mito	SEM	n	Mito + WI	SEM	n
2-HG	3.84E-01	1.96E-01	2	1.45E+00	5.48E-01	3	4.55E-01	8.54E-02	3	1.30E+00	4.49E-01	3	2.73E-01	1.36E-01	2	1.30E+00	3.78E-01	3	1.09E-01	1.09E-01	1	1.59E+00	5.06E-01	3
3-Hydroxybutyrate	7.53E+00	2.91E+00	3	8.83E+00	1.44E+00	3	8.93E+00	3.94E+00	3	1.23E+01	1.57E+00	3	6.68E+00	2.47E+00	3	9.70E+00	3.69E-01	3	2.57E+00	8.37E-01	3	3.34E+00	4.52E-01	3
3-Phosphoglycerate	6.92E-01	2.76E-01	3	1.68E-01	6.53E-02	3	7.19E-01	2.14E-01	3	3.19E-01	1.08E-01	3	4.38E-01	6.79E-02	3	1.59E-01	3.67E-02	3	2.69E-01	8.64E-02	3	4.85E-02	2.53E-03	3
3Phosphoserine	5.03E-02	1.90E-02	3	1.15E-02	2.31E-03	3	6.17E-02	1.96E-02	3	2.19E-02	2.77E-03	3	4.37E-02	8.32E-03	3	2.72E-02	5.68E-03	3	2.11E-02	5.56E-03	3	2.24E-02	5.42E-03	3
Acetylcarnitine	8.57E+01	1.19E+01	3	2.11E+01	8.32E+00	3	9.02E+01	1.42E+01	3	2.56E+01	7.97E+00	3	7.99E+01	1.52E+00	3	2.36E+01	7.54E+00	3	4.36E+01	8.99E+00	3	6.30E+01	1.50E+01	3
AcetylCholine	5.55E+00	1.06E+00	3	5.75E+00	1.37E+00	3	4.91E+00	7.26E-01	3	5.69E+00	1.40E+00	3	4.14E+00	6.46E-02	3	4.78E+00	1.34E+00	3	1.78E+00	5.56E-01	3	3.76E+00	1.06E+00	3
Aconitate	1.73E-01	5.01E-02	3	2.20E-03	1.12E-03	2	1.55E-01	3.86E-02	3	6.89E-04	6.89E-04	1	7.52E-02	2.22E-02	3	2.02E-03	2.02E-03	1	1.49E-01	5.86E-02	3	4.63E-02	1.83E-02	3
Adenine	2.84E+00	2.77E-01	3	1.02E+01	2.00E+00	3	2.11E+00	8.43E-02	3	8.17E+00	1.57E+00	3	1.23E+00	1.48E-01	3	8.52E+00	2.18E+00	3	1.83E+00	2.53E-01	3	8.75E+00	1.02E+00	3
Adenosine	3.69E-01	2.17E-01	2	2.61E+00	1.05E+00	3	1.09E-01	5.47E-02	2	8.60E-01	4.64E-01	3	0.00E+00	0.00E+00	0	7.62E-01	7.62E-01	1	1.75E+00	1.23E-01	3	8.99E+00	2.93E+00	3
adenylosuccinate	3.76E-02	1.18E-02	3	2.42E-03	1.24E-03	2	2.87E-02	1.05E-02	3	3.48E-03	1.43E-03	3	8.58E-03	1.18E-03	3	0.00E+00	0.00E+00	0	0.00E+00	0.00E+00	0	0.00E+00	0.00E+00	0
ADP	4.12E+00	1.09E+00	3	7.53E-01	7.72E-02	3	3.23E+00	7.86E-01	3	6.02E-01	4.30E-02	3	3.22E+00	2.86E-01	3	5.22E-01	2.07E-02	3	3.14E+00	7.40E-01	3	1.06E+00	1.44E-01	3
aKG	2.76E-01	1.43E-01	2	0.00E+00	0.00E+00	0	3.49E-01	7.58E-02	3	1.21E-02	1.21E-02	1	2.62E-01	6.01E-02	3	2.91E-02	2.91E-02	1	4.16E-01	2.54E-01	2	1.14E-01	2.81E-02	3
Alanine	7.45E+00	1.51E+00	3	2.57E+01	3.79E+00	3	7.69E+00	1.70E+00	3	2.39E+01	3.91E+00	3	8.86E+00	9.64E-01	3	2.96E+01	5.74E+00	3	3.11E+00	1.12E+00	3	8.61E+00	1.44E+00	3
Allantoin	6.12E-03	3.41E-03	2	4.68E-02	8.91E-03	3	0.00E+00	0.00E+00	0	6.47E-02	7.21E-03	3	0.00E+00	0.00E+00	0	0.00E+00	0.00E+00	0	0.00E+00	0.00E+00	0	3.18E-03	3.18E-03	1
AMP	2.13E+00	5.73E-01	3	2.80E+00	6.90E-01	3	1.68E+00	2.23E-01	3	2.52E+00	7.57E-01	3	2.43E+00	4.38E-01	3	2.52E+00	6.68E-01	3	4.67E+00	9.93E-01	3	3.47E+00	4.52E-01	3
Arginine	2.33E-01	4.30E-02	3	2.03E-01	3.43E-02	3	1.57E-01	1.78E-02	3	1.44E-01	4.11E-02	3	6.57E-02	4.95E-03	3	2.85E-02	3.01E-03	3	1.11E-01	2.17E-02	3	7.19E-02	1.05E-02	3
Argininosuccinate	3.16E-03	1.47E-03	3	1.62E-03	3.42E-04	3	1.71E-03	5.57E-04	3	9.36E-04	2.04E-04	3	3.64E-04	1.86E-04	2	0.00E+00	0.00E+00	0	1.43E-03	1.18E-03	2	5.06E-03	1.04E-03	3
Aspartate	3.42E+00	7.73E-01	3	1.16E+00	7.09E-02	3	3.76E+00	8.24E-01	3	1.13E+00	1.66E-01	3	3.43E+00	6.57E-01	3	9.82E-01	1.15E-01	3	1.25E+00	4.95E-01	3	1.28E+00	4.93E-01	3
ATP	1.31E+00	4.70E-01	3	4.85E-02	7.75E-03	3	9.60E-01	3.30E-01	3	4.03E-02	9.46E-03	3	3.24E-01	8.59E-02	3	5.23E-03	2.28E-03	3	1.38E-01	2.02E-02	3	4.71E-02	4.53E-03	3
Betaine	4.29E+02	1.16E+02	3	7.16E+02	2.45E+02	3	4.26E+02	1.27E+02	3	6.91E+02	2.43E+02	3	4.23E+02	8.34E+01	3	9.27E+02	3.67E+02	3	3.43E+02	1.04E+02	3	1.03E+03	3.28E+02	3
ButyrylCarnitine	5.22E+00	1.35E+00	3	3.78E+00	1.02E+00	3	5.68E+00	1.45E+00	3	3.35E+00	8.53E-01	3	4.58E+00	1.07E+00	3	2.56E+00	7.01E-01	3	9.23E-01	3.79E-01	3	9.14E-01	2.02E-01	3
Carbamoyl phosphate	1.00E+01	6.93E-01	3	9.04E+00	1.10E+00	3	9.77E+00	1.34E+00	3	9.82E+00	1.08E+00	3	1.21E+01	1.52E+00	3	1.11E+01	1.41E+00	3	7.40E+00	4.75E-01	3	8.62E+00	1.20E+00	3
Carnitine	9.68E+01	2.62E+01	3	1.63E+02	4.30E+01	3	8.92E+01	2.14E+01	3	1.45E+02	3.96E+01	3	7.69E+01	1.18E+01	3	1.29E+02	3.69E+01	3	6.16E+01	2.05E+01	3	8.99E+01	2.38E+01	3
CDP	4.55E-02	1.25E-02	3	3.30E-03	1.28E-03	3	4.24E-02	1.22E-02	3	1.35E-03	4.52E-04	3	3.56E-02	9.55E-05	3	0.00E+00	0.00E+00	0	2.81E-03	1.48E-03	3	6.23E-03	1.75E-03	3
Choline	2.66E+01	6.70E+00	3	8.18E+01	8.24E+00	3	2.39E+01	2.70E+00	3	8.43E+01	8.49E+00	3	2.39E+01	3.37E+00	3	6.91E+01	8.23E+00	3	1.31E+01	5.35E+00	3	4.09E+01	7.95E+00	3
Citrate	4.06E+00	1.62E+00	3	2.38E-01	3.65E-02	3	3.22E+00	4.30E-01	3	1.67E-01	8.19E-02	3	8.35E-01	1.56E-01	3	2.05E-01	2.05E-01	1	1.32E+00	2.05E-01	3	6.91E-01	3.59E-01	3
Citrulline	6.44E-01	3.79E-01	3	2.89E-01	7.12E-02	3	6.98E-01	2.42E-01	3	2.44E-01	7.81E-02	3	2.56E-01	2.02E-02	3	2.38E-01	1.25E-01	3	5.48E+00	1.26E+00	3	5.58E-01	2.82E-02	3
CMP	2.32E-01	5.64E-02	3	1.70E-01	6.50E-02	3	2.16E-01	2.86E-02	3	1.54E-01	6.15E-02	3	2.02E-01	1.38E-02	3	1.41E-01	6.21E-02	3	1.00E-01	1.90E-02	3	1.29E-01	2.91E-02	3
Creatine	4.33E+01	6.17E+00	3	8.59E+01	3.95E+01	3	4.36E+01	8.35E+00	3	7.85E+01	3.83E+01	3	4.65E+01	1.29E+00	3	8.92E+01	4.50E+01	3	2.16E+01	4.85E+00	3	5.23E+01	1.64E+01	3
Creatinine	6.56E+00	1.19E+00	3	3.24E+00	1.05E+00	3	5.59E+00	7.33E-01	3	3.15E+00	1.19E+00	3	5.44E+00	3.44E-01	3	3.35E+00	1.28E+00	3	4.59E+00	1.34E+00	3	4.62E+00	9.37E-01	3
CTP	1.54E-02	5.73E-03	3	0.00E+00	0.00E+00	0	1.18E-02	6.15E-03	3	0.00E+00	0.00E+00	0	1.34E-03	4.82E-04	3	0.00E+00	0.00E+00	0	6.49E-05	6.49E-05	1	0.00E+00	0.00E+00	0
Cystathionine	4.83E-02	1.68E-02	3	3.15E-02	6.31E-03	3	4.62E-02	1.33E-02	3	3.18E-02	7.66E-03	3	2.81E-02	1.28E-02	3	1.99E-02	8.78E-03	3	1.20E-02	6.35E-03	3	2.06E-02	7.70E-03	3
Cysteine	1.34E+01	1.61E-01	3	1.36E+01	6.50E-01	3	1.39E+01	5.76E-01	3	1.47E+01	8.48E-01	3	1.17E+01	2.37E-01	3	1.27E+01	2.00E-01	3	7.81E+00	5.77E-01	3	9.39E+00	4.08E-01	3
Ethanolamine	1.24E-01	3.72E-02	3	4.62E-01	6.30E-02	3	1.18E-01	8.17E-03	3	4.33E-01	5.68E-02	3	1.91E-01	6.23E-03	3	5.64E-01	7.07E-02	3	1.85E-01	6.19E-02	3	2.82E-01	4.27E-02	3
Fructose	1.22E+02	2.06E+01	3	1.15E+02	1.10E+01	3	1.27E+02	2.60E+01	3	1.24E+02	1.52E+01	3	3.34E+02	6.83E+01	3	3.28E+02	4.50E+01	3	8.61E+01	4.52E+01	3	4.85E+01	1.32E+01	3
Fructose 6-Phosphate	4.52E-01	7.67E-02	3	4.19E-01	1.06E-01	3	4.70E-01	6.18E-02	3	4.16E-01	1.08E-01	3	3.32E-01	1.85E-02	3	3.55E-01	1.04E-01	3	4.35E-02	1.88E-02	3	6.61E-02	1.25E-02	3
Fumarate	1.67E+00	3.37E-01	3	6.98E-01	9.33E-02	3	1.75E+00	2.72E-01	3	1.10E+00	1.42E-01	3	1.49E+00	2.46E-01	3	9.09E-01	1.00E-01	3	3.48E-01	2.61E-02	3	8.77E-01	2.35E-01	3
GDP	4.49E-01	1.67E-01	3	1.15E-01	2.12E-02	3	3.10E-01	1.25E-01	3	1.06E-01	3.19E-02	3	2.67E-01	4.72E-02	3	6.64E-02	1.24E-02	3	1.72E-02	6.13E-03	3	4.41E-02	5.97E-03	3
Gluconate	1.87E+00	4.71E-01	3	2.90E+00	4.51E-01	3	1.99E+00	4.68E-01	3	2.77E+00	5.34E-01	3	1.51E+00	2.43E-01	3	2.16E+00	3.86E-01	3	5.77E-01	1.83E-01	3	1.78E+00	1.74E-01	3
Gluconate 6-phosphate	2.07E-02	7.50E-03	3	7.73E-03	6.15E-03	2	2.11E-02	8.41E-03	3	2.16E-02	5.34E-03	3	0.00E+00	0.00E+00	0	7.72E-03	7.72E-03	1	0.00E+00	0.00E+00	0	0.00E+00	0.00E+00	0
Glucose	1.32E+02	2.34E+01	3	2.09E+02	1.91E+01	3	1.38E+02	2.68E+01	3	2.25E+02	2.14E+01	3	3.37E+02	7.62E+01	3	4.00E+02	5.42E+01	3	7.76E+01	3.77E+01	3	1.63E+02	2.57E+01	3
Glucose 6-Phosphate	3.68E-01	4.27E-02	3	3.08E-01	9.13E-02	3	3.68E-01	4.14E-02	3	4.03E-01	1.27E-01	3	3.27E-01	2.24E-02	3	3.59E-01	1.11E-01	3	3.13E-02	1.02E-02	3	6.33E-02	1.51E-02	3
Glutamate	1.73E+01	4.08E+00	3	1.26E+01	4.16E+00	3	1.82E+01	3.80E+00	3	1.17E+01	4.06E+00	3	1.48E+01	1.72E+00	3	1.22E+01	4.72E+00	3	2.54E+01	6.65E+00	3	1.73E+01	4.47E+00	3
Glutamine	4.04E+01	4.29E+00	3	3.32E+01	9.68E-01	3	3.97E+01	1.91E+00	3	2.97E+01	1.22E+00	3	3.98E+01	3.79E+00	3	3.17E+01	5.73E-01	3	3.50E+01	1.24E+01	3	2.58E+01	1.10E+00	3
Glyceraldehyde 3-phosphate	3.64E-01	1.45E-01	3	2.42E-01	2.82E-02	3	5.27E-01	5.15E-02	3	3.10E-01	1.88E-02	3	1.23E+00	1.82E-01	2	5.49E-02	2.81E-02	2	7.05E-02	5.10E-02	3	2.30E-02	1.47E-02	3
Glycerol	4.88E-01	3.17E-01	2	4.53E+00	7.17E-01	3	3.82E-01	1.35E-01	3	5.16E+00	1.53E-01	3	9.19E-01	9.19E-01	1	4.19E+00	4.48E-01	3	3.33E+00	2.58E+00	3	1.38E+00	2.25E-01	3
GlycerylphosphorylCholine	3.95E+01	8.00E+00	3	1.98E+01	2.26E+00	3	3.66E+01	8.81E+00	3	1.72E+01	2.90E+00	3	3.85E+01	3.92E+00	3	1.96E+01	3.68E+00	3	2.63E+01	8.33E+00	3	2.04E+01	2.40E+00	3
Glycerylphosphorylethanolamine	2.39E-01	4.88E-02	3	1.48E-01	1.46E-02	3	2.19E-01	2.91E-02	3	1.54E-01	2.07E-02	3	5.76E-02	2.01E-02	3	4.05E-02	1.34E-02	3	8.64E-02	1.07E-02	3	1.10E-01	1.04E-02	3
Glycine	3.92E-01	8.87E-02	3	5.33E-01	7.82E-02	3	4.24E-01	8.66E-02	3	4.54E-01	8.79E-02	3	2.90E-01	1.67E-02	3	4.21E-01	9.70E-02	3	1.69E-01	6.94E-02	3	1.81E-01	1.76E-02	3

Fig. B.5 Control and 30 min WI liver taurine-normalised ion intensities, ZIC-pHILIC column. 1 of 2.

Metabolite	Hom	SEM	n	Hom + WI	SEM	n	Snt	SEM	n	Snt + WI	SEM	n	Cyto	SEM	n	Cyto + WI	SEM	n	Mito	SEM	n	Mito + WI	SEM	n
GMP	3.70E-01	1.28E-01	3	5.83E-01	8.04E-02	3	3.40E-01	3.27E-02	3	5.81E-01	9.98E-02	3	3.78E-01	2.67E-02	3	5.22E-01	9.13E-02	3	1.30E-01	3.70E-02	3	1.61E-01	1.21E-02	3
GSH	2.76E+01	4.57E+00	3	2.61E+01	4.87E+00	3	2.92E+01	5.82E+00	3	2.47E+01	5.51E+00	3	2.55E+01	1.85E+00	3	2.36E+01	4.72E+00	3	1.99E+01	5.11E+00	3	2.45E+01	3.76E+00	3
GSSG	2.83E-01	1.31E-01	3	3.49E-01	2.95E-02	3	1.59E-01	1.55E-02	3	2.13E-01	3.03E-02	3	5.27E-02	1.94E-02	3	1.00E-01	3.92E-02	3	9.16E-02	1.02E-02	3	2.55E-01	4.64E-02	3
GTP	1.32E-01	4.74E-02	3	6.36E-03	3.10E-03	3	1.06E-01	4.55E-02	3	3.90E-03	1.70E-03	3	2.27E-02	8.61E-03	3	0.00E+00	0.00E+00	0	2.08E-04	2.08E-04	1	1.31E-04	1.31E-04	1
Histidine	1.18E+01	1.24E+00	3	1.24E+01	1.40E+00	3	1.13E+01	1.58E+00	3	1.12E+01	1.30E+00	3	1.41E+01	1.12E+00	3	1.30E+01	1.24E+00	3	1.65E+01	1.55E+00	3	2.11E+01	2.30E+00	3
Hypoxanthine	2.93E-01	4.42E-02	3	2.10E+01	1.96E+00	3	4.56E-02	4.56E-02	1	1.99E+01	2.30E+00	3	0.00E+00	0.00E+00	0	2.21E+01	3.87E+00	3	1.79E-01	3.07E-02	3	2.56E+01	6.47E-01	3
Inosine	0.00E+00	0.00E+00	0	5.54E+00	5.89E-01	3	0.00E+00	0.00E+00	0	5.76E+00	8.20E-01	3	0.00E+00	0.00E+00	0	4.40E+00	6.17E-01	3	1.35E-01	1.35E-01	1	6.66E+00	5.22E-01	3
Lactate	2.48E+01	2.30E+00	3	2.63E+02	4.33E+01	3	2.78E+01	2.07E+00	3	3.13E+02	4.93E+00	3	3.72E+01	8.95E+00	3	2.66E+02	1.20E+01	3	7.59E+00	4.19E+00	2	1.05E+02	1.32E+01	3
Linoleic acid	2.42E+00	3.37E-01	3	2.49E+00	1.19E+00	3	2.60E+00	2.38E-01	3	3.32E+00	2.38E+00	3	3.76E-01	7.69E-02	3	3.15E-01	1.49E-01	3	1.27E-03	1.27E-03	1	2.98E-02	1.05E-02	3
Lysine	5.18E+00	7.68E-01	3	5.82E+00	1.49E-01	3	5.13E+00	7.09E-01	3	5.66E+00	3.94E-01	3	3.60E+00	4.85E-01	3	4.04E+00	2.12E-01	3	1.01E+00	2.96E-01	3	1.76E+00	3.73E-01	3
Malate	3.59E+01	9.39E+00	3	1.64E+01	3.40E+00	3	3.68E+01	6.94E+00	3	2.22E+01	4.20E+00	3	3.30E+01	3.53E+00	3	1.87E+01	2.64E+00	3	1.14E+01	3.26E+00	3	2.68E+01	7.80E+00	3
Mannitol/Sorbitol	0.00E+00	0.00E+00	0	1.08E-01	4.01E-02	3	0.00E+00	0.00E+00	0	9.46E-02	3.93E-02	3	0.00E+00	0.00E+00	0	7.78E-03	3.94E-03	2	0.00E+00	0.00E+00	0	1.44E-02	6.92E-03	3
Methionine	2.32E+00	2.41E-01	3	3.11E+00	4.63E-01	3	2.08E+00	2.78E-01	3	2.80E+00	4.98E-01	3	2.52E+00	2.23E-01	3	3.40E+00	7.23E-01	3	1.14E+00	3.31E-01	3	2.48E+00	1.16E+00	3
Myristic acid	1.10E+00	5.16E-02	3	8.66E-01	1.91E-01	3	9.06E-01	2.27E-02	3	1.01E+00	5.15E-01	3	1.78E-01	7.35E-03	3	1.57E-01	4.53E-02	3	0.00E+00	0.00E+00	0	1.67E-01	1.95E-02	3
Myristoylcarnitine	7.88E-02	1.35E-02	3	2.99E-03	2.01E-03	2	2.48E-02	1.20E-02	3	2.48E-03	2.48E-03	1	0.00E+00	0.00E+00	0	0.00E+00	0.00E+00	0	0.00E+00	0.00E+00	0	0.00E+00	0.00E+00	0
N-AcetylAspartate	1.55E-01	3.23E-02	3	7.03E-02	3.88E-02	2	1.56E-01	2.87E-02	3	6.38E-02	4.16E-02	2	7.33E-02	1.63E-02	3	4.74E-02	2.52E-02	2	5.47E-03	5.47E-03	1	0.00E+00	0.00E+00	0
Oleic acid	2.34E+00	3.31E-01	3	4.41E+00	2.26E+00	3	2.46E+00	2.17E-01	3	6.03E+00	4.46E+00	3	5.32E-01	6.52E-02	3	8.55E-01	3.71E-01	3	0.00E+00	0.00E+00	0	1.04E-01	7.31E-02	2
Oleylcarnitine	2.40E-01	4.77E-02	3	9.06E-02	3.27E-02	3	9.87E-02	4.21E-02	3	4.70E-02	3.47E-02	3	1.57E-02	6.19E-03	3	1.56E-03	7.90E-04	2	0.00E+00	0.00E+00	0	0.00E+00	0.00E+00	0
Ornithine	1.66E+00	3.64E-01	3	2.79E+00	4.41E-01	3	1.74E+00	2.90E-01	3	2.66E+00	4.12E-01	3	1.60E+00	1.55E-01	3	2.40E+00	3.84E-01	3	3.35E-01	6.74E-02	3	9.46E-01	1.12E-01	3
Palmitic acid	5.85E+00	7.07E-01	3	6.41E+00	2.28E+00	3	4.92E+00	6.79E-01	3	7.47E+00	4.51E+00	3	1.60E+00	3.02E-01	3	1.78E+00	3.73E-01	3	0.00E+00	0.00E+00	0	5.43E-01	3.28E-02	3
Palmitoleic acid	4.04E-01	7.17E-02	3	8.31E-01	5.31E-01	3	4.22E-01	5.19E-02	3	1.21E+00	9.78E-01	3	0.00E+00	0.00E+00	0	3.91E-02	3.91E-02	1	0.00E+00	0.00E+00	0	0.00E+00	0.00E+00	0
Palmitoylcarnitine	2.04E-01	3.92E-02	3	6.51E-02	2.38E-02	3	9.27E-02	2.58E-02	3	3.31E-02	2.76E-02	3	1.57E-02	7.52E-03	3	7.57E-04	7.57E-04	1	0.00E+00	0.00E+00	0	0.00E+00	0.00E+00	0
Phenylalanine	4.81E+00	4.65E-01	3	9.93E+00	1.73E+00	3	4.79E+00	4.11E-01	3	9.33E+00	1.76E+00	3	5.21E+00	4.95E-01	3	1.11E+01	2.43E+00	3	3.03E+00	6.13E-01	3	1.26E+01	1.65E+00	3
Phosphoenolpyruvate	2.06E-01	9.36E-02	3	2.89E-02	1.16E-02	3	2.60E-01	7.81E-02	3	8.18E-02	1.85E-02	3	1.12E-01	3.96E-02	3	7.13E-02	2.09E-02	3	4.08E-02	2.00E-02	3	5.62E-02	3.51E-02	3
Picolinamide	2.97E+01	1.00E+01	3	1.94E+01	5.03E+00	3	2.43E+01	5.57E+00	3	1.66E+01	5.69E+00	3	2.42E+01	4.77E+00	3	1.46E+01	5.83E+00	3	6.38E+01	1.82E+01	3	8.39E+01	5.49E+00	3
Proline	6.21E+00	8.49E-01	3	2.47E+01	2.39E+00	3	6.91E+00	6.52E-01	3	2.21E+01	2.75E+00	3	5.10E+00	8.05E-02	3	2.04E+01	3.42E+00	3	4.03E+00	8.76E-01	3	1.26E+01	1.87E+00	3
Propionylcarnitine	2.66E+00	8.71E-01	3	1.07E+01	3.85E+00	3	2.72E+00	7.92E-01	3	1.05E+01	3.66E+00	3	2.07E+00	3.72E-01	3	6.33E+00	2.50E+00	3	8.54E-01	3.00E-01	3	9.46E+00	3.89E+00	3
Pyruvate	3.62E+00	4.45E-01	3	5.37E+00	7.55E-01	3	3.69E+00	7.83E-01	3	5.52E+00	1.12E+00	3	8.71E+00	1.55E+00	3	1.03E+01	2.04E+00	3	0.00E+00	0.00E+00	0	1.47E+00	4.47E-01	3
Riboflavin	1.88E-02	4.12E-03	3	3.34E-02	4.90E-03	3	9.79E-03	1.81E-03	3	2.02E-02	4.43E-03	3	6.20E-03	6.20E-03	1	0.00E+00	0.00E+00	0	9.57E-02	3.00E-02	3	3.72E-01	1.00E-02	3
Ribose/Ribulose-5Phosphate	1.92E-01	5.09E-02	3	3.90E-01	5.96E-02	3	2.64E-01	2.96E-02	3	4.78E-01	6.40E-02	3	2.19E-01	4.02E-02	3	3.43E-01	7.92E-02	3	0.00E+00	0.00E+00	0	4.03E-02	2.31E-03	3
S-Adenosyl-Homocysteine	3.53E-01	8.07E-02	3	1.32E+00	2.56E-01	3	2.26E-01	2.75E-02	3	1.08E+00	2.55E-01	3	1.01E-01	1.60E-02	3	8.20E-01	2.60E-01	3	1.99E-01	3.06E-02	3	1.76E+00	2.30E-01	3
S-Adenosyl-Methionine	2.54E-01	8.17E-02	3	8.67E-02	3.20E-02	3	2.34E-01	6.47E-02	3	6.72E-02	2.47E-02	3	1.64E-01	1.90E-02	3	4.48E-02	2.95E-02	3	1.75E-01	3.21E-02	3	1.34E-01	2.47E-02	3
Sedoheptulose 7-phosphate	3.91E-01	5.48E-02	3	9.69E-01	1.59E-01	3	4.15E-01	6.00E-02	3	9.72E-01	1.28E-01	3	2.52E-01	1.90E-02	3	8.31E-01	1.90E-01	3	1.33E-03	1.33E-03	1	5.87E-02	1.54E-02	3
Serine	2.53E-01	5.97E-02	3	8.55E-02	1.59E-02	3	2.61E-01	5.87E-02	3	6.88E-02	2.00E-02	3	1.74E-01	8.04E-03	3	5.42E-02	1.30E-02	3	1.16E-01	2.29E-02	3	3.06E-02	2.82E-03	3
Serotonin	1.77E-02	1.31E-02	3	2.39E-03	1.21E-03	2	3.41E-02	5.09E-03	3	5.79E-03	2.46E-03	3	0.00E+00	0.00E+00	0	2.36E-03	1.39E-03	2	2.19E-01	8.84E-03	3	1.68E-01	4.69E-02	3
Stearic acid	2.88E+00	5.42E-01	3	2.11E+00	3.44E-01	3	2.27E+00	5.86E-01	3	2.17E+00	9.52E-01	3	5.75E-01	1.09E-01	3	6.63E-01	4.87E-02	3	2.01E-02	2.01E-02	1	1.11E-01	5.56E-02	2
Stearoylcarnitine	7.31E-02	1.53E-02	3	5.00E-02	2.16E-02	3	5.21E-02	1.75E-02	3	3.56E-02	2.64E-02	3	6.27E-03	3.50E-03	3	6.14E-04	6.14E-04	1	0.00E+00	0.00E+00	0	0.00E+00	0.00E+00	0
Succinate	3.82E+00	2.99E-01	3	2.27E+01	2.87E+00	3	3.53E+00	3.74E-01	3	2.04E+01	2.62E+00	3	3.88E+00	7.75E-01	3	1.77E+01	2.61E+00	3	1.47E+00	3.81E-01	3	3.52E+00	3.55E-01	3
Succinic_Glutathione	1.19E-02	4.34E-03	3	5.77E-03	1.92E-03	3	1.05E-02	2.36E-03	3	5.79E-03	1.91E-03	3	1.17E-03	6.16E-04	2	6.33E-04	6.33E-04	1	2.58E-04	2.58E-04	1	2.13E-03	3.61E-04	3
Sucrose	6.17E+02	9.85E+01	3	6.87E+02	7.19E+01	3	6.90E+02	1.19E+02	3	6.47E+02	7.45E+01	3	1.82E+03	3.00E+02	3	1.70E+03	2.64E+02	3	1.03E+03	4.62E+02	3	6.68E+02	1.03E+02	3
Taurine	1.00E+02	0.00E+00	3	1.00E+02	0.00E+00	3	1.00E+02	0.00E+00	3	1.00E+02	0.00E+00	3	1.00E+02	0.00E+00	3	1.00E+02	0.00E+00	3	1.00E+02	0.00E+00	3	1.00E+02	0.00E+00	3
Threonine	2.15E+00	3.67E-01	3	3.42E+00	3.71E-01	3	2.19E+00	4.27E-01	3	3.15E+00	5.48E-01	3	2.13E+00	9.24E-02	3	2.94E+00	5.09E-01	3	9.09E-01	2.25E-01	3	1.39E+00	2.44E-01	3
Tryptophan	6.20E-01	8.08E-02	3	1.09E+00	2.13E-01	3	4.92E-01	6.64E-02	3	1.11E+00	2.70E-01	3	5.50E-01	6.95E-02	3	9.76E-01	2.33E-01	3	6.49E-01	6.24E-02	3	2.69E+00	3.38E-01	3
Tyrosine	6.87E-01	7.97E-02	3	1.93E+00	3.65E-01	3	6.07E-01	3.90E-02	3	1.86E+00	3.71E-01	3	3.12E-01	7.55E-02	3	1.30E+00	3.45E-01	3	3.92E-01	3.54E-02	3	2.21E+00	2.59E-01	3
UDP	3.43E-02	1.11E-02	3	2.06E-04	2.06E-04	1	2.58E-02	8.51E-03	3	0.00E+00	0.00E+00	0	1.19E-02	5.57E-04	3	0.00E+00	0.00E+00	0	1.55E-03	1.55E-03	1	0.00E+00	0.00E+00	0
UMP	1.87E-01	5.54E-02	3	5.72E-02	1.10E-02	3	1.47E-01	2.52E-02	3	4.97E-02	1.07E-02	3	1.77E-01	1.17E-02	3	3.85E-02	1.52E-02	3	1.25E-01	2.43E-02	3	3.11E-02	5.29E-03	3
Urea	7.93E-01	1.85E-01	3	5.12E-01	6.74E-02	3	7.52E-01	1.52E-01	3	5.28E-01	7.88E-02	3	9.93E-01	5.43E-02	3	5.66E-01	1.04E-01	3	1.05E+00	5.28E-01	3	2.92E-01	8.11E-02	3
UTP	5.49E-03	2.25E-03	3	0.00E+00	0.00E+00	0	5.44E-03	2.77E-03	3	0.00E+00	0.00E+00	0	1.60E-04	1.60E-04	1	0.00E+00	0.00E+00	0	0.00E+00	0.00E+00	0	0.00E+00	0.00E+00	0
Xanthosine	0.00E+00	0.00E+00	0	1.69E+00	2.09E-01	3	0.00E+00	0.00E+00	0	1.52E+00	2.25E-01	3	0.00E+00	0.00E+00	0	1.06E+00	1.74E-01	3	0.00E+00	0.00E+00	0	1.38E+00	1.49E-01	3

Fig. B.6 Control and 30 min WI liver taurine-normalised ion intensities, ZIC-pHILIC column. 2 of 2.

Metabolite	Hom	SEM	n	Hom + WI	SEM	n	Snt	SEM	n	Snt + WI	SEM	n	Cyto	SEM	n	Cyto + WI	SEM	n	Mito	SEM	n	Mito + WI	SEM	n
2-HG	9.84E-01	1.59E-01	3	2.25E+00	5.73E-01	3	1.65E+00	5.00E-01	3	4.26E+00	1.72E+00	3	4.39E-01	4.39E-01	1	1.40E+00	4.16E-01	3	1.87E+00	1.16E+00	2	3.83E+00	3.08E+00	2
3-hydroxybutyrate	1.79E+00	9.62E-01	2	4.96E+00	5.75E-01	3	3.90E+00	1.12E+00	3	7.72E+00	1.55E+00	3	8.36E-01	8.36E-01	1	4.31E-01	4.31E-01	1	9.30E-01	4.85E-01	2	6.09E-01	6.09E-01	1
Acetylcarnitine	1.12E+02	2.39E+01	3	3.12E+01	5.32E+00	3	1.67E+02	6.49E+01	3	5.96E+01	2.36E+01	3	1.07E+02	2.12E+01	3	2.03E+01	3.90E+00	3	4.61E+01	1.49E+01	3	5.28E+01	1.81E+01	3
AcetylCholine	7.78E+00	5.93E-01	3	1.16E+01	2.58E+00	3	1.09E+01	1.22E+00	3	1.43E+01	3.19E+00	3	6.07E+00	1.04E+00	3	5.43E+00	1.33E+00	3	1.56E+00	5.35E-01	3	4.04E+00	1.05E+00	3
Adenine	4.18E+00	4.11E-01	3	1.58E+01	1.64E+00	3	3.48E+00	6.67E-01	3	1.79E+01	5.84E-01	3	1.34E+00	1.77E-01	3	9.10E+00	2.43E-01	3	1.15E+00	1.81E-01	3	4.01E+00	2.41E-01	3
Adenosine	8.74E-01	2.94E-01	3	6.15E+00	2.18E+00	3	3.53E-01	2.09E-01	2	1.88E+00	4.46E-01	3	6.66E-03	6.66E-03	1	1.27E+00	6.57E-01	3	9.84E-01	4.13E-01	3	7.59E+00	1.08E+00	3
Alanine	1.05E+02	1.05E+01	3	4.35E+02	3.94E+01	3	1.41E+02	2.53E+01	3	4.99E+02	2.79E+01	3	7.11E+01	1.37E+01	3	2.23E+02	2.19E+01	3	1.24E+01	3.97E+00	3	5.10E+01	9.84E+00	3
Allantoin	2.16E+00	5.17E-01	3	5.96E+00	9.99E-01	3	2.90E+00	9.62E-01	3	7.16E+00	1.14E+00	3	7.55E-01	2.94E-01	3	2.83E+00	3.35E-01	3	6.95E-01	2.22E-01	3	4.33E+00	9.74E-01	3
AMP	3.32E+01	3.25E+00	3	5.91E+01	7.89E+00	3	3.64E+01	4.06E+00	3	6.48E+01	2.82E+00	3	3.14E+01	2.66E+00	3	2.49E+01	3.35E+00	3	1.71E+01	4.20E+00	3	1.96E+01	1.95E+00	3
Arginine	9.84E-01	2.00E-01	3	1.09E+00	1.64E-01	3	8.58E-01	2.60E-01	3	1.02E+00	2.84E-01	3	7.54E-02	2.91E-02	3	0.00E+00	0.00E+00	0	1.96E-01	1.45E-01	2	1.06E-01	3.38E-02	3
Ascorbic acid	6.08E+00	3.66E+00	2	0.00E+00	0.00E+00	0	2.34E+01	3.51E+00	3	0.00E+00	0.00E+00	0	1.15E+01	4.67E+00	3	1.07E+00	5.88E-01	2	2.21E-01	1.61E-01	2	0.00E+00	0.00E+00	0
Asparagine	1.28E+00	4.13E-01	3	2.71E+00	6.98E-01	3	1.53E+00	4.30E-01	3	2.80E+00	9.99E-01	3	6.68E-01	5.64E-02	3	1.96E+00	2.17E-01	3	3.12E-01	3.97E-02	3	1.24E+00	2.44E-01	3
Aspartate	1.86E+01	6.60E+00	3	1.12E+01	8.06E-01	3	2.05E+01	3.12E+00	3	1.06E+01	3.68E+00	3	1.10E+01	4.17E+00	3	5.37E+00	1.18E-01	3	6.07E+00	1.55E+00	3	6.40E+00	7.75E-01	3
Betaine	2.36E+02	1.02E+02	3	7.02E+02	1.20E+02	3	2.71E+02	1.16E+02	3	5.30E+02	2.51E+02	3	1.39E+02	1.09E+02	3	4.65E+02	1.10E+02	3	3.84E+01	3.14E+01	3	2.24E+02	1.31E+02	3
ButyrylCarnitine	1.05E+01	3.98E+00	3	8.46E+00	2.05E+00	3	1.76E+01	5.53E+00	3	1.04E+01	2.25E+00	3	9.87E+00	4.12E+00	3	2.69E+00	5.25E-01	3	1.13E+00	7.03E-01	3	1.12E+00	2.72E-01	3
Carnitine	1.51E+02	6.92E+01	3	1.97E+02	2.88E+01	3	2.16E+02	9.05E+01	3	3.07E+02	1.06E+02	3	1.18E+02	2.91E+01	3	9.97E+01	2.15E+01	3	6.11E+01	2.93E+01	3	8.67E+01	3.71E+01	3
Choline	8.12E+01	3.02E+01	3	1.92E+02	2.38E+01	3	1.02E+02	2.28E+01	3	2.54E+02	1.77E+01	3	6.75E+01	2.25E+01	3	8.94E+01	7.51E+00	3	2.04E+01	1.31E+01	3	5.34E+01	6.80E+00	3
Citrulline	3.92E+00	1.34E+00	3	2.09E+00	3.03E-01	3	5.70E+00	2.06E+00	3	2.29E+00	2.08E-01	3	1.74E+00	6.11E-01	3	9.00E-01	9.19E-02	3	7.92E+00	2.86E+00	3	1.11E+00	1.78E-01	3
Creatinine	9.41E+00	1.63E+00	3	6.51E+00	1.66E+00	3	1.12E+01	1.26E+00	3	5.93E+00	7.38E-01	3	8.17E+00	1.44E+00	3	2.57E+00	6.63E-01	3	2.63E+00	8.17E-01	3	1.92E+00	6.43E-02	3
Cysteine	3.35E+00	4.74E-01	3	1.35E+01	1.60E+00	3	4.98E+00	1.54E+00	3	1.44E+01	4.59E+00	3	1.81E+00	3.25E-01	3	8.24E+00	8.76E-01	3	3.45E-01	1.65E-01	3	8.37E-01	2.45E-01	3
Cytidine	3.99E-01	2.93E-02	3	1.52E-01	5.52E-02	3	5.77E-01	9.08E-02	3	1.83E-01	8.02E-03	3	1.41E-01	4.84E-02	3	1.42E-02	2.18E-03	3	4.87E-02	2.70E-02	3	3.33E-02	9.85E-03	3
Dihydrothymine	3.45E-01	1.43E-01	3	2.86E-01	1.29E-01	3	3.69E-01	1.23E-01	3	4.15E-01	1.62E-01	3	1.96E-01	4.12E-02	3	3.00E-01	5.88E-02	3	3.41E-02	1.72E-02	2	6.81E-02	2.40E-02	3
Fructose	9.85E+01	5.61E+01	2	3.03E+02	4.48E+01	3	1.93E+02	9.51E+01	3	2.36E+02	1.18E+02	2	1.82E+02	1.69E+02	3	4.41E+02	5.43E+01	3	7.10E+00	7.10E+00	1	1.86E+01	1.83E+00	3
Fumarate	2.53E+00	6.44E-01	3	1.05E+00	1.63E-01	3	3.55E+00	1.10E+00	3	1.71E+00	3.78E-01	3	1.77E+00	2.82E-01	3	1.07E+00	2.59E-01	3	5.91E-01	2.50E-01	3	6.77E-01	2.40E-01	3
GABA	5.06E-01	2.50E-01	3	6.55E-01	1.18E-01	3	4.90E-01	1.95E-01	3	4.12E-01	2.07E-01	3	2.01E-01	1.71E-01	3	2.93E-01	6.20E-02	3	2.51E-01	8.94E-02	3	2.16E-01	8.79E-02	3
Glucose	4.46E+02	1.60E+01	3	5.31E+02	7.85E+01	3	5.85E+02	1.86E+02	3	9.24E+02	1.52E+02	3	9.46E+02	1.26E+02	3	6.09E+02	7.05E+01	3	3.39E+02	1.02E+02	3	4.50E+02	1.22E+02	3
Glutamate	3.13E+02	3.71E+01	3	2.94E+02	6.49E+01	3	3.92E+02	3.04E+01	3	2.76E+02	5.78E+01	3	1.86E+02	3.26E+01	3	1.24E+02	3.10E+01	3	1.23E+02	2.06E+01	3	1.12E+02	2.07E+01	3
Glutamine	5.58E+02	6.46E+01	3	5.72E+02	3.24E+01	3	7.44E+02	3.74E+01	3	6.40E+02	4.96E+01	3	4.13E+02	4.83E+01	3	2.74E+02	1.65E+01	3	8.51E+01	1.57E+01	3	9.32E+01	1.99E+01	3
Glycerylphosphorylcholine	2.25E+01	5.30E+00	3	1.16E+01	3.40E+00	3	3.25E+01	1.26E+01	3	2.39E+01	7.19E+00	3	1.85E+01	6.96E+00	3	4.24E+00	7.20E-01	3	3.91E+00	1.70E+00	3	3.83E+00	4.61E-01	3
Glycine	6.25E+01	3.06E+00	3	1.01E+02	6.77E+00	3	8.89E+01	1.28E+01	3	1.10E+02	6.28E+00	3	4.21E+01	5.64E+00	3	4.97E+01	2.20E+00	3	7.39E+00	1.52E+00	3	1.29E+01	2.66E+00	3
GMP	8.93E-01	4.63E-01	2	2.64E+00	6.25E-01	3	1.31E+00	2.85E-01	3	3.93E+00	1.02E-01	3	1.07E-01	1.07E-01	1	9.17E-01	7.84E-02	3	1.43E-02	8.16E-03	2	1.95E-01	8.06E-03	3

Fig. B.7 Control and 30 min WI liver taurine-normalised ion intensities, ZIC-HILIC column. 1 of 2.

Metabolite	Hom	SEM	n	Hom + WI	SEM	n	Snt	SEM	n	Snt + WI	SEM	n	Cyto	SEM	n	Cyto + WI	SEM	n	Mito	SEM	n	Mito + WI	SEM	n
GSH	3.43E+02	5.98E+01	3	4.42E+02	7.03E+00	3	4.48E+02	7.98E+01	3	3.92E+02	9.15E+01	3	2.05E+02	6.46E+01	3	2.57E+02	1.25E+01	3	6.53E+01	1.96E+01	3	1.41E+02	3.36E+01	3
GSSG	1.67E-01	1.43E-01	3	1.81E-01	1.04E-01	3	8.40E-02	6.65E-02	2	6.40E-01	5.36E-01	3	0.00E+00	0.00E+00	0	5.82E-03	3.14E-03	2	1.32E-01	1.30E-01	2	2.74E-01	1.16E-01	3
Histidine	1.22E+01	2.25E+00	3	1.31E+01	6.38E-01	3	1.81E+01	4.01E+00	3	1.87E+01	2.47E+00	3	9.29E+00	2.25E+00	3	6.33E+00	4.39E-01	3	5.04E+00	1.46E+00	3	7.17E+00	4.76E-01	3
Homocysteine	9.13E-02	6.04E-02	2	4.15E-02	2.09E-02	2	2.84E-01	9.26E-02	3	2.51E-01	5.76E-02	3	2.69E-01	1.14E-01	3	2.68E-01	8.20E-02	3	5.77E-03	5.77E-03	1	0.00E+00	0.00E+00	0
Hypotaurine	7.36E-01	4.15E-01	3	7.05E-01	6.07E-02	3	6.96E-01	2.73E-01	3	6.12E-01	2.92E-01	3	3.63E-01	2.99E-01	2	4.68E-01	4.60E-02	3	9.22E-02	3.14E-02	3	3.32E-01	1.41E-01	3
Hypoxanthine	5.76E-01	5.36E-02	3	6.22E+01	3.90E+00	3	1.26E-01	9.17E-02	2	6.18E+01	6.52E+00	3	0.00E+00	0.00E+00	0	2.80E+01	1.46E+00	3	8.25E-02	4.62E-02	2	3.43E+01	5.99E+00	3
Inosine	3.90E-01	1.11E-01	3	5.45E+01	4.84E+00	3	5.00E-02	5.00E-02	1	5.99E+01	4.62E+00	3	0.00E+00	0.00E+00	0	2.19E+01	2.14E+00	3	1.50E-02	7.54E-03	2	2.29E+01	1.16E+00	3
Lactate	2.38E+01	3.87E+00	3	3.52E+02	5.60E+01	3	3.42E+01	7.24E+00	3	4.10E+02	7.15E+01	3	2.00E+01	4.00E+00	3	1.40E+02	1.07E+01	3	1.08E+01	3.18E+00	3	1.40E+02	2.20E+01	3
Leucine	3.36E+01	5.53E+00	3	1.34E+02	2.76E+01	3	6.58E+01	2.51E+01	3	1.28E+02	2.91E+01	3	2.91E+01	6.10E+00	3	3.97E+01	7.89E+00	3	7.50E+00	2.89E+00	3	2.91E+01	1.46E+01	3
Lysine	4.41E+01	1.16E+01	3	5.95E+01	6.34E+00	3	6.02E+01	1.50E+01	3	7.63E+01	1.17E+01	3	2.59E+01	7.63E+00	3	1.85E+01	1.56E+00	3	5.10E+00	2.92E+00	3	1.01E+01	3.08E+00	3
Methionine	6.38E+00	2.24E+00	3	1.11E+01	2.60E+00	3	8.04E+00	1.46E+00	3	1.31E+01	4.86E+00	3	5.81E+00	2.19E+00	3	4.07E+00	6.05E-01	3	1.55E+00	7.77E-01	3	2.95E+00	1.82E+00	3
N-AcetylAspartate	1.55E+00	2.03E-01	3	1.61E+00	1.94E-01	3	1.81E+00	1.49E-01	3	1.39E+00	1.33E-01	3	7.74E-01	1.20E-01	3	6.97E-01	7.55E-02	3	1.14E+00	4.33E-01	3	7.58E-01	2.13E-01	3
Nicotinamide	1.94E+02	2.43E+01	3	2.04E+02	2.36E+01	3	2.41E+02	2.52E+01	3	2.63E+02	1.20E+01	3	1.35E+02	2.67E+01	3	9.82E+01	9.57E+00	3	8.01E+01	2.20E+01	3	1.31E+02	3.38E+01	3
Ornithine	2.57E+01	3.60E+00	3	4.72E+01	1.69E+00	3	3.33E+01	5.70E+00	3	5.69E+01	3.94E+00	3	1.50E+01	2.73E+00	3	1.65E+01	2.06E+00	3	1.57E+00	8.42E-01	2	8.62E+00	2.46E+00	3
Pantothenic acid	1.50E-01	4.65E-02	3	1.19E+00	3.66E-01	3	2.84E-01	1.76E-01	3	1.35E+00	1.22E-01	3	6.66E-02	3.80E-02	2	7.55E-01	3.68E-01	3	1.29E-03	1.29E-03	1	2.92E-01	2.79E-02	3
Phenylalanine	1.81E+01	3.90E+00	3	5.29E+01	9.16E+00	3	2.50E+01	9.12E+00	3	5.83E+01	8.24E+00	3	1.17E+01	2.04E+00	3	1.64E+01	2.23E+00	3	5.29E+00	1.88E+00	3	3.65E+01	1.11E+01	3
Proline	1.57E+01	2.51E+00	3	5.56E+01	1.40E+01	3	1.94E+01	1.00E+00	3	7.33E+01	1.47E+01	3	1.32E+01	7.59E-01	3	3.76E+01	6.99E+00	3	2.80E+00	7.99E-01	3	8.37E+00	2.37E+00	3
Propionylcarnitine	4.64E+00	1.31E+00	3	2.47E+01	6.99E+00	3	6.75E+00	1.82E+00	3	3.05E+01	9.90E+00	3	2.85E+00	8.99E-01	3	8.54E+00	2.32E+00	3	8.05E-01	4.56E-01	3	1.51E+01	6.73E+00	3
Pyroglutamic acid	1.67E+01	8.70E-01	3	2.79E+01	1.03E+00	3	2.42E+01	3.23E+00	3	3.32E+01	5.26E+00	3	1.57E+01	4.98E-01	3	1.41E+01	1.29E-01	3	1.48E+00	2.84E-01	3	3.79E+00	6.93E-01	3
Serine	2.31E+01	6.51E-01	3	1.26E+01	1.96E+00	3	3.40E+01	6.45E+00	3	1.27E+01	1.63E+00	3	1.73E+01	3.98E+00	3	6.25E+00	7.13E-01	3	3.33E+00	6.21E-01	3	4.12E+00	2.51E+00	3
Succinate	1.42E+01	6.02E+00	3	4.57E+01	1.43E+00	3	1.26E+01	6.03E+00	3	5.98E+01	2.25E+01	3	8.74E+00	3.60E+00	3	1.58E+01	1.35E+00	3	6.37E+00	1.72E+00	3	1.02E+01	4.91E+00	3
Sucrose	2.02E+02	1.22E+02	3	1.84E+02	7.06E+01	3	2.58E+02	1.29E+02	3	3.35E+02	1.89E+02	3	3.62E+02	8.75E+01	3	1.12E+02	5.61E+01	3	1.15E+02	5.30E+01	3	1.32E+02	2.37E+01	3
Taurine	1.00E+02	0.00E+00	3	1.00E+02	0.00E+00	3	1.00E+02	0.00E+00	3	1.00E+02	0.00E+00	3	1.00E+02	0.00E+00	3	1.00E+02	0.00E+00	3	1.00E+02	0.00E+00	3	1.00E+02	0.00E+00	3
Threonine	1.58E+01	6.55E-01	3	2.85E+01	5.81E+00	3	2.08E+01	2.65E+00	3	3.13E+01	6.86E+00	3	1.07E+01	1.95E+00	3	1.44E+01	2.59E+00	3	2.34E+00	2.44E-01	3	5.07E+00	2.19E+00	3
Tryptophan	2.51E+00	2.99E-01	3	9.06E+00	2.30E+00	3	3.90E+00	1.09E+00	3	8.50E+00	1.51E+00	3	1.37E+00	2.16E-01	3	2.90E+00	4.67E-01	3	7.04E-01	2.46E-01	3	5.01E+00	1.58E+00	3
Tyrosine	4.81E+00	4.98E-01	3	1.56E+01	3.82E+00	3	5.33E+00	5.15E-01	3	2.01E+01	3.33E+00	3	2.44E+00	4.52E-01	3	7.97E+00	1.20E+00	3	1.31E+00	2.52E-01	3	7.90E+00	1.76E+00	3
Uracil	0.00E+00	0.00E+00	0	3.24E+00	7.61E-01	3	0.00E+00	0.00E+00	0	3.78E+00	1.34E+00	3	0.00E+00	0.00E+00	0	1.42E+00	3.54E-01	3	0.00E+00	0.00E+00	0	2.97E-01	1.53E-01	3
Urea	1.20E+02	9.05E+00	3	1.52E+02	6.94E+00	3	1.60E+02	2.11E+01	3	1.73E+02	1.17E+01	3	9.03E+01	2.14E+01	3	8.82E+01	4.27E+00	3	1.93E+01	3.05E+00	3	2.43E+01	6.71E+00	3
Uric acid	1.94E-02	1.38E-02	3	1.40E+00	1.18E-01	3	2.10E-03	1.10E-03	2	1.33E+00	4.44E-01	3	0.00E+00	0.00E+00	0	3.58E-01	1.00E-01	3	1.41E-03	1.41E-03	1	2.77E+00	1.89E-01	3
Uridine	2.69E-02	2.69E-02	1	4.69E+00	1.09E+00	3	4.18E-02	2.11E-02	2	7.29E+00	2.70E+00	3	0.00E+00	0.00E+00	0	1.81E+00	3.88E-01	3	0.00E+00	0.00E+00	0	3.37E+00	6.41E-01	3
Valine	4.31E+02	1.07E+02	3	7.06E+02	1.23E+02	3	6.21E+02	2.48E+02	3	1.14E+03	4.08E+02	3	3.36E+02	5.73E+01	3	4.66E+02	1.10E+02	3	2.20E+02	6.03E+01	3	4.78E+02	1.60E+02	3
Xanthine	1.13E-01	1.84E-02	3	1.24E+01	9.50E-01	3	2.17E-02	1.40E-02	2	1.47E+01	3.59E+00	3	3.10E-03	3.10E-03	1	3.85E+00	1.37E-01	3	7.03E-02	5.43E-02	2	2.49E+01	2.85E+00	3
Xanthosine	0.00E+00	0.00E+00	0	1.55E+01	6.91E-01	3	2.82E-03	2.82E-03	1	1.55E+01	2.33E+00	3	0.00E+00	0.00E+00	0	6.31E+00	1.63E-01	3	0.00E+00	0.00E+00	0	7.36E+00	7.13E-01	3

Fig. B.8 Control and 30 min WI liver taurine-normalised ion intensities, ZIC-HILIC column. 2 of 2.

Appendix C

LC-MS bar graphs

C.1 Control & 30 min WI Heart

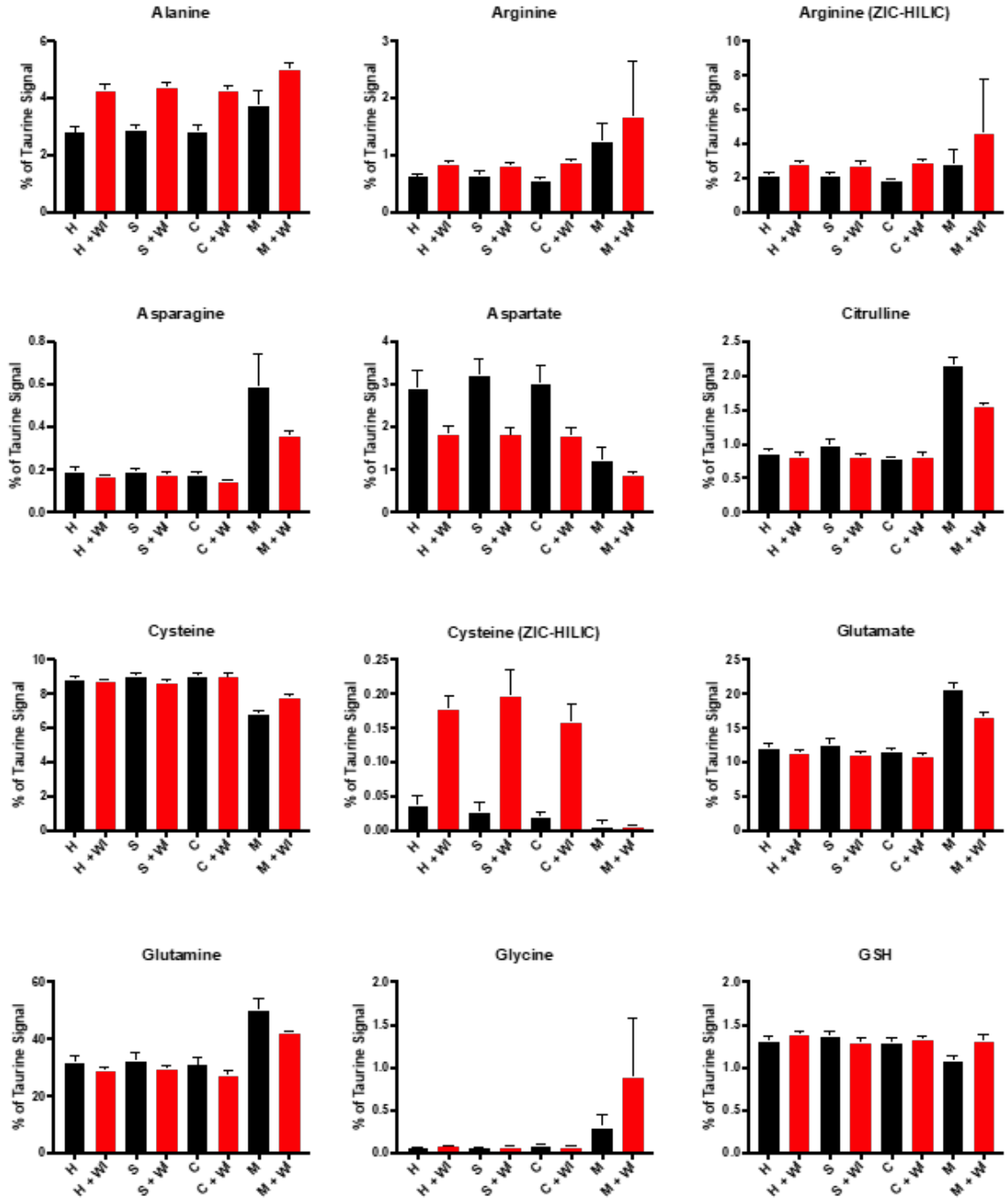

Fig. C.1 Amino acids & peptides in control and 30 min WI mouse heart homogenate, supernatant, cytosol and mitochondria. Metabolite ion intensities from the control and 30 min WI heart data sets were normalised to taurine. Data is from ZIC-pHILIC column unless otherwise stated as from ZIC-HILIC column. Data is average of 6 biological replicates, presented as mean ±SEM. H: Homogenate; S: Supernatant; C: Cytosolic fraction; M: Mitochondrial fraction. NF: Not found.

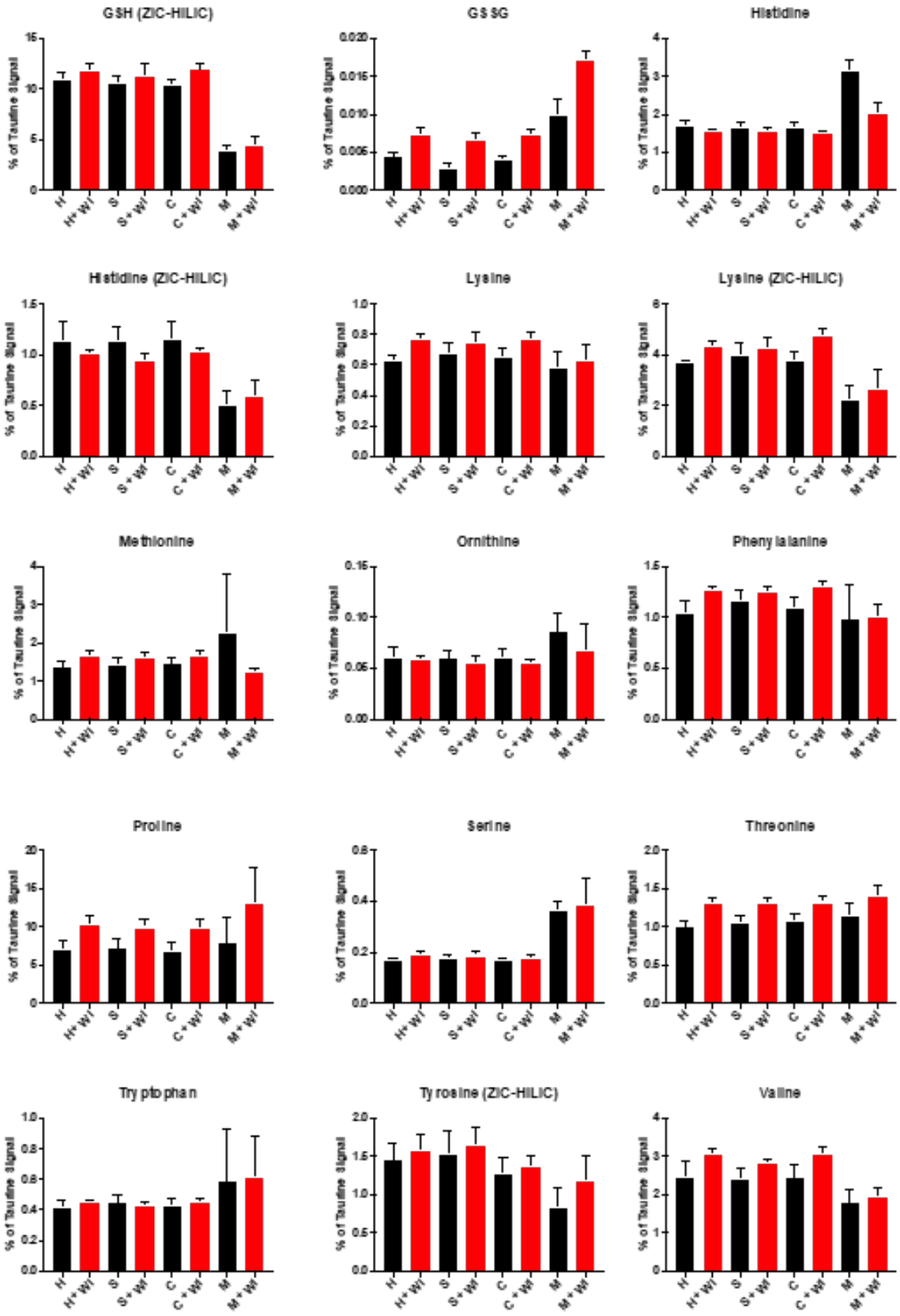

Fig. C.2 Amino acids & peptides in control and 30 min WI mouse heart homogenate, supernatant, cytosol and mitochondria (ctd.). Metabolite ion intensities from the control and 30 min WI heart data sets were normalised to taurine. Data is from ZIC-pHILIC column unless otherwise stated as from ZIC-HILIC column. Data is average of 6 biological replicates, presented as mean ±SEM. H: Homogenate; S: Supernatant; C: Cytosolic fraction; M: Mitochondrial fraction. NF: Not found.

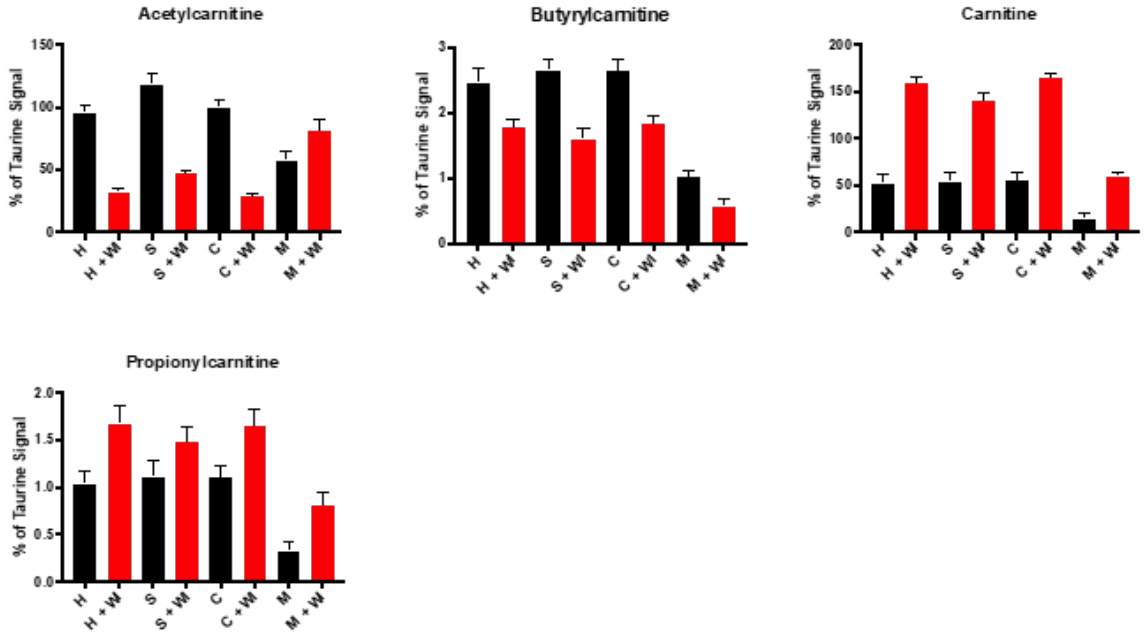

Fig. C.3 Carnitines in control and 30 min WI mouse heart homogenate, supernatant, cytosol and mitochondria. Metabolite ion intensities from the control and 30 min WI heart data sets were normalised to taurine. The fatty acids and carnitines myristic acid, oleic acid, palmitic acid, stearic acid, stearoylcarnitine, oleoylcarnitine, palmitoylcarnitine and myristoylcarnitine were excluded from the analysis due to 3 or more zero values in each fraction. Data is from ZIC-pHILIC column unless otherwise stated as from ZIC-HILIC column. Data is average of 6 biological replicates, presented as mean ±SEM. H: Homogenate; S: Supernatant; C: Cytosolic fraction; M: Mitochondrial fraction. NF: Not found.

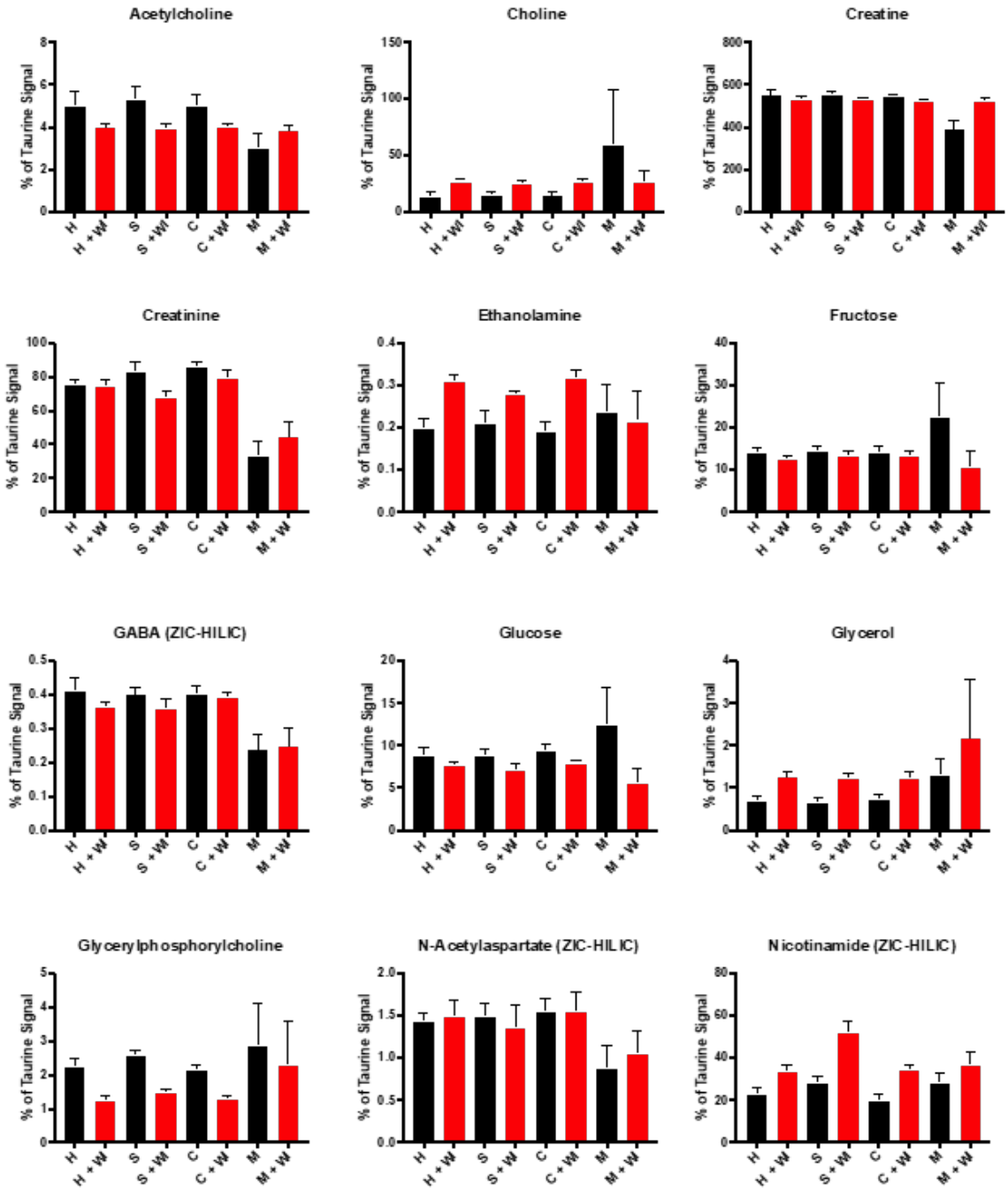

Fig. C.4 Miscellaneous metabolites in control and 30 min WI mouse heart homogenate, supernatant, cytosol and mitochondria. Metabolite ion intensities from the control and 30 min WI heart data sets were normalised to taurine. Data is from ZIC-pHILIC column unless otherwise stated as from ZIC-HILIC column. Data is average of 6 biological replicates, presented as mean ±SEM. H: Homogenate; S: Supernatant; C: Cytosolic fraction; M: Mitochondrial fraction. NF: Not found.

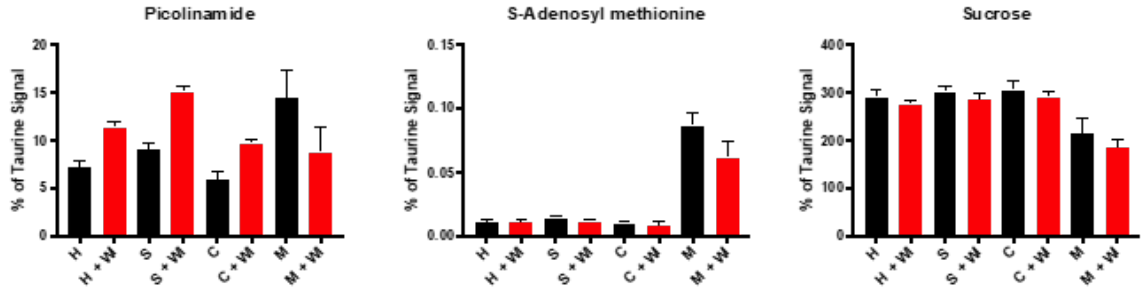

Fig. C.5 Miscellaneous metabolites in control and 30 min WI mouse heart homogenate, supernatant, cytosol and mitochondria (ctd.). Metabolite ion intensities from the control and 30 min WI heart data sets were normalised to taurine. Data is from ZIC-pHILIC column unless otherwise stated as from ZIC-HILIC column. Data is average of 6 biological replicates, presented as mean ±SEM. H: Homogenate; S: Supernatant; C: Cytosolic fraction; M: Mitochondrial fraction. NF: Not found.

C.2 Control & 30 min WI Liver

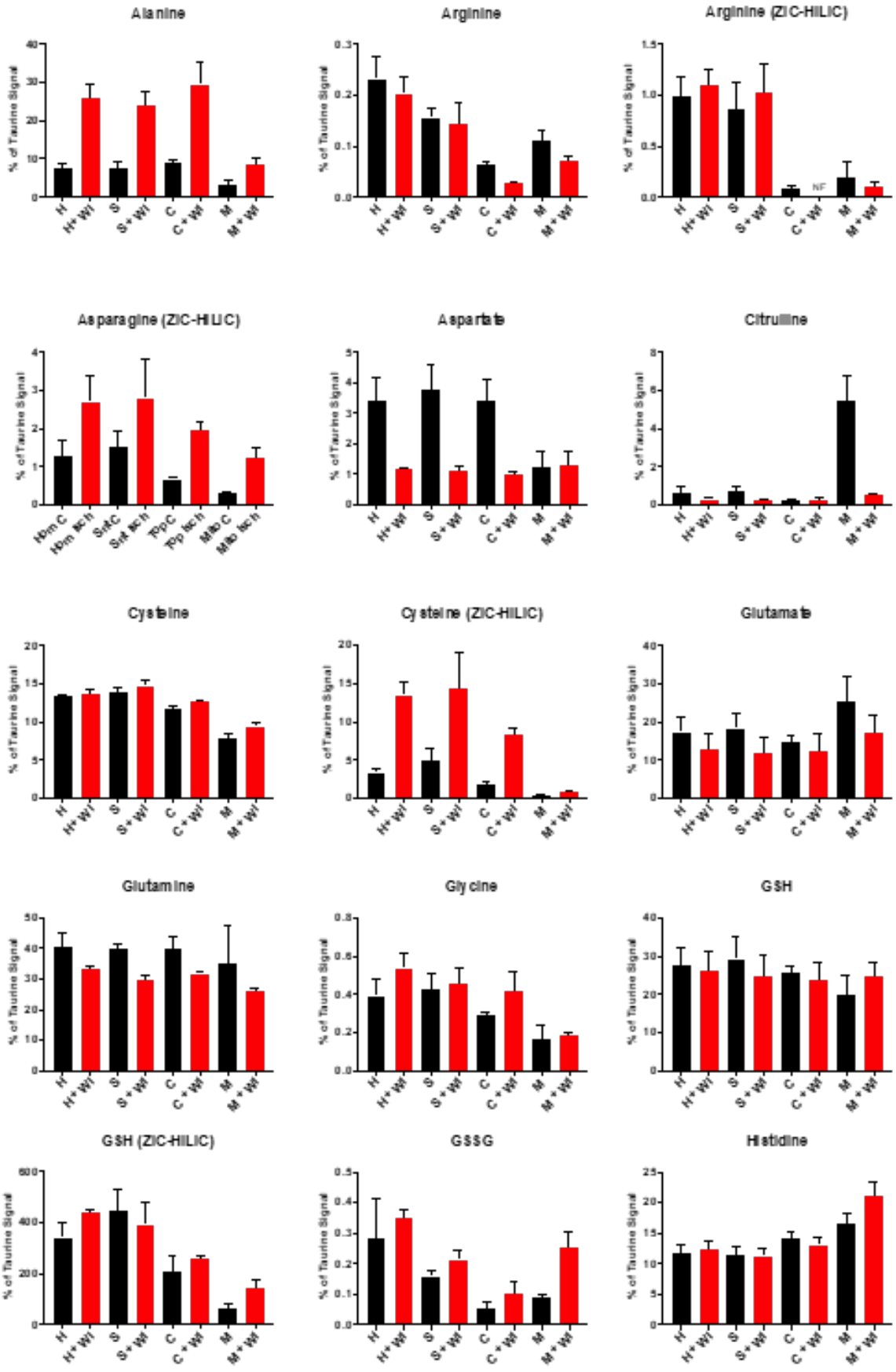

Fig. C.6 Amino acids & peptides in control and 30 min WI mouse liver homogenate, supernatant, cytosol and mitochondria. Metabolite ion intensities from the control and 30 min WI liver data sets were normalised to taurine. Data is from ZIC-pHILIC column unless otherwise stated as from ZIC-HILIC column. Data is average of 3 biological replicates, presented as mean ±SEM. H: Homogenate; S: Supernatant; C: Cytosolic fraction; M: Mitochondrial fraction. NF: Not found.

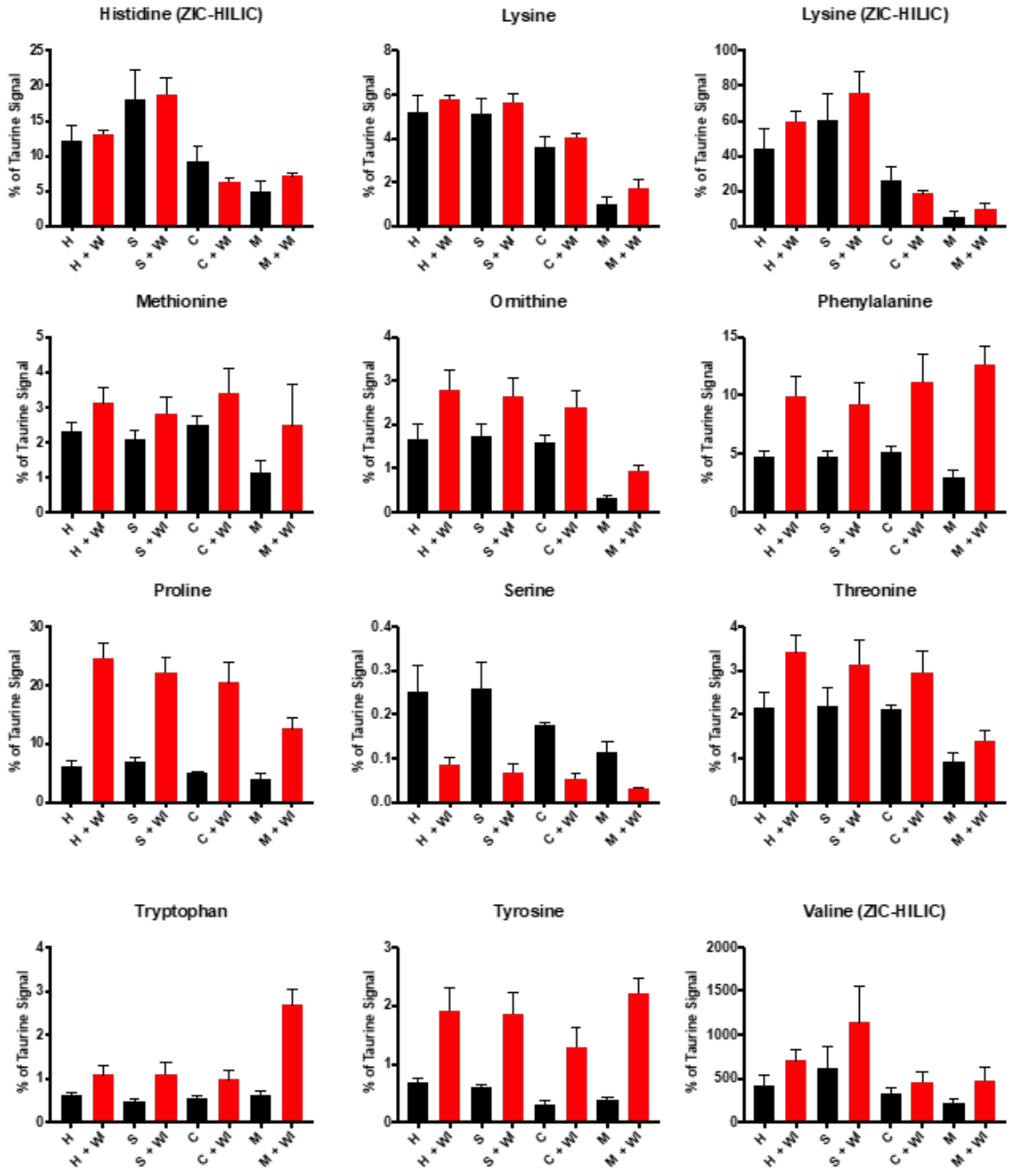

Fig. C.7 Amino acids & peptides in control and 30 min WI mouse liver homogenate, supernatant, cytosol and mitochondria (ctd.). Metabolite ion intensities from the control and 30 min WI liver data sets were normalised to taurine. Data is from ZIC-pHILIC column unless otherwise stated as from ZIC-HILIC column. Data is average of 3 biological replicates, presented as mean ±SEM. H: Homogenate; S: Supernatant; C: Cytosolic fraction; M: Mitochondrial fraction. NF: Not found.

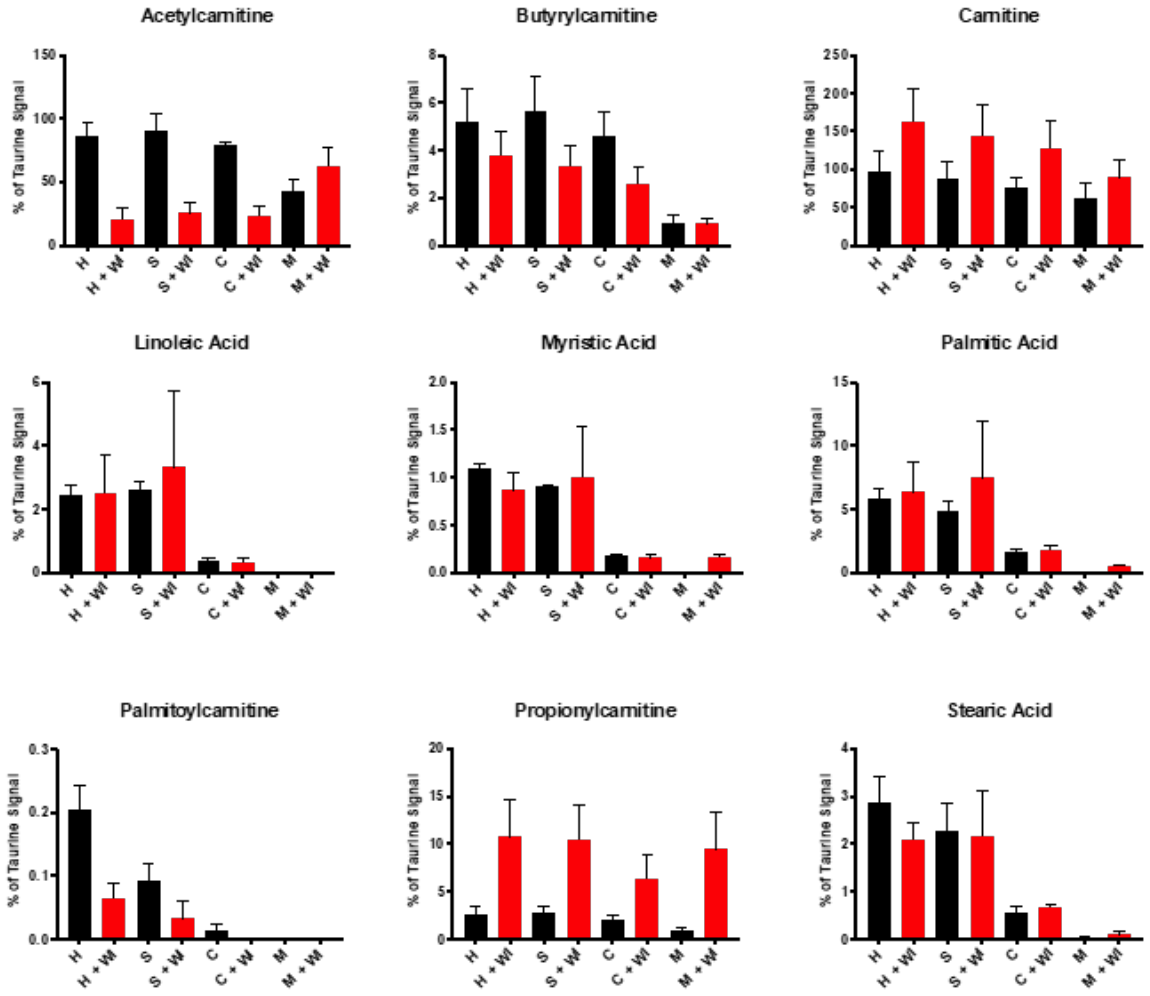

Fig. C.8 Fatty acids & carnitines in control and 30 min WI mouse liver homogenate, supernatant, cytosol and mitochondria. Metabolite ion intensities from the control and 30 min WI liver data sets were normalised to taurine. Palmitoleic acid and myristoylcarnitine were excluded from the analysis due to 3 or more zero values in each fraction. Data is from ZIC-pHILIC column unless otherwise stated as from ZIC-HILIC column. Data is average of 3 biological replicates, presented as mean ±SEM. H: Homogenate; S: Supernatant; C: Cytosolic fraction; M: Mitochondrial fraction. NF: Not found.

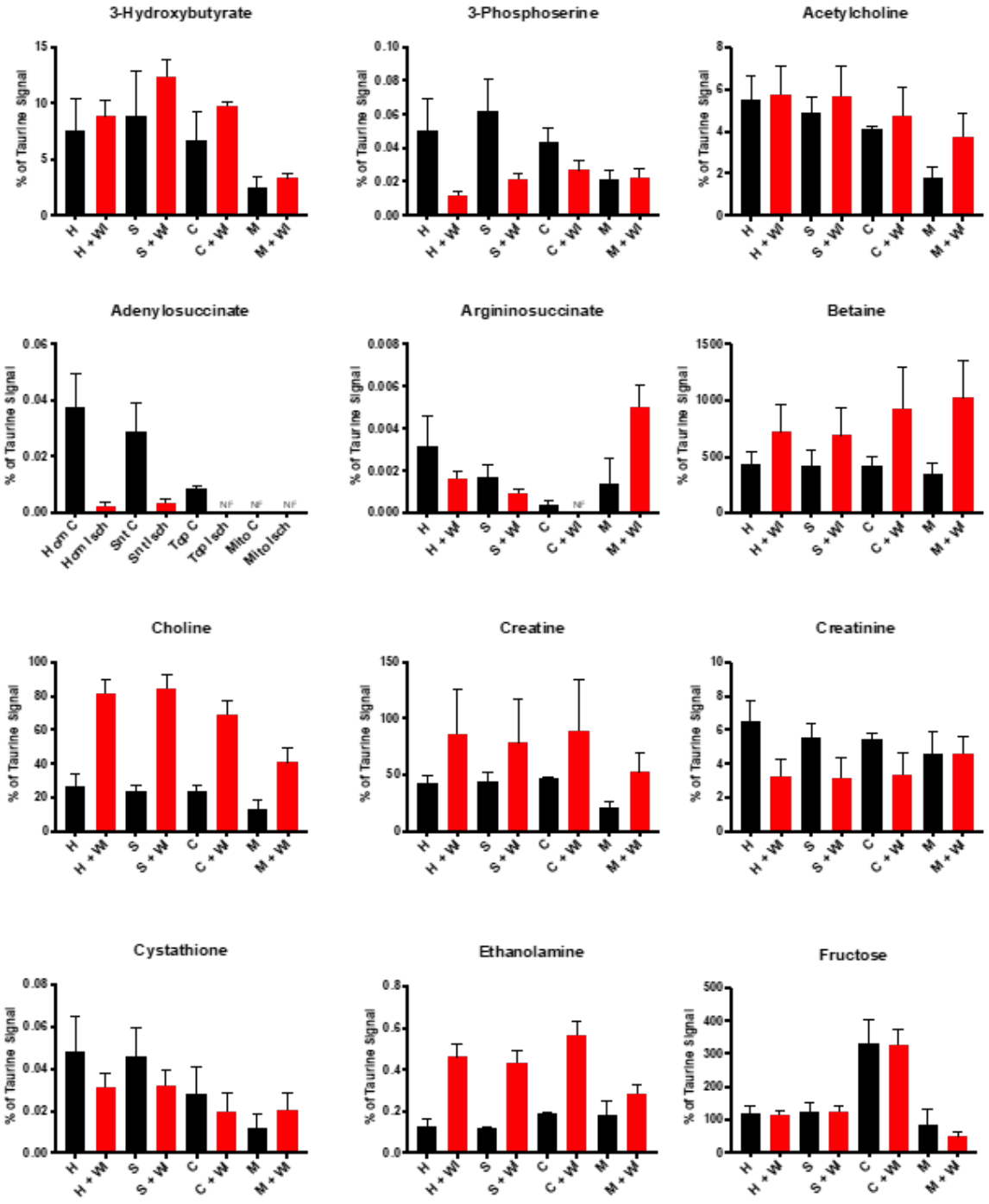

Fig. C.9 Miscellaneous metabolites in control and 30 min WI mouse liver homogenate, supernatant, cytosol and mitochondria. Metabolite ion intensities from the control and 30 min WI liver data sets were normalised to taurine. Data is from ZIC-pHILIC column unless otherwise stated as from ZIC-HILIC column. Data is average of 3 biological replicates, presented as mean ±SEM. H: Homogenate; S: Supernatant; C: Cytosolic fraction; M: Mitochondrial fraction. NF: Not found.

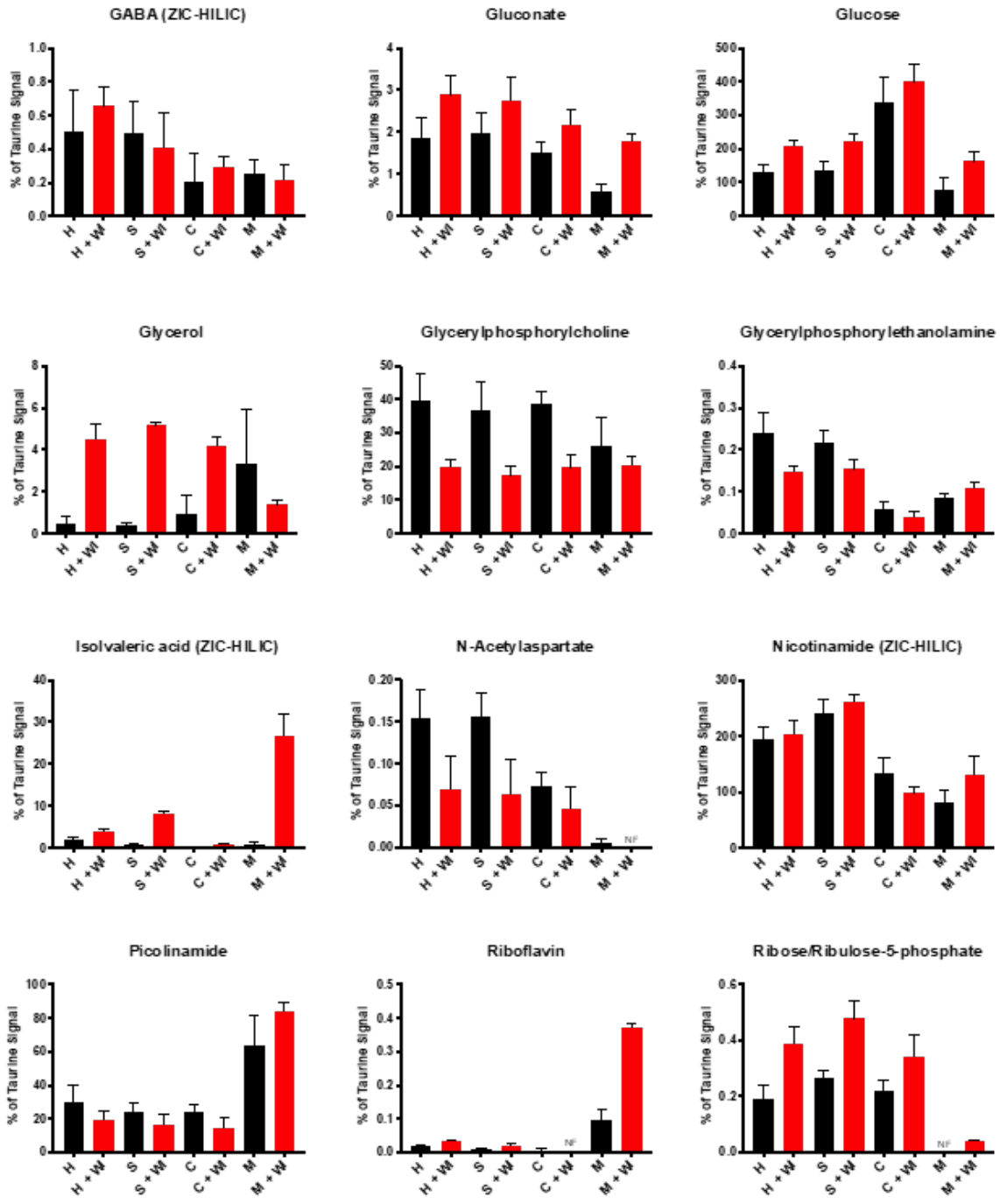

Fig. C.10 Miscellaneous metabolites in control and 30 min WI mouse liver homogenate, supernatant, cytosol and mitochondria (ctd.). Metabolite ion intensities from the control and 30 min WI liver data sets were normalised to taurine. Data is from ZIC-pHILIC column unless otherwise stated as from ZIC-HILIC column. Data is average of 3 biological replicates, presented as mean ±SEM. H: Homogenate; S: Supernatant; C: Cytosolic fraction; M: Mitochondrial fraction. NF: Not found.

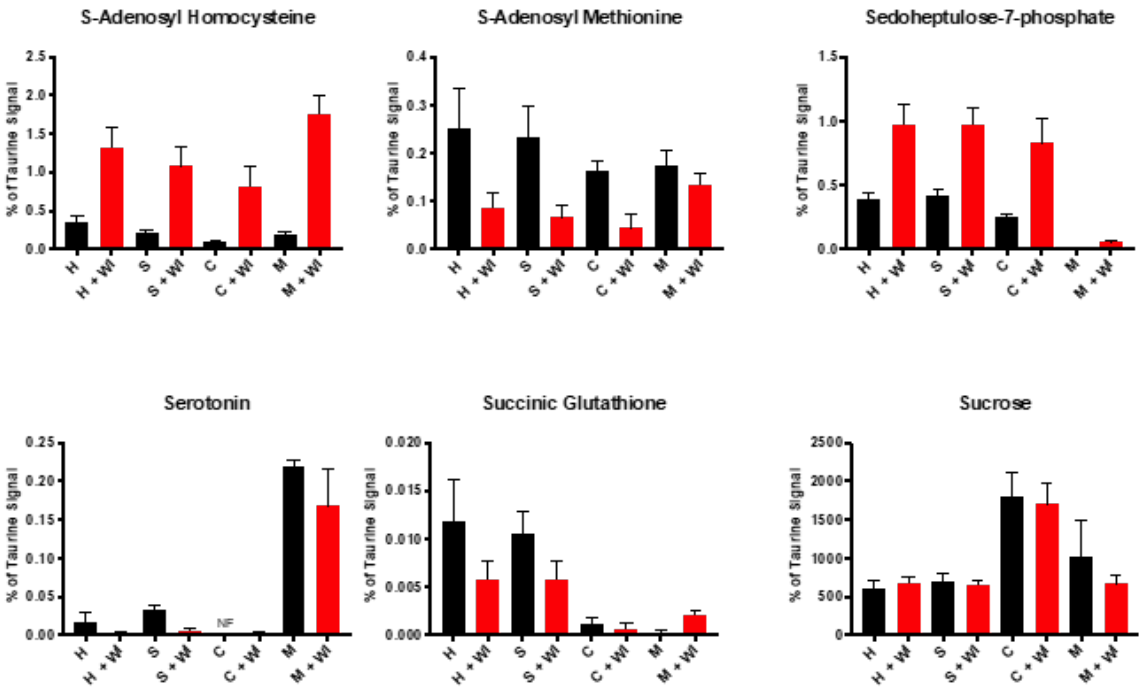

Fig. C.11 Miscellaneous metabolites in control and 30 min WI mouse liver homogenate, supernatant, cytosol and mitochondria (ctd.). Metabolite ion intensities from the control and 30 min WI liver data sets were normalised to taurine. Data is from ZIC-pHILIC column unless otherwise stated as from ZIC-HILIC column. Data is average of 3 biological replicates, presented as mean ±SEM. H: Homogenate; S: Supernatant; C: Cytosolic fraction; M: Mitochondrial fraction. NF: Not found.

C.3 Heart WI time course

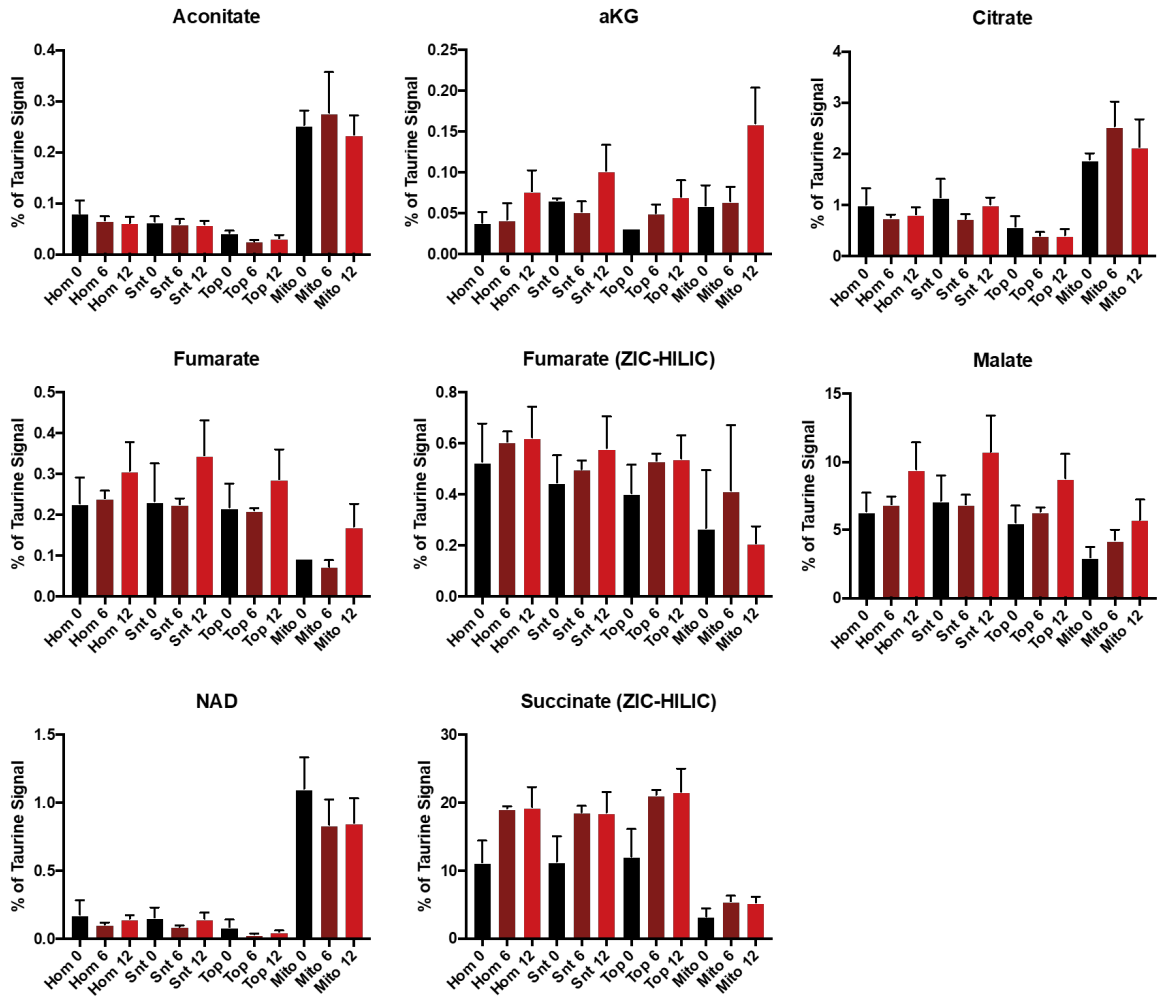

Fig. C.12 Changes in TCA cycle intermediates in mouse heart during a time course of WI. Metabolite ion intensities from the control, 6 and 12 min WI heart data sets were normalised to taurine. Data is from ZIC-pHILIC column unless otherwise stated as from ZIC-HILIC column. Data is average of 3 biological replicates for controls and 6 biological replicates for all other time points, presented as mean ±SEM. H: Homogenate; S: Supernatant; C: Cytosolic fraction; M: Mitochondrial fraction. NF: Not found.

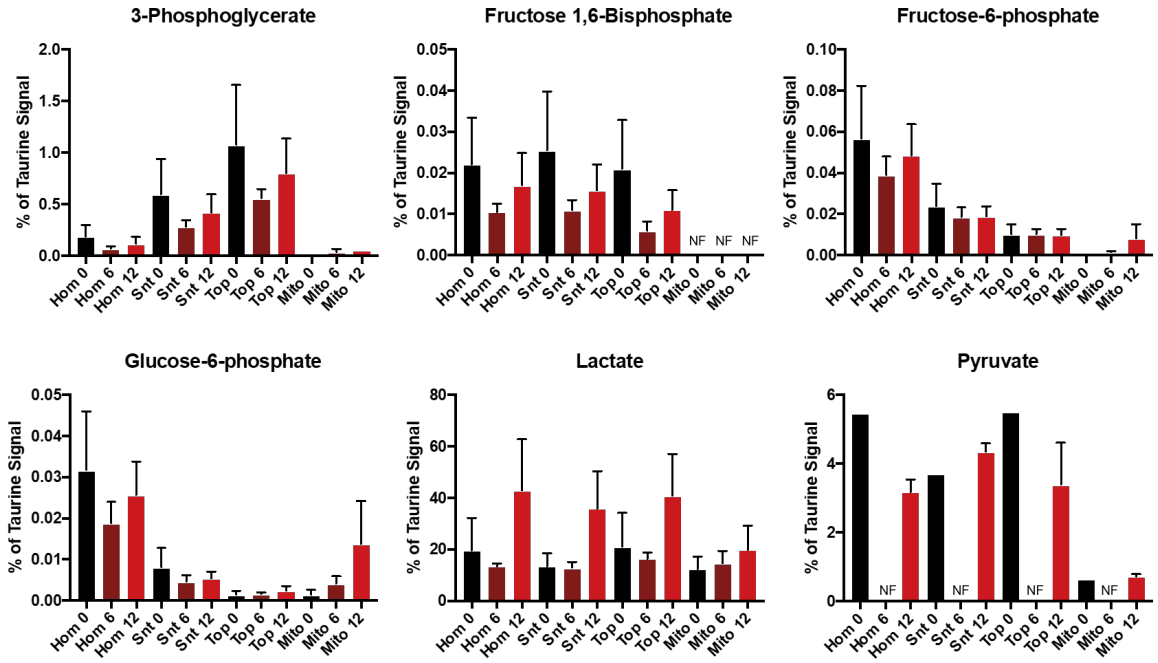

Fig. C.13 Changes in glycolytic intermediates in mouse heart during a time course of WI. Metabolite ion intensities from the control, 6 and 12 min WI heart data sets were normalised to taurine. Data is from ZIC-pHILIC column unless otherwise stated as from ZIC-HILIC column. Data is average of 3 biological replicates for controls and 6 biological replicates for all other time points, presented as mean ±SEM. H: Homogenate; S: Supernatant; C: Cytosolic fraction; M: Mitochondrial fraction. NF: Not found.

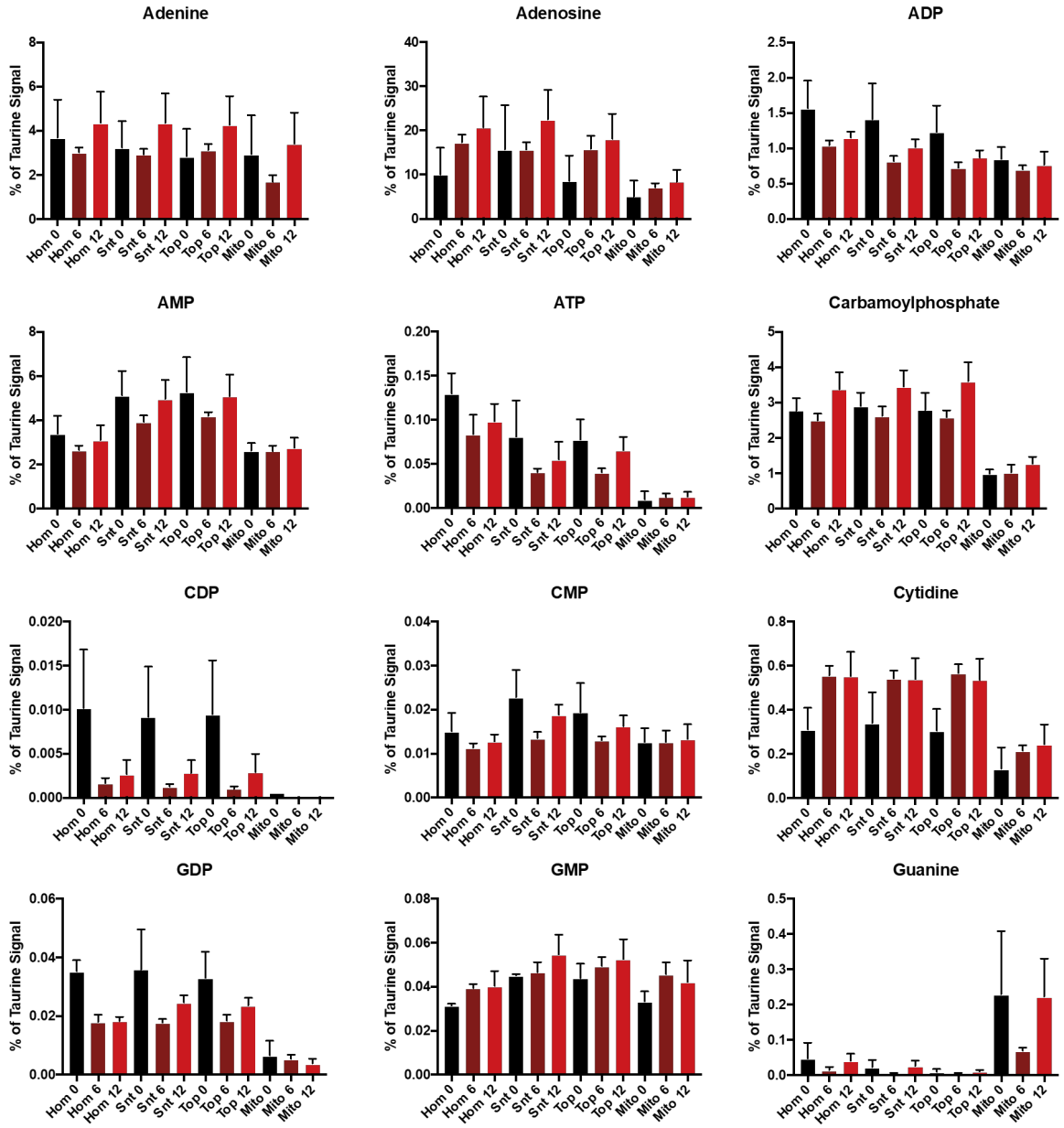

Fig. C.14 Changes in nucleotides & breakdown products in mouse heart during a time course of WI. Metabolite ion intensities from the control, 6 and 12 min WI heart data sets were normalised to taurine. Data is from ZIC-pHILIC column unless otherwise stated as from ZIC-HILIC column. Data is average of 3 biological replicates for controls and 6 biological replicates for all other time points, presented as mean ±SEM. H: Homogenate; S: Supernatant; C: Cytosolic fraction; M: Mitochondrial fraction. NF: Not found.

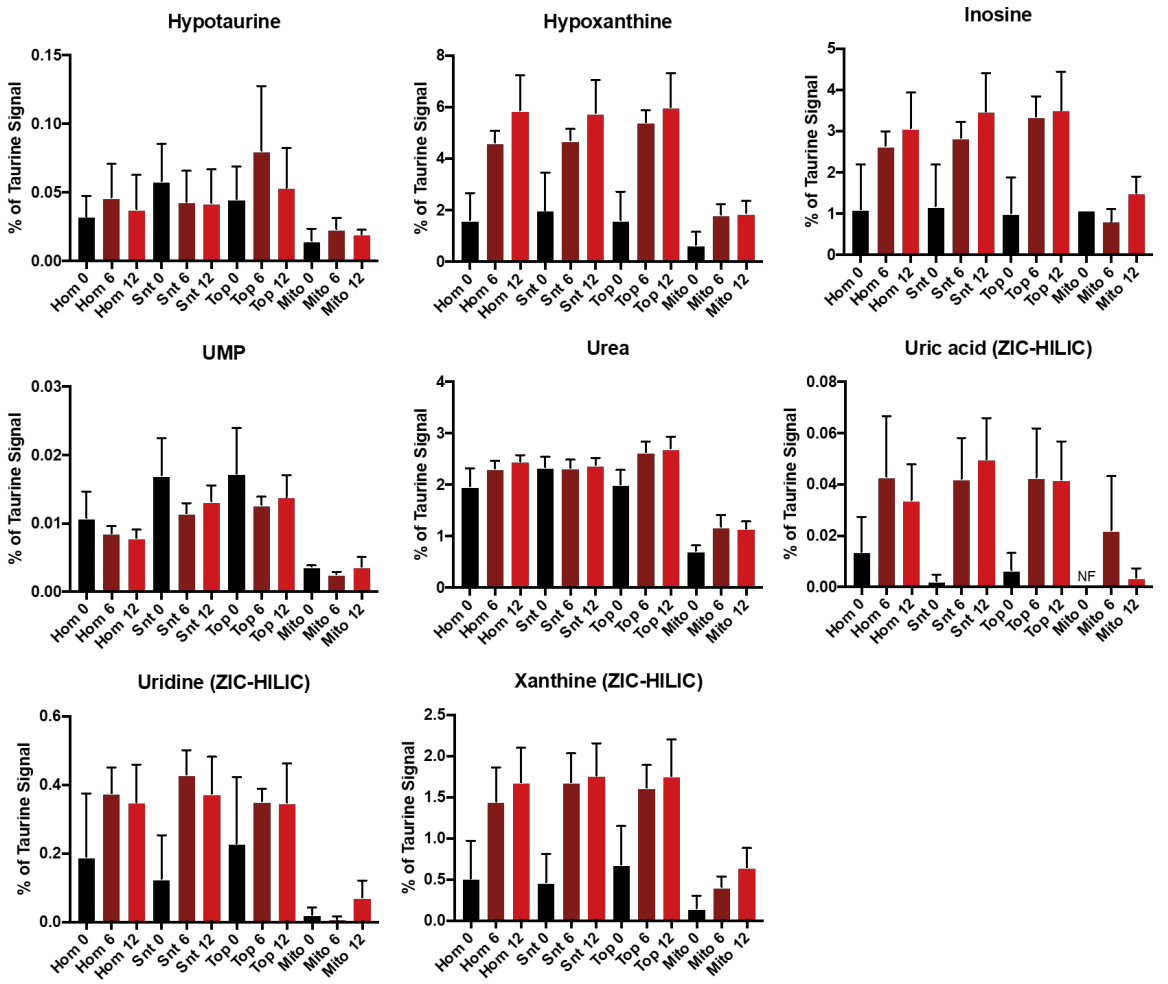

Fig. C.15 Changes in nucleotides & breakdown products in mouse heart during a time course of WI (ctd.). Metabolite ion intensities from the control, 6 and 12 min WI heart data sets were normalised to taurine. Data is from ZIC-pHILIC column unless otherwise stated as from ZIC-HILIC column. Data is average of 3 biological replicates for controls and 6 biological replicates for all other time points, presented as mean ±SEM. H: Homogenate; S: Supernatant; C: Cytosolic fraction; M: Mitochondrial fraction. NF: Not found.

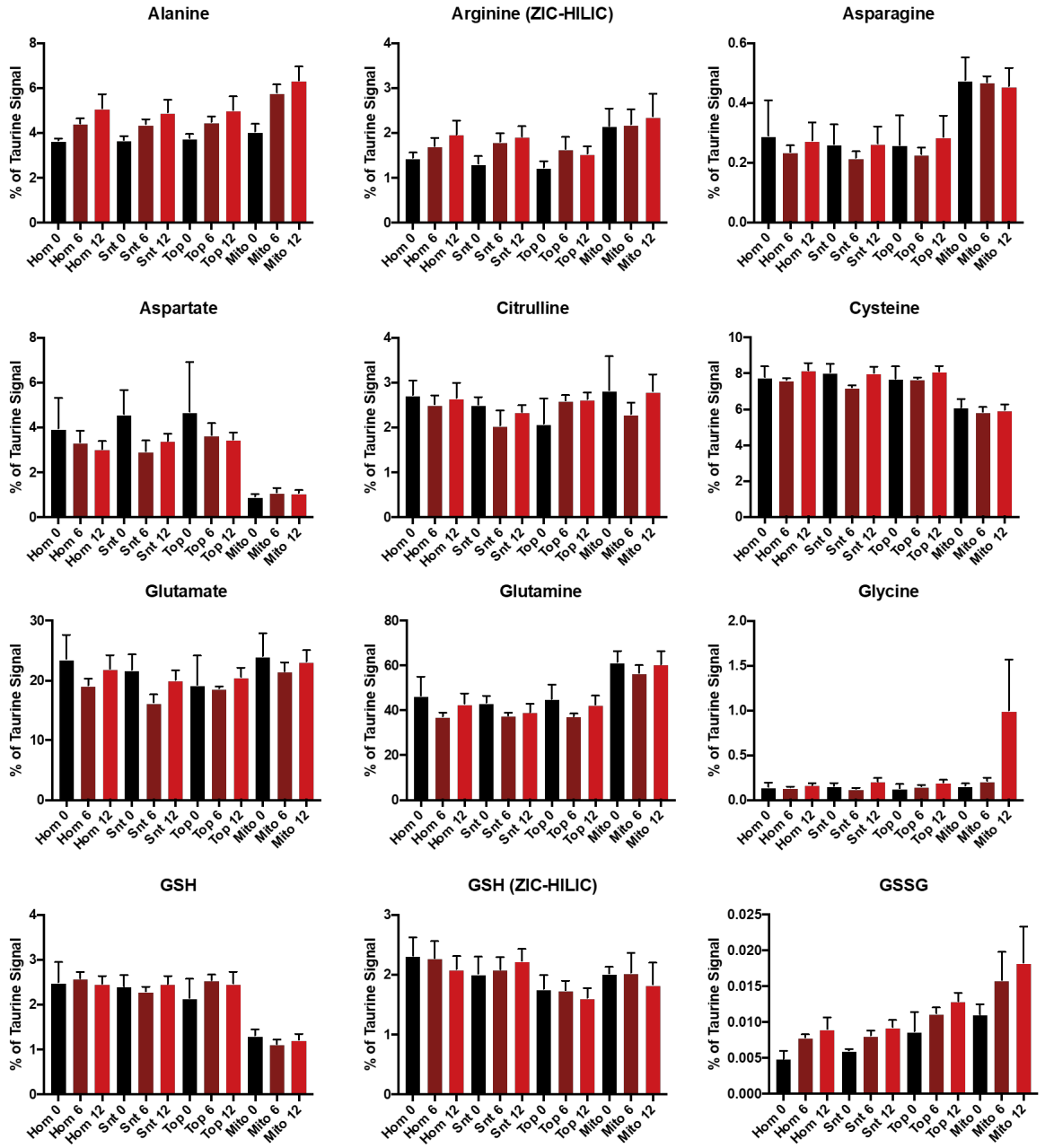

Fig. C.16 Changes in amino acids & peptides in mouse heart during a time course of WI. Metabolite ion intensities from the control, 6 and 12 min WI heart data sets were normalised to taurine. Data is from ZIC-pHILIC column unless otherwise stated as from ZIC-HILIC column. Data is average of 3 biological replicates for controls and 6 biological replicates for all other time points, presented as mean ±SEM. H: Homogenate; S: Supernatant; C: Cytosolic fraction; M: Mitochondrial fraction. NF: Not found.

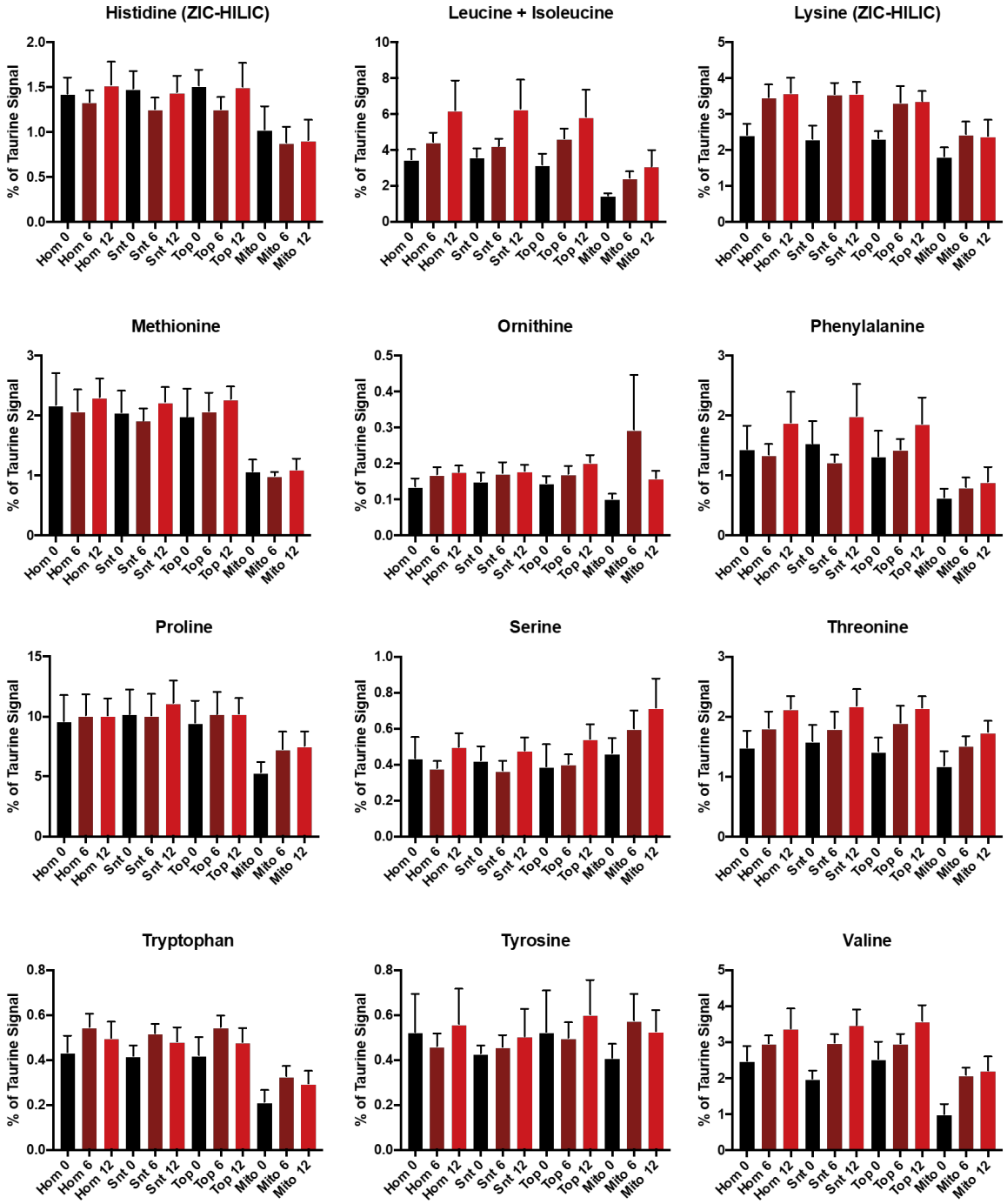

Fig. C.17 Changes in amino acids & peptides in mouse heart during a time course of WI (ctd.). Metabolite ion intensities from the control, 6 and 12 min WI heart data sets were normalised to taurine. Data is from ZIC-pHILIC column unless otherwise stated as from ZIC-HILIC column. Data is average of 3 biological replicates for controls and 6 biological replicates for all other time points, presented as mean ±SEM. H: Homogenate; S: Supernatant; C: Cytosolic fraction; M: Mitochondrial fraction. NF: Not found.

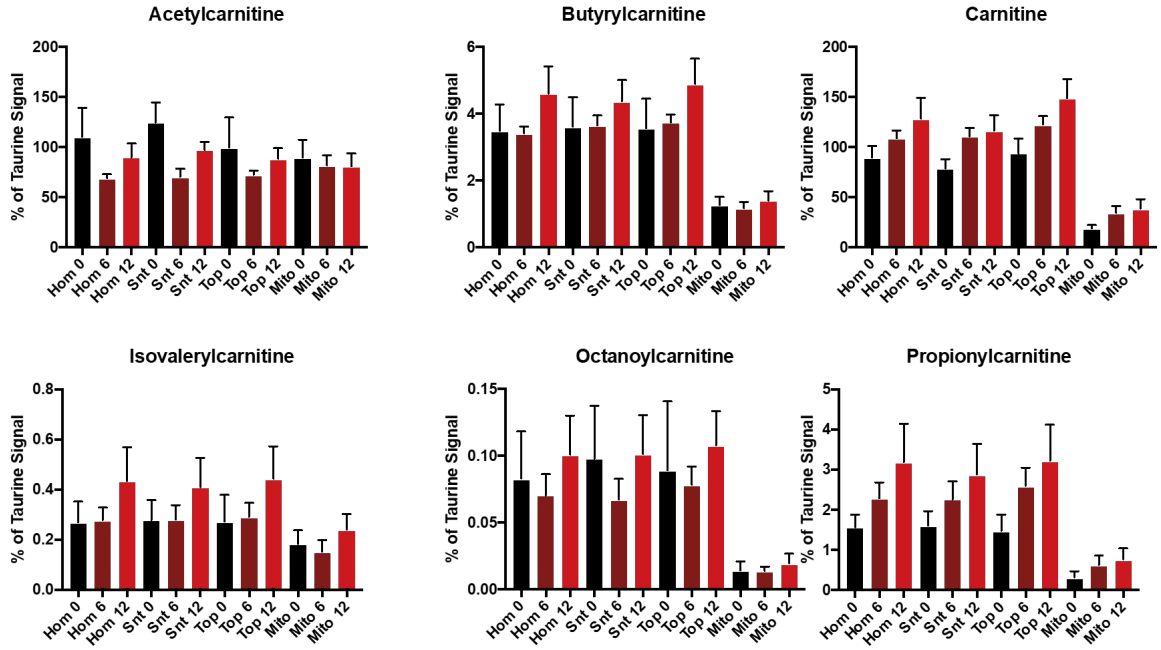

Fig. C.18 Changes in amino acids & peptides in mouse heart during a time course of WI (ctd.). Metabolite ion intensities from the control, 6 and 12 min WI heart data sets were normalised to taurine. Data is from ZIC-pHILIC column unless otherwise stated as from ZIC-HILIC column. Data is average of 3 biological replicates for controls and 6 biological replicates for all other time points, presented as mean ±SEM. H: Homogenate; S: Supernatant; C: Cytosolic fraction; M: Mitochondrial fraction. NF: Not found.

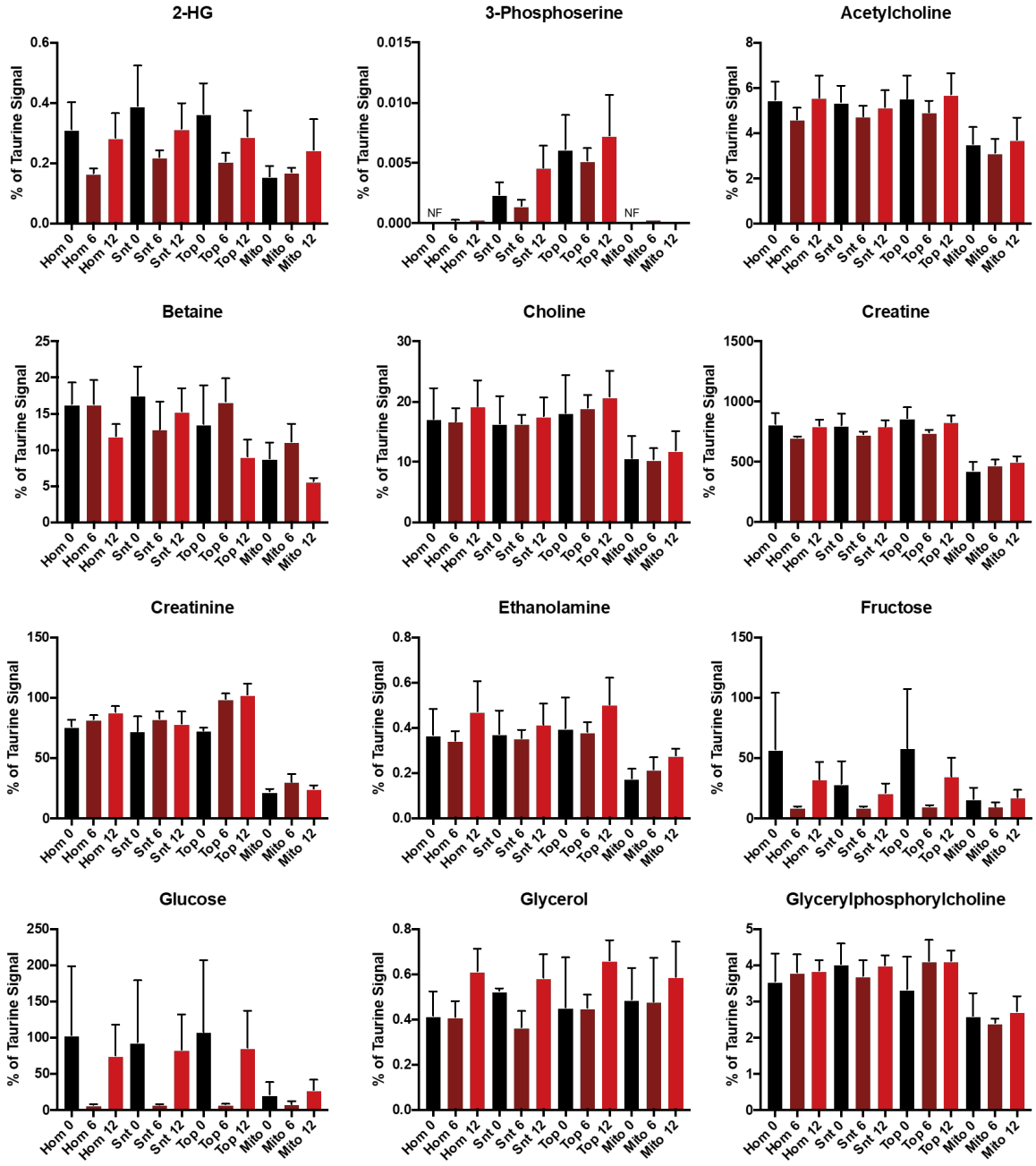

Fig. C.19 Changes in miscellaneous metabolites in mouse heart during a time course of WI. Metabolite ion intensities from the control, 6 and 12 min WI heart data sets were normalised to taurine. Data is from ZIC-pHILIC column unless otherwise stated as from ZIC-HILIC column. Data is average of 3 biological replicates for controls and 6 biological replicates for all other time points, presented as mean ±SEM. H: Homogenate; S: Supernatant; C: Cytosolic fraction; M: Mitochondrial fraction. NF: Not found.

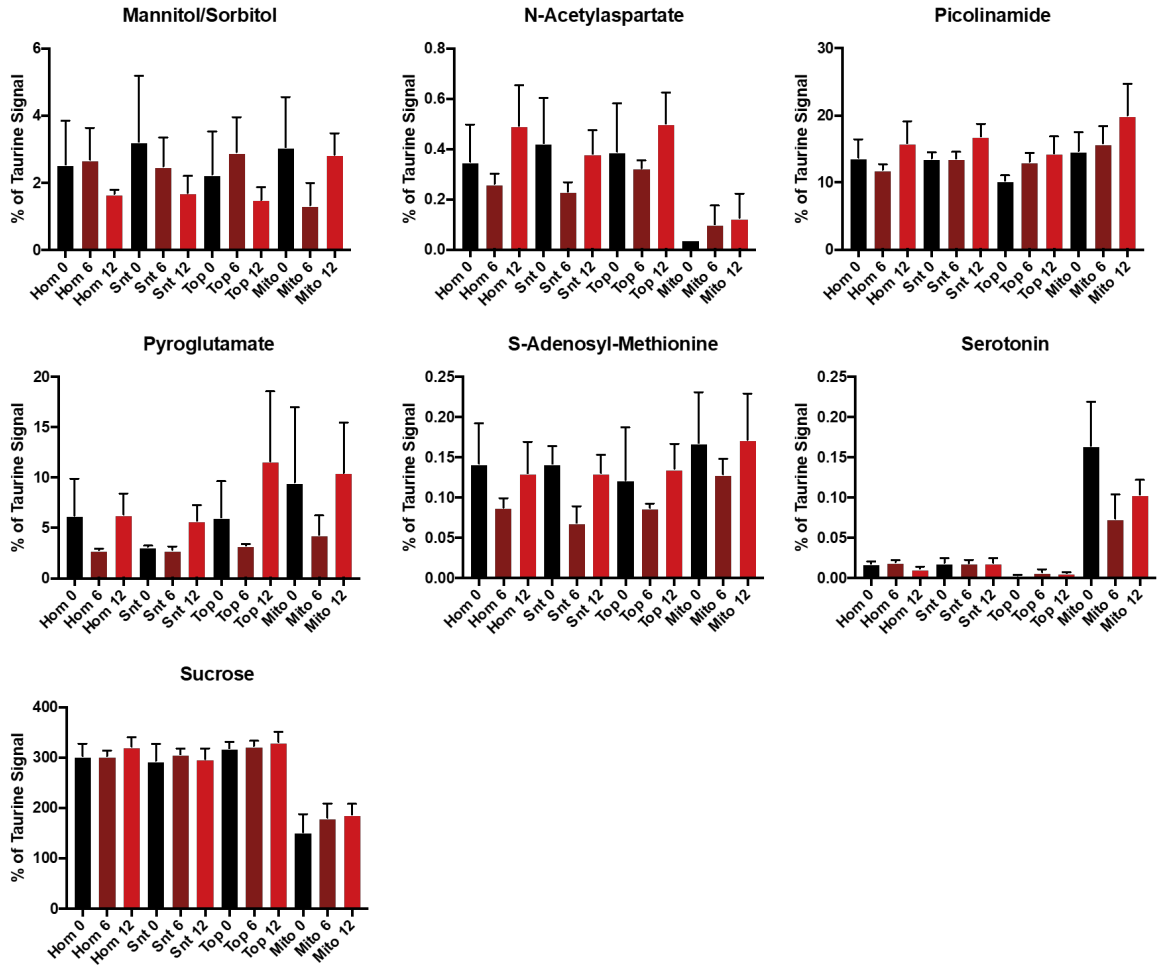

Fig. C.20 Changes in miscellaneous metabolites in mouse heart during a time course of WI (ctd.). Metabolite ion intensities from the control, 6 and 12 min WI heart data sets were normalised to taurine. Data is from ZIC-pHILIC column unless otherwise stated as from ZIC-HILIC column. Data is average of 3 biological replicates for controls and 6 biological replicates for all other time points, presented as mean ±SEM. H: Homogenate; S: Supernatant; C: Cytosolic fraction; M: Mitochondrial fraction. NF: Not found.

C.4 Liver WI time course

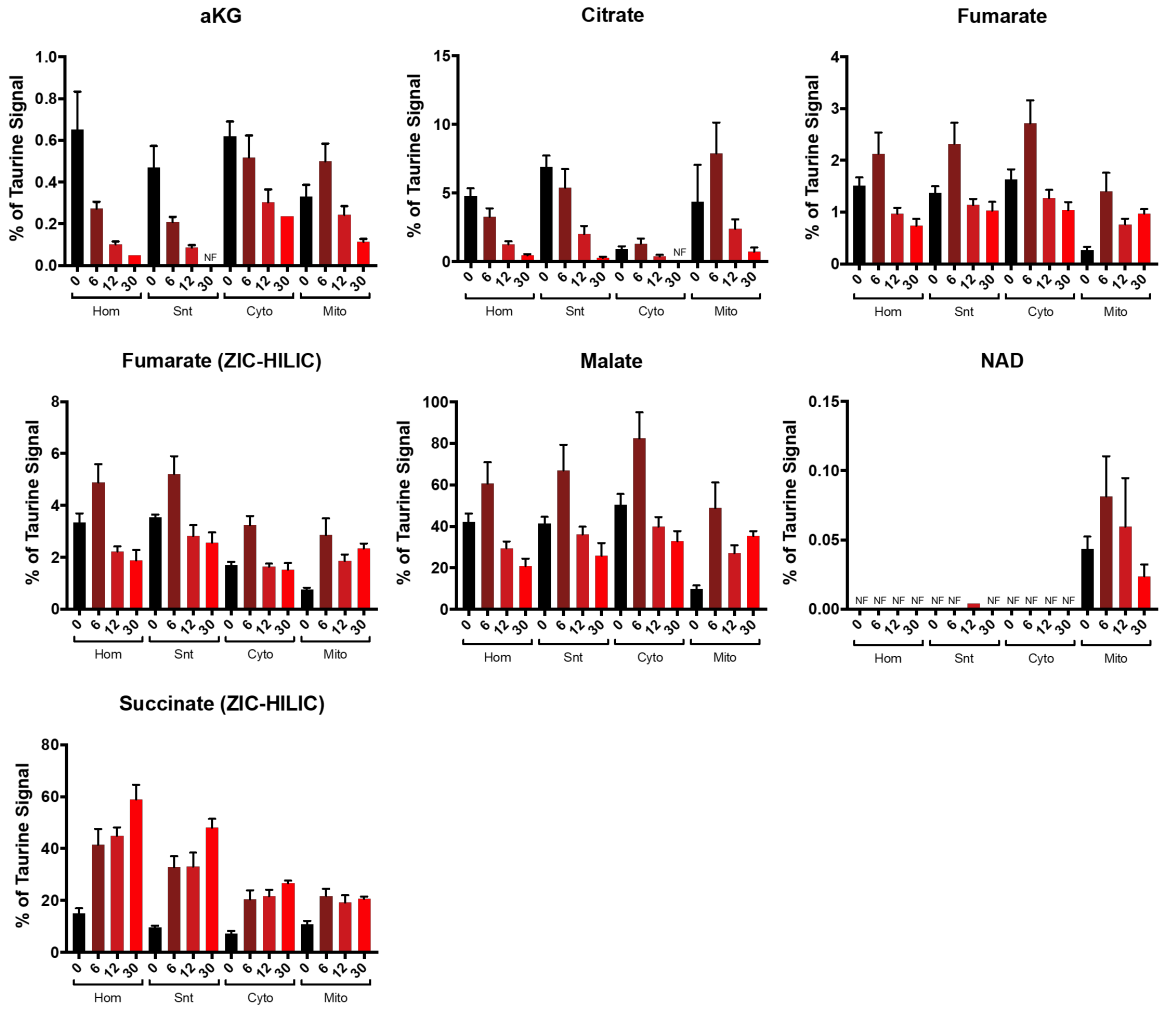

Fig. C.21 Changes in TCA cycle intermediates in mouse liver during a time course of WI. Metabolite ion intensities from the control, 6, 12 and 30 min WI liver data sets were normalised to taurine. Data is from ZIC-pHILIC column unless otherwise stated as from ZIC-HILIC column. Data is average of 3 biological replicates for controls and 6 biological replicates for all other time points, presented as mean ±SEM. H: Homogenate; S: Supernatant; C: Cytosolic fraction; M: Mitochondrial fraction. NF: Not found.

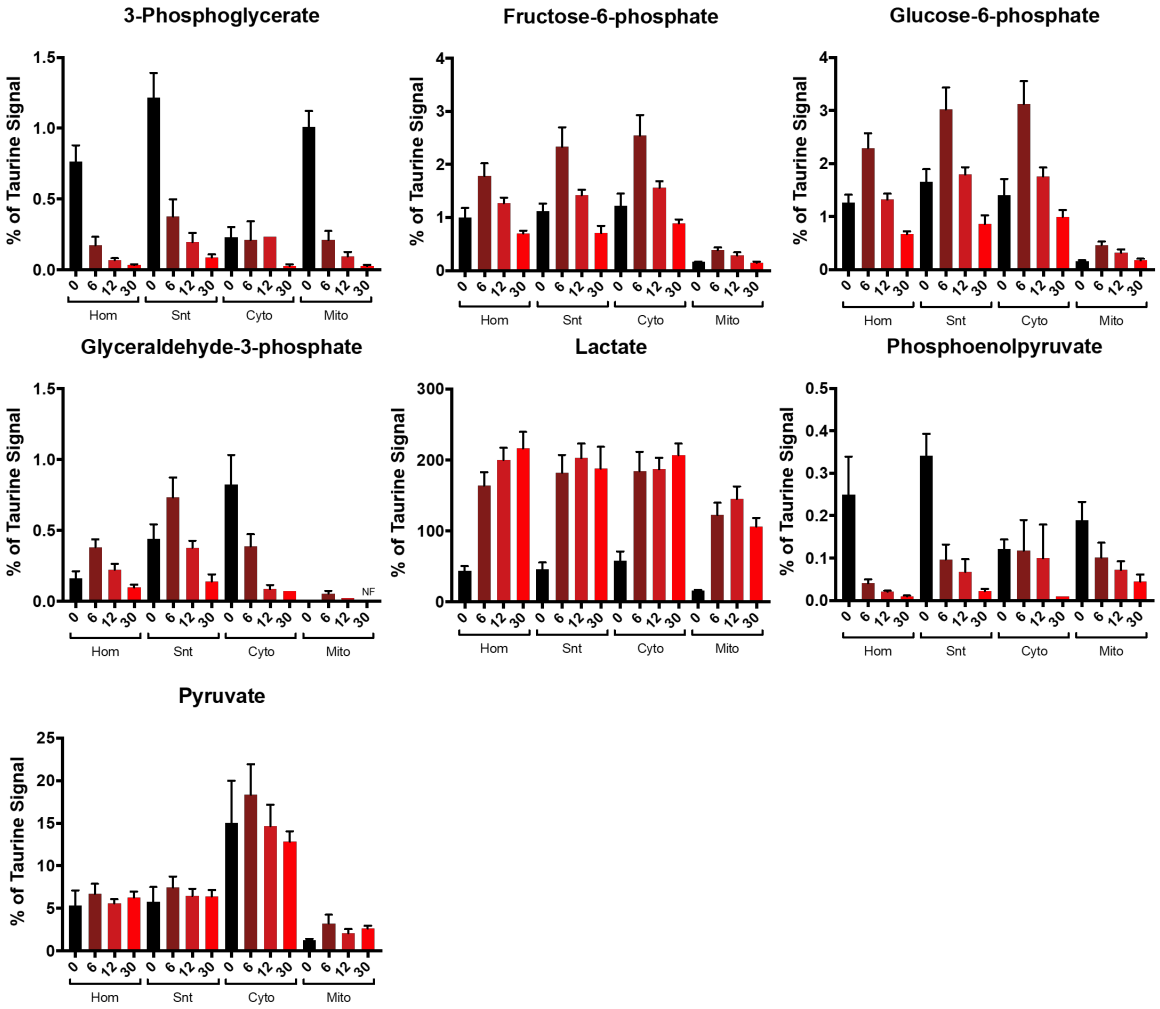

Fig. C.22 Changes in glycolytic intermediates in mouse liver during a time course of WI. Metabolite ion intensities from the control, 6, 12 and 30 min WI heart data sets were normalised to taurine. Data is from ZIC-pHILIC column unless otherwise stated as from ZIC-HILIC column. Data is average of 3 biological replicates for controls and 6 biological replicates for all other time points, presented as mean ±SEM. H: Homogenate; S: Supernatant; C: Cytosolic fraction; M: Mitochondrial fraction. NF: Not found.

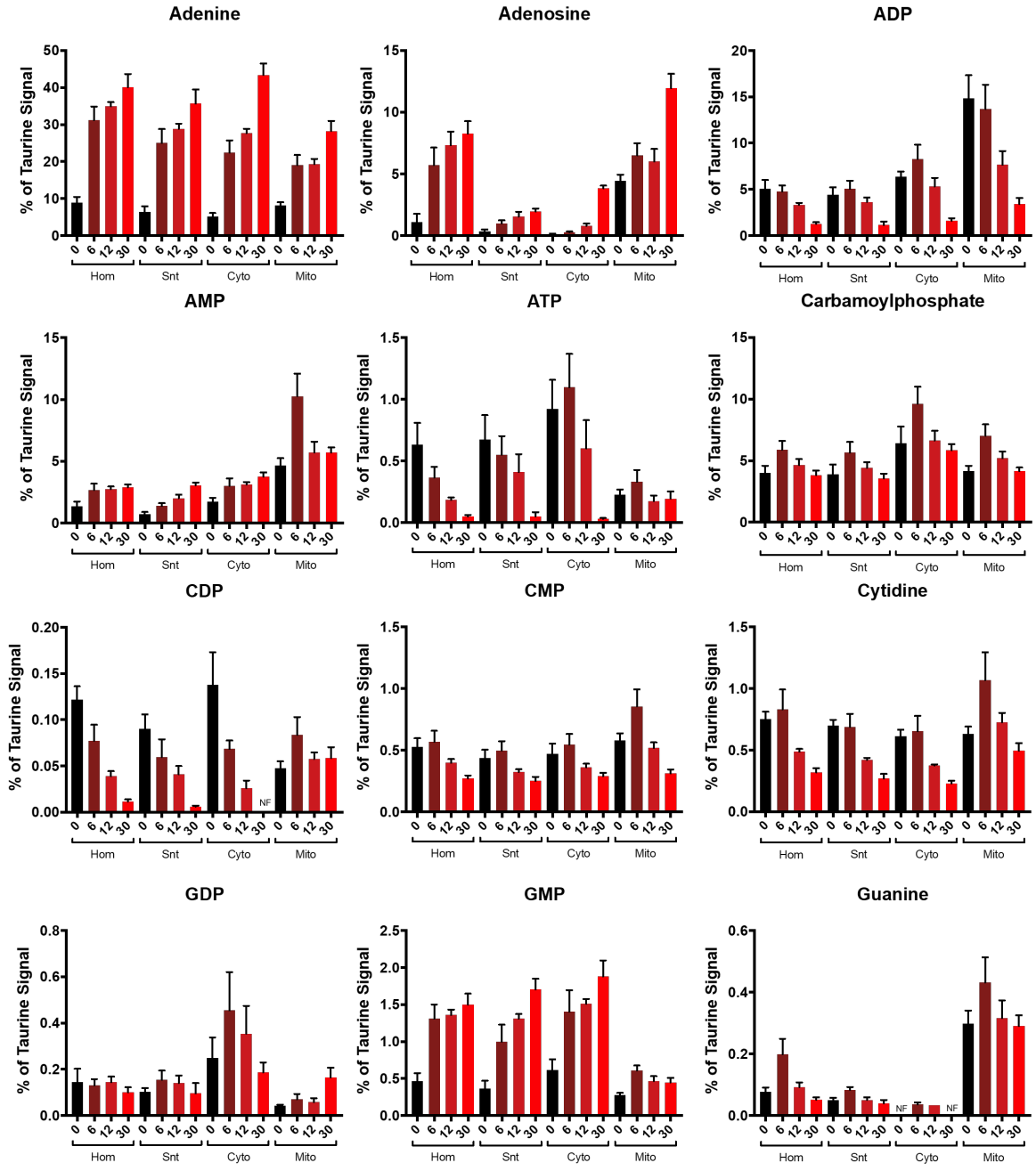

Fig. C.23 Changes in nucleotides & breakdown products in mouse liver during a time course of WI. Metabolite ion intensities from the control, 6, 12 and 30 min WI liver data sets were normalised to taurine. Data is from ZIC-pHILIC column unless otherwise stated as from ZIC-HILIC column. Data is average of 3 biological replicates for controls and 6 biological replicates for all other time points, presented as mean ±SEM. H: Homogenate; S: Supernatant; C: Cytosolic fraction; M: Mitochondrial fraction. NF: Not found.

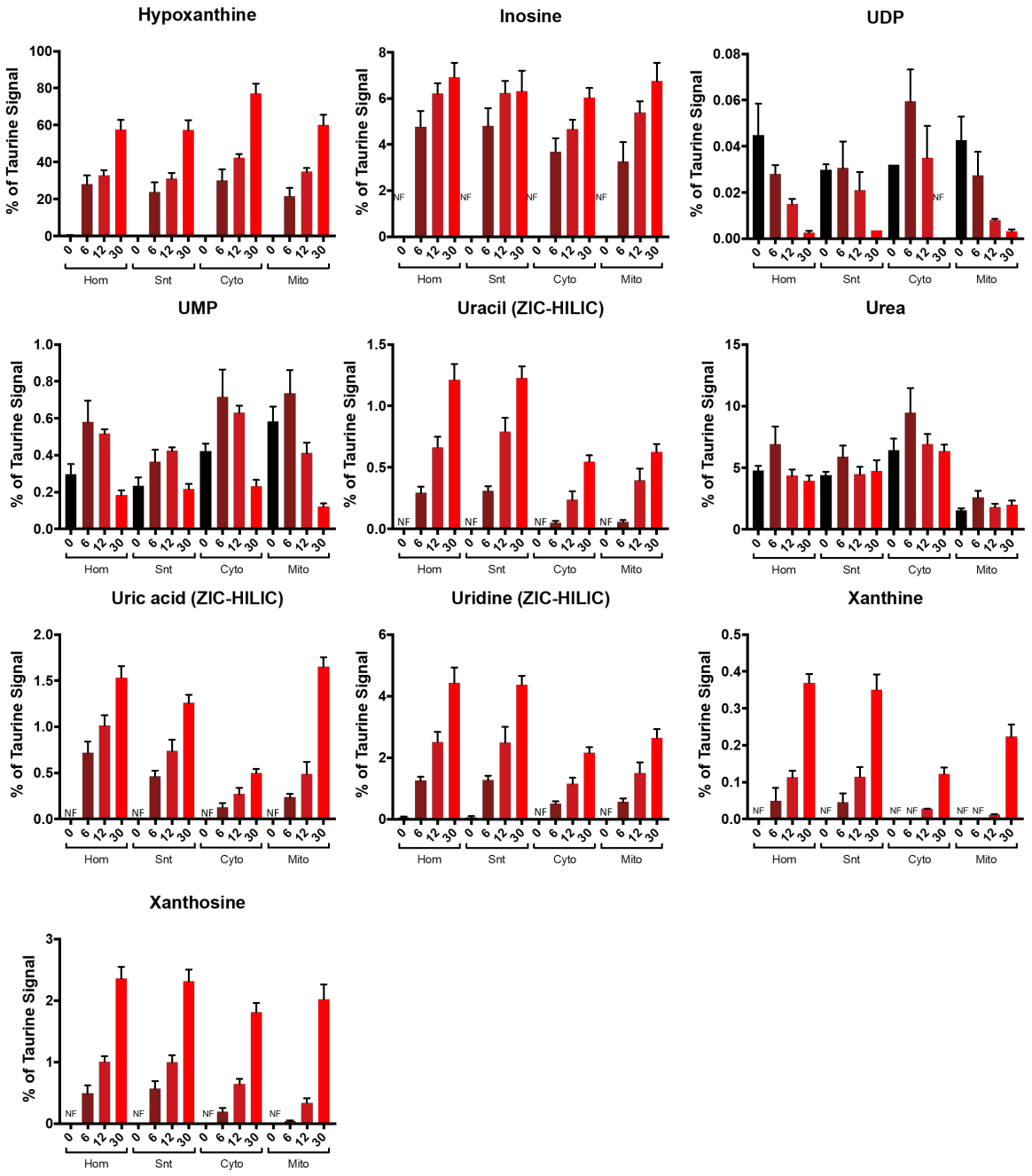

Fig. C.24 Changes in nucleotides & breakdown products in mouse liver during a time course of WI (ctd.). Metabolite ion intensities from the control, 6, 12 and 30 min WI liver data sets were normalised to taurine. Data is from ZIC-pHILIC column unless otherwise stated as from ZIC-HILIC column. Data is average of 3 biological replicates for controls and 6 biological replicates for all other time points, presented as mean ±SEM. H: Homogenate; S: Supernatant; C: Cytosolic fraction; M: Mitochondrial fraction. NF: Not found.

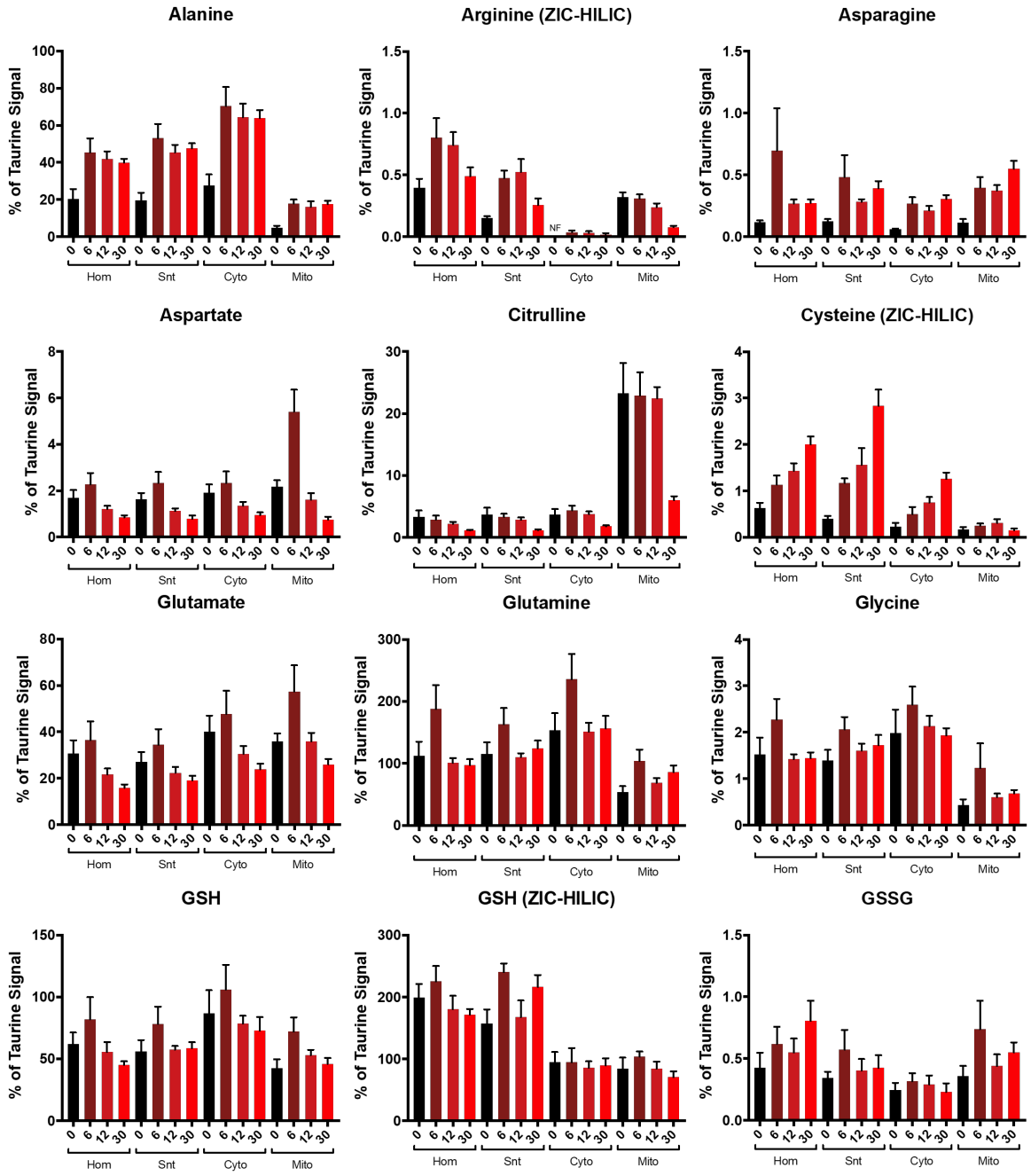

Fig. C.25 Changes in amino acids & peptides in mouse liver during a time course of WI. Metabolite ion intensities from the control, 6, 12 and 30 min WI liver data sets were normalised to taurine. Data is from ZIC-pHILIC column unless otherwise stated as from ZIC-HILIC column. Data is average of 3 biological replicates for controls and 6 biological replicates for all other time points, presented as mean ±SEM. H: Homogenate; S: Supernatant; C: Cytosolic fraction; M: Mitochondrial fraction. NF: Not found.

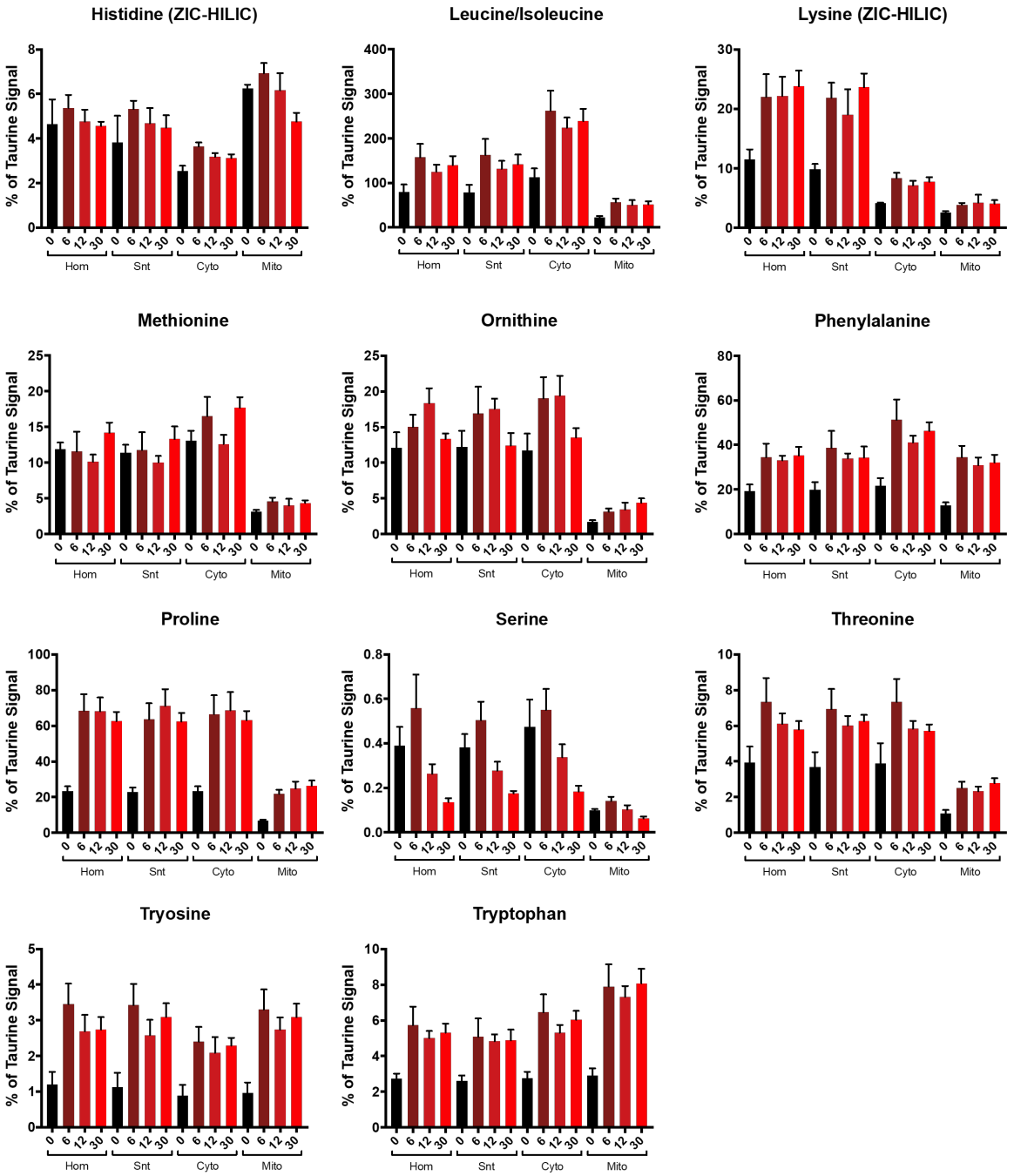

Fig. C.26 Changes in amino acids & peptides in mouse liver during a time course of WI (ctd.). Metabolite ion intensities from the control, 6, 12 and 30 min WI liver data sets were normalised to taurine. Data is from ZIC-pHILIC column unless otherwise stated as from ZIC-HILIC column. Data is average of 3 biological replicates for controls and 6 biological replicates for all other time points, presented as mean ±SEM. H: Homogenate; S: Supernatant; C: Cytosolic fraction; M: Mitochondrial fraction. NF: Not found.

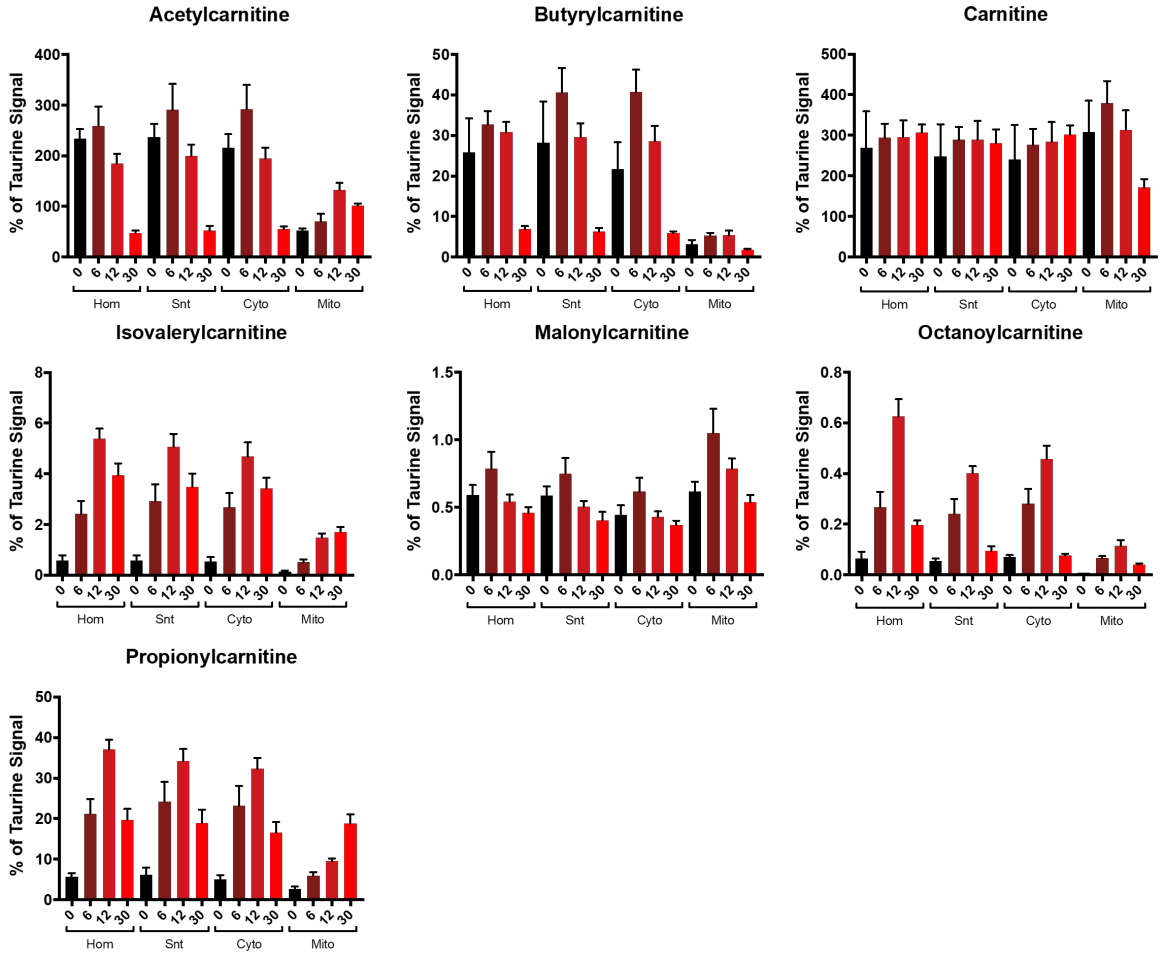

Fig. C.27 Changes in amino acids & peptides in mouse liver during a time course of WI (ctd.). Metabolite ion intensities from the control, 6, 12 and 30 min WI liver data sets were normalised to taurine. Data is from ZIC-pHILIC column unless otherwise stated as from ZIC-HILIC column. Data is average of 3 biological replicates for controls and 6 biological replicates for all other time points, presented as mean ±SEM. H: Homogenate; S: Supernatant; C: Cytosolic fraction; M: Mitochondrial fraction. NF: Not found.

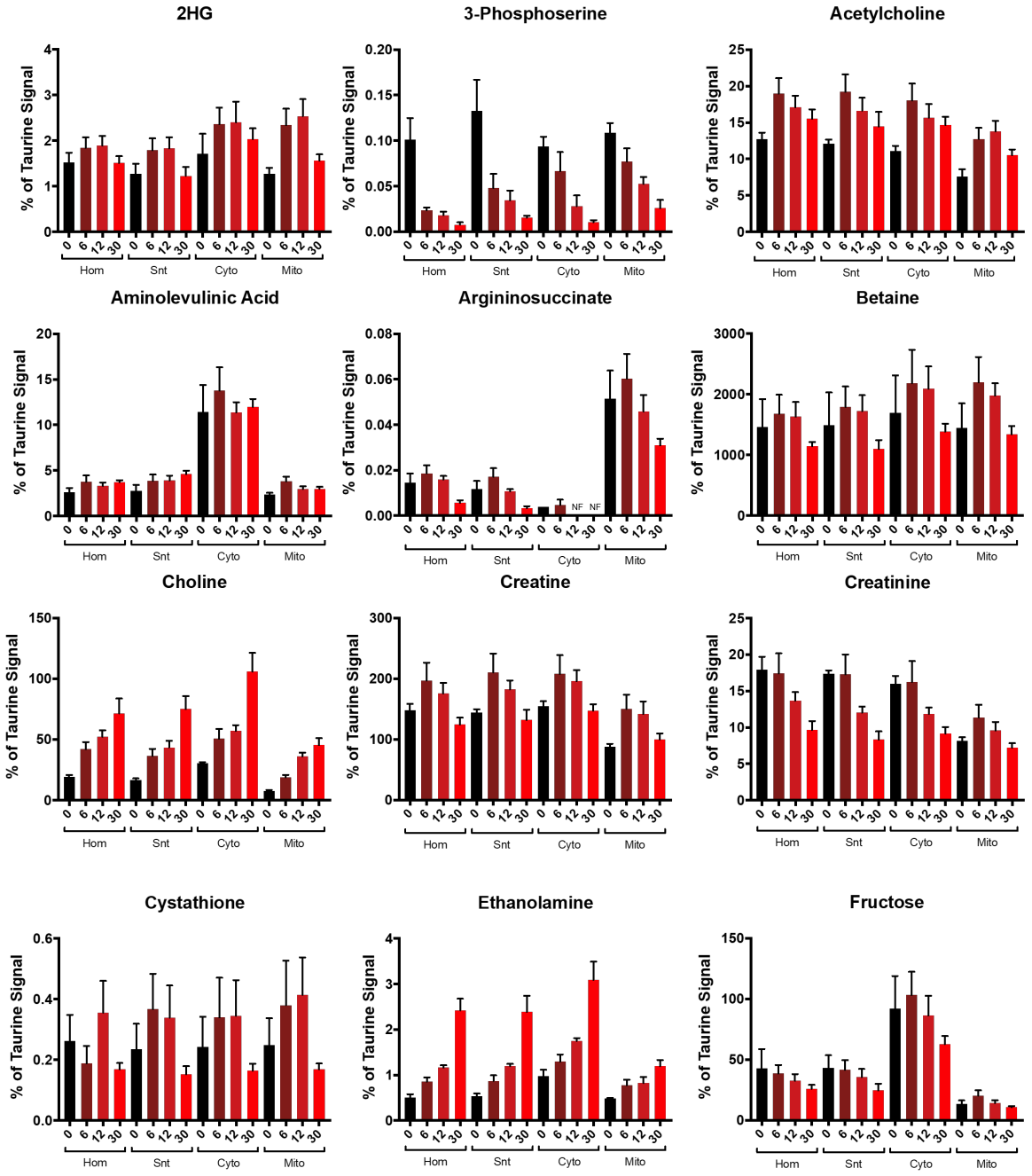

Fig. C.28 Changes in miscellaneous metabolites in mouse liver during a time course of WI. Metabolite ion intensities from the control, 6, 12 and 30 min WI liver data sets were normalised to taurine. Data is from ZIC-pHILIC column unless otherwise stated as from ZIC-HILIC column. Data is average of 3 biological replicates for controls and 6 biological replicates for all other time points, presented as mean ±SEM. H: Homogenate; S: Supernatant; C: Cytosolic fraction; M: Mitochondrial fraction. NF: Not found.

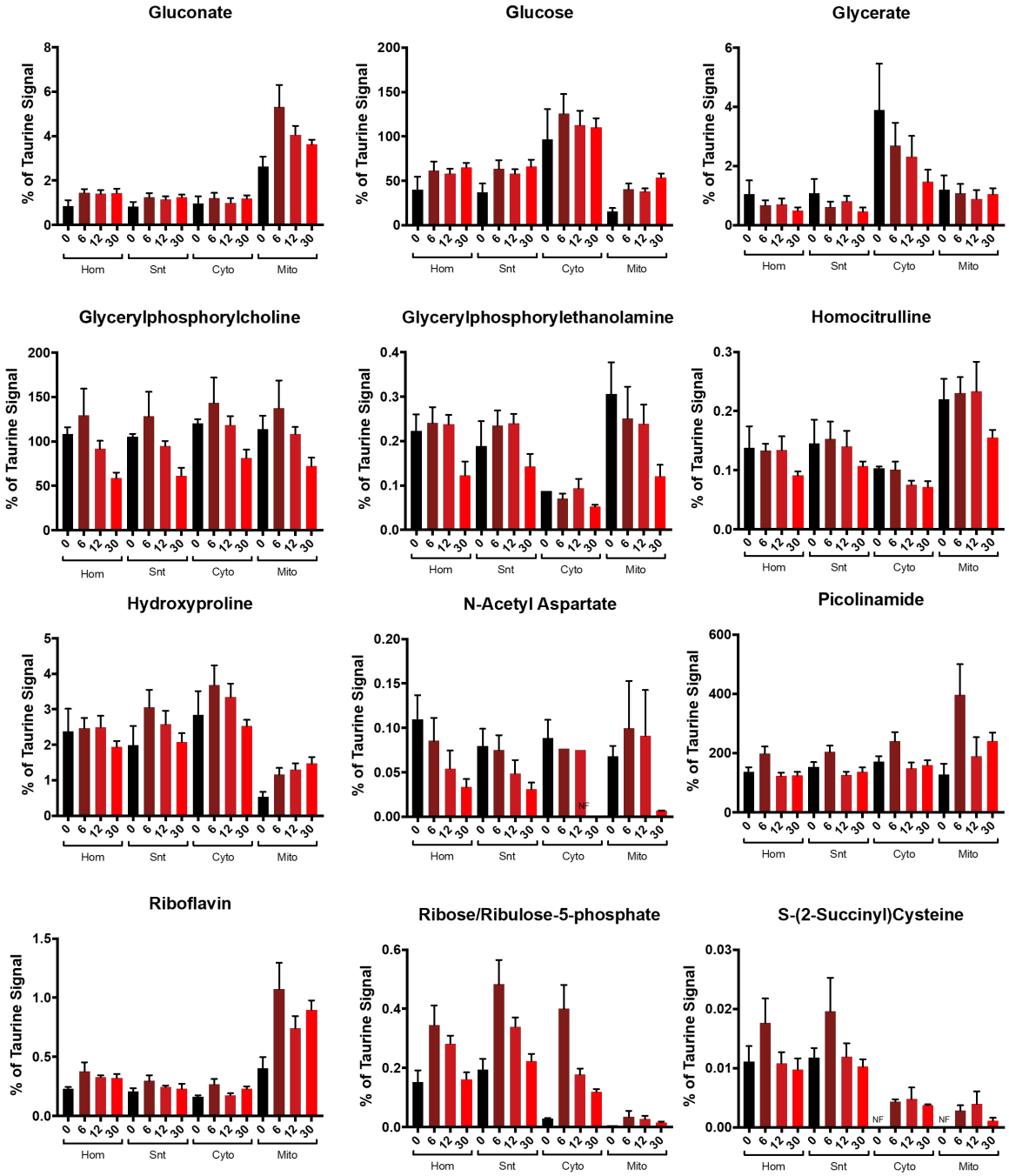

Fig. C.29 Changes in miscellaneous metabolites in mouse liver during a time course of WI (ctd.). Metabolite ion intensities from the control, 6, 12 and 30 min WI liver data sets were normalised to taurine. Data is from ZIC-pHILIC column unless otherwise stated as from ZIC-HILIC column. Data is average of 3 biological replicates for controls and 6 biological replicates for all other time points, presented as mean ±SEM. H: Homogenate; S: Supernatant; C: Cytosolic fraction; M: Mitochondrial fraction. NF: Not found.

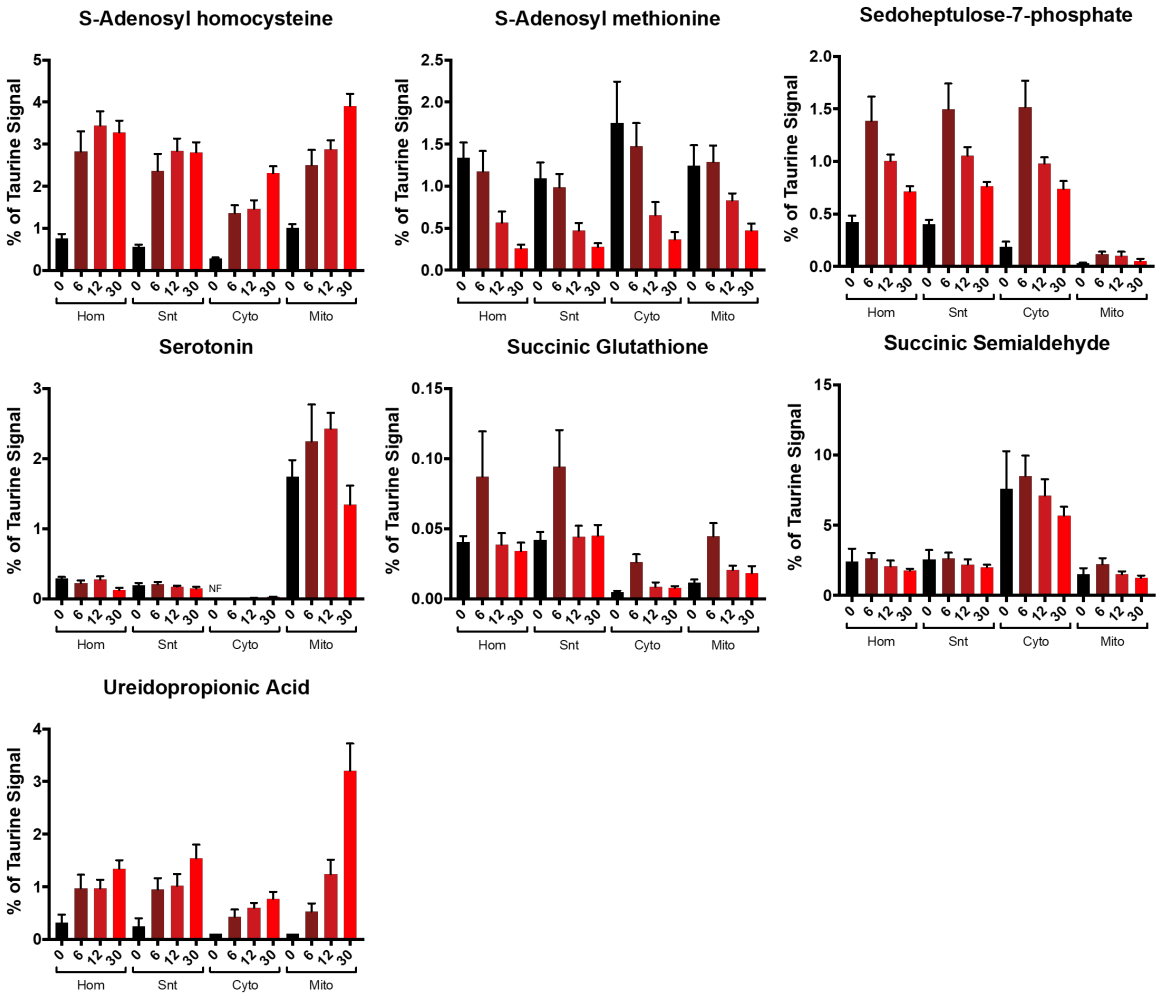

Fig. C.30 Changes in miscellaneous metabolites in mouse liver during a time course of WI (ctd.). Metabolite ion intensities from the control, 6, 12 and 30 min WI liver data sets were normalised to taurine. Data is from ZIC-pHILIC column unless otherwise stated as from ZIC-HILIC column. Data is average of 3 biological replicates for controls and 6 biological replicates for all other time points, presented as mean ±SEM. H: Homogenate; S: Supernatant; C: Cytosolic fraction; M: Mitochondrial fraction. NF: Not found.